

МІНІСТЕРСТВО ОСВІТИ І НАУКИ УКРАЇНИ
ДВНЗ «Прикарпатський національний університет імені Василя Стефаника»

Кафедра фізики і хімії твердого тіла

Фізико-хімічний інститут

Навчально-дослідний центр напівпровідникового матеріалознавства

Державний фонд фундаментальних досліджень

АКАДЕМІЯ НАУК ВИЩОЇ ШКОЛИ УКРАЇНИ

НАЦІОНАЛЬНА АКАДЕМІЯ НАУК УКРАЇНИ

Інститут фізики напівпровідників ім. В.Є. Лашкарьова

Інститут хімії поверхні ім. О.О. Чуйка

Інститут металофізики ім. Г.В. Курдюмова

Інститут загальної і неорганічної хімії ім. В.І. Вернадського

Українське фізичне товариство

Інститут інноваційних досліджень

XVI МІЖНАРОДНА КОНФЕРЕНЦІЯ З ФІЗИКИ І ТЕХНОЛОГІЇ
ТОНКИХ ПЛІВОК ТА НАНОСИСТЕМ

(присвячена пам'яті професора Дмитра Фреїка)

Матеріали

Івано-Франківськ, 15-20 травня, 2017

Ivano-Frankivsk, May 15-20, 2017

Materials

**XVI INTERNATIONAL CONFERENCE ON PHYSICS AND
TECHNOLOGY OF THIN FILMS AND NANOSYSTEMS**
(dedicated to memory Professor Dmytro Freik)

MINISTRY OF EDUCATION AND SCIENCE OF UKRAINE

Vasyl Stefanyk Precarpathian National University

Physics and Chemistry of Solid State Department

Physical-Chemical Institute

Educational Research Centre of Semiconductor Material

State Fund of Fundamental Research

ACADEMY OF SCIENCE OF HIGH SCHOOL OF UKRAINE

NATIONAL ACADEMY OF SCIENCE OF UKRAINE

V.E. Lashkarev Institute of Semiconductor Physics

Chuiko Institute of Surface Chemistry

G.V. Kurdyumov Institute of the Physics of Metals

V.I. Vernadsky Institute of General and Inorganic Chemistry

Ukraine Physics Society

Institute of innovation research

УДК 539.2
ББК 22.373.1
П 80

XVI Міжнародна конференція з фізики і технології тонких плівок та наносистем (присвячена пам'яті професора Дмитра Фреїка). *Матеріали.*
 / За заг. ред. проф. Прокопів В.В. – Івано-Франківськ : Прикарпатський національний університет імені Василя Стефаника, 2017. – 388 с.

Представлено сучасні результати теоретичних і експериментальних досліджень з питань фізики і технології тонких плівок та наносистем (метали, напівпровідники, діелектрики, провідні полімери; методи отримання та дослідження; фізико-хімічні властивості; нанотехнології і наноматеріали, квантово-розмірні структури, нанoeлектроніка, тощо. Матеріали підготовлено до друку [Програмним комітетом](#) конференції і подано в авторській редакції.

Для наукових та інженерних працівників, що займаються проблемами тонкоплівкового матеріалознавства та мікроелектроніки.

Рекомендовано до друку науково-технічною радою Фізико-хімічного інституту ДВНЗ «Прикарпатський національний університет імені Василя Стефаника»

XVI International Conference Physics and Technology of Thin Films and Nanosystems (dedicated to memory Professor Dmytro Freik). *Materials.* / Ed. by Prof. Prokopiv V.V. – Ivano-Frankivsk : Publisher Vasyl Stefanyk Precarpathian National University, 2017. – 388 c.

The results of theoretical and experimental researches in directions of the physics and technology of thin films and nanosystems (metals, semiconductors, dielectrics, and polymers; and methods of their investigation; physic-chemical properties of thin films; nanotechnology and nanomaterials, quantum-size structures; thin-film devices of electronics, are presented. The materials preformed for printing by Conference's Organizational Committee and Editorial Board, are conveyed in authoring edition.

For scientists and reserchers on the field of thin-film material sciences and nanoelectronics.

©ДВНЗ «Прикарпатський національний університет імені Василя Стефаника», 2017

© Vasyl Stefanyk Precarpathian National University, 2017

PROGRAM COMMITTEE / EDITORIAL BOARD

Editor-in-Chief

Prof. Volodymyr PROKOPIV

Vasyl Stefanyk Precarpathian national University (Ivano-Frankivsk, Ukraine)

Vice Editors-in-Chief

Acad. Volodymyr LITOVCHENKO

V.E.Lashkarev Institute of Semiconductors Physics, NAS in Ukraine (Kyiv, Ukraine)

Prof. Andriy ZAGORODNYUK

Vasyl Stefanyk Precarpathian national University (Ivano-Frankivsk, Ukraine)

Program Committee

Prof. Juozas AUGUTIS (*Kaunas, Lithuania*); Prof. Mahammad BABANLY (*Baku, Azerbaijan*); Prof. Slavko BERNIK (*Ljubljana, Slovenia*); Prof. Attila CSÍK (*Debrecen, Hungary*); Prof. Mykola DMYTRUK (*Kyiv, Ukraine*); Prof. Petro FOCHUK (*Chernivtsy, Ukraine*); Prof. Bruce GNADE (*Dallas, USA*); Prof. Gaetano GRANOZZI (*Padova, Italia*); Prof. Yuri GUREVICH (*Mexico City, Mexico*); Prof. Eugeny IVAKIN (*Minsk, Belarus*); Acad. Orest IVASISHIN (*Kyiv, Ukraine*); Prof. Zhao HUI (*Harbin, P.R. China*); Prof. Ivan KABAN (*Dresden, Germany*); Acad. Vasyl KLADKO (*Kyiv, Ukraine*); Prof. Sandor KÖKÉNYESI (*Debrecen, Hungary*); Prof. dr. hab. Marek KUNABRONIOWSKI (*Lublin, Poland*); Prof. Georgy LASHKAREV (*Kyiv, Ukraine*); Dr. Petro LYTVYN (*Kyiv, Ukraine*); Prof. Bingbing LIU (*Changchun, P. R. China*); Prof. Georgy MALASHKEVICH (*Minsk, Belarus*); Prof. Georgy MLADENOV (*Sofia, Bulgaria*); Acad. Anton NAUMOVETS (*Kyiv, Ukraine*); Prof. Ivan PROTSENKO (*Sumy, Ukraine*); Prof. Olena ROGACHEVA (*Kharkiv, Ukraine*); Prof. Eduard SHPILEVSKY (*Minsk, Belarus*); Dr. Petro SMERTENKO (*Kyiv, Ukraine*); Prof. John STOCKHOLM (*Vernouillet, France*); Prof. Tomasz STORY (*Warsaw, Poland*); Dr. Zbigniew SWIATEK (*Krakow, Poland*); Acad. Ion TIGINYANU (*Chisinau, Moldova*); Prof. Arnolds ŪBELIS (*Riga, Latvia*); Prof. Grzegorz WISZ (*Rzeszow, Poland*); Prof. Krzysztof WOJCIECHOWSKI (*Kraków, Poland*); Prof. Paweł ŻUKOWSKI (*Lublin, Poland*)



PLENARY SESSIONS



Optical Phenomena and Processes Induced by Ultrashort Light Pulses in Chalcogenide and Chalcohalide Glassy Semiconductors

Blonskyi I.^a, Kadan V.^a, Rybak A.^a, Pavlova S.^a,
Calvez L.^b, Mytsyk B.^c, Shpotyk O.^{d,e}

^a*Institute of Physics of the NAS of Ukraine, Kyiv, Ukraine;*

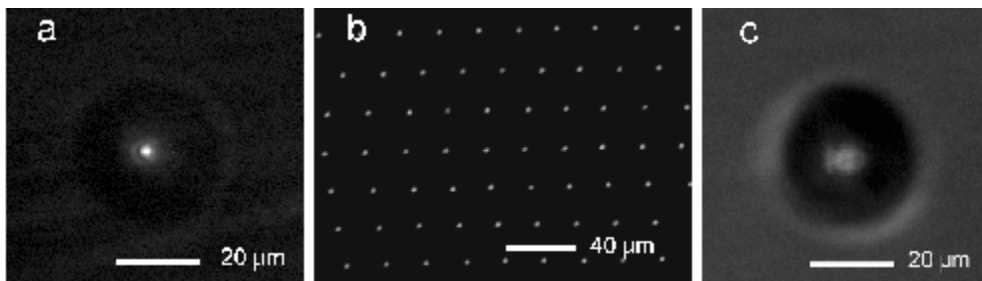
^b*UMR-CNRS 6226, Université de Rennes 1, Rennes Cedex, France;*

^c*Karpenko Physico-Mechanical Institute of the NAS of Ukraine, Lviv, Ukraine;*

^d*Vlokh Institute of Physical Optics, Lviv, Ukraine;*

^e*Institute of Physics of Jan Dlugosz University, Czestochowa, Poland*

The investigation results of new physical phenomena and processes induced by femtosecond laser pulses in chalcogenide (ChG) and chalcohalide (ChH) glassy semiconductors and other optical materials (sapphire, quartz) are reported. The report includes the following three main parts: 1 – experimental study of propagation laws of ultrashort laser pulses in transparent condensed media using new experimental techniques (time-resolved pump-probe microscopy and spectroscopy, Z-scan, pulse temporal compression from 140 to 65 fs), created for this purpose; 2 – study of nonlinear transient phenomena in such media, particularly the peculiarities of filamentation and conical emission in positively and negatively birefringent crystals, attractive and repulsive interaction of two filaments, spectral peculiarities of filament-induced supercontinuum and conical emission; 3 – optical breakdown caused by femtosecond laser pulses in optical materials and its use for precision laser micromachining. We report new femtosecond fabrication technologies of microoptical elements (microlenses, micromirrors, microwaveguides and their arrays) which are promising for telecom use. Particularly, we present a simple two-step fabrication process of diffraction-limited micromirrors and arrays of micromirrors. As an example, the figure shows focal spot of a single micromirror (a), foci of micromirrors array (b), and an image (letters IΦ) created by a single micromirror (c), which demonstrate diffraction-limited performance of the micromirror (resolution $\sim 2 \mu\text{m}$).



The authors acknowledge support from the STCU-NASU (project 6174), NASU-TÜBİTAK (joint project), as well as from the Ukrainian State Fund for Fundamental Research (Project F73/23805).

Effect of the Electric Field on the Energy of Quantum Transitions in Impurity Quantum Dots

Boichuk V.I., Kropyvnytska K.M., Leshko R.Ya.

Drohobych Ivan Franko State Pedagogical University, Drohobych, Ukraine,
teorfizyka@gmail.com

Impurities play an important role in the analysis of the properties of semiconductors which are used in the fabrication of devices. Even a small concentration of impurities increases the semiconductor conductivity by several orders. In the recent few decades, there has been increased attention to the problem of impurity states due to great perspectives of low-dimensional semiconductor structures such as quantum wells, quantum wires and quantum dots (QDs). Due to quantum confinement of impurity electrons (holes) there is a possibility to engineer the electronic structure and tune the energy spectrum to obtain desirable optical transitions through modification of sizes and shapes of quantum dots [1 - 3]. These characteristics are useful for the development of optoelectronic devices with tunable emission and transmission properties and ultra-narrow spectral linewidths.

One of the important factors which influence the physical properties of the quantum dot is the external electric field. It causes a shift of energy levels and field dependence of the carrier lifetime of quantum dots. Therefore, the impurity and the applied electric field effects on the optical properties of quantum dots are of great interest for both fundamental physics and device application.

In the present work we investigated the optical properties of a spherical quantum dot with the parabolic confinement potential in cases of the presence of donor and acceptor impurities, and the electric field. The results show that the oscillator strengths for impurities of different sign are different. The oscillator strength between the ground and the first excited states in the quantum dot has been calculated as functions of the confinement potential and the applied electric field. Based on the results of calculations of the oscillator strength transition, we obtained the linear, nonlinear, the total optical absorption coefficients, and the optical refractive index as a function of the incident photon energy for the different values of the confinement potential and the electric field. The detailed analysis of the dependence of the absorption coefficient and the refractive index on the confinement strength, the applied electric field, and also the type of impurity has been performed.

[1] F. Bassani, G. Iadonisi, B. Preziosi, Rep. Progr. Phys. 37 (1974) 1009.

[2] M.V. Tkach, V.A. Golovac'kij, Ja.M. Berezovs'kij, Physics and Chemistry of Solid State 4(2), 213 (2003).

[3] V. I. Boichuk, I. V. Bilynskyi, R. Ya. Leshko, L. M. Turyanska, Physica E: Low-dimensional Systems and Nanostructures. — 2013. — Vol. 54 — P. 281–287

Metal Nanostructures on Semiconductor Surface as a Basis for Plasmonic Optoelectronics

Dmitruk N.L., Korovin A.V., Malynych S.Z.

Institute for Physics of Semiconductors, National Academy of Sciences of Ukraine
Kyiv, Ukraine, E-mail: dmitruk@isp.kiev.ua

Nowadays much interest has been devoted to nanoscale metal structures (dots, nanowires, etc.) on semiconductor for both fundamental research and practical use. Some different modes can be excited: 1) “surface plasmon polariton” (SPP) on periodical system of nanodots or nanowires on dielectric (semiconductor); 2) surface electromagnetic waves (SPP) along the surface of separate nanowire on the air-metal interface; 3) waveguide TM, TE modes in thin overlayers (TCF); 4) surface (local) plasmon (SP) in nanodot or nanowire.

Besides, the array of metal nanowires creates a multifunctional grid: for surface plasmon polaritons excitation, for current collection, for decrease of the surface recombination velocity, for forming the current-carrying contact on texturized front surface.

A number of practical applications of gold and silver nanoparticles and nanoparticle arrays for needs of photonics [1], nonlinear spectroscopy [2], submicron visualization [3], surface-enhanced Raman and infrared spectroscopy [4, 5], photovoltaics [6], and various sensors [7] has been suggested so far. The fundamental background of all the mentioned processes is a resonant enhancement of light interaction with metal nanoparticles, and it is crucial to minimize the losses caused by absorption of incident light, wasted as heat, by the metal nanoparticles for efficient energy transfer into the active materials.

The main way to design photovoltaic devices of new generation is confinement of light absorption (light trapping) in ultra-thin area nearby the p-n or metal-semiconductor junction separating electron-hole pairs. This increases the number of collected carriers.

Several principal techniques of plasmonic photovoltaics was described in our previous works:

i) increasing the light transmission into the photoactive base in the case of anti-correlated reliefs of both sides of emitter (metal) film of surface-barrier heterostructure due to excitation of surface plasmon polaritons [8];

ii) light absorption enhancement due to light scattering by big noble metal nanoparticles in the wave zone (far-field) [9], e.g. optical radiation efficiency defined by the ratio of the scattering cross-section to the extinction one, for Ag nanoparticles with diameter over 90 nm exceeds 90% [10];

iii) near-field concentration of light nearby metal nanoparticles or nanowires due to excitation of surface (local) plasmons (SP) or SPPs [11] with following generation of non-equilibrium current carriers.

The last technique that allows additional electron-hole pairs generation and therefore SC efficiency enhancement has been considered in this work.

This work was supported by the NATO SPS grant NUKR.SFPP984617 “Nanostructured Metal-Semiconductor Thin films for Efficient Solar Harvesting”.

1. W.L. Barnes, A. Dereux, T.W. Ebbesen, Surface plasmon subwavelength optics // *Nature*. – 2003. – v.424. – P. 824-830.
2. H. Shen, B. Cheng, G. Lu, et al., Enhancement of optical nonlinearity in periodic gold nanoparticle arrays // *Nanotechnology*. – 2006. – v.17. – P. 4274-4277.
3. R.J. Blaikie, D.O.S. Melville, Imaging through planar silver lenses in the optical near field // *J. Opt A: Pure Appl. Opt.* – 2005. – v.7. – P. S176-S183.
4. W.E. Doering, S.M. Nie, Single-molecule and single-nanoparticle SERS: examining the roles of surface active sites and chemical enhancement // *J Phys Chem B*. – 2002. – v. 106. – P. 311-317.
5. T.R. Jensen, R.P. Van Duyne, S.A. Jonson, V.A. Maroni, Surface-enhanced infrared spectroscopy: a comparison of metal island films with discrete and nondiscrete surface plasmons // *Appl. Spectrosc.* – 2000. – v.54. – P. 371-377.
6. K.R. Catchpole, A. Polman, Plasmonic solar cells // *Optics express*. – 2008. – v.16, No. 26. – P. 21793-21800.
7. N.L. Dmitruk, S.Z. Malinich, Surface plasmon resonances and their manifestation in the optical properties of nanostructures of noble metals // *Ukr. J. Phys. (Reviews)*. – 2014. – v.9, No.1. – P. 3-37.
8. N.L.Dmitruk, A.V.Korovin, I.B.Mamontova. Efficiency enhancement of surface barrier solar cells due to excitation of surface plasmon polaritons // *Semicond. Sci. Technol.* – 2009. – V.24. – P. 125011 (7p) doi:10.1088/0268-1242/24/12/125011.
9. N.L.Dmitruk, A.V.Korovin. Plasmonic photovoltaics: photocurrent enhancement by metal nanoparticles on solar cells interface // *Proc. of the 24th European Photovoltaic Solar Energy Conference*. 21-25 September 2009. Hamburg, Germany. – P. 566-569.
10. Dmitruk N.L., Malynych S.Z., Moroz I.Ye., Kurlyak V.Yu. Optical efficiency of Ag and Au nanoparticles // *Semiconductor Physics, Quantum Electronics & Optoelectronics*. – 2010. – v.13, No.4. – P. 369-373.
11. Dmitruk N.L., Korovin A.V. Plasmonic photovoltaics: metal nanowires on solar cell interface // *Proc. of 25th European Photovoltaic Solar Energy Conference and Exhibition and 5th World Conference on Photovoltaic Energy Conversion*, Feria Valencia, Convention & Exhibition Centre, 6–10 September 2010, Valencia, Spain. – P.385-388.

Thermoelectric Properties and Defect Subsystem of Lead Telluride Thin Films and Crystals

Galushchak M.O.

Ivano-Frankivsk National Technical University of Oil and Gas, Ivano-Frankivsk, Ukraine

The features of the direct conversion of heat into electricity in recent years are becoming more widespread practical application. Thermoelectric generators and coolers, which are characterized by long life created on the basis of thermoelectric phenomena. These devices characterized the lack of fast wearing moving parts, quiet and reliable performance, low weight and high specific energy consumption, no pollution of the environment, the ability to create combined systems of power and space heating, etc. To effectively convert of the thermal energy into electricity must have a thermoelectric material, which is the main parameter – the thermoelectric figure of merit Z ($Z = a^2 s / c$), where a is the coefficient of thermal-EMF, s is specific electrical conductivity, c is the coefficient of thermal conductivity. The main obstacle in the way of modification of material properties for maximum thermoelectric figure of merit is mutually connected of these values. In particular, the increasing of conductivity by doping causes to decreases of thermal-EMF and growth of coefficient of thermal conductivity.

The Lead telluride is considered as promising material for thermoelectric energy converters, photodetector devices, and emitting structures of middle and far infrared optical spectrum.

This paper is devoted to the influence of both the technological factors and alloying on processes of defect formation and properties of PbTe crystals and films. There were obtained nest research results on the base of experimental and theoretical research:

1. It was proposed the quasi-chemistry description of equilibrium defects concentration in electronic crystals PbTe saturated by Lead and doped by Thallium. There are received the equilibrium constant and the enthalpy of formation of vacancies tellurium (V_{Te}^{2+}) and interstitial waist (TI_i^-) and formation of clusters $[V_{Te}^{2+} - TI_i^-]^+$ on the base on comparison of experimental data with calculations results.

2. The mechanism of defects formation in PbTe enriched Tellurium and doped Indium was received. It is shown that the doping processes followed by phenomenon of self-compensating of Indium (In_{pb}^+) (donor) and vacancy of Lead (V_{pb}^{2-}) (acceptor).

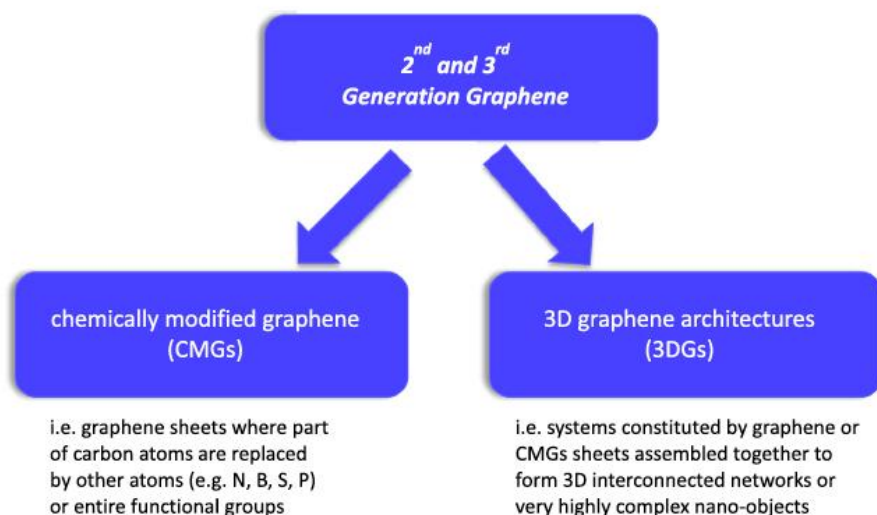
3. Received the two-dimensional and spatial dependence of the concentration of charge carriers from the deposition temperature (T_n), partial pressure of lead vapor (P_{pb}) in the field of deposition and impurities concentration (N_{tl}) in the “hot wall” method for Thallium doped Lead Telluride films. Established that the increase of Thallium content and increase of T_n leading to reduction of major carriers of electronic material, and create of n-p-transition and growing of holes concentration.

4. Were developed the technological basis of modification of PbTe crystals and films with low concentration of free charge carriers that suitable for making elements of optoelectronic transducer and optimized methods of producing of Lead Telluride thin films large values of thermopower and mobility of charge carriers.

Second and Third Generation Graphene related Materials: a Rational Design of Advanced Nanoarchitectures for Energetics

Granozzi G.

*Surface Science & Catalysis Group,
Department of Chemical Sciences, University of Padova, Padova, Italy*



Graphene (G) is an extremely intriguing material that is arousing a formidable interest in many different fields since it was first produced in a conscious manner in a lab in 2003. So many words have already been spent to emphasize its peculiar properties that it is needless to add more efforts to convince scientists on the actual breakthroughs that graphene can provide. Nowadays, the forefront of G research has progressed from the simple preparation and characterization of G toward second generation G-based materials, i.e. chemically-modified graphene (CMGs), and third generation 3D systems based on the assembly of G and/or CMG sheets (3DGs).

In the present lecture Prof. Granozzi will report on recent advances in the field of nanostructures for energetics attained in the Surface Science & Catalysis Group of the University of Padova. A rigorous Surface Science based approach has been adopted to delineate a rational design of G based nanostructures to be adopted in the field of electrocatalysis and photoelectrocatalysis.

Some relevant references:

- *Single- and Multi-Doping in Graphene Quantum Dots: Unraveling the Origin of Selectivity in the Oxygen Reduction Reaction, ACS Catal. 2015, 5, 129*
- *The nature of the Fe-graphene interface at the nanometer level, Nanoscale, 2015, 7, 2450*
- *New Strategy for the Growth of Complex Heterostructures Based on Different 2D Materials, Chem. Mater., 2015, 27, 4105*
- *Fast One-Pot Synthesis of MoS₂/Crumpled Graphene p-n Nanonjunctions for Enhanced Photoelectrochemical Hydrogen Production, ACS Appl. Mater. Interfaces 2015, 7, 25685–25692*
- *Unveiling the Mechanisms Leading to H₂ Production Promoted by Water Decomposition on Epitaxial graphene at Room Temperature, ACS Nano 10, (2016) 4543–4549*

The Properties of NiO Thin Films Grown at Different Magnetron Sputtering Conditions on Si and Glass Wafers

Ievtushenko A.I.¹, Karpyna V.A.¹, Lytvyn P.M.², Korchovyi A.A.², Olifan O.I.¹, Tkach S.V.³, Baturin V.A.⁴, Karpenko O.Y.⁴, Lashkarev G.V.¹

¹*I. Frantsevich Institute for Problems of Material Science, NASU, Kyiv, Ukraine,*

²*V. Lashkarev Institute of Semiconductor Physic, NASU, Kyiv, Ukraine*

³*V. Bakul Institute for Superhard Materials, NASU, Kyiv, Ukraine*

⁴*Institute of Applied Physics, NASU, Sumy, Ukraine*

NiO is a wide direct band gap p-type semiconductor material ($E_g=3.5-4.0$ eV at room temperature). It is an attractive material for the development of p-type transparent conductive films, ultraviolet detectors, solar cells, spin-valve giant magnetoresistive sensor, memory, electrochromic window devices, gas sensors, etc due to its low cost, electrochemical stability and great durability as well as unique optical, electrical and magnetic properties [1]. The development of high-quality p-NiO/n-ZnO p-n heterojunctions is important for creating a new type of solar cells (SC) so-called UV active transparent SC [2] that have additional possibilities for application in window systems for houses, greenhouses comparison with the traditional arrangement of SC on roofs of houses. Therefore, the deposition of high structure and optical quality NiO films are needed for UV active transparent SC.

The different physical and chemical vapour deposition methods such as magnetron sputtering, pulsed laser deposition, plasma-enhanced chemical vapour deposition, electrochemical deposition, sol-gel and spray pyrolysis have been used for NiO films deposition. Among all these methods, reactive magnetron sputtering (MS) is considered to be the most useful widespread method for film deposition due to a good films adhesion, high deposition rates, films uniformity of over large areas of the substrates and easy control over the composition of the deposited films [3]. It is obviously that the enhancement both crystal quality of NiO films and their optical and electrical properties can be reached by the optimization of film growth parameters. Early, we proposed the layer-by-layer growth method for magnetron sputtering pure and doped ZnO films characterized improved crystal quality comparison to films deposited traditional single-stage MS [3].

Therefore, our report is devoted to investigation of the influence of such technological parameters of MS as substrate temperature, oxygen and argon pressures, magnetron power and substrate bias on structure, morphology and optical properties of NiO thin films deposited on Si and glass substrates by layer-by-layer growth method at MS. X-ray diffraction, atomic force microscopy, energy dispersive X-ray spectroscopy and optical transmission measurements were applied to study the influence of technological parameters on the properties of NiO films.

The XRD analysis confirms the formation of polycrystalline textured NiO films with main diffraction peak of rock salt structure (111) (accordingly with JCPDS card number 04-0835) (Fig.1,a). The EDX analysis shown the presence of only Ni and O without other additive impurities (Fig.1,b). The optical transmittance and optical band gap of NiO films varied in the range from 10 % to 75 % and 2.9 to 4.0 eV, respectively. AFM measurement shows (Fig.1,c) that the average grain size and surface roughness change in the range 16-55 nm and 1.21-4.72 nm, respectively. The effect of different magnetron sputtering conditions on the properties of NiO thin films will be discussed and presented.

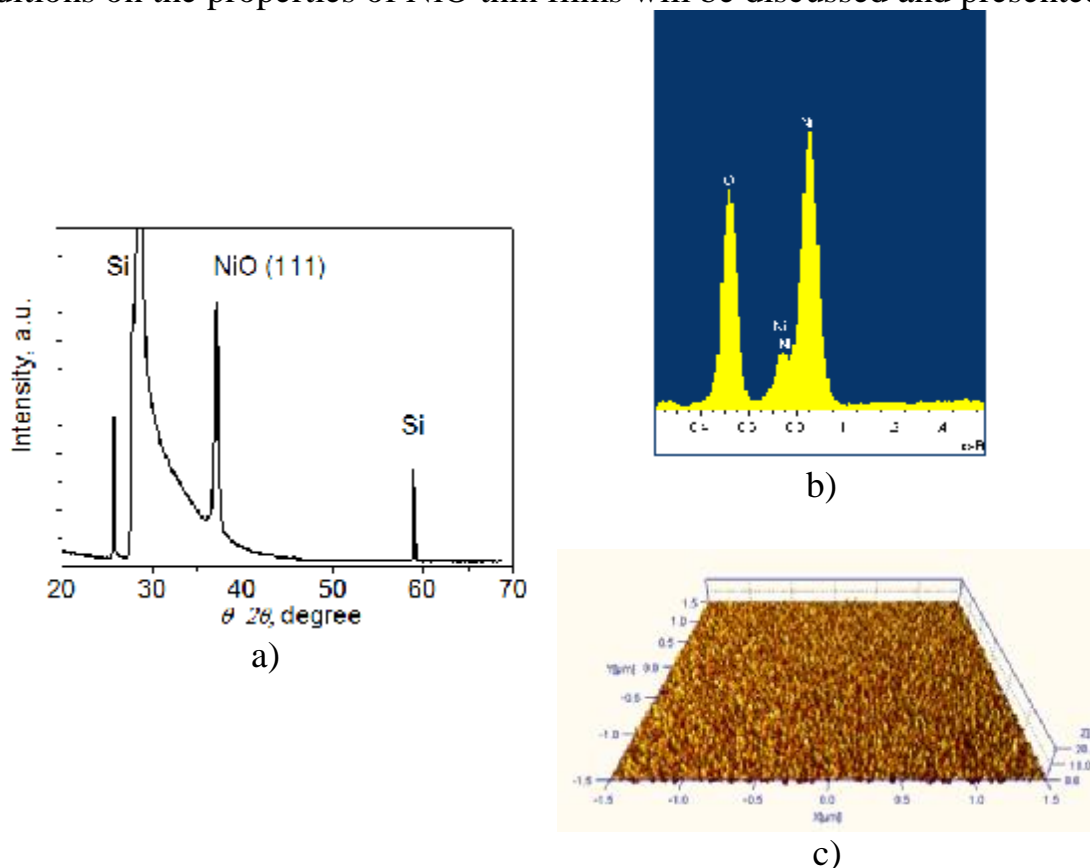


Fig.1. The typical XRD pattern (a), Energy dispersive X-ray spectrum (b) and AFM 3D image (c) of NiO thin film.

1. M.Guziewicz, J. Grochowski, M.Borysiewicz, et al., Electrical and optical properties of NiO films deposited by magnetron sputtering // *Optica Applicata*. – 2011. – V. **XLI**, No. 2. –P. 431-440.
2. R. Karsthof, P. Racke, H. von Wenckstern, M. Grundmann, Semi-transparent NiO/ZnO UV photovoltaic cells // *Phys. Status Solidi A*. – 2016. – V. **3**, No. 1. – P. 30-37.
3. A.I. Ievtushenko, V.A. Karpyna, V.I. Lazorenko, et al., High quality ZnO films deposited by radio-frequency magnetron sputtering using layer by layer growth method // *Thin Solid Films*. – 2010. – **518**. – P. 4529 - 4532.

Synthesis and Transient Grating Thermal Characterization of Nanostructured PbTe:(Bi, Sb) Films

Ivakin E.V.¹, Kisialiou I.G.¹, Nykyruy L.I.², Yavorskiy Y.S.²

¹*Institute of Physics, National Academy of Sciences of Belarus, Minsk, Belarus*

²*Vasyl Stefanyk Precarpathian National University, Ivano-Frankivsk, Ukraine*

Impurities of the periodic table group V are known to influence differently the energy spectrum of electrons in Pb chalcogenides, which is associated with their amphoteric properties. Sb and Bi are donor impurities, which makes it possible to control the concentration of electrons in PbTe thin film structures and provides low values of lattice thermal conductivity component as well.

In this studies we have improved our vacuum heaters design, which allowed us to obtain series of vapor-phase condensation in a common cycle under different technological factors: (I) different thickness at constant substrate temperature T_s , or (II) constant thickness at various T_s . Thin films prepared by pre-synthesized compounds PbTe:Bi(Sb) evaporation in open vacuum have been investigated. Evaporation and substrate temperatures were 970 K and 420 to 520 K respectively. Condensate thickness could be varied by time of vapor deposition from 15 to 240 seconds and was controlled by microinterferometer.

Thermoelectric parameters of condensate were measured at room temperature at constant magnetic and electric fields. Automated device of original configuration provided the electrical parameters measurement and initial data processing. Silver films served as Ohmic contacts. The current through the sample was estimated to be about 1 mA. Magnetic field of 1.5 Tesla normal to the film surface was applied.

In-plane thermal diffusivity χ of films have been studied by the method of transient grating (TG) [1] with the laser-based system “Optopicotest”, worked out in the Institute of Physics, NAS of Belarus. Thermal surface-relief TGs of varied fringe spacing Λ were induced by laser pulses of 8 ns duration at 532 nm wavelength. The excited zone of the film was probed simultaneously by the beam from CW He-Ne laser. Transients of diffracted beam intensity were recorded in reflection mode and decay constants τ of a signal were measured. The χ values in direction along film surface were calculated via ratio $\chi = \Lambda^2/4\pi^2\tau$.

It is well-known [2], that film deposited on substrate can be thermally characterized under conditions of surface heating if film thickness exceeds grating spacing. In order to minimize influence of substrate on the results of measurements, samples with 1.5 to 2.5 μm thick films were chosen for experiment. Thermal TGs of spacing 2.5; 5.0; 12.0 and 25.0 μm were recorded sequentially and their lifetimes were determined. The $\tau(\Lambda)$ function was controlled. If the ratio Λ^2/τ stays approximately constant irrespective of Λ value, we assume that the substrate takes no part in heat transfer in a film-substrate

system. Hence, proper value of Λ^2/τ can be used for χ calculation. Thermal resistance at film-substance boundary plays positive role in this process.

Transients of signals diffracted by thermal TGs with different grating spacing are shown in Fig.1. As soon as the condition $\Lambda^2/\tau \approx \text{constant}$ is fulfilled for all Λ used, the result of χ calculation is considered to be correct enough.

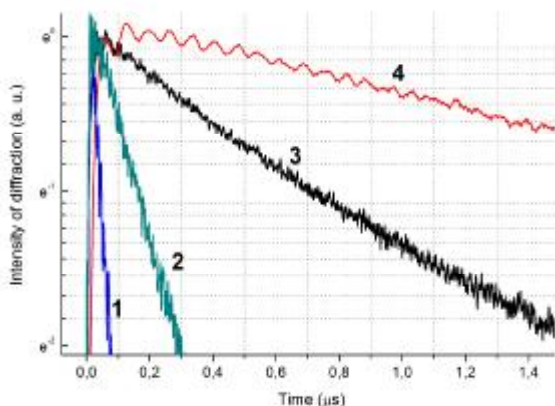


Figure 1. 2.45 μm thick film PbTe:Bi deposited on muscovite
 $\Lambda = 2.5$ (1), 5(1), 12(3) and 25(4) μm

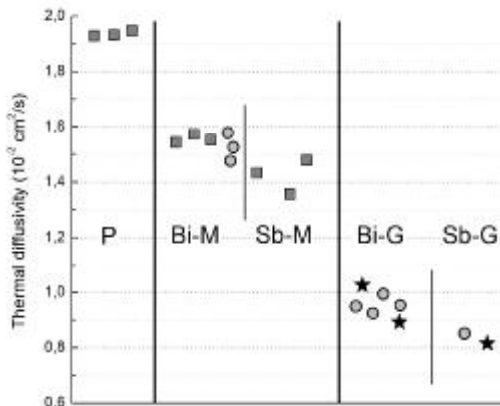


Figure 2. Thermal diffusivity of >1.5 μm thick films PbTe(P), PbTe:Bi and PbTe:Sb on glass G and muscovite M

Summary. We have developed the technology of PbTe:Bi(Sb) film deposition under open vacuum, which governs the processes of nucleation, growth, and formation of individual nanostructures. The values of mean free path of current carriers were determined, as well as their mobility affected by carrier scattering on the film surface and on the intergrains of nanocrystals. It was shown that the surface scattering mechanisms prevail over scattering on the intergrain borders, which is due to large sizes of nanocrystals in thin-film structures. Totals of contactless thermal characterization of the films are given in Fig.2. The most noticeable effect of the in-plane thermal diffusivity decrease as compared to pure PbTe film is observed in films PbTe:Sb deposited on glass substrates. Acoustic 13,6 MHz oscillations in the film/air interface are well seen in scan (4). It is an evidence of surface character of pump radiation absorption.

Acknowledgements. This work was supported by Belarussian Republican Foundation for Fundamental Research through the joint projects №№ Ф13K-063 and Ф16K-054, as well as by the State Fund for Fundamental Research, project N#F73/104.

1. Ivakin E.V., et al. Measurement of thermal conductivity of polycrystalline CVD diamond by laser-induced transient grating technique // Quantum Electronics. - 2002. - Vol.32 (4). - P. 367-372.

2. J.A. Johnson, et al. Phase-controlled heterodyne laser-induced transient grating measurements of thermal transport properties in opaque material // J. Appl.Phys.- 2012. - Vol. 111, 023503; <http://dx.doi.org/10.1063/1.2675467>.

Thin Diamond-Like Carbon Films: Properties and Application in Photovoltaics and Infrared Optics

Klyui N.I.^{1,2}, Litovchenko V.G.²

¹*College of Physics, Jilin University, Changchun, People's Republic of China*

²*V. Lashkaryov Institute of Semiconductor Physics, NAS of Ukraine, Kyiv, Ukraine*

Optical properties of diamond-like carbon (DLC) films in dependence on deposition conditions were investigated. It was established that that the films having refractive index from 1.6 to 2.3 may be obtained. The film optical bandgap and hardness may be changed from 1.5 to 4 eV and from ~1 to ~20 GPa, correspondingly. It has been shown that deposition of single or two-layer diamond-like carbon antireflection coatings enables the solar cells efficiency to be improved 1.35-1.5 times. The improvement is connected with decreasing of reflection losses and passivation of recombination active centers.

Thick (1300-1500 nm) DLC films deposited on a working side of the silicon solar cell (SC) allow us to increase their stability relating to effect of proton and ultraviolet (UV) irradiation. So, one-stage (E=50 keV) or multi-energy (50+100 keV) implantation of proton into protected SC (the SC+DLC films system) did not practically influence the SC parameters. Moreover, SC covered by DLC film after UV irradiation show improvement of efficiency both for implanted and unimplanted samples. At the same time, the unprotected SC deteriorated after those treatments.

We also studied the properties of optical elements for the IR spectral range based on semi-insulating gallium arsenide (SI-GaAs) and antireflecting DLC films. Particular attention has been paid to the effect of penetrating γ -radiation on transmission of the developed optical elements. It was shown that DLC film deposition essentially increases degradation resistance of the SI-GaAs-based optical elements to γ -radiation. Particularly, the transmittance of the DLC/SI-GaAs structure after γ -irradiation with a dose $9 \cdot 10^4$ Gy even exceeds that of initial structures. The possible mechanism that explains the effect of γ -radiation on the SI-GaAs crystals and the DLFC/SI-GaAs structures at different irradiation doses was proposed. The effect of small doses is responsible for non-monotonic transmission changes in both SI-GaAs crystals and DLFC/SI-GaAs structures. At high γ -irradiation dose $1.4 \cdot 10^5$ Gy, passivation of radiation defects in the SI-GaAs bulk by hydrogen diffused from DLFC leads to increasing the degradation resistance of the SI-GaAs crystals coated with DLFC as compared with the crystals without DLFC.

Nanostructured Semiconductor Heterostructures for Ultraviolet Sensors, Solar Cells and Semitransparent Diodes Manufactured by Chemical and Electrochemical Methods

Klochko N.P., Khrypunov G.S., Kopach V.R., Klepikova K.S.,
Lukianova O.V., Korsun V.E., Lyubov V.M., Zaitsev R.V., Kirichenko M.V.

National Technical University “Kharkiv Polytechnic Institute”, Kharkiv, Ukraine

E-mail: klochko_np@mail.ru; klochko.np16@gmail.com; khrip@ukr.net

The creation and research of devices for micro- and nanoelectronics by means of solution-based technologies suitable for mass production, including transparent and flexible electronics, is an emerging science and technology field focused on producing lightweight, “invisible”, pliable electronic circuitry and optoelectronic devices. Applications include consumer electronics, new energy sources, ultraviolet (UV) sensors, solar cells, semitransparent diodes, transistors, memory, magnetics, photonics and health. At the same time, synthesis and fabrication of these materials, as well as processing into particular device structures to suit a specific application is still a challenge. Further, characterization of these materials to understand the tunability of their properties and the novel properties that evolve due to their nanostructured nature is another facet of the challenge.

This work is devoted to the investigation of some nanostructured semiconductor heterostructures manufactured by a combination of electrochemical and chemical methods. We research regularities concerning the influence of pulsed electrodeposition parameters on crystal structure, surface morphology, optical and electrophysical properties of the obtained nanostructured zinc oxide arrays. Then we create and research UV detector on the base of one-dimensional (1-D) ZnO nanostructured arrays. Thereafter, visible active Ag/ZnO nanostructured arrays were obtained by a combination of electrochemical and chemical methods. In order to enhance a solar activity of the electrodeposited in a pulsed mode nanostructured zinc oxide arrays Ag nanoparticles were deposited from silver sol and Ag/ZnO nanocomposites thereon were obtained. We analyzed morphology, structure, electrical, electronic and optical properties of the electroplated 1-D ZnO as well as Ag nanoparticles deposited from silver sol and Ag/ZnO nanocomposites formed by applying Ag nanoparticles to the ZnO surface. The investigated electrical and electronic parameters of ZnO and Ag/ZnO, which we obtained from their current-voltage and capacitance-voltage characteristics, are the electrical resistivity ρ , the height ϕ of the Schottky barriers in the electron depletion regions, the concentration of the fully ionized donor impurity N_d , the density N_{SS} of surface states and the width of the electron depletion region ω . The improved UV sensitivity of the electrodeposited in the pulsed mode 1-D ZnO and enhanced solar activity of Ag/ZnO were valued by dark and light current-voltage characteristics and

through their temporal response curves under the influence of UV and visible sunlight. Analysis of the electronic and electrical parameters, response and recovery performance of the obtained 1-D ZnO arrays and Ag/ZnO nanocomposites thereon let us to select the optimum manufacturing conditions for the creation of solar active plasmonic Ag/ZnO nanostructured arrays with high photosensitivity, fast response and reset times, and reproducible characteristics. So, our studies have allowed the development of a new solar active Ag/ZnO material for photocatalytic oxidation-reduction processes that can be used as photoelectrode for photocatalytic degradation of organic contaminations or for green hydrogen production by water splitting.

In order to create a new design of solid-state quantum dot sensitized solar cell (QDSSC) with pulse electrodeposited 1-D *n*-ZnO arrays as well as applications of SnS quantum dots and thin film of wide band gap semiconductor *p*-CuSCN by Successive Ionic Layer Adsorption and Reaction (SILAR) have been used. The morphology, structure and optical properties of all semiconductor layers are demonstrated. Diode characteristics of the layer composition confirm its functionality for a new design of QDSSC, which we have developed.

Further, we create barrier *n*-ZnO/*p*-CuI heterostructure based on the electrodeposited in a pulsed mode zinc oxide nanostructured arrays and copper iodide films made by SILAR. This semitransparent *p*-CuI/*n*-ZnO barrier heterostructure investigated as a forward-looking device diode base for a near UV detector. The analyses of the crystal structure, electrical and optical properties of the pulse electrodeposited zinc oxide nanoarrays and copper iodide films made by SILAR were performed, on the base of which the *n*-ZnO/*p*-CuI barrier heterostructure sensitive to UV radiation in the spectral range 365-370 nm was created. By means of current-voltage characteristics the shunt resistance $R_{sh} S_c = 880 \text{ Ohm}\cdot\text{cm}^2$, the series resistance $R_s S_c = 8.5 \text{ Ohm}\cdot\text{cm}^2$, the diode rectification coefficient $K = 17.6$, the rectifying barrier height of the *p*-*n* junction $\Phi = 1.1 \text{ eV}$ and the diode ideality factor $\eta = 2.4$ were obtained. It is shown that the both recombination and tunneling of charge carriers are at small forward biases $0 < U < 0.15$. When the voltage is above 0.15 V the transfer mechanism becomes tunnel-recombination. Values of the diode saturation current densities J_o are $6.4 \cdot 10^{-6} \text{ mA}\cdot\text{cm}^{-2}$ for the recombination and tunneling mechanism and $2.7 \cdot 10^{-3} \text{ mA}\cdot\text{cm}^{-2}$ for the tunnel-recombination mechanism of charge carrier transport. Thus, semiconductor heterostructures for ultraviolet sensors, solar cells and semitransparent diodes were made by using chemical and electrochemical methods for the preparing of semiconductor layers and nanoparticles, their structure, optical and electrical properties and output electronic parameters were investigated.

Synthesis, Luminescent and Structural Properties of the $\text{Cd}_{1-x}\text{Cu}_x\text{S}$ and $\text{Cd}_{1-x}\text{Zn}_x\text{S}$ Nanocrystals

Korbutyak D.V.¹, Kladko V.P.¹, Safryuk N.V.¹, Gudymenko O.Y.¹,
Budzulyak S.I.¹, Ermakov V.M.¹, Lotsko O.P.¹, Tokarev V.S.², Ilchuk H.A.²,
Shevchuk O.M.², Petrus R.Y.², Bukartyk N.M.², Tokarev S.V.², Dolynska L.V.²

¹*V.E. Lashkaryov Institute of Semiconductor Physics, NASU, Kyiv, Ukraine,*
kdv45@isp.kiev.ua

²*Lviv Polytechnic National University, Lviv, Ukraine*

The formation of polymer films with the embedded nanocrystals (NCs) was carried out in several stages. Initially, a solution of the copolymer PRC, PEG-200 and a mixture of cadmium acetate CdAc_2 with zinc acetate $\text{Zn}(\text{Ac})_2$ or cuprum acetate CuAc_2 in dimethylformamide was prepared at the ratios of $\text{CdAc}_2 : \text{MeAc}_2$ from 100 : 1 to 1 : 100 and the theoretical content of $\text{Cd}_{(1-x)}\text{Me}_x\text{S}$ nanocrystals in the film 20%. At the first stage, thin polymer films containing Cd^{2+} and another metal ions (either Zn^{2+} or Cu^{2+}) were deposited by spin-coatings on the glass plates, afterwards at the second stage these films were subjected to annealing and cross-linking at $T = 393 \text{ K}$ for 2 hours. It was found that under these conditions a high degree of cross-linking of the polymer films was achieved, the content of the gel fraction in them reached 96% and higher. At the third stage, NCs of ternary semiconductor compounds were formed in the polymer films during exposure to gaseous hydrogen sulphide (H_2S) for 6 hours at $60 \text{ }^\circ\text{C}$. An average thickness of the films thus obtained was about 20 nm.

Previously we didn't observed any changes of $\text{Cd}_{1-x}\text{Cu}_x\text{S}$ NCs' lattice parameters with small Cu concentration ($x \leq 0,1$). In this work for concentration $x \geq 0,1$ we obtained reducing of lattice parameters from $a = 5,83 \text{ \AA}$ ($x = 0$) to $a = 5,789 \text{ \AA}$ ($x = 0.33$), i.e. we observe compound $\text{Cd}_{1-x}\text{Cu}_x\text{S}$ with cubic structure. But under concentration of Cu increases ($x = 0.75-1.0$) structure of NCs becomes hexagonal. The smallest NCs' sizes were formed in samples with Zn concentration ($x = 0.50 - 0.75$). The lowest value of relative deformation were observed for the sample with Zn concentration $x = 0.75$

Photoluminescence (PL) spectra of the NCs $\text{Cd}_{1-x}\text{Cu}_x\text{S}$ and $\text{Cd}_{1-x}\text{Zn}_x\text{S}$ consist of two impurity bands and weaker than the intensity of the exciton band. It was found that the impurity band formed after the capture of nonequilibrium local centers created interstitial impurity ions of sulfur. PL intensity of the bands $\text{Cd}_{1-x}\text{Cu}_x\text{S}$ determined by the concentration of interstitial ions S - with increasing of Cu concentration leads to decreasing of interstitial S ions, formation of the CuS molecules, and PL intensity decreases. At the same time, the monotonic PL intensity of NCs $\text{Cd}_{1-x}\text{Zn}_x\text{S}$ depends on the percentage of Zn, reaching a maximum value for the NC $\text{Cd}_{0,25}\text{Zn}_{0,75}\text{S}$. Therefore concluded that the PL intensity of NCs $\text{Cd}_{1-x}\text{Zn}_x\text{S}$ depends on the strain of NCs - meaning less strain corresponds to the higher value of PL intensity.

Photovoltaic Solar Energy Conversion: Current Status and Development Directions

Kostylyov V.P., Litovchenko V.G., Sachenko A.V., Serba O.A.

*V.E. Lashkarev Institute of Semiconductor Physics NAS of Ukraine, Kyiv, Ukraine,
e-mail: vkost@isp.kiev.ua*

Recently there is significant progress in the development of high efficient photovoltaic solar energy converters – solar cells (SC), which helped increase their efficiencies to the values of one junction SC 28,8% (GaAs) and 25.6% (silicon) under AM 1.5 conditions. For multijunction SC structure of InGaP / GaAs / InGaAs record efficiency is equal to 37.7%. However, practically obtained SC parameters have not yet reached the values predicted by the theory that demonstrates the feasibility of further research(es) in this area. Particularly relevant is now the task to improve the efficiency of SC and reduce their cost.

This report on the basis of the materials of the last European photovoltaic solar energy conferences discuss the main directions of solving marked tasks performed by developers in the world centers:

- decreasing the intensity of recombination processes;
- using of multijunction tandem (cascade) SC;
- using concentrating solar power;
- increasing of quantum efficiency in the short (down conversion) and long-wave (up conversion) spectral regions;
- using thin films and organic compounds;
- using surface (localized) plasmons (plasmon photovoltaics) and others.

Are discussed three generation of SC - based on single-crystal substrates (I), thin films (II) and advanced solutions (III).

The report is presented an overview of the research and development results on physical and technological principles of creating high efficiency (up to 20% efficiency, AM1,5) space and terrestrial SC based on silicon multilayer structures with combined field-diffusion barrier [1], SC with rear barriers and contact metallization, SC with electrostatically charged ferroelectric layer, SC based on the c-Si with triplet-triplet annihilation layer for up-conversion efficiency boosting, concentrator SC and systems on their based, performed in the department of physical fundamentals of semiconductor photovoltaics NAS of Ukraine. The results of work on creation of the certified by authorized state bodies Center for testing solar cells and photovoltaic panels V.E. Lashkaryov Institute of Semiconductor Physics are also presented.

Reference

1. Oksanych A.P. Modern production technology of silicon and silicon photovoltaic solar energy converters [in Ukrainian] / A.P. Oksanych, V.A. Terban, S.O. Volokhov, M.I. Klyui, V.A. Skryshevsky, V.P. Kostylyov, A.V. Makarov. – Kryvyi Rig: Mineral. – 2010. – 266 p. – 300. – ISBN 978-966-7830-IS-0.

Synthesis and Characterization ZnO and ZnS_xSe_{1-x} Nanocrystals

Kovalenko A.V., Bulaniy M.F., Vorovskiy V.Yu., Khmelenko O.V.,
Plakhtiy E.G.

Oles Gonchar Dniprovskiy National University, Dnipro, Ukraine

This paper reports the application of x-ray diffraction, scanning electron microscopy, photoluminescence at high excitation level for characterization of physical properties of ZnSe nanocrystals grown on GaAs (100) substrate by vapor phase epitaxy. The applied characterization techniques show the evidence for coexistence of two sets of nanocrystals with rather different characteristic sizes (dimension ~ 73-82 nm and 7-8 nm). Besides, it was also shown that at relatively intense excitation an extra band has arose in photoluminescence spectra due to biexcitons confined in nanocrystals of 7-8 nm sizes. The binding energy of these biexcitons was as large as 23 meV. It has been investigation the photoluminescence, x-ray diffraction and EPR spectra of ZnS:Mn microcrystal (dimension ~ 25µm) obtained by mechanosynthesis and ZnO:Mn nanocrystals (dimension ~ 37-56 nm) synthesis by ultrasonic spray pyrolysis, which having magnetic properties at room temperature.

The paper deals with the results obtained nanocrystals of ZnS_xSe_{1-x}:Mn (dimension ~ 60nm) by selfpropagating high temperature synthesis (SHS).

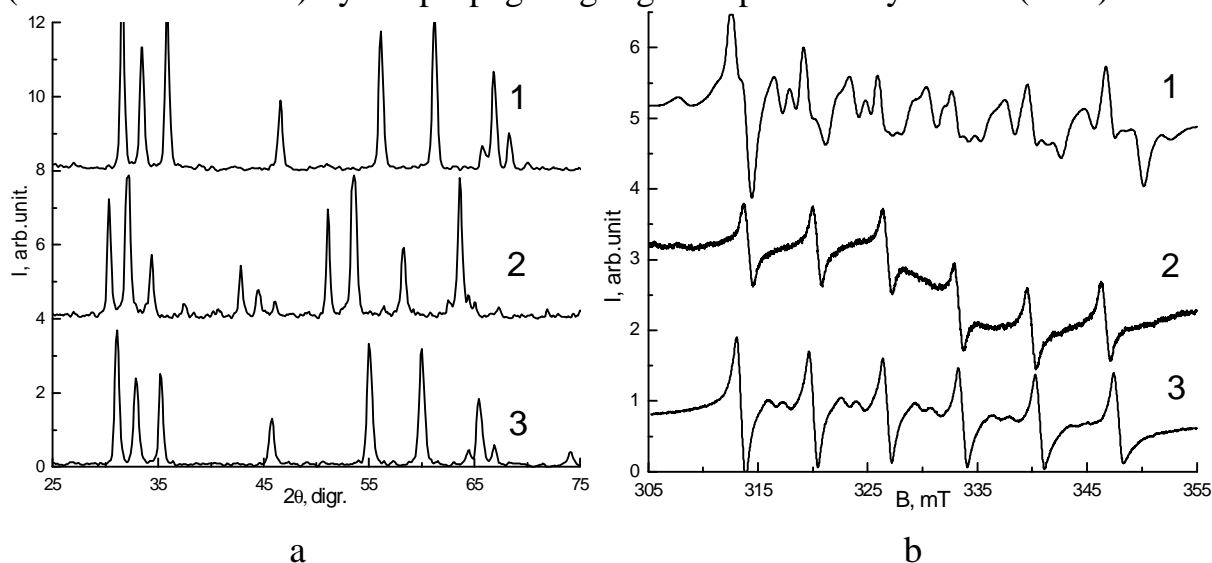


Fig. 1. Data of x-ray diffraction analysis (a) and EPR spectra (b) nanocrystals ZnS:Mn (1), ZnSe:Mn (2), ZnS_{0.8}Se_{0.2}:Mn (3) obtained by SHS method.

Preparation of ZnS_xSe_{1-x} nanocrystals by SHS method was effected in a quartz reactor from mechanical mixture of metallic Zn and S, Se in the different ratio. EPR spectrum consist of a broad line against which the prescribed six superfine structure lines characteristic of paramagnetic centres ions Mn²⁺ in these nanocrystals (Fig.1). It has been analyzes the redistribution intensity of individual bands of photoluminescence in nanocrystals compared with volume crystals of ZnS_xSe_{1-x}:Mn.

Laser Technologies in Nanoelectronics and Spintronics

Krupa M.

Institute of Magnetism National Academy of Science, Kyiv, Ukraine

In the present article we want to consider some features of not thermal influence of laser pulses on multilayer heterogeneous nanofilms to present the results of our experimental researches of change of the roughness of a surface and magnetic characteristics of permalloy films after their irradiation nanosecond laser pulses and the results of measurement of dynamics of magnetic reversal of magnetic tunnel nanostructures with one and two magnetic nanolayers. It is shown that the photon drag effect of electrons can not only generate an electric potential difference between the input and output surfaces in a semiconductor, but may also lead to a drift of the impurities. The results of our research show that in the thin CdS single crystals can be obtained stimulated emission of electromagnetic radiation in the terahertz frequency range.

Giant Thermoelectric Power in Films of Mezoscopic Ferromagnetic Nanocomposites Co/Al₂O₃

Baibara A.E.¹, Bugaiova M.E.¹, Lashkarev G.V.¹, Radchenko M.V.¹, Knoff W.², Story T.², Stelmakh Ya.A.³, Krushynskaya L.A.³, Dmitriev A.I.¹

¹*I.M. Frantsevych Institute for Problems of Material Science, National Academy of Sciences of Ukraine, Kyiv, Ukraine*

²*Institute of Physics, Polish Academy of Sciences, Warsaw, Poland*

³*E.O.Paton Electric Welding Institute, Kyiv, Ukraine*

Earlier in Co/Al₂O₃ nanocomposite (NC) films with compositions below percolation threshold we observed the giant thermoelectric power (GTEP) which achieved 0,1V/K in magnetic field $H \approx 5$ KOe [1]. The low-temperature damping of GTEP, superparamagnetic (SPMR) and ferromagnetic (FMR) resonances also were noticed [1,2,3]. The phenomenological model GTEP will be developed.

Magnetic NC containing Co in the form of nanoparticles (NP's) were grown on polycore substrates using two-crucible electron beam facility [1].

The scattering of the electron with the spin rotation in the Kondo effect is a mezoscopic phenomenon. This rotation is suppressed by a magnetic field. Mezoscopic phenomena occur in our system below percolation threshold, at hopping length exceeding the distance between magnetic centres of localization (MCL), containing separate Co atoms and their NP's.

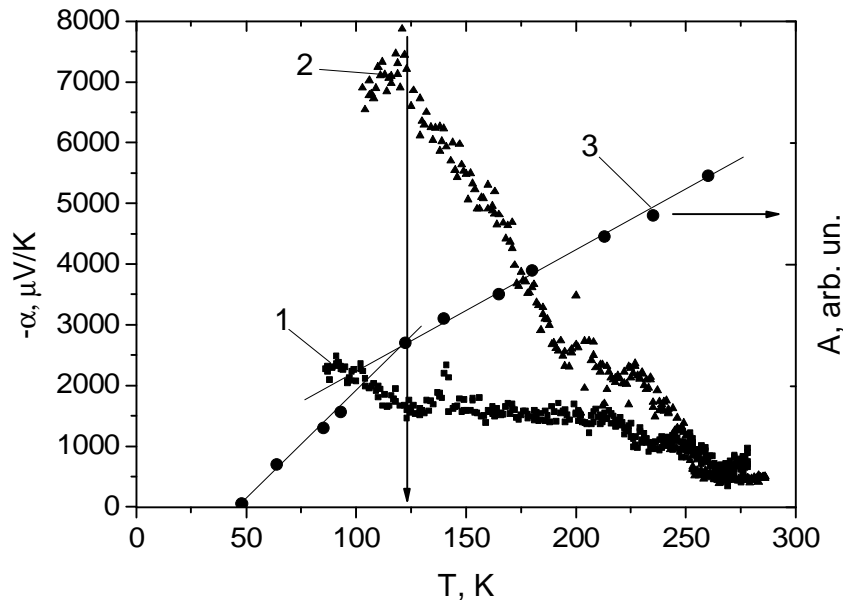


Fig. The dependence of thermoelectric power on temperature and magnetic field in the NC below the percolation threshold (19,3 at.% Co): $H = 0$ (1) -TEP; $H = 4.8$ kOe (2) – GTEP; amplitude SPMR, (A) (3).

We suppose that the GTEP is a result of the large diminishing for electron scattering at MCL with spin rotation. This is possible when MCL are oriented by the field H . At $T < 120$ K the field H_V of oxygen vacancies appears [4], which disrupts the collinearity of MCL magnetic moments. This leads to GTEP damping and TEP increase (curve 1 in Fig.) The latter is a result of the perturbation MCL orientation by the field H_V .

The violation for Co NP's magnetic moments precession by the field H_V leads to SPMR amplitude damping at $T < 120$ K curve 3 in Fig.).

The observed dampings were analyzed taking into account the complicated structure of NP's shells. The possible source of perturbations is an ensemble of magnetic oxygen vacancies on the interface Co-CoO-Al₂O₃. Pair interaction of the two doubly charged identical surface defects (oxygen vacancies) has an integer spin 1 (bosons ?) and their ensemble forms the ferromagnetic state [5,6].

Therefore nontrivial damping in SPR, FMR and GTEP in nanocomposites of Co/Al₂O₃ films probably is due to the conflict between ferromagnetic Co NP's and bosons-type magnetic states of oxygen vacancies in NP's shells.

1. Radchenko M.V., Lashkarev G.V., Bugaiova M.E., Dmitriev A.I., Lazorenko V.I., Penrosian L.I., Knoff W., Story T., Pozniak I.I. Ferromagnetic nanocomposites as spintronic materials with controlled magnetic structure //42nd International School & Conference on the Physics of Semiconductors, Jaszowiec 2013 ThP57, p. 252.

2. Dmitriev A.I., Lashkarev G.V., Radchenko M.V., Bugaiova M.E., Knoff W., Story T. Comparative analysis of superparamagnetic and ferromagnetic resonances on films for Co/Al₂O₃ // 45th "Jaszowiec" International School & Conference on the Physics of Semiconductors, Krynica-Zdrój, Poland, June 20-25. –2016. –WeP7. – P. 203.

3. Dmitriev A.I. Low temperature damping of the magnetodependent phenomena in Co/Al₂O₃ nanocomposite films // (USCPS-7), Ukraine, Dnipro, 26-30 september. –2016. – P. 103-104.

4. Dmitriev A.I. Induced magnetic anisotropy in Co/Al₂O₃ nanocomposite films// (NANSIS-2016), Ukraine, Kyiv, 1-2 december. –2016. – P. 2-3.

5. Morozovska A.N., Eliseev E.A., Glinchuk M.D., Blinc R. Anion vacancy-driven magnetism in incipient ferroelectric SrTiO₃ and KTaO₃ nanoparticles // Phys. B . –2011. –V.406, Is.9 . –P. 1673-1688.

6. Dmitriev A.I. Magnetic oxygen vacancies in Co/Al₂O₃ nanocomposite films // Proceedings of the International conference on nanomaterials: application & properties (NAP-16) –2016.–V.5, № 2. P. 1-2.

Formation of a New Type of Catalytically Active Layers by Changing the Structure of the d-Orbitals, Which Are Passive in the Initial State of Transition Metals

Lytovchenko V.G., Gorbanyuk T.I.

*V. Lashkaryov Institute of Semiconductor Physics of NASU, Kyiv, Ukraine,
e-mail lyg@isp.kiev.ua*

Catalytically active material (for example, Pt-Pd group) is still a basic in developing industrial catalysis and gas sensor till now. The disadvantage of this approach is its expensive and rather high temperature of process [1, 2, 4].

In our previous works outlined other approaches [2, 3], such as: 1) use of nanoscale structures; 2) the active replacement of filling in d-orbitals nanoclusters by acceptor type chemical reactions that can effectively change the filling of d-orbits in the direction of the shift in energy and the formation of unfilled d-orbits and lead to activation of collapse reactions of relevant molecules. In the present article are provides a new experimental data and comparing them with data by electronic orbitals of some non-catalytic active (in normal position) inexpensive transition metals unlike of Pt-Pd family of expensive noble chemical elements.

The theoretical analysis of mechanisms of adsorbo-catalytic activation of complex transition metal compounds was held and a model of high catalytic activity of composites, which are made from porous silicon nanoparticles incorporated transition metals (Pd, W, Cu), was proposed. The impact of atoms of acceptor elements (O, S, F, Cl) at the created of surface nanoclusters of transition metal oxides, which are able to make the filling d-orbits and thus increase the catalytic activity of metals, including inactive metals with completely filled d -shells (Cu, W) was established. The results of experimental studies of the effect are presented and the analysis of experimental research of charge adsorption isotherm of hydrogen and hydrogen sulfide for the surface of the nanostructured silicon composite with nanoclusters of copper oxide, wolfram and palladium in the pores are done. It has been found their adsorption increased sensitivity compared to conventional nanostructured silicon layer. It was established that for small times the physical adsorption mechanism is implemented, and for a large and long times - chemical adsorption (Fig. 1). This conclusion is consistent with data obtained from calculations by type of adsorption isotherms which give meaning $\sim 0,3-0,5$ eV, which is typical for physical adsorption with moderate binding energy.

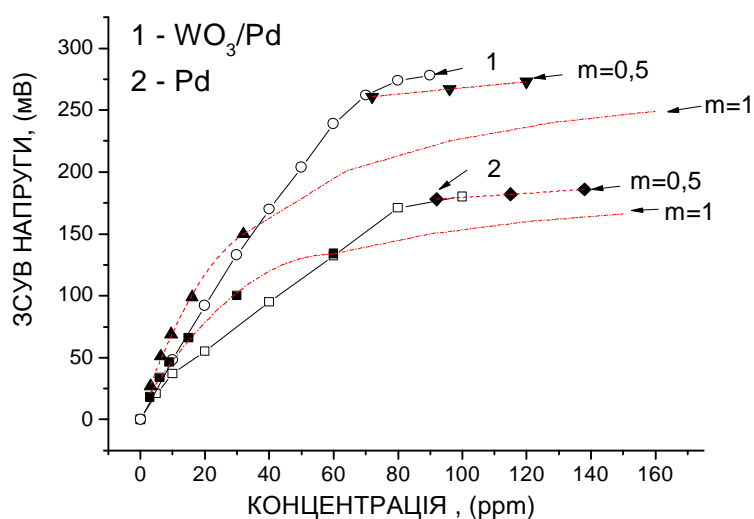


Fig. 1. Dependence of the charge signal response MIS – structures made with porous silicon layer and the nanostructured film (1) of the composite WO₃ – Pd; (2) Pd under adsorption of hydrogen sulfide. Calculated curves of the equation Freundlich isotherm is indicated by dashed lines.

References

1. V.F. Kiselev, O.V. Krilov, Adsorption and catalysis on transition metals and their oxides (Springer, Heildelberg, 1989).
2. Litovchenko V.G. Adsorbo-jelektricheskie jeffekty v sloistyh sistemah dijelektrik – poluprovodnik / Zhurnal Fiz. Him.–1978. – № 52. – С.3063-3070.
3. V.G. Litovchenko, T.I. Gorbanyuk, V.S. Solntsev. New adsorption active nanoclusters for ecological monitoring// Nanodevices and Nanomaterials for Ecological Security - NATO for Peace and Security. Series B: Physics and Biophysics, Springer. – 2012, pp. 297-306.

UV Radiation Sensors on the $\text{GeO}_2\text{-Eu}_2\text{O}_3\text{-Au(Ag)}$ Films

Malashkevich G.E.¹, Kouhar V.V.¹, Chukova O.V.², Nedilko S.G.²,
Shevchenko G.P.³, Bokshyts Yu.V.³

¹*B.I. Stepanov Institute of Physics, NAS of Belarus, Minsk, Belarus*

²*Kyiv National Taras Shevchenko University, Kyiv, Ukraine*

³*Research Institute of Physicochemical Problems of BSU, Minsk, Belarus*

The purpose of this research is the creation of sensors of vacuum and solar blind UV radiation on the basis of Eu-containing germanate films. Such sensors are required for the cosmic radiation detection, long-range detection of forest fires and corona discharges, usage in military engineering and plasma displays, and a number of other applications. Besides, they may be of interest as visualizer of microscopic UV images. For the research, we use the films prepared using layer-by-layer deposition by centrifugation of the GeO_2 sol doped with solution of a tartrate complex of Eu(III) and HAuCl_4 or AgNO_3 onto a silica substrates. The samples were investigated by EPR, phase, microscopic and spectral-luminescent techniques. The monitoring of the luminescence spectra and luminescence excitation ones was carried out with the use of pulse-periodic synchrotron radiation at the SUPERLUMI station of the DESY scientific center (Hamburg, Germany).

It has been established that formation of the Au or Ag nanoparticles (NPs) in the films leads to multiple enhancement in the Eu^{3+} ions luminescence intensity at excitation by the UV radiation as it is shown for the film with AuNPs in Fig. 1. Similar spectra are characteristic and for the film with AgNPs. Their difference consists generally in small long-wavelength shift of excitation bands and higher relative intensity in the region of 200–350 nm.

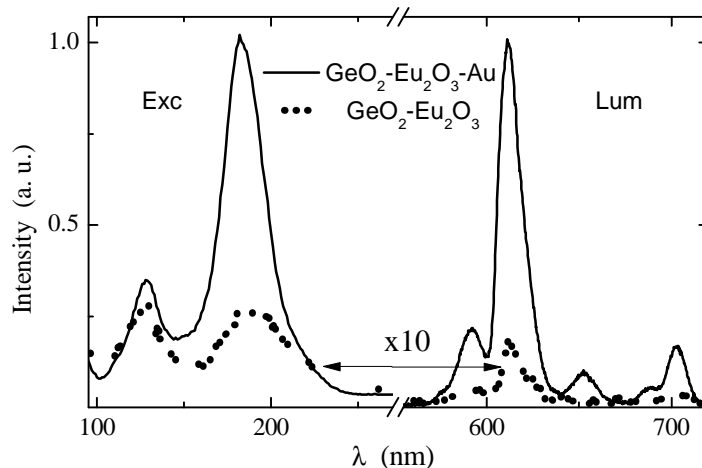
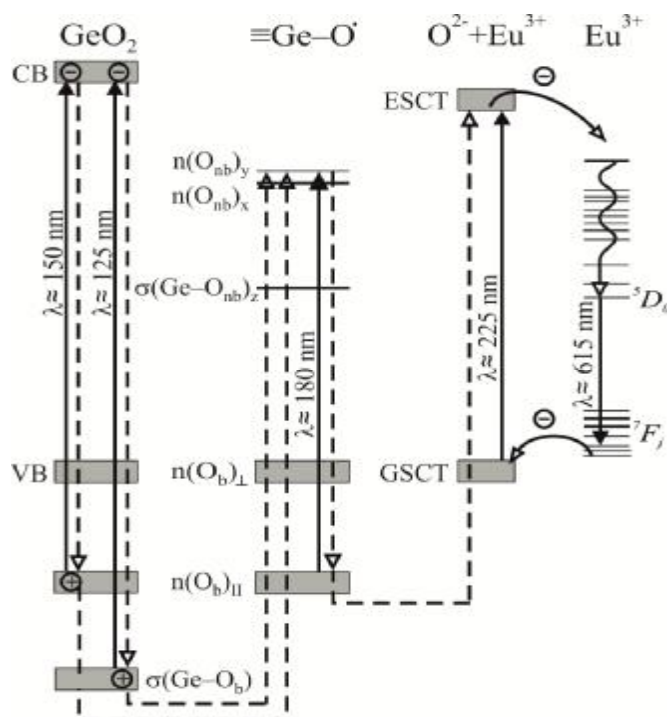


Fig. 1. Luminescence and luminescence excitation spectra.

The enhancement is caused mainly by rise in the non-bridging oxygen hole centers ($\equiv\text{Ge-O}^\bullet$) concentration as a result of breakage of the O–Eu bonds in the $\equiv\text{Ge-O-Eu=}$ bridges by the forming NPs. The $\equiv\text{Ge-O}^\bullet$ centers are characterized with a strong and wide absorption band of $\lambda_{\text{max}} \approx 180$ nm and may sensitize the

Eu^{3+} ions luminescence via the charge transfer state of the $\text{O}^{2-} + \text{Eu}^{3+}$ complexes as it is shown in Scheme 1 [1]. By-turn, the $\equiv\text{Ge}-\text{O}^\bullet$ centers are sensitized by excitons absorbing in a wide band centered at $\lambda \approx 125$ nm. An additional contribution in the luminescence enhancement makes the weakening of reverse passivation of the $\equiv\text{Ge}-\text{O}^\bullet$ centers by the hydrogen atoms formed on the breakage of the end OH^- groups under the action of UV radiation as a result of photocatalytic evolution of H^\bullet to a molecular state on the AuNPs surface [2]. In case of AgNPs, an additional sensitization of the Eu^{3+} ions luminescence by silver ions and clusters stabilized on a surface of the nanoparticles takes place that increases by many times the luminescence intensity at excitation in the region of 200–350 nm.



Scheme 1. Energy states and processes of the Eu^{3+} ions luminescence sensitization. Here GSCT and ESCT are ground and excited states of the $\text{O}^{2-} + \text{Eu}^{3+}$ complexes.

Uncovered influence of noble metals NPs on rare-earth ions luminescence in oxide matrixes may be used for drastic increase of the efficiency of conversion of the ultraviolet radiation (including vacuum and solar blind) into the visible and NIR regions of the spectrum.

1. Malashkevich G.E., Chukova O.V., Nedilko S.G., et al. Influence of gold nanoparticles on luminescence of Eu^{3+} ions sensitized by structural defects in germanate films // *J. Phys. Chem. C.* – 2016. – Vol. **120**, №28. – P. 15369–15377.
2. Rayalu, S.S., Jose, D., Mangrulkar Priti A., et al. Photodeposition of AuNPs on metal oxides: Study of SPR effect and photocatalytic activity // *Int. J. Hydrogen Energy.* – 2014. – Vol. **39**. – P. 3617–3624.

Effect of Microwave Radiation on the Band Structure and Electronic Parameters of the Heterosystems with Fullerenes

Matveeva L.A., Konakova R.V., Kolyadina E.Yu., Neluba P.L.,
Shynkarenko V.V.

*V. Lashkaryov Institute of Semiconductor Physics NAS of Ukraine,
Kyiv, Ukraine, matveeva@isp.kiev.ua*

The discovery of C_n molecules with an even number of carbon atoms (fullerenes) promoted the emergence of a new class of carbon materials and heterosystems based on them. The C_{60} molecules are the most symmetrical and stable. They form a molecular crystal with semiconductor properties. Heterosystems with C_{60} films are used in electronic engineering, sensorics and medicine. Internal mechanical stresses that change the band structure and electronic parameters of the film and substrate appear in films on a foreign substrate. Their properties are determined by the conditions for the production of films and external influences.

The report is devoted to a complex study by the authors of the effect of thermal annealing, ultraviolet, microwave and γ -irradiation on the stability of C_{60} molecules, the band structure, electronic parameters, and mechanical stresses of heterosystems with C_{60} fullerenes. They were deposited from Knudsen's cell by thermal evaporation in a vacuum of C_{60} powder on Si [1]. Substrates were not heated to remove mechanical stresses of thermal nature. The sign and the value of the stresses in the film were determined by the Stoney formula. Prior to our research there were no data on the change in the band gap of the C_{60} films under the influence of internal stresses. From the electroreflectance and absorption spectra of light, we determined the width E_g of the band gap of the film, and from the bending of the heterosystem we calculated the mechanical stresses P in the film and obtained the value $\partial E_g / \partial P = -2.8 \cdot 10^{-10}$ eV/Pa [2].

To reduce mechanical stresses in heterosystems with C_{60} , γ - and UV-irradiation, thermal annealing and microwave irradiation were used. The structural perfection and composition of the films were determined from the Raman and electroreflectance spectra. Microwave irradiation with a frequency of 2.45 GHz and a specific power of 1.5 W/cm^2 was carried out in air for 10 seconds with an interval of 2-3 seconds. Fullerenes C_n contain 12 pentagons and hexagons $n - 12$. Hexagons are bound by shorter double bonds, and the pentagon with hexagon has a longer single bond. With the breakage of this bond, a carbon phase appears at the frequency of 1560 cm^{-1} for the film. The decrease in the intensity of the 1470 cm^{-1} line and the appearance of an additional carbon phase in the Raman spectra were used as a basis for studying the effect of external influences on heterosystems with C_{60} fullerenes.

Since fullerenes decayed during thermal heating and UV irradiation, their decay was eliminated by placing the samples in a vacuum to exclude the interaction of oxygen with the film surface. During thermal annealing in air, the fullerenes decayed at 120 °C. In a vacuum, their collapse did not occur when the C₆₀ was heated in an evaporation cell to 800 °C. C₆₀ films without an amorphous carbon phase were also obtained from the fullerenes remaining in the cell. During γ -irradiation, a GeO_x protective coating was preliminarily applied to the film to eliminate the interaction of fullerenes with oxygen. The relaxation of mechanical stresses in the heterosystem led to a decrease of the band gap width in the film (the compressive stresses decreased) and to the shift of the electroreflectance spectrum in the Si substrate at the interface to the high-energy region (tensile stresses decreased).

Microwave irradiation of C₆₀/Si heterosystems was carried out in air without protective coating on the films. During the irradiation, the samples did not heat up, the composition of the films did not change, the signal at 1600 cm⁻¹, characteristic for the carbon amorphous phase, was absent in the Raman spectra. After 10 seconds of irradiation, the scattering of charge carriers in the film decreased (the parameter Γ changed from 235 to 69 meV, the relaxation time of charge carriers increased from 2.8·10⁻¹⁵ to 1.08·10⁻¹⁴ seconds). Mechanical stresses disappeared after 10 seconds of total irradiation. The obtained results indicate the advantage of using short-term microwave irradiation of C₆₀/Si heterosystems in comparison with other types of external action.

Low-temperature polymer technologies with use of semiconductor properties of C₆₀ fullerenes are applied for the production of photosensitive and solar cells. When studying the effect of the metallization type on the resistance of ohmic contacts at the microwave irradiation of composite polymer films with C₆₀ fullerenes, the advantage of titanium metallization in comparison with gold is revealed. The efficiency of microwave irradiation to reduce the resistance of both contacts increased with its duration in connection with titanium carbidization by forming a chemical bond of Ti-C in the hybridization of the orbitals of *d*-metallic and *p*-fullerenes. After 10 seconds of pulsed microwave irradiation, the resistance ratio of R_{Ti}/R_{Au} decreased by 50 times. This fact is explained by the presence of processes of radiation-stimulated diffusion in the contact region of the Ti-polymer and Au-polymer, which usually improves the ohmicity of contacts in the process of microwave irradiation. But in the case of titanium metallization, the formation of Ti_xC_{60y} carbides occurs in the upper and lower contact areas.

1. Neluba P.L. Peculiarities of fullerenes condensation from molecular beam in vacuum // Technol. Konstr. Elektron. Appar. – 2011. – № 6. – P. 35-39.

2. Kolyadina E.Yu., Matveeva L.A., Neluba P.L., Venger, E.F. Analysis of the fundamental absorption edge of the films obtained from the C₆₀ molecular beam in vacuum and effect of internal mechanical stresses on it // SPQEO. – 2015. – Vol. 18, № 3. – P. 349-353.

Electronic States on the Rough GaAs (100) Surface Created by the Surface Acoustic Wave and Adsorbed Atoms

Peleshchak R.M., Seneta M.Ya., Gal' Yu.M., Uhryn Yu.O., Metsan Kh.O.

Drohobych Ivan Franko State Pedagogical University, Drohobych, Ukraine,
peleshchak@rambler.ru

The development of modern micro- and nanoelectronics needs the research of mechanisms of electronic states excitation on the semiconductors surface and on the semiconductors boundary. The inhomogeneous deformation of the semiconductor surface layer is one of these mechanisms. This deformation is caused by the surface acoustic wave (SAW) and adsorbed atoms. The interaction between the adsorbed atoms and the surface acoustic wave is caused by the deformation potential.

The electronic characteristics of semiconductor surface are researched in this work. The semiconductor rough surface is created by quasi-Rayleigh acoustic wave and adsorbed atoms. The interaction between the adsorbed atoms and the deformation field of surface acoustic wave is described within the deformation potential.

The surface electronic states on rough boundary are found from non-stationary Schrödinger equation

$$i\hbar \frac{\partial \mathbf{y}(x, z, t)}{\partial t} = -\frac{\hbar^2}{2m^*} \left(\frac{\partial^2 \mathbf{y}}{\partial x^2} + \frac{\partial^2 \mathbf{y}}{\partial z^2} \right) + V_0 e^{-k_l z} e^{ikx - i\omega t} \mathbf{y} \quad (1)$$

with deformation potential created by the surface acoustic quasi-Rayleigh wave and adsorbed atoms; where $V_0 = -\frac{|I| \sqrt{\epsilon} N_{0d} q^2 (2 - \alpha_0) c_t^2}{k_l c_l^2}$, I is the constant of

deformation potential, $\frac{1}{k_l}$ is the depth of sound penetration in semiconductor, α_0 is a quantity depended on the ratio between the longitudinal c_l and transversal c_t sound velocity, $\sqrt{\epsilon} N_{0d} = |u_z^l(0)| + |u_z^t(0)|$ is the rough height; components $u_z^l(0)$, $u_z^t(0)$ of the displacement vector of surface points are found from the solution of dynamic equation [1].

It is shown that there are two areas in the surface states spectrum which are separated by a band gap, and their properties are due to quasi-Rayleigh wave and the concentration N_{0d} of adsorbed atoms.

1. Peleshchak R.M. Interaction between the surface acoustic wave and the adsorbed atoms / R.M. Peleshchak, M.Ya. Seneta // Condensed Matter Physics – 2016. – Vol. 19, No 4. – P. 43801: 1–9.

Amorphous Chalcogenides in Nanoplasmonics

Rubish V.M.¹, Lytvyn P.M.², Trunov M.L.¹,
 Kyrylenko V.K.¹, Horvat Yu.A.¹, Yasinko T.I.¹

¹ *Institute for Information Recording, NAS of Ukraine, Uzhgorod, Ukraine*
center.uzh@gmail.com

² *V. Lashkaryov Institute of Semiconductors NAS of Ukraine, Kiev, Ukraine*

The properties of amorphous chalcogenides can be easily modified by irradiation with light from their absorption edge and can be restored following by thermal annealing. It opens up new possibilities of their practical applications, such as optical storage drives with high-density recording, fast and durable photosensitive drums for photocopying and photoresists for lithography, the elements of infrared laser equipment, holograms and elements of integrated optics, electronic switches, etc. Significant attention has been recently paid to the possibility of using amorphous chalcogenides in nanoplasmonics.

Presented report is devoted to investigation of a novel type of photosensitive materials that uses spontaneous or coherent plasmonic signal generation by gold nanoparticles (NPs Au) in “NPs Au/ chalcogenide films” structures.

It was shown that controlled changes in the surface topography of chalcogenide films are possible through near-field illumination which occurs at the excitation of localized surface plasmons. The measurements of the evolution of surface topography were carried out in real time by *in-situ* AFM scanning. Depending on a chalcogenide film composition, the material moves either towards the areas of maximum intensity of light or from them, that is enhanced by plasmon fields.

The investigation have shown the possibility of changing the surface topography of a chalcogenide film by means of changing the shape, size and geometry of gold nanoparticles. Effects, realised in “NPs Au/ chalcogenide film” structures, can be applied for fabrication of locally driven information recording media, mapping the distribution of the electromagnetic field of surface plasmons and development of the sensors of polarization, intensity and shape distribution of the laser radiation wave front (with wavelength near the fundamental absorption edge of chalcogenide amorphous film).

Ukrainian Worldwide Contribution to Natural Sciences (Second Half of XIX – XX Centuries)

Babichuk I.V., Shenderovskij V.A.

Institute of Physics of Ukrainian Nat.Acad.Sci., Kiev, Ukraine

Knowledge of the past is life determining factor in human community, especially when a state is forming. World-renowned Wolodymyr Vernadsky emphasized that "knowledge of science history is a major factor in spiritual consciousness change ..." and "... no idea, no scientific thought, no scientific work, no scientific discovery exists without a person..." The fact that Ukrainian land gave mankind a gallery of geniuses isn't in doubt. However, for many reasons, most of them were hushed up or removed by Soviets from encyclopedias and all textbooks.

Here are some names: Iwan Pulujs, the pioneer of X-rays; Alexander Smakula, the renowned physicist-optician of whom Carl Zeiss in Jena and the Massachusetts Institute of Technology in Boston were proud; the world's first Minister of health prominent chemist and biologist Iwan Horbaczewski. Son of distinguished poet Pawlo Hrabowski Borys created first completely electronic television system. mathematician Michael Ostrogradsky, engineer Stepan Tymoshenko, a prominent economist Michael Tuhan-Baranowski, and mathematician Michael Kravchuk also occupy their places of honor in this glorious gallery.

Global scientific community recognized Ukrainian scientists and naturalists: Wolodymyr Vernadsky, Nicholas Hryshko, Danylo Zabolotny, Wolodymyr Lipsky, Nicholas Melnyk, Eugene Oppokiv, Paul Tutkovsky, Nicholas Kashchenko, Boris Balinski, Vasyl Omelianski, Nobel Prize 2007 winner hydrologist Eugene-Zenon Stachiw, and one of the greatest microbiologists "hunter of microbes from Golden-Domed Kiev" discoverer of chemosynthesis Sergei Winogradski; physicists George Gamow, Dmytro Ivanenko, Yuriy Kistyakovsky that made significant contributions to nuclear physics; founder of the Institute of Biophysics in Germany Boris Rajewski, founder of the Institute for crystal physics in Berlin Ostap Stasiw, and the founder of the Institute for Molecular Biophysics at the University of Florida Michael Kasha.

This is only a small part of Ukrainian scientific constellation in the field of natural science.

Metallfullerene Films: Preparation and Properties

Shpilevsky E.M.¹, Filatov S.A.¹, Matveeva L.A.²

¹*Heat and Mass transfer Institute, NAS of Belarus, Minsk, Belarus, eshpilevsky@rambler.ru*

²*Institute of Semiconductor Physics, NAS of Ukraine, Kiev, Ukraine, matveeva@isp.kiev.ua*

Of all the family of fullerene C₆₀ molecules we chose because they have the highest symmetry and the greatest temperature stability [1, 2]. In this work we are studying the structure of metal-fullerene films (Ag-C₆₀, Cu-C₆₀, Sn-C₆₀) obtained in vacuum from the combined flow of metal atoms and molecules of the fullerene C₆₀.

The films obtained in a vacuum on the "VUP-4" condensation of the combined atomic-molecular flow at a pressure of $1 \cdot 10^{-4}$ Pa. residual vapors Air. The starting materials were used extra pure metals (copper, aluminum, titanium) and C₆₀ fullerite powder purity 99.9%, made by a previously described [3] technology. Getting the films was carried out in a vacuum at a residual air pressure of not more than $1 \cdot 10^{-4}$ Pa. Since the fullerenes begin to sublime at temperatures below 700 K, and the evaporation temperature of metals is much higher, then for the metal-fullerene films using two evaporator (separately for metals and fullerenes). Warming up the evaporators was provided by passing an electric current. As the evaporator for metals used molybdenum boat, for C₆₀ - tantalum. The substrates were oxidized silicon and sieves.

Phase composition of films was controlled by X-ray diffractometer "DRON-3.0" in copper K α radiation. The structure of the films was investigated using an atomic force microscope and scanning electron microscope "LEO 1420VP".

The structure of condensed on the substrate in a vacuum from the combined atomic-molecular flow of metal-fullerene films are influenced by the concentration of the components and process parameters (substrate temperature, flux density and the energy arriving at the substrate atoms and molecules). The size and shape of grains of the alloy depend on the type of metal, its concentration and temperature of the substrate. Thus, for the Ag-C₆₀ grains mainly take the form of pyramids, for the system Cu-C₆₀ - elongated dome, and for the system Sn-C₆₀ - hemispheres.

Found that the doped metal fullerenes leads to a significant increase in the strength of the material, reducing friction, changes in the electrical, optical and other properties of the material [4]. The metal-fullerene films under certain equity ratio of metal atoms and C₆₀ molecules are structurally conductive system of metal particles, separated by small gaps of the semiconductor nanoparticles. Such structures are electrically equivalent to a series connected capacitors and, consequently, their impedance decreases as the frequency of the alternating current.

It is shown that the addition of C_{60} molecules in the metal film substantially reduces the size of structural elements to the nanometer, and the formation of heterogeneous structures consisting of phases: metal, fullerite, solid solutions of metal atoms in the fullerenes and fullerene molecules in crystalline or amorphous states, and for some assessed compositions of metal and fullerenes ($Cu-C_{60}$, $Sn-C_{60}$) discovered ordered stable phase Me_xC_{60} .

Reference

1. Sidorov L.N., Jurovskaja M.A. Fullereny. M.: MGU 2004. – 688 c.
2. Vityaz P.A., Svidunovich N.A. Basics of nanotechnology and nanomaterials. Minsk: Vysheishaya shkola. 2010. - 302 p.(in rus.)
3. Shpilevsky E.M., Shpilevsky E.M., Prylutsky Y.I., Matzuy L.Y., Zakharenko M.I., F.Le Normand. Structure and properties of C_{60} fullerene films With titanium atoms.// Mat.-wiss.u.Werkstofftech. 2011. Vol.42. №1. PP.59-63.
4. Shpilevsky E.M., Zhdanok S.A., Schur D.V. Containing carbon nanoparticles materials in hydrogen energy. Hydrogen Carbon Nanomaterials in clean Energy Hydrogen Systems- II. Dordrecht: SpringerScience, 2011. PP. 23-39.

Classical Quasi-Ballistic and Ballistic Transport in Thin Metal Films

Stasyuk Z.V., Bihun R.I.

Ivan Franco Lviv national university, Lviv, Ukraine.

Thin layers of condensate substance are basic elements of many devices of modern electronic techniques. The further development of electronics is impossible without microminiaturisation of electronic systems, in particular, by techniques of electrically stable ultrathin-thickness condensate. Properties of ultrathin slabs can essentially differ compare properties of bulk material due to dimensional effect which are used in nowadays engineering. This difference first of all is caused by prevailing influence of the surface phenomena on ultrathin layer structure and electric parameters.

The current theoretical and experimental researches on electron charge transport in ultrathin (layer thickness are 2-10 nm) electrically continuous metal films (temperature coefficient of resistance $\beta > 0$) under the condition $d < l$ were analyzed and reviewed, where d is the film thickness, l is the charge mean free path. The peculiarities of film structure are meant as crystal lattice parameters and the crystalline average linear sizes. The fabrication of ultrathin electrically continuous metal film on dielectric substrate surface is a problem of considerable difficulty due to the action of surface tension forces. These phenomena lead to a coalescence of metal particles. As a result there is some critical thickness layer d_c at which current starts to flows (*percolation threshold* is observed here). The technological features of metal film growth (the speed of material condensation, the substrate temperature at layer deposition, the modes of further heat treatment) defines the average of d_c as well as the properties of condensate material, in particular fusion temperature. Essential decrease of d_c may be reached at metal film epitaxial growth on the oriented substrate. The other effective way of d_c decreasing is preliminary deposition of surfactant underlayers of superficially active substances of a subatom thickness on dielectric substrate or so called “quench condensed” method wich prevent coalescence of metal condensates. This technique allowed the formation of ultrathin conductive connectors. In particular, the Hall voltage investigation on 1-3 nm thickness chrome films deposited on surfactant germanium underlayer was performed in [1]. The electron transport phenomena are essentially influenced by electron scattering on film surface when the mean free path of electron becomes commensurable to the thickness of a metal film d . Thus the contribution of surface scattering in the total electron relaxation time is close to the contribution of bulk scattering. The thickness dependence of kinetic parameters of electrically continuous metal films is described within the framework of the classical and internal size effect theories [2].

With further reduction of metal layer thickness when the electron mean free path satisfies the condition $d < l$, the quasi-ballistic electron transport in film (without changes of electron power spectrum in metal film) is presented. Thus

charge carriers surface scattering in metal film becomes dominating. The contribution of surface scattering has essentially influenced on macroscopic surface inhomogeneity because the mean linear grain sizes are commensurable to film thickness. The quasi-ballistic electron transport in metal films can be described by size dependencies of kinetic coefficients proposed in Namba and Wissman theories [2]. The treatment of experimental data by the mentioned theories allows the reliable calculation of the average amplitude of one dimensional surface asperity h . The calculated values of h is well coordinate with experimental data of direct STM and AFM measurements.

When the film thickness does not exceed 5 - 8 nm the ballistic dimensional effect is observed. Quantum size effects are most brightly displayed in semimetal films because of electron de-Broglie wave length in 10 times exceeds interatomic distances in contrast to metal and consequently the interference of electronic waves is influenced poorly by imperfections of film surface. In metal films the situation is essentially different as a de-Broglie electron wave length is commensurable to interatomic distances. Therefore, to observe oscillations of the kinetic coefficients in thin metal layers it is necessary to provide high perfection surface structure. In the quantum electron transport range of films thickness the laws of residual conductivity size dependens $\sigma_{res}=1/[\rho(d)-\rho_{\infty}]$ takes place. The theoretical expressions are most convenient for direct experimental comparison with theoretical data has been received by Fishman and Calecki [3]. Modern theoretical approaches of quantum size effect in kinetic phenomena of metal films are based on assumption that the metal electronic structure is the same as in bulk materials. Quantum size effect in metal film is a consequence of electron system limitation in direction perpendicular to film surface. One dimension model of metal films conductivity in Boltzmann approach for quantum electron transport was developed. The fluctuation of film boundary has dramatic influents on electron spectra. It changes electron scattering under quantum size effect. In the frame work of developed model size dependences of metal films conductivity were calculated. The developed model was successfully used for quantitative description of the experimental data of monocrystalline $CoSi_2$ films and fine-grained films of varies metals. In the film thickness ranges of the quantum electron transport and transition to the semiclassical electron transport the comparison of calculations results of size dependences metal film conductivity were compared for this model with other theoretical approaches. The developed quantum model of charge transport in films with metallic conductivity can more successfully describe the transition from purely quantum to semiclassical charge transport in comparison to other quantum theories [4]. It was possible because proposed model considers the perturbation energy states in the whole volume of the film due to the existence of macroscopic asperities on the metal film surface.

[1] Schroder K., Zhang L. Phys. Stat. Sol. B.– 1994.– Vol.183.– P.k5-k8.

[2] Bihun R. I., Buchkovska M. D., Koltun N. S., Stasyuk Z. V, Leonov D. S. Metallofizika i noveishie tekhnologii.– 2013.– V.35, № 12.– P. 1659-1674.

[3] Calecki D., Fishman G., Phys.Rev.Lett.–1989.– Vol. 62.– P. 1302-1305.

[4] R.I. Bihun, Z.V. Stasyuk, O.A. Balitskii. Physica B.– 2016.– Vol. 487.– P. 73-77.

Suspended Graphene on Ferroelectric Domain Wall

Strikha M.V.^{1,2}, Kurchak A.I.¹, Morozovska A.N.³

¹ V.Lashkariov Institute of Semiconductor Physics, NAS of Ukraine, Kyiv, Ukraine;

² Taras Shevchenko Kyiv National University, Kyiv, Ukraine;

³ Institute of Physics, NAS of Ukraine, Kyiv, Ukraine.

In [1,2] we have studied p-n junction in graphene on ferroelectric domain wall (DW), but did not consider there piezoelectric effect in ferroelectric. However, if the voltage is applied to a gate, one domain elongates and another one becomes shorter depending on the voltage polarity. The piezoelectric coefficients of $\text{PbZr}_x\text{Ti}_{1-x}\text{O}_3$ film near the morphotropic composition $x \approx 0.48$ can reach $(0.5 - 1) \text{ nm/V}$ depending on the film thickness and temperature. Hence it leads to the surface displacement of ferroelectric substrate at distance $h \sim (0.5 - 1) \text{ nm}$ for the gate voltage $\sim 1 \text{ V}$ (Fig. 1). The physical gap between the graphene and ferroelectric $d \sim 0.5 \text{ nm}$ is determined by Van der Waals interaction. The density of the binding energy J is generally not more than 0.5 J/m^2 [3], on the contrary Young's modulus of graphene is extremely high ($Y = 1 \text{ TPa}$). Therefore if h is large enough, the separation of graphene from the substrate occurs. The length of a separated section of channel can be estimated within simple model, presented in Fig.1b: $l = h^3 \sqrt{Yd/2J} \sim 10h$. Therefore the stretched section can be of 10 nm order and even longer. This suspended section can cause many interesting effects. First, the conduction of graphene channel in diffusion regime increases essentially, because electrons in this section scatter on acoustic phonons [4]. Second, mechanic vibrations of MHz range can be realised here [5]. Third, high pseudo-magnetic fields were reported for stretched graphene [6].

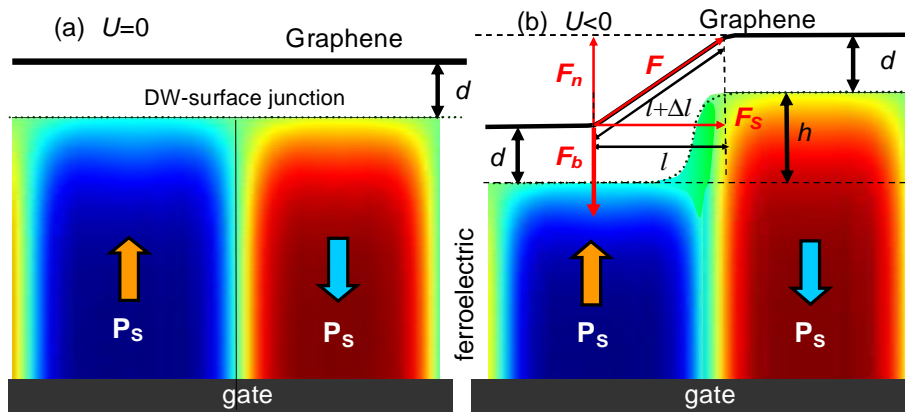


Fig. 1. Suspended graphene induced by a piezoelectric effect at the DW. (a) $U=0$ and (b) $U<0$.

1. A.N.Morozovska, E.A.Eliseev, and M.V.Strikha. *Appl. Phys. Letters* **108**, 232902 (2016).
2. M.V.Strikha and A.N.Morozovska. *J. Appl. Phys.* **120**, 214101 (2016).
3. S.P.Koenig et al. *Nature Nanotechnology* **6**, 543 (2011).
4. Yu. A. Kruglyak, M. V. Strikha. *Ukr. J.Phys. Rev.*, **10**, 3 (2015).
5. J.S.Bunch et al., *Science* **315**, 490 (2007).
6. N.Levy et all, *Science* **329**, 544 (2010).

Phase Transitions and Thermal Evolution of Multilayer Films Morphology

Petrushenko S. I., Dukarov S. V., Samsonik A. L., Sukhov V. N.

*V. N. Karazin Kharkiv National University,
Kharkiv, Ukraine, petrushenko@univer.kharkov.ua*

This work is devoted to the study of supercooling during crystallization of a liquid phase of a fusible component (Pb, Bi, Sn, In) located between layers of more refractory substances (C, Mo, Cu), and thermal stability of single and multilayer films.

The samples under study were obtained by the method of successive condensation in vacuum of 10^{-6} – 10^{-7} Torr. The value of supercooling was determined using two independent methods: an indirect method, based on the measurement of electrical resistance, and direct in situ electron diffraction studies. The samples for studying thermal stability were prepared by a method of a variable content and a variable state: the films were condensed onto lengthened substrates that could either be heated to a chosen temperature, or a suitable temperature gradient could be created along them. Movable shields made it possible to condense films of different composition along the width of the substrate.

It has been established that the crystallization of a fusible component in the multilayer films usually occurs in a certain temperature range. This is explained by the fact that the fusible component is in the films in the form of separate particles, which crystallize independently. Avalanche crystallization is observed in Cu-Bi-Cu and Mo-Bi-Mo samples deposited at room temperature. This is a result of the presence in them of a single system of fusible inclusions.

While studying films thermal stability, it was found that de-wetting of single-component films (Cu, Pb, Bi, Sn, In) occurs due to through pores growth. The activation energy of surface self-diffusion in the systems under study has been estimated. It has been shown that pores are formed in the triple junctions of crystalline grains even before heating. It was found that annealing of copper films 50 nm thick at 150°C for two hours increases the temperature of their de-wetting by 120 K. According to TEM studies, this is due to the increase in the average size of crystallites composing the film. The addition of lead (more than 3 wt. %) sharply changes copper films dispersion. Regardless of the preliminary annealing, Cu-Pb films 50 nm thick break up into separate islands at the melting point of lead, which is much lower than de-wetting temperatures of pure copper films of the same thickness. The activation energy of de-wetting is only 0.2 eV, which makes it possible to classify this process as liquid-phase mass transfer. It is probable that an important role in facilitating the dispersion of films can also be played by an increase in the solubility in thin films, which was detected in this work by in situ electron diffraction studies.

Electronic and Structural Nanomodification of Titanium Dioxide by the Carefully Anion-Doped Process

Telbiz G.M., Yukhymchuk V.O.* , Manorik P.A.

L.V. Pisarzhevsky Institute of Physical Chemistry, NAS of Ukraine. Kiev, Ukraine;

**V.E. Lahskaryov Institute of Semiconductor Physics, NAS of Ukraine, Kiev, Ukraine*

E-mail: gtebiz@yahoo.com

The anion-doping displays a significant scientific interest and practical importance for the enhancement of TiO₂ properties while the structural aspects of the anion integration in TiO₂ structure are still debatable. For example, the sulphur amount and its distribution in the TiO₂ structure are to great extent influenced by the synthesis conditions and can be included in form of S⁴⁺ and S⁶⁺ on the surface or integrated in the TiO₂ lattice forming S–Ti–O bonds. In the present work, synthesis based on the interaction between sulphuric acid titanium tetraisopropoxide was applied for doping of titanium. The integration of the doping elements and genesis of nanocomposites characterized by a number of physical methods (XRD, XPS, FTIR, UV-VIS, TGA, TD MS, SEM, TEM etc) for revealing the structural aspects of the doping process. XRD and Raman data of the hydrothermally synthesized S-doped TiO₂ nanostructures show that the lattice strain became larger with increasing dosage of H₂SO₄. Interaction of sulfate ion during sol-gel synthesis leads to the formation on the surface of anatase bidentate structures that regulate acidic properties of the surface of the composite. At optimal concentration of the dopant, the composite structure has significant hydrophilicity, high density of OH groups on surface that, stable at temperatures up to 350°C and enhanced, relative to other samples, proton conductivity. The results explain the formation in situ synthesis surface nanolayers which, according to the data of XRD, IR and Raman spectroscopy has titanilsulfate structure and motives of titanium oxysulfate have been revealed. The crystallite size of samples decreased due to the presence of sulphate ion in the system. The SEM studies of S-TiO₂ nanoparticles shown, that obtained particles have irregular morphology. From the FTIR and XPS spectra could be concluded that incorporation of S into the TiO₂ lattice can be substitutional or interstitial, and the S⁶⁺ can substitute Ti⁴⁺ into the TiO₂ lattice. The calculated value the OH surface density of the S doped samples shown their growth compare with standart materials. Was found that the S-doped TiO₂ materials catalysts successfully promote selective gas-phase oxidation of ethanol when illuminated with UV light. The rates of photocatalytic reaction are more than twice as high in the case of S-doped TiO₂ compared with Degussa P25. The fact may be directly ascribed to influence of the morphology, structure, OH-density in doped sample.

Phosphate Materials for Modern Green Energy Technologies

Zatovsky I.V.

College of Physics, Jilin University, Changchun, P.R. China

With the reduction of fossil fuel resources and the rapid growth of global energy demands, much attention has been paid to alternative solutions in energy generation and usage. The successful integration of sustainable and renewable sources generated by solar and wind plants requires the development of low-cost energy storage devices in order to smooth the supply of electricity into the power grid or transformation energy in other forms (example, hydrogen as an ideal source of clean energy). It is stimulate efforts to search new materials for development of high energy and high power ion batteries, solid electrolytes for ion conduction, low-cost electrocatalysts for water splitting and other. I In this respect, much attention is devoted to investigation of complex phosphates of transition metal as electrode materials in ion batteries, asymmetric solid-state supercapacitors and catalysts for water splitting.

The report examines the future prospects of the practical application of this family of compounds for modern of green energy technologies. In particular, this report represents a number of results on the synthesis and study of complex phosphates NASICON (NAtrium Super Ionic CONductor) and olivine-type, layered 2D-framework phosphates as solid electrolyte and bases for cathode or anode materials in Li- and Na-ion batteries. Also, it is considered the fabrication possibility of new amorphous phosphate films and nanoparticles as electrocatalysts for water splitting.

The Dependence of Electronic Structure of Nanosystems from Synthesis Conditions and the Influence Characteristics Charge State of Ions to Interact with Lithium Cations

Zaulychnyy Ya.V., Yavorskyi Y.V.^a, Dudka O.I.^a, Kozak I.M.^a,
Lytyvnenko A.A.^a

^a *Physical Engineering Faculty, National Technical University of Ukraine “Kyiv Polytechnical Institute”, Kyiv, Ukraine, yar-yra@ukr.net.*

Studying the redistribution of valence electrons in the dispersion to nanoscale materials with different types of interaction and atomic crystal structure elucidated electronic energy conditions and mechanisms of interaction of nanoparticles and surface ion environment.

We show that narrowing of the energy distribution of the valence electrons in nanosystems is the result of disappearance of the splitting of energy levels and changes their position is a result of relaxation processes at break atomic bonds.

Due to the increasing number of broken ion-covalent bonds while reducing the size of oxide nanoparticles, found relocation of electrons from high-energy states are not binding state of anions to the energy levels of cations. This leads to increase the surface energy nanosize oxides and ability to interact with other systems.

The effect of the shock-vibration handle mixtures of nanoscales oxides and pyrogenic synthesis of nanocomposites form their electronic structure. Showed that when shock-vibration processing amorphous and crystalline nanosize particles interconnect, formation in the interface of them (*O-O*)*p*_π-bonds, due to overlap of *Op*-orbitals and additional splitting of energy levels and fill of the electron binding transitioned from metal. The increase, therefore of charges of anions leads to increased Coulomb attraction Li^+ ions to the anions on the surface and structural defects nanocomposites. This leads to a sharp increase in charge capacity of lithium power sources with composite cathodes.

Established inability Li^+ to recombination with *Op*-bound electrons and recovery of lithium. Therefore, on the surface of the nanoparticles are not formed lithium oxide film and after 2-nd cycle deintercalation level of introduction of lithium in the cathode increased 1.5 times.

Also shown that increase high energy electrons settlement is not binding levels leads to the recovery of lithium through recombination $Li^+ + e^- = Li$.

Features of Depth Profiling of PbTe Crystals by Ar Plasma

Zayachuk D.M.¹, Slynko V.E.², and Csik A.³

¹*Lviv Polytechnic National University, Lviv, Ukraine*

²*Institute for Problems of Materials Science NASU, Chernivtsy branch, Chernivtsy, Ukraine*

³*Institute for Nuclear Research, Hungarian Academy of Sciences, Debrecen, Hungary*

Depth profiling is known to be an effective method for composition analysis of multicomponent and doped solids. Here we present the summarized results of features of depth profiling of PbTe crystals by Ar plasma depending on the conditions of sputtering and the origin of sputtered surface. Sputtering experiments were carried out at the conditions of Secondary Neutral Mass Spectrometry (SNMS). The sputtering energy of Ar⁺ ions was changed in the range of 50 to 550 eV, the sputtering time – from 5 to 50 minutes. Two types of crystals were studied: the crystal grown from melt by the Bridgman method (growing of the crystal under mechanical stress caused by the quartz container) and the crystal grown from vapor phase (free growing of the crystal). Different types of crystal surfaces were treated by Ar⁺ plasma: the natural faceted surfaces corresponding to the crystallographic planes of high symmetry, the natural lateral surfaces of crystal ingots, and surfaces mechanically processed during the cutting of the crystals. The sputtering experiments were complemented with Scanning Electron Microscopy and Energy Dispersive X-ray analysis.

The new phenomena were observed. Primarily it is aperiodical oscillations of Pb and Te sputtering rates during the depth crystal profiling. The amplitude and frequency of oscillations were found dependent on the sputtering energy. As the sputtering energy increases, the average frequency of oscillations increases too, and the amplitude of oscillations decreases. At that there are no correlations between the phases of changes of Te and Pb intensities. At one point during sputtering these changes can occur in phase, at the other – in antiphase, going through any intermediate value.

Another important phenomenon is huge preference of Te sputtering. It can reach more than two orders of magnitude at the beginning of the sputtering process under the lowest plasma energy of 50 eV. Moreover, the Te integrated sputter yield significantly exceeds the Pb yield also for prolonged sputtering by low energy (50-160 eV) plasma.

There is also atypical behavior of the average intensity of Pb and Te sputtering over sputtering time – either towards growth or towards reduction depending on the plasma energy. For low sputtering energy (less than 160 eV) the average sputtering intensity of both components decreases when sputtering time increases. In the range of Ar⁺ beam energy between 160 and 350 eV the direction of changes of the average intensity changes to the opposite, from decrease to increase. At that the direction of changes of Te and Pb intensity over time for any Ar⁺ ion beam energy is always the same.

We have revealed that the depth profiling processes of PbTe crystals, especially the crystals grown from melt or the mechanically processed samples, are accompanied by the processes of re-deposition of the sputtered species on the sputtering surface. The relief of sputtered surfaces as well as the average size, shape, and density of the surface structures re-deposited on the sputtered surface are significantly modified when both duration of sputtering and sputtering energy are changing. In general case the sputtered phase of PbTe crystals and the Pb and Te output analysed at SNMS measurements are formed as the result of superposition of two simultaneous processes – sputtering of PbTe crystal by the Ar plasma and re-deposition of the sputtered species on the sputtering surface, intensity of which depends on the origin of sputtered surface. The best conditions for nucleation of the re-deposited surface structures are provided by the initial lateral surfaces of the PbTe crystals grown from melt by the Bridgman method as well as the surface of the mechanically processed samples. The surface structures originate on both the natural growth defects and dimples of sputtered lateral surfaces of the PbTe crystal samples. Under constant sputtering energy the smaller is the duration of surface sputtering, the smaller is the average size of re-deposited microscopic surface structures, but the higher is their surface density. The same behaviour of the re-deposited microscopic surface structures take place under constant sputtering time of PbTe samples when the sputtering energy changes. The crystal surface pre-modified by Ar+ plasma largely loses the ability to nucleation. Probability of nucleation is also quite low under sputtering of the free natural facet surface and the lateral surface of the crystal grown from vapor phase.

To compare the composition of the sputtered surface and the structures re-deposited on it, the EDX analysis of the sample subjected to sputtering for 50 minutes by Ar plasma with energy of 50 eV was carried out. Within accuracy of the method the un-sputtered surface of the PbTe crystal sample was stoichiometric. The composition of sputtered surface was found to be slightly enriched with lead. The composition of the predominant re-deposited pyramidal structures was found to be intermediate between the compositions of the un-sputtered and sputtered surfaces. In much smaller quantities it is observed the re-deposited structures strongly enriched with lead or tellurium.

It is demonstrated that the observed non-uniform sputtering may be caused by the peculiarities of the charge states of the interstitial Pb and Te in PbTe crystal matrix and the processes of formation and re-sputtering of both the sub-critical nuclei and the post-critical re-deposited surface structures. It is concluded that vast majority of the nuclei are formed on the sputtering surface of PbTe crystal at the early stages of sputtering and re-deposition process. At the later stages of dominates predominant process is a redistribution of material between the small surface structures that gradually disappear and the larger ones that grow. The longer the PbTe crystal surface is sputtered, the less efficiently the new nuclei of re-depositing phase are formed on it.



ORAL REPORTS

Session 1

Thin films technology (metals, semiconductors, dielectrics, conductive polymers) and their research methods



Electrodeposition of Ni-Re Thin Films From Sulfamic and Citrate Electrolytes

Bersirova O.L., Kublanovsky V.S.

*V.I. Vernadskii Institute of General and Inorganic Chemistry, NAS of Ukraine,
Kiev, Ukraine, e-mail: bersibol@ukr.net*

Ni-Re alloys were electrolytically synthesized from sulfamic and citrate electrolytes with current densities ranging from 0.3 up to 5 A·dm⁻² at temperatures 15 and 40 °C (288 and 313 K). For films deposited from sulfamic electrolyte, current density increase leads to rhenium content reduction in the nascent alloy. For citrate electrolyte, an important role is played by the rhenium salt concentration: with low (0.01M) potassium perrhenate concentrations, deposits were obtained with low (5-30%) rhenium content in the alloy. Doubling the rhenium salt concentration in the solution (up to 0.02 M) leads to formation of deposits high in rhenium (90-95%). In citrate solution, with the perrhenate concentration increase up to 0.02M, and with current density increase, quantitative composition of the deposited Ni-Re alloy remains virtually unchanged. Independence of tungsten content in the metal phase on the current density can be typical for this type of electrolytes for electrodeposition of Re-containing alloys with iron group metals. Raising up the electrolyte temperature during the electrodeposition of alloy from citrate solution slightly affects the rhenium content, but significantly improves the uniformity of obtained films composition. The obtained alloys deposits grain size ranges from 5 up to 35 nm; and their structure is nanocrystalline. With the increase of the rhenium content in the deposit, its grain size decreases (Fig. 1).

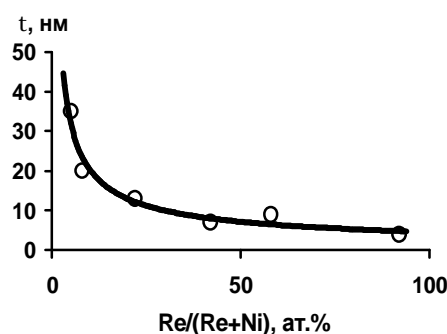


Fig. 1. The dependence of the calculated deposit grain size (τ) on the rhenium content in the electrodeposition of Ni-Re alloy.

It can be concluded from the obtained deposits corrosive properties studies results that higher corrosion resistance of films is connected with a lower rhenium content in it. The highest corrosion resistance is characteristic for alloys containing 8-10% of rhenium. A comparative evaluation of corrosion resistance of nickel alloys containing tungsten and rhenium was carried out. It was found that these alloys can be arranged in the following series by its corrosion resistance: Ni-W-Re > Ni-Re > Ni-W.

Plasma Thermocycling Nitriding: An Improved Method for Surface Treatment

Dolgov N.A., Rutkovsky A.V.

Pisarenko Institute for Problems of Strength, Nat. Ac. Sci. of Ukraine, Kiev, Ukraine

The surface hardening of steels using plasma nitriding is an efficient and reliable method that can be used in the manufacturing and machining industries primarily to treat engine component, machine tools as well gears. The process has been traditionally used to improve their wear, corrosion and fatigue resistance [1]. In this study we present the results of the surface treatment of high-chromium steel 40Kh13 (0.4C, 13Cr, 0.8Si, 0.8Mn) by plasma nitriding followed by thermal cycling. Each cycle induce high temperatures in a short time, followed by an also fast cooling down.

Plasma nitriding of steel samples has been carried out using pulse DC glow discharge. Plasma nitriding was carried out in an atmosphere of a 25% N₂ and 75% Ar mixture under a pressure of 100 Pa at temperature ranging from 510 to 560°C for 16 h. The gas flow rate was controlled by a mass flow meter. After nitriding for required time, the specimens were cooled to the room temperature in vacuum chamber.

The plasma nitrided specimens showed important surface property improvements. The dissolved nitrogen and the volume expansion of nitrides precipitation cause a compressive residual stress in the diffusion layer. It was found that the tensile strength and yield strength of the steel were not affected by the treatment. However, the tensile elongation decreased from 32.8% to 30.8% after plasma nitriding. The stress–strain curves exhibited similar shapes before and after nitriding. Microhardness results were obtained using a Vickers microhardness tester. Microhardness was measured with the load of 200 g. Microhardness measurements showed significant increase in the hardness from 164 HV (for untreated specimens) up to 520 HV (for nitrided specimens).

Studies have shown that the microstructure of the surface layer can be affected by changing process parameters such as temperature ranging, time and gas mixture ratio. The change of the microstructure of surface layer affects mechanical properties of materials such as surface hardness.

Literature

1. A.V. Rutkovsky, A.U. Kumurzhi, “Abrasive wear proofness of 40X13 steel hardened by thermocyclic ion nitriding method,” *Problems of Frictions and wear.*– No. 57. – P. 240 – 250 (2012).

Formation of GaAs (AlGaAs) Epitaxial Layers by LPE Method for Phototransducer

ІІ'chuk H., Krukovskyi S., Krukovskyi R.

Lviv Polytechnic National University, Lviv, Ukraine

Significant increasing of the photoactive absorption of sunlight in the solar cells is possible by using multiple stages made of semiconductor material bandgap which increases to the surface of epitaxial structure. Another way is based on using heterogeneous (graded-gap) active layers phototransducer. Spatial heterogeneity of structure can be seen as an additional degree of freedom inherent in graded-gap material, which makes the new features in the flow of many physical phenomena, including photovoltaic.

Today is not fully realized the possibilities of graded-gap structures in photoconversion. In this work introduced the results of researches properties of the active region heterostructures based on GaAs (AlGaAs) including graded-gap obtained by LPE using complex doping with rare earth elements and izovalent elements.

The feature of such doping is an effective cleaning of epitaxial layers from uncontrolled impurities. Reducing the number of uncontrolled impurities decrease the carrier concentration and increase their mobility. Thus, there is a significant increase in the drift-diffusion length of minority carriers. Was founded that the optimal concentration of ytterbium-gallium melt is $(1-3) \times 10^{-3}$ at%, diffusion length of electrons in GaAs layers up to 10-12 microns.

This value is significantly greater than the thickness of the base region of phototransducer. Therefore most of the carriers reach the region of space charge in p-n-junction. This can significantly improve the efficiency of solar energy conversion.

Sensitive Elements of Digital Signal Processing Noninvasive Measurement Devices Blood Glucose

Kotyk M.V., Yanitskyi V.Y.

Vasyl Stefanyk Precarpathian National University, Ivano-Frankivsk, Ukraine, mikot@i.ua

This article is devoted to the problem of diabetes and device for non-invasive control of blood glucose level (BGL) based on glucose absorption of infrared (IR) radiation in one of the maximums (940 nm).

The objective was to manufacture a prototype device for non-invasive determination of blood glucose.

The device model for non-invasive determination BGL was developed. The experimental device has following elements: LED type TSAL6100 and phototransistor type BPT-BP2931. This device has implemented new methods of signal filtering. Bandpass filter with a wavelength of 940 nm was used for filtering optical signal, and for filtering the electrical signal - a low frequency bandpass filter.

During the performance, it was found that the sensitivity phototransistor BPT-BP2931 were not enough, and in this regard it was decided to develop on its basis an advanced sensor, through which could reduce the error of this type of equipment. The basis of the development was taken analytical microsystem-on-chip with the structure of silicon-on-insulator. Also, to improve the processing of information received from the object, it was suggested to include analytical microsystem-on-chip operational amplifier and the inverter element (fig.1).

The modes and electrical scheme of experimental noninvasive device for measuring the BGL and the model of AMSoC were simulated. [1]

The experimental results are the basis for optimizing this type of devices that creates perspectives for further work.

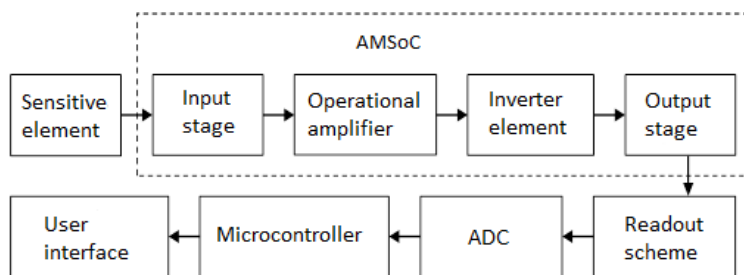


Fig. 1. Functional diagram of processing information for non-invasive blood glucose meters using AMSoC

1. Druzhinin A. Electrical and layouts simulation of analytical microsystem-on-chip elements for high frequency and low temperature applications / A. Druzhinin, Yu. Khoverko, V. Dovhij, I. Kogut, V. Holota // UkrMiCo'2016. – Kyiv, 2016. – P. 29-32

Influence of the $C_4H_6O_6$ Concentration Change on the of InAs, GaAs and InSb, GaSb Polishing Process

Levchenko I.V., Tomashyk V.M., Stratiychuk I.B.,
Malanych G.P., Korchovyi A.A.

V. Lashkaryov Institute of Semiconductor Physics, NAS of Ukraine, Kyiv, Ukraine

The features of the InAs (001), GaAs (111), InSb (112) and GaSb (112) chemical-dynamic polishing (CDP) using $(NH_4)_2Cr_2O_7$ –HBr– $C_4H_6O_6$ etchants with different $C_4H_6O_6$ initial concentration have been investigated. The etching compositions were prepared using 26 % $(NH_4)_2Cr_2O_7$, 42 % HBr, 27 % and 40 % $C_4H_6O_6$. The researched interval of the etchant solutions (in vol. %): (2-22) $(NH_4)_2Cr_2O_7$, (10-98) HBr and (0-80) $C_4H_6O_6$ was chosen.

The semiconductors etching rate decreases more effective when the 40 % initial concentration of the tartaric acid is used.

InAs and GaAs crystals dissolve slower ($v_{max}=5,6-7,5$ $\mu\text{m}/\text{min}$) in comparison with InSb and GaSb substrates ($v_{max}=7,9-8,4$ $\mu\text{m}/\text{min}$) and also this process is not depends on the using of the $C_4H_6O_6$ initial concentration.

The etchants based on the 27 % and 40 % $C_4H_6O_6$ are polishing for arsenides and they are limited by the interval (in vol. %): (2-19) $(NH_4)_2Cr_2O_7$: (10-98) HBr : (0-80) $C_4H_6O_6$. In the case with antimonides, the etchant solutions (in vol. %): (2-19) $(NH_4)_2Cr_2O_7$, (10-98) HBr, (0-80) $C_4H_6O_6$ are characterized by polishing properties. The film formed on the InSb and GaSb surfaces when the solutions (in vol. %): (19-22) $(NH_4)_2Cr_2O_7$, (69-81) HBr and (0-11) $C_4H_6O_6$ were used and it's not depend on the initial concentration of the tartaric acid.

The metallographic analysis data suggests that the use of the 40 % $C_4H_6O_6$ provides more effective surface polishing in comparison with 27 %. AFM investigation of the surface roughness obtained after treatment in the etchants with 40 % $C_4H_6O_6$ have shown that the polishing of the antimonides surface is a little more effective in comparison with arsenides: $R_a(\text{InSb})=2,8$ nm, $R_a(\text{InAs})=3,3$ nm.

Electrochemical Potential of Charge Carriers in Nanostructured Films of High-Temperature Metals with a Cylindrical Defects Filling Volume

Marenkov V.I.

Odessa I.I. Mechnikov National University, Odessa, Ukraine

Development of element base of modern electronics, which would have preserved the performance in aggressive conditions of high temperatures and pressures characteristic of space technology, taking into account the latest achievements of nanotechnology in the field of processing and creation of new high-temperature materials, “focuses” the attention of researchers on the problems of the description of electronic properties of nanostructured materials, in particular heat-resistant membranous structures based on high temperature metals and semiconductors with nanoinclusions in the volume [1]. Since “uniting” subsystem for base material (BM) films and multiple defects of filling of the volume (DVF) a gas of conduction electrons, which penetrate into the volume and are emitted from the volume of the defects in the BM, and outside of film structure, main point, given the urgent imperative of our time, regarding the development and implementation of nanotechnology is the development of new approaches to the creation of an adequate theory to describe electronic properties of nanostructured systems [2]. Methods “functional of the electronic density” very well at solving the problems of the description of local electronic features in a separate nanodetector, but the presence of a large number of “adjustable parameters” greatly complicates their applicability to the description of average properties of carriers in the macro-systems with many distributed in the volume nanodefects [3]. “Plasma” approach proposed in this work is based on the “cell concept” of the description of the electronic properties of heterogeneous plasma (HP) with a condensed macro particles (MP), exchanging electrons with a gas plasma subsystem. Due to the significant differences of relaxation times “particles” and electronic subsystems of HP local thermodynamic equilibrium (LTE) as a result of the Coulomb long-range interaction are first installed in a LTE-regions of the volume that contain the individual MP. In accordance with the principle of minimum free energy, this fact leads to the existence of instantaneous areas of electroneutrality in the HP – quasi-neutral cells C_{ξ}^Z . Nano inclusions (NI), in particular defects of the filling volume (DFV) nanostructured films are also in dynamic equilibrium with the electronic subsystem, and due to the electromagnetic interaction of the carriers with the ion subsystem of the base material film, forming local electrostatic inhomogeneity in the vicinity of the DFVs, that is, each time “breaking” the volume of the film on the electroneutral region – cells C_{ξ}^Z . Statistical averaging over the ensemble of cells provides the opportunity irreducible problem of the

interaction of micro fields and charges in the film with DFVs to translate the rank of the effective electrostatic problem in an averaged cell C_{ξ}^z electroneutrality. Ultimately, the solution to the model system of the conservation equations and the kinetics is reduced to the solution of the conjugate equations Poisson-Fermi (EPF) and Poisson-Boltzmann (EPB) for the distribution of the self-consistent electrostatic potential in a cylindrical cell of electroneutrality of the nanostructured film with DFVs. RPF and RPB for nanostructured films contain a cylindrical DFVs after a series of transformations and transition to dimensionless coordinates, respectively: the logarithm of the dimensionless distances normalized on the Fermi-length of electrons of the base material (BM) films and the Debye radius of the electrons of the DFV ; and the self-consistent potential, respectively, normalized to the Fermi energy of carriers in the BM and their thermal energy in the defects are reduced to a single transcendental equation relative to the level of electrochemical potential in the film with nano defects .

The developed approach gives a possibility based on the basic physical parameters of the film (work function of the material of the metal film – W^0 , the energy of the bottom of the conduction heat-resistant metal – E_c^0 , the dielectric constant of the metal – ϵ_p) and parameters of the plurality of DFV (concentrations in volume nanocluster – n_p geometrical parameters: the height – h_c and base radius – r_p) to define an effective Fermi level carriers in nanostructured films structures, based on modern high temperature technologies. For a number of high-temperature metals that are used in space technology, conducted model calculations dependences electrochemical potential of the carriers on the temperature and nanoclusters' geometry. Noticed a good correlation of model calculations with available experimental data.

[1]. Marenkov V.I. Fermi Level of Carriers in the Volume Filling Defects structure Based in Heat-Resistant Metals// Nanomaterials: Applications& Properties (NAP-2011).-2011. - P. 82-84.

[2]. Marenkov V.I. Local Electrostatic Field and Carrier Density in the Heat Resistant Metals with the Regular Matrix of Volume-Filling Nano-Defects. - In Book: Physics and Technology of Thin Films and Nanosystems, XIV-International Conference, Conference Proceedings.- May 20-25, 2013 year,Ivano- Frankivsk, Ukraine. - P. 317-318.

[3]. Marenkov V.I. The Influence Cylindrical Nano Defects Filling Volume on Heat- Resistant Metals Thin Films Effective Electronic Characteristics. - In Book: Physics and Technology of Thin Films and Nanosystems, XIV-International Conference, Conference Proceedings. - May 11-16, 2015, Ivano-Frankivsk, Ukraine. - P. 34-35.

Preparation of Textured Bismuth Films by Electrochemical Deposition

Shendyukov V.S., Perevoznikov S.S., Tsybul'skaya L.S., Poznyak S.K.

*Research Institute for Physical Chemical Problems, Belarusian State University,
Minsk, Belarus*

Bismuth is a semimetal and demonstrates a large magnetoresistance [1] which makes it promising for magnetic field sensor application. Bismuth was also found to have a strong dependence of magnetic properties on its microcrystalline structure. In this way, an amazing challenge is to develop the method of synthesis of textured bismuth films with defined magnetic properties. Electrodeposition method allows obtaining smooth compact coatings with a high deposition rate of about 200 $\mu\text{m/h}$ when concentrated bismuth perchlorate acidic electrolyte is used. Preliminary research revealed a significant difference in electrochemical parameters of the deposition process when some types of organic additives were added to electrolyte which indicates a change of the electrodeposition mechanism. In this work, bismuth films (50 μm thick) were electrodeposited at various cathodic current densities from perchlorate electrolytes without additives and with safranin dye (SD), and microcrystalline structure and texture of the obtained deposits were studied by SEM and XRD.

XRD analysis showed that in additive-free electrolyte, the deposited Bi has the preferable orientation of {012} plane, irrespective of the current density (Fig. 1a). Increasing the current density from 0.18 to 2.30 A/dm^2 leads to decreasing the grain size from 7–12 μm to 2–5 μm . Addition of SD to electrolyte results in changing the preferred orientation of Bi, deposited at 0.18 A/dm^2 , from {012} to {110} (Fig. 1c). As the current density grows from 0.18 to 2.30 A/dm^2 , the preferred orientation is changed to {202} (Fig. 1b) and the grain size decreases from 20–25 to 10–12 μm .

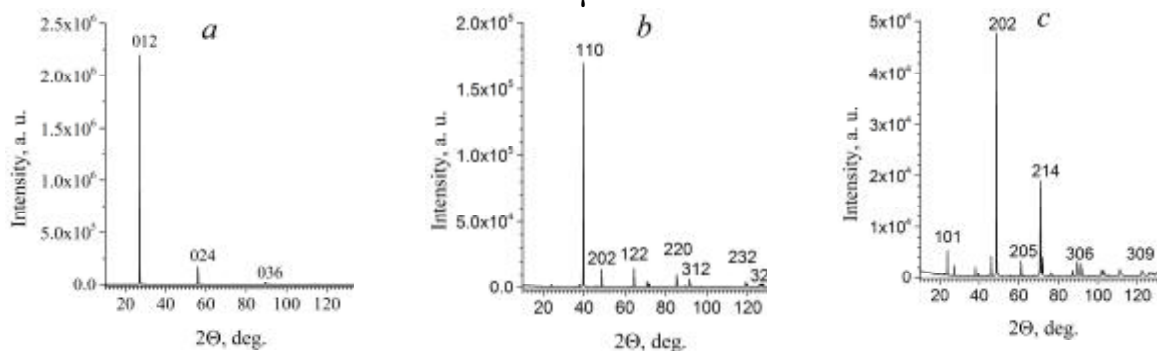


Figure 1 – XRD patterns of Bi films electrodeposited in perchlorate electrolyte without additives at 0.18 A/dm^2 – (a), with SD at 2.30 A/dm^2 – (b), with SD at 0.18 A/dm^2 – (c)

The obtained results provide a great opportunity for creation of multi-layered Bi coatings with controllable magnetic properties.

1. Yang F. Y. [et al.] Large magnetoresistance of electrodeposited single-crystal bismuth thin films // Science. – 1999. – Vol. 284. – P. 1335–1337.

Application of Phototransformations of Bacteriorhodopsin and Its Mutants in Polymer Film for Nanoprocessing

Savchuk A.¹, Stepanchikov D.², Korchemskaya E.^{1,3}

¹*International Center “Institute of Applied Optics”, National Academy of Sciences, Kiev, Ukraine, Alla.Savchuk@iao.kiev.ua ;*

²*Zhytomir State University, Zhytomir, Ukraine, dstep123@gmail.com ;*

³*Institute of Physics, National Academy of Sciences, Kiev, Ukraine, elkorch@hotmail.com*

An analogy of nanotechnology can be found in nature, where biological systems have been operating at the nanoscale for billions of years [1]. The bacteriorhodopsin (BR) protein molecules are arranged at 120 degrees into trimers forming a two-dimensional hexagonal crystalline lattice with a space of 62 Å in the purple membrane fragment of the microorganism *Halobacterium salinarium*. The crystalline structure causes astonishing stability of the retinal protein BR toward chemical and thermal degradation. The light-adapted BR (bR570 state) transports protons and undergoes reversible light-induced transitions through a set of photocycle intermediates. The bR570 state has its absorption peak at 570 nm, while the shortwavelength-absorbing intermediate state M412 has its absorption peak at 412 nm.

In this work, we found that a probability of a transformation to the intermediate M412 of one, two or three molecules in BR trimers is a function of intensity of the linearly polarized exciting light beam [2]. The low-power cw He-Ne laser irradiance was used. For BR genetic mutant E204Q, we have shown that a two-state photochemical cycle model, bR570↔M412, should be replaced by three-state photochemical cycle, bR570→M412→O640→bR570, at increasing humidity where accumulation of the red-light absorbing intermediate O640 in the E204Q BR gelatin film becomes progressively pronounced [3]. Using the BR genetic mutant E204Q as an example, we have developed a design of the functional macromolecular block in the chromoproteins with crystalline structure by means of light.

1. Wagner N.L., Greco J.A., Ranaghan M.J., R.R. Birge. Directed evolution of bacteriorhodopsin for applications in bioelectronics // J. R. Soc. Interface. – 2013. – Vol.**10(84)**. - 20130197.

2. Stepanchikov D.A., Savchuk A.V., Korchems'ka O.Ya. Anizotropna fotoselektsiya molekul bakteriorodopsynu v purpurniy membrani z heksahonal'noyu krystalichnoyu reshitkoyu trymeriv // Uzhhorod University Scientific Herald. Series Physics. – 2016. - Vol.39. - P.73-81.

3. Korchemskaya E., Stepanchikov D., Burykin N., Dyukova T., Balashov S., Savchuk A. Dynamic holography recording on E204Q bacteriorhodopsin gelatin films in red-light range at different humidity values // Molecular Crystals and Liquid Crystals. – 2014. – Vol.**589**. - P.232–241.

Fabrication and Investigation of Graphite/n-CdZnTe Schottky Diodes Prepared by the Transfer of Drawn Graphite Films on CdZnTe

Solovan M.M.¹, Mostovyi A.I.^{1,2}, Brus V.V.^{1,3}, Dymko L.M.¹,
Ulyanytsky K.S.¹, Maryanchuk P.D.¹

¹*Chernivtsi National University, Department of Electronics and Energy Engineering,
Chernivtsi, Ukraine, e-mail: m.solovan@chnu.edu.ua*

²*Department of Chemical Physics, Lund University, Lund, Sweden*

³*Institute for Silicon Photovoltaics, Berlin, Germany*

Carbon based materials are of a great interest for the research and development of next generation low-cost electronic and optoelectronic devices. The low resistivity and high transparency of graphene make it applicable for the fabrication of low-cost ITO-free transparent electrodes, which can be used in photodiodes and organic solar cells. Moreover, graphene becomes more and more attractive as a “window” material in graphene based Schottky-type heterojunction solar cells and photodetectors [1].

The aim of this paper is to propose a simple approach for the fabrication of low-cost photosensitive heterojunctions based on the graphite films. Therefore, we use a simple transfer method of the graphite films, drawn on salt (NaCl) substrates, for the fabrication of high quality photosensitive pencil-on semiconductor heterojunctions. The uniform graphite films were drawn on the prepared rough salt substrates by a pure graphite rod 1 mm in diameter under a constant pressing forth of 1 N. Afterward, the samples were carefully placed on the surface of deionized water (graphite film on top). The salt substrate dissolves in a minute and finally we get a substrate free dry drawn graphite film floating on water surface [2]. The floating dry drawn graphite films were transferred on the freshly cleaved n-CdZnTe single crystal substrates with prepared back ohmic contacts.

The obtained heterojunctions possessed sharply defined rectifying properties. The dominating current transport mechanisms through the heterojunctions were determined at forward and reverse biases. The analysis of capacitance-voltage (C–V) characteristics was carried out at different frequencies of the small amplitude AC signal.

1. Brus V.V., Maryanchuk P.D. Photosensitive Schottky-type heterojunctions prepared by the drawing of graphite films // *Applied Physics Letters*. – 2014. – V. **104**. – pp. 173501-1-173501-3.

2. Brus V.V. , Maryanchuk P.D. Graphite traces on water surface – A step toward low-cost pencil-on-semiconductor electronics and optoelectronics // *Carbon*. – 2014. – V. **78**. – pp. 613-616.

Growth Mechanisms of Lead Chalcogenide Films Grown by Pulsed Laser Deposition

Virt I.S.^{1,2}, Lopatynskiy I.Y.³, Frugynskiy M.S.³, Tur Y.²,
Lusakowska E.⁴, Luka G.⁴

¹*Drogobych State Pedagogical University, Drogobych, Ukraine, ivirt@email.ua*

²*University of Rzeszow, Rzeszow, Poland*

³*Lviv Polytechnic, National University, Lviv, Ukraine*

⁴*Institute of Physics PAS, Warsaw, Poland*

An increased interest in $A^{IV}B^{VI}$ compounds stems from their excellent ability to detect infrared (IR) radiation in a wide wavelength range. This explains practical applications of these compounds in various optoelectronic devices. Lead chalcogenides (PbS, PbSe and PbTe) are especially good materials for mid-wave IR (wavelength of 2500 nm) detection.

In this work, we obtained and studied lead chalcogenide films - PbTe, PbSe and PbS, that were grown by pulsed laser deposition (PLD) and have using stoichiometric targets. We used a YAG:Nd³⁺ laser with the following parameters: the laser wavelength was 1064 nm, the energy maximum in a pulse was 0.4 J, the power density was $5 \cdot 10^8$ W/cm², the pulse duration was 10 ns, and the pulse frequency was 0.3 Hz. The pressure inside the PLD chamber was 10^{-5} Pa, and the substrate temperature was 200°C. We used KCl(001), Si(111), and Si₃N₄/Si substrates. The Si₃N₄ layer thickness was 100 nm. The thickness of each lead chalcogenide film was ~2000 nm.

The structure and homogeneity of the synthesized PLD target materials were studied by X-ray diffraction (XRD) using a DRON-3 diffractometer with CuK_α radiation and θ - θ scanning. They also have good chemical, mechanical stability and structural quality. The degree of texture slightly varied among the three chalcogenides and was the highest for the PbS layer. The highest structural order of PbS was associated with the smoothest surface morphology, the highest density of dislocations that formed at the film/substrate interface, and the highest compressive strain in the film plane direction. The surface geometry (roughness) of the films grown on Si₃N₄ was studied by means of the power spectral density analysis. Different growth modes, ranging from plasma plume condensation to bulk diffusion, resulting in observed film morphologies were identified. The investigations were complemented by electrical characterization of the chalcogenide films.

1. Alvira F.C., Cabrera L. P., Mendoza Y. P., Ricci M.L.M., Videla F. Pulsed laser deposition of PbTe under monopulse and multipulse regime// Optics and Lasers in Engineering. – 2017. – Volume 90, Iss. 3. – P. 284–290

Especially Obtained of Nanocrystals ZnO: Mn by Ultrasonic Spray Pyrolysis

Vorovsky V.Yu., Kovalenko A.V., Khmelenko A.V.

Oles Gonchar Dniprovskiy National University, Dnipro, Ukraine

The method of ultrasonic aerosol pyrolysis is widely used in the preparation of diluted magnetic semiconductors (DMS) based on ZnO by doping it with manganese. The contradictory results of studies of these materials are related to the existence of certain features of the process of doping of zinc oxide by Mn^{2+} ions. Manganese at high synthesis temperatures can form oxides of different valence levels: MnO_2 , Mn_2O_3 , Mn_3O_4 . This leads to the appearance of impurity phases that affect the physical properties of synthesized DMS. It should also be borne in mind that the formation of ZnO: Mn nanocrystals with this method of synthesis occurs in short-term, very nonequilibrium conditions, causes a large number of defects in nanocrystals and does not allow their effective doping with impurities. Taking these features into account, the optimal conditions for the synthesis of the ZnO:Mn nanopowder were studied by ultrasonic pyrolysis of aerosol. The possibility of obtaining ZnO:Mn nanocrystals, which have ferromagnetic properties at room temperature, has been shown. It was found that the optimal temperature for the synthesis of ZnO: Mn nanocrystals with a manganese concentration of 2% is in the range $T = 450-550^\circ C$ and annealing in air at $T = 550^\circ C$ and $800^\circ C$ for a 1 hour time leads to a decrease and disappearance of ferromagnetic properties (Fig.1). The significant increase in the amplitude of the lines of the superfine structure in the EPR spectrum after annealing at $T = 850^\circ C$ indicates that only in this way there is the possibility for effective doping of ZnO nanocrystals with Mn^{2+} .

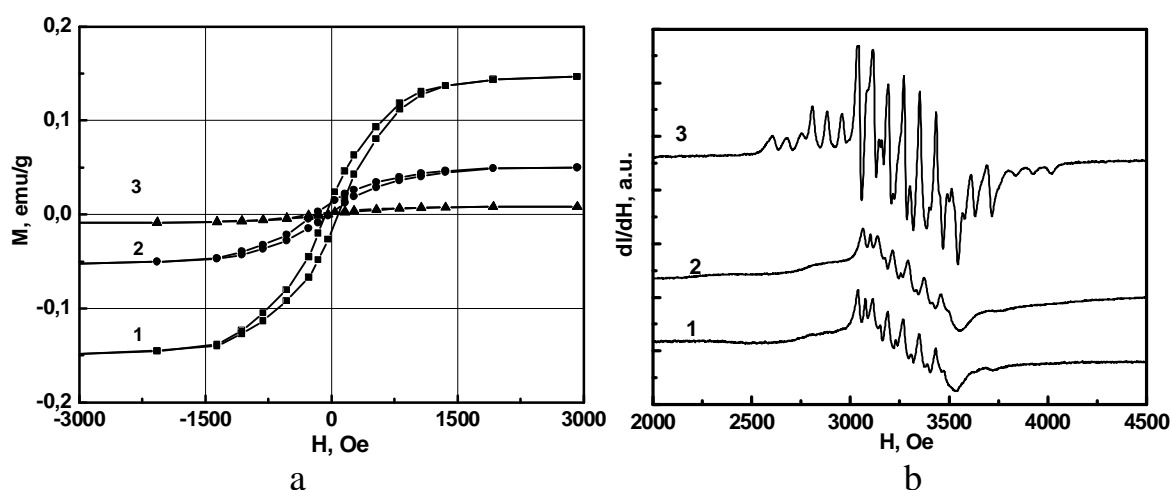


Fig. 1. The magnetization curves (a) and EPR spectra (b) nanocrystals of ZnO: Mn (2%) synthesized at $T = 550^\circ C$ before annealing (1), after annealing in air for a 1 hour time at $T = 550^\circ C$ (2) and $T = 850^\circ C$ (3).



ORAL REPORTS

Session 2

Nanotechnologies and nanomaterials, quantum-size structures



The Influence of Carbon and Oxygen Ion Implantation on Thermodonor Generation in Cz and Fz-Silicon Layered Structures

Babich V.M., Popov V.G., Romanyuk B.M., Gudymenko O.Yo., Kladko V.P., Oberemok O.S., Dubikovskiy O.V.

*V.Lashkaryov Institute of Semiconductor Physics of NAS of Ukraine, Kyiv, Ukraine;
romb@isp.kiev.ua*

Investigation of oxygen complexes in Cz and Fz - silicon are presented. Carbon (C^+) and oxygen (O_2^+) ion implantations with subsequent thermal treatments have been used for creation of thermostable shallow thermodonors (STD). That allows forming a thin n-type surface layer in p-type silicon. Such structures can be used as a p-n junction [1].

The main purpose of present work was creation of the high STD concentration ($\geq 5 \times 10^{16} \text{ cm}^{-3}$) in p-type silicon surface layer. Such STD concentration is sufficient for p-n structure formation.

It was shown that the STD concentration depends on the implanted carbon dose and annealing temperature. The necessary STD concentrations were obtained in the layer with 80 nm thickness after carbon ion implantation with dose of $1 \times 10^{14} \text{ cm}^{-2}$ and subsequent annealing at 650°C during 30 minutes.

STD concentration in the n-type layer correlates with the concentration of microdefects (MD). This is confirmed by the transmission electron microscopy method (TEM). The defects have a round (1 nm) and extended (>2 nm) shapes. Investigation by TEM and diffuse X-ray scattering on defects indicate their interstitial character. Namely these MD are the donor type oxygen-carbon complexes and to act as thermally stable STD. Electro physical studies indicate that the thermodonor activation energies are 12 and 14 eV for Cz- and Fz – silicon (at additional implantation of O_2^+), respectively.

The test p-n structures have been fabricated from various initial p-Si materials. For the first time the n-type thin-layer region was formed on the STD base for the creation of p-n junction by the C^+ ion implantation with corresponded thermal treatments. Analysis of current-voltage characteristics (CV) for such structures indicates the real possibility of p-n junction formation with high breakdown voltage and low reverse current ($\approx 10 \text{ nA}$).

Increasing of implanted oxygen dose in Fz – silicon and also annealing time lead to appear the SiO_2 phase in the oxygen distribution region near the TD centers. CV of such structures have unstable (N-form) areas for direct biased p-n junction. This effect requires a more detailed study.

1. Romanyuk B. et al. Structural and electrical properties of oxygen complexes in Cz and Fz silicon crystals implanted with carbon ions // *Nanoscale Research Letters*. – 2014. – T. 9. – №. 1. – C. 1-6.

Methods and Algorithms of the Realistic Physical and Chemical Portrayal of Nanoscale Systems

Balabai R.M., Kravtsova D.Yu.

*Kryvyi Rih State Pedagogical University, Kryvyi Rih, Ukraine,
balabai@i.ua, gritsulia.dariya@kdpu.edu.ua*

Our presentation is devoted to fundamental theoretical models in nanoscale materials science. Based on accurate first-principle pseudopotentials, the electron density functional method and momentum space formalism the software package was developed and tested by the authors. It allows calculating the spatial distribution of the electron density and its cross section, the total energy of atomic systems, Coulomb potential, the forces that act on the atom from side of all other atoms etc [1].

Various results of our investigations are discussed in the report that includes environmental effects on nanomaterials, predictions of their properties, correlations with experiments etc.

For example, the nanocrystals of the composite of diamond and cubic boron nitride (cC-cBN) are one of the investigated materials. The hardness and the chemical inertness were interested us. For information about the hardness of the material there is necessary to calculate the forces with which the atomic cores of the lattice and electron subsystem act on the observed atom. Logical to assume that the force, which resists indentation load, is the difference between forces generated in no deformed and deformed material. It was revealed that crystal of cC-cBN composite has a record high hardness when deformed at the top. In addition, so-called "orientation defect"[2] is manifested in these models, which can be seen in Fig. 1. You can observe an increase concentration of the electron density along the deformed chemical bond.

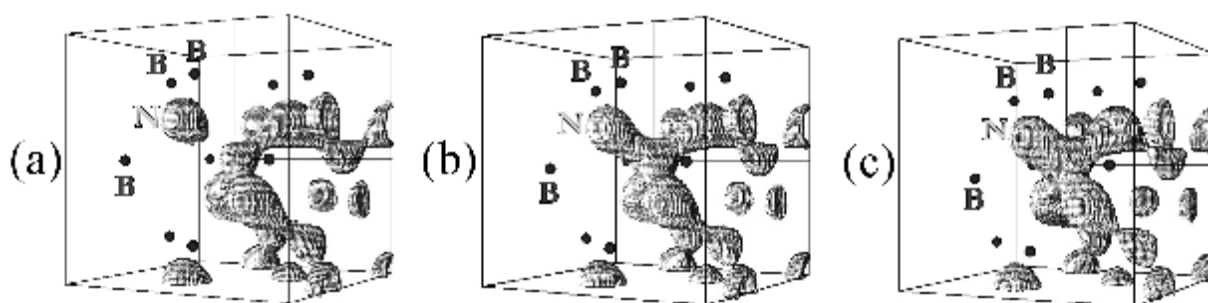


Fig.1. The spatial distribution of the valence electron density for the no deformed (a) and deformed (b,c) nanocrystals of cC-cBN

1. Ab initio calculation [E-resource] – Mode access to the resource: <http://sites.google.com/a/kdpu.edu.ua/calculationphysics>.
2. Vavilov V. Mehanizmy obrazovaniya i migracii defektov v poluprovodnikah / V. Vavilov, A. Kiv, O. Nijazova. – Moskva: Nauka, 1981. – 368 s.

Structural and Electrochemical Properties of β -Ni(OH)₂/RGO Composite

Bandura Kh.V.¹, Kotsyubynky V.O.¹, Hrubciak A.B.², Fedorchenko S.V.¹

¹Vasyl Stefanyk Precarpathian National University, Ivano-Frankivsk, Ukraine

²Institute of Metal Physics, National Academy of Science, Kyiv, Ukraine

Nowadays transition metals oxide-hydroxides / reduced graphene oxide (RGO) composites are one of the most promising electrode material for highly efficient hybrid supercapacitors. The impact of structural and conductive properties of composite β -Ni(OH)₂/RGO on its electrochemical parameters was investigated. Ultrafine β -Ni(OH)₂ was synthesized by surfactant assisted (polyethylene glycol 6000) hydrothermal method. Graphene oxide (GO) was obtained by Hummers method. The reduction of GO was carried out under hydrothermal conditions using hydrazine hydrate. β -Ni(OH)₂/RGO composite with mass ratio of 2:1 was obtained by ultrasonic dispersion. The phase state of origin RGO and β -Ni(OH)₂ were tested by XRD (Fig.1). XRD pattern of β -Ni(OH)₂ is characterized by broadening reflex (001). The thickness of separate particles is about 15-20 nm (calculated from (001) reflex broadening). The presence of sticking faults doesn't affect the width of (001) reflex. Only weak intensity increasing in 25-30° range is observed on β -Ni(OH)₂/RGO composite XRD pattern. The (100) and (101) reflexes broadening implies the sticking faults appearance. It may be suggested that ultrasonic dispersion is accompanied with the intercalation of RGO fragments in the β -Ni(OH)₂ interplanar space. Cyclic voltammetry was used for the comparison of obtained materials' electrochemical properties in 1M KOH and calculating its specific capacitance (fig. 2). The surface faradic reactions will proceed according to the following reaction β -Ni(OH)₂ + OH⁻ → β -NiOOH + H₂O + e⁻. The anodic peak (oxidation of β -Ni(OH)₂ into β -NiOOH) and the cathodic peak (reverse process) for β -Ni(OH)₂/RGO are more clear that indicates the improved mass transportation and electron conduction of composite. The average specific capacitances of β -Ni(OH)₂ and β -Ni(OH)₂/RGO (calculated from the CV curves, scan rates of 2 mV/s) were 271 and 372 F/g, respectively.

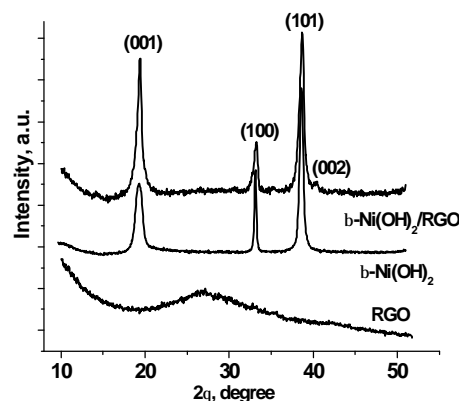


Fig.1. XRD patterns of β -Ni(OH)₂, RGO, β -Ni(OH)₂/RGO

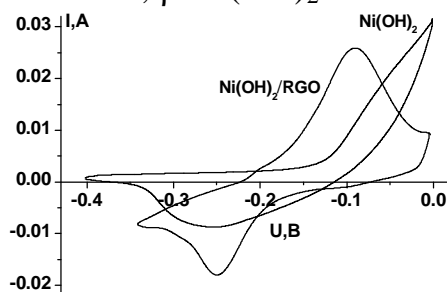


Fig.2. Cyclic voltammograms of β -Ni(OH)₂ and β -Ni(OH)₂/RGO

Y-doped BaTiO₃ Ceramics with Mn Additives as Ferroelectric-Semiconductor with Nanosize Inner Interfaces

Belous A.G., V'yunov O.I., Reshytko B.A.

*Vernadskii Institute of General and Inorganic Chemistry,
National Academy of Sciences of Ukraine
e-mail: vyunov@ionc.kiev.ua*

Ferroelectric-semiconductor polycrystalline structures with nanosize inner interfaces attract interest due to their high (colossal) permittivity ($\epsilon > 1000$) offering promising opportunities in the development of high-energy-density storage devices. It is known that the semiconducting grains and insulating nanosize grain boundaries of the ceramic samples contribute to their colossal permittivity which can be used for instance in the internal barrier layer capacitors (IBLCs). The colossal permittivity is the characteristic of BaTiO₃-based ceramics, and can be explained by internal barrier layer capacitance [1], hopping polarization [2], and external barrier between electrode and ceramics [3]. The present work is devoted to a deeper understanding of the nature of colossal permittivity of BaTiO₃-based ceramics with the view of its further enhancement.

Polycrystalline Y-doped BaTiO₃-based solid solutions with different amount of Mn additives have been synthesized using a solid-state reaction technique. Structural and electrical properties of the samples have been studied in details to understand the impact of different polarization mechanisms in the total value of permittivity. All of the samples demonstrated single-phase composition, and tetragonal symmetry at room temperature. It has been found that relatively high permittivity ($\sim 10^4$) of the ferroelectric-semiconductor solid solutions based on barium titanate can be achieved over the wide range of measurement temperatures. However, the dielectric losses of the materials with colossal ϵ values are too high enough to limit their potential applications. Impedance spectroscopy shows that the impact of various polarization mechanisms to the permittivity decreases in the range: “internal barrier layer capacitance \rightarrow external barrier between electrode and ceramic \rightarrow hopping polarization \rightarrow spontaneous ferroelectric polarization”.

This research was supported by the Program on Fundamental Studies of the National Academy of Science of Ukraine “Fine Chemicals”.

1. Lunkenheimer, Peter, *et al.* "Colossal dielectric constants in transition-metal oxides." *The European Physical Journal-Special Topics* 180.1 (2009): 61-89.
2. Guillemet-Fritsch, Sophie, *et al.* "Colossal permittivity in ultrafine grain size BaTiO_{3-x} and Ba_{0.95}La_{0.05}TiO_{3-x} materials." *Adv. Mater.* 20.3 (2008): 551-555.
3. Hess, Harald F., *et al.* "Giant dielectric constants at the approach to the insulator-metal transition." *Physical Review B* 25.8 (1982): 5578.

Enhancement of Efficiency of Surface-Barrier Solar Cell Due to Metal Nanowires on Quasiperiodical Microrelief

Dmitruk N.L., Korovin A.V., Borkovskaya O.Yu, Mamontova I.B.,
Kotova N.V.

Institute for Physics of Semiconductors, National Academy of Sciences of Ukraine
Kyiv, Ukraine, E-mail: dmitruk@isp.kiev.ua

Texturization of front surface of solar cell (SC) is one of the effective methods to enhance the SC efficiency by reduction of optical losses due to randomization of light propagation. For this purpose a random microrelief is being used. However, in the case of some special quasigrating microrelief (QG) of metallized semiconductor surface/interface an excitation of surface plasmons (SP) and surface plasmon polaritons (SPP) is possible [1]. The surface microrelief of quasigrating-type has been manufactured on n-GaAs (100) with 10^{16} - 10^{17} cm⁻³ doping impurities concentration by chemical anisotropic etching. Parameters of microrelief (mean period and depth of grooves) were varied by a change of the technological regime and were determined by AFM technique. These parameters were used in the theoretical modeling [2] and calculation of optical (transmittance, reflectance and absorption) spectra for *p*- and *s*-polarized light. The structures with different mean period (from 0.7 to 2 μm) and some period distribution were fabricated to investigate the influence of quasigrating relief parameters on the photocurrent enhancement of surface barrier solar cells induced by metal (Au) nanowires deposited on ridges of microrelief.

The comparison of the experimental results with those of the theoretical analysis of quasiperiodical microrelief parameters influence on optical properties of structures with metal nanowires allowed to ascertain the basic mechanisms of the photocurrent enhancement and to choose parameters of structures (and technology of fabrication of them) the more perspective for solar cells application.

Thus, in this report it has been performed the comprehensive investigation of solar cell efficiency enhancement due to light trapping via excitation of SPs and SPPs in metal nanowires and propagation of SPPs in 1D periodical array of these wires.

This work was supported by the NATO SPS grant NUKR.SFPP984617 “Nanostructured Metal-Semiconductor Thin films for Efficient Solar Harvesting”.

[1] N.L.Dmitruk, A.V.Goncharenko, E.F.Venger. Optics of small particles and composite media. Kyiv, Naukova Dumka, 2009, 386 p.

[2] N.L.Dmitruk, A.V.Korovin. Plasmonic photovoltaics: near-field of a metal nanowire array on the interface for solar cell efficiency enhancement. Semiconductor Science and Technology, 2013, Vol. 28 (5). P. 055013-055020.

Raman Scattering Spectra of CeO_x on Graphene Nanoparticles for Catalitical Application.

Dovbeshko G.¹, Gnatyuk O.¹, Kraszkieicz P.², Boiko V.¹,
Kovalska E.³, Stubrov Yu.⁴, Mista W.², Strelchuk V.⁴, and Klimkiewicz R.²

¹*Institute of Physics of NAS of Ukraine, Kyiv, Ukraine;*

²*Institute of Low Temperature and Structure Research, PAS, Wroclaw, Poland.*

³*Department of Physics, Bilkent University, Ankara, Turkey*

⁴*Institute for Physics of Semiconductors, NAS of Ukraine, Kyiv, Ukraine*

Ceria over graphene supported catalyst was synthesized and characterized by Raman, IR spectroscopy, electron microscopy and TPR measurement. It was done to study new effective catalyst for transformation of oxygenates.

The results of Raman spectroscopy showed that CeO_x particles are distributed non-homogenously on the surface of graphene particles with a strong interactions in the site of location. Raman spectra were registered with 0.488 μm laser radiation under power excitation from 0.1 to 10 mW. The band of CeO_x on graphene in the region of 447-451 cm⁻¹ was found to be shifted in comparison to analogous to those for CeO_x on CNT (456 cm⁻¹). We registered drastic changes of this line intensity of CeO_x under laser radiation power tuning from 1 to 10 mW and supposed chemical reduction of CeO_x on graphene surface under laser radiation. This process could be connected with laser induced charge transfer between CeO_x and graphene. Ratio D/G mode that characterises the graphene defects increases in the site of CeO_x interaction with graphene. Electron-phonon interaction calculated from position of 2D mode in the CeO_x - graphene system, decreases with increase CeO_x content. Data of Raman spectroscopy is in accordance with TRP measurement and discussed.

Acknowledgements: This work was supported by project STCU № 6175 and Ukrainian-Polish joint research project.

Effect of Low-Temperature Annealing on the Electrical Conductivity of Amorphous SiO_x Films

Kizjak A.Yu.¹, Evtukh A.A.^{1,2}, Steblova O.V.²

¹*V. Lashkaryov Institute of Semiconductor Physics, NAS of Ukraine,
e-mail: anatoliy.evtukh@gmail.com*

²*Taras Shevchenko Kyiv National University, Institute of High Technologies, Kyiv, Ukraine.*

Amorphous oxide films have wide applications in electronics and optoelectronics. Nowadays the silicon enriched SiO_x films attract much attention due to the possibilities of new device realization on their base. For this the SiO_x films with required physical parameters are needed.

The results on influence of the low-temperature annealing of SiO_x film at T = 450°C in hydrogen and vacuum on their electrical conductivity are presented here. The initial SiO_x films 20-30 nm thick were deposited on Si substrate by ion-plasma sputtering method at a temperature of 150°C. The Al / SiO_x / n-Si / Al structures have been prepared for electrical measurements. The current-voltage (I-V) characteristics were obtained in wide range of voltage and measurement temperatures.

The influence of low-temperature annealing in hydrogen on I-V characteristics are presented in Fig. 1. As can be seen, the different influence is observed in two voltage regions. The annealing in hydrogen increase the conductivity in region 0 – 2.4 V. On the contrary, the conductivity of SiO_x films decreases after annealing in H₂ in region U > 2.4 V. Such unusual behavior is explained by the existing of different type of traps (energy position, concentration) in the bandgap and peculiarities of their passivation by hydrogen.

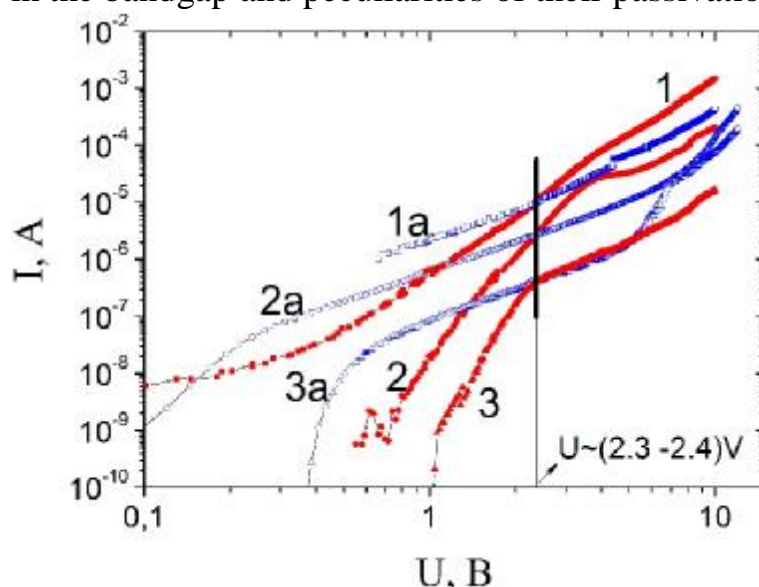


Fig.1. I-V characteristic of the Al/SiO_x/n-Si/Al structure (1-3 – initial films, 1a-3a – after annealing in hydrogen); measurement temperature: 1, 1a – T=330 K; 2, 2a – T=224 K; 3, 3a – T=107.

Electronic Properties of Fullerene Molecule C₆₀, That is Coated With a Single-Layer Film of Silicon Dioxide

Filonenko O., Lobanov V.

A.A. Chuiko Institute of Surface Chemistry, National Academy of Sciences, Kyiv, Ukraine. E-mail: filonenko_ov@ukr.net

It is known that low solubility, thermal instability and tendency to clustering of molecules limit the practical application of fullerenes. The incorporation of fullerene molecules into a polymer matrix, such as silica gel, expands the area of their application, in particular optics.

Using DFT method with a functional that takes into account the dispersion interaction, we calculated the equilibrium spatial structure and electronic structure of a model system: fullerene molecule covered with a layer of silicon-oxygen frame corresponding to gross formula (HOSiO_{1,5})₆₀.

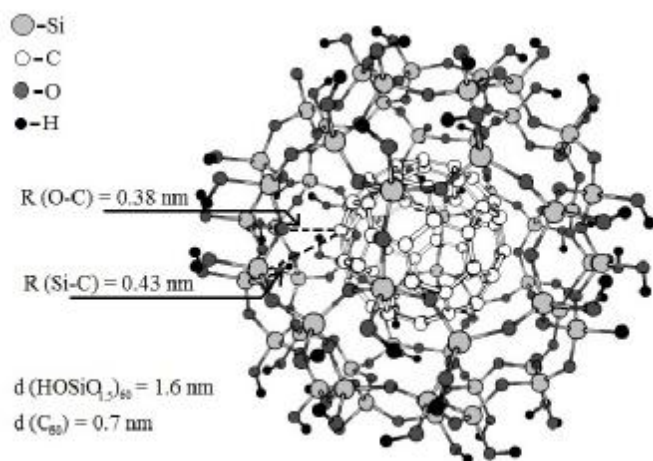


Fig. Equilibrium spatial structure of the system (HOSiO_{1,5})₆₀@C₆₀

(HOSiO_{1,5})₆₀@C₆₀ with respect to individual molecules in its composition is -44.6 kJ/mol, which indicates possible spontaneity of the corresponding process. The main contribution to E_b is made by two components: the term caused by the charge transfer and the dispersion interaction one.

An analysis is made of the density of electronic states of the molecules C₆₀, (HOSiO_{1,5})₆₀ and complex (HOSiO_{1,5})₆₀@C₆₀. It has shown that the main contribution to energy of formation of the system is made by the energy of dispersion interaction. When considering the partial densities of electronic states of atoms C of C₆₀ molecule and of the complex (HOSiO_{1,5})₆₀@C₆₀, it has been revealed that when transiting from molecule C₆₀ to complex the structure of the valence band does not change, and the bottom of the valence band shifts toward lower energies. This is because the C₆₀ molecule undergoes the spherical electrostatic field of the outer shell.

The structure of hollow spherical molecule (HOSiO_{1,5})₆₀ is derived from the structure of C₆₀ molecule by replacing C–C bond with a triatomic fragment Si–O–Si, which consists of two silicon-oxygen tetrahedra connected via vertices. A hydroxyl group was attached to each silicon atom to eliminate the valence unsaturation of Si. The binding energy (E_b) of the system

Topical Directions of Use of Ionizing Radiation in Nanotechnology

Gaidar G.P.

Institute for Nuclear Research of National Academy of Sciences of Ukraine, Kyiv, Ukraine

Nanotechnology is one of the most rapidly developing directions in the science and technology [1]. The possibility to influence on various properties of nanomaterials is a necessary condition at the development of new methods in nanotechnology. Meanwhile, the problem of the creation of appropriate types of tools for nanostructuring of surfaces or the synthesis of nano-objects sharply arises. The ionizing radiation it proved to be a useful tool for synthesis of nanomaterials and nanostructures, as well as for modification of their properties (both in the bulk and on the surface) [2].

The potential of use of ionizing radiation in nanotechnology has been evident from the earliest stages of research. This is due to the fact that: a) the radiation forms the primary nanostructure in any homogeneous condensed medium; b) early stages of the radiation-induced processes (transfer of excitation, migration of hole, thermalization of electrons) develop in the nanometer scale; c) radiation makes it possible to obtain the chemically active particles – "building blocks" for nanoassembly – in any molecular mediums without special reagents.

Radiation technologies include researches in the following areas: receipt of nanoparticles, nanoclusters, metal-polymer nanocomposites, ion-track membranes, nanohydrogels, 3D lithography (electronic, ionic) for obtain of nanoproducts and others. Besides the usual gamma- and electron-beam sources, a number of promising applications use new types of radiation such as synchrotron radiation of X-ray range or the focused ion beams. The creation of nanoporous membranes with high uniformity of geometry is a striking example of the industrial application of ionizing radiation. Radiation can play a significant role in the many applications of the nanostructures and nanoparticles such as catalysis, bio-probing, nanoelectronics, magnetic applications, tissue engineering, biocompatible implants, molecular computers.

The overview of the most important directions of application of ionizing radiation in the nanotechnology researches is proposed, that covers the different technologies of nanostructure fabrication, including three-dimensional, the modification of nanoscale materials, the synthesis of the metal nanoparticles, some medical applications, as well as the problems of nanotechnology application and irradiation in the field of biotechnology.

1. Kireev V. Nanotechnologies: history of origination and development // Nanoindustry. – 2008. – № 2. – С. 2-10.

2. Kostyuk G.I. Nanotechnology: theory, experiment, technics, prospects: Monograph. – Kiev: Publishing House of the International Academy of Science and Innovative Technologies, 2012. – 648 c.

Conditions of High Figure of Merit and Methods of Search for Promising Superlattice Thermoelectric Materials

Gorskyi P.V.

Institute of Thermoelectricity, Chernivtsi, Ukraine

Interest in superlattices as thermoelectric materials arose due to hopes for their thermoelectric figure of merit improvement due to reduction of structure dimensionality. However, these hopes were not fully justified in the sense that no thermoelectric superlattice materials with high figure of merit were created, though it was established, including in empirical way, that other things being equal, the thermoelectric figure of merit of superlattice material can be even an order of magnitude greater than that of conventional single crystal of the same composition. Nevertheless, even the best of resulting superlattices possessed thermoelectric figure of merit that did not exceed or, at least, was not much better than the figure of merit of conventional materials based on bismuth telluride and the alloys of Bi(Sb)-Te(Se) system. However, both theoretically and experimentally it was shown that this figure of merit is drastically reduced with increasing, for instance, superlattice period. The above circumstances motivated the author of this paper to perform a more detailed analysis of factors that might produce both positive and negative impact on the figure of merit of superlattice thermoelectric materials.

When performing the above analysis, the Fivaz model was used in the framework of which charge carrier motion in plane of superlattice layers was described by the effective mass method, and in transverse direction – by the tight-binding method. To describe charge carrier scattering on acoustic phonons, use was made of mean free path approximation which is independent of quantum numbers, but inversely proportional to temperature. The lattice thermal conductivity of material was conventionally considered to be known and also inversely proportional to temperature.

Calculations showed that thermoelectric figure of merit of superlattices drastically grows as a result of increasing the ratio of the Fermi energy of ideal two-dimensional gas to miniband half-width determining the interlayer motion of charge carriers, however rather drastically decreases with increasing the distance between superlattice layers. Based on this, methods of search for promising superlattices with the use of quantizing magnetic fields were proposed.

Anisotropy of Lattice Thermal Conductivity of Zinc and Cadmium Antimonides

Gorskyi P.V., Vikhor L.N.

Institute of Thermoelectricity, Chernivtsi, Ukraine

Though zinc and cadmium antimonides as thermoelectric materials have been known for a long time, interest in them has weakened to a certain extent due to the discovery of bismuth telluride and the production of numerous sufficiently high-quality thermoelectric materials on its basis. The latter are practically unique materials for thermoelectric coolers and prevalent materials (except for high-temperature range) for generators. However, recent times have seen a surge of interest in zinc and cadmium antimonides. This surge is caused by a variety of factors, among which mention should be made of high cost, toxicity and limited tellurium reserves. Moreover, the thermoelectric figure of merit of cadmium and zinc antimonides, though not high at room and lower temperatures, drastically grows with a rise in temperature, and can be increased even more due to optimization by doping with specially selected impurities in proper concentrations. Thus, zinc and cadmium antimonides could be worthy of competition with conventional tellurium-containing materials and generator ones, especially in the temperature range of 400-600K. Besides, a very important practical feature of these materials is pronounced anisotropy of their kinetic coefficients which allows their use, for instance, for creation of anisotropic thermoelements, including optical.

In this connection, the authors of the present paper have analyzed the mechanism for origination of the anisotropy of lattice thermal conductivity of cadmium and zinc antimonides. It was established that this anisotropy can be correctly described only with regard to frequency dependence of phonon relaxation time. The anisotropy of lattice thermal conductivity of cadmium and zinc antimonides is caused by the anisotropy of the following parameters of these materials: sound velocity, the Grunesien parameter and umklapp coefficient. The latter characterizes the degree of dependence of phonon-phonon umklapp scattering intensity on phonon frequency. Consecutive account of phonon umklapp scattering is important because it determines the final value of lattice thermal conductivity of cadmium and zinc antimonides in the temperature range which is relevant for their application. The results of the calculations are involved in the interpretation of the experimental data.

Structural, Optical and Photocatalytic Properties of Nanodispersed γ -Fe₂O₃ Synthesized by Hydrothermal Method

Hrubiak A.¹, Kotsyubynsky V.², Moklyak V.¹, Moklyak M.²

¹*Institute of Metal Physics National Academy of Science, Kyiv, Ukraine*

²*Vasyl Stefanyk Precarpathian National University, Ivano-Frankivsk, Ukraine*

Nanostructured mesoporous γ -Fe₂O₃ was synthesized by hydrothermal treatment (120°C, 20 hours) of iron citrate sol [1] with the next annealing of xerogel at 250°C. The obtained material (XRD) is monophase γ -Fe₂O₃ with average sizes of coherent scattering regions (close to particle size) about 7 ± 1 nm. The specific surface area is about 97 m²/g. The distribution of pores volume with pores size (Fig. 1, a) is characterized by the peak at 3.6 nm; the diameter of about 72% pores is in a range of 2.5-4.5 nm.

Optical properties of γ -Fe₂O₃ were studied by UV-vis spectroscopy. The obtained materials have direct optical band gap about 2.73 eV. Thus, the band gap values of the synthesized iron oxide nanoparticles are higher than that of bulk maghemite for which E_g is 2.06 eV. Band gap enlarging in a result of quantum confinement effect due to delocalized close to the Fermi level electronic states. The calculated dependence of the band gap on the particle size (based on the Bruce equation) gives the possibility to do the estimation of the average particle sizes. The obtained results (7.5 nm) very good correlate with the XRD data.

Photocatalytic properties of mesoporous γ -Fe₂O₃ were investigated by the heterogeneous photo-Fenton process of methylene blue dye ($C_0=40$ mg/l) degradation (assisted by hydrogen peroxide as an electrons acceptor). The dependence $\ln[C_0/C](t)$ (Fig. 1, c) has enabled to establish kinetic characteristics of dye reaction destruction: reaction constant rate $K=0.01$ min⁻¹ and half-life time $t_{1/2}=28.6$ min.

1. Kotsyubynsky V.O., Hrubiak A.B., Moklyak V.V., Mokhnatska L.V. Electrochemical Properties of Mesoporous γ -Fe₂O₃ synthesized by Sol-gel Citrate Method // JNEP. – 2016. – 8(1), 1004-1.

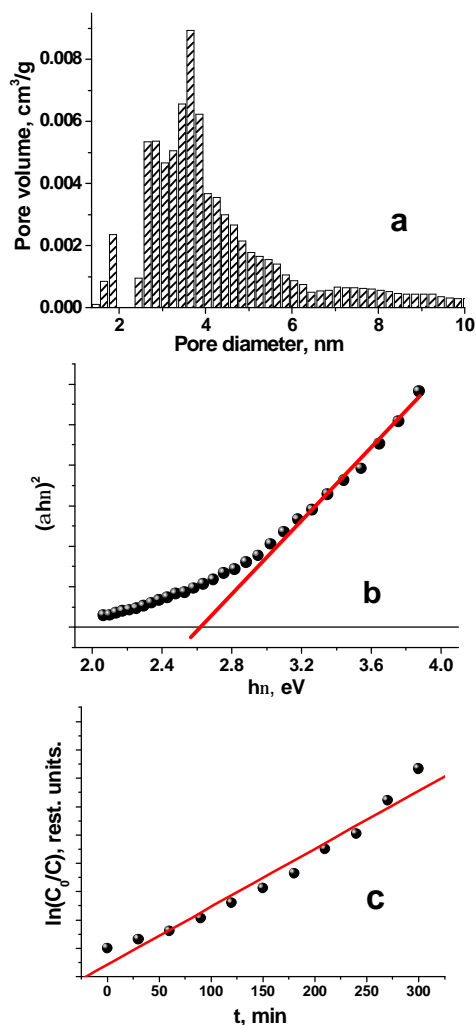


Fig. 1. Pore size distribution (a) and dependence $[\alpha \cdot hv]^2/(hv)$ (b) and $\ln[C_0/C](t)$ (c)

Nanostructuring of $Zn_xCd_{1-x}Te$ Surface in the Gold Nanoparticles Presence

Ivanits'ka V.G., Dzyubinska N., Fochuk P.M., Mar'yanchuk P.D.

Yuriy Fed'kovych Chernivtsi National University, Chernivtsi, Ukraine

A large active area of nanostructured semiconductor surface is the cause of light absorption increasing and of the photogenerated carrier's efficiency separation. The purpose of the study is $Zn_xCd_{1-x}Te$ surface modification for creating of nanostructured heterojunctions with the reproducible electrical, photoelectric and gas sensory properties.

Samples under investigation were cut from $Zn_{0.1}Cd_{0.9}Te$ single crystals grown by Bridgman technique. Study of surface morphology was carried out by using atomic force microscopy. Information on the methods of CdTe and $Zn_xCd_{1-x}Te$ surface nanostructuring was not found, so we used the technique of porous silicon obtaining [1]. In order to fabricate the porous nanostructures on the $Zn_{0.1}Cd_{0.9}Te$ surface, the gold nanoparticles were synthesized from tetrachloroauric acid ($HAuCl_4$) aqueous solution, with the sodium citrate ($Na_3C_6H_5O_7$) addition. $Zn_{0.1}Cd_{0.9}Te$ samples, coated by gold nanoparticles were treated with a different selective etchants. Etching process was performed for 1-5 min. The best results were obtained using the $HF:HNO_3:C_3H_6O_3$ (lactic acid) etchant composition and optimal etching time was 3 minutes. After treatment the darkening of crystal surface was observed. An AFM image of etched samples has confirmed the nanostructured surface layer formation (fig.1).

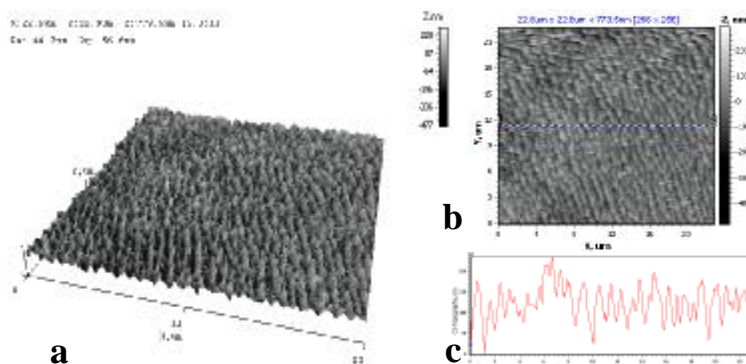


Figure 1. Three-dimensional (a) and two-dimensional (b) AFM image of the $Zn_{0.1}Cd_{0.9}Te$ sample surface and its cross-section (c)

Thus, the obtaining of porous $Zn_{0.1}Cd_{0.9}Te$ surface structure can be carried out in two stages: the creation of gold nanoparticles film on the semiconductor surface, and its etching in $HF:HNO_3$:lactic acid solution by the method described above.

References:

1. Zhipeng Huang, Nadine Geyer, Peter Werner, Johannes de Boor, and Ulrich Gösele. Metal-Assisted Chemical Etching of Silicon: A Review. // Adv. Mater. – 2011. – Vol. 23. – P. 285-308.

Volt-Watt Sensitivity of Macroporous Silicon Structure with Polymeric Nanocoating

Karas N., Karachevtseva L., Litvinenko O., Onyshchenko V.

V. Lashkaryov Institute of Semiconductor Physics, NASU, Kyiv, Ukraine

Macroporous silicon structures are promising for use in optoelectronic and photoelectronics. This is due to the fabrication of structures with the required geometry, large surface area and peculiarities of photoelectric properties determined by the processes on the macropore surface. It is of interest to use macroporous silicon also in photovoltaics to convert solar energy into electricity. One of the photovoltaic characteristics of solar cells is the volt-watt (V/W) sensitivity. The aim of this work is to study the volt-watt sensitivity of macroporous silicon structures with a nanocoating “polyethyleneimine - carbon nanotube”.

Macroporous silicon structures were formed by photoelectrochemical etching with the cylindrical macropore depth $h = 100 \mu\text{m}$, diameter $4 \mu\text{m}$, thickness of the polymer nanocoating is 30 nm . The measurements were carried out according to a standard scheme consisting of structure of macroporous silicon and load resistance. Measurements were made at a wavelength of $0.93 \mu\text{m}$ with a perpendicular incidence of light on the surface of a macroporous silicon structure. The volt-watt sensitivity was calculated as $\Delta V/\Delta P$ at the initial linear portion of the curve shown in the figure.

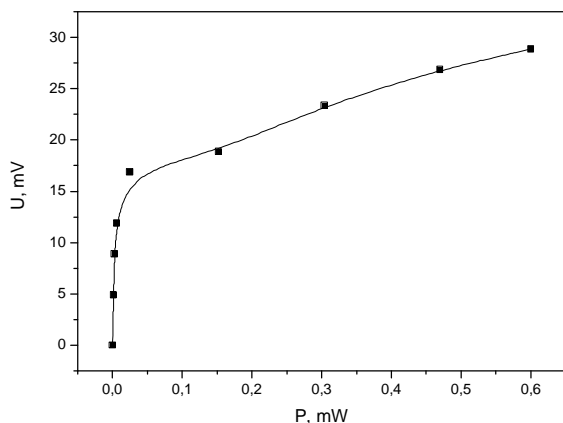


Figure:

The volt-watt sensitivity of a macroporous silicon structure with a nanocoating “polyethyleneimine - carbon nanotube”.

Thus, we obtained the value of the volt-watt sensitivity 2700 V/W . This value significantly exceeds the previously obtained by us value of the the volt-watt sensitivity 1691 V/W for the structure of macroporous silicon with an oxide nanocoating.

Physical and Chemical Properties of Carbon Nanoclusters with Graphene-Like Structure - Quantum Chemical Calculations

Lobanov V.V., Karpenko O.S., Demianenko E.M., Kartel N.T.

Chuiko Institute of Surface Chemistry of the NAS of Ukraine, Kyiv, Ukraine

The unique properties of graphene – an infinite in two dimensions single-layer crystal lattice consisting of sp^2 -hybridized carbon atoms – were first theoretically elucidated long before the production of its reproducible samples. In this case, a simple approximation of the tight-binding was used; the interaction of the nearest neighbors was taken into account. In particular, it has been shown that the areas of the first hexagon-like Brillouin zone of graphene are points; the valence band and the conduction band of $2p_z$ -electrons come into in these points where the dispersion law of electrons near contact zone is linear. These important results were later confirmed by more accurate methods.

It is clear that the tight-binding approximation is not suitable for examination of graphene-like clusters, since it neglects a lot of their properties that are very important from the point of view of a chemist. First of all, this refers to the equilibrium spatial structure of such clusters, the spin state of their ground electronic level (GEL), the influence of various types of defects (mono- and polyatomic vacancies) and doping by electron-donor and electron-accepting atoms on the width of the forbidden gap and the density of one-electron states at the Fermi level.

A theoretical evaluation of all these properties can be carried out using the methods of modern quantum chemistry for example the density functional theory with the 6-31G** basis.

The report presents the results of calculations of these properties using of a graphene-like cluster as an example C_{96} ; it has exclusively zigzag-shaped edges. The most of chemical and physical properties, that cannot be determined using tight-binding approximation and which are manifested exclusively in quantum-chemical calculations, have been identified.

In particular, it has been shown that the GEL of many clusters is not singlet, the peripheral conjugated ring of carbon atoms is connected with the rest of the cluster by ordinary C–C bonds, and the distribution of molecular electrostatic potential is clearly anisotropic. The results obtained are compared for purely carbonaceous clusters and corresponding polyaromatic molecules of similar structures.

Synthesis and Electrochemical Properties Nanostructured α -MnO₂

Ostafiychuk B.K., Kotsyubinsky V.O., Kolkovskyi P.I., Kolkovskyi M.I.

Vasyl Stefanyk Precarpathian National University Ukraine, Ivan-Frankivsk

Nowadays hybrid capacitors (HC) is the most perspective direction of electrochemical energy sources development due to the high of specific power and energy. HC occupy an intermediate position between lithium power sources and electric double layer capacitors and operate using fast surface reversible redox reactions. MnO₂ is one of the most perspective electrode materials due to the successful combination of electric and structural parameters (availability of channels along the crystallographic c axis, Fig. 1, a). For the purpose studies on the relationship between of α -MnO₂ structural characteristics and electrochemical properties. Thus, the synthesis of α -MnO₂ was carried out two methods by controlled hydrothermal synthesis (S1) and the microemulsions synthesis (S2) [1].

We report for the synthesis of monophasic α -MnO₂ for S1 sample (average size of coherent scattering region is about 10-12 nm) and amorphous for S2 with tetragonal structure motives (Fig. 1, b). The values of the specific surface area were 60 and 92 m²/g for of the S1 and S2 samples, respectively. The electrochemical behavior of obtained materials were investigated in 1M Li₂SO₄ aqueous solution by cyclic voltammetry method (Fig. 1, c). The specific capacitances of S1 and S2 materials at scan rate 3 mV/s were 62 and 19 F·g⁻¹, respectively. As a result the material crystallinity is positive factor for increase of ultrafine α -MnO₂ electrochemical performance (in particularly specific capacitances) as electrode materials of hybrid capacitors.

1. Devaraj S., Munichandraiah N. Effect of crystallographic structure of MnO₂ on its electrochemical capacitance properties //The Journal of Physical Chemistry C. – 2008. – T. 112. – №. 11. – C. 4406-4417.

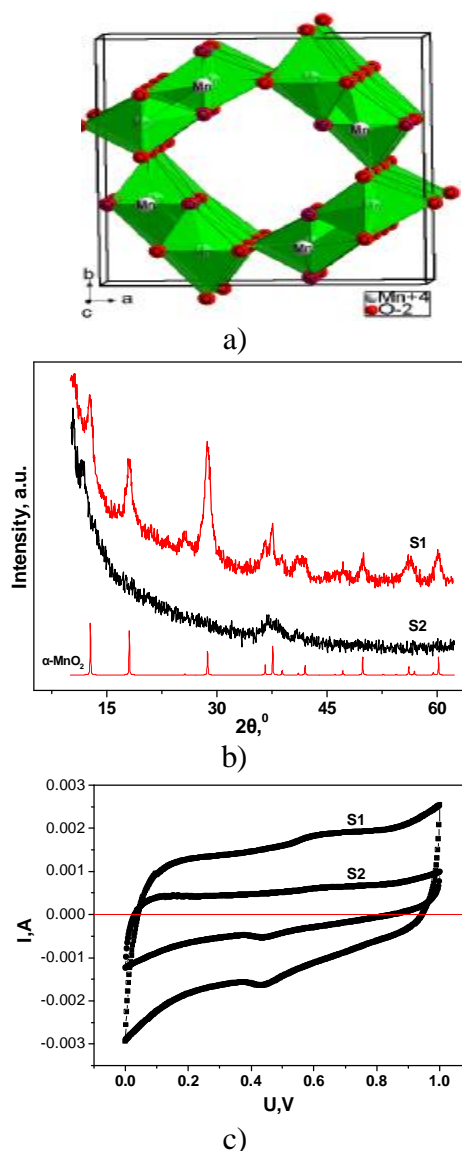


Fig. 1. The crystal structure of α -MnO₂ (a) and the experimental diffraction (b) and CV curves (c) for samples S1 and S2.

Parameters of Charge Transport in Conjugated Polymers Doped by Carbon Nanotubes

Konopelnyk O.I.¹, Aksimentyeva O.I.², Horbenko Yu.Yu.²

¹*Physical Department of Ivan Franko National University of Lviv, Lviv, Ukraine,
E-mail: konopel@ukr.net*

²*Chemical Department of Ivan Franko National University of Lviv, Lviv, Ukraine,
E-mail: aksimen@ukr.net*

Conducting polymer systems present electron delocalization, arising from conjugated double bonds in the polymer backbone. They show electrical conductivity in doped states and are insulators when they are undoped (neutral) state. As a result of doping-dedoping processes the electronic properties (e.g. band gap) of the conjugated polymers can be essentially varied.

Among the family of conducting polymers the polyaniline, polythiophene and their derivatives have the advantages due to thermal and oxidative stability, good workability and higher conductivity [1]. Nanosystems based on conducting polymers doped by carbon nanoclusters (graphene, fullerene, carbon nanotubes) are promising materials for memory devices, plastic solar cells, and sensors [2].

In order to estimate the effect of doping on the parameters of charge transport in the polymer nanocomposites we studied the structures and temperature dependence of conductivity of conjugated polymers - polyaniline (PAn), poly-ortho-toluidine (PoT) and poly-3,4-ethylenedioxythiophene (PEDOT) doped by multiwall carbon nanotubes (MWCNT) in the interval of $T = 273-403$ K.

The activations energy of charge transport (E_a) for PAn is 0.072 ± 0.001 eV, for PoT $E_a = 0,168 \pm 0,003$ eV and for PEDOT $E_a = 0,196 \pm 0,001$ eV. Introduction of carbon nanotubes in concentration near percolation threshold (0.13 - 0.64%) leads to increase of conductivity in PAn, PoT and PEDOT nanocomposites. Simultaneously the activation energy of charge transport increasing for nanocomposites conjugated polymers - MWCNT comparatively with undoped polymers.

According to X-ray powder diffraction a process of polymer doping leads to increasing polymer crystalline level in result of formation the crystalline “domains” in the amorphous polymer matrix. This structural streamlining leads to an increase of energy required overcoming areas of amorphous phase and charge carriers are localized in the areas of crystallinity.

1. Konopelnik, O.I., Aksimentyeva, O.I., Tsizh, B.R., Chokhan, M.I. Physical and Technological Properties of the Sensor Materials Based on Conjugated Polyaminoarenes. Physics and Chemistry of Solid State. 2007, 8 (4), 786-790.
2. O.I. Aksimentyeva, O.I. Konopelnyk, V.P. Dyakonov, V.A. Shapovalov, Yu.Yu. Horbenko. Charge separation in polyphenylacetylene – fullerene nanostructures / In book: "Fullerenes and nanostructures in condensed matter". Minsk: Edit. Center of BSU. 2011. P. 178-183.

Effect of Dielectric Substrate on Optical Absorption of Metal Nanofilm

Korotun A.V., Pogosov V.V.

Zaporozhye National Technical University, Zaporozhye, Ukraine

Interest in the optical properties of the metal nanofilms in recent decades is associated with the improvement of both the technologies and investigation of solid ultrathin metal films. In this case, for the interpretation of experimental results, as a rule, either the classical Drude theory or the generalized Drude-Smith model is used [1]. However, the nonmonotonic size dependence of the optical characteristics on the film can be due to the transitions between the energy subbands [2]. The question of the substrate effect to the oscillation of the optical characteristics remains open.

The aim of this work is to investigate the dielectric confinement effect on the optical absorption of a metallic nanofilm.

The expression for the absorption coefficient has the form

$$\eta(\omega) = \frac{2\omega}{c} \text{Im} \sqrt{\mathfrak{d}(k_\omega)},$$

where $\mathfrak{d}(k_\omega)$ is the dielectric function of a metallic film of thickness L ,

$$\mathfrak{d}(k_\omega) = 1 - \frac{4m_e e^2}{\pi \mathfrak{d}_0 \hbar^4 L} \sum_{m,m'} \frac{(k_F^2 - k_{xm}^2) |p_{ij}|^2}{(k_{xm}^2 - k_{xm'}^2) [(k_{xm}^2 - k_{xm'}^2)^2 - k_\omega^4]},$$

where p_{ij} is the matrix element of the electron momentum operator, $\hbar k_{xm}$ is its quantum-sized component [3], $\hbar k_F$ is the Fermi momentum taking into account the substrate.

It is shown that taking into account the dielectric environment leads to an increase in the maxima and a shift in the peaks on the frequency dependences of the absorption coefficient and the dielectric function.

1. Walther M., Cooke, D. G., Sherstan, C., Hajar, M., Freeman, M. R., Hegmann F. A. // *Phys. Rev. B.* – 2007. – V. 76, No 12. – id. 125408.
2. Kurbatsky V. P., Korotun A. V., Pogosov V. V., Vasyutin E. V. // *Phys. Sol. St.* – 2008. V. 50. – P. 949 – 956.
3. Korotun A.V. // *Phys. Sol. St.* – 2015. V. 57. – P. 391 – 394.

Self-Organization Effects During Plasma Arc Synthesis of Carbon Nanotubes

Kosminska Yu.O., Perekrestov V.I.

Sumy State University, Sumy, Ukraine

Plasma arc synthesis is one of the main routes for carbon nanotubes (CNT) fabrication. This method has been developing since the early work of S. Iijima published in the Nature journal, 1991, and still it remains of great research interest due to low defects in CNT. Besides, there are also other techniques based on catalyst and catalyst-free, physical, chemical and mixed approaches. Thus, CNT can be fabricated by so various ways as to suggest that some similar thermodynamical conditions should be inherent in the techniques. We offer to consider relative supersaturation of deposited vapours as a key to understanding conditions of CNT growth. It is known that under high supersaturations nucleation goes faster but at the same time the fluctuating diffusive field determines joining of adatoms to overcritical nuclei. As a result, continuous films are usually formed without specific structural features. Therefore, one should use low supersaturations to get atom-by-atom formation of specific structures such as nanotubes.

To address the above idea, we have analyzed available experimental data on arc synthesis of CNT and have formulated physical and mathematical model of the major processes taking place in arc discharge during CNT synthesis. The essence of the model is self-organization of technological conditions which results in self-organization of growing structures such as CNT. In the arc each electrode undergoes action of various factors either heating or cooling it, which are considered in the model. The basic factors leading to self-organization are the following. In steady mode of arc discharge operation, a heated cathode made of copper or graphite emits electrons through thermofield mechanism. The electron flux heats a graphite anode up to ~3500 K. The anode ablates. Carbon flux is directed to the cathode and is ionized at near-cathode sheath. The carbon ions are accelerated by electric field in collision-free near-cathode region and are deposited onto cathode surface. Because of high cathode temperatures, a part of carbon adatoms reevaporates, and thus near-cathode region becomes an accumulation area for carbon material until it condenses in the form of CNT.

Mathematically, we write a system of three equations representing interdependent time changes of the cathode temperature, the anode temperature and the carbon concentration in near-cathode accumulation area. The equation system is analyzed and solved using phase portraits method. The solution features the only stable singular point (the stable node) at supersaturation of $\sim 10^{-3}$ and the temperatures values being in experimentally observed ranges. This confirms self-organization of the technological conditions allowing CNT growth.

Nanostructured Structural Features of the Surface of the Catalyst Cu_nCl_m on γ-Al₂O₃

Mykytyn I., Kurta S., Ribun V.

Vasyl Stefanyk Precarpathian National University, Ivano-Frankivsk, Ukraine

Structure of CuCl₂ active catalyst centres used for ethylene oxidative chlorination (EOC) on the γ-Al₂O₃ carrier was described. Namely two types of catalysts were considered - deposited catalyst X1 of the firm «Harshow», with copper chlorides supported onto an alumina surface, and permeated MEDC-B catalyst located in the internal pores of the support of the firm «Sud-Chemie Catalysts». CuCl₂ interactions with γ-Al₂O₃ surface groups (≡Al-OH) lead to complex compounds formation with [CuCl₄]⁻² and [CuCl₂]⁻¹. A new mechanism of metal-complex catalysis of the ethylene oxidative chlorination reaction into 1,2-dichlorethane with Al₂O₃[CuCl₄]⁻² and Al₂O₃[CuCl₂]⁻¹ surface metal complexes reacting with ethylene, hydrogen chloride, and oxygen was proposed.

Differential thermal analysis modeling catalysts' industrial tests. MEDC-B catalyst has higher dehydration and dehydrochlorination rate, and higher 210-220 °C EOC temperature range compared with X1 catalyst (200-210 °C). MEDC-B catalyst is more stable, but less active in the lower 190-210 °C EOC temperature range, thus its optimal EOC temperature range is 210-220 °C. Lower total weight loss of 17% during MEDC-B catalyst heating compared with 20% for X1 is caused by the smaller amounts of the adsorbed and structured water, and by smaller dehydrochlorination losses. Average process rates comparison for the three samples is quite interesting. MEDC-B catalyst dehydration rate increases as a result of [CuCl₄]^{-2,-1} and γ-Al₂O₃ interactions. Modified [CuCl₄]^{-2,-1} catalyst acts as chlorine transmitter during its reduction and dehydrochlorination in the 200-250 °C range which is within the 215-225 °C range of ethylene oxidative chlorination catalyst working temperature. X1 catalyst dehydration and dehydrochlorination temperature range is 180-250 °C (ΔT=70 °C) while for MEDCB it is 200-250 °C (ΔT=50 °C). Working temperature range reduction by 20 °C for MEDC-B compared with X1 catalyst is beneficial for ethylene oxidative chlorination reaction into 1,2-EDC and significantly increases process selectivity. Deposited X1 catalyst has a larger 190-210 °C working range which causes side reactions of ethylene combustion and oxidative chlorination into trichloroethylene. While X1 catalyst selectivity does not exceed 95-97%, MEDC-B selectivity is 97-99%. Based on industrial tests ethylene combustion to CO and CO₂ diminishes to 1.5-2% for MEDC-B. The amount of the permeated MEDC-B catalyst active phase is evenly distributed throughout γ-Al₂O₃ structure which diminishes carrier influence on ethylene combustion observed in industrial EOC technological processes.

1. Sergiy A Kurta, Igor M Mykytyn, Tetiana R Tatarchuk. Structure and the catalysis mechanism of oxidative chlorination in nanostructural layers of a surface of alumina // Springer Journal: Nanoscale Research Letters 15.06.2014, №9\1,-P.357 <http://www.nanoscalereslett.com/content/>

2. Sergey Kurta . Catalysis of ethylene oxychlorination into 1,2-dichlorethane in the presence of CuCl₂/CuCl active centres on the surface of γ-Al₂O₃ // CHEMISTRY & CHEMICAL TECHNOLOGY / Vydav. Nats. Un-tu "L'vivs'ka politekhnika", L'viv, Ukrayina Vol. 6, No.1, 2012.r.1-8 ISSN: 1996-4196.

Interband and Intraband Absorption of Electromagnetic Waves Caused by the Neutral Impurity a Spherical Quantum Dot

Boichuk V.I., Leshko R.Ya., Ivanchyshyn I.B., Toma I.P.

*Drohobych State Pedagogical University named after Ivan Franko,
Drohobych, Ukraine, E-mail: leshkoroman@gmail.com*

Among the modern directions of nanosystem research, significant place has led by heterostructures with *CdS* quantum dots (QDs). Such QDs will be able become by the substitute of organic substance in the biologic sensors and other optical electronic devices. Therefore the last years many researchers had paid attention to elaborate of the new technology of production high-quality and stable *CdS* QD in the solid state and polymer matrix. Buy high-quality do not guarantee that those nanosystems have no impurities. The presence of impurity can change absorption of electromagnetic waves by this system.

First of all we consider the external electromagnetic wave with quant energy range $\hbar\omega \in [0, U_{0e}]$ (where U_{0e} is maximum value of the electron confinement potential) which irradiates the QD with impurity. There are two possible cases:

1) the impurity's electron from the ground state can transit into excited states (p-states according to dipole selection rules) and absorb the quant $\hbar\omega$ (intraband transition);

2) the electron from the valence band can transit into allowed levels near conductive band and the exciton will be created which moved in the average field which caused by the impurity and confinement in the QD (interband transition). The second case can be realized if the confinement potential is large then band gap in the QD. For the *CdS* $U_{0e} = 2.7$ eV and $E_g = 2.5$ eV. And this case is also possible.

In this work we study those two cases. According to this, we calculate impurity spectrum and exciton spectrum in the presence of the impurity in the QD. Based on this results, we found the optical parameters of the nanosystem, which caused by the interband and intraband transition. We compared this two cases and got the dependence of the absorption coefficient on the QD size and on the electromagnetic wave frequency. Also we found conditions when interband or intraband transition are dominant.

Best of Two Worlds: Combination of Magnetic and Semiconductor Properties in (Ga,Mn)(Bi,As) Nanostructured Thin Films

Levchenko K.¹, Andrearczyk T.¹, Sadowski J.^{1,2}, Lusakowska E.¹, Domagala J.Z.¹, Trzyna M.³, Jakiela R.¹, Radelytskyi I.¹, Figielski T.¹ and Wosinski T.¹

¹ Institute of Physics, Polish Academy of Sciences, Warsaw, Poland

² MAX-IV Laboratory, Lund University, Lund, Sweden

³ Faculty of Mathematics and Natural Sciences, University of Rzeszów, Rzeszów, Poland

In a highly-demanding time of the Information Age requirements for new ideas to push the classical limits of the electronics are very high. Several technological approaches are evolving simultaneously: miniaturization to quantitatively increase number of active units per area (e.g. transistors on a microprocessor chip), search of new/enhanced materials with improved characteristics and state of the art development of alternative concepts [1]. In our research [2] we try to combine all three of this methods within a spintronic nanostructures made from quaternary alloy of (Ga,Mn)(Bi,As) thin ferromagnetic semiconductor.

In order to provide an overall description of the material, a quick overview of the III-V ferromagnetic semiconductors theory is given, ensured by samples structure and magnetization characterization check. Results for a wide range of non-destructive techniques, applicable for thin layers investigation, will be presented: typical superconducting quantum interference device (SQUID) magnetic measurements, general layers quality description by X-ray diffraction (HR-XRD) and secondary mass ion spectroscopy (SIMS).

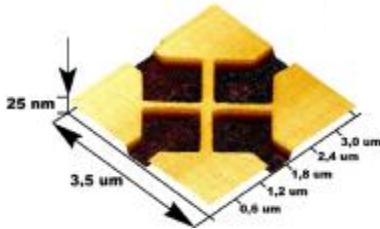


Fig. 1: Atomic force microscopy (AFM) image for the cross-shaped nanostructure of (Ga,Mn)(Bi,As) thin epitaxial layer grown on semi-insulating GaAs. The darker contrast corresponds to non-conducting areas etched to the substrate.

Furthermore, we'll show cross-like (Fig. 1) and ring-shape geometries of nanostructures, tailored using electron-beam lithography patterning and chemical etching from 10-nm thick (Ga,Mn)(Bi,As) epitaxial layers with 6% Mn and 1% Bi contents. An interplay between original magnetic in-plane anisotropy of the material, that arose from the lattice mismatch with a substrate during growing procedure and patterned-induced anisotropy, introduced via the lithography process, creates well-defined magnetic defects (domains). As a result, we achieve resistance difference between contacts pairs, that can be driven by an applied low magnetic field or a spin-polarized current and increased as a result of enhanced spin-

orbit coupling by bismuth incorporation. Series of thorough magneto-transport and magnetic measurements on similar structured thin layers of (Ga,Mn)(Bi,As) / GaAs and earlier concepts [3] based on well-known (Ga,Mn)As / GaAs semiconductor proves stability and utility of such a magnetic memory unit.

[1] T. Dietl and H. Ohno, *Rev. Mod. Phys.* **86**, 187 (2014).

[2] K. Levchenko, T. Andrearczyk, J. Z. Domagala, J. Sadowski, L. Kowalczyk, M. Szot, R. Kuna, T. Figielski and T. Wosinski, *J. Supercond. Nov. Magn.* **30**, 825 (2017).

[3] T. Wosinski, T. Andrearczyk, T. Figielski, J. Wrobel and J. Sadowski, *Physica E* **51**, 128 (2013).

Magnetoresistance of BiSe Whiskers at Low Temperature

Liakh-Kaguy N.S.¹, Druzhinin A.A.^{1,2}, Ostrovskii I.P.^{1,2}, Khoverko Yu.N.^{1,2}

¹Lviv Polytechnic National University, Lviv, Ukraine

²International Laboratory of High Magnetic Fields and Low Temperatures Wroclaw, Poland
e-mail: druzh@polynet.lviv.ua

Magnetotransport properties of various semiconductor whiskers such as Si, Ge, InSb, GaSb at low temperatures have been widely studied in our previous works [1-4]. Transverse magnetoresistance of BiSe whiskers with doping concentration $1 \times 10^{19} \text{ cm}^{-3}$ is studied in the temperature range 4.2 – 77 K and in magnetic fields 0 – 10 T. Temperature dependence of resistance for heavily doped n-type BiSe whisker at a zero magnetic field is shown in Fig.1.

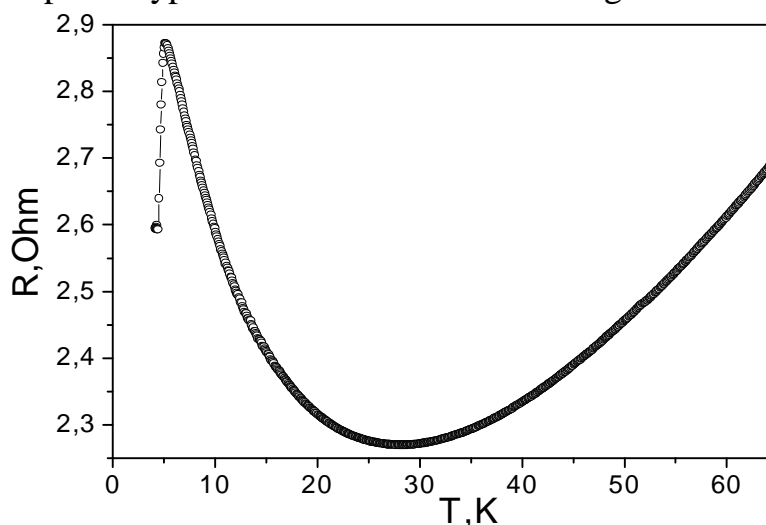


Fig.1. Temperature dependence of resistance for n-type BiSe whisker

A sharp drop at temperature below 4.2 K and minimum at temperature about 30 K are found on the temperature dependence of resistance in BiSe whiskers. The revealed sharp drop of resistance below 4.2 K indicates possible partial superconductivity in the whiskers. The observed minimum on the temperature dependence of resistance for n-type

BiSe whiskers is connected with contribution of Kondo effect in the whiskers. Studied properties of doped BiSe whiskers at low temperatures and high magnetic fields allow to design the sensitive sensor of magnetic field induction and thermoelectric convertors operated at the range of cryogenic temperatures.

1. Druzhinin A.A., Ostrovskii I.P., Khoverko Yu.N., Liakh-Kaguy N.S., Vuytsyk A.M. Low temperature characteristics of germanium whiskers // *Functional Materials*. – 2014. – Vol. 21, No.2. – P.130-136.

2. Druzhinin A., Ostrovskii I., Khoverko Yu. and Liakh-Kaguy N. Negative magnetoresistance in indium antimonide whiskers doped with tin // *Low Temperature Physics*. – 2016. – Vol. 42.– P. 453-457.

3. Khytruk I., Druzhinin A., Ostrovskii I., Khoverko Yu., Liakh-Kaguy N., Rogacki K. Properties of doped GaSb whiskers at low temperatures // *Nanoscale Research Letters*. – 2017. – Vol. 12:156.

4. Druzhinin A.A., Maryamova I.I., Kuttrakov O.P. GaSb whiskers in sensor electronics // *Functional Materials*. – 2016.– Vol. 23, No.2. – P. 206-211.

A New Approach to the Problems of Precision Diagnostics in Micro- and Nanotechnology

Makoviychuk M.I.

Yaroslavl Branch of the Institute of Physics and Technology of RAS, Yaroslavl, Russia

The systematic theoretical and experimental studies carried out in recent years have shown that, in a wide class of natural phenomena, the random nature of the medium, despite its seemingly disorganizing effect, can induce a much richer variety of regimes than those that are possible under the corresponding deterministic conditions.

Unlike internal fluctuations, which are negligibly small for macroscopically large systems, the fluctuations due to the randomness of the medium are very important. The main difference between internal fluctuations and external noise is that the fluctuations of the medium behave not as inverse powers of the characteristic size of the system. In addition, unlike internal fluctuations, the stochastic of the medium is not of microscopic origin. External noise often manifests itself in a turbulent, or chaotic, state of the environment and reflects the dependence of external parameters on a large number of interrelated environmental factors. Because of this, the fluctuations of the medium change not in proportion to the inverse of the characteristic size of the system. That is why they do not disappear at the macroscopic level of the description of the system.

The intensity of external noise within certain limits can be controlled - if the experiment is carefully set up, the noise level can be lowered. On the other hand, the intensity of the fluctuations of the medium can be controlled in a controlled manner to investigate its effect on the behavior of the system. This is another difference between external noise and internal fluctuations, making it much more malleable "material" in the hands of the experimenter.

Thus, taking into account the foregoing, a special place among the new electrophysical methods of information analysis that meet the requirements of defect-impurity engineering is the method of joint measurement of the sheet resistance and its spectral density of flicker fluctuations in the structures - the defect-impurity flicker-noise spectroscopy [1].

1. Makovijchuk M.I. Flicker-shumovaja spektroskopija. Strukturno-neuporjadochennye poluprovodniki. - Saarbrjukken, Germanija: Izdatel'skij Dom «LAP LAMBERT Academic Publishing», 2013. – 168s.

Promising Electrode Material Based on Iron Oxide Hydroxide β -FeOOH

Mokhnatska L.V., Kotsyubynsky V.O., Hrubciak A.B.

Vasyl Stefanyk Precarpathian National University, Ivano-Frankivsk, Ukraine,
knoopka@ukr.net

Nowadays ultrafine β -FeOOH with controlled morphology one of the most promising electrode materials for high-performance hybrid supercapacitor with improved energy and power densities. The iron hydroxides β -FeOOH with tunnel structure and rod-like morphology was synthesized by controlled precipitation. All samples were monophasic β -FeOOH (XRD and Mossbauer spectroscopy data). Three systems (F1, F2 and F3) were obtained at different $\text{FeCl}_3 \cdot 6\text{H}_2\text{O}$ molar concentration in the initial solution (0.1M, 0.37M and 0.55 M, respectively). The increasing of iron-containing precursors causes the decrease of material crystallinity: the average sizes of coherent scattering domains (CSD) for F1 sample are about 15-20 nm, F2– 5-6 nm (calculated from XRD reflexes broadening, Fig.1). At the same time F3 sample is close to amorphous. Morphological differences between synthesized samples were observed by adsorption porosimetry method. The specific surface areas for F1, F2 and F3 systems were 138, 143 and 190 m^2/g . Mesopores size distribution for F1 sample in is very uniform in the 2-25 nm range and micropores are present. Mesopores sizes for F2 sample are localized in 6-16 nm. F3 sample is characterized the narrow mesopores distribution in a range 2-10 nm with the micropores presence (up to 10 %). Cyclic voltammetry (CV) was used for investigation of the capacitive behavior of obtained samples. CVA curves CV curve of β -FeOOH electrode in 1 M Li_2SO_4 electrolyte at the scan rate of 1-20mV/s at the potential window of -0.8-0.0 V vs. Ag/AgCl. The surface faradic reactions will proceed as $\beta\text{-FeOOH} + \text{OH}^- \rightarrow \beta\text{-FeOOH} + \text{H}_2\text{O} + e^-$. One quasi-reversible electron transfer process is visible in all CV curves that indicate the capacitance is mainly based on redox mechanism. The average specific capacitances of β -FeOOH (calculated from the CVA data integrating the area under the current-potential curves) are about 26-29 F/g. We can suggest that the ultrafine β -FeOOH can be recognized as a promising candidate for the supercapacitor applications.

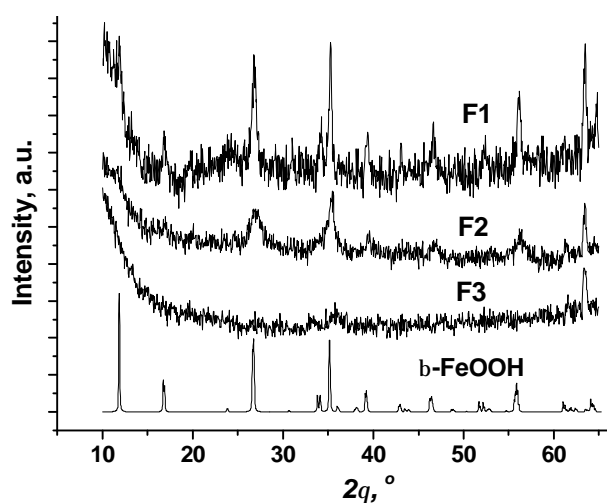


Fig.1. XRD patterns of β -FeOOH obtained at different $\text{FeCl}_3 \cdot 6\text{H}_2\text{O}$ molar concentration

Using Perovskite-Like Materials in Lithium Power Sources

Mokhnatskyi M.L., Yaremiy I.P.

*Vasyl Stefanyk Prekarpathian University, Ivano-Frankivsk, Ukraine,
mark351000@gmail.com*

Perovskite oxides have been widely recognized as promising interconnect materials for solid oxide fuel cells. High conductivity, resistance to external factors and cheap ways of obtaining make these materials very promising in other areas such as lithium power sources.

The samples were synthesized by sol-gel method with auto burning. The initial materials for the synthesis were nitrates' crystal hydrates of the appropriate metals. The structure of obtained material was checked by x-rays diffractometer fig.1.

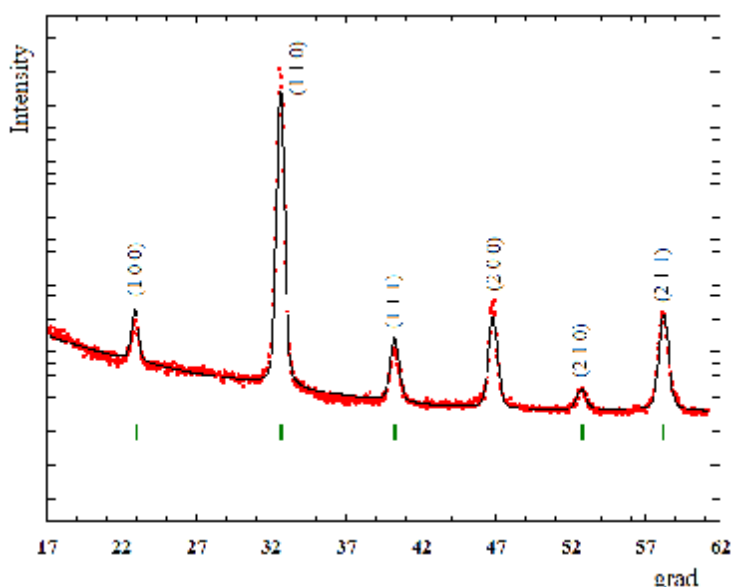


Fig. 1 Radiograph of the perovskites structure.

The average size of coherent scattering regions of monophase powders was found to be in the range of 15 to 30 nm. Theoretical calculation of particle size in approaching the sphere particles gave a size for LaCrO_3 -46 nm, LaFeO_3 -94 nm. It means that particle consists of 2-4 coherent scattering regions.

Gained materials had checking for operational capability as cathode material for the lithium source current. For the best results obtained powders was mixed with carbon and linked material in proportion 17:2:1. Of the mixture were made cathodes on a thin aluminum foil. Model of lithium source current with such cathode has a specific capacity 380 A·h/kg.

Functional Elements Formation Based on the Ordered Arrays of Magnetic Nanoparticles

Kostyuk D. M., Cheshko I. V., Protsenko S. I.

Sumy State University, Sumy, Ukraine, cheshko.iryana@gmail.com

The work presents study results of the structure, phase composition, magnetoresistive and optical properties of ordered arrays of Fe_3O_4 , CoFe_2O_4 and NiFe_2O_4 nanoparticles by spin-coating and Langmuir - Blodgett methods on $\text{SiO}_2(500 \text{ nm}) / \text{Si}(001)$ substrates or in conducting thin film Ag matrix (see more details [1]). The nanoparticles were prepared by chemical synthesis by authors [2] in the solutions form with 15 – 200 mcG / mL concentration solids.

It was found that start of nanoparticles ordered arrays continuous layer defragmentation with networks and cluster nanostructures forming observed at concentrations of nanoparticles in solution at $25 \div 100 \text{ mcG/mL}$ and value of spin-coating rotation speed at $10 \div 75 \text{ rp/m}$, respectively.

It is shown that after the heat treatment of nanoparticle arrays in vacuum at temperatures $T_v = 1100 \text{ K}$ are formed particles with an iron oxide core and $\gamma\text{-Fe}_2\text{O}_3$ shell. Changes in the samples optical properties and parameters wetting after annealing up to $T_v = 600 \text{ K}$ indicate the effective surfactants removal on nanostructures surfaces. In the case of samples with conducting thin film Ag matrix determined that annealing at $T_v = 600 \text{ K}$ leads to increase of magnetoresistance value in 2- 3 through increase of nanoparticle / conducting matrix separation boundaries area. The maximum value of magnetoresistance 12 % observed at thicknesses Ag 5 – 15 nm, with increasing Ag thickness to 20 nm magnetoresistance is reduced to 2 % value.

Calculations based on a modified phenomenological model of granulated film alloy electrical properties confirm the magnetoresistive properties of nanoparticles / conducting thin film matrix type structures dependence on matrix thickness and treating conditions that is consistent with experimental dates.

The analysis and generalization of the obtained results suggested the spintronics memory element functional structures formation with thermally stable and predicted characteristics in spin-valve type nanostructure based on Co and Cu or Fe and Au and magnet nanoparticles by layers sequential deposition by thermal vacuum condensation with additional functional layers in $[\text{Co/Cu}]_n$ or $[\text{Fe/Au}]_n$ multi-layers (with the repetitions number $n = 4 - 14$) and ordered arrays of Fe_3O_4 , CoFe_2O_4 and NiFe_2O_4 nanoparticles in conducting thin film Ag matrix.

Work was done as part of State Project №0116U002623.

1. Kostyuk D. M., Cheshko I. V., Protsenko S. I. et al. Magnetoresistive properties of solid iron oxide nanoparticles in the conducting matrix // *J. nano-electron. phys.* – 2015. – Vol. 7, № 4. – P. 04039-1 – 04039-7.
2. Ivanko J., Luby S., Jergel M. Nitric dioxide and acetone sensors based on Iron Oxide nanoparticles // *Sensor Lett.* – 2013. – Vol.11, №12. – P.2322 – 2326.

Influence of Ultrasound on Formation of Uniform Quantum Dots

Peleshchak R.M.¹, Kuzyk O.V.¹, Dan'kiv O.O.¹,
Velchenko A.A.² and Bryzhko V.S.¹

¹*Drohobych Ivan Franko State Pedagogical University, Drohobych, Ukraine*

peleshchak@rambler.ru

²*Belarusian State Agrarian Technical University, Minsk, Belarus*

In recent years, a new approach to controlling the properties of semiconductor quantum dot (QD) heterostructures has been developed. Progress in the development of nanotechnology and the physics of nanostructures has led to the practical implementation of various types of optoelectronic devices based on InAs QD arrays on wide gap GaAs substrates. Therefore, the main problem in growing QDs is to control their morphology: the average size, density, uniformity, etc [1]. All of these QD characteristics can be controlled by varying the technological parameters of the growth process.

The non-linear diffusion-deformation theory of self-organization of nanoclusters of dot defects in semiconductor exposed to ultrasound treatment that considers the interaction of defects among themselves and with atoms of a matrix via the elastic field created by dot defects and an acoustic wave is developed. Within this theory the influence of ultrasound on the conditions of formation of spherical nanoclusters and their radius is investigated.

The presence of ultrasound leads to a decrease of dispersion of radius of the spherical nanocluster. And increase in amplitude of an ultrasonic wave leads to decrease of dispersion of the nanocluster size. Besides, the ultrasonic treatment expands intervals of the concentration of defects and temperature ranges within which the formation of self-organized nanoclusters is possible.

Thus, treatment by ultrasound of semiconductor materials in the growth process of the self-organized nanoclusters (for example, under the influence of laser irradiation, in the process of the molecular beam epitaxy, etc.) will promote the formation of the nanoclusters, uniform in the sizes. It can be explained by the emergence of additional deformation flux at the expense of the inhomogeneous deformation created by an ultrasonic wave that leads to the restriction of mobility of atoms of the nanocluster. The obtained results qualitatively agree with the experimental data of work [2]. Namely, it was found that the ultrasonic treatment of semiconductor quantum dots for 5 – 90 *min* in the course of their synthesis allows one to obtain nanoclusters that are more uniform by dimensions.

1. R.M. Peleshchak, O.V. Kuzyk, O.O. Dan'kiv, Journal of nano- and electronic physics, V.8 (2016), P. 02014: 1 – 6.
2. W. Yang, B. Zhang, Ultrasonics Sonochemistry, V.30 (2016), P. 103 – 112.

The Formation and Morphology of n-type Porous Silicon

Oksanich A. P., Pritchich S. E. Kohdas M. G.³

¹ *Kremenchuk Mykhailo Ostohradskiy National University,
Kremenchuk, Ukraine, Oksanich@kdu.edu.ua*

Porous silicon (PS) is a material formed by anodic dissolution of single crystalline silicon in HF containing solutions. Since its discovery more than four decades ago, a large number of investigations have been undertaken, the results of which revealed that PS has extremely rich morphological features and the formation process of PS is a very complex function of numerous factors. Accordingly, many theories have been proposed on the various mechanistic aspects on formation and morphology of PS.

PS was obtained by one-sided polished n-type silicon plates (doped with phosphorus) with a dopant concentration of $1.49-6.33 \times 10^{18} \text{ cm}^{-3}$, 625-700 μm thick and oriented $\langle 100 \rangle$. Platinum (Pt) (99.95%) was used as the electrode, with a diameter of 0.013 inches. Hydrofluoric acid (HF) (49%) and ethanol (95%).

PS was successfully prepared from doped n-type Si substrates under periods of short etching times, from 30 to 300 s and at a low current density of 30 mA cm^{-2} . The morphology of the as-prepared PS changed from a narrow columnar structure with side branching at 30 s to larger, non-branched columns at 500 s. At 530 s, however, electro-polishing set in, signifying that the critical current density (J_{ps}) had dropped below the applied current density. The pore diameter and inter-pore distance remained practically unchanged while the porosity increased as the etching time was prolonged. The PS surface showed an increasing trend with regard to the roughness, upon increasing the etching time from 30 to 180 s. The above results suggest that the electrochemical and chemical dissolutions occurred concurrently, albeit at different rates.

The consistent direct electrochemical dissolution propagated pores into the bulk Si with occasional branching as the etching time was increased. The then exposed Si atoms were subjected to electrochemical oxidation which led to an oxidised surface, ultimately giving rise to a PS with columnar structures with similar pore diameters, shapes and inter-pore distances etc. However, the chemical dissolution caused a smoothening of the pore wall with a subsequent enlarging of the pore bottom as well as of the PS surface. Meanwhile, the conductivity of the PS layer was reduced with increasing etching times due to the limited mobility of charge carriers as the porosity of the PS layer increased.

Porous GaAs-Based Gas Sensor with Rapid Response for Biomedical Applications

Oksanich A.P., Pritchyn S.E., Holod A.G.

*Kremenchuk Mykhailo Ostrohradskyyi National University
Kremenchuk, Ukraine, pritchinse@gmail.com*

The paper considers the possibility of using a semiconductor sensor based on porous GaAs to determine the markers of biochemical processes for the diagnosis of a number of diseases. The possibility of using sensors based on porous GaAs to determine gases such as acetone is shown in [1].

The porous GaAs samples were created on a substrate of GaAs:Te with $\rho=10^{-2}$ Ohm \times cm. The porous layer was obtained by anode etching method in H₂SO₄: H₂O: H₂O₂ at a concentration of 1.0: 1.0:0.5 at a current of 15 mA and at etching time of 20 minutes. The film thickness was measured by a weight method and was 26 μ m. The film structure was determined by SEM at a voltage of 10 kV with an increase of 1500 x.

The ohmic contacts to porous GaAs were created by the AuGe deposition method (100 nm), with the contact resistance of 1.6 k Ω . The sensor tests were carried out in a vacuum flask with a discharge of 10-2 mmHg. at room temperature.

Gases that are markers for diagnosing various diseases, such as: CO, CO₂, NO, C₃H₆O, NH₃, CH₄ [2] at a concentration in the range of 10 to 500 ppm were researched.

As a result of the conducted researches it was established that there is a direct relationship between the change in the gas concentration and the change in the intercontact resistance. The maximum change in resistance for gases CO and C₃H₆O, NH₃ has an extremely weak effect. The reaction time for absorption and desorption at 50% of the value of resistance is 40 seconds For CO and 70 seconds for NH₃.

Conclusions. The possibility of using gas sensors on porous GaAs working at room temperature for analyzing the markers of biochemical processes in the diagnosis of diseases is shown.

Literature:

1. Milovanov Y.S. Influence of gas adsorption on the impedance of porous GaAs / Y.S. Milovanov, I.V. Gavrilenko, S.V. Kondratenko, A.P. Oksanich, S.E. Pritchyn, M.G. Kogdas // *Functional materials*. – 2017. – Vol.24, No.1. – p. 52-55.
2. Lukash S.M. Problems of the diagnosis of certain diseases in exhaled air // *Computer means, networks and systems*. – 2010. – № 9. – c. 62 – 71.

Compositional Dependencies in the Vibrational Properties of GeAsSe Chalcogenide Glasses Studied by Raman Spectroscopy

Revutska L. O.¹, Shportko K. V.², Paiuk O. P.², Stronski A. V.², Baran J.³,
Gubanova A. O.⁴

¹*National Technical University of Ukraine “KPI”, Kyiv, Ukraine,
e-mail: liubov.revutska@gmail.com.*

²*V. Lashkaryov Institute of Semiconductor Physics NAS of Ukraine, Kyiv, Ukraine.*

³*Institute of low temperatures and structure research, PAS, Wroclaw, Poland.*

⁴*Kamianets-Podilsky National University, Kamianets-Podilsky, Ukraine.*

Chalcogenide glasses based on Ge-As-Se system are widely used in versatile technological applications such as infrared optical elements and all-optical switching devices, holography recording media etc.

This work is devoted to investigation of structural properties of $\text{Ge}_x\text{As}_y\text{Se}_{100-x-y}$ glasses, where $x=0, 2.1, 6.4, 8.5, 10.6$ and $y=35.8, 36.6, 37.4$ and 39.2 . Raman spectra were measured in the spectral range from 60 to 600 cm^{-1} at room temperature using a FRA-106 Raman attachment to Bruker IFS 88 (Nd:YAG laser with $\lambda_{\text{ex}}=1.06\text{ }\mu\text{m}$).

Observed bands in the Raman spectra of Ge-As-Se samples can be explained in the terms of vibrational modes As_2Se_3 and GeSe_2 glasses. The Gaussian decomposition of obtained Raman spectra was fitted for a quantitative analysis of their compositional dependencies using home-made software CoRa. The fitted Raman spectra showed that the backbones of the studied samples consist of $\text{AsSe}_{3/2}$ pyramidal units (226 cm^{-1}), As_4Se_3 entities (237 cm^{-1}), corner- and edge-shared GeSe_4 tetrahedral units (198 and 213 cm^{-1} respectively), As-Se (245 cm^{-1}) and Se-Se-bonds (258 cm^{-1}). The bands located in the $100\text{--}200\text{ cm}^{-1}$ region confirm the presence of structural units containing As–As bonds and/or Ge–As vibrations.

Compositional dependences indicate that intensity of the bands corresponding Ge-related bonds and nonstoichiometric molecular fragments with homopolar As-As, is increased with the growth of Ge content. Intensity of Se-Se bonds is decreased with higher Ge content.

Thus, Raman data show that Ge-As-Se glasses contain different nanophases whose concentration is changing along chosen compositional cross-section.

Ця робота була частково підтримана проектом МОН № держреєстрації: 0117U000422

Microstructure Characterization of Undoped and Phosphorus Doped Nanocrystalline Silicon Thin Films

Nakhodkin N.G., Rodionova T.V.

Taras Shevchenko National University of Kyiv, Kyiv, Ukraine E-mail: rodty@univ.kiev.ua

The nanocrystalline silicon thin films have attracted significant attention because of their potential use to produce low-cost and large-area electronic devices such as solar cells or thin-film transistors [1,2].

The microstructure of undoped and phosphorus doped amorphous-crystalline silicon films deposited by low pressure chemical vapor deposition has been investigated by transmission electron microscopy.

It was shown that phosphorus doping significantly influences the structure of amorphous-crystalline silicon films. There are two morphological species of nanocrystallites observed in P-doped films: 1 – elliptical crystallites which contain twin boundaries along the major axis. The major axis of each ellipse is about three times longer than the minor one. Twin boundaries are found to lie along the $\langle 112 \rangle$ direction with the average length of 200 nm. The elliptical crystallites shape is due to the anisotropic growth of crystal in amorphous silicon along different orientation and implies that these formation is controlled by the slowest growing planes, i.e. (111); 2 – fan-like crystallites with average size about 50 nm. This is only one species of crystallites is observed in undoped amorphous-crystalline silicon films – fan-like crystallites. Such difference is determined by various crystallite formation mechanisms in these two cases. In undoped silicon films crystallite formation is controlled by deposition temperature and proceeds in amorphous surrounding. As far as P-doped silicon films is concerned, the analogy with ion-implanted layers allow us to suppose that in situ doping results in disordered amorphous layers.

1. Mao H.-Yu, Lo S.-Yu., Wu D.-S., Wu B.-R., Ou S.-L., Hsieh H.-Yu, Horng R.-H. Hot-wire chemical vapor deposition and characterization of p-type nanocrystalline Si films for thin film photovoltaic applications // *Thin Solid Films.* – 2012. – Vol. **520.** - P.5200–5205.

2. Mukhopadhyay S., Chowdhury A. Nanocrystalline silicon: A material for thin film solar cells with better stability // *Thin Solid Films.* – 2008. – Vol. **516,** - P. 6824-6828.

Nanostructured Carbon Films Obtained from Accelerated C_{60} Ion Flows

Rudchenko S.O., Pukha V.E.

*National Technical University «Kharkiv Polytechnic Institute», Kharkov, Ukraine.
svetlana.rudchenko14@gmail.com*

Superhard carbon films and coatings which called as diamond-like carbon (DLC) are forms of amorphous carbon. DLC films containing up to 88% sp^3 bonds are called tetrahedral carbon (ta-C) and have nanocluster structure with unique combination of physical, chemical and mechanical properties similar to properties of diamonds, which identified a wide opportunities for practical application of DLC films as multifunctional coatings.

The synthesis of such carbon materials from accelerated C_{60} ions with energies of 100-1000 eV leads to polymer structures forming, condensates with complex 3D molecular structures and fragments of graphene planes. The results of theoretical modeling of interaction between C_{60} ions with energies more than 1 keV and surface indicate the possibility of forming new types of carbon films.

In this work the DLC films were obtained by deposition of mass-separated ion beam with average energy of C_{60} ions $E = 5$ keV at substrate temperatures (T_s) from 100°C to 400°C.

Taking into account the structural, mechanical and optical studies it was established that: change T_s from 100 to 400°C leads to the consecutive formation of DLC films with amorphous state and superhard nanocomposites consist of nanographite crystals (1-2 nm) surrounded by diamond-like amorphous matrix; hardness of films is ~ 50 GPa and don't change at transition from an amorphous state to nanocomposites; for amorphous films the band gap (E_g) is 1.2 - 1.4 eV. On optical absorption spectra for nanocomposite films there are two energy components: with $E_g \sim 1$ eV that is associated with 3D nanocrystals of graphite and with wide optical gap ($E_g = 3.45-3.55$ eV) that corresponds to the diamond-like amorphous matrix of nanocomposite.

Such a two-component model for nanocomposites obtained at high substrate temperatures (300-400°C) is confirmed by the results of scanning tunneling microscopy (STM) and tunneling spectroscopy (TS). According to these data, the size of graphite nanocrystals is about 1-2 nm and amorphous layer surrounding graphite nanocrystals has a thickness of about 1.5 nm. The graphite component of composite has $E_g = 1.4$ eV and n-type conductivity and amorphous component has $E_g = 4.2$ eV and p-type conductivity. The electrical conductivity of such semiconductor nanocomposite is higher to 6 orders in comparison with DLC film in the amorphous state and is value more than $\sim 10^3$ S/m. These facts open the perspective of using proposed materials in electronics, opto- and nanoelectronics engineering and other industries.

Considering of Temperature Component Parameters by Metrological Characteristics of Safety Production

Rudyk Yu.I., Dominik A.M.

Lviv State University of Life Safety. Lviv, Ukraine

The need arises to develop methods of use of nanomaterial and quantum-dimensional structures to prevent technogenic emergency situations (fire, electrical, hazardous technology processes, transport, etc.) and adaptation means to perform of tasks to rescue people and elimination emergency and their consequences [1].

Nanotechnologies become a revolutionary foundation of society development. Unfold opportunities synthesis unknown in nature systems not only in composition but also in structure and, above all, the properties, and hence, by functional abilities.

Characteristics of existing measuring instruments not fully meet these requirements. So important is the search for new methods and tools for measuring the parameters of tiny objects. Development of theoretical principles, models and techniques make it possible in the future to solve the important problem of proper metrological characteristics of contact less, for example, temperature measurements of small size objects. Often different authors put different meaning in the same definition.

Not defined by various authors used the terms "pinpoint objects", "small size", for which suitable metrological characteristics and suitability to his measurements in the nanometer size range measurement object. Also in this case there is need to clarify the methodological component device error as the main development on it consider its reduction only with respect to the calibration function for converting the secondary circuit of the optical scheme [2].

Thus, expands the measurement range, new methods and tools for measuring dimensions, temperature and other parameters of hazardous objects, providing their essential metrological characteristics, since accurate maintenance of temperature in most dangerous processes is a key parameter which determines the safety of the final product or process.

LITERATURE

1. Rudyk Yu., Lavrivska O. Methods of nanotechnology application to the prevention and elimination of emergency situations / Physics and Technology of Thin Films and Nanosystems. Materials of XVI International Conference / Ed by Honored engineer and techniques of Ukraine, Dr. Chem.Sci., Prof. Freik D.M. – Ivano-Frankivsk: A publish-designing department of 'Vasyl Stefanyk' Precarpathian National University, 2013. – P. 188.

2. Kryvenchuk Y. Research Raman frequency shift of carbon nanotubes with temperature change / O. Sehed, Y. Kryvenchuk, N. Zamishchak // Metrology and devices. – 2013. – # II(40). – P.215-219.

Properties of the Phonon Spectrum of Anisotropic Wurtzite Nanostructures

Seti Ju.O., Tkach M.V., Voitsekhivska O.M.

*Yuriy Fedkovych Chernivtsi National University,
Chernivtsi, Ukraine, email: j.seti@chnu.edu.ua*

The modern quantum cascade lasers and quantum cascade detectors [1] produced at the base of isotropic nanocrystals (InAs, GaAs, AlAs and their ternary compounds) are operating in the middle and far infra red range with the near infrared range is not reached. In order to approach the near infra red range, there was realized the idea to create the quantum cascade lasers and detectors [2] at the base of nitride semiconductors (GaN, AlN, InN and their ternary compounds), which have the wurtzite structure and, thus, the anisotropic properties.

The optical phonons play an important role of the canal of electron energy relaxation due to radiationless quantum transitions in the functioning of the abovementioned devices with anisotropic nanolayers of wurtzite type, the same as with isotropic ones. Therefore, it is important to study the properties of phonons and their interaction with other quasi-particles in such nanostructures.

In the proposed paper, the consistent theory of the complete phonon spectra in anisotropic wurtzite-like nanostructure (AlN/GaN/AlN/Al_xGa_{1-x}N/AlN), being the basic active element of the separate cascade of quantum cascade detector operating in near infra red range [3] is developed. It allows to establish and explain the new specific properties of the spectra of all phonon modes (interface, confined, half-space and propagating) of nanostructure. In particular, it is shown for the first time, that the complicated phonon spectra of three-layer nanostructure (AlN/GaN/AlN/Al_xGa_{1-x}N/AlN) with two layers of binary compounds and one layer with ternary compound are the specific superposition of the separate spectra of this subsystems (AlN/GaN/AlN, AlN/Al_xGa_{1-x}N/AlN).

It is shown that the type of phonon's mode in nanostructure does not depend on the geometrical parameters of the layers but is determined only by the relationship between the components of the tensor ($\epsilon_{\perp}/\epsilon_{\parallel}$) of anisotropic dielectric constants in all layers. The dependences of the energies of different phonon modes on quasi-momentum are caused both by the sizes of nanolayers and by the relationships between the energies of optical vibrations in the respective bulk crystals.

1. B. Schwarz et al., *Appl. Phys. Lett.* **107**, 071104 (2015).
2. S. Sakr et al., *Appl. Phys. Lett.* **101**, 251101 (2012).
3. M. Beeler, E. Trichas, E. Monroy, *Semicond. Sci. Technol.* **28**, 074022 (2013).

Influence of Pulsed Magnetic Field on the Charge State of the Surface Layers of Zirconia Nanoparticles

Shylo A.V.¹, Doroshkevich A.S.^{1,2}, Kirillov A.K.³, Konstantinova T.E.¹,
Danilenko I.A.¹, Troitskiy G.A.³

¹*Donetsk Institute for Physics and Engineering of the NAS of Ukraine, Kyiv, Ukraine,*
artyom_shilo@mail.ru

²*Joint Institute for Nuclear Research, Dubna, Russia;* doroh@jinr.ru

³*Donetsk Institute for Physics of Mining Processes of the NAS of Ukraine, Dnipro, Ukraine,*
kirillov1953@inbox.ru

Investigation of self-organization processes of nanopowder oxide dispersed systems (NODS) and search of ways to use them in a synthesis of nanostructures with predetermined properties is a topical task today. One way to solve this problem is to use low-energy fields. Thermodynamically nonequilibrium structural elements of nanopowder dispersed systems are sensitive to influence of such fields [1]. One of them is weak pulsed magnetic field (PMF). To date, system analysis of magnetically induced phenomena in media with poorly expressed magnetic properties was carried out, a model of a possible mechanism of their realization was proposed [2]. As applied to NODS, acceleration effects of dehydration and disaggregation processes caused by action of PMF were established [3]. Investigation of influence of PMF on the structural-energy state of zirconia nanopowder was the aim of this study.

Electrochemical impedance spectroscopy (EIS), nuclear magnetic resonance and thermogravimetry were used as research methods. The excitation factor was a low-frequency PMF ($H=10^5-10^6$ A/m). An essential change in charge state of near-surface layer of nanoparticles and in binding energy of adsorbates with nanoparticles surface after treatment with PMF was established. It was shown that after processing of a powder by a PMF with a pulse repetition rate of 1 Hz, the total conductivity of the nanoparticle material and the activation energy of desorption from the surface of water molecules are almost reduced by half. It was concluded about the presence in the material of nanoparticles near the surface of a space charge region involved in the formation of a chemical bond with adsorbed molecules.

The feature established in this paper can be used to control physical and chemical properties of nanopowder systems during technological operations.

1. Serov I.N. Resonance phenomena in nanoscale structures // Engineering Physics. - 2004. - No. 1. - P.18 -32.
2. Golovin Yu. I. Magnetoplasticity of solid states. // Moscow: Mechanical engineering. - 2003. - 107 p.
3. Danilenko I.A. Influence of microwave radiation and pulsed magnetic field on crystallization of zirconia // Physics and technics of high pressures - 2004. - Vol. 14, No. 3. - P. 49 -57.

The Phenomenon of Resonant Tunneling in SiO_x(Si) Structures

Steblova O.V.¹, Evtukh A.A.^{1,2}, Kizjak A. Yu.², Bartsikhovskiy V.V.¹

¹Institute of High Technologies of Taras Shevchenko National University of Kyiv, Kyiv, Ukraine; e-mail: steblovia@gmail.com

²V. Lashkaryov Institute of Semiconductor Physics NAS of Ukraine, Kyiv, Ukraine, anatoliy.evtukh@gmail.com

The resonant tunneling diodes play important role in development of nanoelectronics devices. One of their unique feature is the presence of region with negative differential conductivity in current-voltage characteristic that widely used to create the superfast oscillators and logic devices.

The results on realization of resonant tunneling in SiO_x(Si) film are presented here. Resonant tunneling structures based on SiO_x(Si) films were formed by ion plasma sputtering (IPS) of Si target in O₂+Ar ambient on single crystalline Si substrate (*n* – type, $\rho = 4.5 \Omega \times \text{cm}$ (100)). The properties of SiO_x(Si) films were changed by low-temperature annealing (450 °C) in vacuum and H₂. The resonance peaks have been revealed in current-voltage characteristics in measurement temperature range (100 < T < 222 K) in case of unannealed film and films annealed in vacuum after annealing in hydrogen (Fig. 1a). The intensity of peaks increased with the decrease of temperature. On the contrary, after annealing in hydrogen the resonant peak disappeared. The barrier height $q\phi_b = 0.31 \text{ eV}$ was calculated from the slope of the I-V curves in Fowler-Nordheim coordinates.

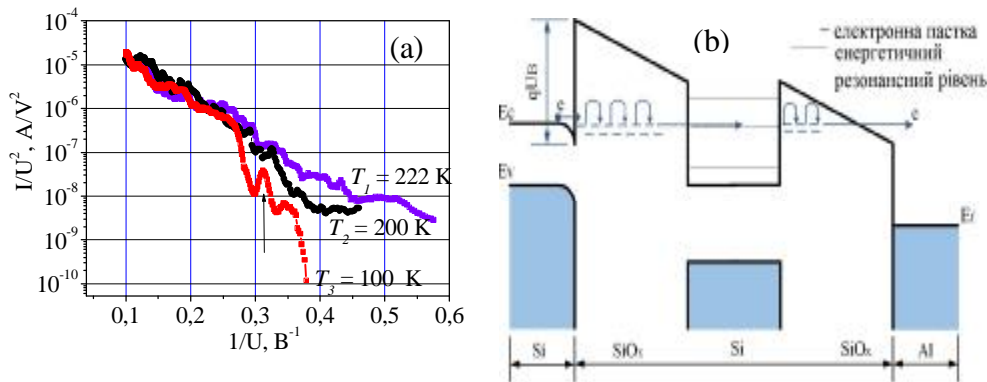


Fig.1 (a) I-V characteristics of unannealed SiO_x(Si) films in Fowler-Nordheim coordinates 100 < T < 222 K, (b) Schematic energy diagram of resonant tunneling SiO_x(Si)structure.

The model based on resonant tunneling through film with Si nanoclusters has been proposed for explanation of experimental results (Fig. 1b). In this case the SiO_x sublayers are the barriers and Si nanoclusters are the quantum well. The theoretical calculation of current flow through such structure confirmed the experimental results.

CdTe Nanoparticles and Their Bioconjugate with Human Serum Albumin for Fluorescence Imaging

Stolyarchuk I.D.¹, Wojnarowska-Nowak R.², Polit J.², Nowak S.³,
Romerowicz-Misielak M.³, Sheregii E.M.²

¹*Ivan Franko Drohobych Pedagogical University, Drohobych, Ukraine, istolyarchuk@ukr.net*

²*Centre for Microelectronics and Nanotechnology, University of Rzeszow, Rzeszow, Poland*

³*Institute of Applied Biotechnology and Basic Sciences, University of Rzeszow, Poland*

Nanotechnology plays a central role in the recent technological advances in the areas of disease diagnosis, drug design and drug delivery. The nanotechnological applications to disease treatment, diagnosis, and to the control of biological systems have been referred to as “nanomedicine” [1]. Research on semiconductor nanocrystals (NCs), also known as quantum dots (QDs), and their application in nanomedicine, has intensified rapidly in the past few decades.

From a point of view of biomedical applications the II-VI based QDs have particular interest due to broad absorption spectra, narrow photoluminescence spectra, size-tunable spectra and high sensitivity. These nanoparticles are brightly fluorescent, enabling their use as imaging probes both in vitro and in vivo study [2]. Moreover, a semiconductor QDs are able to fluorescence resonance energy transfer process (FRET) and this effect can be commonly used as a biological molecular probes. In the present work, the results of research dedicated to the CdTe quantum dots interaction with human serum albumin and human cell culture are reported.

Three different CdTe QDs with average radiuses of 2.8 nm, 2.9 nm and 3.1 nm were obtained and their interactions with HSA were investigated. The intrinsic fluorescence of HSA was quenched through static quenching mechanism. Obtained data enable us to find optimal QDs concentration in CdTe QDs-HSA constructs useful for labeling this molecule. However, in case of CdTe QDs-HSA biocomplex using for carcinoma cells bioimaging, the concentration of QDs should be higher. The low toxicity as well as high stability of the CdTe QDs and CdTe QDs-HSA bioconjugates in the case of their using as bio-imaging probes for the 143b osteosarcoma cells has been demonstrated.

[1] [Nanotechnology in biomedical applications: a review](#) / V.S. Saji, H.C. Choe, and K.W.K. Yeung // *Int.J. Nano and Biomaterials* 2010, V.3, No. 2, p. 119-139.

[2] [Recent progress in the bioconjugation of quantum dots](#) / J.B. Blanco-Canosa, M. Wu, K. Susumu, E.Petryayeva, T.L. Jennings, P.E. Dawson, W.R. Algar, and I.L. Medintz // *Coord. Chem. Rev.* 2014, V. 263– 264, p.101-137.

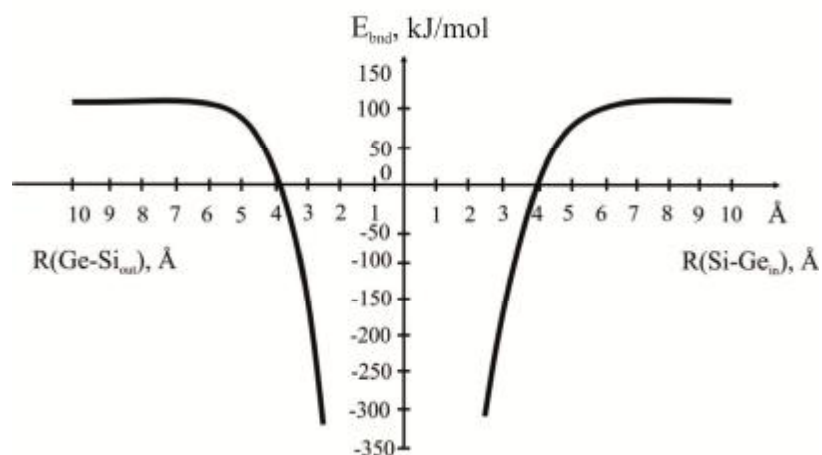
Substitution of Substrate Silicon Atoms During the Formation of the Adsorption Ge Film on the Si(001) Surface: Energetic Aspects

Terebinska M.I., Tkachuk O.I., Krivoruchko Ya.S., Lobanov V.V.

*Chuiko Institute of Surface Chemistry of National Academy of Sciences of Ukraine
Kyiv, Ukraine E-mail: terebinska_m.i@bigmir.net*

In the course of the epitaxial formation of germanium quantum dots on the Si(001) surface, Ge₂ dimers are formed due to the surface diffusion. However, that process is accompanied by the penetration of germanium atoms into surface and subsurface layers of the substrate simultaneously with the migration of silicon atoms from the bulk crystal to the surface, followed by the formation of both pure and mixed dimers (>Si–Si< and >Si–Ge<, respectively).

We present the results of Kohn-Sham DFT calculations (B3LYP functional, 6–31G** basis set) of the interaction energy of the germanium atom with the (Si₆₃H₅₂), cluster which simulates a typical fragment of the Si(001) surface. As one can see from Figure below, large separations between the incident Ge atom and the surface Si atom of the substrate correspond to the positive binding energy within the Si₆₃H₅₂Ge system which vanishes as R(Ge···Si_{in}) drops to ca. 4 Å. Further decrease of R(Ge···Si_{in}) leads to a significant binding in the system under consideration. Similar situation is observed upon the abstraction of the Si atom from the Si₆₃H₅₂Ge adsorption complex.



Activation energy for the replacement of the Si atom by Ge atom has been calculated using simpler cluster Si₆₃H₅₂Ge₂ (too large initial cluster Si₆₃H₅₂Ge caused computational difficulties). Direct localization of the activated complex between the initial and final states (Ge atom in the pure surface dimer >Ge–Ge< vs. that inside the bulk substrate, respectively) has yielded 5.6 eV for the activation energy. Such a large value should be considered as a preliminary upper estimate of the activation energy, since a number of structure-related effects has been neglected.

Energy Spectrum of Electron-Phonon Complex States in Two-Level System of Localized Quasi-Particles at Low Temperatures

Tkach M.V., Pytiuk O.Yu., Voitsekhivska O.M., Seti Ju.O.

*Yuriy Fedkovych Chernivtsi National University,
Chernivtsi, Ukraine, email: j.seti@chnu.edu.ua*

The rapid development of the physics of low-dimensional systems (quantum dots, wires and layers) caused the active investigation of complex states arising due to the interaction between quasi-particles and quantized fields (photons, phonons). Without the consistent theory it is impossible to establish the optimal geometrical design of active regions and extractors (injectors) of quantum cascade detectors (lasers) for the sake of their effective operating, since the electron-phonon complex states play an important role in their functioning.

In the proposed paper the energy spectrum of the system is studied in the model of two-level localized quasi-particles, interacting with polarization phonons. The Hamiltonian of the system has the form

$$\hat{H} = \sum_{m=1}^2 E_m \hat{a}_m^+ \hat{a}_m + \sum_q \Omega \left(\hat{b}_q^+ \hat{b}_q + \frac{1}{2} \right) + \sum_{m_1, m_2=1}^2 \sum_q j_{m_1 m_2} \hat{a}_{m_1 q}^+ \hat{a}_{m_2 q} \left(\hat{b}_q + \hat{b}_{-q}^+ \right)$$

where the quasi-particle energy (E_μ), the phonon energy (Ω) and binding function ($j_{m_1 m_2}$) are assumed as known.

The renormalized spectrum is obtained using the method of Feynman-Pines [1] diagram technique for the Fourier-image of quasi-particle Green's function related with the mass operator by the Dyson equation.

$$G_{m\bar{m}}(\omega) = \left\{ \omega - E_m - M_{m\bar{m}}(\omega) - |M_{m\bar{m}}(\omega)|^2 [\omega - E_{\bar{m}} - M_{\bar{m}\bar{m}}(\omega)]^{-1} \right\}^{-1} \quad (m, \bar{m}=1,2)$$

Here the indexes m and \bar{m} are bound, when $m=1$, then $\bar{m}=2$ and vice versa. The calculation and analysis of the energy spectrum of the system of localized quasi-particles weakly interacting with polarization phonons show that:

1. At low temperatures (formally $T=0K$) both energy levels shift into the low-energy region proportionally, to the square of binding function ($|j_{m\bar{m}}|^2$) due to the interaction with phonons.

2. When the energy distance between the both levels is far from the resonance with phonon energy, one can see two series of bound states with the energies $\tilde{E}_{m(n)} \cong E_m - |j_{m\bar{m}}|^2 \Omega^{-1(1+n)}$ where $n=0,1,2,\dots,\infty$; $\mu=1,2$ in the high-energy region.

3. When the energy distance between the both levels is close to the resonance ($E_2 - E_1 \approx \Omega$), one can see the new complex states and the equidistant energy spectrum is strongly broken due to the anti-crossing effect.

1. A.S. Davydov, Theory of Solids, Nauka, Moscow (1976).

Influence of the Insulating SiO₂ Film on the Structure and Properties of Adsorption Germanium Complexes on the Si(001) Surface

Tkachuk O.I., Terebinska M.I., Krivoruchko Ya.S., Lobanov V.V.

*Chuiko Institute of Surface Chemistry of National Academy of Sciences of Ukraine
Kyiv, Ukraine E-mail: tkachuk_olya@bigmir.net*

Epitaxial germanium films on a pure Si(001) surface are widely used as building blocks for modern microelectronic devices. However, further miniaturization of the latter has stimulated the development of integrated structures that include an insulating layer (often made of amorphous SiO₂) between germanium islands and conducting silicon support. Since experimental studies of such structures are rather laborious and expensive, their quantum-chemical modelling seems to be extremely helpful.

To model germanium adsorption complexes on the Si(001) surface covered by a SiO₂ film, we employed a cluster composed of two parts simulating Si(001) surface and SiO₂ film, with brutto formulas Si₁₁₃H₈₀ and Si₁₈O₃₀H₁₆, respectively. Spatial structure and electronic properties of that cluster have been extracted from our Kohn-Sham DFT calculations using B3LYP functional and 6-31G** basis set. We have considered three structures that differ from each other by a number of Ge atoms and a way of their interaction. Our calculations have shown the binding energy of the first Ge atom with the SiO₂ film to be 6.2 eV, while that for the second Ge atom reduces to 3.9 eV (per adsorbed atom). As far as a dimer Ge₂ is formed on the surface of the insulating film, its binding energy reaches 10.6 eV that stabilizes the entire system.

Silicon atoms of the SiO₂ film bear rather large positive charge (1.06 a. u.) which is significantly higher than that of Si atoms located on the Si(001) surface (0.05 a. u.) As a consequence, a considerable electron density transfer from the adsorbed Ge atom to the SiO₂ film followed by the formation of long-living localized positive charges on germanium atoms takes place. Further dimerization of Ge atoms results in an insignificant reduction of the total charge of Ge₂ complex.

To summarize, the structures like those considered in this work seem to be promising as building blocks in microelectronics due to their ability to act as positive charge traps.

Effect of the Medium of Poly (Titanium Oxide) Formation on the Properties of Organic-Inorganic Interpenetrating Polymer Networks

Tsebrienko T.V., Alekseeva T.T., Babkina N.V.

Institute of Macromolecular Chemistry of the NAS of Ukraine, Kyiv, Ukraine

The hybrid organic-inorganic materials are great interest due to the possibility of obtaining of the polymer compositions with the improved physico-chemical properties compared to the initial materials. Using TiO_2 as an inorganic component is perspective due to the wide range of its application for the realization of photochemical reactions. The uniform distribution of the inorganic component in the organic matrix may be achieved by sol-gel process.

The organic-inorganic interpenetrating polymer networks (OI IPNs) based on cross-linked polyurethane (PU), poly(hydroxyethyl methacrylate) (PHEMA) and poly(titanium oxide) ($(-\text{TiO}_2-)_n$) were obtained. The samples were obtained at the same ratio of components PU/PHEMA/ $(-\text{TiO}_2-)_n$ (49,8/49,8/0,4, wt%), but formation of $(-\text{TiO}_2-)_n$ was carried out via reactions of hydrolysis-condensation of titanium isopropoxide in the different medium – poly(propylene glycol) (PPG) and 2-hydroxyethyl methacrylate (HEMA). The initial IPNs were obtained based on PU and PHEMA without the gel of $(-\text{TiO}_2-)_n$.

The features of the kinetics of OI IPNs formation relatively to IPNs were studied by the differential calorimetry method. It was established, that the rate of HEMA polymerization as a component of OI IPNs in the presence of $(-\text{TiO}_2-)_n$, synthesized in HEMA medium reduced by 12 and 9 times relatively to the initial IPNs and OI IPNs, containing $(-\text{TiO}_2-)_n$ synthesized in PPG medium. The reduction of the rate of HEMA polymerization occurs due to the grafting of $(-\text{TiO}_2-)_n$ to HEMA and it leads to decrease of the initiation efficiency.

The viscoelastic properties of OI IPNs were investigated by dynamic mechanical analysis. The data indicate that OI IPNs with $(-\text{TiO}_2-)_n$, obtained in PPG medium demonstrate higher phase separation and lower cross-linking density of polymer networks relatively to IPNs and OI IPNs with $(-\text{TiO}_2-)_n$, synthesized in HEMA medium.

The results of thermogravimetric analysis were shown, that the resistance to thermo-oxidative destruction is higher for OI IPNs with $(-\text{TiO}_2-)_n$, obtained in HEMA medium due to the high cross-linking density of polymer networks that promotes more effective antioxidant protection of the polymer matrix.

Optical Properties of Chemically Syntheses of ZnS, ZnSe Semiconductor Nanoparticles

Vaksman Yu.F., Nitsuk Yu.A.

I.I. Mechnikov National University, Odesa, Ukraine

ZnSe semiconductor nanoparticles and their analogs are a promising material for developing a modern perspective photomultiplier devices (LED, solar cells) and fluorescence imaging. To create high quality color images, you must obtain nanoparticles ranging in size from 2 to 8 nm, most narrow dispersion. Emission of such nanoparticles must lie in the spectral range of 400-700 nm. For fluorescence imaging is optimal radiation is in the near-infrared range.

The paper presents a series of techniques to obtain semiconductor nanoparticles ZnSe, ZnS, containing hydrothermal technology and methods of the controlled deposition. Zinc chloride, sodium selenite (selenosulfate) or sodium sulfide were used as reactant materials. Polyvinyl alcohol was used as a stabilizing growth agent for nanoparticles.

The influence of technological conditions on the size and dispersion of nanoparticles, optical and luminescent properties.

It is established that in all the samples studied the absorption edge is shifted to the region of high energies in comparison with the absorption edge of single crystals, which indicates the presence of quantum size effects in the samples. In this case, the displacement of the absorption edge increased with a decrease in the concentration of sodium selenite (selenosulfate) or sodium sulfide.

From the absorption spectra, the nanoparticles sizes in the samples were estimated. The mean radius of the nanoparticles R was estimated from the absorption spectra along the edge of the absorption band from the change in the band gap (ΔE_g) relative to the bulk crystal, using the effective-mass approximation in accordance with

$$R = \frac{h}{\sqrt{8\mu\Delta E_g}}$$

It is shown magnitude of the shear size determined nanoparticles that were 6-10 nm.

In the photoluminescence spectra of zinc selenide nanocrystals, broad luminescence bands are observed at the range 500-850 nm at 300 K. In zinc sulphide nanocrystals wide bands of photoluminescence were at the range 400-600 nm. The change in the size and temperature of the crystallites does not lead to a shift in the position of these bands, which may indicate the presence of radiative transitions within the donor-acceptor pairs.

Similar emission lines were observed earlier in bulk ZnSe and ZnS crystals.

A comparison of the elementary emission bands with the bulk crystals emission bands establishes the nature of the investigated nanocrystals radiative transitions.

The Influence of Irradiation of Bremsstrahlung Gamma Rays and High Energy Electrons on Properties of Zirconium Silicate

Vasylyeva H.¹, Kylivnyk Yu.²

¹ *Uzhgorod National University, Chair of theoretical physics, Department of physic of high energies, Uzhgorod, Ukraine h.v.vasylyeva@hotmail.com*

² *Institute of Sorption and Endoecology problems NAS of Ukraine, Kyiv, Ukraine, ispe@ispe.kiev.ua*

The effect of Bremsstrahlung gamma rays and high energy electron on the surface parameters of microporous amorphous zirconium silicate and on its ability for sorption is studied. The samples were irradiated using a Betatron (electron accelerator) with the maximal energy of the γ -quanta of 10 MeV and 22 MeV, energy flux 10^8 gamma-quanta/cm²s, and Microtron M-10 with the energy of electron 8,6 MeV, and electron flux 10^{11} e/cm²s. The surface characteristics of the sorbents were studied by low-temperature adsorption/desorption of nitrogen. The experimental data were processed by BET, DR, and BJH methods. The results show that under exposure to Bremsstrahlung gamma rays the micropores of the sorbent under investigation are partly transformed in mesopores. Under the high-energy-electrons irradiation we get a similar effect.

The ability of zirconium silicate to absorb Sr²⁺ ions from an aqueous solution of strontium chloride is shown to increase noticeably after irradiation by 22-MeV Bremsstrahlung gamma rays. Since some of the zirconium isotopes (⁴⁰₉₁Zr, ⁴⁰₉₂Zr, and ⁴⁰₉₀Zr) have low gamma ray activation thresholds it is supposed that a certain role in the increased Sr²⁺ ion sorption is played by Zr ion activation which can lead to the formation of vacancies in the sorbent matrix.

We made a suggestion, that the main mechanism of influence on properties of sorbent is formation of radiation defect due to IT decay of Zr nuclear.

A similar effect is also observed for another zirconium-containing inorganic sorbent – hydrated zirconium dioxide and zirconium phosphate – and is considerably reduced at the decrease of the gamma radiation energy down to 10 MeV or under high-energy-electrons exposure.

Effect of Electric Field on Energy Spectrum and Intersubband Absorption Spectra of Electron in Spherical Multilayered Quantum Dots CdSe/ZnS/CdSe

Holovatsky V.A., Yakhnevych M.Ya.

Chernivtsi National University, Chernivtsi, Ukraine

Semiconductor spherical quantum dots, intensively researched from the end of last century, are called the artificial atoms. They are characterized by discrete energy spectra, which are determined by material and sizes of nanocrystals.

Recently, particular interest of the researchers is paid on semiconductor multilayered spherical nanostructures, consisting of the core and several spherical layers, which are widely applied in medicine and electronics. The fluorescent labels with the high quantum yield, sources of simultaneous radiation electromagnetic waves with different demanded frequencies, biosensors and other semiconductor devices for modern nanoelectronics can be created using multilayered quantum dots.

Investigation of the effect of external electrical field on the optical properties of nanostructures is important in terms of their practical applications in the modern electronics. This field violates spherical symmetry and changes the electron location, that are displayed on the optical properties [1].

In this paper, the energy spectrum of electron and complete set of exact wave functions are obtained in the framework of effective mass approximation and rectangular potential barriers model for the nanostructure CdSe/ZnS/CdSe. Using the matrix method the numeric calculations are performed for the electron energy spectrum in multilayered quantum dot as function of electric field intensity. The polarization potentials, appearing due to the different values of dielectric constants in different layers of nanostructure and external medium are taken into account.

It is shown that the effect of electric field on the electron, which is located in the core in the ground state causes its tunneling into the outer potential well. Thus, the overlap of wave functions is essentially varied, that influences on the dipole moments of quantum transitions and light absorption coefficient.

1. Holovatsky V. Effect of magnetic and electric fields on optical properties of semiconductor spherical layer / V. Holovatsky, I. Bernik // *Semiconductor Physics, Quantum Electronics and Optoelectronics*. – 2014. – V. 17, № 1. – P. 7-13.

The Dependence of the Charge Capacity of Lithium Batteries with Cathodes SiO₂/TiO₂ from Changes of Structural and Morphological Characteristics, Electronic Structure Due to Shock-Vibration Treatment Nanocomposites

Yavorskyi Y.V.^a, Zaulychnyy Ya.V.^a, Karpets M.V.^b, Kotsyubynsky V.O.^c,
Kononenko Ya.A.^a, Zaretska N.S.^a

^a Physical Engineering Faculty, National Technical University of Ukraine “Kyiv Polytechnical Institute”, Kyiv, Ukraine, yar-yra@ukr.net.

^b Frantsevich Institute for Problems of Materials Science, Kyiv, Ukraine, mkarpets@ukr.net.

^c Vasyl Stefanyk Precarpatian National University, Ivano-Frankivsk, Ukraine

By the method ultrasoft X-ray spectroscopy investigated the influence of mechanical activation method on energy redistribution of *Sisd-*, *Tisd-* and *Op-* valence electrons in pure SiO₂, TiO₂ and mixtures with a ratio of titanium oxide and silicon dioxide 90/10, 60/40, 40/60 80/20, respectively. The phase composition and characteristics of the crystal structure of samples, namely the region of coherent scattering and lattice parameters was investigated by X-ray diffraction analysis. Considered and analyzed changes in the morphology of nanocomposites with different weight ratio of incoming precursors and after shock-vibration treatment. In analyzing the results, it was concluded that the high local pressure and temperature, which accompany the process of shock-vibration treatment, facilitate the formation of atomic bonds between SiO₂ and TiO₂ nanoparticles. At the same time an increase in the population of *Op_π*-hybrid states (Fig.1, Grey lines correspond to the bands of mechanical mixture. Black lines represent the bands of mechanically). This leads to a decrease in the ability of recombination of ions Li⁺, which prevents the formation of lithium oxide films around the nanoparticles. As a result, the charge capacity stabilized during cycles LPS.

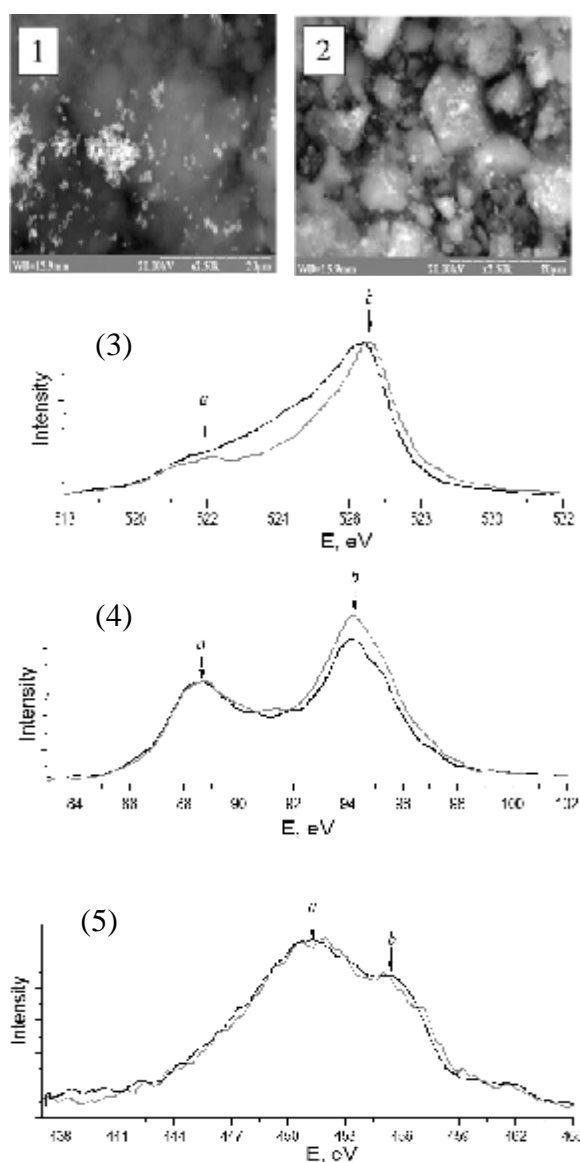


Fig. 1. Change of morphology (1,2), OKα-(3), SiLa-(4), TiLa-(5) emission spectrum due to shock-vibration treatment nanocomposite 20% TiO₂/80% SiO₂.



ORAL REPORTS

Session 3

Physical-chemical properties of thin films



Formation of Thin Beryllium Oxide Films on the Mo(112) Substrate

Afanasieva T.V.¹, Fedorus A.G.², Naumovets A.G.², Rumiantsev D.V.³,
Strizheus D.²

¹*Taras Shevchenko National University of Kyiv, Kiev, Ukraine.*

²*Institute of Physics, Natl. Acad. of Sci. of Ukraine, Kiev, Ukraine.*

³*Physical-Technical Educational Centre of NASU, Kiev, Ukraine.*

Formation of a monolayer BeO film is obtained under adsorption of oxygen on supermonolayer beryllium coverage prepared on the Mo(112) surface before oxygen adsorption. Experimental studying the process of thin film formation is carried out by means of low-energy electron diffraction (LEED), Auger electron spectroscopy (AES) and retarding field contact potential difference (CPD) techniques providing information on the atomic structure and elemental composition of the surface, the work function changes, and the changes in the electronic state of surface Mo, Be, O atoms resulting from the adsorption and surface chemical processes. For the O/Be/Mo(112) surface structures identification, the density functional theory (DFT) calculations were performed in the generalised gradient approximation (GGA), using the ABINIT code.

Oxidation of Be deposit on the Mo(112) surface occurs while adsorption of oxygen at room temperature and as high temperature as up to 1000 K. The oxidation process was registered through the emergence and next growth of the specific “chemical” shift in energy and split of the Be Auger peak. Further, the obtained BeO-Be-Mo(112) sandwiches were annealed at progressively rising temperatures and their properties (work function changes, surface structure and elemental composition) were investigated. Since Be, BeO and adsorbed O species desorb from the Mo(112) surface in the diverse temperature intervals, there is an opportunity to obtain a single BeO/Mo(112) system and establish its properties. Depending on the original thickness of Be deposit and accumulated oxygen amount, different modes of the BeO/Mo(112) coverage formation have been found: a BeO monolayer commensurate with the Mo(112) substrate (analogue of Frank-van der Merwe mode) and BeO 3D islands (Volmer-Weber mode). BeO coverage reduces the electron work function by 1.0-1.2 eV. Conclusion concerning the formation of the commensurate BeO monolayer (nanosheet) structure is based on the observation of rather clear (1×1) LEED patterns for adlayers covering the most of the substrate surface (according to the AES data). Feasibility of the BeO monolayer formation is validated by DFT calculation. Obtained results for the BeO/Mo(112) system may be helpful not only for nuclear reactor application but also for the development of ideas about 2D nanoobjects.

Structural Phase Transformations Mixture of Paraffin and Carbon Nanoparticles

Nasyeka Yu.M., Bardashevskya S.D., Budzulyak I.M., Budzulyak S.I.,
Stubrov Yu.Yu.

Vasyl Stefanyk Precarpathian National University, Ivano-Frankivsk, Ukraine

Heat accumulating material is the basis for thermal batteries, polymer matrix for the synthesis of colloidal nanocrystals and carbon quantum dots. Therefore, the study of vibrational and optical properties are important in terms of focused practical use.

We obtained temperature dependences of vibrational spectra of paraffins and mixtures with heat conductive powder. The temperature dependences of Raman spectrum and structural parameters for pure waxes and mixtures with carbon heat conductive fillers helped to identify the main phase transition temperature, both technically paraffin and reinforced heat conductive particles of different chemical composition submillimeter sizes. It is established and explained the difference in the dynamics of structural phase transitions of pure paraffin and reinforced heat conductive fillers. It is revealed the increase of thermal conductivity, more uniform distribution of thermal field and reduction the temperature of the main phase transitions in reinforced heat accumulating substances, that increase the efficiency of the thermal battery type.

It is shown an effectiveness and efficiency of Raman and IR spectroscopy for diagnostic support technology development of thermal batteries based on phase transition materials, namely to establish the synthesized and modified properties under heat accumulators working with nanoparticles of carbon compounds and mixtures in order to obtain optimal parameters of thermal conductivity, thermal storage etc. These findings are important and relevant to the development of domestic thermal storage technology based on phase transition materials.

1. Acharya A., Panda B., Mohanty M. Roy G. Study of the characteristics of nanocrystal CdS, CdSe, CuO and nanocomposite CdS–PTh, CdSe–PTh by XRD–analysis // *Researcher*. – 2011. – Vol. 3, № 1. – P. 108–112.

Controlled Changes in the Hydrophilic Properties of Polystyrene Films

Beketov G.V., Liptuga A.I., Shynkarenko O.V.

*V. Lashkaryov Institute of Semiconductor Physics, NAS of Ukraine, Kyiv, Ukraine,
gbeketov@isp.kiev.ua*

Human beings, like other biological species, are deemed to confront pathogenic microorganisms. New diseases are emerging and are constantly evolving. Modern healthcare allows early diagnosis of many diseases by analyzing biological fluids. The development of science and medicine knowledges lead to a number of new methods of disease identification in the presence of certain human diseases. At the same time, a growing need for new sensors that can reflect the state of health of the patient as a whole.

We are reporting on simple, inexpensive, and environment-friendly method for hydrophilization of polystyrene surface which has strong potentiality for use in manufacturing of enzyme-linked immunosorbent assay (ELISA) plates as an adsorption-promoting technique.

ELISA is a biochemical assay widely used in immunological diagnostics for detection of peptides, proteins, antibodies, hormones etc. It is an essentially heterogeneous assay, in which separation of some component of the liquid analytical probe is performed by adsorbing them specifically onto a physically immobilized solid phase. The solid support is usually constructed as a multiple-well polystyrene plate known as the "ELISA plate". The critical issue in manufacturing the ELISA plates is achievement of an optimal adsorption capacity and affinity for the specified biomolecules used as a ligand. The world-leading brands (TermoFisher Nunc, Corning etc.) widely use proprietary hydrophilization technologies for this purpose.

Availability of an independently developed hydrophilization technology will promote competitiveness of emerging local manufacturers of ELISA-related products and facilitate access to advanced medical care for all sections of the population.

Results of investigation of the hydrophilized polystyrene surfaces using FTIR-spectroscopy, scanning probe microscopy, contact angle measurements, and adsorption properties for selected classes of biomolecules are presented. Possible mechanisms of hydrophylyzation are discussed on the ground of characteristic reactions of the phenil core and formation of polar functional groups at the polystyrene surface.

O.V. Shynkarenko gratefully acknowledges partial support provided by the Swiss National Science Foundation (SNSF, Bern) under grant No. IZ73Z0_152661 (SCOPES).

Thin Films of Organic-Inorganic Perovskites $\text{CH}_3\text{NH}_3\text{PbI}_3$: Control of Microstructure and Properties

Belous A.G.¹, V'yunov O.I.¹, Kobylanskaya S.D.¹,
Ishchenko O.O.², Kulinich A.V.²

¹*Vernadskii Institute of General and Inorganic Chemistry,
National Academy of Sciences of Ukraine
e-mail: vyunov@ionc.kiev.ua*

²*Institute of Organic Chemistry, National Academy of Sciences of Ukraine*

Organic-inorganic metal halide perovskites APbX_3 ($\text{A}=\text{CH}_3\text{NH}_3$, $\text{X}=\text{Cl}$, Br , I) attract scientific interest as efficient solar energy absorbers [1]. These compounds show excellent photovoltaic parameters together with relatively low production costs [2]. Hybrid lead iodide perovskites can be synthesized from solutions at low temperatures.

Our work shows the effect of starting reagents ($\text{CH}_3\text{NH}_3\text{I}:\text{PbI}_2$) with different ratios in raw solutions on the microstructure, phase composition, absorption, and luminescence spectra of the films of organic-inorganic perovskites $\text{CH}_3\text{NH}_3\text{PbI}_3$.

Starting reagents (PbI_2 and $\text{CH}_3\text{NH}_3\text{I}$) were taken in different ratios, dissolved in DMF, and stirred at 70 °C until optically clear solutions are formed. A relative humidity during synthesis was not above 10%. The resulting solutions were spin-coated on the glass substrates.

It has been found that the temperature range corresponding to the formation of a single-phase product is limited by the incomplete interaction of starting and intermediate phases (below 80 °C) as well as the decomposition of organic-inorganic lead iodide perovskite to form PbI_2 (above 150 °C). In the case of stoichiometric ratio of starting reagents, the films consist of needle-like particles. When the amount of methyl ammonium iodide increases, the rounded-shape particles and then faceted-shape particles are formed. This is accompanied by more selective absorption in the optical range: the intensity of the spectral band in the range 350-400 nm increases.

This research was supported by the Targeted Research Program of the National Academy of Science of Ukraine “Novel Nanomaterials”.

1. Green, Martin A., *et al.* "Solar cell efficiency tables (version 49)." *Progress in Photovoltaics: Research and Applications* 25.1 (2017): 3–13.

2. Zhao, Yixin, and Kai Zhu. "Organic–inorganic hybrid lead halide perovskites for optoelectronic and electronic applications." *Chemical Society Reviews* 45.3 (2016): 655–689.

Liquid-Like Migration of Solid Ni Islands on Amorphous Carbon Substrate

Bogatyrenko S.¹, Kryshtal A.²

¹*V. N. Karazin Kharkiv National University, Kharkiv, Ukraine*

²*AGH University of Science and Technology, Krakow, Poland*

Thin film structures, such as, protective high-temperature coatings, elements of micro-, nano- and optoelectronics, highly effective solar cell elements, information storage devices, multilayer periodic structures for X-ray optics, etc. are widely used in modern technologies. However, nanofilms applications have faced the problem of durability of the devices created on their basis. Ultimately, the stability of such structures is determined by the kinetics of phase transitions, diffusion and relaxation processes. The same problem also arises for isolated nano-sized particles on a substrate. For example, active surface area of the nanocatalyst in low-temperature fuel cells with a carbon ion-exchange membrane is lost during the electrochemical reaction. Several possible mechanisms of cathode degradation are discussed in the literature, e.g.: migration and coalescence of particles, separation of catalyst particles from the substrate due to corrosion of carbon, Oswald ripening, dissolution in the ionomer. However, there are no direct experimental proofs in favor of any mentioned mechanism up to this moment. Therefore, the study of temperature stability of nanoscale transition metals in contact with a carbon substrate is an urgent task.

In this work we present the results of investigation of the morphological structure thermal evolution of an island Ni film formed on or between amorphous carbon films. This choice has been motivated by nickel catalytic activity and the fact that this metal belongs to the platinum group. In addition, nickel has the same type of interaction with carbon as platinum and palladium. All these systems are characterized by phase diagram of a simple eutectic type.

Ni film with thickness of about 5 nm was formed on a carbon sublayer (approximately 25 nm thick) by means of electron-beam evaporation from independent sources at a vacuum of $1 \cdot 10^{-7}$ Torr. Such a thickness of the carbon film provides mechanical strength of the samples in the whole investigated temperature range. The morphological and crystalline structures of the films were studied in a transmission electron microscope TEM-125K during heating. For this purpose, an in-house holder was used. This holder has been designed to heat samples directly in an electron microscope to a temperature of 1100°C. The Ni/C films were almost instantaneously heated to a temperature of 550°C, and the change in the morphology of the nickel film was registered in real time. The accuracy of the samples temperature determination was estimated as 2%.

The effect of a liquid-like migration of crystalline nickel nanoparticles on carbon sublayer has been observed during two hours of isothermal annealing at 550°C. Possible mechanisms of this phenomenon are discussed.

Strain Analysis of Heterostructures and Multilayered System by X-Ray Multiple Diffraction

Borcha M., Fodchuk I., Solodkyi M., Kroitor O., Kshevetsky O., Tkach O.

Chernivtsi National University, Chernivtsi, Ukraine, m_borcha@ukr.net

The study of multilayered heterostructures using X-ray multi-beam diffraction (MBXRD) and modified calculating technique that provides high-precision of lattice parameter [1] and strain determination in each layer taking into account anisotropy are presented in this report.

Kinematic approximation of theory of X-ray scattering [2] in the case of multi-beam X-ray diffraction is used to calculate multi-beam diffraction patterns (Renninger scans) for the crystalline $Zn_{1-x}Mn_xSb$ thin layers and $Al_xIn_{1-x}Sb$ heterostructures. Required conditions (primary reflection and X-ray wavelength) were proposed for each individual layer in heterostructures to implement three-beam coplanar or four-beam noncoplanar coincidental diffraction. This tool reduces the influence of instrumental errors on the accuracy of the lattice parameter determination.

The peculiarity of multi-beam X-ray diffraction pattern is the existence of several systems of related structurally equivalent peaks. Studying the geometry of their angular displacements gives possibility to determine directions and values of changes of lattice parameters more precisely.

The possibility to evaluate the tetragonal distortion [3] of unit cell have been shown for relaxed and non relaxed heterostructures using analysis of displacements of different multi-beam reflexes that have different behaviour under compressive or stretching strains (displacement direction depends on the strain sign).

1. Borcha M. Lattice parameter determination by coincidental multi-beam X-ray diffraction / M. Borcha, I. Fodchuk, I. Krytsun // *Physica status solidi A*. – 2009. – **206**, № 8. – P. 1699-1703.
2. Rossmannith, E., Hupe, A., Kurtz, R., Schmidt, H. & Krane, H.-G. // *J. Appl. Cryst.* – 2001. – **34**. – P.157-165.
3. Ashwin, M. J., Morris, R. J. H., Walker, D., Thomas, P. A., Dowsett, M. G., Jones, T. S. & Veal, T. D. // *J. Phys. D: Appl. Phys.* – 2013. – **46**. – P.26400.

Gibbs Grand Potential in the Theory of Kinetic Properties of Conductive 3D and 2D crystals

Budjak Ya.S., Malyk O.P.

Lviv Polytechnic National University, Lviv, Ukraine

At present paper using the grand Gibbs potential the kinetic tensors of the well known in nonequilibrium thermodynamics generalized equations of conductivity and thermal conductivity were justified. These tensors define the computational algorithms of material tensor of the conducting crystals and coefficients of the various galvanomagnetic and thermomagnetic effects. The influence of spatial quantization in 2D (thin film with microscopic thickness d) crystal on all its fundamental kinetic properties was shown.

In [1,2] it was shown that these algorithms are the pragmatic formulas in computational problems of the kinetic properties of crystals and in the tasks of prognostication of semiconductor crystals with desired properties.

In the cited works it was shown that the entire set of kinetic properties of the 3D crystals are described by the such functional relation.

$$J(i, j, \mathbf{m}^*, T)_{3D} = \int_0^\infty \left(\frac{e}{kT} \right)^i u(e)^j G(e)_{3D} \left(-\frac{\partial f_0}{\partial e} \right) de, \quad (1)$$

And for 2D crystal by relation:

$$J(i, j, \mathbf{m}^*, T)_S = \int_0^\infty \left(\frac{e}{kT} \right)^i u(e)^j G(e)_{3D} \left(-\frac{\partial f_0}{\partial e} \right) de \times \left(1 - \frac{1}{2d} \frac{\int_0^\infty \left(\frac{e}{kT} \right)^i u(e)^j G(e)_{2D} \left(-\frac{\partial f_0}{\partial e} \right) d}{\int_0^\infty \left(\frac{e}{kT} \right)^i u(e)^j G(e)_{3D} \left(-\frac{\partial f_0}{\partial e} \right) d} \right) =$$

$$= J(i, j, \mathbf{m}^* T)_{3D} \left(1 - \frac{1}{2d} \frac{J(i, j, \mathbf{m}^*, T)_{2D}}{J(i, j, \mathbf{m}^*, T)_{3D}} \right) \quad (2)$$

The properties of these functionals are carefully described in the cited studies, and functional (2) shows the analytical dependence of 2D crystal properties on its thickness d resulting from the spatial quantization of the carrier's energy spectrum in the crystal.

[1]. Ya. S. Budjak, L.O. Vasylechko. Fundamentals of the statistical theory of thermal and kinetic properties of semiconductor crystals. Lviv. Liga-Press. 2016. 281 P.

[2]. Ya. S. Budjak, O.P. Malyk. Great canonical Gibbs distribution in the calculation of the kinetic properties of 3D and 2D crystals. Physical and technological problems of transmission and processing of information storage in information and communication systems. Proceedings of 5th International scientific-practical conference. 3-5 November 2016. Chernivtsi. Misto. 2016. P.136.

Ti/Au Ohmic Contacts to Diamond

Dub M.M.

V.E. Lashkaryov Institute of Semiconductor Physics,
Kiev, Ukraine, maksimdub19f94@gmail.com

Diamond is a promising material for high power microwave, optoelectronic devices, sensors of ionizing radiation, ultraviolet detectors [1]. Our goal was to define possible usage of metal-diamond contacts and measure its parameters.

The samples were fabricated using bulk n-type diamond grown on the silicon substrate. After growing the diamond layer with 100 μm thickness the silicon substrate was etched. For measuring the contact resistivity, the transmission line method (TLM) was used with linear geometry of contact pads. The layered structure Ti (60 nm)-Au(100 nm) was deposited through TLM mask by magnetron sputtering on the substrate heated to 350 °C in a single process cycle. Investigated samples were treated by rapid thermal annealing (RTA) in vacuum at 600 °C during 60 s.

The contact resistivity of manufactured sample has a significant temperature dependence (Fig. 1a) in the wide range from 100 up to 380 K (ρ_c changed from 8.6 kOhm·cm² to 14 Ohm·cm²) and the specific surface resistance of the semiconductor diamond varies from 407 GOhm to 0.02 GOhm.

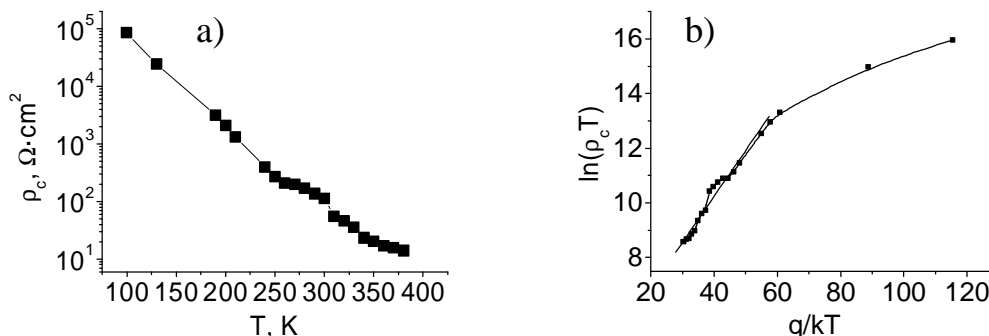


Fig.1. a) Temperature dependencies of contact resistivity $\rho_c(T)$; b) Temperature dependence of the contact resistance in the coordinates thermionic emission

The study of electrical parameters shows that at temperatures over 190 K predominant mechanism of current transport is thermionic emission with barrier height of ~ 0.17 V. The contact resistivity is smaller than total contact resistivity (less than 1%) at temperature higher than 280 K. In this case, I-V curves of contacts are linear and symmetrical. Obtained structures are prospective for future devices based on diamond. Since diamond substrates are used as heat sink for high-power RF devices, such type contact system could effective measure diamond film temperature.

1. V.V. Basanec, N.S. Boltovec, A.V. Gucul, i dr. //ZhTF. – 2013. – V.83., №3. – P. 113–117.

Properties of Nano-Structured Carbon Materials with Optimal Pore Size Distribution and Their Application for Supercapacitor Production

Izotov V.Yu.^{1,2}, Havrikov D.S.^{1,2}, Koltsov I.V.¹, Selikhova A.V.¹,
Belyaev O.E.², Burlaka I.M.², Iarmolenko D.O.²

¹*College of Physics, Jilin University, Changchun, People's Republic of China.*
E-mail: vizotov@bigmir.net

²*V. Lashkaryov Institute of Semiconductor Physics, National Academy of Sciences of Ukraine, Kyiv, Ukraine. E-mail: belyaev@isp.kiev.ua*

One of the main disadvantages of modern supercapacitor (SC) is their low, in comparison with batteries, specific energy capacity. For the best samples of SC it varies from 4 to 6 W*h/kg. Therefore, the search for ways to increase the specific energy capacity of supercapacitors is one of the actual tasks of modern energy. The purpose of this work was to find the optimal ratio between the pore sizes of the activated carbon material from which the electrodes are made and the size of the ions of the organic electrolyte, which allows obtaining the maximum capacity for symmetric SC. The work was carried out by searching for the optimal ratio between the pore size and the electrolyte ions size. In the process of chemical activation occurred carbon combustion within the pores, which increased specific surface area of the carbon material and as a result, lead to increase of the specific energy capacity of electrodes for SC. The example of an electrochemical system of a porous carbon electrode/organic electrolyte shows that the maximum capacity is reached when the pores of the carbon material become equally accessible both for cations and for anions. It is shown that not only the pore area but also the surface of the carbon powder, from which the electrodes are made, has a significant effect on the capacitance of the SC. The approach allows us to obtain porous carbon materials with required pore size distribution those are promising for the production of SC with high specific power.

Adsorption of the Volatile Organic Molecules in the Langmuir-Blodgett Phosphorylated Calix[4]Arenes Films

Kazantseva Z.I.¹, Koshets I.A.¹, Kalchenko V.I.²

¹*Institute of Semiconductor Physics, National Academy of Sciences of Ukraine, Kiev, Ukraine*

²*Institute of Organic Chemistry, National Academy of Sciences of Ukraine, Kiev, Ukraine*

Nowadays a great attention is paid to creation and development of miniaturized, low-cost, smart chemical sensing systems based on various physical and chemical principles, which provide accurate and reliable real-time control of ambient medium. One of the most important problems under creation of such systems for pattern recognition of smells is the choice of appropriable sensitive materials for coating of sensor. Sensitive layers should provide good and quick response to the presence of analyzed molecules in surrounding air, from the other hand sensor must have sensitivity to the interfering molecules as less as possible. As well, sensor should be easily cleaned. From this point different types of functionalized calixarenes are very promising materials and many researchers focus their attention on investigation of selective and sensitive properties of calixarene films [1,2].

This work reports on the results of investigation of quartz crystal microbalance (QCM) sensors coated with novel phosphorylated calixarenes (CA) to wide range of volatile organic molecules. The influence of introduction of various functional groups into calixarene molecule macrocycle to sensitivity towards different organic molecules has been analyzed. Sensors coated with phosphorous-containing calixarenes showed a high sensitivity and an excellent selectivity towards volatile organic compounds (aromatics, chlororganics, ketones and aliphatic alcohols). Sensor response was found to be depended on chemical structure of calixarenes under study, particularly, on the substituting group of molecule.

Films of the phosphorylated calixarenes demonstrated fast and reversible adsorption to wide range of analyte except the situation when stable complex “host-guest” was formed. The phosphorylated calix[4]arenes were synthesized in the Institute of Organic Chemistry in Kiev. The chloroform solutions of calixarenes were used for deposition onto quartz crystals by Langmuir-Blodgett technology.

1. F.L.Dickert, O.Schuster, Supramolecular detection of solvent vapours with calixarenes // *Mikrochimica Acta*, 1995, v.119 (1-2) p.55-62.

2. D.Diamond, K. Nolan, Calixarenes: designer ligands for chemical sensors // *Analytical Chemistry*, 2001, v73 (1) p.23-35.

Effect of Diamond-Like Carbon Films on the Properties of Semi-Insulating Gallium Arsenide

Klyui N.I.^{1,2}, Lozinskii V.B.^{1,2*}, Liptuga A.I.², Lukianov A.M.^{1,2},
 Temchenko V.P.², Lozinska Yu.V.³, Gorbulik V.I.²

³ *Vadym Hetman Kyiv National Economics University, Kyiv, Ukraine*

¹ *College of Physics, Jilin University, Changchun, People's Republic of China*

² *V. Lashkaryov Institute of Semiconductor Physics, NAS of Ukraine, Kyiv, Ukraine*

Owing to its optical properties the semi-insulating gallium arsenide (SIGA) is widely used in fabrication of optical elements for IR optics. The important issue for efficient work of such devices is the high quality of the initial crystals and their stability in various degradation conditions. The penetrating irradiation holds a special place among other degradation factors due to huge difficulties in protecting from it optical devices and elements. The generation of radiative defects causes the degradation of device parameters based on SIGA. For example, the generation of radiative defects under the γ -irradiation occurs due to the Kompton effect. In order to prevent such effects, the protective covers can be used. In case of IR optical elements based on GaAs the protective films should also reduce optical losses caused by light reflection, such covers have to be antireflective.

In this study the optical properties of SIGA crystals in the IR wavelength range were studied. The crystals were fabricated by Czochralski method with liquid hermetisation. The antireflective diamond-like carbon (DLC) films were deposited using PE-CVD setup with the plasma power 200 W. Prior the DLC deposition the crystal surface was treated with hydrogen or argon plasma for cleaning, partial relaxation the mechanical stress and improving the resistance for following treatments. The irradiation of the initial crystal GaAs and structures DLC-GaAs by γ -quanta was conducted using the Co⁶⁰ source with consecutive dose increasing.

It was shown that the deposition of DLC film led to the sufficient improvement the stability of the optical element based on the SIGA. The possible mechanism of the effect of γ -quanta on the SIGA crystals and DLC-GaAs structures for different levels of irradiation dose was proposed. It was revealed that application of preliminary plasma treatments with hydrogen and especially argon are promising for improvement the degradation stability of the studied structures DLC-GaAs under the γ -irradiation.

Optical Absorption Dye Bases in Solutions and Films

Kobzar P.Y.¹, Pavlenko O.L.¹, Kulish M.P.¹, Dmytrenko O.P.¹, Studzinski S.L.¹,
Kurdyukov V.V.², Kachkovsky O.D.³

¹Taras Shevchenko National University of Kyiv, Kyiv, Ukraine

²Institute of Organic Chemistry NAS of Ukraine, Kyiv, Ukraine

³Institute of bioorganic chemistry and petrochemistry NAS of Ukraine, Kyiv, Ukraine
spiritofspirt@gmail.com

Dye is derived asymmetric polymethine dyes containing two coordinated nitrogen atoms. Due to their electronic properties with prospects for application in molecular electronics. At high concentrations dyes can form aggregates that should occur in spectrum absorption. We explored the donor-acceptor dye structural formula which, together with the absorption spectra in a solvent CH₂Cl₂ (curve 1) and the film (2) obtained by watering with this solution is shown in Figure 1.

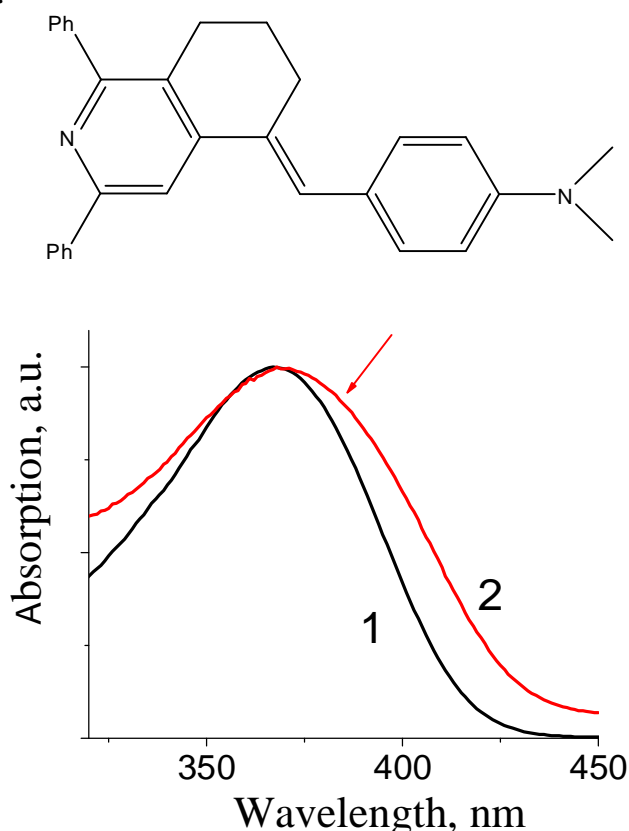


Fig. 1. The structural formula and absorption bases, in a solvent CH₂Cl₂ (curve 1) and the film (2) obtained by watering with this solution.

As shown in the figure, the maximum absorption solution is at 367 nm, and the film range is become wider, maximum shifted to 372 nm, there is also the long-wave shoulder at 384 nm, which shows there is interaction between the molecules and requires further study.

Chalcogenides and Fluorides of Metals as Basis of Film-Forming Materials for IR Optics

Zinchenko V.F.¹, Kocherba G.I.², Magunov I.R.¹, Eremin O.G.¹

¹*A.V. Bogatsky Physico-Chemical Institute of NAS of Ukraine,
Odessa, Ukraine, e-mail: vfzinchenko@ukr.net*

²*JV "New Materials and Technologies", Odessa, Ukraine, e-mail: nmt@paco.net*

Materials for interference optics, or, otherwise, the film-forming (optical) materials (FFM) developed for an enlightenment of optics still in 30-40th years of 20-th century, find more and more wide application in laser technics, optoelectronics, semiconductor devices, etc. [1].

As FFM with a favorable combination of refractive indices ($n^1 = n^2$) and desirable operational properties are widely applied chalcogenides (sulfides, less often - selenides and tellurides) and fluorides of metals. Opportunities of improvement of properties of the coatings received from simple chalcogenides ZnS, ZnSe, PbTe or fluorides MgF₂, YF₃, PbF₂ due to perfection of technologies of FFM reception or drawing of coatings, are practically exhausted. For last 15-20 years the scale of essentially new FFM is developed. Their application made it possible essential improving operational (mechanical durability, thermal and climatic resistance, beam durability) and optical (an optical transparency, uniformity) parameters of interference optics [2, 3]

Two basic types of such FFM are considered: complex compounds (sulfides, fluorides, sulfofluorides) or composites.

As a rule, complex compounds (except for sulfofluorides) are characterized by congruent evaporation while composites undergo essential rectification at thermal evaporation in vacuum. Depending on FFM nature and conditions of evaporation and condensation on a substrate, the x-ray amorphous (nanocrystalline) or mixed amorphous-crystalline coatings with prevalence of one of the component are formed, that essentially affects properties of coatings. Influence of composition and crystal structure of initial FFM on character of coatings is established.

1. Optical Technologist's Handbook / Antonov E.A., Baigozhin A. et al. / Ed.by Okatov M.A.-The 2-nd edition.-St.Petersburg: Politekhnic, 2004.-679 pp.
2. Zinchenko V.F. Scientific bases of prognostication and creation of the film-forming materials for interference optics / Opticheskiy Zhurnal.-2006.-V.73, No.12.-P.72-77.
3. Zinchenko V.F., Sobol' V.P., Kocherba G.I., Timukhin Ye.V. Optical and operational properties of thin-film systems for interference optics (review) / Phys. Chem. Solid State.-2007.-V.8, No.3.-P.441-450.

Optical Recording of Phase Reliefs in Amorphous Chalcogenide and Polymer Layers

Molnar S.¹, Burunkova J.², Zhuk D.², Bohdan R.¹, Makauz I.³, Csarnovics I.¹, Takacs V.⁴, Kokenyesi S.¹

¹*Institute of Physics, University of Debrecen, Hungary*

²*ITMO University, St.Petersburg, Russian Federation*

³*Uzhgorod National University, Uzhgorod, Ukraine*

⁴*Institute for Nuclear Research, Hungarian Academy of Sciences, Debrecen, Hungary*

New materials and technologies for photonic elements are intensively developing last time due to the increasing demands of photonics, infocommunication technologies and data processing, sensorics. Among the wide number of materials and proper fabrication methods optical, holographic recording in photo-sensitive materials, polymers is one of the most known, perspective although the selective etching, development of optical reliefs causes essential shortcomings. The goal of the present work was the targeted development of previously investigated amorphous chalcogenide and acrylate-based materials [1], which can be used for optical recording at certain laser wavelengths (green, red or near-IR), in continuous or pulsed regimes (DPSS or femtosecond lasers) with direct surface relief formation.

The multi-beam interference method was used for one step, direct formation of 1-, 2-D photonic structures in functional acrylate nanocomposites, which contain SiO₂ and Au nanoparticles and which are sensitized to blue and green laser illumination. Amorphous chalcogenide layers from As-Se-Te system were optimized for visible and near-IR spectral range. It is essential, that no additional treatments of the material after the recording are necessary and the elements possess high transparency and low scattering levels. Stability or erasing of surface and volume phase reliefs was investigated with aim to select materials for producing applicable photonic elements.

The support of the GINOP-2.3.2-15-2016-00041 project is acknowledged.

1. Molnar, S., Bohdan, R., Csarnovics, I., Burunkova, I., Kokenyesi, S., Amorphous chalcogenide layers and nanocomposites for direct surface patterning, Proceedings of SPIE , volume 9359, (2015), Article number 935908.

Thermoelectric Properties of Vapor-Phase Condensates PbAgSnTe

Kostyuk O.B.

Vasyl Stefanyk Precarpathian National University, Ivano-Frankivsk, Ukraine

Compounds based on PbTe are a high-performance thermoelectric materials. Recently, a new thermoelectric material PbAgSbTe, named LAST was received based on PbTe, with high thermoelectric figure of merit. There are many modifications of the LAST compounds such as LASTT ($\text{Ag}(\text{Pb}_{1-x}\text{Sn}_x)_m\text{SbTe}_{2+m}$), Na $_{1-x}$ Pb $_m$ Sb $_y$ Te $_{m+2}$ (SALT), and Pb $_{1-x}$ Sn $_x$ Te-PbS. Thermoelectric properties of these compounds are very sensitive to the chemical composition. In this work the patterns of thermoelectric parameters of films based on compounds Pb-Sn-Ag-Te (LATT) are researched. Compounds PbAgSnTe both n- and p-type can be obtained by regulating the chemical composition, which makes the system particularly promising for use in power generation. So it makes sense to optimize the composition for better thermoelectric properties.

On the transition to film condensate the properties of the material are significantly different from the bulk samples. In addition, the exposure of films on the air due to the acceptor effects of oxygen on the surface are formed a layer, which is enriched of carriers of p-type conductivity. This layer makes a significant contribution to the thermoelectric properties of condensate.

The dependence of thermoelectric parameters from the thickness of films based on compounds PbSnAgTe is investigated, which are obtained of the vapor phase on fresh chips (0001) of mica-muscovite substrates. The obtained results are interpreted by the adsorption of oxygen on the surface.

Films for the investigation are received by the deposition of the vapor on pre-synthesized material Pb $_{14}$ Sn $_4$ Ag $_2$ Te $_{20}$, Pb $_{16}$ Sn $_2$ Ag $_2$ Te $_{20}$ та Pb $_{18}$ Ag $_2$ Te $_{20}$ in vacuum on the fresh chips (0001) of mica-muscovite. The measurement of the thermoelectric parameters of condensates was realized at the room temperature in the constant magnetic and electric fields on the developed automated installation. This installation provides as a process for measuring the electrical parameters, as initial registration and as initial data processing.

It was shown that condensates thickness $d < 500$ nm are characterized by improved thermoelectric properties. In addition, thin films based on compounds Pb $_{14}$ Sn $_4$ Ag $_2$ Te $_{20}$ have the highest thermoelectric figure of merit compared to other investigation chemical composition. Therefore, a film based on Pb $_{14}$ Sn $_4$ Ag $_2$ Te $_{20}$ can be used as p-branches of highly efficient thermoelectric energy converters.

Investigation of the Hall effect in PbTe:Sb thin films

Kryskov Ts.A., Lyuba T.S., Optasyuk S.V., Rachkovsky O.M.

*Ivan Ohienko Kamyanets-Podilsky National University,
Kamyanets-Podilsky, Ukraine. E-mail: optasyuk@gmail.com*

A^{IV}B^{VI} thin films are widely used as solar cells, sources and detectors of medium and far infrared range of optical spectrum and are the basic material for making thin-film thermoelectric energy converters. Among all semiconductor compounds, such thin films are unique because of their fundamental characteristics: the band gap, radiation resistance, and high concentration and high mobility of charge carriers. Investigation of galvanomagnetic phenomena in thin films is a powerful method in research of the electrical parameters of such compounds and also as an approach for the control of the technological processes in micro- and nanoelectronic devices. Our findings on the Hall effect in PbTe:Sb thin films are presented in this work.

PbTe:Sb thin films of different thickness were the object of research. These films were obtained by the vacuum thermal deposition method. The thickness of the film was determined by an interference microscope. Electrical parameters were determined by Hall effect using the transverse potential difference method at constant electric and magnetic fields in different directions. The value of constant magnetic field was 0.91 T, temperature of 300 K.

Charge carrier mobility for films of different thicknesses was calculated on the experimental data obtained with the consideration of the average values of Hall voltage and measurements of current and magnetic field in two different directions

$$m_{n,p} = |R_H| S = \frac{|R_H|}{r} \quad (1)$$

Based on calculations of main electrical parameters, the dependencies of mobility and carrier concentration on the film thickness were built. Two specific features should be marked. The first one - a decrease in the sample thickness results in the increased concentration of free charge carriers. Probably, the increase of concentration could be due to several factors: the thinner film is, the more significant is the influence of substrate on concentration and mobility of charge carriers in the film; technological conditions of films growing when the film thickness can change the charge transfer mechanism. A change in concentration of charge carriers can be due to an acceptor effect of oxygen, since the impact of surface oxidized layer depends on the film thickness. It should also be noted that the inversion of the conductivity from n to p type occurs upon decreasing of the film thickness to 90 nm.

Electrical Properties of the CdS: Au NPs/CdTe Heterostructures

Kusnezh V.V.¹, Il'chuk H.A.¹, Petrus' R.Yu.¹, Płaczek-Popko E.², Gwózdź K.²,
Zmiiowska E.O.¹, Ukrainets N.A.¹

¹Lviv Polytechnic National University, Physics Department, Lviv, Ukraine

²Wroclaw University of Science and Technology, Wroclaw, Poland

The metallic nanoparticles can increase the photoconversion efficiency of the thin-film solar cells (SC). Important and underestimated issue of metallic NPs application is compatibility with SC that does not change the device architecture, can be easily added to one of the solar cell layers and does not initiate composition changes of the SC layers. The location of NPs on top, in the window layer or on back contacts, the period, and width of the nanostructures for optimized light trapping is the matter of investigations. The light trapping in the CdS/CdTe SC has not yet been studied systematically, only several articles were published [1].

Magnetron rf-sputtering method of the CdS and CdTe thin films with an AuNPs arrays chemical growth was combined to fabricate CdS: Au NPs/CdTe solar cells. Created structures exhibit rectifying properties with positive polarity of CdTe film at a forward bias. Room temperature current-voltage and capacitance-voltage dependences (fig. 1) of the CdS/CdTe SC with AuNPs array embedded in CdS window layer were investigated. Obtained results were compared with the results for the reference CdS/CdTe cell without AuNPs.

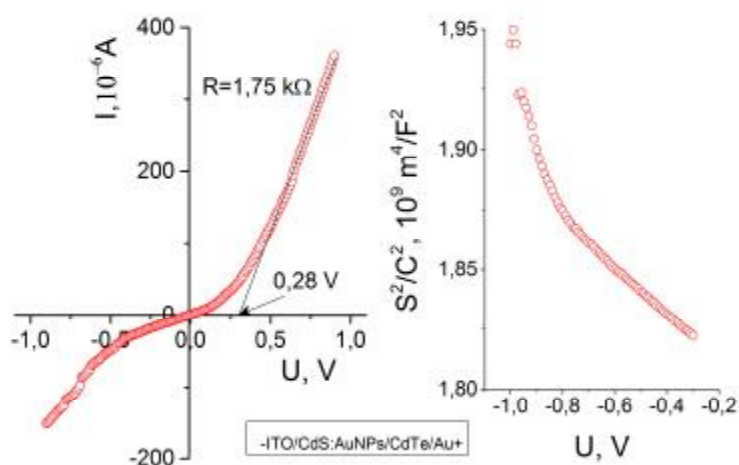


Fig. 1. Current-voltage and S^2/C^2 -voltage dependences of the CdS: AuNPs/CdTe heterostructure.

1. Spalatu N., Hiie J., Maticiuc N., Krunk M., Katerski A., Mikli V., Sildos I. Plasmonic effect of spray-deposited Au nanoparticles on the performance of CSS CdS/CdTe solar cells // Applied Surface Science. –2015. – Vol.350.– P. 69-73.

Spin-dependent giant thermoelectric power in magnetic field for Co/Al₂O₃ nanocomposites

Lashkarev G.¹, Radchenko M.¹, Baibara A.¹, Bugayova M.¹, Stelmakh Y.², Krushinskaya L.², Knoff W.³, Story T.³

¹*I.M. Frantsevych Institute for Problems of Material Science, National Academy of Sciences of Ukraine, Kyiv, Ukraine e-mail: radch@isp.kiev.ua*

²*E.O. Paton Electric Welding Institute, Academy of Sciences of Ukraine, Kyiv, Ukraine*

³*Institute of Physics, Polish Academy of Sciences, Warsaw, Poland*

The thermoelectric power (α), electrical resistivity and magnetic properties of ferromagnetic nanocomposites (FMNC) Co/Al₂O₃ were investigated in the concentration region 23,7-25,5 at.% of Co in the temperature range (4,2-300) K and in magnetic fields (H) up to 5 kOe.

Earlier in samples of Co/Al₂O₃ below percolation threshold of Co concentrations, the giant thermoelectric power in a magnetic field (GMTEP) in the temperature range above 85 K was found, exceeding the thermoelectric power at the same temperature but without a magnetic field in 3-5 times. This phenomenon was explained by the hopping mechanism of electron transfer through magnetic centers containing Co in a dielectric matrix in the conditions of a temperature gradient. In such case the influence of the magnetic field, in our opinion, causes a decrease in the electrons scattering with spin rotation due to the cooperative orientation of magnetic moments of electrons and magnetic localization centers.

We observed maximum $\alpha(T)$ in the minimal temperature (the growth of α about ~160 times) when sample was cooled without a magnetic field H. However, when it was cooled in the switched-on magnetic field, GMTEP did not appear. An explanation of the giant α in the last case can be a transition from the superparamagnetic state of FMNC to ferromagnetic one due to the orientation of magnetic moments for Co nanoparticles and centers of localization by an appearing internal magnetic field. As a result, the external magnetic field changes insufficiently. Thus there must be a correlation of the temperature for the maximum $\alpha(T)$ with the transition to the spin glass state.

Thereby, GMTEP is a multifunctional effect that depends on temperature, magnetic field, composition (and hence on the concentration of magnetic centers) and the prehistory of various factors action on the sample. Thus, discovered effect is the complicated one and needs additional experimental studies and calculations.

The influence of thermal annealing on the GMTEP phenomenon and the electrical properties of FMNC was investigated.

The Influence of Electron Irradiation on Optical, Electrical and Structural Properties of ZnO:Al Films

Lashkarev G.¹, Myroniuk D.¹, Godlewski M.², Pietruszka R.², Maslyuk V.³, Dranchuk M.¹, Karpyna V.¹, Timofeeva I.¹, Vasilkovskaya M.¹, Petrosyan L.¹

¹Frantsevich institute for problems of materials science NAS Ukraine, Kyiv, Ukraine,
e-mail: geolash@materials.kiev.ua

²Institute of Physics, PAS, Warsaw, Poland

³Institute of electron physics NAS Ukraine, Uzhgorod, Ukraine

Transparent conductive film materials have wide applications in optoelectronic devices, gas sensors, reflecting coatings on windows. Several types of solar cells for space applications require transparent electrodes which should be resistant to ionizing radiation.

ZnO is used as a window, component of heterojunction and electrode layer for thin film solar cells based on ternary photovoltaic materials (CuInSe₂, CuInS₂). The main requirements for such material are low resistivity and high transparency.

We carried out the influence of electron irradiation on the optical, electrical and crystal structure properties of the ZnO films doped by aluminum within 0.5 to 7 %. The films were deposited on glass substrates by atomic layer deposition. The samples were irradiated by electrons with high energy of 10 MeV up to the fluences 10^{15} and $2 \cdot 10^{15} \text{ cm}^{-2}$ using the microtron electron accelerator M-30. Electronic devices can obtain these fluences by moving in the Van Allen belt during 10 and 20 years, correspondingly. The effect of electron irradiation on the properties of aluminium doped ZnO films is discussed here.

The crystal structure of films was investigated by X-ray diffraction analysis using diffractometer DRON-4 (Cu-K α , $\lambda = 0.1542 \text{ nm}$). The method of atomic layer deposition provides a perfect polycrystalline ZnO films with XRD reflections (100) and (110) indicated preferred orientation of crystallites main c-axis in the film plane. Temperature dependences of electrical resistance, mobility and carrier concentration were measured in the temperature range 77÷300 K. It was established that in all cases after irradiation the electron mobility increases and electrical resistance decreases. It is important that improving the electrical properties is not accompanied by changes in the microstructure, the size and orientation of crystallites and tension. So, defects at grain boundaries are sensitive to radiation annealing. Thus, the latter reduces the height of the intergrain barriers, which leads to higher values of the mobility. Another important fact is a great enhancement of electrical activity of Al donor impurity after electron irradiation. For example, two times increasing in Al electrical activity was observed for ZnO films with low (0.5 at. %) concentration of Al.

Influence of Quantum Size Effect on Superparamagnetic Properties of Co/Cu(111) Nanofilms

Lukienko I.M.¹, Kharchenko M.F.¹, Stetsenko A.N.².

¹*B. Verkin Institute for Low Temperature Physics and Engineering of the National Academy of Sciences of Ukraine, Kharkiv, Ukraine, lukijenko@ilt.kharkov.ua*

²*National Technical University “Kharkiv Politechnical Institute”, Kharkiv, Ukraine*

Quantum size effect is known as important factor that influence on formation of morphological peculiarities of thin metallic films. Here results of experimental investigations of the magneto-optical Kerr and Faraday effects for multilayer Co/Cu(111) nanofilms are submitted. Magnetic field dependences of the magneto-optical Kerr angles have been approximated by Langevin functions with using log-norm distribution of superparamagnetic clusters. It was detected decreasing of the averaged cluster magnetic moments for the films with thickness of the Cu layers, which ensure the antiferromagnetic exchange coupling between Co layers, similarly to results, obtained from magnetoresistive data (Fig.1). Additionally, comparative analysis of magnetic field dependencies of the Kerr and Faraday effects has been carried out taking into account the impact of the magneto-dipole shape anisotropy of ferromagnetic granules in films on magnetization at magnetic field, oriented parallel and transverse to the film plane. It is found that parameters of the initial linear parts of the magneto field dependences for the Faraday and Kerr effects are non-controversial, if we assume the existence of dependences of geometrical parameters for ferromagnetic grains and pins on thickness of Cu layers in films (Fig. 2). It is suggested, that the observed regularities in formation of the specific grains in the [Co/Cu(111)]₂₀ films are caused by rearrangement of the charge density in the Co/Cu interfaces, induced by the electronic quantum size effect in the Cu layers.

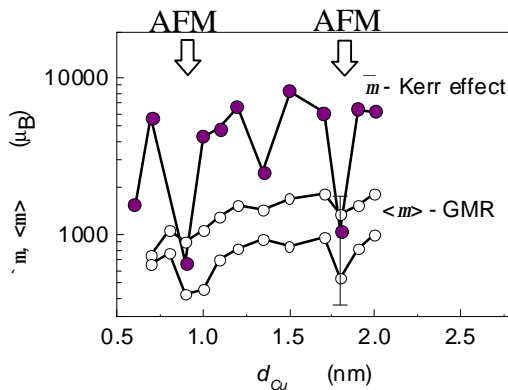


Fig. 1 Averaged magnetic moments of the SPM clusters in the [Co/Cu]₂₀ films in dependence of the copper layer thickness, obtained from Kerr and GMR effect data.

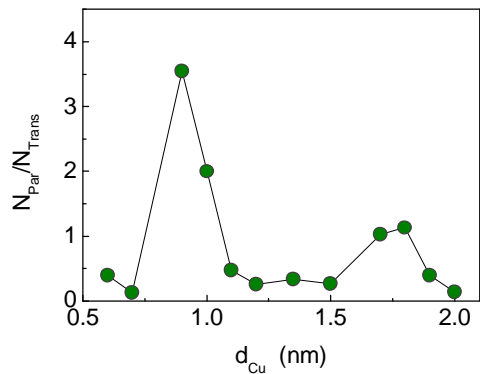


Fig. 2 The ration of the demagnetization factors for FM grains in directions parallel and transverse to the film plane.

Effect of Thermal Annealing on the Optical Properties of Thin Films of Cadmium Telluride

Mazur T.M.¹, Makhniy V.P.², Prokopiv V.V.¹, Slyotov M.M.²

¹Vasyl Stefanyk Precarpathian National University,

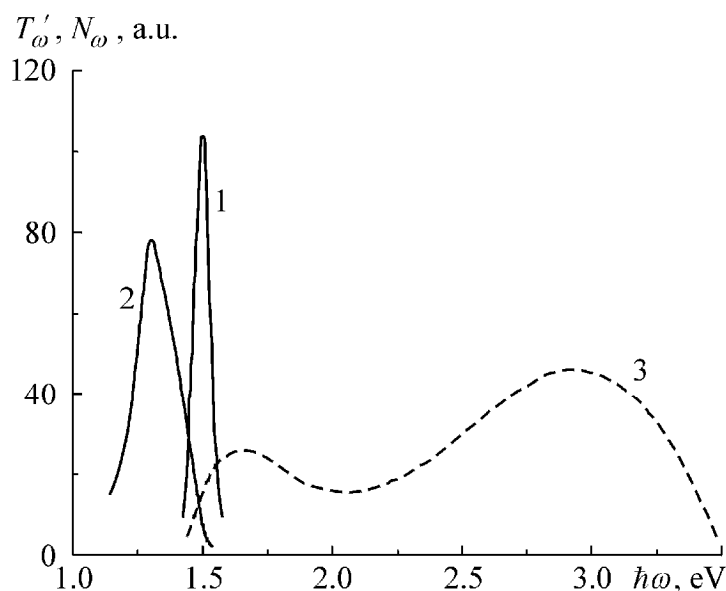
Ivano-Frankivsk, Ukrain, tetyana.m.mazur@gmail.com

²Yuriy Fedkovych Chernivtsi National University, Chernivtsi, Ukraine

CdTe occupies a special place among semiconductor solar cells suitable for forming. It has a number of advantages over the materials currently used. These include, in particular, significantly higher temperature and radiation stability than in Si, as well as a simpler and less expensive technology of growing CdTe crystals allows the use of thin film technology in producing solar cells, which can lead to further reduction of costs of materials and of products.

In this regard, currently, intensive large scale search for effective methods of synthesis of relatively simple thin films of CdTe is being made. Since the parameters of grown films do not always meet the necessary requirements, additional processing technologies are applied for correcting them.

This paper examines the effect of annealing temperature on transformation of optical transmission spectra and photoluminescence films CdTe, obtained by the method of the hot wall on mica substrat. Maximums of transmission T'_ω (curve 1) is located at $\hbar\omega_m = 1.5$ eV and is consistent with E_g cadmium telluride. Annealing of the films in the air under the conditions that lead to the formation of nanostructures on the surface of single crystal substrates CdTe,



result in the displacement of the maximum of the curve T'_ω to ~ 1.3 eV (curve 2), and the emergence of a wide spectrum of photoluminescence (curve 3) in the field of energies greater than E_g teluridu of cadmium.

The mechanisms responsible for the optical properties transformation of the objects of research are discussed.

Thermal Instability and Self-Organizing Processes in the Thin Film Structures of a Non-Crystalline Materials

Mar'yan M., Yurkovych N.

Uzhhorod National University, Uzhhorod, Ukraine

At presence significant deviations from state equilibrium or significant external fields crucial role in shaping the ordering, creation and storage of functional organizations are implemented synergistic effects and mechanisms of energy transformation. In these materials presented research model of thermal instabilities and the formation of dissipative structures of the amorphous solids *Ge-As-Te* under the action of continuous infrared radiation (wavelength is $\Lambda = 10.6 \text{ mkm}$, power is $P = (3 \div 5) \text{ W/sm}^2$ and duration of exposure is $t_p = (1 \div 30) \text{ s}$) and comparing with experimental data.

Radiation with Gaussian distribution on the beam cross section normally falls to the surface layer axially z and totally absorbed in the substrate. The dynamics of temperature T change on the surface of the amorphous layer and the substrate which describes a system of the non-linear differential equations taking into account the process heat generation, its distribution and heat transfer to the substrate and the thin film amorphous layer. We found that stabilization of thermal instability is realized through self-regulatory mechanisms that lead to saturation of absorption nonlinearity and leveling the rate of growth of the absorbed energy and heat. This bifurcation diagram of temperature dependence of the radiation power of the material explains the non-monotonic behavior optical density D amorphous condensates *Ge-As-Te* and helps identify the exposure threshold range of laser radiation are considered. For powers $P > P_c = (7.6 \div 8.5) \text{ W/sm}^2$ (intensity is $I = 0.3 \text{ W}$, the effective radius of the beam is $r_0 = 0.11 \text{ sm}$) exposure duration threshold at which the growing instability manner $(0.35 \div 0.4) \text{ s}$ corresponding exposure in the range of non-monotonic behavior D . Typical values scale spatial heterogeneity of the temperature profile are $L_c \approx (0.3 \div 0.5) \cdot r_0$, the lifetime of dissipative structures are $t_{life} \approx (10^{-1} \div 10^{-2}) \text{ s}$, consistent with experimental data. It is shown that radial-ring structure with the number of beams $m \geq 3$ formed by irradiation power density $P \geq 18.6 \text{ W/sm}^2$.

Surface Polariton Excitation in $Mg_xZn_{1-x}O$ Films at Optical Anisotropic Al_2O_3 Substrates

Venger E.F.¹, Venger I.V.¹, Melnichuk L.Yu.², Melnichuk O.V.²

¹*V.Lashkarev Institute of semiconductor physics NANU, Kyiv, Ukraine*

²*Nizhyn Gogol State University, Nizhyn, Ukraine*

Today is a fairly significant number of scientific papers which studied the optical and electrophysical properties of the films of metal oxides for dielectric and semiconductor optical isotropic and optical anisotropic substrates. This is due both to the growing scientific interest to the films of metal oxides because of their miniature, high efficiency over a wide frequency range, the ability to integrate with other microelectronic elements and with the possibility of wide practical use in optical and nanoelectronics. The report presents the results of studies of surface phonon and plasmon-phonon polariton excitation (PP) in undoped and heavily doped films of triple compounds $Mg_xZn_{1-x}O$ at concentrations of electrons from 10^{16} to $5 \cdot 10^{18} \text{ sm}^{-3}$ on dielectric Al_2O_3 substrates by the method of spectroscopy of total impaired internal reflection (TIIR) in the sphere of residual film rays and substrate orientation at $E \perp C$ i $E \parallel C$. Feature of research of triple compounds $Mg_xZn_{1-x}O$ with the range $Mg_2 +$ from 0 to 20 at.% is a hexagonal lattice preservation and display of optically anisotropic properties in the infrared spectrum. When $x > 0,2$ for triple compounds of $Mg_xZn_{1-x}O$ characterized by a cubic lattice.

$Mg_xZn_{1-x}O$ films were synthesized by electron-ray evaporation by using a modernized industrial plant VU-1A with automatic control of technological process (temperature control, pressure valves, etc.). The growth rate of the $Mg_xZn_{1-x}O$ films at $x < 0,2$ at Al_2O_3 substrates was 0,1-0,15 mkm / h. The thickness of the films was determined with an interferometer MYY-4 varied from 1 to 40 mkm.

With the help of a spectrophotometer IKS-31 using adapters NPVO-2 conducted the registration of TIIR spectra in p -polarized light in the current frequency range of $Mg_xZn_{1-x}O$ film and Al_2O_3 substrate (400 - 1200 cm^{-1}) at $T = 300 \text{ K}$.

Theoretical study of surface polariton excitations conducted using by manyoscillator mathematical model of additive contribution of oscillators to dielectric permeability of heavily doped $Mg_xZn_{1-x}O$ film at substrates with orientations $E \perp C$ i $E \parallel C$ and under consideration of phonon and plasmon-phonon interaction of films.

Using analysis of variance spectra of TIIR double-layer structure in the area 400 - 1200 cm^{-1} defined optical and electrophysical characteristics of the $Mg_xZn_{1-x}O$ film at Al_2O_3 substrates with specified orientations.

The authors set criteria of excitation and distribution of SP in $Mg_xZn_{1-x}O$ films at Al_2O_3 substrates. Theoretical study of possibilities of existence and spread of surface plasmon-phonon polaritons has conducted. Found that the number of the dispersion branches in $Mg_xZn_{1-x}O$ at Al_2O_3 substrates varies by changing the orientation of the substrate and the concentration of free charge carriers in the heterostructure of $Mg_xZn_{1-x}O$. It is shown that the maximum number of dispersion branches for strongly doped $Mg_xZn_{1-x}O$ film/ Al_2O_3 is five. Found that the surface plasmon-phonon polariton excitation of third and fourth types are limited range of values of the wave vector.

Size Effects in Thin PbTe<In> Films

Menshikova S.I., Rogachova O.I.

National Technical University "Kharkiv Polytechnic Institute", Theoretical & Experimental Physics Department, Kharkiv, Ukraine, olhovskaya.sveta@gmail.com

Nowadays the intensive development of nanophysics and nanotechnology stimulates the study of thin film properties.

In the case, when thin film thickness d is comparable with the de Broglie wavelength λ_F or mean free path l of charge carriers, quantum (QSE) or classical size effects (CSE), respectively, can be observed. Earlier we observed [1,2] the manifestation both of CSE and QSE on thickness dependences of kinetic properties of stoichiometric and doped with chlorine PbSe films.

The oscillatory behavior of thermoelectric properties under increasing PbTe<In> thin films thickness in the $d = 20-60$ nm range was observed, which was described as QSE [3]. The d -dependence of Seebeck coefficient S in this range was interpreted in the frame of size quantization approximation, taking into account the d -dependence of the Fermi energy and contributions to kinetic coefficients from multiple energetic subbands, but there was no interpretation of the behavior of kinetic properties at $d > 60$ nm.

The goal of the present work is to carry out the theoretical interpretation of Seebeck coefficient variation depending on PbTe<In> thin films thickness in the $d > 60$ nm range.

Theoretical calculation of d -dependence of the Seebeck coefficient was performed using MatLAB 6.5 software package.

The character of Seebeck coefficient thickness dependence in the $d > 60$ nm range (the increase of S with increasing d) was attributed to the manifestation of CSE and was interpreted in the framework of the Mayer theory. It was shown that at thickness dependences of PbTe<In> thin films kinetic coefficients one can isolate an oscillatory and monotonic components, which are attributed to the manifestation of the QSE and CSE, respectively.

1. Rogacheva E.I., Nashchekina O.N., Ol'khovskaya S.I., Dresselhaus M.S. Size effects in thin PbSe films // J. Thermoelectricity. – 2012. – № 4. – P. 25-32.

2. Menshikova S.I., Rogacheva E.I., Sipatov A.Yu., Krivonogov S.I., Matychenko P.V. Size effects in chlorine doped PbSe thin films // J. Thermoelectricity. – 2015. – № 2. – P. 22-31.

3. Menshikova S.I., Rogacheva E.I., Sipatov A.Yu., Zubarev Ye.N. Size effects in thin n -PbTe films // Functional Materials. – 2015. – V. 22. – № 1. – P. 14-19.

On the Liquid Phase Stability in Nanoscale Layered Bi-Ge Films: an *in situ* TEM Study

Minenkov A.A.^a, Bogatyrenko S.I.^a, Kryshtal A.P.^b

^a*V.N. Karazin Kharkiv National University, Kharkiv, Ukraine*

^b*AGH University of Science and Technology, Krakow, Poland*

Nanostructured materials, which are e.g. thin films and nanoparticles, exhibit plenty of interesting and novel properties, which are different from those of macroscopic polycrystalline materials. The majority of these features have been commonly explained by the increase ratio of "surface" and "bulk" atoms numbers, i.e. by the rise of the surface energy contribution to the systems overall free energy. Although the technological interest in nanostructured materials relies mainly on their special magnetic, optical or mechanical properties, they also exhibit the evolution of thermophysical ones. Moreover, the changes in thermophysical properties such as the melting point depression or diffusivity enhancement are crucial for nano-objects stability. Unfortunately, available experimental data are scant and don't allow to trace the phase state of the nanostructured material in a wide size range. Thus, further investigation becomes an actual objective.

In this work we present the results of systematic and complex experimental studies of the effect of scale on the liquid phase stability in Bi-Ge binary system. Selection of the object under study was motivated by the fact that Bi-Ge binary system has the phase diagram of a simple eutectic type with negligible mutual solubility of components in the solid state. Thus, layered Bi-Ge film is a convenient model object for phase transitions in binary nanosystems studying. The eutectic composition is formed at 99.9 at.% Bi and the temperature of 271°C.

Our experimental approach involves the study of crystalline structure and morphology of the three layer Ge/Bi/Ge films of various thicknesses during *in situ* TEM heating in the 20 – 275°C temperature range. Continuous tracing of the samples diffraction pattern during heating-cooling cycle allows us to precisely determine eutectic and crystallization temperatures, thus to define the liquid phase stability boundaries. The samples were produced at room temperature by sequential thermal evaporation of components from independent sources at a vacuum of $5 \cdot 10^{-8}$ Torr.

As a result of investigation, the Bi-Ge eutectic T_e and crystallization T_g temperatures have been systematically measured as a function of film layer mass thickness (3-50 nm). Significant lowering of T_e and T_g with the layer thickness reduction was registered. It has been revealed that the liquid-phase formation in the system at the eutectic temperature takes place only if bismuth film mass thickness value is greater than the threshold one (≈ 5 nm). While the onset temperature for liquid phase formation at the metal-semiconductor interface was found as $\approx 190^\circ\text{C}$. The observed effect can be consistently explained in terms of thermodynamic approach.

Dopant Activation in Super-Thin P⁺ Ion Implanted Germanium Layer by Low-Temperature RF Hydrogen Plasma

Yukhymchyk V.O.¹, Gomeniuk Yu.V.¹, Okholin P.N.¹, Glotov V.I.²,
Lysenko V.S.¹, Nazarova T.M.³, Duffy R.⁴, Napolitani E.⁵, Nazarov A.N.¹

¹*Lashkaryov Institute of Semiconductor Physics NAS of Ukraine, Kyiv, Ukraine,*

²*Institute of Microdevices NAS of Ukraine, Kyiv, Ukraine*

³*NTUU “KPI”, Dep. General and Neorganic Chemistry, Kyiv, Ukraine*

⁴*Tyndall NI, Lee Maltings, Prospect Row, Cork, Ireland*

⁵*Università di Padova and CNR-IMM Matis, Padova, Italy*

Shallow p-n junction formation is a key requirement in production of advanced Si and Ge devices. Germanium has considerable advantages in comparison with silicon due to high electron/hole mobility, however, diffusion coefficients for donor impurities in germanium, are rather high, which hampers the formation of shallow n⁺/p junctions. Therefore in the case of Ge-based devices one should avoid the high-temperature annealing that is traditionally used to eliminate the implantation-induced defects and to activate implanted impurity. The present work considers low-temperature RF hydrogen plasma annealing of the amorphous P⁺ ion implanted Ge layer. A comparison with standard thermal annealing (TA) and rapid thermal annealing (RTA) is also performed; effect of nonthermal processes on annealing of the amorphous Ge layer is considered.

The phase composition of the implanted layer was studied by Raman scattering spectroscopy at room temperature; the analysis of the thickness and composition was performed with a SIMS CAMECA IMS- 4f spectrometer; a profile of activated implanted impurity was obtained by electrochemical C-V profiling. Surface sheet resistance and estimation of doping concentration in the implanted layer were performed by four-point probes method.

It was shown that low-temperature RF plasma treatment at temperature about 200°C resulted in a full recrystallization of amorphous Ge layer implanted by P⁺ ions and activation of implanted impurity up to $6.5 \times 10^{19} \text{ cm}^{-3}$ with a maximum concentration about 20 nm in depth from surface. RTA (15 sec) and TA (10 min) in nitrogen ambient demanded considerably higher temperatures for the recrystallization and activation processes that resulted in diffusion of implanted impurity inside of Ge bulk. It was demonstrated that RF plasma treatment of the samples with front implanted side resulted in significantly stronger effects of recrystallization and activation than the same treatment from the back unimplanted side. The experiment shows that non-thermal processes play an important role in enhanced recrystallization and dopant activation during the RF plasma treatment. Mechanisms of enhanced modification of the subsurface implanted Ge layer under plasma treatment are analyzed.

TPD-MS Study of Desorption of Water From Kaolinic Clay Minerals

Nichiporuk Yu.M.¹, Payentko V.V.¹, Matkovsky A.K.¹, Gun'ko V.M.¹,
Balakin D.Yu.²

¹*Chuiko Institute of Surface Chemistry, NAS of Ukraine, Kyiv, Ukraine,*
yury_nichiporuk@ukr.net

²*Institute of Physics of NAS of Ukraine, Kyiv, Ukraine*

For applications of clay materials in medicine, pharmaceutical, food and cosmetic industry, it is important to know features of interaction of water with a surface of the minerals. This is an important criterion in preparation of any composite materials because this interaction determines the operational use of them in typical environment.

Clays of kaolinic series are used as supplements to the diet because of the structure and mineral composition. They are characterized by the presence of water mostly at the surface, not in the interlayer space, and, therefore, we have studied the interaction of water with the surface of clay minerals.

Table 1 shows the results of determination of hygroscopic moisture (M, 105-110°C) loss on ignition(LOI,%) and water absorption (W%) over saturated solution of NH₄Cl at 20-25°C.

Table 1. Water amounts bound to clay minerals

Clay	M, %	LOI, %	W,%
Kaolin	0.59	15.84	0
White-blue kaolinic clay	1.1	11.3	1.43

Desorption of water from the surface of clay minerals depends on the chemical structure of the surface, structure of particles, type and concentration of surface hydroxyls. In thermograms of clay(kaolin-1, white-blue kaolinic clay -2) there is hydrogen (m/z 2), H₂O (18) C (12), O (16), CO (28) and CO₂ (44).

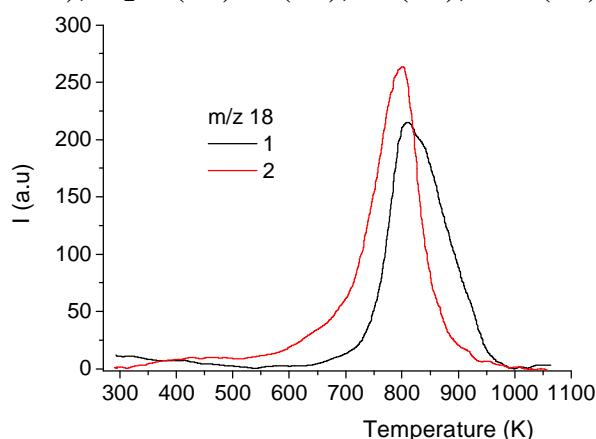


Fig. 1. TPD MS thermograms at m/z 18 (H₂O) for kaolin - 1, white-blue kaolinic clay - 2

Observed desorption of water and CO from white-blue kaolinic clay is greater than that for kaolin. The obtained data are seeing associative desorption and adsorbed water, which is hire for white-blue kaolinic clay (Fig. 1). In the case of kaolin, water desorption peaks partially shifted toward higher temperatures. TPD-MS as a sensitive method allows to distinguish surface hydroxyl structures of different types and to investigate the effect of time of adsorption / re-adsorption water.

Coercivity of Film Materials Based on Fe and Ge

Vlasenko O.V., Zakharchenko N.M., Odnodvoretz L.V.

Sumy State University, Sumy, Ukraine, e-mail: larysa.odnodvoretz@gmail.com

The ability to adjust the orientation of the spins in semiconductors (SC) allows you to form the new materials - magnetic semiconductors (hybrid structure based ferromagnet and SC) transistors and spin. Wide prospects of these nanomaterials are connected with the possibility of a SC layer detector that responds to changes in the magnetic state of a ferromagnet. Poorly understood in terms of the practical application of such materials as sensitive elements of the sensors, the question remains correlation between the coercive force (B_c) and the thickness of the individual layers, so the purpose of the work was to investigate the influence of the thickness of the SC layer film systems based on Fe and Ge on the value of the coercive force, which is calculated based on the measurement of magneto-optical Kerr effect (MOKE).

Film nanomaterials were prepared by layering ceramics condensation on the substrate (S) in a vacuum installation VUP-5M (residual atmospheric gas pressure $\sim 10^{-4}$ Pa) and thermal annealing of automatically on the temperature range 300 - 800 K for 3-4 cycles «heating \leftrightarrow cooling».

Results of the study magneto-optical properties of three-layer film of Fe(10nm)/Ge(5-20nm) / Fe (10nm) /S in the initial state showed that increasing the thickness of the SC layer from 5 to 20 nm the coercive of film systems decreased from 42 to 15 mT (non-annealed samples) and from 8 to 70 mT (annealed to 800 K). Change the value of the coercive force after annealing of systems associated with formation of iron germanium phases FeGe_x ($1 \leq x < 2$) throughout the sample volume [1]. We observed as a «stepped» hysteresis loop dependence of the Kerr angle of the magnetic field, which indicates the implementation of two magnetic states in their ability to control and speed-sensitive sensor element based binary films based on ferromagnetic metals and semiconductors in a magnetic field and temperature.

The work is done within the framework the state budget project №0115U000689 (2015 – 2017 years).

1. Vlasenko O.V., Odnodvoretz L.V., Protsenko I.Yu. // Probl. Atomic Sci. Technol.: Phys. Radiat. Effects Radiat. Mater. Sci. – 2014. – V. 92, №4. – P. 130 – 133.

Kinetic Properties of NiO Thin Films

Parkhomenko H.P., Maryanchuk P.D.

Yuriy Fedkovych Chernivtsi National University
Chernivtsi, Ukraine, e-mail: h.parkhomenko@chnu.edu.ua

Metal-oxide thin films are of great interest both for fundamental research and practical applications. Transparent conducting layers are widely used in electronic, optoelectronic, and photovoltaic devices [1]. Nickel oxide (NiO) is a transparent conducting material with p-type conductivity and is characterized by good electrical and thermoelectric properties and a high chemical stability.

The NiO thin films were deposited onto the preliminarily cleaned glass and ceramic glass substrates $10 \times 5 \times 1$ mm in size using a LeyboldHeraeus L560 universal vacuum installation with the help of the magnetron reactive sputtering of the pure nickel target in a mixture of argon and oxygen with a DC voltage.

During the sputtering process, the partial pressures in the vacuum chamber were $\sim 4 \cdot 10^{-3}$ mbar for argon and $\sim 4 \cdot 10^{-3}$ mbar for oxygen. The magnetron power was ~ 100 W. The sputtering process lasted for ~ 10 min at a substrate temperature of $T_s \approx 373$ K and $T_s \approx 523$ K. The kinetic conductivity coefficients were investigated in a temperature range of 77–290 K. The samples for the Hall effect and electrical conductivity measurements had four Hall contacts and two current ohmic contacts, which were formed using a mask by the magnetron reactive deposition of nickel at a room temperature. Kinetic coefficients were measured at the dc current in a constant magnetic field. The influence of side (“parasitic”) galvanomagnetic and thermomagnetic effects on the measurement results was excluded by means of averaging the results of measurements at various directions of the current and the magnetic field.

The temperature dependence of the Hall coefficient for the NiO thin films indicates that the films are of the semiconductor type of conduction (R_H decreases as T increases).

Using the measurements of the Hall coefficient, it is established that the hole participate in the transfer phenomena, i.e., NiO films have the p-type conduction. Carrier concentration at room temperature were $p \approx 4.1 \cdot 10^{19}$ cm⁻³ ($T_s \approx 373$ K) and $p \approx 4.3 \cdot 10^{18}$ cm⁻³ ($T_s \approx 523$ K). The electrical conductivity of thin films is of a semiconductor nature and at room temperature were $\sigma \approx 0.56$ cm⁻¹·Ω⁻¹ ($T_s \approx 373$ K) and $\sigma \approx 0.34$ cm⁻¹·Ω⁻¹ ($T_s \approx 523$ K). The Hall mobility of NiO films at room temperature were $\mu_H \approx 0.75$ cm²/V·s ($T_s \approx 373$ K) and $\mu_H \approx 7.8$ cm²/V·s ($T_s \approx 523$ K).

1. Sasi, B., Gopchandran, K. G., Manoj, P. K., Koshy, P., Rao, P. P., Vaidyan, V. K. Preparation of transparent and semiconducting NiO films. // *Vacuum*. – 2002. – 68(2). – 149-154.

Supercooling During Bi-Sn Alloys Crystallization in Contact with a Copper Film

Petrushenko S. I., Dukarov S. V., Sukhov V. N., Nevgasimov A. O.

*V. N. Karazin Kharkiv National University,
Kharkiv, Ukraine, petrushenko@univer.kharkov.ua*

At present significant prospects in modern technologies are associated with the use of nanocomposite materials, in which nanoparticles are in contact with a more bulk matrix. These structures are considered as functional elements of advanced nanoelectronic devices, elements of renewable energy, biosensors, etc. These devices operation can be based on the phase transitions occurring in them. This makes the problem of determining stability limits of the liquid phase in such systems, as well as the development of techniques for controlling the temperatures of phase transitions, urgent. This work is devoted to the study of supercooling during Bi-Sn melts crystallization with different concentration of components in contact with copper.

The samples were obtained by vacuum condensation at a residual gas pressure of 10^{-6} Torr by sequential deposition of components. Phase transition temperature was determined by the two independent methods: electrical resistance measurement and in situ electron diffraction studies during film systems heating and cooling. Condensation of the components was performed on substrates at room temperature, which were polished glass plates with electrical contacts and fresh cleavages of KCl single crystals.

It has been found that tin-free Bi/Cu films crystallization is avalanche-like. This is explained by the formation in them of a single fusible structure, found by SEM methods. Crystallization becomes a multistage process and gradually blurs in a certain temperature range with tin concentration increasing. In this case the microstructure of the samples changes. The connected structure of the fusible component breaks up into separate islands, which apparently crystallize independently. The decay of this structure begins at eutectic temperature and accompanied by an irreversible increase of electrical resistance. It should be noted, that the temperature interval in which crystallization occurs, increases rapidly with an increase of tin concentration. This interval stops to change with a concentration approximately corresponding to the maximum solubility of tin in solid bismuth. The crystallization temperature changes with increasing tin concentration, however, the relative supercooling at content of tin in the 3-70 wt.% range does not change and has a value of about 0.25 of the liquidus temperature of the corresponding concentration.

Magnetoresistive Properties of Granular Film Alloys Based on Ag and Fe or Co

Protsenko I.Yu., Odnodvoret L.V., Tkach O.P.,
Shabel'nyk Yu.M., Shumakova M.O.

Sumy State University, e-mail: i.protsenko@aph.sumdu.edu.ua

The results of studies of crystal structure and magnetoresistive properties of granular films based alloys Ag and Fe or Co were are presented. Samples with total thickness to 50 nm formed by simultaneous ((Ag+Fe)/S) and ((Ag+Co)/S) or layering (Fe/Ag/Fe/S or Co/Ag/Co/S) condensation of separate components in the ratio of equiatomous. The thickness of the Ag intermediate layer was not more than 25 nm. Three-layer film systems homogenized by thermal annealing to $T_a = 700 - 900$ K, which allowed to form granular alloys based on solid solutions (s.s.) Ag(Fe) or Ag(Co). At the simultaneous condensation of separate component the elements of granular state formed directly at the condensation process and significantly improved at the next thermal annealing to 700 K.

The electron diffraction studies indicate that the phase composition of film samples of both types corresponds to fcc-phase of solid solutions based on the lattice fcc-Ag. The lattice parameter s.s. different from the lattice parameter of film fcc-Ag on the value $\pm 0,002$ nm, indicating the formation of limited s.s. At the same time, no extra reflections from granules with hexagonal or bcc lattice Co or α -Fe, respectively, indicates a low concentration of granules of relatively large size, which is confirmed by electron microscopic studies (see also [1]).

Study magnetoresistive properties in three geometry measurements indicate that in the samples, which was formed by our methods, observed are only signs of GMR with maximum amplitude $\sim 0,1\%$, although the distinction of value in different measurement geometries suggests its anisotropic character. The absence of GMR-effect «in its pure form» indicates inefficiency of spin dependence scattering of electrons in film s.s. with low concentration of magnetic granules is relatively large size.

The work is done within the framework the state budget project №0115U000689 (2015 – 2017 years).

1. Odnodvoret L.V., Protsenko I.Yu., Tkach O.P., Shabel'nyk Yu.M., Shumakova N.I. // *J. Nano- Electron. Phys.* – 2017. – V.9, №2. – P.02021(1) – 02021(4).

Probabilistic Approach to Analysis of Long-Term Transformation of GaN Radiative Recombination Spectra Due to Microwave Treatment

Red'ko R.A., Milenin G.V., Milenin V.V., Red'ko S.M.

V. Lashkaryov Institute of Semiconductor Physics, National Academy of Sciences of Ukraine, Kyiv, Ukraine, redko.rom@gmail.com

Objects of our study were the structures of epitaxial GaN obtained by MOCVD- method on sapphire substrate and doped with Si (carrier concentration was $\sim 8 \cdot 10^{17} \text{ cm}^{-3}$), thickness $\sim 2.2 \text{ }\mu\text{m}$. We studied the photoluminescence (PL) at 300 K within the spectral range 2.0-3.5 eV with exciting 3.94 eV. The PL spectra of samples were measured during the extended period after microwave treatment (up to 90 days). Microwave treatment was carried at the frequency 2.45 GHz and power 7.5 W/cm^2 . The duration of exposure was 60 s.

Initial PL spectrum of GaN-structure consisted two bands peaked about 3.42 and 2.34 eV. The first peak is attributed to near-edge emission. The second one is assigned to complex with V_{Ga} cooperation and apparently not trivial. Changing of the PL bands intensity after the microwave irradiation treatment was nonmonotonous. At the first the increase of the band's intensity but latter the decrease to the initial values or close to them were detected. The obtained results testify about the change of impurity-defect composition of near-surface layer of GaAs crystals due to the influence of microwave radiation.

Non-monotonic change of PL intensities of impurity bands of the semiconductor material is a special feature due to the microwave radiation treatment. It caused by a non-trivial character of the relaxation of excited subsystem of structural defects. To explain this feature, one can use the assuming that the intensities of the oscillations are caused by random events (e.g., the appearance of local regions enriched (depleted) by point and extended defects). Accordantly to Weibull-Gnedenko distribution dependence of normalized PL intensity via the time after treatment could be expressed:

$$I(t) = I_{in} + I_0 \left\{ \left[1 - e^{-\left(\frac{t}{\tau_1}\right)^{m_1}} \right] e^{-\left(\frac{t}{\tau_2}\right)^{m_2}} \right\},$$

where τ_1, τ_2 – are the time constants of random events; m_1, m_2 are the form factors of the distribution function of time to a corresponding random event, I_{in} is the initial value of the intensity of the photoluminescence band, I_0 is the proportionality factor. One can note a good agreement between the experimental and theoretical results. Moreover, some of parameters of these approximations are very similar for both the impurity and edge PL bands (τ_1, τ_2 and m_2) for GaN and GaAs, respectively. The others ones (I_0, m_1) are different. Detailed properties of fitted parameters, its depending on the impurity-defect composition and initial state of structure under investigation will be analyzed in other work.

Growth ZnO:N Thin Films Using N₂ as the Dopant Source

Rogozin I.V.

Berdyansk State Pedagogical University, Berdyansk, Ukraine

We investigate the p-type doping in ZnO prepared by the original method of radical beam gettering epitaxy using N₂+O₂ mixture as the oxygen source and nitrogen dopant. The basic principle of this process is that thermal annealing leads to the growth of layers on a crystalline substrate via atomic oxygen (radicals) sorption from the gas phase and gettering of zinc atoms from the substrate bulk. The growth was at temperatures in the range of 400-800°C. All N-doped ZnO films were grown on semi-insulating ZnSe (220) substrates. The substrates were degassed by heating in a vacuum (5×10^{-3} Pa) at 500°C for 30 s. The N₂+O₂ mixture was used as the oxygen and N-dopant source. The chamber pressure was 1 Pa. Atomic oxygen and nitrogen were obtained in RF-discharge with the power 100 W. Separation of charged particles was carried out using a strong permanent magnetic field.

The structure and crystalline orientation of the films were studied using an X-ray diffractometer with the use of Cu K_α radiation. Low temperature photoluminescence measurements were performed using N₂ laser with a wavelength of 337.1 nm as an excitation light source.

The typical thickness of the grown films that are studied in this work is about 0.5 μm. An X-ray diffraction $2\theta \sim 34.45^\circ$ can be clearly seen. It suggests that the ZnO films exhibit the (0002) preferential orientation with the *c*-axis perpendicular to the substrate. The full width at half-maximum of the peak (0002) for N-doped ZnO films was measured and equals 0.136°

Secondary ion mass spectroscopy measurements demonstrate that N is incorporated into ZnO film in concentration of about $\sim 6 \times 10^{18}$ cm⁻³. The electrical properties of samples were measured by Hall analysis in the van der Pauw configuration at a room temperature, using a direct current of 0.01 mA in a magnetic field of 0.5 T. The Hall data were compiled employing both negative and positive currents and magnetic fields and the results were averaged. In all cases, the size of the substrates was 10×10×2 mm. Aluminum and gold contacts to the n- and p-layers, respectively, were deposited at a substrate temperature of 200°C in a VUP-5 vacuum system. The hole concentration of the N-doped p-type ZnO films was $\sim 4 \times 10^{17}$ cm⁻³, and the hole mobility was ~ 0.9 cm²/Vs as demonstrated by Hall effect measurements. The activation energy of the nitrogen acceptor was obtained by temperature-dependent Hall-effect measurement and equals about 145 meV. The emission peak of 3.312 eV is observed in the photoluminescence spectra at 4.2 K of N-doped p-type ZnO films, probably neutral acceptor bound. The nature of donor-acceptor band of 3.23 eV and green band is discussed.

The Kinetic Effects, Caused by Thickness Fluctuations of Quantum Semiconductor Wire

Ruvinskii M.A., Ruvinskii B.M., Kostyuk O.B.

Vasyl Stefanyk Precarpathian National University, Ivano-Frankivsk, Ukraine

In thin semiconductor wire quantization of electron energy spectrum leads to quantum size effects, which are found in the kinetic parameters of quasi-one-dimensional system, which are depended also on the mechanism of carriers scattering. In modern nanoelectronics technologies can not, generally speaking, ignore the influence of random field associated with fluctuations in the thickness of semiconductor quantum wires [1]. The aim of this work is to generalize and refine previous studies [2,3] the proliferation impact of such fluctuations on the basic kinetic characteristics of semiconductor quantum wire.

In this work the model of semiconductor quantum wires with cross sizes, limited by thickness d (in the direction of coordinate axis z) by one-dimensional a potential pit $V(z)$ with infinitely high walls and for the width (towards y) parabolic potential βy^2 ($\beta > 0$) are considered.

According to calculations for wires A3B5 materials (eg, GaAs [1,2,3]) and A4B6 mechanism of relaxation of charge carriers at random roughness of boundaries is essential at low temperatures $k_B T < \hbar^2 / 4m\Lambda^2$ for clean enough samples and nanometer thicknesses.

The effects of localization type, which arising in quasi-one-dimensional systems in heavy clutter (or at very high concentrations of impurities) which can not be explained within the theory of weak scattering in our work are not considered. So we obtained temperature dependence of conductivity significantly different from the consequences of the theory of localization.

Based on the expressions of the relaxation time of charge carriers, conductivity, thermoelectric power and thermal conductivity of quantum semiconductor wire are shown that the mechanism of relaxation is caused by a random field Gauss fluctuations in the thickness of wire may be effective for sufficiently thin and clean wire from the material A3B5 and A4B6 in thicknesses of nanometric size. The possibility of increasing some kinetic parameters of quasi-one-dimensional systems is revealed.

1. P.K. Basu, P. Ray. Calculation of the mobility of two-dimensional excitons in a GaAs/ $Al_xGa_{1-x}As$ quantum well // *Phys. Rev. B* – 1991 –V. 44, №4 – P. 1844-1849.
2. M.A. Ruvinskii, B.M. Ruvinskii. On the influence of thickness fluctuations on the static electroconductivity of quantum semiconductor wire // *FTP* – 2005 – V. 39, №2 – P. 247-250.
3. B.M. Ruvinskii M.A. Ruvinskii. The effect of thickness fluctuations on the static electrical conductivity of a semiconductor quantum wire//*Semiconductors* – 2005 –V. 39, №2 – P. 231-234

Features of Carrier Transport Mechanism for Ohmic Contacts to Indium Nitride

Sai P.O., Shynkarenko V.V.

V.E. Lashkaryov Institute of Semiconductor Physics, Kiev, Ukraine, sajpasha@gmail.com

In spite of the extremely fast development of the microelectronic devices based on III-Nitrides, the potential of these semiconductors is far from being exhausted. Indium Nitride (InN) holds a special place in this group due to its narrow band gap and superior electric properties. Experimental realization of these predominant features faces severe difficulties mainly caused by growth of InN films with high defect density that effects on ohmic contact formation.

For investigation of transport mechanism the Pd/Ti/Au metallization layers were deposited on heated semiconductors films to 300°C in vacuum. At the last step TLM patterns were formed for contact resistivity measuring.

The experimental temperature dependence of contact resistivity (ρ_c) is shown in Fig. 1 (dots). Its behavior differs significantly from the typical dependences $\rho_c(T)$ for non-rectifying (ohmic) Schottky contacts in the entire range of temperature measurements 100 – 380 K. As in our previous study [1] of such type ohmic contacts to InN with free electron density $2 \cdot 10^{18} \text{ cm}^{-3}$ the increasing dependences $\rho_c(T)$ were explained by current flow through dislocations associated with metal shunts at lower temperature down to 4.2 K.

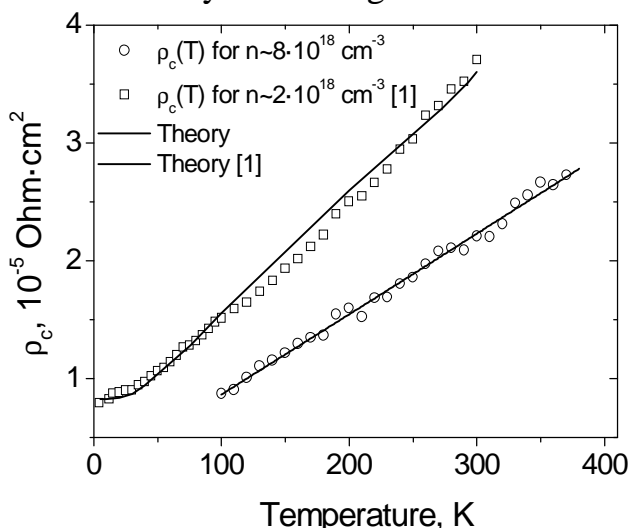


Fig.1. Temperature dependencies of contact resistivity $\rho_c(T)$: dots – experimental data, line – theory

Good agreement between theoretical and experimental dependences is achieved in wide temperature range from 4.2 up to 380 K at different free electron density. In this case the flowing current is limited by the total resistance of the metal shunts and the density of conductive dislocations is $\sim 8.8 \cdot 10^9 \text{ cm}^{-2}$. High dislocation density was confirmed by X-ray diffraction method, the total density of screw and edge dislocations in the structure exceeds $9 \cdot 10^9 \text{ cm}^{-2}$.

Consequently we obtained ohmic contacts to InN films with high defect density that currently are crown by modern epitaxial technology. It was shown that the increasing dependences of the contact resistivity can be explained by current flow through dislocations associated with metal shunts.

1. Sachenko A. V., et al. Temperature dependences of the contact resistivity in ohmic contacts to n+-InN // Semiconductors – 2015. – 49(4). – P. 461-471.

On the Possibility of the Size-Independent Temperature Hysteresis of the First Order Phase Transition in a Nanoscale Metallic Powder

Shirinyan A.¹, Bilogorodskyy Y.^{2,3}, Makara V.^{1,3}

¹ *“Physical-chemical materials science” center of Kyiv Taras Shevchenko National University and National Academy of Sciences of Ukraine, Physics Faculty, Kyiv, Ukraine*

² *Cherkasy regional ecological-naturalistic center, MA of Sciences, Cherkasy, Ukraine*

³ *Department of metals physics, Kyiv Taras Shevchenko National University, Kyiv, Ukraine*

The work presents the description of the evolution of a nanoscale powder during the thermal cycling treatment and the first order phase transition. For example of $\gamma\text{-Fe}\rightarrow\alpha\text{-Fe}$ transformation in the temperature cycling interval $800\text{K}\leftrightarrow 1450\text{K}$ one obtains the thermal hysteresis (temperature difference of forth and back transitions).

Such hysteresis is determined by the superposition of the size-dependent kinetic hysteresis on the size-dependent thermodynamic hysteresis [1]. It is shown that the thermal "thermodynamic" hysteresis arises due to the asymmetry of transforming paths of the nanosystem with respect to the initial conditions, kinetic constraints on the transition modes, different probabilities of forth and back transitions and multiple states separated by different energy barriers [2].

It results three different cases of the size dependence of the width of the hysteresis loop of the new phase volume fraction. For the first time the possibility of a weak size effect or its absence in the case of the compensation of kinetic and thermodynamic hysteresises is substantiated. The correlations between the size of the nanopowder particles, cycling rate and the width of the hysteresis loop of the volume fraction of the new phase exhibit a logarithmic dependence.

Literature

- [1]. **Shirinyan, A.** (2015): Two-phase equilibrium states in individual Cu-Ni nanoparticles: size, depletion and hysteresis effect / Beilstein Journal of Nanotechnology, Vol. **6**, 1811-1820.
- [2]. **Shirinyan, A., Bilogorodskyy, Y.** (2009): Size-induced thermal thermodynamic hysteresis in nanopowder undergoing structural transitions – from particular case to general behaviour. / Journal of Phase Transitions, **82**, 551-565.

Gold Nanofilms and Surface Plasmon Resonance Excitation for Investigation of Bioobjects

Shynkarenko O.V.¹, Beketov G.V.¹, Wojnarowska R.², Prohorenko S.V.^{2,3},
Shergii E.M.²

¹*V. Lashkaryov Institute of Semiconductor Physics, NAS of Ukraine, Kyiv, Ukraine,*
gbeketov@isp.kiev.ua

²*Center for Microelectronics and Nanotechnology, University of Rzeszów. Rzeszów, Poland*

³*Lviv Polytechnic National University. Lviv, Ukraine*

Gold nanofilm placed at the interface can promote surface plasmon resonance excitation under conditions of total internal reflection. In the surface plasmon resonance (SPR), a polarized light beam is reflected from the interface of a noble metal surface and an adjacent dielectric layer at an angle exceeding to the total internal reflection angle.

Within this reflection process, a certain part of the light energy is coupled into an evanescent field that excites longitudinal charge density fluctuations of the free electron gas of the metal layer (surface plasmon waves) and propagates into the proximate dielectric medium with a decaying length of a few hundred nanometers.

The incident angle of the light beam under which a maximum excitation of the surface plasmon waves occurs (surface plasmon resonance angle) is dependent on the wavelength of the exciting light source and the refractive index of the dielectric medium at the interface. Therefore, variation of the optical properties and by this a change in refractive index of this dielectric layer will produce a measurable sensor response as a change of the reflected light intensity.

The SPR effect results in enhancement of the electromagnetic field strength thus intensifying the light scattering.

Results of investigation of the bioobjects using SPR excitation on gold nanofilms are presented.

O.V. Shynkarenko gratefully acknowledges partial support provided by the Swiss National Science Foundation (SNSF, Bern) under grant No. IZ73Z0_152661 (SCOPES).

Structure and Properties of CdSb and ZnSb Thin Films Obtained by High Frequency Cathode Sputtering

Strebezhev V.V., Pylypko V.G., Kleto G.I., Yuriychuk I.M., Strebezhev V.M.

Chernivtsy National University, Chernivtsi, Ukraine

The method of high frequency cathode sputtering was used to obtain a number of thin film CdSb(ZnSb)-Cd_{1-x}Mn_xTe and CdSb(ZnSb)-In₄(Se₃)_{1-x}Te_{3x} heterojunctions. CdSb and ZnSb compounds have strongly different partial vapor pressure of the components and decompose when spraying in a vacuum. Therefore, deposition of CdSb and ZnSb thin films have been carried out in an atmosphere of Ar at high frequency power of 10-30 W, substrate temperatures was of 100°-160° C, and deposition rate was of 4-6 Å/s. The thickness of the grown films was of 0.8-1.5 microns. Electron diffraction studies showed that quasi amorphous, polycrystalline, or textured films are obtained depending on the power of high frequency cathode sputtering.

The transformations of shape and size of grains, nonequilibrium states such as stable and metastable phase modifications, structural disturbances of crystal perfection under laser pulse have been studied by SEM and AFM. The mechanism of the formation of large crystallites after the laser action on CdSb and Cd_{1-x}Zn_xSb films due to coalescence of nanometer size grains has been established (Fig. 1). The method of electron probe microanalysis was used to study the distribution of precipitates and conditions for obtaining stoichiometric films.

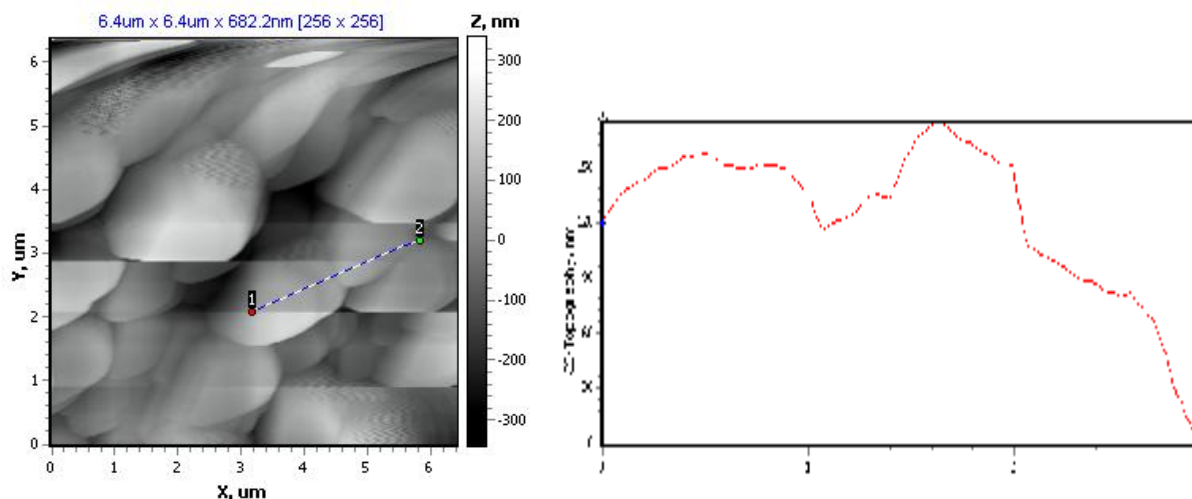


Fig.1. The structure of CdSb film after laser treatment (YAG-laser: $\lambda=1.06 \mu\text{m}$, $\tau=1.5 \text{ ms}$, $E=0.6 \text{ J/cm}^2$).

Spectral characteristics of photosensitivity and electrical I - V and C - V characteristics of obtained thin film CdSb-Cd_{1-x}Mn_xTe and CdSb-In₄(Se₃)_{1-x}Te_{3x} heterojunctions were studied.

Models of Native Defects in Thermally Annealed n-InSb Single Crystals

Sukach A.V., Tetyorkin V.V., Tkachuk A.I.¹, Trotsenko S.P.

V. Lashkaryov Institute of Semiconductor Physics, NAS Ukraine

¹*V. Vinnichenko Kirovograd State Pedagogical University, Ukraine*

The *p*-type conversion was observed in n-InSb single crystals subjected to furnace annealing at rather low temperatures [1]. The nature of this phenomenon is not clear so far. It is well known that the most important native point defects in InSb semiconductors are vacancies, interstitials, antisites and antisite pairs. Generally, In_{Sb} antisites can be neutral, singly and doubly negatively charged defects. Accordingly, Sb_{In} antisites can be neutral, singly and doubly positively charged ones. Due to small band gap of InSb can limit the formation of charged defects, only the neutral and -1 charge states for In_{Sb} and the +1 and neutral charge states for Sb_{In} are possible. Sb_{In} antisites are more stable than In_{Sb} under Sb-rich condition, whereas under In-rich condition In_{Sb} antisites are favored over Sb_{In}. The antisite pairs In_{Sb}-Sb_{In} are assumed to be neutral. The formation energies for In_{Sb} and Sb_{In} antisites under stoichiometric condition are 1.46 and 1.29 eV, whereas formation energies of In and Sb vacancies for the same condition are 2.57 and 1.69 eV, accordingly [2,3].

Obviously, Sb vacancies can not be responsible for the conductivity type conversion due to donor-like nature. In order to explain experimental data it has been assumed that vacancies generated due to evaporation and segregation of volatile component (Sb) are unstable with respect to formation of In_{Sb} antisites, which are acceptors in InSb. Antisite defects more easily generate at the surface resulting in the band bending and formation of an accumulation layer. This leads to suppression of recombination of minority carriers (electrons) at the surface and to increase of photoresponse in the annealed samples [1]. The density of antisites is estimated to be of the order of (2-4) 10¹⁴ cm⁻³ in samples annealed at 300, 370 and 400 °C for 30 min.

1. Stariy S.V., Sukach A.V., Tetyorkin V.V., Yuhymchuk V.O., Stara T.R. Effect of thermal annealing on electrical and photoelectrical properties of n-InSb // SPQEO.- 2017.- 20, N7.- P.105-109.
2. Chroneos A., Tahini H.A., Schwingenschlögl U., and Grimes R.W. Antisites in III-V semiconductors: Density functional theory calculations // J. Appl. Phys. – 2014.- **116**, N2.- P. 023505.
3. Tahini H.A., Chroneos A., Murphy S.T., Schwingenschlögl U. and Grimes R.W. Vacancies and defect levels in III–V semiconductors // J. Appl. Phys. -2013.- **114**, N6.- P. 063517.

Nature of the Conductivity Dispersion of the Lithium-Iron Spinel Substituted by the Rare Earth Elements

Gasyuk I.M., Sulym P.O.

Vasyl Stefanyk Prekarpathian University, Ivano-Frankivsk, Ukraine, sulympo@gmail.com

Spinel lithium ferrites have a wide range of applications, mainly in the electronics and telecommunications industry because of their universal electrical and magnetic properties. However, in the literature there is almost absent the information about the research spinel lithium-iron alloy doped by the rare earth elements (REE). Although, as you know, even a slight substitution of spinel ferrite REE leads to structural deformation of the crystal lattice, thereby the rise of the electrical and magnetic parameters [1]. Furthermore such systems are interesting in terms of their practical application. In this work the frequency dependence of conductivity spinel with structure $\text{Li}_{0.5}\text{Fe}_{2.475}\text{Ln}_{0.025}\text{O}_4$, ($\text{Ln} = \text{Pr}, \text{Eu}, \text{Ho}, \text{Er}$). For all samples there are observed variance conductivity as shown in Fig. 1.

In the frequency region $f \leq 10^3$ Hz the conductivity is almost independent of frequency to Pr substituted spinel and undoped lithium ferrite. However, at $f > 10^3$ Hz it is observed the frequency dependence of conductivity for these systems. Also, there is a monotonic increase in conductivity across the frequency range for systems substituted by *Eu*, *Ho* and *Er*. Such dispersion can be explained by Kups' theorem. According to this theorem the obtained structure can be seen as a multilayer capacitor in which the grains and grain boundaries have different properties. From these characteristics, it follows that for some samples the effect of the multilayer capacitor increases with frequency only above a certain frequency ($f > 10^3$ Hz), and for the other samples it has a permanent character and as a result of this the conductivity is increased.

1. Ravinder D, Kumar K, Balaya P 2001 High-frequency dielectric behavior of gadolinium substituted Ni-Zn ferrites Mater. Lett. **48** 210–214.

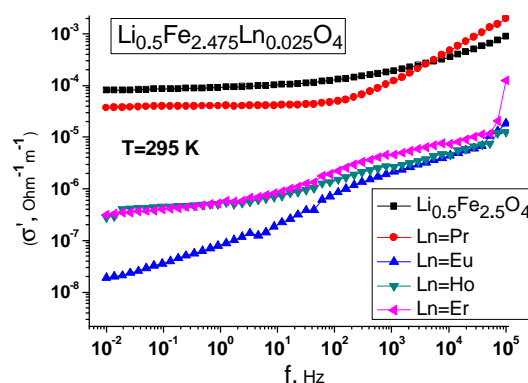


Fig. 1. The dependence of the real part conductivity (σ') of the frequency of systems $\text{Li}_{0.5}\text{Fe}_{2.475}\text{Ln}_{0.025}\text{O}_4$, ($\text{Ln} = \text{Pr}, \text{Eu}, \text{Ho}, \text{Er}$).

Composite Thin Films Based on Lead Chalcogenides

Tur Yu.V., Virt I.S.

Ivan Franko Drohobych State Pedagogical University, Drohobych, Ukraine

tur2014@meta.ua

In recent years, thermoelectric effects get increasingly practical application. The unique set its parameters thermoelectric generators created on its basis are used in space, underwater and land equipment [1].

Efficiency of using the thermoelectric material is primarily determined by its ability to achieve high values of thermoelectric good quality [2]:

$$ZT = \frac{\sigma S^2 T}{k}$$

Here σ – specific electrical conductivity, S - Seebeck coefficient, thermal conductivity, $T = (T_1 + T_2) / 2$ - working or average temperature (T_1 and T_2 – temperatures of hot and cold contacts, respectively), k - thermal conductivity.

Compounds $A^{IV}B^{VI}$ are perspective semiconductor materials for making thermoelectric devices that operate at temperatures ranging from room temperature to 800-900K. PbTe favorably differ from the plumbum chalcogenides by its properties [3].

Not less important factor in determining efficiency of thermoelectric materials, and in this case of plumbum telluride (PbTe), is a thermoelectric power:

$$P = S^2 \sigma$$

Thin films of PbTe with inclusions of Bi_2Te_3 were used for research [3]. To prepare the targets of PbTe and Bi_2Te_3 the elements Bi, Te and Pb semiconductor purity 4N (99.999%), which in stoichiometric ratio were placed in evacuated quartz containers, were used. Target material deposited on the heated to 180-220 ° C single crystal substrates Al_2O_3 (0001) and since fresh KCl or NaCl (001).

- [1] Freik D. M., Galushchak M. O., Krynytskyi O. S., Matkivskyi A. M. New nanocomposite thermoelectric materials // Physics and Chemistry of Solid - 2013 - T.14, №2 - P.317.
- [2] Virt I. S., Kurylo I. V., Rudyi I. O., Lopatynskyi I. E., Fruzhynskyi M. S. Structure and electrical properties of thin films Bi_2Te_3 , Sb_2Te_3 i Bi_2S_3 and uperstructures $Bi_2Te_3 - Sb_2Te_3$, received by pulsed laser deposition // Visn. Nat. Univ. "Lviv Polytechnic". - 2007. - № 592: Electronics. - P. 115-121.
- [3] Pei Y.-L. Electrical and thermal transport properties of Pb-based chalcogenides: PbTe, PbSe, and PbS / Y.- L. Pei, Y. Liu // Journal of Alloys and Compounds. - 2012. - number 514 - P. 40 - 44.

Interfacial Superconductivity in A^{IV}B^{VI} Semiconductor Heterostructures

Yuzepovich O.I.^{1,2}, Bengus S.V.^{1,2}

¹*B.Verkin Institute for Low Temperature Physics and Engineering of NAS of Ukraine, Kharkiv, Ukraine*

²*International Laboratory of High Magnetic Fields and Low Temperatures, Poland Academy of Sciences, Wroclaw, Poland,
e-mail: yuzepovich@ilt.kharkov.ua*

We review complex investigations of the interfacial superconductivity in the PbTe/PbS, PbTe/PbSe, and PbTe/YbS heterostructures. Superconductivity of these heterostructures is an unusual property, because the individual semiconductor films are not superconductors. The “joining” of the crystal lattices of the semiconductors occurs through the formation of a periodic grid of misfit dislocations at the interface. It is shown that we deal with dislocation-induced superconductivity at the interface.

We discuss the superconducting properties of multilayers and two-layered heterostructures and demonstrate the dependence of superconducting properties on the samples’ structure. It is shown that the dimensionality and the period of the interfacial superconducting nanostructures can be changed by the choice of semiconductors, the thickness of the semiconductor layers, and by their number. It is possible to produce: arrays of quantum dots with single Josephson weak links; continuous superconducting nano-nets, quasi-3D structures – multilayers.

New investigations in high magnetic fields show the possibility of the realization of the magnetic field induced superconductor-insulator transition.

1. Yuzepovich O.I. et al. Interfacial superconductivity in bilayer and multilayer IV–VI semiconductor heterostructures // *Low Temp. Phys.* – 2008. – V.**34**. – p.985.

2. Bengus S.V., Sipatov A.Yu., Yuzepovich O.I. Suppression of superconductivity by strong magnetic fields in PbTe/PbS heterostructures with a superconducting interface // *Low Temp. Phys.* – 2013. – V.**39**. – p.695.



ORAL REPORTS

Session 4

Thin film compounds for electronic devices, nanoelectronics



The Formations and Characteristics of Nanocomposite Materials Based on Nanoparticles of 2D Layered Crystal InSe and GaSe and Solid Me(NO₃) Ion Salts (Me K, Na, Rb, Cs)

Bakhtinov A.P., Kovalyuk Z.D., Vodopyanov V.N., Tkachuk I.G.,
Netyaga V.V.

*Institute for problems of materials science. And. M. Frantsevich of NAS of Ukraine, Chernivtsi
Department, Chernovtsy, Ukraine, E-mail: chimsp@ukrpost.ua*

For the manufacture of nanocomposites based on ionic MeNO₃ salts (Me=K,Na,Rb,Cs) and 2D nanoparticles of InSe and GaSe used the results of studies of ionic self-organization of nanostructures on van der Waals surfaces of layers of oxides of In and Ga in the implementation of the melts of the ionic salts in the space between the layers of these crystals . Taking into account : different wetting by molten ionic salt crystal surfaces with molecular linkages and surfaces of oxides, which is due to different values of the surface energy of the interphase boundaries; thermal decomposition of ionic molten salts according to the chemical reaction $2 \text{MeNO}_3 = 2 \text{MeNO}_2 + \text{O}_2\uparrow$ and burnim is accompanied by release of molecular oxygen, which creates excessive pressure on the layers of crystal and oxidizes their surface; the processes samospravny ion salts in the wetting of nanoscale oxides; the formation nanoni composites type “oxide-ion salt ”with high ionic conductivity at the boundaries of 2D nanoparticles. The structure, composition and morphology of oxides and ionic nanostructures was studied by x-ray diffraction, optical spectroscopy, x-ray photoelectron spectroscopy, scanning atomic force and tunneling microscopy. It is established that the thickness 2D of the nanoparticles (~tens nm) is determined by the processes of the stages of implementation of the melts between the layers of crystals, and their lateral dimensions – deformation processes in pyramidal planes of the crystals. It is established that the oxidation only covers the individual layers of the crystal InSe in places of penetration of ionic melts. This allows you to create heterogenic between the oxide and the semiconductor, with a minimum concentration of defects, which reduces electron scattering and increases mobility in 2D nanoparticles. Ion electrical properties of nanocomposites are determined by the formation of the electric double layer, which is formed according to an electrochemical concept ions of solid electrolyte and electrons in the oxidized 2D nanoparticles. When under constant stress there is an effect of the field, which can lead to electrostatic doping of the semiconductor surface and affects the energy barriers for heterogenized, that is, the conductivity of these materials.

Effect of Thermocycling on Electrical Properties of InSb MOS Structures

Beketov G.V., Sukach A.V., Tetyorkin V.V., Tkachuk A.I.¹, Trotsenko S.P.

V. Lashkaryov Institute of Semiconductor Physics, Kyiv, NAS Ukraine

¹*V. Vinnichenko Kirovograd State Pedagogical University, Kropivnitskiy, Ukraine*

The surface of active regions in InSb photodiodes are usually passivated using thin layers of anodic oxide (AO). Since operation of InSb photodiodes includes multiple thermal cycling, the important problem is to study its effects on electrical properties of MOS structures. AO was grown on the surface of (100) InSb substrate with electron concentration $(1-2) \cdot 10^{14} \text{ cm}^{-3}$ at $T=77 \text{ K}$ using an electrolyte of 0.1N KOH in a mixture of 90% ethylenglycol and 10% H_2O . Anodization was carried out in two steps. At the first step the AO was grown in a galvanostatic mode at a current density $0,1 \text{ mA/cm}^2$ until voltage 28 V on the electrochemical cell has been reached. At the second one, potentiostatic step anodization was continued at 28 V until anodic current drops down to $\sim 10 \mu\text{A/cm}^2$. The thickness of deposited AO layers was about 450 nm. Indium electrodes with diameter of 0.75 mm were deposited on the surface of AO. The investigated structures were thermocycled between 77 K and 300 K for 40 complete cycles. The thermocycle includes fast cooling down to 77 K and slow warming to room temperature. After each of ten thermocycles the current-voltage characteristics were measured. It is found that the thermal cycling results in increase of dark current from $\sim 5 \cdot 10^{-7}$ to $\sim 3 \cdot 10^{-4} \text{ A}$ at a bias voltage of 1 V at temperature 77 K. The most rapid change of current was observed at the initial stages of thermal cycling. At the bias voltage less than 0.7 V the current was not dependent on the polarity of the applied voltage. At higher voltages rectifying effect was observed for negative polarity of bias voltage applied to In electrode. The measured characteristics were linearized in Schottky coordinates $\ln I - U^{1/2}$. For positive polarity of applied bias linear $I-U$ dependences were observed. After forty thermocycles temperature dependences of dark current were measured at fixed bias voltages of different polarity. The activation dependences were observed with energies of 55 meV and 120 meV at temperatures 120-150 K and 77-95 K, respectively. Experimental evidences were obtained for electron conductivity type of anodic oxide, comprising In_2O_3 component, as well as ohmic behaviour of In contacts. The nature of the dark current increase in the investigated structures under thermal cycling is discussed.

The Dependence Between Lithium Diffusion Coefficient in the Spinel Structure and the Discharge Current Value

Boichuk A.M., Gasyuk I.M., Ilnitsky R.V.

Vasyl Stefanyk Precarpathian National University, Ivano-Frankivsk, Ukraine

Materials with spinel structure are successfully used in lithium batteries and hybrid electrochemical systems. Important is their ability to work under conditions of high power. This is possible subject to high conductivity and stable single phase spinel structure. In the case of lithium-manganese spinel it can be achieved by iron substituting. This paper describes the study of spinel $\text{LiMn}_{1.95}\text{Fe}_{0.05}\text{O}_4$ in aqueous electrolyte at different currents by galvanostatic intermittent titration technique (GITT).

This nanosized spinel was synthesized by sol-gel method and was annealed at the temperature of 1070 K. On its basis, anode mixture was formed (75% - spinel, 25% - carbon black). Electrochemical measurements were conducted using a cell with three electrodes in an aqueous electrolyte based on Li_2SO_4 . The experiment included a discharge of cell (20 s) and its relaxation during 60 s.

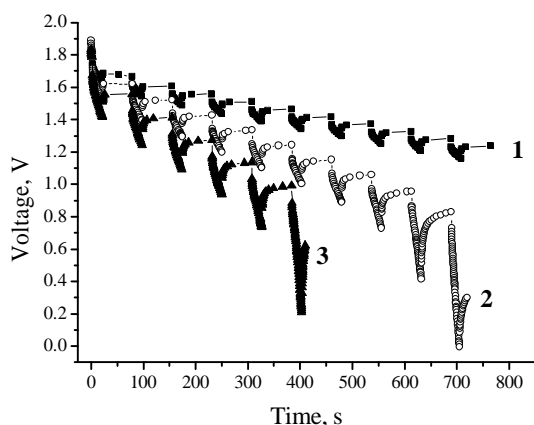


Fig. 1. GITT - curves for different discharge currents impulse (1- 1C, 2- 2C, 3- 3C)

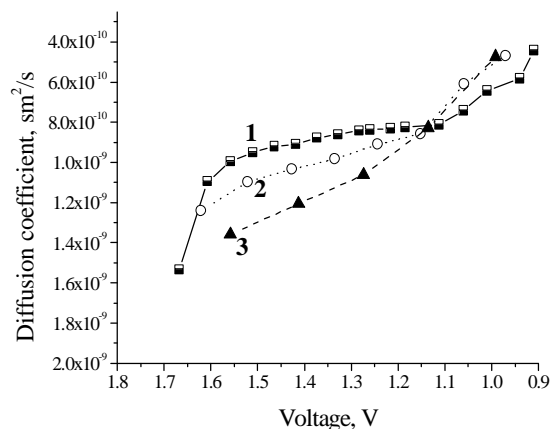


Fig. 2 The dependence between diffusion coefficient and the voltage at various currents

Increasing of discharge current value leads to growth of potential recession and its relaxation. Stability of these values saved up to cell voltage 0.8 V regardless of the current density (fig. 1). We can assume, that in this voltage ends the intercalation process and begins the drawdown of lithium ions on the spinel surface. Even at a current of 3C calculated value of lithium diffusion coefficient in aqueous electrolyte is $(5 \cdot 10^{-10} - 2 \cdot 10^{-9}) \text{ cm}^2/\text{s}$. Such high values allow to use spinel as electrode materials for electrochemical systems with high power density.

Electronic Parameters of a New Thin Film Composition for Kesterite Solar Cell

Klochko N.P., Khrypunov G.S., Kopach V.R., Lukianova O.V.,
Lyubov V.M. , Kirichenko M.V.

*National Technical University “Kharkiv Polytechnic Institute”, Kharkiv, Ukraine,
E-mail: klochko_np@mail.ru; klochko.np16@gmail.com; khrip@ukr.net*

Currently, a quaternary compound kesterite $\text{Cu}_2\text{ZnSnS}_4$ (CZTS) has drawn much renewed interest as a potential candidate to meet a global energy demand on a terawatt scale. $\text{Cu}_2\text{ZnSnS}_4$ is a *p*-type semiconductor with a direct bandgap of 1.4–1.5 eV and an absorption coefficient $\sim 10^4 \text{ cm}^{-1}$. Besides it, CZTS contains only earth-abundant and non-toxic elements and its thin films can be fabricated by using relatively inexpensive processes. A generally accepted view is that the not high efficiencies of the best CZTS solar cells (9.66 %) indicate that the current status of their fabrication is far from optimum. So, the preparation of the device quality $\text{Cu}_2\text{ZnSnS}_4$ films by a simple and low-cost technique is of great importance for photovoltaic applications. Presently, there is no consensus on the best way to prepare CZTS thin films. In this work new thin film composition for kesterite solar cell on the base of *n*-ZnS/*p*- $\text{Cu}_2\text{ZnSnS}_4$ heterojunction has been successfully made using inexpensive and suitable for large-scale production liquid-phase methods. Investigation of dark current-voltage characteristics of Al/ZnS/ $\text{Cu}_2\text{ZnSnS}_4$ /Mo/Al has shown that nanograin SILAR-deposited $\text{Cu}_2\text{ZnSnS}_4$ layer effectively prevents shunting of the main kesterite layer obtained by sulfurization of the electrodeposited Cu/Sn/Zn stack precursors and allows obtaining of the rectifying barrier structure. Diode and electronic parameters calculated on the basis of the sets of current-voltage and capacitance-voltage characteristics confirm the promise of this approach for creating of efficient semiconductor device structure. Additionally, suitable crystal structure and optical properties of nanograin SILAR-deposited ZnS and kesterite layers enable the use of such heterojunction in thin film kesterite solar cell that can efficiently absorb sunlight and transform its energy into electricity. The work shows the results of analysis of diode characteristics of the developed ZnS/ $\text{Cu}_2\text{ZnSnS}_4$ heterostructures (series resistance R_s , shunt resistance R_{sh} , ideality factor n_d and the saturation current densities J_o). Other investigated electrical and electronic parameters obtained from the current-voltage (*I-U*) and capacitance-voltage (*C-U*) characteristics are the electrical resistivities ρ_{CZTS} and ρ_{ZnS} , the ZnS/ $\text{Cu}_2\text{ZnSnS}_4$ rectifying barrier Φ , the height φ of symmetrical double Schottky barriers in the grain boundary regions in the polycrystalline kesterite layers, the width of the electron depletion regions ω , the concentration of the fully ionized donor impurity N_d in *n*-ZnS and acceptor impurity N_a in *p*- $\text{Cu}_2\text{ZnSnS}_4$, the density N_{SS} of the surface states in the kesterite layers.

Structure and Optical Properties CdS and CdTe Films on Flexible Substrate Obtained by DC Magnetron Sputtering for Solar Sells

Kopach G.I., Mygushchenko R.P., Khrypunov G.S.,
Dobrozhan A.I., Harchenko M.M.

National Technical University «Kharkiv Polytechnic Institute», Kharkiv, Ukraine

Thin-film solar cells based on CdS/CdTe heterosystem of are prospective for an industrial production and large-scale ground application. One of the economical and high-tech methods for obtain thin films is direct current magnetron sputtering (DC magnetron sputtering). However, there are some technological problems during the deposition of semiconductor films by this method. They are caused by low conductivity of CdS and CdTe pressed powder targets and sufficiently low emission ability of these materials. Therefore at first the influence of physics and technological condensation modes by the method of DC magnetron sputtering on the structure and optical properties of CdS and CdTe films on a glass substrates was studied.

The laboratory method of DC magnetron sputtering with preheating of the target for CdS and CdTe films on glass substrates was developed. The band gap in obtained hexagonal CdS films is $E_g=2,38-2,41$ eV. Optical transparency of CdS films is 80-90%, which allows to use such films as a transparent window layer in solar cells based on heterojunctions of CdS/CdTe.

When plasma discharge current density is $2,2-5,4$ mA/cm² and the deposition rate is 200 nm/min., CdTe layers with hexagonal structure up to 5 μ m thick was obtained. The transmittance of CdTe films with hexagonal structure in the wavelength range of the visible spectrum is up to 5%, and in the infrared spectral range is about 60%. The band gap in obtained CdTe layers of different thickness is 1,52-1,54 eV. After the Cl treatment with subsequent annealing in air at $T=430^0$ C for 25 min. as a result of the phase transition wurtzite-sphalerite investigated CdTe films contain only the stable cubic structure. Value of lattice constant is $a = 6,4905$ Å, that less than by 0,2% deviate from the tabular value. Such CdTe films can be used as a base layer of solar cells based on heterojunctions of CdS/CdTe.

The influence of the technological DC magnetron sputtering modes of CdS/CdTe heterosystem deposited on flexible substrates on the output parameters of solar sells is studied. It is shown that the preliminary cooling of the CdS layer and its transfer to the air before deposition of the CdTe layer leads to an increase in the open circuit voltage and the fill-factor of the illuminated UI-characteristic and decreasing the series resistance of the solar cell. As a result, the efficiency of ITO/CdS/CdTe/Cu/Au flexible solar cell on the CdTe base layer increases from 2,6% to 3,1%.

Effect of the Doping Level on the Gas Sensitivity of Si p-n Junctions

Ptashchenko O. O.¹, Ptashchenko F. O.², Gilmutdinova V. R.¹, Kyrnychuk O.S.¹

¹Odessa National I. I. Mechnikov University, Odessa, Ukraine

²National University "Odessa Maritime Academy", Odessa, Ukraine

Si p-n junctions as wet ammonia vapors sensors have a lower threshold of sensitivity than Si nanowires and porous Si membranes. In this work, the characteristics of Si diffused p-n junctions as water and ammonia sensors were experimentally studied over a range of the impurity concentration gradient a from $a_m=1 \cdot 10^{21} \text{ cm}^{-4}$ to $a_M=5 \cdot 10^{23} \text{ cm}^{-4}$.

Adsorption of water and wet ammonia vapors significantly increased the direct and reverse currents of the studied p-n structures. The gas sensitivity of a sample was estimated as

$$S_I = \Delta I / \Delta P \Big|_{V=const}, \quad (1)$$

where ΔI is the change in the current (at a fixed voltage) due to a change ΔP in the corresponding gas partial pressure. The threshold of sensitivity to wet ammonia vapors P_m was estimated from the intersection of $I(P)$ curve with the line $I = I_w = const$, where I_w was the current, measured in saturated water vapors.

The experimental data showed that H₂O and NH₃ molecules adsorption forms an n-conducting channel in the p-region, which shorts the p-n junction. The threshold of sensitivity to wet ammonia vapors P_m increased with the doping level over the whole doping range studied. It can be explained taking into account an neutrality equation for the homogeneous channel section

$$N_{ns} = N_i^+ - N_s^- - N_{sA}^- + N_{sD}^+, \quad (2)$$

where N_{ns} is the free electrons surface density in the channel; N_i^+ is the surface density of adsorbed donor like ions; N_s^- denotes the density of the ionized acceptor surface centers; N_{sA}^- is the surface density of ionized acceptors in the surface depletion layer; N_{sD}^+ is the surface density of ionized donors. It is seen from (2), that the electrons number N_{ns} in the channel decreases by N_{sA}^- growth, i. e. by doping level at a fixed number of adsorbed ions.

At $P > 10$ Pa, the gas sensitivity S_I of p-n structures was practically independent from the doping level. At those pressures, expression (2) reduces to

$$N_{ns} = N_i^+ - (N_s^- + N_{sA}^- + N_{sD}^+), \quad (3)$$

which explains this effect.

The obtained results can be used for the optimization of the gas sensors structure on p-n junctions and nanomaterials.

Yellow Luminescence in High-Power Ultraviolet AlInGaN LED 365 nm

Veleschuk V.P.¹, Vlasenko O.I.¹, Vlasenko Z.K.¹, Khmil' D.N.¹, Petrenko I.V.²,
Tartachnyk V.P.²

*V.E. Lashkaryov Institute of Semiconductor Physics of the NAS of Ukraine, Kyiv, Ukraine
Institute for Nuclear Research, NAS of Ukraine, Kyiv, Ukraine*

Over the last 10 years, ultraviolet (UV) high-power light emitting diodes (LEDs) ($\lambda_{\text{peak}} = 365 \text{ nm}$, $P_{\text{electr}} = 1..3 \text{ W}$) are increasingly used in industry and science. However for AlInGaN structures inherent undesirable tunnel effects, that causes yellow electroluminescence (EL) from defects [1]. Also, UV radiation excites photoluminescence (PL) in themselves AlInGaN structures in the entire visible range, which leads to additional losses of useful UV-radiation. At using UV LEDs for PL excitation such "parasitical" radiation creates problems with adding up to photoluminescence from materials and structures that emit in the same spectral range. Observed EL and PL in the UV LED as a yellow-white light is useful for visualization of UV LED radiation at switching on/off. On the other hand, there is a loss of useful UV radiation.

We found that yellow EL in UV LED $\lambda_{\text{peak}} = 365 \text{ nm}$, $I_{\text{nom}}=350 \text{ mA}$ occurs at a voltage of 2.55 - 2.6 V at a current 1 - 5 mA, i.e. before to the switching voltage of UV band ($U = 2,9 \text{ V}$). Up to 2.9 V was observed the yellow band (peak at 560 nm) without the UV band at 365 nm, as in [1]. Yellow EL for UV LED at $T = 77 \text{ K}$ is absent, but with current increasing was observed the appearance of the yellow band with a maximum of 545 nm. For the separation of EL and PL, PL was measured at excitation from other UV LED 365 nm, the measured EL and PL spectra differs.

The appearance of yellow EL in UV LED 365 nm at $T = 77 \text{ K}$ is very similar to the appearance of the red band EL for GaAs_{0,15}P_{0,85}:N/GaP: N, Zn-O light emitting diodes at current increasing at $T = 77 \text{ K}$. In these GaAsP LEDs red band of EL is responsible oxygen and zinc, for the green band - nitrogen atoms.

Thus in the UV-LED a significant role in the yellow luminescence is probably playing the oxygen atoms, because, according to one of the standard, elsewhere accepted model, yellow EL and PL caused by the recombination of shallow donor (for example O, Si) on a deep acceptor (complex $V_{\text{Ga}} - O_{\text{N}}$).

LITERATURE

1. V.T.Shamirzaev, V.A. Gaisler, T.S. Shamirzaev. Edge and defect luminescence of powerful ultraviolet InGaN/GaN light-emitting diodes // Semiconductors (2016) **50**, 1493. doi:10.1134/S1063782616110233.



ORAL REPORTS

Session 5

Functional crystalline materials: growth, physical properties and applications



The Influence of the Dislocation Structure of CdTe Crystals on the X-Ray Intensity Distribution Near the Reciprocal Lattice Site

Fodchuk I.¹, Gutsuliak I.¹, Dovganyuk V.¹, Solodkyi M.¹, Maslyanchuk O.¹, Roman Yu.¹, Safriuk N.², Kladko V.^{2,3}, Barchuk M.³

¹*Yuriy Fedkovych Chernivtsi National University, Chernivtsi, Ukraine, ifodchuk@ukr.net*

²*Institute of Semiconductor Physics of NASU, Kyiv, Ukraine*

³*Institute of Materials Science, TU Bergakademie Freiberg, Freiberg, Germany*

Cadmium telluride (CdTe) is one of the most promising materials for highly efficient detectors of X- and γ -radiation working without cryogenic cooling with sensitivity extended to the region of high photon energies compared with Si detectors [1,2]. The series of MoO_x/p-CdTe (111)-oriented heterostructures with different degrees of imperfection manufactured by reactive magnetron sputtering was chosen for our research. The experimental investigations in different X-ray diffraction geometries (symmetrical 333, forbidden 222 reflections as well as asymmetrical one 331) were performed on Philips X'Pert PRO diffractometer.

The samples are known to possess different types of defects namely dislocation loops, Lomer-Cottrell junction, inclusions etc. Therefore, the simulation of reciprocal space maps (RSM) for (333) and (331) X-ray reflections were performed using the model of real crystal, which contains complexes of structural defects [3]. The influence of this system on the diffraction pattern is comparable to the set of edge dislocations with dislocation lines perpendicular to the surface and different directions of Burgers vector in this plane: $a/2[\bar{1}10]$ and $a/2[110]$. The density of these dislocations was determined as $2.86 \cdot 10^6 \text{ cm}^{-2}$ and $2.38 \cdot 10^6 \text{ cm}^{-2}$. In particular, a case of stacking faults was considered according to which a large dislocation loop restricts the region with small point defects and inclusion of another phase. The characteristic intensity distribution around reciprocal space nod indicates the presence of individual blocks separated by small-angle boundaries with the angle of misorientation about 0.5 degrees.

1. Sordo S.D., Abbene L., Caroli E., Mancini A.M., Zappettini A., Ubertini P. Progress in the development of CdTe and CdZnTe semiconductor radiation detectors for astrophysical and medical applications // *Sensors*. – 2009. – V. 9, №5. – P. 3491-3526.
2. Szeles C. CdZnTe and CdTe materials for X-ray and gamma ray radiation detector applications // *Physica Status Solidi*. – 2004. – V. 241, №3. – P. 783-790.
3. Sun C., Paulauskas T., Sen F.G., Lian G., Wang J., Burma C., Chan M. K. Y., Klie R. F., Kim M. J. Atomic and electronic structure of Lomer dislocations at CdTe bicrystal interface // *Scientific Reports*. – 2016. – V. 6. – doi: 10.1038.

Using of the Improved Model of "Penetrating Core" at Indentation Diamond at High Temperature

Galanov B.A.¹, Milman Yu.V.¹, Ivakhnenko S.A.², Suprun O.M.², Golubenko A.A.¹,
Chugunova S.I.¹

¹ *Institute for Problems of Materials Science, National Academy of Sciences of Ukraine, Kiev, Ukraine, milman@ipms.kiev.ua*

² *Institute for Superhard Materials, National Academy of Sciences of Ukraine, Kiev, Ukraine, alona.suprun@gmail.com*

On the complex of its properties diamond occupies an exceptional position among advanced materials. It is chemically and radiation resistant, extremely firm, therefore there is the prospect for the use of diamond in high-tech areas of science and technology. Indentation of single diamond crystals is a of nondestructive testing method, an effective tool in solving many problems of plastic deformation and fracture, forecasting reliability and brittle fracture. For non-destructive testing in industrial and scientific purposes the main goal is the ability to define complex physical and mechanical properties of the material.

Indentation was conducted on the faces (100) single crystal diamond obtained by the temperature gradient in thermodynamic stability at 900 ° C in the modernized installation VIM-1. Experiments were conducted by the pyramidal indenter with different angles between the axis of the pyramid and its edge ($\gamma_i = 60, 62.5, 65, 67.5$ and 70 degrees). The temperature of 900 ° C is most appropriate for the diamond indentation due to the microplasticity within it.

With improved model of "penetrating core" defined size elastic-plastic zones in the indenter and sample effective angles between the axis of the pyramid and its edge (for indenter and sample), and the borders of their fluidity, characteristics of plasticity and elastic, plastic and total deformation [1]. The value of microhardness and liquid limit increases with decreasing angle at the top of the indenter (with increasing degree of deformation) from 40,46 to 59,56 GPa and 43,28 to 68,23 respectively. Transition to a sharp indenter deformation leads to growth of 4,14 to 8,31%, hence the increase in hardness. Characteristics of plasticity, which is defined using this technique $\delta_H \approx 0,2 - 0,4$ is significantly lower from the critical value (0,9), which is observed macroscopic ductility but sufficient for quality prints hardness.

Using the model of "penetrating core" made it possible to investigate the stress-strain state indenter samples and determine their yield strength and ductility characteristics. It was also investigated strain hardening diamond. The strain curve diamond was built which coordinated tension - total deformation.

1. B. A. Galanov, Yu. V. Milman, S. A. Ivakhnenko, et. al. Journal of superhard materials 38 (5), 289 (2016)

The Composite Thermoelectric Materials Based on Lead Telluride with Nano inclusions of ZnO and TiO₂

Horichok I.V., Lishchynsky I.M., Matkivskyi O.M.,
Dzumedzey R.O., Dron R.P. Potyak V.Yu.

*Vasyl Stefanyk Precarpathian National University, Ivano-Frankivsk, Ukraine,
e-mail: HorichokIhor@gmail.com*

Now very widely used method of pressing the powder for the manufacture of thermocouples, which have number of advantages over the methods of obtaining single-crystal samples. In particular, the method is highly productive and provides examples of different geometric shapes with precisely specified size. For metal tellurides of fourth subgroup important is the fact that the decline of thermo efficiency of pressed samples is small compared to the single crystals. Importantly, that between the pressed sample and the starting materials is virtually no correlation of thermoelectric parameters. This shows the complete reconstruction of defective subsystems of material and in particular, the ability to manage technological conditions by selecting pressing and annealing the samples.

One of the properties optimization pressed samples is used of micro dispersive powder of base material with the addition of powder nano dispersive of other material (usually with higher melting temperature, such as SiO₂, SiC, NC). For such systems increase of thermoelectric figure of merit, primarily caused by the significant decrease in conductivity of the material, due to effective phonon scattering on the nano grains.

In this paper the influence nano dispersive powder ZnO and TiO₂ on thermoelectric properties of PbTe was established. The synthesis of the materials carried out in evacuated quartz ampoules with residual pressure of 10⁻⁴ Pa. Was used the tellurium with main component containing of 99.999% Te and lead - 99.99% Pb. The resulting length of ingots <10 sm and transverse dimensions <1.5 sm ground in an agate mortar and the resulting powder is mixed with the nanoparticle of zinc oxide and titanium dioxin. The content of ZnO, TiO₂ amounted to 3 wt. %. The resulting mixture was compressed under pressure of 1.5 GPa, and the resulting cylindrical samples with d = (5-8) mm and h ≈ (8-12) mm were subjected to annealing at different temperatures in the range T = (200-500) °C.

Found that effect of reducing the thermal conductivity of composites essentially depends on the size fractions of the base material. Furthermore, the addition of nanopowder of ZnO and TiO₂ significantly affects on the conductivity of the material and its microhardness.

Work carried out in the framework of the research project of MES of Ukraine (State registration number 0117U002407).

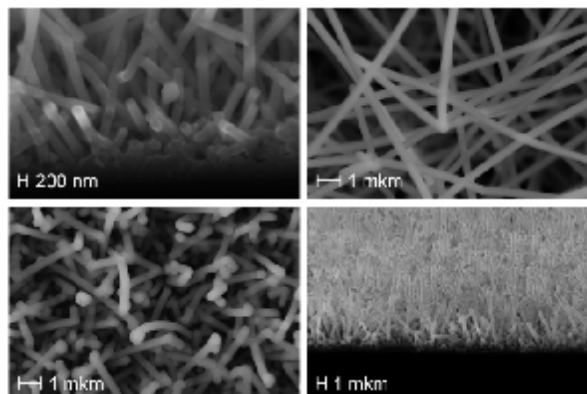
Growth of Silicon Nanowires by Self-Assembled CVD-Technology

Kalashnyk Yu.Yu., Klimovskaya A.I., Oberemok O.C., Pedchenko Yu.M.,
Voroshchenko A.T., Lytvyn P.M.

*Lashkaryovs Institute of Semiconductor Physics, National Academy of Sciences, Kyiv,
Ukraine*

Silicon nanowires (SiNWs) are promising material for applications in micro-, opto- and bio-electronics and information technologies.

We present some features of SiNWs growth technology based on gold enhanced chemical vapor deposition (CVD). The technology used consists of two main stages:



AFM images of SiNWs

1. Formation of growth-seeds, which includes initial refining and treatment of a substrate surface, deposition of a metal film and following its annealing.

2. Growing of nanowires by decomposition of Si-containing gas-molecules at catalytic particle, following transport of rejected silicon atoms through or/and across the catalyst particle and incorporation of Si-atoms into solid phase.

We studied relationship between conditions of the formation of growth-seeds and their composition, morphology, size distribution, density and aggregative state. These peculiarities defined properties of the SiNWs grown on the second stage of the nanowire formation. To grow SiNWs, we used various growth temperature, composition, pressure and flow of gas mixture (silane and hydrogen). To provide one-dimensional growth of nanowires, a special attention has been paid to initial refining the surface of substrate and methods formation of growth-seeds.

In spite of the fact that, a great deal of experimental research has been implemented, there is a lack of good understanding of this phenomenon to exert control over important properties of the system, though it presents the simplest system like gold on silicon substrate. To find the best conditions to grow SiNWs with specified properties, we studied different technological regimes both of growth-seed formation and conditions of SiNWs growth.

The results of our study allow us to grow arrays of SiNWs on the silicon substrate with pre-determined properties (length, diameter, density nanowires).

Semiconductor Diamond Crystallization in Magnesium–Based Systems

Kovalenko T.V., Ivakhnenko S.O, Lysakovskiy V.V.

Institute for Superhard Materials NAS of Ukraine, Kyiv, Ukraine,
tetiana.v.kovalenko@gmail.com

Diamond is attractive material in the science and industrial field, because of its excellent physical and chemical properties. Due to its unique atomic structure diamond materials is widely used in various fields. Nitrogen and boron is the main impurities in diamonds. Doping with boron impurities is an effective way to change electrical properties of diamond. To produce semiconductor diamond at high pressures and temperatures traditionally boron or boron-containing components addition are usually used.

This paper reported the semiconductor diamonds growth in magnesium-based systems without adding of boron or boron-containing components in “toroid” high pressure apparatus (TS-20) at 7,0–8,5 GPa and 1350–2240 °C.

It is shown that in the Mg–C system the boron content in grown crystals increases from $3.4 \cdot 10^{17} \text{ cm}^{-3}$ to $1.1 \cdot 10^{18} \text{ cm}^{-3}$, depending on the growing temperature from 1770 to 2000 °C. It is established that boron content in crystals grown in the Fe–Mg–C system with magnesium content of 30, 50, 70 at. %, increases in the range $(0.68\text{--}1.34) \cdot 10^{17} \text{ cm}^{-3} \rightarrow (1.23\text{--}2.10) \cdot 10^{17} \text{ cm}^{-3} \rightarrow (1.75\text{--}2.86) \cdot 10^{17} \text{ cm}^{-3}$, respectively. Crystals are semiconductors, are of the type IIb and can be obtained without adding of boron or boron-containing compounds to growth system.

Doping of the Fe–C system with Al and Mg in an amount of 7-8 at. % and 10-25 at. %, respectively, allows the application of the temperature gradient method for growing structurally perfect single crystals of type IIa; further increase in magnesium content in this system makes it possible to obtain semiconductor crystals of type IIb.

Boron content in the uncompensated impurity form in single diamond crystals determines the semiconducting properties of crystals grown in magnesium–based systems; the specific electric resistance of such crystals is within the range $(1.4 \cdot 10^7\text{--}2.2 \cdot 10^2) \text{ Ohm} \cdot \text{cm}$.

All these features of the change in the diamond defect-impurity content can be explained by the change in the thermodynamic activity of the main impurities in the diamond crystal lattice (nitrogen and boron) on crystallization front depending on the composition of the growth system and the growing temperature.

The main feature of the change in thermodynamic activity is that boron, which enters as a small amount in the carbon source ($<1 \cdot 10^{-5}$ wt. %), enters the crystal in significant quantities due to an increase in its activity at the crystallization front.

Optical Absorption and Piezoelectric Effect Studies of Single Crystal $\text{AgGaGe}_3\text{Se}_{7.6}\text{Te}_{0.4}$ Solid Solution

Krymus A.S., Ryzhuk A.O., Denysiuk M.I.

Lesya Ukrainka Eastern European National University, Lutsk, Ukraine,
KrymusAS@rambler.ru

The quaternary crystalline compound $\text{AgGaGe}_3\text{Se}_8$ and their derivatives caused recently an enhanced interest [1] due to a high possibility of its use as a material for optically operated piezoelectricity and nonlinear optics. This one opens a possibility to apply it to different quantum electronics and piezoelectric devices [2]. This compound possesses melting temperature equal to about 993K. The space group of the titled crystal is $Fdd2$. The study of $\text{AgGaGe}_3\text{Se}_8$ has shown that these crystals are promising for optoelectronic applications, infrared devices and nonlinear optics. This crystal has perfect optical, electrical, piezoelectric and nonlinearoptical [3] features. Substitution of Ga by In or Ge by Si allows to vary piezoelectric features of the titled single crystals in a wide range of corresponding susceptibilities.

However, up to today, it was not explored a possible influence of Te ions on the complex photoinduced piezoelectric and piezooptical features which are very promising to the presence of delocalized p-TE orbitals. The latter orbitals possess delocalized states which may principally change the delocalization of the electrons and ensure an excellent charge transfer responsible for the corresponding dipole moments and hyperpolarizabilities.

Spectral features of absorption were studied for novel $\text{AgGaGe}_3\text{Se}_{7.6}\text{Te}_{0.4}$ solid state alloys at different temperatures. During increasing of temperature from 100 K up to 300 K, the energy gap of $\text{AgGaGe}_3\text{Se}_{7.6}\text{Te}_{0.4}$ decreases linearly from 2.05 eV up to 1.94 eV at a rate $5,7 \times 10^{-4}$ eV/K. The magnitudes of piezoelectric coefficients are significantly changed and demonstrate substantial anisotropy. At room temperature, these values are equal to 5.2 pm/V (d_{11}), 31.5 pm/V (d_{22}) and 35.5 pm/V (d_{33}). It is crucial that with an increasing temperature the piezoelectric efficiencies are increased. We have explored temperature and laser-induced changes of piezoelectric coefficients.

1. A.O. Fedorchuk, G.P. Gorgut, O.V. Parasyuk, G. Lakshminarayana, I.V. Kityk, M. Piasecki, IR operated novel $\text{Ag}_{0.98}\text{Cu}_{0.02}\text{GaGe}_3\text{Se}_8$ single crystals, *J. Phys. Chem. Solids* 72 (2011) 1354–1357
2. W. Kuznik, P. Rakus, K. Ozga, O. V. Parasyuk, A. O. Fedorchuk, L. V. Piskach, A. Krymus, I. V. Kityk, Laser-induced piezoelectricity in $\text{AgGaGe}_{3-x}\text{Si}_x\text{Se}_8$ chalcogenide single crystals, *Eur. Phys. J. Appl. Phys.* 70 (2015) 30501
3. V. Badikov, K. Mitin, F. Noack, V. Panyutin, V. Petrov, A. Seryogin, G. Shevyrdyaeva, Orthorhombic nonlinear crystals of $\text{Ag}_x\text{Ga}_x\text{Ge}_{1-x}\text{Se}_2$ for the mid-infrared spectral range, *Opt. Mater.* 31 (2009) 590–597

Investigation of the Physical Parameters of the Composition for the Single Crystals System $Pb_{1-x}Sn_xTe_{1-y}Se_y$

Luchytskyi R.M., Nyzhnykevych V.V.

*Ivano-Frankivsk National University of Oil and Gas, Ivano- Ivankivsk, Ukraine,
E-mail: galuschak@nung.edu.ua*

The most important task for solid state physics is to establish a quantitative relationship of physical and chemical properties of crystals on their atomic structure. The search for new IV-VI-like materials with special properties have led to need to obtain multicomponent solid solutions with their ability smoothly and predictably manage their changes by replacing component in both sublattices.

The method for predicting physical properties is required to grow the single crystals of $Pb_{1-x}Sn_xTe_{1-y}Se_y$ solid solution. Such method is an interpolation analysis. With knowing both the properties of binary compounds and the nature of developments in the ternary solid solutions can predict them for any condition of solid solution. And also, the composition of single crystals with desired physical properties.

We have received several expressions to determine the nature of the changes of band gap (1.1), lattice constant (1.2), effective charge (1.3), density (1.4), average atomic weight (1.5), and ionic parameter (1.6) depending on the degree of substitution in isovalent anion (X) and cationic (Y) crystal cell at room temperature:

$$E_g(X, Y) = 0,32 - 0,03Y - 0,5X - 0,39XY \quad (1.1)$$

$$a(X, Y) = 6.46 - 0,3335Y - 0,133X + 0,01XY \quad (1.2)$$

$$g(X, Y) = 0,18 + 0,21Y + 0,15X + 0,15XY \quad (1.3)$$

$$\rho(X, Y) = 8,25 + 0,01Y - 1,80X - 0,281XY \quad (1.4)$$

$$A(X, Y) = 167,4 - 44,255X - 24,32Y \quad (1.5)$$

$$\lambda(X, Y) = 0,39 + 0,05X + 0,07Y + 0,05XY \quad (1.6)$$

All formulas derived assuming a linear change the composition of these parameters in the corresponding ternary solid solutions.

It is need to know the temperature of crystallization for growth of crystals $PbSnTeSe$. In paper was analyzed the crystallization temperature change for compositions that crystallize in the cubic structure. This analysis showed that the solidus curves can accurately describe the quadratic dependence of composition:

$$T_c(X, Y) = 925 - 150X - 97Y + 28X^2 + 252Y^2 + 96XY - 28X^2Y - 406XY^2 \quad (1.7)$$

The temperature curves of solidus for $Pb_{1-x}Sn_xTe_{1-y}Se_y$ system received using formula (1.7).

XPS Studies of Tl_4HgI_6 Single Crystals

Luzhnyi I.^a, Khyzhun O.Y.^a, Parasyuk O.V.^b, Levkovets S.I.^b,
Yurchenko O.M.^b, Piskach L.V.^b

^a Frantsevych Institute for Problems of Materials Science, NAS of Ukraine, Kyiv, Ukraine

^b Lesya Ukrainka Eastern European National University, Lutsk, Ukraine

Tl_4HgI_6 single crystal belongs to a quite large group of compounds A_4BX_6 and was actively studied in recent years. Tl_4HgI_6 exhibits potential applications in ionizing radiation detectors, ionic conductors and temperature sensors.

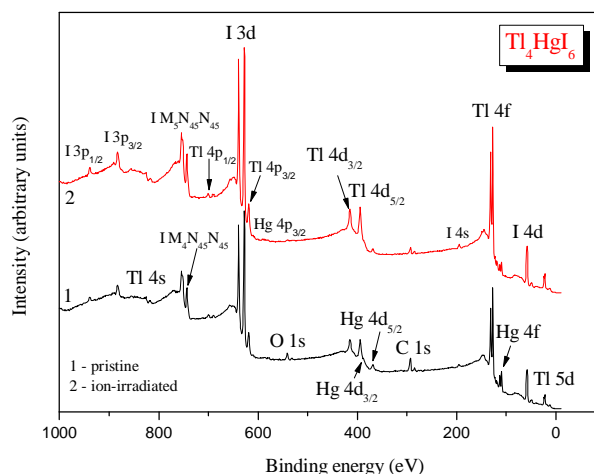


Fig. 1. Survey XPS spectra measured for (1) pristine and (2) Ar^+ ion-bombarded surfaces of the Tl_4HgI_6 single crystal.

In the present work we employ X-ray photoelectron spectroscopy (XPS) to study the electronic structure of pristine and Ar^+ ion-bombarded surfaces of the Tl_4HgI_6 single crystal. The results are presented in Fig. 1. It is obvious that chemical interaction of the Tl_4HgI_6 single crystal surface with oxygen and carbon is very weak during its exposure to air for long time (several weeks). The Ar^+ -bombardment of the Tl_4HgI_6 single crystal surface adopting the technique [1] induced a decrease of the mercury content in the top surface layers by about 29%. This fact indicates that in the Tl_4HgI_6 compound, the chemical Hg-I bonds are substantially weaker in comparison with the Tl-I bonds. Furthermore, the Tl_4HgI_6 single crystal surface is characterized by low hygroscopic nature which is important when handling this compound in optoelectronic or nano-electronic devices applications, working at ambient conditions.

References

[1] O.Y. Khyzhun, M. Piasecki, I.V. Kityk, I. Luzhnyi, A.O. Fedorchuk, P.M. Fochuk, S.I. Levkovets, M.V. Karpets, O.V. Parasyuk. *Journal of Solid State Chemistry* 242 (2016) 193–198.

Optical, Electrical and Photovoltaic Properties of $Tl_{1-x}Ga_{1-x}Sn_xSe_2$ ($x=0,05; 0,1$) Crystals

Makhnovets H.V., Muronchuk G.L., Zamuruieva O.V., Klots O.M.

¹*Lesya Ukrainka Eastern European National University,
Lutsk, Ukraine, anjutka_mv@mail.ru*

Crystals as $TlGaSe_2$ are perspective materials that are used in the different devices of the modern electrical engineering. Interest of researchers is megascopic in the last few years in so solids on the basis of $TlGaSe_2$ conditioned by a strong anisotropy them physical properties.

Therefore expansion of $A^{III}B^{III}C_2^{VI}$ class exactly of the stratified semiconductors as, including $TlGaSe_2$, receipt of perfect single crystals and further study of complex those physical properties are actual tasks in area of modern physics of solid. Because these crystals are perspective for wide application in sources, transceivers, transformers, strengtheners of different types of energy and creation on their basis of different functional elements of optoelectronics.

The aim of our work was research of influence of change of composition of connection of so solids of the system $Tl_{1-x}Ga_{1-x}Sn_xSe_2$ ($x=0.05; 0.1$) on their optic electric and photoelectric properties, that gives important information about nature and spectrum of power levels, non-communicative in the restricted area investigated semiconductors and about their zone structure.

The investigated single-crystals are high-resistance semiconductors. In obedience to the sign of coefficient of thermo emf they are materials with the p-type of conductivity. At the megascopic x type of conductivity remains permanent.

Therefore, we determined the temperature range 260-300 K, which is 0.41 eV and 0.37 eV for 90mol% $TlGaSe_2$ -10mol% $SnSe_2$ and 95mol% $TlGaSe_2$ -5mol% $SnSe_2$ - accordingly found that the studied crystals are photosensitive materials. A characteristic feature of the spectral distribution of photoconductivity is caused by the presence of two peaks intrinsic and impurity photoconductivity.

1. Gurbulak B. The Urbach tails and optical absorption in layered semiconductor $TlGaSe_2$ and $TlGaS_2$ single crystals / B. Gurbulak, S. Duman, A. Ates. // Czechoslovak Journal of Physics. – 2005. - Vol. 55. - No. 1. - P.93-103.
2. O. V. Zamurueva, G. L. Myronchuk, G. Lakshminarayana, O. V. Parasyuk, L. V. Piskach, A. O. Fedorchuk, N. S. AlZayed, A. M. El-Naggar, I. V. Kityk. Structural and Optical Features of Novel $Tl_{1-x}In_{1-x}Ge_xSe_2$ Chalcogenide Crystals// Opt. Mater. – 2014. – Vol. 37. – P. 614–620.

Scattering Mechanisms in Crystals PbTe p-type Conductivity

Nyzhnykevych V.V., Lutchytskyi R.M.

*Ivano-Frankivsk National University of Oil and Gas, Ivano-Frankivsk, Ukraine,
E-mail: galuschak@nung.edu.ua*

The theoretical analysis of scattering mechanisms of carriers by thermal vibrations of crystal lattice is done. The calculation provided of the mobility of carriers in a wide temperature (4,2 – 300 K) and concentration ($10^{16} - 10^{20} \text{ sm}^{-3}$) bands in view of interacting conduction of holes of deformation potential acoustic and optical phonons and polarization potential of optical phonons.

Kinetic parameters of semiconductor materials are largely determined by the scattering mechanisms of carriers. Scattering mechanisms of carriers in lead chalcogenides have been studied repeatedly by different authors. But despite this, at present there is no consensus on the concentration and temperature limits the dominance of certain types of scattering. In this paper, based on comparison of theoretical calculations with the experimental Hall mobility data of specified concentration and temperature limits the use of approximate models of the band structure and the prevailing scattering mechanisms of charge carriers in lead selenide crystals p-type conductivity.

The dominant scattering mechanisms of carriers in hole lead selenide crystals are the scattering of short-range potential vacancies for the concentrations of $10^{19} - 10^{20} \text{ sm}^{-3}$ and the lattice thermal vibrations.

Scattering of phonons gives a correct picture of the quality necessary to characterize transport phenomena. The role of polar optical phonon significant at temperatures of 77 and 300 K for concentrations of $10^{16} - 10^{18} \text{ sm}^{-3}$. When increasing the concentration scattering on optical phonons is reduced due to screening.

At high concentrations (higher 10^{19} sm^{-3}) scattering on optical phonons is manifested through their deformation potential, whose influence on the total scattering at certain concentrations is very essential at room temperature. Scattering of carriers by acoustic phonons significant for all temperatures in the considering the whole studied concentration range. For temperature 77 K influence on the total scattering dominates deformation potential scattering on optical phonons.

1. Ravich Yu.L., Efimova B.A., Tamarchnko V.I. Scattering of current carriers and transport phenomena in lead chalcogenides. I. Theory // Phys. Stat. Sol. – 1971. – Vol.43, № 1. – P. 11-33.
2. Freik D.M., Nykyrui L.I., Ruvinsky M.A., Shperun V.M., Nyzhnykevych V.V. Scattering of charge carriers in lead chalcogenides crystals n-type // Physics and Chemistry of Solids. – 2001. – Vol.2, № 4. – P. 681-685.

Phosphate Glass-Ceramics in the System Na-Ni-P-O: Formation and Electrochemical Application Aspects

Odynets I.V., Zatonvsky I.V., and Klyui N.I.

College of Physics, Jilin University, Changchun, P.R. China

Li-ion batteries (LIBs) are essential for the development of portative electronic devises and many other consumer products these days. For further successful development of huge energy storage systems, the next generation of ion batteries are needed. Due to the intensive research, sodium ion batteries (NIBs) are considered as alternative secondary batteries to save material cost. The energy density of the NIBs is increasingly become equal to that of conventional LIBs. But in the case of sodium-based materials the abundance of initial reagents is much higher. Poly-anion phosphates of sodium and 3d-metals are widely described as active cathode materials in sodium half cells. These materials are stable and safe in Na ion batteries as the same as LiFePO_4 in Li ion batteries.

The glass-ceramic processing (i.e., crystallization of glasses) is a nice technique, to prepare a lot of complex oxides. In this work, we successfully applied the glass-ceramic technique for studying of compounds formation in $\text{Na}_2\text{O-NiO-P}_2\text{O}_5$ system for SIBs. Initial components in ratio $\text{Na}_2\text{O:NiO:P}_2\text{O}_5 = 22.2\div 40\%:20\div 33.3\%:33.3\div 44.4\%$ were used to obtain glass-ceramics with following compositions: NaNiPO_4 , $\text{Na}_4\text{Ni}_5(\text{PO}_4)_2(\text{P}_2\text{O}_7)_2$, $\text{Na}_2\text{NiP}_2\text{O}_7$ and $\text{Na}_2\text{Ni}_3(\text{P}_2\text{O}_7)_2$ and comparatively high theoretical capacity 152, 116, 96 and 94 mAh/g, respectively. Starting mixtures were melted at 1050-1150 °C during 30-120 min in a platinum crucible. Then, homogenous melts were quickly poured onto a copper plate and pressed by another plate. Obtained glasses were subsequently annealed at 300-700 °C, this procedure promotes formation of crystalline phases in bulk material. The glass transition and crystallization temperatures were determined by differential thermal analysis (DTA). Further, samples were ground by mechanical milling in a planetary ball mill. In order to confirm glass formation and to characterize crystallized phase, all samples were investigated by FTIR spectroscopy, X-ray powder diffraction, SEM and TEM analysis. By combining of these compounds with carbon black the composite materials were prepared. Obtained composites were deposited onto nickel foam and used as positive electrode in electrochemical studies. In particular, the author studied the current-voltage characteristics for aqueous and non-aqueous electrolytes, polarization curves, capacitance and cyclic stability of the charge-discharge process in the materials.

In the report, it is discussed the results obtained by electrochemical tests and the possibility of practical application of the glass-ceramics as cathode materials for NIBs, supercapacitors and electrocatalysts for water decomposition.

Structure Simulation and Thermodynamic Properties of II-VI Crystals

Parashchuk T.O.¹, Volochanska B.P.², Bojchuk V.M.²

¹ *Ivano-Frankivsk National Medical University, Ivano-Frankivsk, Ukraine*

² *Vasyl Stefanyk Precarpathian National University, Ivano-Frankivsk, Ukraine*

In the paper based on the crystal and electronic structures of ideal stoichiometric zinc and cadmium chalcogenides ZnX, CdX (X = S, Se, Te) and paying attention to their physical and chemical properties, the cluster models for calculating the thermodynamic parameters of sphalerite and wurtzite have been proposed. The simulations of structure and thermodynamic properties calculations are based on density functional theory method.

First step of the cluster properties calculation was determination of the lowest energy configuration. All computations started with SCF convergence and geometry optimization; after obtaining a stable minimum, the frequencies were calculated. The calculations carried out using density functional theory using SBKJC parameterization. DFT simulation performed obtaining Becke's three parameter hybrid method with Lee, Yang, and Parr (B3LYP) gradient corrected correlation functional using the FireFly program packages. The visualization of the spatial structures carried out in Chemcraft. The adequacy of the proposed calculation method is confirmed by number of papers on this subject and convergence of calculated data with experimental results [1,2].

Using the first principles' calculations we defined energy ΔE , enthalpy ΔH , Gibbs free energy ΔG , entropy ΔS for sphalerite phases of ideal stoichiometric crystals ZnS, ZnSe, ZnTe and CdS, CdSe, CdTe for wide temperature range: (100-1000) K for ZnX and (50-700) K for CdX respectively. These results can be used to predict properties of II-VI crystals during annealing. Although we obtained isochoric C_V and isobaric C_P molar heat capacities for zinc and cadmium crystals and their temperature dependences. For stoichiometric crystals of zinc chalcogenides provided the equality of Gibbs free energy of sphalerite $\Delta G_1(T)$ and wurtzite $\Delta G_2(T)$ phases have been defined the transition temperature of "sphalerite-wurtzite" that are falling in the line ZnS→ZnSe→ZnTe and equal to 1454 K, 1427 K, 1382 K, respectively.

1. Rasëit Ahiska, Dmytro Freik, Taras Parashchuk, Igor Gorichok. Quantum chemical calculations of the polymorphic phase transition temperatures of ZnS, ZnSe, and ZnTe crystal // Turkish Journal of Physics. – 2014. – **V.38**. – P. 125-129.

2. Dmytro Freik, Taras Parashchuk, Bohdana Volochanska. Thermodynamic parameters of CdTe crystals in the cubic phase // Journal of Crystal Growth, Elsevier, – 2014. – **V.402**, P. 90-93.

Evolution of Al-SiO₂-Si Structure Subsurface Layer During the Formation of Radiative Recombination Centers

Pavlyk B.V., Kushlyk M.O., Slobodzyan D.P.

Ivan Franko National University of Lviv, Lviv, Ukraine

It is shown the formations of oxygenous and hydrogenous complexes with dislocations in subsurface layer of p-Si (111). Uniaxial deformation and annealing stimulate diffusion of point defects акщъ volume to surface. Difference in lattice parameters of Al film and Si crystals is the cause of deformation potential in subsurface layer (1,5 ÷ 3 mm) presence. The availability of such potential accompanied by the formation and delight in the surface layer of dislocation-impurity complexes. Research of structural defects restructuring processes by using MCSDL method in comparison with spectra of radiation allowed us to show that the energy levels $E_v + 0.08$ eV (60° dislocation), $E_v + 0.14$ eV (dislocation - V), $E_v + 0.23$ eV (dislocation - SiI), $E_v + 0.26$ eV (dislocation - O), correspond to luminescence centers [1].

Research IR spectra of vibrational levels and VFC analysis and calculation of surface states distribution density showed the presence of thin (100 ÷ 200 nm) layer of SiO₂. Also, results of study show a complex structure both electrically active and neutral defects in the surface layer of silicon (Tab. 1) with different distribution in depth from the crystal surface (Fig. 1). It is shown increasing of SiO₂ nanoinclusion concentration in silicon subsurface layer, that reflected in efficiency of infrared radiation scattering.

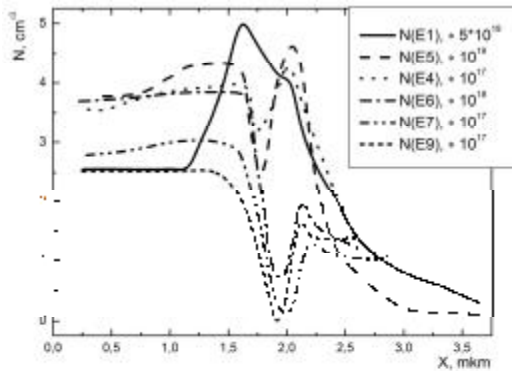


Fig. 1. Profiles concentration distribution of defects on the thickness of silicon crystals subsurface layer (after deformation and annealing)

Tab.1. Impurity-defect complexes in Al-Si (p) samples

Marker	Level position in E_g , eV	Type of defect
E1	$E_v + 0.14$	dislocation – V
E4	$E_v + 0.04$	V
E5	$E_c - 0.08$	60° dislocation
E6	$E_v + 0.23$	dislocation – SiI
E7	$E_v + 0.26$	dislocation – O
E9	$E_v + 0,31$	CI – OI

1. B.V. Pavlyk, M.O. Kushlyk, D.P. Slobodzyan About the nature of electroluminescence centers in plastically deformed crystals of p-type silicon // J. Nano- Electron. Phys. – 2015. – Vol. 7, No 3. – pp. 03043-1-5.

Point Defects of Silver Doped Lead Telluride

Prokopiv V.V.¹, Horichok I.V.¹, Turovska L.V.², Mazur T.M.¹

¹*Vasyl Stefanyk Precarpathian National University, Ivano-Frankivsk, Ukraine, prkvv@i.ua*

²*Ivano-Frankivsk National Medical University, Ivano-Frankivsk, Ukraine*

The issue of improving the efficiency of converting heat into electricity has gained a special importance in recent years in connection with the awareness of exhaustion of fossil fuels and significant emissions of harmful gases into the atmosphere during combustion that pollute the environment, damage the ozone layer and cause global climate changes.

Among all thermoelectric materials lead telluride (*PbTe*) should be noted, as its basic parameters can be changed effectively by doping and forming solid solutions. Especially promising impurity is silver.

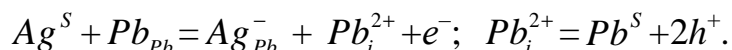
In this work, silver doped lead telluride has been synthesized, and its defect structure and thermoelectric properties have been studied.

It has been found that the samples of undoped material and the samples containing impurity < 0.3 at. % are single-phase regardless of the annealing temperature, and at the impurity concentration > 0.5 at. % phase of pure lead (Pb) is presented in *PbTe:Ag* samples, which is caused by reaching the solubility limit of impurity.

The dependence of the Hall concentration and mobility of free charge carriers on the amount of introduced silver is characterized by non-monotonic dependence with a maximum, which position depends on the annealing temperature of samples. At annealing temperature 228 °C a maximum corresponds to concentration 0.5 at. % Ag, and at annealing temperature 300 °C it corresponds to 0.3 at. % .

Samples of undoped lead telluride obtained from the ingot with stoichiometric mixture by cold pressing with the annealing in air at 228 °C are characterized by *n*-type conductivity. Silver doping leads to a significant decrease in conductivity, but there is no transition to *p*-type.

To establish the causes of acceptor action of silver in *PbTe*, crystal-quasichemical and quasichemical approaches to analysis of *PbTe:Ag* defect subsystem have been used. It has been concluded about the replacement of lead atoms by silver by way of their displacement into the interstices with the subsequent precipitation:



Since the interstitial atom of lead is a double-charged donor Pb_i^{2+} and silver atom in cationic site is singly charged acceptor Ag_{Pb}^- , it could be an explanation of weak acceptor action of silver.

These assumptions about the mechanism of defect formation in silver doped lead telluride are confirmed by established increase of lattice constant with growth of Ag content and appearance of traces of phase of pure lead (*Pb*).

Phase Composition and the Thermoelectric Properties Material System Pb-Ag-Te

Semko T.O¹, Mudryy S.I.², Haluschak M.O.³, Lopyanko M.A.¹
Maksymiuk N.T.¹.

¹*Vasyl Stefanyk Precarpathian National University, Ivano-Frankivsk, Ukraine*

²*Lvivskyy National University named after Ivan Franko, Lviv, Ukraine*

³*Ivano-Frankivsk National Technical University of Oil and Gas, Ivano-Frankivsk, Ukraine*

In this work the phase composition and the thermoelectric properties of doped silver lead telluride with impurity concentration of 0.3, 0.5, 1.0 at.% and solid solutions $\text{Pb}_{18-x}\text{Ag}_2\text{Te}_{20}$ ($x = 0, 0.5, 1.0$), $\text{Pb}_{17}\text{Ag}_3\text{Te}_{20}$ are researched. Synthesis of materials carried out in evacuated quartz ampoules. The resulting ingots ground in an agate mortar and highlighting fraction size (0.05 - 0.5) mm and pressed under pressure of 1.5 GPa. The obtained samples with $d = (5-8)$ mm and $h \approx (8-12)$ mm subjected to additional annealing.

Based on X-diffraction studies found that the introduction of impurities in silver in PbTe samples are shown traces of phase pure lead. For all samples of solid solutions Pb-Ag-Te in diffraction pattern observed additional phase and $\text{Te Ag}_{10,6}\text{Te}_7$.

The coefficient of thermal emf samples containing impurities 0.3 and 0.5 at. % Ag are almost identical and monotonically decreasing values of 500 mV / K at 100 C, to values of 350 mV / s at 350 C. The temperature dependence of the thermopower samples containing impurities 1 at. % Ag characterized by non-monotonic dependence with a maximum of 400 mV / s at 200 C. Thermal conductivity increases with little increase in the number of impurities.

Unlike the doped material for all formulations investigated $\text{Pb}_{18-x}\text{Ag}_2$ (₃) Te_{20} ($x = 0, 0.5, 1.0$) was obtained stable-type conductivity. The conductivity of the material is higher compared to the doped material. There is a marked increase in the value of σ with reduction of lead in solution, although holding by measuring the concentration of media virtually unchanged. Thermopower factor for all compositions $\text{Pb}_{18-x}\text{Ag}_2\text{Te}_{20}$ is almost the same and is ≈ 300 mV / s at 300 C. Thermal conductivity decreases with the decrease of lead in solution, which can be explained by the increase in the number of vacancies of lead, which scattered phonons. Lowest value of k samples characterized $\text{Pb}_{17}\text{Ag}_3\text{Te}_{20}$. It is important that this sample is the most intense peaks of additional phases $\text{Ag}_{10,6}\text{Te}_7$.

Perspective of Acoustic Hall Method Research of "near Dislocation" Point Defect Clusters in CdTe Crystals

Olikh Ya.M.¹, Safriuk N.V.¹, Tymochko M.D.¹, Ilashchuk M.I.²

¹*V.Ye. Lashkaryov Institute of Semiconductor Physics, NAS of Ukraine, Kyiv, Ukraine.*

²*Yuriy Fedkovych Chernivtsi National University, Chernivtsi, Ukraine.*

It is considered that the electrophysical (EPh) properties of doped semiconductor crystals A_2B_6 are mainly determined by the point defect complexes (PDC). Taking into account the high density of dislocations ($N_{Dis} \sim 10^{10} m^{-2}$) we suppose that the local inhomogeneities of the deformation field and the potential barriers are forming primarily in the near-dislocation (ND) regions of the crystal. Direct methods of NDPDC electrical activity investigations are unavailable. At the same time, detected significant acoustic-induced (AI) changes of EPh sample parameters in-situ ultrasonic (US) loading indicate a high acoustosensitivity of NDPDC [1]. In fact, as the mechanism of US waves interaction in A_2B_6 crystals is acoustic-dislocation, and charge carriers scattering contribution directly at the dislocations (up to $N_{Dis} \sim 10^{12} m^{-2}$) is insignificant [2], so there is a high probability to explain the observed changes from the positions of AI NDPDC structure rebuilding.

In order to study the specific correlation of regularities between initial characteristics (a composition and dopant concentration, electron concentration and mobility, dislocation density) in the low-ohmic resistance CdTe samples and there adequate AI changes temperature investigations of the Hall effect and the acoustoconductivity relaxation kinetics $\sigma(t)$ at US switching-on/off were conducted. To explain the mechanism that connects the "instant" increase $\sigma(t)$ with AI decreasing large-scale potential fluctuations amplitude as a result of increasing the NDPDC effective cross section scattering was used; long-term temperature-dependent relaxation ((50-500) sec) are determined by the PD diffuse rebuilding in the middle of the cluster.

Thus, we found that: 1) the composite PDC in A_2B_6 crystal in US loading can be labile at low temperatures (<300K); 2) CdTe samples is a convenient model material for acoustic-dislocation-electron interaction in semiconductors in general; 3) the acoustic Hall dynamic method is perspective for the complex electrically active dislocation systems in semiconductor structures studies, in particularly containing a high density of dislocations (thin film, epitaxial and nanostructures etc.).

[1] Ya.M. Olikh, M.D. Tymochko, *Ukr. J. Phys.* **61** (5), 381 (2016).

[2] D.C. Look, J.R. Sizelove, *Phys. Rev. Lett.* **82**, 1237 (1999).

Computation of the Thermodynamic Properties of Chalcogenide Crystals Using Firefly (PC Gamess) Software

Volochanska B.

Vasyl Stefanyk Precarpathian National University, Ivano-Frankivsk, Ukraine

The determination of the relative placement of the electron clouds in examined compounds is the basic values for obtaining of main properties of solids, in particular, semiconductor materials. The *ab initio* calculation is convenient method for such investigation. The charges of nuclear and their position in solid are used as initial data. However, the inability to obtain exact solutions encourages researchers to use any approximations. And, the final results are directly dependent on the appropriateness of such approach.

For simulation of the semiconductor crystals properties as part of *ab initio* calculation the most accurate results were obtained using Becke-Lee-Yang-Parr hybrid-functional (LYP, BLYP, B3LYP). Selecting of functional sort is predetermined by the main task and nature of materials [1, 2]. Therefore, comparison of the calculation results of thermodynamic properties for lead chalcogenide crystals by using the above-mentioned approximations. We can conclude from the comparative analysis that effectiveness of these approximations and perform further calculations using the chosen approach. Most suitable for calculations of the thermodynamic properties of PbX (X=S, Se, Te) is representation the exchange-correlation interactions within the crystal as B3LYP functional.

Comparison of the obtained characteristics allows identify the contribution which takes into account during the calculation of the exchange-correlation interactions. It should be noted that the obtained results of calculations using of basic Becke-Lee-Yang-Parr functions are higher than using parameterized basic functions throughout the temperature range.

[1]. Nemoshkalenko, V.V., Kucherenko, Yu.N. Computing physics theory Methods for Solid State — Kyiv: Naukova dumka, 1986 — 296 p.

[2]. Yong D. C. Computational chemistry: a practical guide for applying techniques to real-world problems — New-York: Wiley J.& Sons, Inc., 2001 — 370 p.

Study of Interaction in Systems Germanium – Metal Oxide by Spectroscopic Methods

Zinchenko V.F., Magunov I.R., Nechyporenko G.V., Sadkovska L.V.

A.V.Bogatsky Physical and Chemical Institute of NAS Ukraine, Odessa, Ukraine

The new type of functional materials based on composites of composition Germanium - metal chalcogenide (oxide) is developed. Historically the first example of such materials is system Ge-ZnS showing properties of so-called a CVD ("Chemical Vapor Deposition") - composite. The feature of CVD - composites is ability of their components to evaporate simultaneously at temperatures, lower in comparison with that for each of them. Many of them at condensation form nano-structured coatings (nano-composites) with high mechanical durability.

Among oxide systems, first of all, it is necessary to specify a natural CVD - composite - Germanium (II) oxide. Compound GeO exists only in a gaseous state, and at condensation it decomposes under the scheme [1]:



Thus, the solid substance consists of ultra-micro-dispersed particles of Germanium and mainly vitreous Germanium (IV) oxide, therefore GeO is amorphous substance irrespective of conditions of its reception. Composite of GeO composition evaporates at various temperatures depending on the size of composing particles. As an example of CVD - composites systems of Ge-GeO₂, Ge-SnO₂ type, possessing certain features of spectral characteristics, in particular, IR transmittance spectra can serve. On their basis thin-film coatings with a certain set of optical and operational parameters are received. At the same time, in systems Ge-ZnO and Ge-In₂O₃ at heating and, especially, at thermal evaporation in vacuum interaction on other mechanism which is distinct from pure CVD-process takes place. In case of the first of systems poorly volatile oxide Zn₂GeO₄, and for the second - almost pure GeO₂ of hexagonal modification are formed.

Even more complicated character carries interaction in systems Germanium - complex oxide, for example, Ge-In₂SnO₅, Ge-LnInO₃ (Ln - La, Sm, Eu etc.). The temperature of the beginning of evaporation of one of volatile products, In₂O in certain degree depends on composition of oxide component of a composite.

Research of such systems is important for working out materials for interference optics of an IR range of a spectrum.

1. Tananaiev I.V., Shpirt M.Ia. *Khimiia germaiia.*—Moscow: Khimia, 1967.—451pp.



ORAL REPORTS

Session 6 Innovative methods for teaching



Modern Peculiarities of Teaching Physics in The Technical University

Dyakonenko N.L., Petrenko L.G., Lyubchenko E.A.

National Technical University "Kharkiv Polytechnic Institute", Kharkov, Ukraine

At present, the progress in development of education system is largely determined by intensive introduction of modern computer and information technologies into educational process. The education of students in technical university should be directed not only to obtaining knowledge of fundamental and special disciplines, but also to the formation of professional skills in use of computer technology in future professional activities.

In this regard, the traditional forms and methods of education are undergoing significant qualitative changes. The use of modern multimedia systems, lecture presentations and other technologies, providing an opportunity to set out the information in an accessible and qualitative way, takes an increasing place in the process of teaching physics. But this does not cancel the traditional, "verbal" way of lecturing. It is the combination of these two techniques that make it possible to improve substantially the assimilation efficiency of the proposed material. Computer technologies allow us to offer a demonstration of interesting physical experiments, phenomena and processes, to give illustrative examples that contribute to a better understanding. Live communication, in turn, allows adjusting the proposed material in accordance with the level of its perception by students, checking the understanding directly during the lecture and answering the emerging questions. At the same time, lecture demonstrations and physical experiments shown by the lecturer, especially if students can take part in them, not only contribute to a more complete understanding of the topic under consideration, but also cause a natural interest in the subject as a whole.

The second priority is to teach students to solve physical problems, since this skill is the criterion for understanding theoretical material and the ability to apply the knowledge gained in practice. In practical exercises it is useful to use different types of tasks: traditional calculation tasks, qualitative questions, and computer tests.

The third important component of the learning process is the work of students in physical laboratory. To increase the effectiveness of training, it is possible to combine traditional physical experiments and measurements with computer laboratory work, especially in the cases where it is impossible to observe real processes and phenomena in a conventional laboratory.

Such methods, using traditional and modern teaching methods, are widely used at the Department of Physics of NTU "KhPI" when studying the discipline "General Physics" and special courses.

Determination of the Structural State and Limit of Fluidity is in Coverages the Method of Instrumental Indentation

Gorban' V. F.

Kiev Frantcevich Institute for Problems of Materials Science NAS of Ukraine, Kiev, Ukraine
 E-mail address: gvf@ipms.kiev.ua

On the basis of the known relations used in an instrumented indentation method the equation is obtained analytically. It establishes direct relation between hardness H_{IT} , reduced modulus E_r and parameters of the indentation diagram - displacement values h_s and h_c : $H_{IT}/E_r = K \cdot (h_s / h_c)$; for the Berkovich indenter $K = 0.3206$. This equation is a fundamental indentation equation, since it reflects regularities of the indentation process and immediately establishes a relation between material strength properties (i. e. stresses and strains) in completely elastic (E_r) and elastic-plastic (H_{IT}) deformation regions and indentation diagram parameters. The equation is calibration dependence of instrumented indentation method.

On the basis of this equation the new methodology of processing and the analysis of results of an instrumented indentation of modern materials with various types of atomic bonding and the structural states, possessing special properties (nanomaterials, amorphous, gradient, semi-crystals, films, etc.) is developed. It allows not only characteristics of elasticity, strength and deformation of materials to be calculated, but also their structural state to be identified. The methodology is express and effective. Indentation constants, which reflect availability of a basic possibility of existence of limit numbers for indentation depth and hardness of materials, are established. Experimental confirmation of methodology was obtained at an indentation on several hundreds materials. $\geq 100 \text{ nm} \leq 100 \text{ nm}$. Figure 1, 2 shows the correlation results.

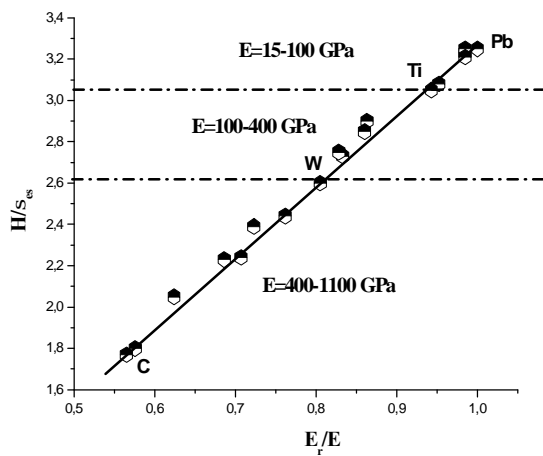


Fig. 1.

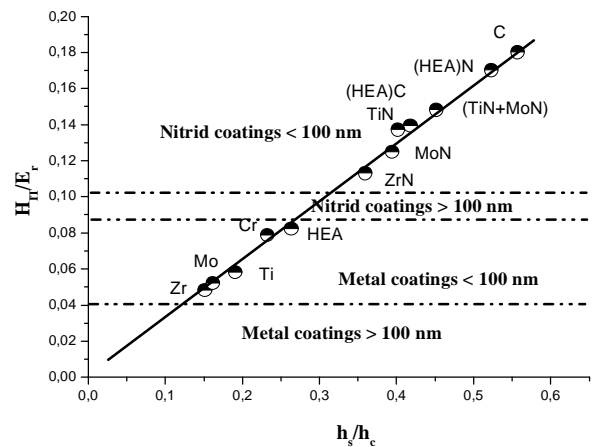


Fig. 2.

The Formation of Critical-Constructive Thinking of Future Teachers of Physics in the Process of Analysis of Contradictions in Electrodynamics

Solomenko A.O.

Kryvyi Rih State Pedagogical University, Kryvyi Rih, Ukraine

The theoretical analysis of science-methodical literature, textbooks in electrodynamics show the existence contradictions in argumentations of some electrodynamics phenomena and processes. The urgency of necessity of their eliminations stresses the aim of the active to show their essence of these contradiction and didactical possibilities of processes of their analysis as the way of developing of critical-constructive thinking of students of physics of pedagogical university.

It is proved that one of the most important function of critical-constructive thinking is finding deficiently and contradiction and their eliminations in future. So, it is given by us some contradictions which take place in the process of studying electrodynamics and take some making definitions [1; 2], mainly:

- $$\mathbf{r}_+^0 = -\frac{\mathbf{r}_-^0}{\sqrt{1-b^2}} = -\mathbf{r}_- \text{ – it is widespread conditions of neutrality}$$

of conductor with direct current which has some contradiction;

- incompatibility of Biot-Savarts's law
$$d\mathbf{B} = \frac{\mu_0 i}{4\pi r^3} \cdot [d\mathbf{l}, \mathbf{r}]$$
 and Coulomb law which are often used together in scientific literature;

- the absence of physical explanation origin magnetic field of direct current;

- Faraday's law of induction
$$\mathbf{rot} \mathbf{E} = -\frac{\dot{\mathbf{B}}}{\partial t}$$
 doesn't show two physics reasons which are in the basis of this phenomenon;

We consider that a deep analysis of these contradictions in the method of studying of electrodynamics makes the process of formation critical-constructive thinking possible for future teachers of physics.

1. Konoval O. A. Theoretical and methodical bases of studying electrodynamics on bases of special theory of relativity : [monography] / O. A. Konoval ; Ministry of Education and Science of Ukraine ; Kryvyi Rih State Pedagogical University. – Kryvyi Rih : Publishing House, 2009. – 346 p.
2. Solomenko A. O. Didactical ways of formation critical-constructive thinking of student of physical while independent analysis condition of neutrality conductor with direct current / A. O. Solomenko, O. A. Konoval // The search of young. – Kherson, 2014. – Issue 13. – p. 60-65.

STEM-Education is One of the Way of Studying Technical Subjects

Voitkiv H.

*Ivano-Frankivsk Regional Institute of Postgraduate Teachers Education,
Ivano-Frankivsk, Ukraine*

Today engineers, specialists of high-tech industries are working to improve efficiency manufacturing. This requires knowledge in engineering and manufacturing, the foundations of design, construction, high intellectual abilities, spatial imagination, creativity in the development of new techniques and technologies. Therefore, a priority in education today is STEM-education – Science, Technology, Engineering and Mathematics. STEM-education implemented in educational institutions in order to increase the competitiveness of countries in science and technology

At present, we have not STEM-programs for secondary school that's why the aim of the study is to highlight ways to implement STEM-education through the development of technical creativity of pupils at physics lessons at school.

In the scientific literature, technical creativity of students is treated as the ability to perform mental and practical action in the course of research to create new devices subjective or alter their function [1, 2].

Teaching character of child technical creativity is not the result of creative activity, but in preparation for her in future, the accumulation of experience specific activities, such as design, construction, development of technologies, rationalization and invention [2].

Primary role in the development of technical creativity of students in the educational process in physics plays an educational physical experiment. Through educational physical experiment, pupils acquire practical experience of the experiment serves as a method of educational knowledge, provides experimental skills and research skills, so in the minds of the student form new connections and relationships.

Great contribution to the development of technical creativity makes activities connected with the production of physical devices. The production of device includes two phases: design - the formation of a design in the form of ideas and the visual image of the future technical construction.

The activity of pupils should organize as an educational creative project, that involves performed a set of operations - from conception to its future production.

Thus, one way to implement Stem-education lessons in physics is the development of technical creativity of pupils. The ways of development of technical creativity of pupils in physics is physics experiment, laboratory work, project activities related to manufacturing equipment. The important during these activities is the experience of organizing and conducting technical activities acquired technical knowledge, intellectual and heuristic capabilities.

1. Honcharenko S. Ukrainian Pedagogical dictionary / Semen Goncharenko. - Kyiv: Lybid, 1997. - 376 p.

2. Tarara A. The technical work of secondary school pupils in the process of design and technological activities: educational - methodical manual / Tarara A.- K., Educational thought, 2014.- 134 p.



POSTER REPORTS

Session 1

Thin films technology (metals, semiconductors, dielectrics, conductive polymers) and their research methods



Influence of Morphology of Surface and Structural Orientation Features of Vapor-Phase Condensates SnTe: 1% Sb on Their Thermoelectric Parameters

Bushkov N.I.

Vasyl Stefanyk Precarpathian National University, Ivano-Frankivsk, Ukraine

The paper presents the electrical properties and morphological characteristics of structures on the surface of films based on crystalline SnTe doped Sb, deposited on substrates of amorphous sital and polycrystalline mica. The patterns of process temperature dependences of concentration and mobility of free charge carriers of semiconductor films and spatial orientation and symmetry crystalline forms on the surface are analyzed.

Electrical conductivity of thin films deposited on sital is 2 times larger than the films deposited on mica for the temperature range 200 – 300°C. The concentration of carriers in thin films deposited on sital is 2 times larger than on mica for temperatures of 125 – 200°C. However, the carrier mobility in films on mica and sital behaves the same way. Concentration with increasing deposition temperature decreases and mobility increases.

Electrical conductivity of thick films does not depend on the type of substrate. The concentration of charge carriers in films deposited on sital 2 times larger than on mica for temperatures in the vicinity 200°C. However, the mobility of carriers in the films on sital 2 times smaller than on mica for temperatures in the same neighborhood of 200°C. Carrier concentration with increasing deposition temperature passes through a maximum in the vicinity of 150°C and decies and mobility incies in the 250°C.

The Process of Formation, Topology and Thermoelectric Properties of Thin Films Based on PbTe

Bylina I.S.

*Vasyl Stefanyk Precarpathian National University, Ivano-Frankivsk, Ukraine,
E-mail: vanjabylina@gmail.com*

Now the work of many scientists aimed at developing new materials and devices based on nanotechnology. This causes the development and improvement of research methods nanostructures. Atomic force microscopy (AFM) opens up new opportunities for observing and analyzing the stages of growth of nano-objects of different levels.

In particular, special attention to itself attracts Lead telluride. He is an efficient thermoelectric materials for middle temperatures (500-750 K) of high enough quality factor $ZT = 1$. Doping of PbTe impurities fifth group (Sb, Bi) causes the improvement of its properties. An important stage in the development of technology obtaining nanostructures with desired properties is study features nucleation mechanisms and the kinetics of growth.

Vapor-phase condensates on based PbTe obtained by the method of open evaporation in a vacuum on a substrate of pyroceram and mica. The sizes of nanostructures determined using the method watershed. The analysis of AFM-images constructed histogram distribution of nanostructures on the surface of the film at normal (h) and lateral (D) size (Fig.1)

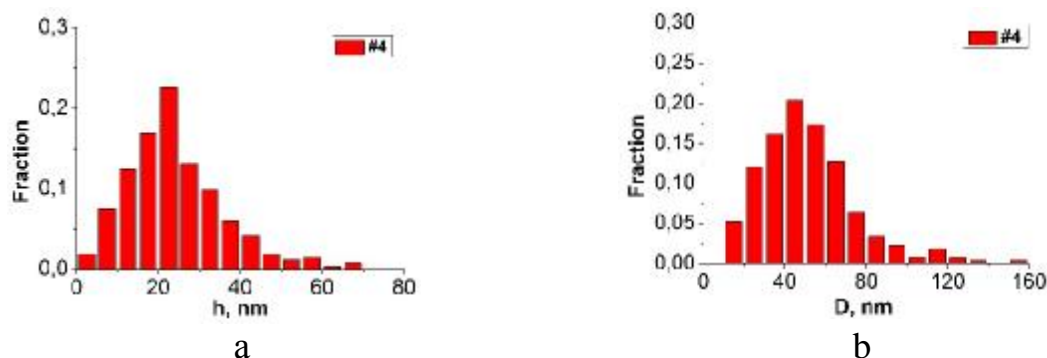


Fig.1. Histograms distribution of nanostructures vapor-phase condensation PbTe:Bi for height (a) and lateral sizes (b).

The dependence of the average sizes of nanocrystals in normal (h_m) and lateral (D_m) to the substrate surface direction of deposition time τ . Revealed that the size distribution histograms are asymmetrical shape and increase the duration of deposition leads to the shift of the maximum distribution towards higher values. Confirmed root dependence medium size of the duration deposition. Established that with increasing duration deposition of nanostructures increased form factor for all samples based on PbTe.

Removing of Thin Layers from the CdTe and Zn_xCd_{1-x}Te Surfaces by the HBr – K₂Cr₂O₇ – Ethylene Glycol Etching Compositions

Chayka M.V.¹, Tomashyk Z.F.², Tomashyk V.M.², Denysyuk R.O.¹

¹*Zhytomyr Ivan Franko State University, Zhytomyr, Ukraine, laridae92@gmail.com*

²*V.E. Lashkaryov Institute for Semiconductor Physics NAS of Ukraine, Kyiv, Ukraine, tomashyk@isp.kiev.ua*

The investigation was carried out on the single crystals of CdTe and Zn_{0,1}Cd_{0,9}Te, which have been grown by Bridgman's method, and Zn_{0,04}Cd_{0,96}Te obtained from the gas phase. We have developed a method of getting a high quality surfaces of these semiconductors and removing from them a thin layer of them that consists of the following steps: grinding of the plates by abrasive powders marks M10-M1 → mechanical polishing with diamond paste → chemical etching to remove the damaged layer (80-100 μm) → finishing polishing by new slow etchants.

Finishing step is the process of chemical-dynamic polishing (CDP) using the method of disc rotating at T = 284 K and disk rotation speed $\gamma = 82 \text{ min}^{-1}$. The etching mixtures were prepared using 40 % HBr, 10,9 % aqueous solution of K₂Cr₂O₇ and ethylene glycol (EG). Putting in the etchant composition EG as viscous component, can partially regulate the interaction of HBr and K₂Cr₂O₇ with evolving of Br₂ and promotes the better dissolution of interaction products of etchant with semiconductor. This is an opportunity to get high-quality surface without films and sediments.

The choice of polishing etchants compositions were performed in the concentration range (in vol. %): (20-80) HBr : (20-50) K₂Cr₂O₇:(0-60) EG. The dependence of the chemical dissolution of the CdTe and Zn_xCd_{1-x}Te rates versus solutions concentration, mixing, temperature, nature of semiconductor material, and time of solutions storage has been investigated. It was established that the polishing area occupies the most of the researched concentration interval, and the rate of dissolution is in the range: 1.8-6.7 μm/min for CdTe; 1.7-7.5 μm/min for Zn_{0,04}Cd_{0,96}Te and 1.8-7.9 μm/min for Zn_{0,1}Cd_{0,9}Te. It was found that the dissolution process is limited by the diffusion stages ($E_a < 30 \text{ kJ/mol}$). After finishing CDP the samples must be washed by 0.1 M aqueous solution of Na₂S₂O₃, then with large quantity of distilled water and dry in air flow. Polished plates can be stored in isopropanol for several weeks.

The results of metallographic and profilometric analysis of plates surface after finishing CDP showed that etched semiconductor surfaces are characterized by high quality ($R_z < 0,05 \text{ μm}$) and good luster. Optimized composition of etchants can be recommended for controlled reducing of the plates thickness to the specified size, removing of thin layers of material from the surface and finishing CDP of CdTe and Zn_xCd_{1-x}Te solid solution.

Sensory Properties of Poly-Ortho-Toluidine Films

Dzeryn M. R.¹, Horbenko Yu. Yu.², Tsyzh B. R.^{1,3}

¹*Lviv National University of Veterinary Medicine and Biotechnologies named after S. Gzhytskyj, Lviv, Ukraine; marjawka232@ukr.net*

²*Ivan Franko National University of Lviv, Lviv, Ukraine;*

³*Kazimierz Wielki University in Bydgoszcz, Bydgoszcz, Poland*

Gas sensor technology is one of the most important branches of modern electronics, due to the need of environmental control and monitoring of gaseous media in the food industry, etc. Sensitive elements of sensory devices fabricated by using conjugated polymers such as polypyrrole, polyaniline, polythiophene and their derivatives attract attention thanks to their high sensitivities and short response time, simple and cheap method of manufacture [1,2].

Poly-ortho-toluidine (PoT) is the promising material to develop sensitive elements of sensors due to interesting physical and electrochemical properties caused by electron donating substituent - methyl group in ortho position to the amino group, that leads to the deformation of the polymer chain, which in turn reduces its stiffness.

The work is devoted to the study of optical absorption spectra of PoT films under the influence of gases of different nature (NH₃, HCl, H₂S) and their possible application in optical sensors.

PoT films have been obtained by electrochemical and chemical oxidative polymerization. As optically transparent substrates the glass plates coated on the one side with a thin conductive layer of SnO₂ have been used.

Significant changes in the intensity and displacement of the absorption maximum as a result of the action of ammonia and hydrogen chloride vapor have been shown.

It was established that the character of optical changes in PoT films depends on acid-base properties of detected gases and it can be used for the selective determination of basic and acid gases in the atmosphere and industrial environments.

This work was supported by the project of Ministry of Education and Science of Ukraine «Development of new sensory environments for gas analysis in food and processing industry» (state registration number 0116U004740).

1. Bai H., Shi G. (2007). Gas Sensors Based on Conducting Polymers. Sensors (Basel). 7 (3), 267–307.
2. Tsyzh B. R., Chokhan M. I., Aksimentyeva O. I., Konopelnyk O. I., Poliovyi D. O. (2008). Sensors based on conducting polyaminoarenes to control the animal food freshness. Mol. Cryst. Liq. Cryst. (497), 254–260.

Spectral Transformation of Merocyanines in Thin Films

Iakovyshen R.S.¹, Pavlenko E.L.¹, Kulish N.P.¹, Kachkovsky O. D.²,
Kurdyukov V.V.³

¹ Faculty of Physics, Taras Shevchenko National University of Kyiv, Kyiv, Ukraine,

E-mail: iakovyshen@ukr.net

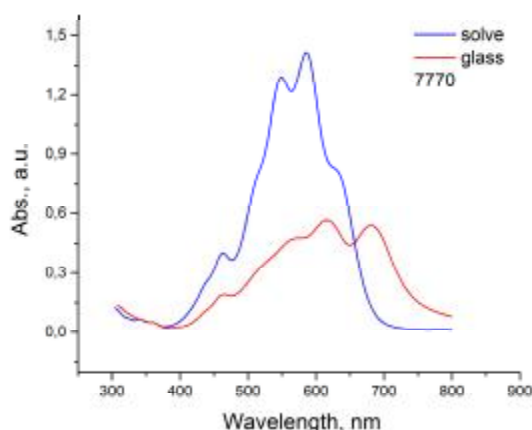
² Institute of Bioorganic Chemistry and Petrochemistry, NAS of Ukraine, Kyiv, Ukraine

³ Color and Structure of Organic Compounds, Department of Institute of Organic Chemistry,
National Academy of Sciences of Ukraine, Kyiv, Ukraine

The progress of new technologies provides the area of the application of well-known polymethine dyes and their neutral derivatives because of their strong and selective absorptions across broad spectral regions, as well as their fluorescence characteristics, firstly, high quantum yield [1].

Spectral and quantum-chemical investigation of transformation of the absorption spectra of merocyanines was investigated upon going from solution to thin film *Fig.1*. It was established that the wide longwavelength spectral band of the merocyanine solution is connected with intensive vibrational structure.

Quantum-chemical calculation of optimized molecular geometry were performed by HF/6-31(d,p) and DFT/CAM-B3LYP//6-31(d,p) methods, while the characteristics of the electron transitions in the individual dye molecules and their dimer were obtained by TD-DFT and ZINDO/S methods.



In the thin films obtained by spin-coating method, the planar conjugated systems of dyes produce the molecular ensembles bonded by stack π -interactions, what is accompanied by significant transformation absorption spectra.

[1]. S. R. Marder. Organic nonlinear optical materials: where we have been and where we are going Chem. Commun., 2006, 131–134

Electroactivity of Al in Al-Doped ZnO Films

Ievtushenko A.I.¹, Dranchuk M. V.¹, Karpyna V.A.¹, Lytvyn O.S.^{2,3},
Tkach S.V.⁴, Baturin V.A.⁵, Karpenko O.Y.⁵, Lashkarev G.V.¹

¹*I. Frantsevich Institute for Problems of Material Science, NASU, Kyiv, Ukraine,*

²*V. Lashkarev Institute of Semiconductor Physic, NASU, Kyiv, Ukraine*

³*Borys Grinchenko Kyiv University, NASU, Kyiv, Ukraine*

⁴*V.Bakul Institute for Superhard Materials, NASU, Kyiv, Ukraine*

⁵*Institute of Applied Physics, NASU, Sumy, Ukraine*

Transparent conductive oxides (TCO) having a wide band gap, high transparency and conductivity are necessary material for fabrication the photovoltaic heterostructure solar cells, transparent conducting electrodes, window materials, displays, etc. Today, the most widely used TCO are indium tin oxide (ITO), which has suitable characteristics. However, ITO has some drawbacks such as the limited deposits of indium in the Earth's crust causes constant increasing in value of indium, high toxicity and environmental hazard ITO industrial-scale production. These negative factors are the reason to replacement ITO on more safe, economically profitable and affordable material. Zinc oxide doped by donor impurities of Al, Ga or In is a promising material for future electronics and optoelectronics demands. In economic terms, aluminum is the most favorable donor impurity.

Al-doped ZnO (ZnO:Al) satisfies all the above mentioned requirements. It is non-toxic material, with prevalence of raw materials in the Earth's crust, having high stability to hydrogen plasma and temperature changes. ZnO has a wide direct band gap ($\sim 3,34$ eV at room temperature) that allows to be highly transparent ($\sim 85-95\%$) in the wide range of wavelengths (300-1000 nm). However, the problem of small electroactivity of donor impurities introduced into ZnO lattice still exists. Therefore, our report devoted to study the influence of Al content on its electroactivity in ZnO film.

ZnO:Al films were grown on Si and glass substrates by reactive magnetron sputtering (MS). To improve the crystalline perfection of the ZnO:Al films and to maintain a constant growth rate we used a new approach in ZnO:Al magnetron sputtering, namely, the layer-by-layer growth method [1]. It is shown that our method allows to grow high quality ZnO:Al films [2]. ZnO:Al films with different concentrations of aluminum impurity were deposited on Si and glass wafers by changing Al concentration in metallic Zn-Al target as well as at sputtering by variation of technological parameters of MS. The set of ZnO:Al films with concentration of Al in the range from 0.2 to 1.2 at.% were grown. For samples characterization, XRD, EDX analysis, atomic force microscopy and transmittance measurements were used. The temperature dependences of electrical resistivity and Hall coefficient were investigated.

The linear character of temperature dependence of resistivity and the value of electron concentration more than $7 \cdot 10^{19} \text{ cm}^{-3}$ suggested that all ZnO:Al films

were degenerate semiconductors. It was shown that with increasing Al impurity concentration in ZnO its electrical activity was decreased (Fig. 1). The reason for such behavior of electroactivity is self-compensation effect (the compensation of introduced donor impurities by generated own acceptor-type defects) and also dispersion on free carriers. So, even relatively small donor doping of ZnO within 0.2 -1.2 at.% leads to problem with electroactivity of introduced donor elements. Therefore, here we face to hard case: in desire to decrease resistivity in ZnO films down to $1 \cdot 10^{-4}$ Ohm·cm we need introduce a large amount of donor impurity the most of which is non-electroactive and, hence, play the role of scattering centers by forming intrinsic defects, even complex, which significantly decrease the electron mobility that is not large in wide-gap semiconductors. Hence, the only way to obtain the extra low resistivity ZnO films to do the best in the technology of Al-doped thin film deposition and maintain both mobility and electroactivity at a high level. Also, the relationship between structure and morphology of ZnO:Al thin films and electroactivity of Al impurity will be discussed.

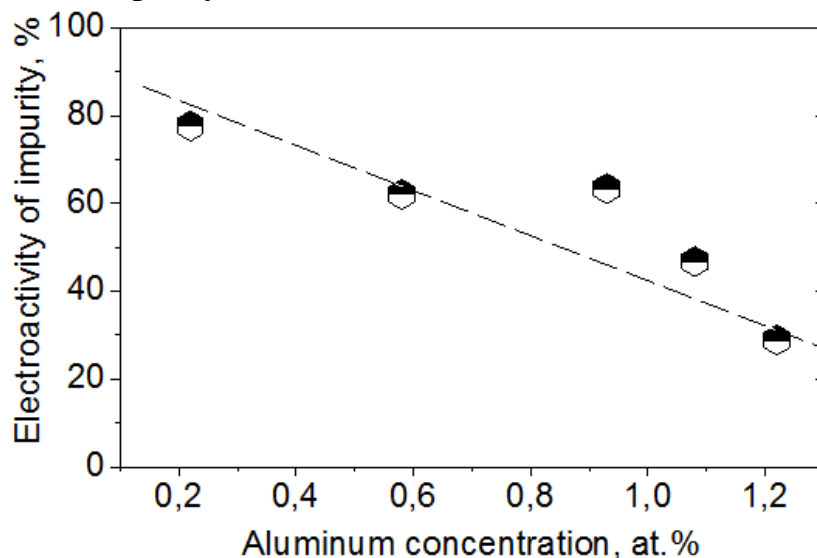


Fig.1. Electroactivity of aluminum impurity in ZnO:Al films. (Dashed line for eye)

1. A.I. Ievtushenko, V.A. Karpyna, V.I. Lazorenko, et al., High quality ZnO films deposited by radio-frequency magnetron sputtering using layer by layer growth method // *Thin Solid Films*. – 2010. – **518**. – P. 4529 - 4532.

2. A.I. Yevtushenko, O.I. Bykov, L.O. Klochkov, ta in., Vplyv tysku kysnyu na vlastyvoli tonkykh plivok ZnO:Al, vyroshchenykh metodom posharovoho rostu pry mahnetronnomu rozpylenni // *Fizyka i khimiya tverdoho tila*. – 2015. – T.16, 4. – S. 667-674.

“Polymer-Carbon Multiwall Nanotube” Nanocoatings on Macroporous Silicon Matrix

Karachevtseva L., Lytvynenko O., Onyshchenko V., Stronska O.

V. Lashkaryov Institute of Semiconductor Physics, NASU, Kyiv, Ukraine

Carbon nanotubes (CNT) are among the most anisotropic materials known and have extremely high values of Young's modulus. The opportunities to enhance the properties of nanostructured surfaces were demonstrated on the composite nanocoatings “polymer-CNT” on 2D macroporous silicon structures.

Carbon high purity multiwall nanotubes of submicron length and 20 nm diameter were formed by catalytic pyrolysis of unsaturated hydrocarbons. The macroporous silicon structures were etched on silicon wafers of [100] orientation and *n*-type conductivity. The “polymer-CNT” nanocoating was obtained from a colloidal solution of polyethyleneimine onto (1) single crystalline Si, (2) macroporous Si, (3) oxidized macroporous Si, and (4) macroporous Si with microporous Si layer.

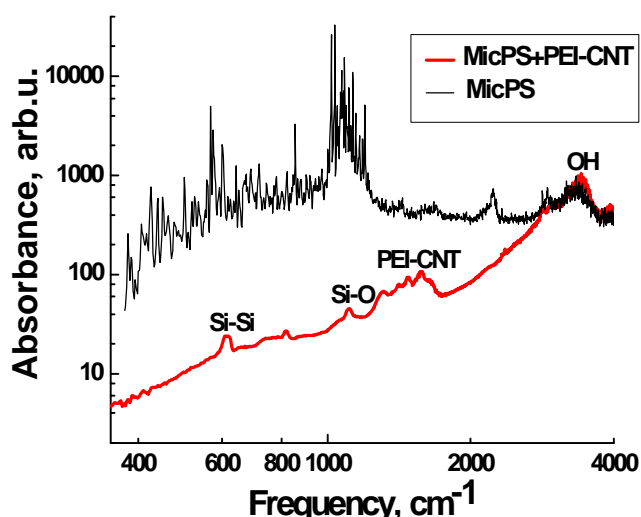


Figure:

The enlightenment effect in IR absorption spectra spectra of macroporous silicon structures with microporous layer (MicPS) and with nanocoatings of polyethyleneimine with carbon multiwall nanotubes (MicPS+PEI-CNT) with Si-Si and Si-O surface bond passivation.

It was found that “polymer-CNT” nanocoatings reduced IR absorption (Figure) by 2-3 orders of magnitude (the enlightenment effect) and actively neutralized (passivated) Si-Si and Si-O surface bonds. The photoluminescence of polyethyleneimine with carbon multiwall nanotubes on macroporous silicon with microporous layer is about six times more intense than photoluminescence of polyethyleneimine with carbon multiwall nanotubes on single crystalline silicon, macroporous silicon and oxidized macroporous silicon. This indicates a non-radiative proton recombination decrease due to hydrogen atoms on boundary silicon matrix with microporous layer and “polymer-nanoparticles” nanocoating.

Polyaniline Films Depositions in Potentiodynamic Mode on the Aluminium-Based Electrodes with Amorphous and Polycrystalline Structure From the Aqueous Solutions of Sulfuric Acid

Kostiv V.T.¹, Yatsyshyn M.M.¹, Boichyshyn L.M.¹, Pandyak N.L.²,
Reshetnyak O.V.¹

¹*Ivan Franko Lviv National University, Lviv, Ukraine, e-mail: m_yatsyshyn@franko.lviv.ua*

²*National Forestry University, Lviv, Ukraine*

Electrochemical polymerization of aniline (An) in potentiodynamic mode is an effective process of the forming of polyaniline (PAn) films on various metallic electrodes. The selection of experimental conditions, namely monomer and electrolyte concentration, the nature of the electrolyte, interval of potential scanning and scanning rate etc., gives a possibility to form the nano- and microstructured polymeric films on the surfaces of working electrode (WE) made of active metals, in particular on the surface of aluminum and its alloys including amorphous alloys (AA) [1]. The samples of polycrystalline aluminium (further in the text - Al-electrode) and ribbon of Al₈₇Ni₈Dy₅ amorphous alloy (further AlNiDy-electrode) in the form of plates 3.5 by 0.5 cm size (working surface was about 1.0 cm², thickness was ~40 μm) were used as a WEs in our studies. The concentration of An was 0.25 M. The aqueous H₂SO₄ solutions with concentration of 0.1, 0.5 and 1.0 M were used as an background electrolyte. The scanning rate of electrode potential was 25, 50, 75 and 100 mV/s, and potential was scanned in the (–200)–(+1200) mV interval. It was detected that the nature of the WE, electrolyte concentration and rate of potential scanning affects on the process of PAn films deposition on the Al-based electrodes. It appears as a formation of microfractal and nanosizes rod-like structures of the polymer on the Al-electrode, while there is formation of “cauliflower”-like deposits on the AlNiDy-electrode. The optimal conditions, namely An and H₂SO₄ concentrations and potential scanning rate, of the formation of nanostructured polyaniline films were determined during studies. Produced PAn-modified electrodes on the base of aluminium were tested in the chemosensors for determination of a number of organic compounds.

[1] Morphology of Polyaniline's Films Electrochemically Deposited on the Surface of Al-Based Amorphous Metal Alloys / M.M. Yatsyshyn, L.M. Boichyshyn, I.I. Demchyna, Yu.A. Hnizdiukh / Computational and Experimental Analysis of Functional Materials / O. V. Reshetnyak, G. E. Zaikov (Eds.) [Series: AAP Research Notes on Polymer Engineering Science and Technology]. – Toronto, New Jersey: Apple Academic Press, CRC Press (Taylor@ Francis Group), 2017. – P. 61–91.

Determination of Noncrystalline Solidification Conditions of Different Types of Metal Melts

Kosynska O.L., Skipochka D.G., Kozoriz V.S.

Dniprovsk State Technical University, Kam'yanske, Ukraine

A mathematical model has been developed for studying the thermal regime and the crystallization kinetics of thin melt layers in contact with a massive heat-conducting substrate. The mathematical basis of the model consists of the Fourier thermal conductivity equation for a thin melt layer (1) and substrate (2):

$$c_1 \rho_1 \frac{\partial T_1(z_1, t)}{\partial t} = k_1 \frac{\partial^2 T_1(z_1, t)}{\partial z_1^2} + \frac{\Delta H_m}{M} \rho_1 \frac{\partial x(t)}{\partial t} \quad (1)$$

$$c_2 \rho_2 \frac{\partial T_2(z_2, t)}{\partial t} = k_2 \frac{\partial^2 T_2(z_2, t)}{\partial z_2^2} \quad (2)$$

and also the boundary conditions that reflect the features of the heat transfer processes under rapid cooling conditions. To determine the crystallized volume fraction using the kinetic equation:

$$x(t) = \frac{4}{3} p \int_{t_m}^t (1 - x(t')) I(t') \left[R_c(t') + \int_{t'}^t (1 - x(t'')) u(t'') dt'' \right]^3 dt' \quad (3)$$

where $T_i(z_i, t)$, c_i , ρ_i , k_i – temperature, specific heat, density and thermal conductivity of the melt ($i=1$) and substrate ($i=2$), respectively; ΔH_m – molar heat of metal melting; M – molar mass of metal; x – fraction of crystallized volume; z_i – coordinate in the direction of heat removal within the melt ($i=1$; $0 \leq z_1 \leq l_1$) and substrate ($i=2$; $0 \leq z_2 \leq l_2$); I – the nucleation rate of crystals with critical size R_c ; u – crystal growth rate; t_m – the time when the melt reaches the melting temperature T_m of the material; $t' \leq t'' \leq t$ – current time moments.

With the help of the presented mathematical model, the possibility of obtaining metals and alloys in an amorphous state was studied. For this purpose, we studied the critical thickness and the critical cooling rate at which the crystalline volume fraction decreases to negligible values that lie beyond the sensitivity of modern methods of structural analysis ($x \approx 10^{-6}$). Calculations were carried out for pure metals Ag, Al, Cu, Ge, Ni and alloys $\text{Fe}_{80}\text{B}_{20}$ and $\text{Cu}_{47}\text{Ni}_8\text{Ti}_{34}\text{Zr}_{11}$.

It is found that among the pure metals, the crystallization processes are most easily, at the lowest cooling rates ($u_m = 4,6 \cdot 10^8 \text{ K} \cdot \text{s}^{-1}$), suppressed in Ge layers 0.6 μm thick, Ni is amorphized in layers with a thickness of 0.15 μm at $u_m = 3 \cdot 10^9 \text{ K} \cdot \text{s}^{-1}$. Ag and Cu are characterized by a lower ability to glass formation, a completely amorphous structure is fixed only at rates of more than $10^{11} \text{ K} \cdot \text{s}^{-1}$, which are not achieved by modern methods of quenching from melt. Al showed a complete inability to amorphization, a completely crystalline structure was fixed throughout the investigated range of thicknesses of quenched foils. The $\text{Fe}_{80}\text{B}_{20}$ alloy exhibits a tendency to amorphization in layers with thick 10 μm at $u_m = 10^7 \text{ K} \cdot \text{s}^{-1}$, and the $\text{Cu}_{47}\text{Ni}_8\text{Ti}_{34}\text{Zr}_{11}$ is amorphized at cross sections 450 μm at $u_m = 1,4 \cdot 10^3 \text{ K} \cdot \text{s}^{-1}$.

Dynamic Destruction Aggregates into Nanosuspensions in Aspect of Create Processing of Thin Films

Kuzma O.V.

Igor Sikorsky NTU“KPI”, Kyiv, Ukraine

Authors in Ref. [1] described the self-organization of BaTiO₃ nanoparticles from PVB-ethanol suspensions - first step for the preparing process for corresponding thin films.

In this abstract were discussed for aggregates with nano inclusions of barium titan at the dynamical failure criterion and corresponding changes on date for effective viscosity. Criterion can be obtained by comparing the interaction force F_i , equals derivation of potential energy U from Ref. [2] for a pair of spherical particles ($r_1 = r_2 = r$) on the distance $h_c = 2r$,

$$F_i = \frac{\partial U}{\partial h} \Big|_{h=h_c} = \frac{\partial}{\partial h} \left[r \left(-\frac{A}{12h} - \frac{B}{h^2} - \frac{64}{k^2} \pi N T \gamma^2 e^{-k_1 h} \right) \right]_{h=h_c}, \quad (1)$$

and generalizing dynamical (rotation, vibration) forces Q_n from the Lagrange equations of motion similar to Ref. [3]. Most active force that failures aggregates into the rotational viscometer is centrifugal force F_{cf} , which depends on rotation velocity or shear rates (ω, D). Next is passive dissipative force F_{dis} depends shear τ and effective viscosity η_{ef} . Summa of first and second attractive terms in (1) for dates Ref. [1, 2] has negative values near $-4 \cdot 10^{-14} N$ for $h = 1.3 \cdot 10^{-7} m$ and becomes less on modulus then positive F_{cf} at $\omega = 2\pi 103 s^{-1}$.

By analysis relations between η_{ef} and D or concentration c of particles, between τ and D , building carves for Krieger-Dougherty and generalized Casson models were obtained intervals of corresponding for dates and was shown that influence of interaction on η_{ef} took place at $D \leq 100 s^{-1}$ and $c \geq 0.1$ -suspension structuring station.

1. M. Zagorny, A.Zhygotsky, A.Ivanchuk, O. Kuzma, A. Pozniy, A.Ragulya. Barium Titanate Nanoparticles Self-organization from PVB-ethanol Suspensions, J. Chem. Eng. Chem. Res. Vol. 2, 4 (2015) 547-555.
2. U.B. Uriev. Physical and chemical dynamics of disperse systems, Russ. Chem. Rev. 73 (2004) 39-62.
3. O.V. Kuzma. The behavior of particles into column of a compressible liquid, disturbed by source of oscillations on the axis of symmetries, Res. Bul. of NTUU “KPI” (Naukovi visti) 4 (2006) 66-72.

Mathematical Methods of Planning and Optimization Processes Growing of Thin Films and Nanostructures $A^{II}B^{VI}$ and $A^{IV}B^{VI}$ from the Vapor Phase

Lopjanko M.A.

Vasyl Stefanyk Precarpathian National University, Ivano-Frankivsk, Ukraine

It is known that semiconductors groups AII BVI and AIV BVI have unique features number that allows them to apply for production of photodetectors and lasers with spectral range of 3-50 microns. Advances for reduce the size of photonic devices closely related with the use of controlled growing of epitaxial thin layers. Despite numerous studies of thin films and nanostructures compounds of AII BVI and AIV BVI, still not fully clarified the impact of growing conditions on the electrical parameters of thin-layer material.

In this paper, using the method of mathematical planning of multifactor experiments received the dependence of the electrical properties of thin layers and nanostructures of PbTe from technological factors of growing from vapor phase by the method of hot wall.

As substrate used fresh chips (111) of crystal BaF₂. To describe the dependence of the electrical parameters of thin layers from technology factors were constructed global polynomial models in 3-factor hyperspace using mathematical modeling. For factors which vary (k=3) were selected substrate temperature (T_S), evaporator temperature (T_V) and chamber walls temperature (T_C) technologically acceptable change range of which are respectively:

$$473 \text{ K} \leq T_S \leq 623 \text{ K}, 758 \text{ K} \leq T_V \leq 878 \text{ K}, 833 \text{ K} \leq T_C \leq 983 \text{ K}.$$

Optimization parameters are: charge carrier mobility (μ), concentration (n), Seebeck coefficient (α), conductivity (σ), thermoelectric power ($\alpha^2\sigma$), and value:

$$Z = \mu/\mu_{\max} + (n/n_{\min})^{-1} + (\alpha^2\sigma)/(\alpha^2\sigma)_{\max},$$

which is a complex optimization parameter.

Choosing the latter option due to the need of researchers to obtain thin layers with maximum values μ_{\max} , $(\alpha^2\sigma)_{\max}$ and minimum concentration n_{\min} . Optimization was performed for summary values:

$$\begin{aligned} \mu &= \mu/\mu_0, \text{ where } \mu_0 = 10^4 \text{ sm}^2 \times \text{V}^{-1} \times \text{s}^{-1}, n' = n/n_0, \text{ where } n_0 = 10^{17} \text{ sm}^{-3}, \\ \sigma &= \sigma/\sigma_0, \text{ where } \sigma_0 = 10^2 \text{ Ohm}^{-1} \times \text{sm}^{-1}, \alpha' = \alpha/\alpha_0, \text{ where } \alpha_0 = 10^2 \text{ B}^1 \times \text{K}^{-1}, \\ (\alpha^2\sigma)' &= (\alpha^2\sigma)/(\alpha^2\sigma)_0, \text{ where } (\alpha^2\sigma)_0 = 10^2 \text{ W} \times \text{K}^{-2} \times \text{sm}^{-1}. \end{aligned}$$

In describing the dependence of the electrical parameters from technological factors identified models of a different order. Borders of adequacy model are defined as the cube which inscribed in hypersphere of planning with radius $R=\alpha$, were α - magnitude shoulder of star.

The data presented in the table and shown in the form of hypersurfaces of response.

Table

Parameters	Regression equation	Values of factors
Charge carrier mobility μ'	$3.89 - 0.20x_1 - 0.12x_2 + 0.22x_1x_2 - 0.36x_1x_3 + 0.23x_2x_3 - 0.76x_1^2 - 0.31x_2^2 - 0.44x_3^2$	$x_1 = \frac{(T_{II} - 548)K}{45K}$
Concentration n'	$1.07 - 0.15x_1 - 0.31x_2 - 0.44x_3 + 0.15x_1x_2 + 0.23x_1x_3 + 0.35x_2x_3 - 0.06x_1^2 + 0.19x_3^2$	
Seebeck coefficient α'	$2.51 - 0.44x_1x_3 - 0.31x_3^2$	$x_2 = \frac{(T_B - 818)K}{35K}$
Conductivity σ'	$2.97 - 0.35x_1 + 0.18x_2 + 0.50x_3 + 0.16x_1x_3 + 0.77x_2x_3 + 0.31x_2^2 + 0.24x_3^2$	
Thermoelectric power $(\lambda^2\sigma)'$	$1.90 - 0.26x_1 - 0.59x_1x_3 + 0.43x_2x_3 - 0.28x_3^2$	$x_3 = \frac{(T_C - 908)K}{45K}$
Z	$2.53 - 0.35x_1x_3 - 0.30x_1^2 - 0.23x_2^2 - 0.38x_3^2$	

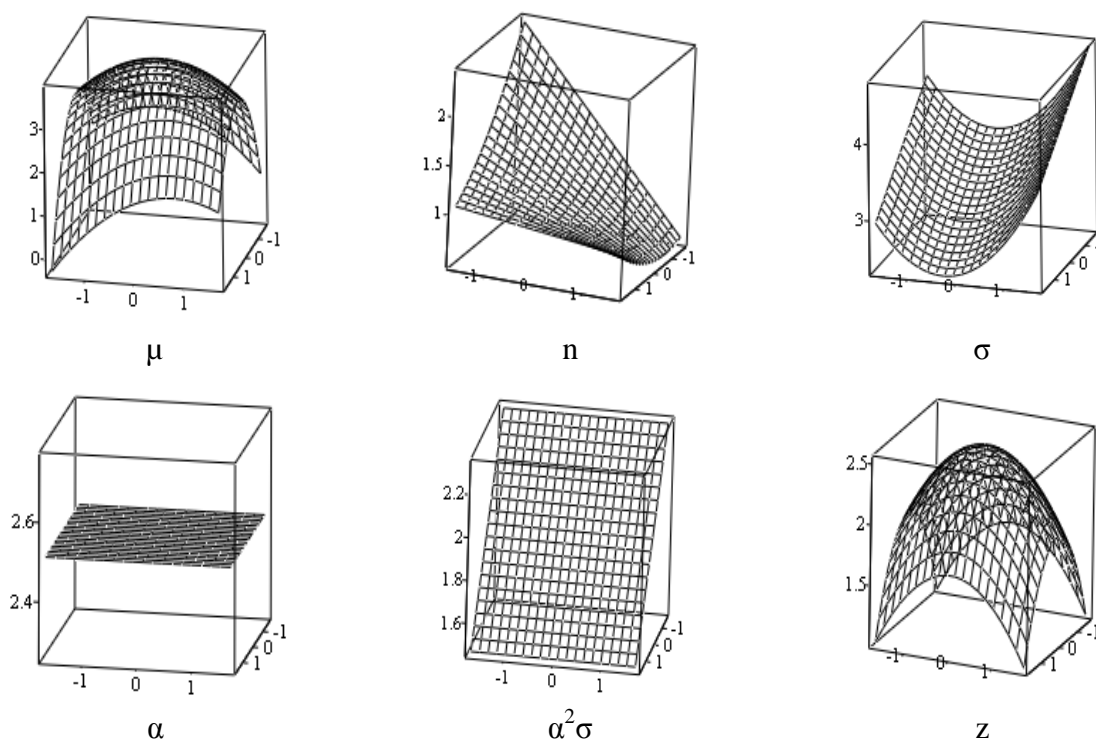


Fig. Response hypersurfaces at a fixed value $x_3=0$.

1. Adler Ju. P., Markova E. V., Granovskij Ju. V. Planirovanie jekperimenta pri poiske optimal'nyh uslovij. – M., 1971. – 255 s.
2. Nalimov V. V., Chernova N. A. Statisticheskie metody planirovanija jeksperimenta. – M., 1965. – 339 s.
3. Beleckij A. V., Kunickij Ju. A., Freik D. M., Shperun V. M. Metody planirovanija i optimizacii fizicheskogo jeksperimenta.- K.: KPI, 1980. – 95 s.
4. Bondar' A. G., Statjuha G. A. Planirovanie jeksperimenta v himicheskoy tehnologii. – K.: Nauka. – 1976. – 247 s.
5. Hartman K., Leckij Je., Shefer V. Planirovanie jeksperimenta v issledovanii tehnologicheskikh processov. – M.: Mir, 1977. – 246 s.
6. Shvedkov E.L. Jeksperimental'naja matematicheskaja statistika v jeksperimental'nyh zadachah materiallovedenija. – K.: Naukova Dumka, 1975. – 216 s

Optimization of Growing Process of the Thin-Film Structures ZnS by Method of Gas-Dynamic Flow of Vapor

Lopjanko M.A.¹, Gaidai S.I.², Leschiiy R.M.³, Kosovan R.P.³, Samojlenko D.V.³

¹Vasyl Stefanyk Precarpathian National University, Ivano-Frankivsk, Ukraine

²Lesya Ukrainka Eastern European National University, Lutsk, Ukraine

³Kalush Polytechnic College, Kalush, Ukraine

In this work is research basic parameters of the deposition process ZnS by gas-dynamic flow of vapor. The dependence of parameters of the deposited material from technological conditions and made optimization for nanostructures and films. Described opportunities for effective recruitment of technological parameters for materials with predictable properties [1-3].

The growth of coefficient values of condensation α and bringing them closer to 1 indicates on the prevalence of the condensation process of reevaporation material particles from the walls surfaces in the high range of values ξ (Fig. 1). This process also illustrates that when $\xi \approx 0,6$ curve of condensation velocity exposed fracture. The dependence of the calculated values of the resulting condensation velocity ω^* from dimensionless coordinate ξ indicates that when $\xi \approx 0,35$ received film have the largest thickness. Evaluation of the reevaporation material makes it possible to specify a region with a structural perfect material which is before the maximum of resulting condensation velocity. Further reduction of the relative density ρ/ρ_1 and increasing degree of vapor phase supersaturation with increasing ξ can be explained by increasing the mean free path of molecules (Fig. 2).

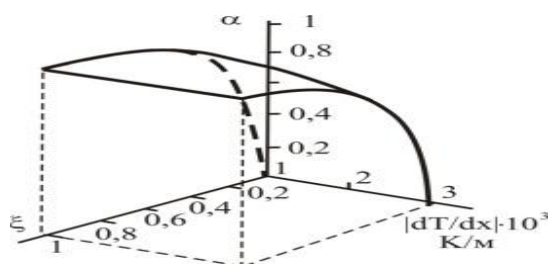


Fig. 1. The dependence of the calculated values of the condensation coefficient α from temperature gradient dT_c/dx and dimensionless coordinates ξ ($T_s = 923$ K, $L = 0,08$ m, $d = 0,05$ m).

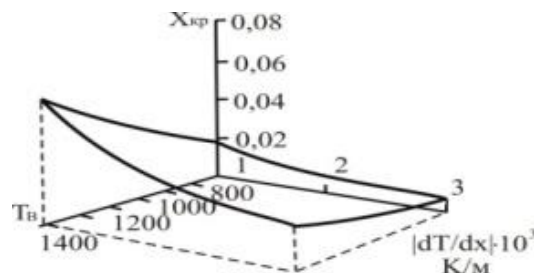


Fig. 2. The dependence of the calculated values of the critical cross section x_{kp} from substrate temperature T_s and temperature gradient dT_c/dx ($L = 0,08$ m, $d = 0,05$ m).

1.C. Ricolleau, L. Audinet, M. Gandais, T. Gacoin, J.P. Boilot. 3D morphology of II-VI semiconductor nanocrystals grown in inverted micelles // *Journal of Crystal Growth*, 203, pp. 486-499 1999.

2. Andrievskij R.A. Nanomaterialy: koncepcija i sovremennye problemy // *Ros.him.zh.*, XLVI(5), ss. 50-56 2002.

3.W.T. Tsang, in: R.K. Willardson, A.C. Beer (Eds.) // *Semiconductors and Semimetals*, Academic Press, New York, 24, pp. 397 1990.

4. Bubnov Ju.Z., Lur'e M.S., Staros F.G., Filaretov G.A. Vakuumnoe nanesenie plenok v kvazizamknutom ob'eme. L. 1975.

Voltammetric Analysis of Phase Composition of Zn-Ni Alloy Thin Films Electrodeposited from Weak Alkaline Polyligand Electrolyte

Maizelis A.A., Bairachny B.I.

*National Technical University «Kharkiv Polytechnic Institute», Kharkiv, Ukraine,
a.maizelis@gmail.com*

Zinc-nickel alloy containing 10-15% of nickel, possess higher corrosion resistance, better mechanical properties and thermal stability against zinc. Such coatings are recommended to replace environmentally hazardous cadmium coatings. Multilayer coating consisting of thin layers of alloy shows higher corrosion resistance. Alkaline electrolytes allow deposition of films of more uniform thickness and composition. Anticorrosive and mechanical properties of the films depend on their phase composition.

The zinc-nickel alloy films of 30–300-nm thickness were electrodeposited on the platinum substrate from weak alkaline ammine-glycinate poliligand electrolyte. The ratio of zinc and nickel ions concentrations in electrolyte and the ligands concentration ratio were varied. Phase composition was analyzed by anodic stripping voltammetry in solution containing 0,5 mol L⁻¹ of Gly⁻ and NH₃(NH₄⁺) each.

From two to four peaks were observed on the voltammograms of anodic dissolution of the deposited Zn-Ni alloy thin films, depending on the deposition conditions. The appearance of anodic peaks may occur due to both oxidation of initial phase of the film, and phase transformation in the dissolution process. Therefore, classical anodic voltammogram analysis was accompanied with voltammogram analysis after accumulation of partial phases, element and X-ray diffraction analysis. The peaks at the voltammograms were separated by partial oxidation at different potentials.

Voltammograms of all films contained alloy peaks corresponding to the oxidation of the initial intermetallic γ -phase (Ni₅Zn₂₁), and all films dissolved with accumulation of α -phase of zinc solid solution in nickel. Films deposited from electrolytes with zinc to nickel ions concentration ratio of 5:1, were dissolved by anodic potential sweep with the appearance of peak corresponding to dissolution of η -phase of zinc solid solution in nickel. Phase content in the coating was determined using ratio of peak areas at the voltammograms. The accumulated deposit after dissolution of all phases before potential values of the last peak is similar to the β -phase by chemical composition (it contains metals in the close to the equimolar ratio).

Thus, the most corrosion resistant γ -phase was observed in the nickel-zinc alloy thin films deposited in weak alkaline ammine-glycinate poliligand electrolyte with a wide range of metal ions and ligands concentration. The films may contain η -phase, depending on the nickel and zinc ions concentration ratio in electrolyte and the current density used for alloy deposition.

Development and Optimization of Conditions for the Surface Treatment of the PbTe Single Crystals by Chemical-Mechanical Polishing

Malanych G.P., Tomashyk V.M.

*V. Lashkaryov Institute of Semiconductor Physics of NAS of Ukraine,
Kyiv, Ukraine, e-mail: galya_malanich@mail.ru*

The purpose of this work is to develop the new effective polishing etchants with a wide range of PbTe etching rates, as well as the high quality of the treated crystal surface after treatment, which includes wire cutting ingots into wafers, mechanical grinding and chemical-mechanical polishing (CMP). Single crystals of PbTe grown by the Bridgman method have been investigated.

Mechanical grinding of the plates was carried out by water suspensions of abrasive powders M10, M5 and ASM 1/0. The disturbed during cutting and grinding layer with the thickness of 100-150 μm was removed by CMP using H_2O_2 – HBr – ethylene glycol etchant at a polishing rate of 185 $\mu\text{m}/\text{min}$. CMP was carried out on a glass polisher covered with lawn cloth with a continuous supply of etchant at a rate of 2-3 ml/min for 2 min and a pressure on the plates in 2-3 kPa. The crystal dissolution rates were registered by reducing its thickness before and after etching using an electronic indicator TESA DIGICO 400 with an accuracy $\pm 0.2 \mu\text{m}$. The etchants were prepared using 48 % HBr, 35 % H_2O_2 , ethylene glycol (EG) and glycerol (GL) (the composition is given in vol. %).

Washing of the samples after the CMP is a very important step, as the rinsing them with deionized water only is ineffective. According to the developed by us method, the samples must be quickly extracted from the etchant and immediately rinsed under the scheme (30 sec in each solution):



Microstructure of the treated surfaces after various stages of the mechanical and chemical treatments was studied using table scanning microscope JEOL JCM-5000 NeoScope. Morphological study of the polished surface of PbTe spent on scanning probe microscope NanoScope IIIa Dimension 3000TM (Digital Instruments, USA).

It was shown that the dilution of the polishing etchants H_2O_2 – HBr – EG (based solution – BS) at the chemical-dynamic polishing and CMP with the etching rates of 8.0 and 185 $\mu\text{m}/\text{min}$, respectively, leads to ameliorate the quality of polished surfaces. Using such dilution, it is possible to change the CMP rate within the interval from 1 to 185 $\mu\text{m}/\text{min}$ at the using the etchants with the volume ratio 100–10 BS : 0–90 GL. The proposed compositions of the (H_2O_2 –HBr–EG)/GL polishing etchants and the developed treatment methods of PbTe single crystals give the possibility to decrease significantly the surface roughness ($R_a < 10 \text{ nm}$) compared with its value obtained after cutting ingots into plates with the next grinding.

Technology of Gas-Dynamical Stream of Vapour for II-VI and IV-VI Nanocrystals

Nykyruy R.I.¹, Shenderovskiy V.A.², Kalytchuk I.V.³, Mazur M.P.⁴, Pavlyuk M.F.⁵

¹Kolomyia Polytechnical College of the Lviv National Polytechnical University, Kolomyia, Ukraine;

²Institute of Physics NAS of Ukraine, Kyiv, Ukraine;

³Snyatyn College of the Kamyanets-Podilskiy Agro-Technical University, Snyatyn, Ukraine

⁴Ivano-Frankivsk National University of Oil and Gas, Ivano-Frankivsk, Ukraine

⁵Vasyl Stefanyk Precarpathian National University, Ivano-Frankivsk, Ukraine

The aim of paper is calculate the parameters of gas-dynamical stream of vapour of semiconductor compounds CdS, ZnS and PbS for predicted control growing process.

Semiconductor nanocrystals CdS, ZnS and PbS were obtained by precipitation in the vacuum cylindrical chamber (diameter $D = 0.05$ m and length $L = 0.08$ m, the evaporation temperature $T_s = 923$ K, and the temperature gradient along the chamber walls was $dT_c/dx = -3 \cdot 10^3$ m⁻¹).

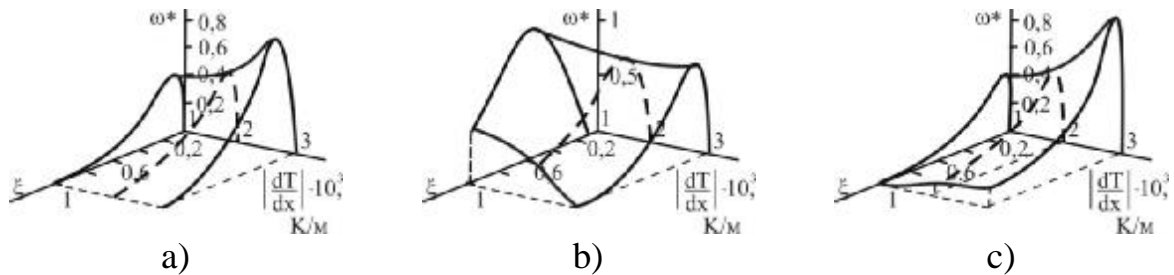


Fig. The dependence of the resulting condensation rate ω^* for the CdS (a), ZnS (b) and PbS (c) due $\frac{dT_c}{dx}$ and dimensionless coordinates ξ .

The parameters of the gas-dynamic stream of vapour calculated (namely, condensation ratio α , the resulting condensation rate ω^* , supersaturated vapor phase ψ). Was established their dependence on temperature gradient dT_c/dx along the chamber walls.

The dependence of the parameters of the gas-dynamic stream of vapour on the composition of the compound due to different values of base units - energy evaporation pressure and vapor density were obtained.

The parameters of gas-dynamical stream of vapour depends to the evaporation temperature T_s , temperature gradient along the chamber walls dT_c/dx , and identifies by locations of condensing substrate ξ (see figure). On the area $\xi = 0$ no vapor condensation ($\alpha = 0$). The sharp growth factor condensation $0 \leq \alpha \leq 0.9$ shown when $0 \leq \xi \leq 0.3$ for CdS, $0 \leq \xi \leq 0.4$ for ZnS, and $0 \leq \xi \leq 0.3$ for PbS. The re-evaporation contribution rate decreases and approaches the unit ($\alpha \sim 1.0$) for dimensionless coordinates.

Synthesis of Ag_8SnSe_6 Argyrodite thin films

Semkiv I.V.¹, Dubiv T.O.², Rodych V.M.¹, Zmiiovska E.O.¹, Lopatynskiy I.Ye.¹,
Honchar F.M.¹

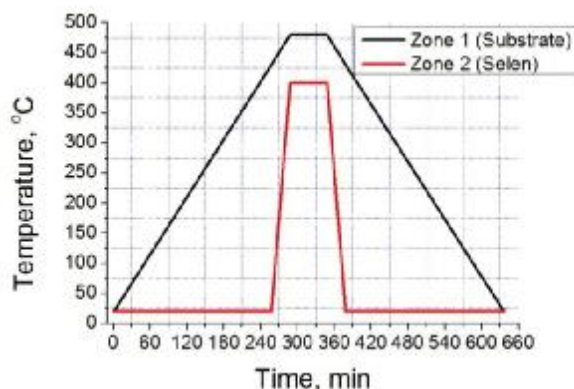
¹Lviv Polytechnic National University, Lviv, Ukraine

²Ivan Franko National University of Lviv, Lviv, Ukraine, Semkiv.Igor.5@gmail.com

Synthesis of argyrodite thin films was carried out by the selenization of Ag-Sn films, taken in stoichiometric ratio of these components in the Ag_8SnSe_6 compound.

The Ag-Sn thin films was deposited by high-frequency magnetron sputtering method from the target (alloy of silver and tin in the following molar ratio of the component $[\text{Ag}]/[\text{Ag} + \text{Sn}] = 0,85$) in an argon atmosphere during 30 minutes. Further obtained films was placed in a quartz ampoule with the elemental selenium of high purity and evacuated to a pressure of 10^{-6} Torr. Filled and evacuated ampoule was placed in a vertical furnace with two controlled zone to synthesis of argyrodite thin films.

Synthesis temperature of Ag_8SnSe_6 films was conducted according to the temperature dependence shown in Figure. During synthesis zone 1 (with the substrates) was slowly heated to 480°C . When the desired temperature is reached to form gaseous Se the rapid heating of zone 2 (with elemental selenium) to 400°C was starting. To order the avoid the formation of selenium clusters that decrease the activity of selenization of Ag-Sn films, between zones 1 and 2 was used additional narrow zone with temperature 700°C . When the required temperatures were reached the temperature exposure during 1 hour was carried out. After this process cooling of the system (see Figure).



Obtained thin films were investigated by X-ray diffractometer STOE STADI P in a reflection mode with $\text{CuK}\alpha_1$ radiation. X-ray diffractogram shows only peaks related to the Ag_8SnSe_6 compound. Crystal structure determination showed that the compound crystallized in orthorhombic structure with space group $Pmn2_1$. The crystal lattice parameters are $a = 7.9081(6) \text{ \AA}$, $b = 7.8189(7) \text{ \AA}$, $c = 11.0464(9) \text{ \AA}$, $V = 683.03(10) \text{ \AA}^3$. This result for the Ag_8SnSe_6 thin films are in good agreement with the results for crystalline samples [1].

1. I.V. Semkiv, B.A. Lukyanets, H.A. Ilchuk, R.Yu. Petrus, A.I. Kashuba, M.V. Chekaylo. Energy Structure of β -phase of Ag_8SnSe_6 Crystal, *Journal of Nano- and Electronic Physics* **8**(1), 01011 (5pp) (2016).

The Phenomenon of Improving of Turbostrate Structure of Carbon Fibers, Subjected Chemo-thermo-mechanical Activation, during Dynamic Contact of Surfaces of Solid States

Sirenko H.O., Soltys L.M.

*Vasyl Stefanyk Precarpathian National University,
Ivano-Frankivsk, Ukraine, soltys86@gmail.com*

The phenomenon of improving of turbostrate (two-dimensional ordered) structure – decreasing interlayer distance and increasing the thickness and length of the packets layers of carbon hexagon of carbon fibers. The fibers were obtained by thermal treatment at temperature of 723-2673 K of final thermal influence on hydrate cellulose, polyacrylonitrile or copolymer organic fibers in an inert atmosphere, such as nitrogen, inert gases, methane or natural gas. The fibers were chemically processed before or after thermal treatment by compounds of phosphorus and boron, for example, sodium tetraborate and diammonium phosphate. After thermal treatment the fibers were subjected to mechanical activation in knife crusher for 2000-12000 rev./min. or in dismembrator or disintegrator for 2000-25000 rev./min. Additionally the fibers were subjected to thermal, complex deformation and tense influence during dynamic contact surfaces of solid states in the bound dispersion with polymer matrix in the node of friction or in the free dispersion, for example, in ball mill for 50-3050 hours.

The effect of improving the structure of fibers differs from three-dimensional ordered (crystalline) structure of artificial or natural graphites in the same conditions, for which interlayer distance increases and the length and thickness of the carbon hexagon packets decreases.

By results of researches were made conclusions:

1. The three-dimensional ordered crystal structures of graphites during chemo-mechanical action, especially during friction and wear, the part becomes amorphous and the most part transforms in the two-dimensional ordered (turbostrate) structure.

2. It has opened the phenomenon of improving of turbostrate (two-dimensional ordered) structure (decreasing interlayer distance and increasing the thickness and length of the packets layers hexagon) of carbon fibers, obtained by chemo-thermo-mechanical activation in the presence of boron-containing and phosphorus-containing compounds during intensive mechanical action. This effect the most appears for carbonated fibers at temperature of 1123-2073 K.

3. It has proposed the hypothesis: it is likely that only at certain perfection of turbostrate structure of carbon fibers and graphites (interlayer distance, thickness and length of the packets layers hexagon) and simultaneously during the leaking of tribochemical, chemo-physico-mechanical and other triboprocesses can achieve the effect of low friction and small magnitude wear.

The Effect of Particle Size Distribution of Graphite on the Properties of Polymer Composites

Sulyma I.V., Sirenko H.O.

Vasyl Stefanyk Precarpathian National University, Ivano-Frankivsk, Ukraine

There are the results of studies of the effect of parameters of particle size distribution of fillers (natural graphite different bands) on physical and mechanical properties of polymer composites based on aromatic polyamide (APA) fenilon C-2. The fillers differed by ash content, moisture and grinding fineness (dispersion). The particle size of the filler and polymer for the theoretical gamma-distribution parameters (perimeter, thickness and diameter) have different values. The particles of graphite have similar values with aromatic polyamide particles on the perimeter. The particles of graphite and aromatic polyamide have the same average value that determines composition on these materials on the effective diameter of roughly. The aromatic polyamide and all graphites are small on the thickness.

The physical and mechanical properties of polymer composites based on aromatic polyamides are highly dependent on dispersion, of ash content and the graphite particles concentration of dispersed phase. Graphite is named the high-ash with 5-15% ash content. And graphite is named the low-ash with 0,05-2,5% ash content.

The influence of ash content and graphite dispersed phase on friction strength APA was investigated. Both factors affect about the same. The regularities for strength during stretching and compression, the specific impact strength, elongation at break were determined. There are discovered to the tribological properties too, which was found in the limit loads mode. The relative durability of samples of colloidal systems based on graphite is growing with a decrease in ash content and dispersity for low-ash graphite and with a increase in ash content and dispersity of high-ash graphite ($\frac{1}{I_C} / \frac{1}{I_P} = \frac{I_P}{I_C}$, where I_C ,

I_P – the intensity of wear of polymer composites and polymer matrix, respectively). A minimum of frictional strength observed by 1,5-5% ash content. The durability of polymer composite have a reliable relationship with a set of bulk mechanical properties according to the research by selected samples.

The linear correlation was determined between the relative durability ($y = I_P/I_C$) on the first (S_1) and second (S_2) friction stages and the gamma distribution θ and λ parameters on the basis of the results to predict areas of application and performance properties of polymer composites. Perimeter particles of graphite was the most informative parameter in polymeric composites. The non-linear correlation was discovered between the wear rate and the distribution parameters of graphite particles.

Technological Features of Manufacturing and Characteristics of Thin Films Obtained by Treating PM with TX100 Detergent

Trikur I.I., Sakalosh I.I., Sichka M.Yu., Rizak V.M.

Uzhgorod National University, Uzhgorod, Ukraine

Fiber optic biosensors of reflective type with a sensitive element on bacteriorhodopsin (BR) have many advantages: high sensitivity, small-size and low-cost. For monitoring of aqueous solutions and for medical researching the usage of water-insoluble sol-gel matrices is required. A large difference in sizes between fragments of purple membranes (PM) and matrix molecules leads to a deterioration in the quality of these films and the sensitivity of sensors on their basis. The given work is devoted to developing technology of obtaining purple membranes fragments of the minimum size at which BR photoactivity and photochromity of films on its basis are preserved.

Solubilization substantially impairs the stability of the BR [1]. Since we are interested not in full solubilization of BR but in PM fragments size reduction, we used a slightly modified procedure described in [2]. PM suspension was diluted in 5 mM Tris-HCl buffer solution (pH 7.0) to a concentration of 10 μ M. Triton X100 with the concentration of 1 to 3 mM was added in the dark to the resulting solution, kept for 2 hours at 35 °C and then centrifuged at 105,000 g for 60 min at 4 °C. The efficiency of solubilization was controlled by determining the maximum transmission ratio of the obtained supernatant solution and the value of maximum absorption at 568 nm in native PM. PM fragments that have not undergone complete solubilization during centrifugation are deposited on the bottom. The precipitated fragments were diluted in distilled water and used for all subsequent studies.

As a result of the study of the spectral characteristics of suspensions and BR films with the addition of detergent TX100, it was found that high concentrations (> 4 mM) lead to the destruction of PM and irreversible changes in the structure of BR by the action of optical radiation. At the same time, at lower concentrations, partial solubilization is observed at which the PM size decreases and a large part of the BR molecules retains their optical properties. Studies of PM treated with detergent TX-100 at a concentration of 2.5 mM using AFM showed that the average size of the fragments was about 1 μ m. The roughness of the surface of the resulting films is 2 times less than that of films of PM untreated by detergent. The obtained results indicate that the use of detergents allows to influence the size of PM fragments and thus increase the optical quality of films based on BR.

References

1. Dencher N. A., Heyn M. A. Preparation and properties of monomeric bacteriorhodopsin // *Methods in Enzymology* Vol. 88, 1982. p. 5-10.
2. T. Sasaki, M. Sonoyamat, M. Dernura, S. Mitaku Photobleaching of Bacteriorhodopsin Solubilized with Triton X-100 // *Photochemistry and Photobiology* Vol. 81, 2005. p. 1131-1137

Dynamic System of Obtaining Thin Films of Materials

Myrovych O.V.¹, Oleskiv R.B.¹, Turovska L.V.²

¹*Vasyl Stefanyk Precarpathian National University, Ivano-Frankivsk, Ukraine*

²*Ivano-Frankivsk National Medical University, Ivano-Frankivsk, Ukraine*

Nowadays, the problem of obtaining statistically homogeneous, reproducible, functional active and passive nanosystems of electronics in the process of deposition of gas-vapor mixture of material on substrates of different chemical nature and electronic structure (amorphous, polycrystalline, crystalline) by vacuum evaporation method, Hot-wall-epitaxy, or molecular beam epitaxy is not fully solved due to complexity of determining the optimum temperature of condensation of gas-vapor mixture on adsorbent to obtain the high structural perfection of adsorbate.

In order to solve this problem, the construction of compact, low energy intensive, sectional electric heater of substrates in a vacuum in the range of 293-893 K, consisting of seven discrete ovens, each of which was individually calibrated for temperature with a difference of 373 K, has been developed and tested. The heater is powered by a constant voltage which is changed to obtain heating temperature of ovens with the difference of 273, 283, 293, 353 K.

In one cycle of evaporation, in the vacuum chamber, the process of obtaining film structure of material at various fixed temperatures of heating the substrate of different chemical nature and the electronic structure is implemented that allows to study one of the important aspects of kinetics of adsorption-desorption processes of formation of adatoms, grain boundaries, two-dimensional islands, and its coalescence, growth, and formation of pseudomorphic superfine layer, and homogeneous thin film at the final stage.

Thickness of a deposited film on substrates of different nature depends directly on the mass of evaporated material in time phase.

It is easy to evaluate the impact of technological factors on properties of materials deposited on substrates of different nature and optimize the function value of the heating temperature of substrate, which characterizes the investigated process, due to using mathematical modelling.

The Changes of Structure and Electrical Properties of Thin Films During Long-Term Aging

Yatsyshyn B.P., Domantsevych N.I.

Lviv University of Trade and Economics, Ukraine, Lviv

As research materials were crystalline thin film of ternary systems which have been identified as compound REMeGe₂, which had long-term aging (20 years) or periodically exploitation as elements of thermoelectric sensors. All samples were obtained in vacuum 10⁻³ Pa at a deposition rate v_p 4 to 30 nm / s. The thickness of the condensate was 60-120 nm.

It was established that long-term aging led to an increase in electrical resistance of crystalline condensates. The deviations from the initial value of resistance depended on the conditions of condensation (mainly in indexes of substrate temperature during deposition T_p , thermodynamic saturation Z_p , the deposition rate v_p , type of material (compounds), conditions of storage or exploitation. The best temporal stability of electrical characteristics were obtained on thin film which condensed at high maximum substrate temperature allowable for the glass ceramic substrates. The slightest deviation from the initial electrical resistance at the long aging characterized by crystalline condensates Y₂₅Fe₂₅Ge₅₀, obtained by coevaporation on a substrate at $T_p = 710$ K at a rate $v_p = 6$ nm per sec, and LaNiGe₂, which were obtained under the same conditions. For the first sample deviation was 15-25%, for the second – 26-40%. The deviation for the first films was 15%, for the second – 26%. The crystalline thin films of ternary compounds with Sc and La, which were obtained by $T_p = 650$ K, characterized by significant abnormalities deflections of electrical resistance (deviation – 80%). The structure of the surface of such films after long decades of aging uniformly smooth, with no visible defects such as pores and cavities. However, the growth of crystal conglomerates predominantly round shape with dimensions $0,5 \cdot 10^{-6}$ m observed. The defects of thin films which had the form of pores were identified as flaws of initially receiving during condensation, which, however, not grew at a long time aging.

The structure of the surface of such films after long decades of aging uniformly smooth, with no visible defects such as pores and cavities. However, the growth of crystal conglomerates predominantly round shape with dimensions $0,5 \cdot 10^{-6}$ m observed. The defects of thin films which had the form of pores were identified as flaws of initially receiving during condensation, which, however, not grew at a long time aging.

CdTe and ZnO for Heterojunctions in Solar Cell

Yavorskyi R.

Vasyl Stefanyk Precarpathian University, Ivano-Frankivsk, Ukraine, roctyslaw@gmail.com

Highly efficient and low cost solar cells remain among the potential choices to solve climate problems and meet the increasing demand of global energy. Research on the so-called “next-generation” solar cells is focused in the development of cost-effective clean sources of energy. In general, the extremely thin absorber solar cell consists of an extremely thin absorbing layer ($E_g \sim 1.1-1.8$ eV) embedded between n and p-type nanostructured electrodes ($E_g > 3$ eV).

The increasing efforts have been devoted to the development of ZnO nanostructures for solar cells due to its wide bandgap energy of 3.3 eV at room temperature, high exciton binding energy of 60 MeV and high electron mobility. On the other hand, CdTe, is highly effective absorbent layer and is considered a good candidate as a shell layer through the energy band gap of 1.45 eV at room temperature and its high rate of optical absorption ($> 10^4$ cm⁻¹). The potential deviation to tellurium decreasing also should be emphasized, as well as demand from the future use of CdTe nanostructures in order to reduce the amount of raw materials consumed.

The ZnO films were deposited on silicon, glass and ITO/glass substrates by PLD using the YAG: Nd³⁺ laser with the 532 nm wavelength (II harmonics), 6 ns pulse time, 10 Hz repetition rate and fluence F in the range 10 J/cm². The laser beam was focused on the target using a quartz lens with focal distance of 600 mm. The growth temperature T_s was kept at (20–400)°C.

The CdTe films were deposited on silicon and glass substrates using the vapor-phase condensation method. The growth temperature T_s was 200 °C, temperature evaporation of the sample pre-synthesized compounds CdTe change within $T_v = (500 - 600)$ °C. The thickness of the thin films asked deposition time $\tau = (60 - 420)$ sec.

The morphological properties and the cross-section of the sample CdTe and ZnO thin films were investigated by Scanning Electron Microscope and the structural by Atomic Force Microscope techniques. On cross section morphology of the sample observed the condensed in columnar type of growth oriented in c direction. In this case type of growth is oriented by temperature of the substrate.

Optical characterization of ZnO and CdTe films contain information about other physical properties, band gap energy and band structure. Optical characteristics indicate on thin and stable films, and samples have an average optical transparency of 60-80% in visible range. The samples CdTe have greater homogeneity of structure. With a reduction deposition time, absorption window of the samples CdTe thin films were expanded.

Study of Morphology and Microhardness of Co-Mo Alloys Films

Shtefan V.V., Yepifanova A.S., Berezovskyi I.S., Shkolnikova T.V.

National technical university „Kharkiv politechnical institute“, Kharkiv, Ukraine

Galvanic alloys of Co-Mo are one of the most perspective materials used in microelectronics and technology of microelectromechanics devices [1]. Depending on correlation of components the property of such alloys can largely change: alloys with high maintenance of cobalt show magnetic properties and can be used in the devices of record and maintenance of information, alloys with high maintenance of molybdenum possess high hardness.

Films of alloy Co-Mo, getting with galvanic method were viewed in this study. The content of the refractory component varied 0 ... 85 wt.%. Structure study was conducted using a Leica DM ILM metallographic microscope with a digital camera Leica DFC 295 maintaining the appropriate hardware and software [2]. Vicker's microhardness (Hv) coatings cobalt-molybdenum alloy was determined by pressing a diamond pyramid hardness tester PMT - 3 by the load of $P = 0,2$ kg and 10 seconds time delay. Hv calculations were calculated using the method [3]. Impedance calculations were performed using the system IPC-Pro and FRA in acidic and neutral aqueous areas, the parameters of the impedance were determined by the technique [3].

Impedance spectra indicate that the equivalent scheme of the electrode-electrolyte were described by the model Eshlera-Rendolsa. The definition of transfer resistance were the maximum and the capacity of the electric double layer - the minimum for films consisted on alloys with a molybdenum content greater than 25 wt.% was defined. The behavior of the spectra and the parameter's definition of impedance indicates about the formation on surface of films compounds of a new phase.

Entering of molybdenum compounds in the electrolyte increases the hardness of the coating, the highest scratch microhardness reaches 429 kg/mm^2 for films with molybdenum content of 50 wt.%. Further increase of the molybdenum content to 85 wt.% In the alloy leads to a reduction of microhardness definition was equal to 313 kg/mm^2 .

1. Shtefan V.V., UA Patent112925, 2016.
2. Shtefan V.V., Bairachnyi B.I., Lisachuk G.V., Smyrnova O.Yu., Zuyok V.A., Rud R.O., Voronina O.V. Corrosion of Aluminum in Contact with Oxidized Titanium and Zirconium // *Materials Science*, 2016, Volume 51, Issue 5, p.p. 711–718.
3. Shtefan V.V., Ved M.V., Sakhnenko M.D., Pomoshnyk L.V., Fomina L.P. Regularities of the deposition of cobalt-tungsten alloys by pulsed currents // *Materials Science*, 2007, Volume 43, Issue 3, pp 429–433.

Synthesis and Investigation of Thick Epitaxial $Y_{3-x}La_xFe_5O_{12}$ (LA:3IG) Films

Yushchuk S.I., Yuryev S.O., Gorina O.M., Dubelt S.P., Loboiko V.I.

National University "Lvivska Polytechnica", Lviv, Ukraine, e-mail: syuryev@mail.ru

The aim of this work is to study the possibility of growing of substituted yttrium-iron garnet (YIG) thick films with homogeneous physical properties and a narrow linewidth of ferromagnetic resonance (FMR) which determines the magnetic losses of high frequency devices. For the expanding of the range and increase the working capacity of microwave devices requires the thick ($\geq 20 \mu m$) films. The YIG films, which have the lattice parameter equal to $a_f = 12,376 \text{ \AA}$, are grown by the method of liquid-phase epitaxy on single crystal substrates of gallium-gadolinium garnet (GGG) with the lattice parameter $a_s = 12,383 \text{ \AA}$.

To eliminate the difference between the lattice parameters a_s and a_f we have replaced the part of the Y^{3+} ions in the films by La^{3+} ions ($x \leq 0,06$) which are non-magnetic and have the large ionic radius. It is possible to increase the lattice parameter of the ferrite film to a value characteristic of the substrate of GGG, and thereby to eliminate mechanical stresses in the film.

The Pb^{2+} ions that entered to the film from the boron-lead melt-solution (MS) during the process of growing increase the linewidth of the FMR, and, consequently, increase the magnetic losses. By the selection of the optimal composition of melt-solution and technological conditions the entry of Pb^{2+} ions were minimized. The La:YIG films with thicknesses up to $60 \mu m$ and FMR linewidth near of $0,6 \text{ oE}$ were obtained.

The growing of substituted La:YIG thick films became possible due to higher distribution coefficient of the ions La^{3+} with the comparison to the Pb^{2+} ions at high of growth temperatures.

The requirements to the results of technical growth conditions have been defined. To reduce the concentration of lead ions in the La:YIG films need to grow them at higher temperatures $\approx 1220 \text{ K}$ and small supercooling of the MS. Also, a mandatory rule during the growth of La:YIG is the continuous temperature decrease of the MS with small velocities ($\approx 0,35 \text{ K/min}$). This is due to the depletion of the MS during the process of the films growth. To ensure the reproducibility of the properties of the La:YIG thick films it is necessary to carry out their growing with the large mass ($\approx 12 \text{ kg}$) of MS and with a high content of oxides.

Nanocellulose as a Functional Part of Electronic Components: *ab initio* Diagnostic Calculation

Balabai R.M., Zdeshchyts A.V.

Kryvyi Rih State Pedagogical University, Kryvyi Rih, Ukraine

On one hand, the lifetime of electronics is becoming shorter; this evolution generates technological challenges and poses a growing ecological problem. On the other hand, paper is ubiquitous in everyday life. It is renewable, portable, and flexible and in addition, cellulose is the Earth's major biopolymer [2]. Besides natural cellulose, nanocellulose is the basis of novel sustainable area to produce cellulose categorized as a renewable source of materials that displays remarkable physical properties, such as transparency, together with low toxicity and cost production, earth-abundance and biocompatibility, besides being able to be integrated in other systems acting as a composite for paper-based electronics [2].

For extension of information about electronic properties of composite structures of graphene and cellulose (fig.1), we are calculated with such methods as electron density functional and first-principles pseudopotential based on own program code [3], the spatial distributions of the valence electrons density, width of the band gap, Coulomb potentials along the chosen directions, the charge's state of atoms.

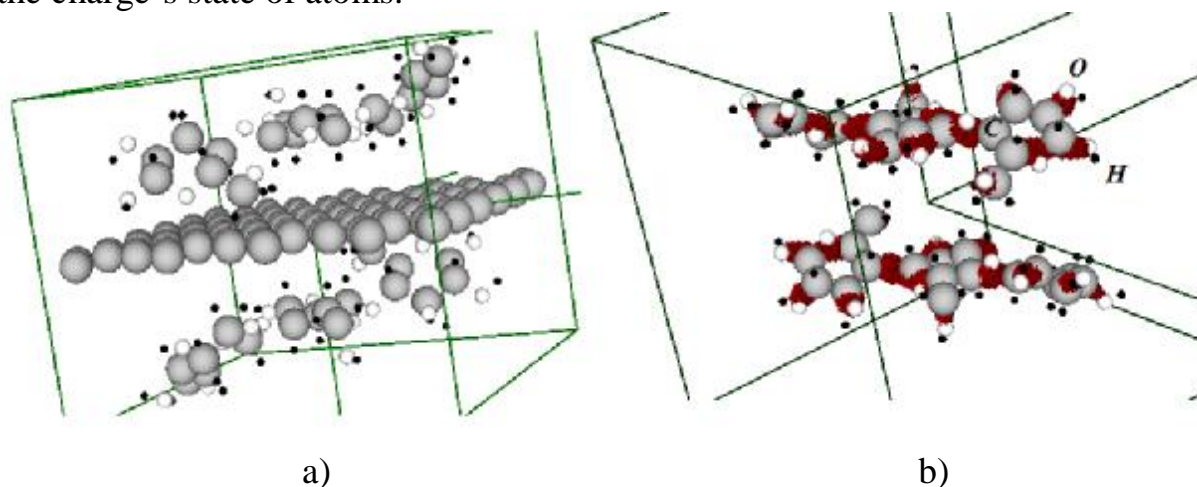


Fig.1. a) hybrid structure based on graphene and cellulose for calculation; b) the spatial distributions of the valence electrons density within the interval of 1.0–0.9 of the maximum value for cellulose

1. S. Ummartyotin, M. Sain. Cellulose Composite for Electronic Devices / Department of Physics, Faculty of Science and Technology, Thammasat University, Thailand. – 2016.
2. HORIZON 2020 - Work Programme 2016 – 2017, Cross-cutting activities (Focus Areas), PILOTS-05-2017: Paper-based electronics.
3. Ab initio calculation [E-resource] – Mode access to the resource: <http://sites.google.com/a/kdpu.edu.ua/calculationphysics>



POSTER REPORTS

Session 2

Nanotechnologies and nanomaterials, quantum-size structures



Influence of Modifiers on Structure and Optical Properties of the Au-Containing Silica Gel-Glasses

Akinshau K.A.

*B.I. Stepanov Institute of Physics, NAS of Belarus, Minsk, Belarus,
e-mail: akinshau@ifanbel.bas-net.by*

The aim of the work is to develop the synthesis technique and to study the structure of Au-containing silica gel-glasses doped with Ce, Mg and B.

The glasses (mass %) 1.0Au-99.0SiO₂ (**1**), 0.5Au-98.5SiO₂ (**2**), 0.5Au-0.4Ce₂O₃-99.1SiO₂ (**3**) и 0.5Au-1.0B₂O₃-98.5SiO₂ (**4**) were synthesized by modified sol-gel method followed by the heat treatment at the various temperatures. DRON 3.0 diffractometer, LEO 1420 SEM-microscope and Cary-500 spectrophotometer were used to study the structure and optical properties of these samples.

It was found that the gold nanoparticles have been already forming at the heat treatment process of xerogels. It is evidenced by appearance of the reddish coloring of samples. The sintered silica glasses absorption spectra (Fig. 1) and SEM pictures show that the most elliptical gold nanoparticles are inherent to B-Au-containing silica glasses, and the most spherical gold nanoparticles are inherent to Ce-Au-containing glasses.

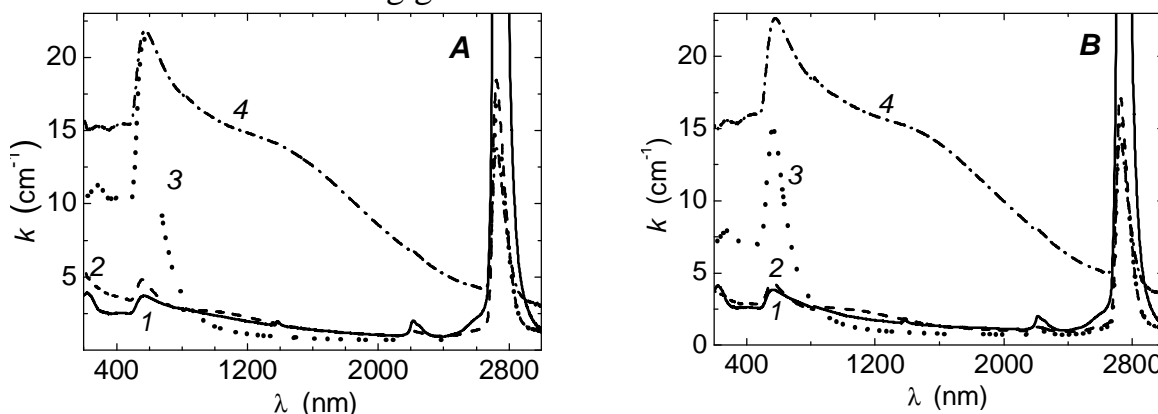


Figure 1 – Absorption spectra of the synthesized glasses (1-4) **A** – initial, **B** – after heat treatment at $T = 970^{\circ}\text{C}$ for 25 hours.

The glasses annealing in the air is accompanying by the noticeable self-oxidation [1], but it slightly affects on the position, shape and intensity of the plasmonic band of both Au-containing glasses and the similar glasses doped with B and Mg. The “spectroscopic behavior” of the Ce-Au-containing glass is more sensitive to such annealing.

The nature of the phenomena and possible applications are under discussion.

[1] G.E. Malashkevich, E.N. Poddenezhny, I.M. Melnichenko, and A.A. Boiko, *J. Non-Cryst. Solids* **188**, 107-117 (1995).

Influence of Ethanol and Water on Physical and Chemical Processes of Splitting of Paracetamol and Glycine

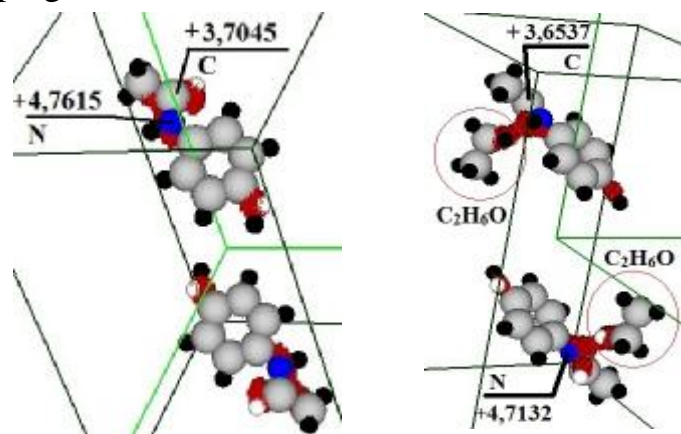
Barilka A.G.¹, Balabai R.M.¹, Chernikova H.M.²

¹Kryvyi Rih Pedagogical University, KryvyiRih, Ukraine, barilkaalena@gmail.com, balabai@i.ua

²Kryvyi Rih National University, Kryvyi Rih, Ukraine, hmchernikova@gmail.com

Information about the interaction of medicinal preparation with other fluids used by the people, important to determine the physical and chemical properties of determinate medicament. For example, there is evidence that the therapeutic properties of paracetamol as a remedy of respiratory diseases, can be toxic to patients receiving both medicines containing ethanol as a solvent [1]. As for glycine, which is an inhibitory neurotransmitter type of action and the regulator of metabolic processes in the central nervous system, the medical practice has shown that it can be combined with ethanol [2].

It is important to define the specifics of pharmacodynamics interactions of medicaments with liquids. So, the aim of this work is detailing at the atomic level physical and chemical processes splitting of paracetamol and glycine molecules in the presence of liquids (water and ethanol) in the framework of the electron density functional and ab initio pseudopotential methods. All calculations the spatial distributions of the valence-electron, the electric charges in the different positions of the atomic molecules, the energy spectrum were carried out with the help of our own program code [3].



Thus, in Fig. 1, the results of calculations for molecules of paracetamol and ethanol. We are showed a change of the electrical charge in the vicinity of the nitrogen and carbon atoms after the supply of ethanol. The charge of an isolated nitrogen core is +5, and carbon +4.

Fig. 1. Spatial distributions of the valence electron density in the paracetamol`s molecules (left) and the paracetamol`s molecules surrounded by the ethanol`s molecules (right) for values of density in interval of 0.9–1 from the maximum.

- 1.Yoon E. et.al. Acetaminophen - Induced Hepatotoxicity: a Comprehensive Update // J. Clin. Transl. Hepatol. – 2016. –V. 4, No.2. – P. 131–142.
- 2.Amin FU, Shah SA, Kim MO. Glycine inhibits ethanol-induced oxidative stress, neuroinflammation and apoptotic neurodegeneration in postnatal rat brain // Neurochem. Int. – 2016. – V. 96. – P.1-12.
- 3.<https://sites.google.com/a/kdpu.edu.ua/calculationphysics/>

A Study of the Reactions Between Silver Nanoparticles and Organic Compounds Under Local Plasmon Resonance Conditions

Boltovets P.M., Kravchenko S.O., Snopok B.A.

V.Ye. Lashkaryov Institute of Semiconductor Physics NAS of Ukraine, Kyiv, Ukraine
paraskeva2013@gmail.com

“Soft” decomposition of potent organic xenobiotics under normal conditions is quite promising approach with regard to the control of the environment safety. Using the natural light induced excitations specific for metal nanostructures of gold and silver is one of the possible ways to realize that. The intensity of electric fields in direct proximity to the metal surface under the surface plasmon resonance (SPR) conditions can reach high values because of characteristic features of the light field distribution. In this case it is possible to lower or completely level out the potential or activation barriers, giving rise to the occurrence of reactions that are impossible under normal conditions, in particular, ones specific for “cutting” of organic molecules.

Silver nanoparticles (Ag NP) are known by their oxidative properties under the illumination at c.a. 410 nm (localized SPR). The most convenient way to study oxidative properties of colloidal silver solutions is test their reactions with some organic dyes, for example, methylene blue (MB) under the controllable illumination conditions (using light-emitting diodes). Taking into account that Ag NP and methylene blue have well distinguishable peaks of absorption, it was reasonable to test initially absorption regions specific for Ag NP and methylene blue. Despite the fact, that localized SPR manifests itself at 408 nm and MB absorbs light mainly in the range of 600-700 nm, illumination in those regions did not induce decomposition. However illumination within the 450±20 nm range efficiently destroys the organic molecules without any specific additions etc. So, it was found that the decomposition of methylene blue occurs only under specific illumination conditions.

The possible mechanism may be related to processes on the nanoparticle surface, between nanoparticles or as the result of generation of active silver ions. Anyway, as a result of exposure to light under local plasmon resonance conditions “dangling bonds” were formed, which include free electrons and free valencies. In this process, the “active form” of silver interacts with methylene blue to form complex compounds. Further electron transfers within the intermediate complexes induce step-by-step conversion of the MB to the products of decomposition of organic matter until elementary compounds.

This research was sponsored by the NATO Science for Peace and Security Programme under grant SPS 985140.

Obtaining Ultra Dispersed Cathode Material for Lithium Power Sources Based on Solid Solutions of Ferro-Alluminate Lithium Synthesized on Ceramic and Sol-Gel Methods

Deputat B.J.¹, Karpets M.V.², Uhorchuk V.V.³, Kaykan Y.S.³, Gasyuk M.I.³

¹Ivano-Frankivsk National Technical University of Oil and Gas, Ivano-Frankivsk, Ukraine

²Institute of Materials Science after Frantsevich NAS of Ukraine, Kyiv, Ukraine

³Vasyl Stefanyk Precarpathian National University, Ivano-Frankivsk, Ukraine

The formation of electrode active matrix of modern lithium power sources requires the achievement of certain values of technologically-controlled parameters, the provision of which is possible only in the case of high intercalation matrix characteristics for cathode or anode system. In addition, that such a substance or item must be of composite or layered canal structure, there is also a necessary condition of its high ionic conductivity and effective transportation of conduction electrons to the place of electrochemical reaction. In this regard, there must be given special attention to the largely dependent on the conditions of synthesis phases of variable composition, particularly characteristic for solid solutions substitution according to general formula $(1-y) \text{LiFe}_5\text{O}_8 + (y) \text{LiAl}_5\text{O}_8$ in the boundary regions of coexistence of different phases and phase modifications for the smooth organization of meso-structural grid for leading and matrix formations.

Structural characteristics and phase composition of solid solutions substitution made by the way of ceramic synthesis at the temperature of 1000 °C with the expected composition $(1-y) \text{LiFe}_5\text{O}_8 + (y) \text{LiAl}_5\text{O}_8$ at $y = 0.5$, which corresponds to the formula of stoichiometric lithium-aluminum-iron spinel, the synthesis heat treatment of which was carried out in two ways: series 1 – speed of cooling $t \approx 0,03$ °C/sec; series 2 $t \approx 4$ °C/sec. Besides, there were the properties of these systems with similar highly-dispersed lithium-aluminum-iron oxide system synthesized by low-temperature sol-gel method, followed by auto-combustion (series number 3) compared.

There was the influence of the method of synthesis of the structural properties and phase composition of synthesized samples depicted. Sustainable significance of lattice structures are presented in Table 1.

Table 1. The dependence of the constant lattice and phase composition of synthesized samples determined by X-ray structural method.

System	lattice a, Å	$\text{LiAl}_{0,5} \text{Fe}_{4,5}\text{O}_8$, %	$\alpha\text{-Fe}_2\text{O}_3$, %
Series №1	8,27649	78,45	21,55
Series №2	8,27605	73,86	26,14
Series №3	8,3229	94,8	5,2

Higher figures of constant lattice of system 3, are apparently caused by small particle size and essential impact of the surface which in the case of nanoparticle morphology significantly affects both the structure and the properties of the

synthesized material. Due to sol-gel method of auto-combustion the size of crystallites was increased in more than 4 times and the specific surface area in 20 times.

The analysis of diffraction patterns of all systems by the method of Rietveld showed high content (> 75%) of lithium-aluminum-iron ferrite spinel phases and small including of $\alpha\text{-Fe}_2\text{O}_3$ for the systems by synthesized ceramic way and almost single phase ferro-aluminate lithium system obtained by sol-gel method (content $\alpha\text{-Fe}_2\text{O}_3$ is about 5%).

It was the phase transition of the "order-disorder" for systems №1 and №3 detected that is their adherence to the space group R4332 [JCPDS No 76-1591], the so-called above arranged spinel structure, as it is revealed by the presence of above structural peaks (110) (210) and (211). This superstructure is caused by an orderly arrangement of lithium ions and iron at a ratio of 1: 3 in the crystallographic direction [110].

Rapid cooling of the system from synthesis temperature virtually has no effect on the phase composition, but promotes the formation of mesoscopic spinel structure characterized by non-statistic order in the sublattice. This disordered change of areas with different types of cationic environment can be seen as colloidal into the distributed volume in areas of different types and values of electron and ion (Li^+) conductivity. However, samples obtained by sol-gel method with an improved structure of above mentioned constant lattice and is highly stoichiometric. Sol-gel method allowed to decrease at about 4 times the size of crystallites, which indicates the high dispersion system of Li-ferrite and increased in 20 times the surface area, as perspective matrix to be used as an electrode-active material of lithium-ion sources of currents.

Heterostructures CdS/Porous-Si and CdS/Porous-CdTe for the Manufacture of Photovoltaic Cells

Dyadenchuk A.F., Kidalov V.V.

Berdyansk State Pedagogical University, Berdyansk, Ukraine

In this paper the receipt of CdS thin films on substrates porous-Si and porous-CdTe surface by chemical vapor deposition later use of the structures for the production of photovoltaic cells.

CdS layer formation by deposition occurred in a chemical bath of aqueous solution. As a substrate for growing CdS film used nanoporous silicon and porous CdTe wafer produced by standard technology of electrochemical etching.

With porous Si as an intermediate layer, contact between the film and CdS crystalline Si material works both ways: both in volume and at the interface, resulting in voltage due to the large mismatch and the difference in thermal expansion coefficient between CdS and Si, can be reduced.

For chemical surface deposition of CdS films used freshly prepared 0,015 M aqueous solution of cadmium chloride CdCl_2 , 1,5 M solution thiourea $\text{CH}_4\text{N}_2\text{S}$, 14,28 M solution of ammonium hydroxide NH_4OH . Because of the low solubility $\text{Na}_2\text{S}_2\text{O}_3$ prolonged heating and mixing for several hours is required. Electrolyte final pH was adjusted to 12. Linings, coated them prepared solution, heated to a temperature of 80°C for 5 minutes.

After a series of experimental studies obtained heterostructures. The following results:

1. The morphology of the surface studied and chemical composition of the films using a scanning electron microscope JSM-6490. CdS layer thickness is uniform and varies from 10 to 30 microns. CdS films with n-type conductivity.

2. Investigated films obtained by the method energodispersive X-ray spectroscopy. Research impurity concentration distribution in depth showed that the volume of CdS films of carbon and oxygen content is reduced by half, the concentration of other impurities not significantly changed.

Formation of ohmic contacts to the silicon substrate and CdS film was performed by indium solder followed by forming an electric pulse.

Measuring light current-voltage characteristics obtained heterostructures CdS/porous-Si was carried out in the mode of lighting AM 1,5. Power cutoff voltage-current characteristics $I(U)$ in the structures of n-CdS/porous-Si is $U_0 \approx 1,9$ in and close to the bandgap E_G porous silicon.

Production of solar cells based on heterojunction between the wide-gap semiconductors (CdS), playing the role of optical windows and narrow-gap semiconductors (Si, CdTe), which is used as an absorbent layer minimizes the loss of carriers due to surface recombination.

Some Aspects of Minimizing of Professional Risks for Working with Nanomaterials

Koshel V.I., Poplavskyy O.P., Dzundza B.S., Poplavskyy I.O.

Vasyl Stefanyk Precarpathian National University, Ivano-Frankivsk, Ukraine

Nanomaterials characterized by small size and a large total surface area, which in combination with other physical and chemical properties, such as the presence of contaminants and metals in surface charge can detect quite unpredictable genotoxic properties. Nanomaterials can cause DNA damage indirectly by promoting an oxidative stress. The particles of small size can penetrate cell membranes and interact directly with DNA in the nucleus [1]. Given the rather large spread and the rapid development of neural nanoindustry it's safe to say that in near future, the humanity will face with nanomaterials almost daily both in production and in daily life. Already nanomaterials began to be used with diagnostic and therapeutic purposes [2]. So, the greatest impact on human neural definitely has a place in the production environment (chronic effect for a long time). Therefore, it is necessary to evaluate the genotoxic potential of such materials in a wide range of real impact to understand the basic mechanisms that can determine toxic effects.

The result of analysis of literature data show us that nanoparticles own more expressed toxicity in comparison with usual microparticles which have circulating and accumulating in body parts and cloths and cause to more definite pathomorphologic changes in internals too, they also have longer period of half-inference from. Nanoparticles toxicity depends on forms and sizes. For example, small spindle-shaped particles cause to more destructive effects in our organism than similar particles spherical form. Also we can clearly trace connection between dose and effect. During recent 5 years amount of published works from nanotoxic effects constantly rises from year to year [2]. But because of not enough data about negative consequences of nanoparticles on our body and on ecosystem in general we can't find one true possibility to prevention.

For detrimental and hazard factors impact minimization it is necessary to use a complex of such measures as creation of a healthier air environment, technical equipment and technologies application, usage of individual security means. Special attention should be paid to remote technologies implementation, as well as to the work performed in closed plants, without transporting materials through air.

1. Demets'ka O. V. Pidkhody do otsinky ryzyku vplyvu nanochastynok ta nanomaterialiv na robochomu mistsi // Ukrayins'kyy zhurnal z problem medytsyny pratsi. – 2011. – T2, #26 – S. 62–67.

2. Prodanchuk N. H., Balan H.M. Nanotoksykologyya: sostoyanye y perspektyvy yssledovanyy // Sovremennyye problemy toksykologyy y perspektyvy yssledovanyy. –2009. –# 3. –S. 4–20.

Microscopic Basis for Engineering of InSe (Ni) Heterostructures

Galiy P.V.¹, Nenchuk T.M.¹, Mazur P.², Poplavskyy I.O.³, Yarovets I.R.¹,
Dveriy O.R.⁴, Buzhuk Ya.M.¹

¹*Ivan Franko Lviv National University, Lviv, Ukraine*

²*Institute of Experimental Physics, University of Wrocław, Wrocław, Poland*

³*Vasyl Stefanyk Precarpathian National University, Ivano-Frankivsk, Ukraine*

⁴*National Academy of Land Forces, Lviv, Ukraine*

Hybrid metal-layered semiconductor nanosystems are attracting the great interest considering their perspective to be base of novel nanosized devices. The engineering of conductive nanowires, nanodot arrays on the surface of two-dimensional semiconductor materials is one of the main streams in nanoelectronics. Besides, the study of such structures is also interesting from fundamental point of view.

We focus on scanning tunneling spectroscopy (STS) study of electronic structures of Ni monolayer intercalated into interlayer gap of InSe, so-called, sandwich structures. Ni_xInSe layered intercalate crystals have been grown by Bridgman-Stockbarger method from previously synthesized melts InSe + x at.% Ni (x ≤ 10%). STS is the surface method but is useful for our study due to easy obtaining cleavage surfaces in layered crystals.

The Omicron NanoTechnology STM/AFM System has been exploited in current imaging tunneling spectroscopy (CITS) mode to study the local distribution of density of states (LDOS) on the cleavage. CITS mode is useful for this purpose because gives 6400 I-V curves over the studied area with 1/80 X (nm) x 1/80 Y (nm) spatial distribution. So, resolution is only affected by choice of studied area size. It's well known, that scanning tunneling microscopy attains 1 Å spatial resolution. So, 10x10 nm² size of studied area is sufficient to obtain atomic resolution. Thus, it could be established to what extent does Ni-derived localized electronic states affect the neighboring InSe surface area.

We conducted detailed mapping of the studied area using CITS 6400 (data points) x 300 (ΔV) matrix. In this case each data point has its own corresponding I-V curve. The analysis of DOS frequency appearance in the matrix above the limited level of noise in the energy gap of InSe allowed to evaluate concentration of metallic Ni sites over the studied area. The derived surface concentration of Ni was estimated as ≈ 1%. This value might be multiplied twice, when considering that after cleavage we deal with one half of Ni content intercalated in the interlayer gap. Besides nickel atoms local surface distribution thus was revealed and also visualized with 3D presentation.

Molecularly Imprinted Polymers (MIPs) as Elements of Nanosensors for Bisphenol A

Gorbach L.¹, Lutsyk O.¹, Sergeeva L.¹, Brovko O.¹, Sergeyeva T.²

¹*Institute of Macromolecular Chemistry, NAS of Ukraine, Kyiv, Ukraine,*
gorbachla@bigmir.net

²*Institute of Molecular Biology and Genetics, NAS of Ukraine, Kyiv, Ukraine*

During the last decade “smart polymers” attracted significant attention of scientists, working in the area of analytical chemistry, as an alternative to antibodies and natural receptors. One of the most effective methods of their synthesis is the method of molecular imprinting. The method allows one to obtain nanostructured molecular imprinting polymers (MIPs) as well as, using colorimetric methods, to develop of easy-to-use inexpensive colorimetric test-systems based on rationally-designed smart polymers for detection of trace levels of organic contaminants like bisphenol A (BPA). Acrylate based nanostructured MIPs specific to BPA were synthesized and colorimetric test-systems based on them were obtained. A capability of MIP to high selectively absorb of BPA and to give a color response was taken into account. A quantity of BPA adsorbed from aqueous solution was controlled by using color qualitative reaction between BPA and 4-aminoantipyrine in presence of potassium ferrocyanide $K_3[Fe(CN)_6]$ in alkaline medium. The coloring intensity of polymer film was shown to depend of BPA concentration and changed from dark crimson to slightly rose-colored. The coloring was kept for a long time. Concentration region (4,4 – 0,0068) mM was fixed within which the application of developed colorimetric test-system was the most effective. Thus, the developed colorimetric test-system worked as a “litmus paper” and to allowed one to fast detect quantitatively and qualitatively BPA in the nature aquatic environment without expensive equipment.

Financial support from National Academy of Sciences of Ukraine

Calculation of Kinetic Parameters Forming InAs Quantum Dots in GaAs Matrix for Low-Temperature CVD-Method

Guba S.K., Petrovich R.Y.

Lviv Polytechnic National University, Lviv, Ukraine

Advances in nanotechnology and physics of nanostructures led to the practical realization of optoelectronic devices based on arrays of quantum dots (QD) [1].

Currently already developed a number of technologies that effectively operate and provide a receipt $\text{In}_{1-x}\text{Ga}_x\text{As}/\text{InAs}/\text{GaAs}$ heteronanostructures for laser use. First of all, this is molecular beam and Metalorganic chemical vapour deposition (MOCVD). Also QD InAs in GaAs matrix can be obtained by chloride hydride epitaxy method (CVD-method) [2]. Kinetics of growth and distribution system voltage QD-matrix affects the size, shape and location in the QD matrix. In addition, the QD geometric dimensions and forms heavily dependent material properties such as a radiative recombination, Auger recombination rates, and so on. However, so far not reached theoretical predictions hetero nanostructures parameter values $\text{In}_{1-x}\text{Ga}_x\text{As}/\text{InAs}/\text{GaAs}$ QDs of InAs nanostructures obtained through low-temperature CVD-method. Therefore, the purpose is to determine the kinetic parameters of self-organization and structural properties of InAs QD in GaAs matrix for low-temperature CVD-method in kinetic mode of growth, based on model concepts covered in [3,4].

We present the results of theoretical study for the kinetic mode of quantum dots InAs formation in the GaAs – $\text{In}_{1-x}\text{Ga}_x\text{As}$ – GaAs system. The estimating characteristics of the kinetics formation of InAs quantum dot in the matrix GaAs, and their structural properties at low-temperature CVD - method. The calculated results can be used to analyze technology heteronanostructures GaAs / QD InAs / $\text{In}_{1-x}\text{Ga}_x\text{As}$ / GaAs for low-temperature CVD - method. Moreover they are useful for modeling the structural properties of InAs quantum dots in the system GaAs – $\text{In}_{1-x}\text{Ga}_x\text{As}$ – GaAs.

[1]. A.E. Zhukov, A.R. Kovsh, E.V. Nikitina, V.M. Ustinov and Zh.I. Alferov // *Semiconductors*. – 2007. – Vol.41. – P. 601

[2]. B.A. Voronin, S.K. Guba, I.V. Kurilo // *TKEA*. – 2008. – 5. – P. 36

[3]. V.G. Dubrovskii // *Semiconductors*. – 2006. – Vol.40. – P. 1123

[4]. S.K. Guba and V.N. Yuzevich // *Semiconductors*. – 2014. – Vol.48, № 7. – P.905

Reversible Surface Modification of Chalcogenide Nanolayers by Coherent Light Irradiation for Advances in Sensing, Ultrafast Photonics and Renewable Solar Energy Technology

Holomb R.¹, Kondrat O.¹, Ihnatolia P.¹, Veres M.², Tsud N.³, Mitsa V.¹

¹ *Institute of Solid State Physics and Chemistry, Uzhhorod National University, Uzhhorod, Ukraine, e-mail: holomb@gmail.com*

² *Wigner Research Centre for Physics, Hungarian Academy of Sciences, Budapest, Hungary*

³ *Charles University, Faculty of Mathematics and Physics, Department of Surface and Plasma Science, Prague, Czech Republic*

The rapid development of light-based technology indicates that in the nearest future we will depend as much on photonics rather on electronics. To control the light and access *all optical* functionality there is a need in new types of nanostructured materials with the dimensions of their structural elements in order of tens nanometers.

The chalcogenide-based photonic media have attracted much scientific interest. In addition to their intrinsic infrared properties, the useful combination of optical activity, structural photosensitivity and high third-order optical non-linearity of chalcogenides they offer a wide possibilities of their applications in information technologies (data storage and ultrafast data processing), renewable energy technologies (high efficiency solar cells, solid electrolytes), thermal imaging, sensing and biosensing *etc.* The structure and its coupling to the fundamental properties of chalcogenides have been the subject of intensive studies for decades. In particular, the special interest is dedicated to the light-matter interactions in various chalcogenide systems.

In this report, we present the results of *in-situ* investigation of As-S nanolayers surface and their modification by using coherent light. The photon-energy dependent photoelectron spectroscopy and surface-enhanced Raman spectroscopy as surface-sensitive experimental techniques have been used together with theoretical density functional theory (DFT) calculations in order to characterize the sample surface. The atomic compositions, short- and medium-range order structures at the surface of As-S nanolayers were determined and their changes under the action of over-bandgap light were analyzed in detail. Results show that both the composition and structure of As-S nanolayers surface can selectively be modified by laser treatment. Furthermore, the reversibility of photo-modification of As-S surface in irradiation-annealing cycles is firmly established and confirmed on different As_xS_{100-x} compositions ($x=40,45,50$). The DFT calculations were also performed in order to facilitate the interpretation of experimental spectra and the microscopic origin of discovered phenomena is discussed in term of structural units and molecular clusters transformations. The observed reversible post-fabrication modification of chalcogenide surfaces can cover a wide range of modern potential applications.

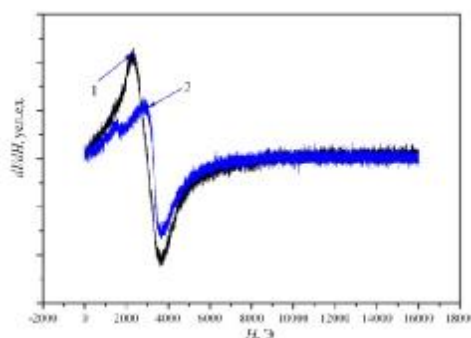
EPR Study of Magnetic Nanoclusters in Conducting Polymer Matrices

Aksimentyeva O.I., Horbenko Yu.Yu.

Ivan Franko National University of Lviv, Lviv, Ukraine,

E-mail: y_bilka@ukr.net; aksimen@ukr.net

Until recently radicals ($\bullet N = O$) were used as paramagnetic probes, which are very harmful to the human body. Therefore, there is the problem of finding a relatively safe and quite informative method of studying the behavior of magnetic centers in organic and biological systems. The basis of this study – the idea to simulate the paramagnetic center surrounded by organic polymer matrix containing besides C and H heteroatoms N, O, S and explore patterns of conversion of EPR spectra of magnetic center at different temperatures. The 3d ions of the iron group are known as a main source of free radicals causing cellular degradation in nervous system. Using the ESR methodologies is promising for the development of new methods in nanomedicine.

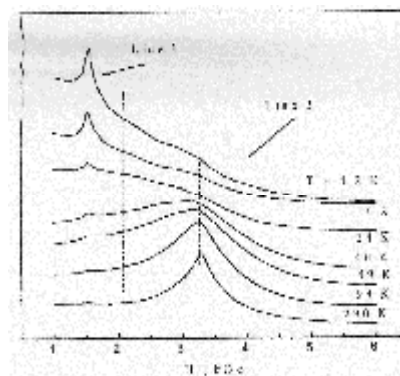


ESR spectra of PAT-Fe³⁺ at T = 298 K (1) and 4,2 K (2)

At the T < 78 K in EPR spectra a second resonance line is appeared with effective value of g₂ depended on nature of molecular surrounding. With temperature changing the redistribution of EPR-signal takes a place. Unusual behaviour also is attributed to width of lines. It is suggested that observed dynamic of magnetic centres in polymer matrices may be used in biology and medicine as paramagnetic sound to monitoring and prognoses behaviour of nervous cells.

The temperature transformation in EPR spectra of poly-*o*-anisidine, poly-*o*-toluidine, poly-3-aminothiazole (PAT) doped by magnetic clusters has been studied. The EPR spectra of model nanosystems at T = 4.2–293 K show the interesting temperature behaviour.

At 298 K only one line with g₁ = 2.01±0.01 is observed (see figures). At the



Redistribution of absorption for PAT-Fe³⁺ system

Horbenko Yu., Aksimentyeva O. Electron paramagnetic resonance of the complexes of polyaminothiazole, doped by ferric chloride // Visnyk of the Lviv University. Series Chemistry. – 2015. – Iss. 56. – P. 334–338.

Kumar Ch. Nanomaterials for medical diagnosis and therapy // Nanotechnologies for the Life Sciences. – 2007. – Vol. 10. – 757 p.

The Influence of Deformation of Nanoheterosystem with Quantum Dots InAs/GaAs on the Binding Energy of Deformation Electron Polaron

Hrushka V.I.¹, Peleshchak R.M.¹, Mironchuk V.I.², Stan'ko M.H.¹

¹*Drohobych Ivan Franko state pedagogical University. Drohobych. Ukraine*

²*Belarusian state agricultural technical University. Minsk, Belarus*

In recent years, great interest is the study of quantum-dimensional structures, and, in particular, quantum dots (QDs), in which the spatial limitation of carriers in all three directions. Materials quantum dots (InAs; CdTe) have large value of the deformation potential, which leads to increased polaron effects in QDs compared to volume materials.

In [1] was studied polaron effects in QD without taking into account deformation of QD and found that with decreasing size of QD polaron effects grow. The gain parameter polaron effects is the ratio of the radius polaron state a_0 to a radius of quantum dots R_0 , that is, $p_0 = a_0 / R_0 \gg 1$. In the case where the material of the quantum dot InAs/GaAs undergoes deformation of compression ($Sp\hat{e}^{(1)} < 0$) the value of the gain parameter p will grow because the size of the quantum dots will decrease with increasing deformation of the material of QD due to mismatch of lattice parameters of, leading to increased polaron effects

compared to not deformed materials $p = \frac{a_0}{R_0(1 - |Sp\hat{e}^{(1)}|)}$, where $Sp\hat{e}^{(1)}$ – the sum of the diagonal components of the strain tensor of the material of the quantum dots, which is found from the condition of mechanical equilibrium $\nabla \text{div} \mathbf{u} = 0$.

The binding energy of the electronic polaron deformation in a deformed quantum dot InAs/GaAs are determined from the Shredinger equation with a deformation potential of the conduction, and the potential of the electron-phonon interaction and own energy of phonons:

$$\left[\hat{H}_e + U_e + \sum_q \hbar \omega_q a_q^+ a_q + e \sqrt{\frac{2p\hbar}{Vee_0}} \sum_q \frac{\sqrt{\omega_q}}{q} (a_q e^{iq\mathbf{r}} + a_q^+ e^{-iq\mathbf{r}}) \right] \psi_{\text{in}}(\mathbf{r}) = E \psi_{\text{in}}(\mathbf{r}),$$

where a_q, a_q^+ – the operators of annihilation and birth of phonons, e – the

optical dielectric constant, $U_e(r) = \begin{cases} 0, & 0 \leq r \leq R_0 \\ \Delta E_c(0) - |a_c^{(1)} e^{(1)}| - |a_c^{(2)} e^{(2)}|, & R_0 \leq r \leq R_1 \end{cases}$.

The binding energy of the electronic polaron in a deformed QD was found from the expression:

$$\Delta E^{(\text{in})} = -\frac{e^2}{2ee_0} \int \frac{(y_{0\text{in}}^{(i)}(\mathbf{r}))^2 (y_{0\text{in}}^{(i)}(\mathbf{r}'))^2}{|\mathbf{r} - \mathbf{r}'|} d^3 r d^3 r', \text{ where } y_{0\text{in}}^{(i)}(\mathbf{r}), y_{0\text{in}}^{(i)}(\mathbf{r}') - \text{the wave function of}$$

an electron in a tense nanoheterosystem with a deformed QD.

1. I. Ipatova, A. Maslov, O. Proshina, FTP 33, No7,832 (1999).

Photoluminescence Excitation in Thin Films of Nanocomposites Polyvinylpyrrolidone/ ZnO

Fediv V.I.¹, Isaieva O.F.², Rudko G.Yu.³, Gule E.G.³, Olar O.I.¹

¹*Bukovinian State Medical University, Chernivtsi, Ukraine, E-mail: vfediv@ukr.net*

²*National University “Kyiv-Mohyla Academy”, Kiev, Ukraine*

³*V. Lashkaryov Institute of Semiconductor Physics of NAS of Ukraine, Kiev, Ukraine*

Recently, many researchers have focused on the fabrication and luminescent properties of nano-phosphors. Inorganic-organic hybrid nanocomposite materials are an example of materials, which have become a creative alternative to the industrially used materials. Improvement of traditional phosphors, development of new phosphors and investigation of luminescence mechanisms are the main aspects of current research. ZnO nanoparticles are widely employed in the fundamental research and commercial applications (field emitters, ultraviolet lasers and diodes, piezoelectric devices, fluorescence labels in medicine and biology) [1,2]. The controlled synthesis of ZnO nanoparticles and in-depth understanding of the physical properties are the key issues for the future development of ZnO-based devices.

Here, we report on the synthesis of ZnO nanoparticles by wet chemical method and production of ZnO-base nanocomposites. Semiconductor ZnO nanoparticles were grown in water solution of Zn acetate and tetramethylammonium hydroxide. Nanocomposite was produced by admixing the obtained ZnO nanoparticles to water solution of polyvinylpyrrolidone (PVP) polymer. The mixture was dried to obtain flexible thin solid films of nanocomposite.

The PVP/ZnO nanocomposite was characterized by various optical methods: absorption, photoluminescence and photoluminescence excitation. It was found that the emission spectrum of nanocomposites is very wide and results from overlapping of at least two dominating emission bands with the enhanced intensity in blue range. The low intensity of green emission, most probably, corresponds to low density of oxygen vacancies in nanoparticles. Dependence of emission spectra on exciting photon energy was studied. The scheme of excitation and emission processes was proposed.

1. Djurisc A.B. ZnO nanostructures for optoelectronics: Material properties and device applications / A.B. Djurisc , A.M.C. Ng, X.Y. Chen // Progress in Quantum Electronics.- 2010.- V.34.- P.191–259.

2. Zhang Z.-Y. Photoluminescent ZnO Nanoparticles and Their Biological Applications / Z.-Y.Zhang, H.-M.Xiong // Materials.- 2015.- V.8.- P.3101-3127.

The Heating Temperature Influence of Activated Carbon on the Capacitance of Electrochemical Capacitor.

Kachmar A.I., Nykoliuk M.O., Rachiy B.I., Budzulyak I.M, Ilnitsky R.V.

Vasyl Stefanyk Precarpathian National University, Ivano-Frankivsk, Ukraine

Carbon raw material were activated with sodiumhydroxide. Activated carbon material (ACM), were used as electrode material for electrochemical capacitorandwereheatedbydifferenttemperatures(600°C – series 1, 700°C – series 2, 800°C – series 3 i 900°C – series 4).All series of samples were washed to neutral pH and were dried to constant mass at 90°C.The resulting symmetrical electrodes were seeped by electrolyte, were separated by sealant and placed into the 2-electrodes cell with typical size “2525”, where after it was sealed. The 33% KOH was used as an electrolyte.

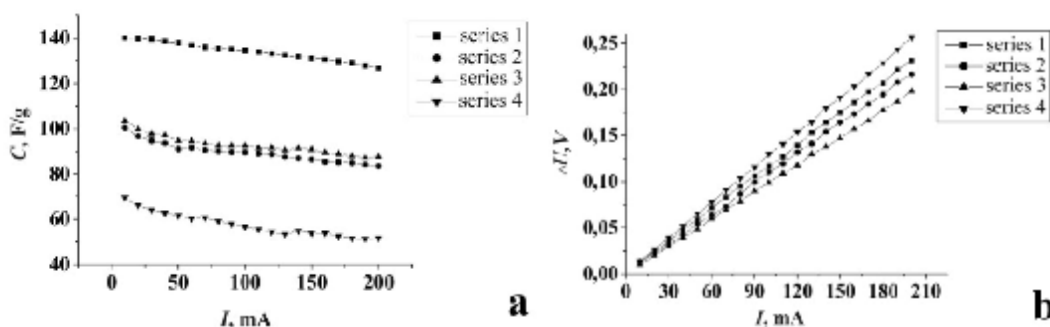


Fig.1. The dependences of porous carbon material capacity C (F/g) (a) and voltage drop (b) from charge/discharge current.

The specific capacity for all series was calculated from galvanostatic and potentiodynamic cycling research, which was done to investigate the heating temperature influence on capacitance of activated carbon. It was established that heating at 600 °C allowsto get carbon material with bigger specific capacity 138 F/g (for others 91 F/g at 700 °C, 95 F/g at 800 °C, 62 F/g at 900 °C) at discharge current at 50 mA.

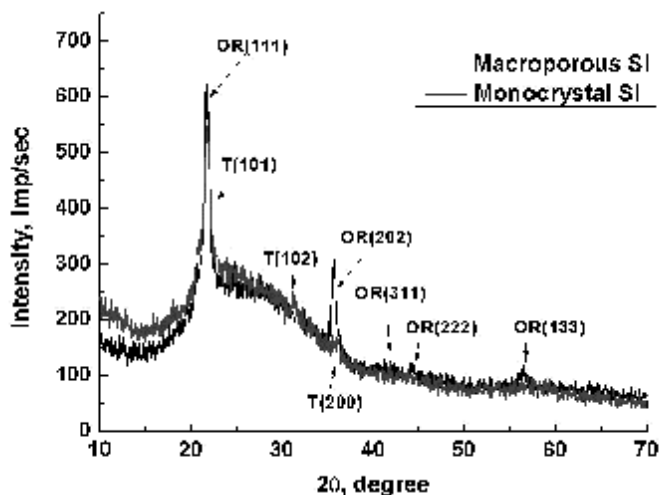
Silicon Oxide Restructuring in Oxidized Macroporous Silicon Structures

Karachevtseva L., Klad'ko V., Gudymenko O., Konin K., Morozovska D.

V. Lashkaryov Institute of Semiconductor Physics, NASU, Kyiv, Ukraine

The effect of cylindrical macropores oxidation in 2D macroporous silicon was investigated taking into account different thermal expansion coefficients of silicon and silicon oxide. The samples were made of *n*-Si plates by photoelectrochemical etching. 4-200 nm thick SiO₂ layers were formed in dry oxygen, 800-1400 nm thick layers were formed in an atmosphere of wet oxygen. The X-ray diffraction measurements were performed with a high-resolution diffractometer using the ICDD database. The splitting energy of TO- and LO-phonons in IR absorption spectra was analyzed too.

The coherent X-ray scattering curves for macroporous silicon with 4÷200 nm thick SiO₂ layers include symmetric deformation without shoulders or tails. This indicates a small residual strain caused by presence of vacancies. X ray analysis of samples with 800÷1400 nm thick SiO₂ layers evaluates presence of SiO₂ tetragonal phase. Besides, the hexagonal tridymite structure and cristobalite β with orthorhombic SiO₂ phase (Figure) are formed at high pressure due to different thermal expansion coefficients of silicon and silicon oxide.



X-ray diffraction of sample with SiO₂ layer 800 nm thick on macroporous and monocrystal parts.

OR point the orthorhombic SiO₂ phase, T points the tetragonal phase.

The splitting energy of TO- and LO-phonons corresponds to growth of stoichiometry on the border between Si and SiO₂, with increasing SiO₂ thickness to 15-20 nm. The minimum of the phonon splitting energy at SiO₂ thickness of 50 nm corresponds to bend dependencies of residual strain and the lattice parameter. By increasing the thickness of SiO₂ to 200 nm, the maximal residual deformation corresponds to phonon splitting energy bending. The reduction of residual strain in the bulk of SiO₂ in excess of 200 nm is accompanied by slowing of stress growth. This is due to restructuring of SiO₂ under high pressure to tridymite and cristobalite (β) structures.

The Use of Ukraine`s Biomass for Synthesis of Carbon Nanomaterials

Keush L.

National Metallurgical Academy of Ukraine, Dnipro, Ukraine, lina.keush@yandex.ua

Carbon nanomaterials are a variety of carbon structures. The most representative structures may be carbon nanotubes (single-walled, double-walled or multi-walled carbon nanotubes), carbon nanoparticles, carbon nanofibers and carbon quantum dots. In the plasma-arc method, various raw materials such as graphite, coal, coke and soot can be a source of carbon for the production of carbon nanomaterials. However, the use of such raw materials, as well as catalysts, which are not subsequently used after purification, makes the plasma arc method not ecological. Therefore, the development of new ways using renewable materials as raw materials can have a huge potential in the production of carbon nanomaterials by the plasma arc method. Biomass in the composition of the electrode can serve as a source of carbon to form new carbon nanostructures, and perform the function of a catalyst. As a necessary requirement for the use of biomass is a high content of carbon and a low content of hydrogen. In Ukraine, the most important raw material for the synthesis of carbon nanomaterials can be the husk of sunflower, which contains ~50 % of carbon and ~5 % of hydrogen and straw, which contains ~40 % of carbon and ~5 % of hydrogen. The advantage of this raw material is that it is sufficiently in large quantities, is a source of "ecological" carbon and cheaper than graphite, coal or coke.

It is also possible to use biomass pyrolysis products, in which the carbon content can reach 97 %. For example, the carbon content in the charcoal is 80-85 %, and the hydrogen content is 6-7 %, which makes it possible to use this material for the production of carbon nanomaterials.

Biomass, as well as its pyrolysis products in the plasma-arc method can be a source of carbon for obtaining various types of carbon nanomaterials.

Kinetics of Degradation Phenomena in Modified $\text{Cu}_{0.1}\text{Ni}_{0.8}\text{Co}_{0.2}\text{Mn}_{1.9}\text{O}_4$ Ceramics

Klym H.¹, Shpotyuk O.², Balitska V.³, Hadzaman I.⁴

¹*Lviv Polytechnic National University, Lviv, Ukraine, klymha@yahoo.com;
halyna.i.klym@lpnu.ua*

²*Vlokh Institute of Physical Optics, Lviv, Ukraine*

³*Institute of Fire Safety, Lviv, Ukraine*

⁴*Drohobych Ivan Franko State Pedagogical University, Drohobych, Ukraine*

Semiconductor spinel ceramics are one of the most perspective materials for device application as negative temperature coefficient thermistors. To eliminate the degradation, the method of chemical modification of ceramics is used. Synthesis of modified thermally-sensitive elements based on $\text{Cu}_{0.1}\text{Ni}_{0.8}\text{Co}_{0.2}\text{Mn}_{1.9}\text{O}_4$ ceramics was performed owing to technological conditions, the content of NiO phase (1 % - batch 1, 8 % - batch 2, 10 % - batch 3, 12 % - batch 4 and 12 % - batch 5 obtained at different amounts of thermal energy transferred at sintering) having decisive role on final ceramics structure.

The results of ageing tests were controlled by relative resistance drift (RRD) caused by ceramics storage at the temperature of 170 °C. With a purpose of adequate mathematical modelling of the kinetics in studied ceramics, the numerical values of different fitting parameters in the typical relaxation functions (RF) were calculated to minimize the mean square deviation of experimentally measured points from chosen RF. It is well known this kinetics behaviour in spinel-type ceramics can be adequately described by stretched-exponential relaxation function $y=h(t)=a(1-\exp[-(t/\tau)^k])$ at $0 < k < 1$. Extraction of additional NiO phase from $\text{Cu}_{0.1}\text{Ni}_{0.8}\text{Co}_{0.2}\text{Mn}_{1.9}\text{O}_4$ ceramics enlarges the dispersivity of the system, while the monolithization of ceramics causes an opposite effect. The ceramics samples of batch 3 demonstrate the best suitability for stretched-exponential RF. Non-exponentiality index k grows from 0.10 (batch 1) to 0.66 for batch 2, the similar increase being character for time constant τ too. However, the further increase in NiO content from 10 (batch 3) to 12 % (batches 4 and 5) is associated with principally different processes of microstructural evolution corresponding to monolithization. The non-exponentiality index k is most close to 1 ($k = 0.66$). Despite nearly the same value of non-exponentiality index $k = 0.46$, the time-constant τ decrease from 189.2 for batch 4 to 65.5.2 h for batch 5 samples. The parameter a , which reflects structural perfectness of ceramics, gives a good correspondence between RRD values for all batches and decrease from 43.5 (batch 1) and 6.45 (batch 2) for fine-grain ceramics with small amount of NiO phase to 3.52 (batch 3) and 3.13 (batch 4) for monolithized ceramics. For batch 5 ceramics this value increases to 20.77 at smaller $t = 65.5$ h in respect to increase in RRD up to 18%.

Viscoelastic Properties of Polymer Nano-Disperse Systems

Kolupaev B.S., Levchuk V.V., Sidletsky. V. A.

Rivne state humanitarian University, Rivne, Ukraine

In the megahertz frequency range of the conducted study of viscoelastic, shear modules, bulk deformation, the coefficients of energy dissipation of the ultrasonic field as well as internal pressure and life time of structural elements of PVC systems depending on the temperature and content of ingredients.

Installed: nanosized metal aggregates (Cu, Ni, CR), obtained by electrical explosion of wire (EEW) and/or chemical electrophysical (F/X) dispersion, represented the new modifier effective viscoelastic properties of PVC systems; the quantitative correlation between the volumetric density of the internal energy of the material and internal pressure. It is shown that under the action of ultrasonic vibrations with a frequency of 0.4 MHz in the system, in the case of longitudinal deformation, the thermal motion is the superposition of mechanical (elastic) fluctuations in the form of waves and quasistationary thermal fluctuations associated with the local temperature changes. The exchange of energy between the thermal fluctuations occurs by conduction, which allowed to calculate the thermophysical characteristics (I, C_p) of the material. It is established that power exchange process in PVC-systems can also be directionally adjusted according to the type metalnanodisperse filler (EVP and/or f/X).

Based on the proposed model, it is shown that the structural part of the volumetric strain has a relaxation nature. The analysis of results concerning elastic and viscoelastic deformation of shear, compression-tension and volume loading of the composite. It is shown that in the case of the volumetric strain of the composite ultrasonic frequencies should take into account the presence of devoting modulus of compressibility, which depends on the frequency of the ultrasonic field, the relaxation time of the elements of the structure and the dynamic viscosity and shear modulus of the material. Set the quantitative relationship between internal pressure, the elastic modulus of the material and the internal energy of the composite is Clarified by the molecular-kinetic nature of the dissipative loss of mechanical energy in the system and the nature of the relaxation process, the stress-strain. Refer to the possibility of practical use of the composite as dampers, acoustic delay lines, sound insulator, coolants. Established analytical relations allow to predict the specific behavior and the use of PVC systems under dynamic and thermal loads.

Nanostructures of CuAl with H₂O and Cl⁻ as Defined by DFT Study

Korniy S., Pokhmurskii V., Kopylets V.

Karpenko Physico-Mechanical Institute of the NAS of Ukraine, Lviv, Ukraine

Water and Cl⁻ (especially in presence of oxygen) form original surface adsorption structures on Al alloys, important in catalysis and corrosion. In frames of quantum-chemical method of density functional theory DFT a model of intermetallics CuAl₂ (100) was proposed to calculate such structures at equilibrium.

Calculations were made with VWN local potentials, DZVP and auxiliary basis sets for all elements as implemented in StoBe2011 software [1]. Geometries of adsorption species were fully optimized while positions of metal atoms were fixed as in experimental data for CuAl₂.

The results are as follows. A single H₂O molecule bonds preferably with Cu plane of the cluster at atop sites (distance 2.926 Å). Multi adsorption of 5 H₂O lowers the atop separations to 2.801 Å. The addition of Cl⁻ ion causes the reversible effect: all particles preface to bond to Al plane of CuAl₂ (100) with Cl⁻, positioned at 4-fold hollow site (distance 2.807 for Cu-Cl⁻ and 2.851 for Cl⁻-H₂O). Four water molecules move over Cl⁻ to larger distances and form Cl⁻-symmetrical outer sphere. We say that chlorine ions substitute water at the surface and activate it to further processes.

The most important result was obtained when molecular oxygen was added to these structures. First of all it was separated at the surface to individual atoms (due to Cu catalytic action, not described here). The newly structure included to O atoms, adsorbed at bridge position of Al plane, next were for water molecules at atop positions and chlorine ion at the largest hollow position.

Finally addition of another two oxygen molecules formed a new structure with one O below the Al surface, two O in the plane of Al and one O at the previous bridge site. Water molecules and Cl⁻ ions remained almost as for two O

Thus we obtained a first stage picture of multi-species adsorption of aggressive ions and molecules in water environment for studying of possible surface reaction mechanisms to predict catalytic activities and corrosion resistance of aluminum alloys.

1. Hermann, K.; Pettersson, L. G. M.; Casida, M. E. et al. StoBe 2011, Version 3.1, 2011.

Influence of Nanofiller Surface Nature on the Formation of Poly (Methyl Methacrylate) Modified by Crosslinked Polyurethane

Kosyanchuk L.F., Ignatova T.D., Shumsky V.P., Antonenko O.I.,
Getmanchuk I.P.

Institute of Macromolecular Chemistry of NAS of Ukraine, Kyiv, Ukraine

A promising method of obtaining of polymer composites with the properties from reinforced elastomers to shock-resistant plastics is reaction formation of blends of different chemical nature polymers. In particular, to improve the impact resistance of poly(methyl methacrylate) (PMMA) semi-interpenetrating polymer networks are formed, where the second component is a crosslinked polyurethane (PU). To achieve high adhesion between the components and improve the mechanical properties of such a mixture compatibilizers are used. Such compatibilizers may be mineral nanofillers which facilitate the dispersion of one phase in another phase and stabilize the morphology of the blend. Changing hydrophilic-hydrophobic properties of solid nanofiller particles one can influence the degree of nanofiller interaction with components of the blend and thus regulate the final properties of the polymer material.

The purpose of this study is the investigation of the influence of surface nature of mineral nanofiller (fumed silica) when it is introduced into the initial reaction mixture on the in situ formation of PMMA/PU blend of 70/30 by weight and the morphology of the final products. Unmodified fumed silica with hydrophilic properties (A-300) and modified fumed silica with hydrophobic properties (AM-300) are used as nanofillers for this blend. Specific surface of these nanofillers is 300 m²/g and particle sizes are 5–10 nm.

It is shown that the introduction of both types of fumed silica has negligible effect on the kinetics of formation of each component. However, the dependence of viscosity on time (rheokinetic curves) during formation a blend essentially depends on the type of nanofiller. For unfilled blend and blend filled with modified fumed silica AM-300 extreme dependence of viscosity on time occurs, indicating that the process of phase separation in the system takes place. For blend filled with unmodified fumed silica extremes in rheokinetic curves are absent. It is the result of "forced" compatibility of components due to intermolecular interaction PU and PMMA with polar groups on the active surface of the A-300. The data of optical microscopy show that the introduction of unmodified fumed silica actually results in a finer morphology of smaller structures compared to the blend without filler or blend filled with modified fumed silica. The modified fumed silica (AM-300) has the inactive surface and this reduces its interaction with PMMA and PU. It is the contributing factor for the phase separation of system and formation structures with larger sizes.

Optical Properties of Au- and Ag-Containing Silica Glasses Co-Doped with Ln

Kouhar V.V.

B.I. Stepanov Institute of Physics, NAS of Belarus, Minsk, Belarus

In present work, we synthesized by the sol-gel method the Au-, Au–Eu-, Au–Yb-, Ag-, Ag–Eu-containing silica glasses and investigated their optical properties.

It is shown that gold nanoparticles (AuNPs) are self-formed in Au-containing glasses during sintering in air, as evidenced by the presence in the absorption spectrum of the corresponding plasmon band with a maximum at $\lambda \approx 565$ nm. An additional doping of the Au-containing glass with Eu and Yb leads to different shift of the NPs plasmon band maximum position and to changing of the band half-width. It is seen from Fig.1 (curves 2 and 3) that the plasmon band maximum for Au–Eu-containing glasses lies at 543 nm, while for Au–Yb-containing glass it lies at 563 nm. These results are discussed.

For air-sintered Ag- and Ag–Eu-containing glasses, self-forming of the AgNPs is not observed that due to incorporation of silver into the glasses in the ionic form. The formation of these NPs takes place only after annealing of the glasses in H_2 -containing gases. The nanoparticles concentration depends on the temperature and duration of this annealing and decreases in the presence of Eu as implied by the plasmon band intensity in Fig. 1 (curves 4–6). We explain relatively low efficiency of silver ions reduction by hydrogen in Ag–Eu-containing glasses by formation of complex optical centers whose structure prevents interaction of hydrogen with europium and silver ions. The decrease in the intensity and the long-wavelength shift in the AgNPs plasmon band with an increase in T_{an} indicates the sequential oxidation of such NPs starting with the smallest ones.

Some prospects of application of such glasses are considered.

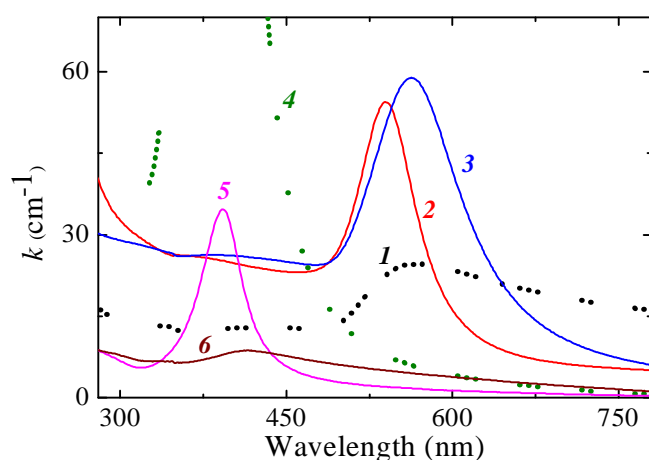


Figure 1. Absorption spectra of (1) Au-, (2) Au–Eu-, (3) Au–Yb-, (4) Ag-, (5, 6) Ag–Eu-containing silica glasses.
 $T_{an}, ^\circ\text{C}$: 900 (5), 950 (4), 1200 (6)

BSA-Based Hybrid Thin Films for Gas Biosensors

Kruglenko I., Burlachenko J.

*V. Lashkaryov Institute of Semiconductor Physics NASU, Kyiv, Ukraine,
kruglenko@yahoo.com*

Biosensors are traditionally used for operation in liquids. There are, however, a number of tasks that involve operation in gas media (analysis of patient breathing, industrial, storage and environmental monitoring etc). With the aim to develop a gas biosensor we use bovine serum albumin (BSA). The sensor system was based on the quartz crystal microbalance (QCM) sensors.

BSA was deposited from the solution onto the surface of QCM's silver electrode and onto previously thermally sputtered 100nm layer of fullerenes C60. Both films were stable and have being demonstrating reversible and reproducible responses during 5 month (storage under room conditions). Figure 1 shows the amplitudes of responses tovapors of different alcohols, acetone, water, brandy and vodka, of sensors with Ag-BSA and C60-BSA coatings.

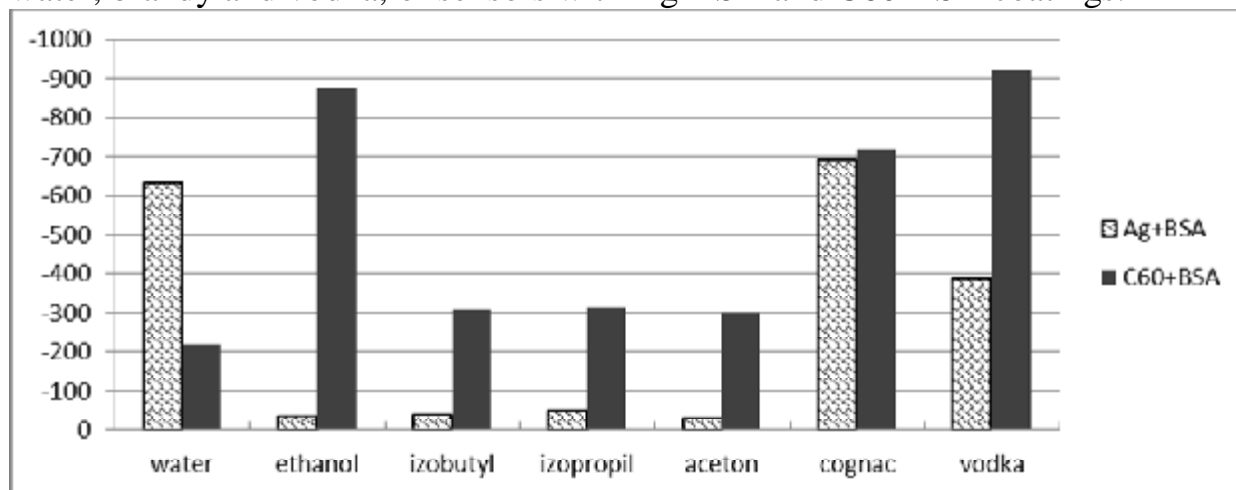


Figure 1 – response amplitudes to vapors of ethanol, isobutyl, isopropyl, water, acetone and alcohol drinks for QCM sensors with two types of sensitive layers:

(1) Ag-BSA, (2) C60-BSA.

As it is seen from the figure, the two sensors demonstrate different selectivity profiles despite they are both based on the BSA layer. This may be explained by different BSA orientation dependently on the bottom surface nature. In such a way, sensors based on Ag-BSA and C60-BSA hybrid films may be used as elements of multisensor arrays.

Self-Assembling Metallic Filler for Electroconductive Polymer Films

Kytsya A.R.¹, Bazylyak L.I.¹, Zavaliy I.Yu.², Pobigun O.I.¹

¹ Department of Physical Chemistry of Fossil Fuels InPOCC, NAS of Ukraine
Lviv, Ukraine, andriy_kytsya@yahoo.com

² Karpenko Physico-Mechanical Institute of NAS of Ukraine, Lviv, Ukraine

Nearly monodisperse nickel spherical shape submicron particles with the mean diameter of 180 nm have been synthesized via reduction of ethylene glycol solution of Ni²⁺ by hydrazine in the presence of sodium hydroxide without any surfactants. It was observed (Fig. 1), that nickel particles form the linear chain-like aggregates due to their magnetization during the synthesis.

Using a simple technique of components mixing, a series of metal-filled polymer compositions based on synthesized submicron nickel particles and butyl acetate solution of methacrylic copolymer with different filler content have been prepared. The values of specific conductance of dried composites have been investigated by van der Pau method. It was shown (Fig. 2), that such compositions are characterized by a low (volume filler fraction is less than 4 %) percolation threshold.

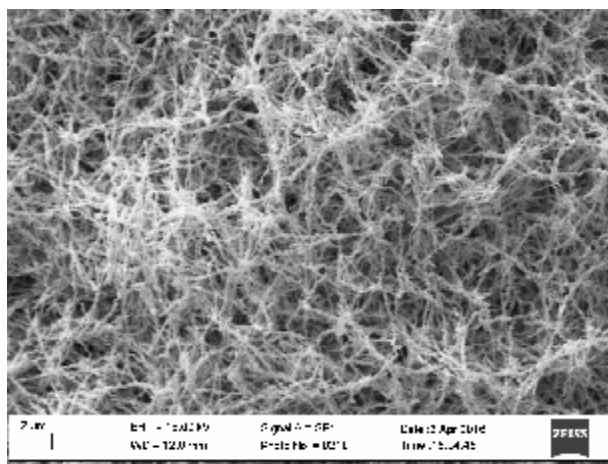


Fig. 1. SEM-image of nickel chain-like aggregates.

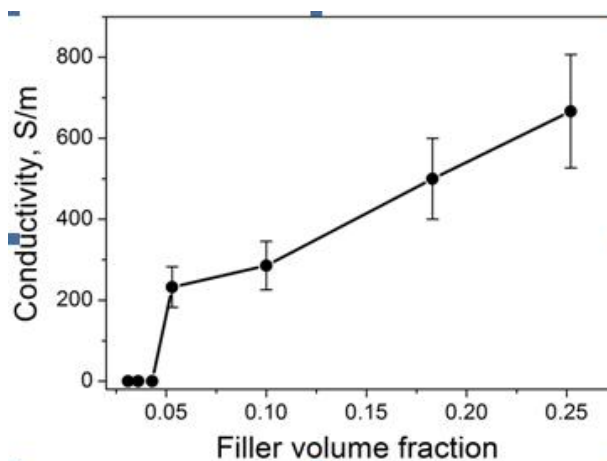


Fig. 2. Specific conductance of nickel-filled composites.

Filler packing factor equal to 0,3 for magnetic nickel submicron particles has been calculated. Such value is less in twice than theoretically calculated by Scher and Zallen for ideal spherical particles that is evidence of some interaction between particles of filler. On the base of comparison of theoretical calculations and results of electron microscopy investigations it was shown that a low value of volume filler fraction of obtained nickel particles at the percolation threshold is caused due to self-assembling of nickel particles and forming of 3D electroconductive network in polymer matrix.

Physical Properties of Nanocomposite Elements Based on Ni

Lepikh Ya.I., Lavrenova T.I., Sadova N.N.

Odessa I.I. Mechnikov national university, Odessa, Ukraine, e-mail: ndl_lepikh@onu.edu.ua

Nanocomposite materials are widely used in microelectronics, in particular, as film conducting elements of hybrid integrated circuits, solar batteries and sensors [1]. As a current-carrying phase use mainly precious materials silver, palladium and gold. In the given work the opportunity of precious materials replacement by conductors on the basis of nickel boride (Ni_3B) is investigated.

The structural-phase and physical properties of the film conducting elements based on Ni_3B , received at annealing with the help of electronic beam (EB) has been investigated. Thermal processing was carried out on the electron accelerator MULU - 8. As initial materials for past composition were used Ni_3B , glass C 279-2 and organic binding agent on a basis of terpeneol. For the analysis of initial functional materials phase structure changes under action of thermal and infra-red-thermal processing, the samples as a entire covering, by thickness of 200 microns on a substrate from ceramics BC-94-1 were prepared. It is established, that glass C 279-2 is stable with respect to processing by an electronic beam in a wide interval of temperatures. Conducting paste at heat treatment by EB gives in an interval of temperatures 800...950⁰ C, the stable structure $\text{Ni}_2\text{B} + \alpha\text{-Al}_2\text{O}_3$ and change of keeping time of composition at high temperatures does not result in change of phase structure.

Dependence of the conductor specific surface resistance on EB processing modes is received: the annealing temperature in the interval 390⁰-960⁰ C; temperature rapidity up to $T = 960^0$ C rise; time of sample keeping at $T = 860^0$ C. It is established, that functional nanocomposite materials which were used for nickel film conductors formation, are stable enough at infra-red-thermal effect. Current-carrying elements based on nickel, annealed with the help of EB, on the electrophysical parameters do not concede

Literature

- [1]. Lepikh Ya.I., Lavrenova T.I. Influence of a glass properties and structural-phase transformations on electrophysical parameters of semiconductor systems "glass - $\text{Pb}_2\text{Ru}_2\text{O}_6$, Ru_2 " // Radio electronics & Info Communications (UkrMiCo), 2016 International Conference, IEEE, 11-16 Sept, 2016. DOI:10.1109/UkrMiCo.2016.7739616, <http://eeexplore.ieee.org/document/7739616/>

Micro- and Nano-Measurements of Local Wettability of the Surface by Optical and Capillary-Force Methods

Efremov A., Lytvyn P., Prokopenko I.

*V. Lashkaryov Institute of Semiconductor Physics, NAS Ukraine
Kyiv, Ukraine, dr.alef007@gmail.com*

Various physical and computational aspects of the atomic force microscopy (AFM) application for quantitative estimations of the local wettability value are analyzed in combination and comparison with optical methods based on condensation of micro-droplets of moisture on the surface.

Expressions are given for capillary forces on various elements of the geometric relief, depending on the sign and radius of curvature and surface energy. It is shown that the first technique works perfectly both on smooth and on real relief surfaces. The use of measurements by several AFM probes (from different materials and with different tip radii) makes it possible to recalculate the obtained maps of capillary forces and surface relief into maps of surface energies with a lateral resolution of several tens of nanometers. This allows us to assume its chemical, corrosive and catalytic activity, the ability to fix nanoparticles, carry out their vibrational transportation and perform other nano-manipulations.

The use of optical techniques with application of condensed droplets makes it possible to carry out the same mapping, but with averaging over areas of a few tens of microns in diameter. In addition to a good qualitative visualization of the inhomogeneities that this method gives, numerical analysis of the droplet-microlens optics makes it possible to obtain a coarsened map of the wetting angles quantitatively. For wetting angles in the range of about 1° - 40° , calculations are carried out by interference rings, and for large angles – by analysis of the light brightness scattered by a drop. The informative nature of the methodology also increases if light of different wavelengths is used. The advantages and prospects of using the combination of measurements of the same property (in this case, wettability) with different degrees of "instrumental" coarsening in micro- and nanoscale are discussed in the report.

Quasi-Equilibrium Thermal Fluctuations of the Electromagnetic Field in Flexibly Polymers Filled With Nanodispersion Metal or Semimetal

Kolupaev B.B.¹, Maksimtsev Yu.R.²

¹*Rivne International Economics and humanitarian University. Rivne, Ukraine, Boris.Kolupaev@ukr.com*

²*Rivne state humanitarian University. Rivne, Ukraine, Maksymtsev@ukr.net*

From the point of view of thermodynamics of nonequilibrium processes described by the dynamics of electromagnetic phenomena in heterogeneous polymer systems (HPS). At the same nanodispersed metals (Cu, Ni, CR, W) and semimetals (graphite various modifications) act as a source of violation of the quasi-equilibrium structure of the elements of flexible polymers (PVC – a typical representative of them).

Schematically, the structure of HPS presented in the form of components: the nanosized particles of metal or semimetal, boundary layer (BL) and a polymer volume; the results of a statistical description of electromagnetic processes in each of them. With regard to the temporal delay and spatial non locality, analyzed the mechanism of current passage through the filler, polymer and BL and the synthesis of the composite. It is shown that for HPS you can create nice minority carriers of the opposite sign of the conductivity of the matrix. In such a bipolar conduction process the passage of current is accompanied by the modulation and the fluctuations of the electromagnetic field. Analyzed the interaction of electromagnetic radiation with HPS. On the basis of balance equations for the energy density of the microscopic fields shown that the kinetics of the elements of the composite structure is satisfactorily described by the Langevin equation for the harmonic oscillator, taking into account the dissipation of energy. Accordingly, consideration of the density of internal energy of the PVC-systems have shown that between the structure-sensitive characteristics of the polymer and composite microplasticity there is a quantitative relationship. Therefore:

$$P = \frac{c\rho \pi}{2\beta \omega \tau},$$

where P is the internal pressure; C – specific heat; ρ – density; β – temperature coefficient of volume expansion of the composite; in accordance ω , τ – frequency oscillations ($0 < \omega < \infty$) and the time of the Maxwell relaxation, as a reference to the speed setting field in the system.

Waystouse PVC composites as HPS in the external electric ($0,1 \text{ KHz} \leq \omega \leq 100,0 \text{ KHz}$), mechanical ($v = 0,4 \cdot 10^6 \text{ s}^{-1}$) and thermal ($T_C \leq T \leq T_C + 10 \text{ K}$, where T_C – temperature of glass transition) fields.

Structure, Morphology and Conductive Properties of C-Al₂O₃ Composites

Mandzyuk V.I.¹, Myronyuk I.F.¹, Bezruka N.A.², Kulyk Yu.O.³

¹Vasyl Stefanyk Precarpathian National University, Ivano-Frankivsk, Ukraine

²Ivano-Frankivsk National Medical University, Ivano-Frankivsk, Ukraine

³Lviv Polytechnic National University, Lviv, Ukraine

The structure, morphology and electrical properties of C-Al₂O₃ composites are explored in the work using small-angle X-ray scattering (SAXS), low-temperature porometry (LTP) and impedance spectroscopy. Composite materials were obtained by encapsulation of 5, 10, and 30 % of fumed Al₂O₃ into carbon matrix. For this purpose a dispersion of oxide material in a saccharose solution was caramelized and heated at 400°C. The resulting composite mixture was activated at 800°C for 30 minutes in the limited access of air.

According SAXS-studies there is a correlation between porosity of samples w , content of Al₂O₃ and the fractal dimension of structure n (Table 1). It is found that increasing the volume of porous material leads to a reduction of its fractal dimension. The formation of fractal structure caused by aggregation of carbon clusters formed on the surface of aluminum oxide.

Table 1. Parameters of C-Al₂O₃ composite materials

Al ₂ O ₃ , %	w	n	S_{SAXS} , m ² /g	S_{LTP} , m ² /g	V_{LTP} , cm ³ /g	σ , Ohm ⁻¹ ·m ⁻¹
0	0.61	2.80	426	356	0.187	26.2
5	0.60	2.45	300	121	0.081	16.5
10	0.75	2.10	440	192	0.106	14.4
30	0.79	1.90	330	14	0.010	0.4

Comparing SAXS and LTP data, we can conclude that closed porosity dominate in nanocomposite materials. The fraction of pores inaccessible to nitrogen molecules increases from 16.4 % (for carbon) to 95.8 % (for 30% content of Al₂O₃).

Adding non-conductive fumed Al₂O₃ (according to [1] its conductivity is 4.3 μOhm⁻¹·m⁻¹) results in decreasing of composite conductivity σ due to destruction of conduction channels in the carbon matrix.

1. V.I. Mandzyuk, I.F. Myronyuk, V.V. Gumenyak. Electrochemical intercalation of lithium ions into composite material Al₂O₃-graphene // Bulletin of Vasyl Stefanyk Precarpathian National University. Chemistry. – 2012. – V. XVI. – P. 95-101.

Influence of Synthesis Method on the Structure and Morphological Properties of Magnesium Ferrite Nanoparticles

Myslin M.V., Mironyuk I.F., Tatarchuk T.R.

Vasyl Stefanyk Precarpathian National University,
Ivano-Frankivsk, Ukraine, marjanysik@gmail.com

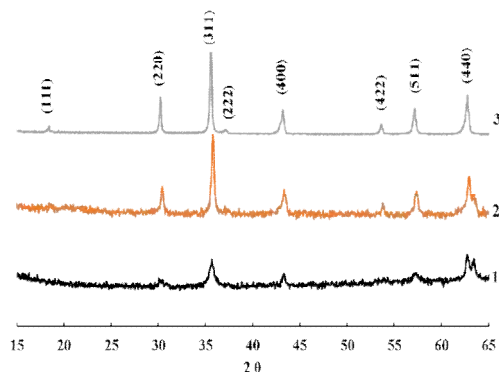


Fig. 1. The X-ray pattern of MgFe_2O_4 .

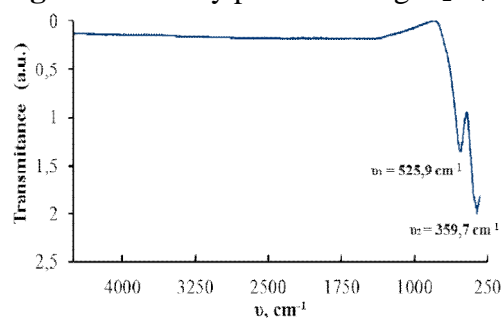


Fig. 2. FT-IR spectrum of MgFe_2O_4 obtained by combustion reaction (alanine + urea).

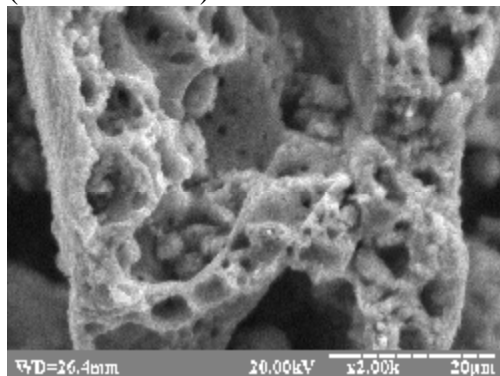


Fig. 3. SEM image of MgFe_2O_4 obtained by combustion reaction (alanine + urea).

In general, nanocrystalline ferrites are the widely investigating due their physical, electrical, optical and magnetic properties which are depend on method of preparation. This is why the investigating of influence of the synthesis method on the structure and morphological properties of nanosized MgFe_2O_4 is actual task. Magnesium ferrite was obtained by three methods: co-precipitation (1) and sol-gel combustion with different fuel (glycine(2) and alanine+urea (3)). The samples was characterized by XRD, FTIR, SEM, EDS and antistructural modeling was also done to get the concentration of active centers. The XRD analysis confirm the formation of single cubic spinel phase. The crystallite size were calculated by Scherrer, Williamson-Hall and size-strain plot method (SSPM). Crystallographic data were obtained from XRD: $a = 0,8381 \text{ nm}$, $u = 0,3707$, $\rho_{\text{XRD}} = 4,512 \text{ g/cm}^3$, $r_{\text{oct}} = 0.1994 \text{ nm}$, $r_{\text{tetr}} = 0.1613 \text{ nm}$. Also interionic distances were calculated: $d(\text{Me(A)}-\text{O}) = 0,1751 \text{ nm}$, $d(\text{Me(A)}-\text{Me(A)}) = 0,3629 \text{ nm}$, $d(\text{Me(B)}-\text{O}) = 0,2132 \text{ nm}$, $d(\text{Me(B)}-\text{Me(B)}) = 0,2963 \text{ nm}$, $d(\text{Me(A)}-\text{Me(B)}) = 0,3475 \text{ nm}$. FTIR spectra of MgFe_2O_4 are shown in Fig. 2 and the appearance of two absorption bands correspond to stretching vibration of tetrahedral and octahedral complexes. The force constants were calculated for tetrahedral site ($K_{\text{T}} = 1.659 \cdot 10^6 \text{ dyn/cm}^2$) and octahedral site ($K_{\text{O}} = 0.943 \cdot 10^6 \text{ dyn/cm}^2$) from the IR absorption data.

EDS elemental analysis confirmed a desired chemical composition of ferrite. SEM image (Fig. 3) reveal porous structure for MgFe_2O_4 obtained by autocombustion method. A new antistructural modeling for describing of active surface centers is discussed.

The Influence of Isothermal Annealing on Electrochemical Properties of Carbon Material

Nykoliuk M.O., Kachmar A.I., Rachiy B.I., Budzulyak I.M, Ilnitsky R.V.

Vasyl Stefanyk Precarpathian National University, Ivano-Frankivsk, Ukraine

The dependence of the specific capacity of electrochemical capacitor from discharge current is an important issue in terms of practical application. Therefore, to increase the value of specific capacity, we have investigated the activated carbon material (ACM), which was obtained from plant materials (shells of apricot seeds) and was subjected to prolonged isothermal annealing at $T = 400\text{ }^{\circ}\text{C}$ for 30, 60, ... , 210, 240 min. From the series of electrodes was formed ACM 2-electrode cell size of "2525". The 33% KOH was used as an electrolyte. The experimental results indicate a slight decline discharge current of 200 mA, which show a positive effect of isothermal annealing of ACM. Thus it shows the possibility of exploitation of capacitor with high current charge/discharge ($> 150\text{ mA}$) with a small surge in the discharge of the capacitor, which also demonstrates small decline in capacity.

Specifically, the decline in capacity for electrochemical capacitor is 9% for the current charge/discharge range from 10 to 200 mA, which was based on carbon material that was annealed for 90 min. Thus, the capacity of the capacitor is 171 F/g at a discharge current of 50 mA, which is 30 F/g more than capacity of electrochemical capacitor based on original ACM. For the electrode material which was annealed for 120 minutes there are a small decline in capacity in this current range, which is 7%, while for original ACM is 22%.

From these studies was found the optimal values of isothermal annealing time in which you can increase specific capacitance characteristics of activated carbon materials for electrochemical capacitors.

Structural Properties of As₂S₃ Doped With Cr

Paiuk O.¹, Stronski A.¹, Gudymenko O.¹, Nasioka Iu¹, Gubanova A.², Vlček M.³

¹ V. Lashkaryov Institute of Semiconductor Physics NAS of Ukraine, Kyiv, Ukraine,
paiuk@ua.fm

² Kamianets-Podilsky National University, Kamianets-Podilsky, Ukraine

³ University of Pardubice, Pardubice, Czech Republic

Chalcogenide glasses are well-known for their unique physical and optical properties such as transmission in the infrared, high refractive index, high nonlinearity, high chemical stability and a large variety of the photoinduced phenomena. Such properties can be controlled by doping with transition metals or rare-earth elements and have enabled many chalcogenide-based applications to be developed in diverse fields including photonics, medicine, environmental sensing and security. This report is concerned with studying the effect of chromium admixtures adding to arsenic sulfide glass on the structural and magnetic properties of glass by means of Raman and IR spectroscopy, X-ray diffractometry and SQUID magnetometer.

The amorphous nature of the bulk samples was confirmed by absence of sharp peaks in X-ray diffraction pattern. Radial electron distribution functions of doped and pure As₂S₃ bulk glasses were obtained and analyzed. In Raman spectra main observed effect under the introduction of Cr dopant into glass matrix was the change of relative concentration of main and non-stoichiometric structural units characteristic for As₂S₃ glasses.

Optical properties doped and undoped samples were studied in mid-IR region. Intensity of the vibrational absorption bands of various structural molecular fragments essentially depends on the chemical composition of glasses. The observed changes are considered to be connected with the interaction between introduced admixtures and the non-stoichiometric structural elements which present in glass as well as inherent impurities of the host glass such as hydrogen and oxygen.

Luminescence of As₂S₃ glass doped with Cr was studied in 800-1600 nm region (T=77K, $\lambda_{ex} = 514nm$). Luminescence intensity increased with the Cr concentration thus showing on the increased level of molecular fragments containing homopolar As-As bonds with the chromium introduction into the glass.

Pure chalcogenide glasses are diamagnetic. Introduction of transitional or rare-earth metals changes the magnetic properties of investigated chalcogenide glasses. There was observed the M(T) dependence, which characteristic for paramagnetics in the fields near 6 T.

Synthesis and Electronic Properties of $\text{Mg}(\text{OH})_2$ / Grafene Oxide Nanocomposites

Kotsubynsky V.O., Poplavsky I.O.

Vasyl Stefanyk Precarpathian National University, Ivano-Frankivsk, Ukraine

The method of deposition from aqueous solution of bischofite $\text{MgCl}_2 \cdot 6\text{H}_2\text{O}$ in colloidal solution environment of reduced graphene oxide has enabled obtaining of nanocomposite material with the expected mass ratio of $\text{Mg}(\text{OH})_2$: carbon equal to 10:1. Its structure with methods of X-ray diffraction and electron microscopy has been installed. The material is porous agglomerates, sizing 50-70 nm, consisting of individual whiskers or prismatic particles, transverse size of which is about 100 nm, and the particles are being observed with planes oriented parallelly to the crystallographic planes (100) and (101).

The research of frequency dependency conductivity of obtained ultrafine magnesium hydroxide, reduced graphene oxide and the composite magnesium hydroxide / oxide graphene restored has been conducted. It has been established that there is a nanocomposite material of qualitatively higher degree of disorientation compared to "clean" materials, and its conductivity in case of a sharp increase in the frequency hopping carrier between the equilibrium position is the best described by Jonscher model.

Length reducing of the connection of Mg-O coordination in the transition from relatively magnesium ions OH groups in $\text{Mg}(\text{OH})_2$ (2.1518 Å) to octahedral magnesium ions in the MgO_6 environment magnesium oxide (2.1157 Å) has to lead to an increase in frequency stretching of connection vibration. However, there has to increase the power of coupling constant Mg-Mg-O and with it the frequency of its vibrations strain. This conception is confirmed by the dynamics of change in the characteristics of infrared spectra of materials obtained by annealing at different temperatures, and the band almost disappeared at 3700 cm^{-1} . On the surface of the material there still recorded chemisorbed carboxyl groups (absorption region in the vicinity of 1440 cm^{-1}).

By the method of X-ray photoelectron spectroscopy there have been revealed changes of nanocomposite magnesium hydroxide / oxide restored graphene range compared to ultra pure magnesium hydroxide. There was, however, a new line in the spectrum of 1s electrons of oxygen atoms with energy of 531.3 eV, which is probably related to oxygen-containing functional groups localized on the package surface of partially restored graphene oxide.

Obtaining, Structure and Physicochemical Properties of Nanopowder Metal Oxides for Gas Sensors

Ostafiychuk B.K.¹, Bovgyra R.I.², Popovych D.I.^{2,3}, Savka S.S.²,
Serednytski A.S.², Venhryn Yu.I.²

¹ *Vasyl Stefanyk Prekarpathian University, Ivano-Frankivsk, Ukraine*

² *Pidstryhach Institute for Applied Problems of Mechanics and Mathematics NAS of Ukraine, Lviv, Ukraine, popovych@gmail.com*

³ *National University "Lvivska Polytechnika" Lviv, Ukraine*

In this paper carried out theoretical and experimental researches of features of the regularities of formation of structure and electronic properties of the metal oxide nanopowders in the gas environment. By methods of molecular dynamics conducted calculations of processes of formation morphology structure of *ZnO* nanoparticles by coagulation and coalescence *ZnO* nanoclusters under laser evaporation of *Zn* targets in chemically active gas environment. Been shown to structure, shape and size of the obtained particles depends from the cooling rate and the concentration of atoms in the volume, found that clusters are formed mainly in three structural phases - amorphous, wurtzite or cubic zinc blende. A density functional theory study [1] of the adsorption of molecules of different gases (*O₂*, *CO*, *NO₂*, *NH₃*) on the surface of nanoclusters *ZnO* were performed. It was determined that the molecules of *CO*, *O₂*, *NH₃* increase the concentration of the main charge carriers in sensor systems, whereas molecule *O₂*, reduce their concentration. The sharpest decrease is observed for *O₂* molecules, and among donor molecules the greatest impact was observed with *CO* and *NH₃* molecules. The features of photoluminescent properties in gases of *ZnO* nanopowder obtained them by means of laser ablation have been studied. Found that laser modified and surface doping of materials with impurities of noble metals can increase sensitivity to the corresponding gas component and purposefully implement catalytic processes on the surface of nanopowders. Established physicochemical regularities of formation of adsorption surface electronic states initial and doped nanopowders during adsorption to gases. The nature of nanopowdered metal oxide gas-sensing properties (adsorption capacity, performance, sensitivity, selectivity) has been established and the design and optimal materials for the construction of the multi-component sensing matrix [2] have been selected.

1. Bovgyra O.V., Bovgyra R.V., Kovalenko M.V., Popovych D.I., Serednytski A.S. The Density Functional Theory Study of Structural and Electronical Properties of ZnO Clusters // *Journal of Nano-and Electronic Physics*. – 2013. – V.5, №1. – P. 1027(6pp).

2. Zhyrovetsky V.M., Popovych D.I., Savka S.S., Serednytski A.S. Nanopowder Metal Oxide for Photoluminescent Gas Sensing // *Nanoscale Research Letters*. – 2017. – V.12. – P. 132(5pp).

XPS Investigation of Adenine Nanolayers on TiO_x Surface

Popovych N.¹, Popovych A.¹, Barta A.¹, Tsud N.², Duchon T.², Veltruska K.²,
Bercha S.², Khalachan I.², Gazova Z.³, Matolin V.², Rizak V.¹

¹*Uzhgorod National University, Uzhhorod, Ukraine*

²*Charles University in Prague, Prague, Czech Republic*

³*Department of Biophysics, Institute of Experimental Physics SAV, Košice, Slovakia*

Recent studies have demonstrated that nano-TiO₂ induces DNA damage and increase the risk of cancer and the mechanism might relate to oxidative stress. To our knowledge, no detailed spectroscopic study is reported on adenine/TiO_x system. Therefore the aim of this work is study of the adenine biomolecules interaction with the polycrystalline TiO_x surface by X-Ray photoelectron spectroscopy (XPS).

TiO_x surface was obtained by thermal oxidation of the cleaned Ti foil at the T=650 K, oxygen pressure 1×10^{-7} torr during (30+30+60) min. The thermal evaporation of adenine at 110°C took place in the preparation chamber (p= 1×10^{-7} torr). Al K α radiation (1486.6 eV) was used to measure the XPS O1s, C1s, N1s and Ti 2p_{3/2} core levels spectra with 1 eV total resolution. Curve fitting was performed after a Shirley background subtraction by a Lorentzian–Gaussian method.

The adenine thin film (d=9 Å) on the surface of titanium oxide were obtained. Analysis of the measured XPS spectra shows that the Ti 2p core level spectra after oxidation consist many components that can be associated with oxides TiO₂, TiO, Ti₂O₃ and titanium nitride and/or titanium carbide. N 1s core level spectra consist the two components (399.4 eV and 400.8 eV), which can be attributed to nitrogen with unsaturated chemical bonds (-N =) and (NH + NH₂), respectively. C 1s core level spectra of adenine film contains two components with 285.3eV and 287 eV binding energies, which can be attributed to carbon in the CC/CH groups and a CN-carbon bonds of the adenine rings respectively.

Then the sample was annealed (1min at 50, 75, 100, 125, 150, 175, 200, 250°C)

After heating in vacuum stepwisely 1 min at T=50, 75, 100, 125, 150 and 200°C thickness of the adenine layer decreases. After annealing at T = 250 C on the surface TiO_x remain only small amount of adenine, as evidenced the C 1s and N 1s core level spectra and AFM images of studied surface structure.

Surface Modification of LiMn_2O_4 for Enhancing its High-Rate Properties

Potapenko A.V., Kirillov S.A.

Joint Department of Electrochemical Energy Systems, Kyiv, Ukraine

Increasing power density of lithium-ion battery materials is one of the key issues for using them in industrial applications. Lithium-manganese spinel is one of the most prospective candidates for novel batteries from the point of view of its low cost, environmental friendliness and the ease of synthesis [1]. As follows from our recent paper [2], lithium manganese spinel synthesized by a citric acid route can endure current loads of 30C ($3990 \text{ mA}\cdot\text{g}^{-1}$) without degradation.

One of the ways enabling one to enhance the high-rate properties of LiMn_2O_4 is modifying its surface by substituted lithium-manganese spinel $\text{LiNi}_{0.5}\text{Mn}_{1.5}\text{O}_4$. In this case, undesirable processes such as Mn dissolution resulting from some side reactions that occur at the electrode/electrolyte interface upon charging/discharging the battery can be avoided. This procedure is called “core-shell” technique.

In this presentation, synthesis and studies of physico-chemical and electrochemical properties of $\text{LiMn}_2\text{O}_4/\text{LiNi}_{0.5}\text{Mn}_{1.5}\text{O}_4$ samples are described. Fig. 1 reveals that the modified sample sustains greater current loads ($9620 \text{ mA}\cdot\text{g}^{-1}$ or 65C) than the non-modified material and shows no degradation upon cycling. This indicates that surface modification is an effective tool for improving material properties and power characteristics.

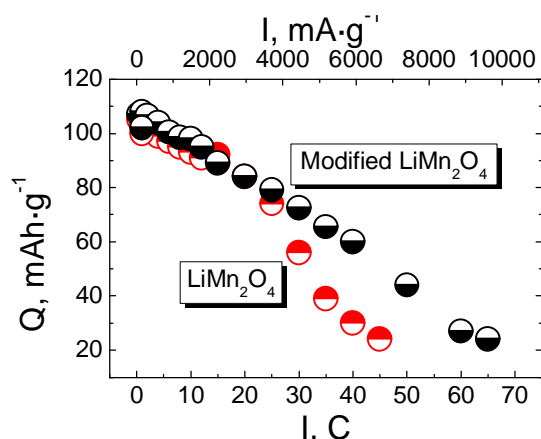


Fig. 1. Dependence of capacities on current load ($1\text{C}=148 \text{ mAh}\cdot\text{g}^{-1}$) for non-modified LiMn_2O_4 and modified $\text{LiMn}_2\text{O}_4/\text{LiNi}_{0.5}\text{Mn}_{1.5}\text{O}_4$ samples.

[1] A. V. Potapenko, S. A. Kirillov. *J. Energy Chem.* (2014) 23:543–558.

[2] A. V. Potapenko, S. I. Chernukhin, S. A. Kirillov. *Mater. Renew. Sustain. Energy* (2014) 3:40-47.

Low-Temperature PL Spectroscopy of ZnO:Mn Nanorods

Nikolenko A.¹, Rarata S.^{1,4}, Strelchuk V.¹, Komarov A.², Chey C.³, Nur O.³, and Willander M.³

¹*V. Lashkaryov Institute of Semiconductor Physics, National Academy of Sciences of Ukraine, Kyiv, Ukraine, rarata@ukr.net*

²*Institute of Physics, National Academy of Sciences of Ukraine, Kyiv, Ukraine.*

³*Department of Science and Technology, Linköping University, Norrköping, Sweden.*

⁴*Taras Shevchenko National University of Kyiv, Kyiv, Ukraine.*

Spintronics suppose constructing of electronic devices where information is carried by electron spin instead of electron electric charge. In the past decade, the wide band gap diluted magnetic semiconductors (DMS) have been considered to have great potential for applications in room temperature spintronic devices. Among these materials, ZnO doped with transition 3d metals has received much attention as one of a few promising materials with predicted room-temperature ferromagnetism. With growing interest to nanomaterials, Mn-doped ZnO nanorods (NRs) have attracted much interest for their potential in spintronic applications. In this work we used low-temperature photoluminescence (PL) spectroscopy as a sensitive tool to study the influence of Mn incorporation on electron energy structure of Mn-doped ZnO NRs grown by low-temperature aqueous chemical growths method.

PL measurements of near band edge emission of pure ZnO and ZnO:Mn NRs doped with nominal Mn concentrations of 15 and 30 at. % were performed at room and liquid helium temperatures. PL spectrum of ZnO NRs at room temperature is dominated by free exciton recombination emission band (FX) at 3.274 eV and its LO-phonon replica. As temperature decrease down to 4.2 K, FX band disappears and PL spectrum becomes dominated by recombination band of donor-bound exciton (DX) at 3.3672 eV, which is more narrow and shifted to higher energies due to increase of the bandgap with temperature.

Position of DX band for Mn-doped ZnO NRs gradually shifts to lower energies with Mn concentration and makes 3.3632 eV and 3.3618 eV for 15% and 30% nominal Mn content, correspondingly. Such low-energy shift agrees with the reduction of bandgap of ZnO:Mn NRs registered earlier in optical absorption measurements [1]. Such reduction in E_g with Mn content is due to s,p-d exchange interaction between band carriers and d-electrons of Mn^{2+} substituting Zn^{2+} ions, and evidence concentration of incorporated Mn for the investigated NRs of up to 1 %, which is significantly less than the nominal ones.

1. Strelchuk V.V. Optical and structural properties of Mn-doped ZnO nanorods grown by aqueous chemical growth for spintronic applications / V.V. Strelchuk, A.S. Nikolenko, O.F. Kolomys, S.V. Rarata [et al.] // Thin Solid Films. – 2016. – V.601. – P. 22-27.

The Minimal Conductivity of Graphene, Caused By An Effective Attenuation of Carriers due to The "Zitterbewegung" Effect

Ruvinskii M.A.

Vasyl Stefanyk Precarpathian National University Ivano-Frankivsk, Ukraine

Considering the features of the free movement of relativistic quantum mechanics based on the Dirac equation, Schrödinger was first discovered appearance of microscopic periodic motion with form of pairs of particles and antiparticles. This movement is called Schrödinger electronic "trembling" ("Zitterbewegung"). Normal physical interpretation associated with the Heisenberg uncertainty principle, when if you trying to determine the exact coordinates than will form electron-positron pair. The aim of this work is to find the minimum conductivity of graphene based on electronic explicit definition of effective damping by means of non-stationary perturbation theory for quantum transition of systems in states with born of the electron-hole pair with followed substitution in known physical kinetics expression.

Internally band conduction can be defined from the kinetic Boltzmann equation in the relaxation time approximation $\tau=1/\Gamma$ in model of massless Dirac fermions and linear response theory. The general expression for the internally band conductivity with taking into account the energy dependence of the inverse relaxation time $\Gamma(\varepsilon)$ has the form [1]:

$$\sigma = -g_s g_v \frac{e^2}{(2\pi\hbar)^2} \int \frac{v_x}{(\Gamma_{tz} - i\omega)} \frac{\partial}{\partial p_x} (\rho_1^0 - \rho_2^0) d^2p, \quad (1)$$

where $v_x = \hbar^{-1} \partial \varepsilon / \partial p_x$, $\rho_1^0 = f_0(\varepsilon - \mu)$, $\rho_2^0 = f_0(-\varepsilon + \mu)$, $f_0(\varepsilon - \mu) = (\exp[(\varepsilon - \mu) / \theta] + 1)^{-1}$ – the Fermi-Dirac function, $\theta = k_B T$, k_B – Boltzmann constant. Transit relaxation time Γ_{tz}^{-1} :

$$\Gamma_{tz} = \frac{1}{\tau_{tz}} = \int_0^{2\pi} (1 - \cos \varphi) \Gamma(\varepsilon_p) d\varphi = 2\pi \Gamma(\varepsilon_p),$$

$$\Gamma(\varepsilon_p) = g_s g_v \frac{L^2}{(2\pi\hbar)^2} \frac{\pi\hbar}{2L^2} \int_0^{2\pi} d\varphi \int_0^\infty \delta(2\varepsilon' - \varepsilon_p) \varepsilon' d\varepsilon' = \frac{\varepsilon_p}{4\hbar}$$

For the static case of ideal graphene substitute in (1) $\omega=0$ and value $\Gamma_{tz}(\varepsilon)$, caused by the effect of "Zitterbewegung" for sufficiently small T i μ . At low temperatures $T \rightarrow 0$ $-\frac{\partial f_0(\varepsilon - \mu)}{\partial \varepsilon} = \delta(\varepsilon - \mu)$. For minimal conductivity at $T = 0$ and $\mu = 0$ using the properties of Dirac δ -function:

$$\sigma_{min} = \frac{4e^2}{\pi\hbar} \left[\int_0^\infty \delta(\varepsilon) d\varepsilon + \int_{-\infty}^0 \delta(-\varepsilon) d\varepsilon \right] = \frac{4e^2}{\pi\hbar}. \quad (2)$$

Thus, the apparent using of effect "Zitterbewegung" leads to the universal expression of σ_{min} , which is confirmed experimentally.

1. M. A. Ruvinskii and O. B. Kostyuk, Minimal Conductivity of Graphene // Metallofiz. Noveishie Tekhnol. – 2015 – V. 37, №12 – P. 1725-1731.

Graphene Nanoparticles at Opal Surface Probed by Raman Spectroscopy

Severin I.^{1,2}, Boiko V.¹, Perederii O.¹, Negriyko A.¹, Posudievsky O.³,
Moiseeko V.⁴, Dovbeshko G.¹

¹*Institute of Physics, NAS of Ukraine, Kyiv, Ukraine*

²*National Technical University of Ukraine,*

“Igor Sikorsky Kyiv Polytechnic Institute”, Kyiv, Ukraine

³*L.V. Pisarzhevskii Institute of Physical Chemistry of NAS of Ukraine, Kyiv, Ukraine*

⁴*Gonchar Dnipropetrovsk National University.*

Graphene-like materials and composites based on them are widely used in numerous electronic and optic applications, including optical and electrical signal enhancement. Photonic crystals (PC) on the synthetic opal basis due to periodicity its structure are able to redistribute a density of electromagnetic field leading to its concentration in specific opal regions. It results in an increase efficiency of interaction between the field and molecules introduced in PC cavities.

We expect to observe an impact of the PC on the optical modes (intensity, halfwidth and spectral position) of graphene infiltrated in PC structure. It will allow us to register enhanced Raman scattering of graphene modes located within stop band spectral region and optical modes which cannot be registered under ordinary circumstances. According to our preliminary data [1] an enhancement of the optical field in the interglobular PC cavities was observed.

Here we registered G, D and 2D modes and showed that GNP infiltrated in opal structure became less disordered than GNP on Si/SiO₂ (this conclusion is based on the half-width of G mode). Creation of bonding between the opal globule defects and GNP reduce number of GNP defects. It was concluded from the I(D)/I(G) ratio. The size of the GNP clusters absorbed by the surface are bigger on the PC domains (particle aggregates on the surface of PC more) than between opal domains. This fact was confirmed by lesser intensity of G-mode of GNP absorbed by the PC surface in comparison with those for GNP between opal domains.

We got 2.6-3 times enhancement for D, G and 2D modes from GNP infiltrated in opal in comparison with those for GNP on Si/SiO₂ surface. This data is in agreement with simulation by FDTD methods.

Acknowledgement: *we thank to FAEMCAR and STCU 6175 projects for financial support*

1. V. V. Boiko, V. R. Romanyuk, O. P. Gnatyuk, E. A. Andreev, O. O. Ilchenko, S.O. Karakhim, A. V. Korovin, and G. I. Dovbeshko. Vibrational spectra of DNA in the confined interglobular volume of photonic crystal. Phys Rev E 2017 accepted for publication.

The Faraday Effect in the Two-Layer Fe/PET Structure

Shapoval K.O., Kasumov A.M., Lashkarev G.V.

Francevich Institute for Problem of Material Science of NASU

Kiev, Ukraine, e-mail: kasumov8@ipms.kiev.ua

It is known that properties of thin films in large extent depend on the substrate properties on which they are deposited. For example, the method of epitaxy is based on such dependence. Microelectronics usually uses inorganic substrates. However, no less interesting are organic polymers substrates having a branched structure consisting of molecular groups of different chemical composition and possessing properties which differ a lot from inorganic compounds.

One of such attractive polymers' is the polyethyleneterephthalate (PET) widely used now in various fields of engineering. In the present work, we investigate the magneto-optic properties for visible light ($\lambda = 0,62 \mu\text{m}$) of thin iron film ($\approx 60 \text{ nm}$) deposited by thermal evaporation on the PET substrate of 0.1 mm thick. The Figure shows the typical dependence of the Faraday rotation angle φ from magnetization of iron film on the glass (1) and on the PET (2). As can be seen from the Figure, the dependence φ (M) for thin Fe films deposited on glass is linear one, which accords with the theory [1]. Fe/PET structure has nonlinear φ (M) dependence and the value of φ is much higher than that of Fe film on glass (30-50 times). Also from this Figure it is seen that with increasing of Fe/PET magnetization, the dependence φ (M) gradually decreases, at, presumably, may be due to the features of an interaction between Fe film and PET.

Simultaneously we observed the changes of the spectral position for IR absorption lines of PET and Fe/PET structures and their splitting in magnetic field. The magneto-optical Faraday rotation in PET and in Fe/PET structure as well as the change of their IR absorption spectra we discovered for the first time.

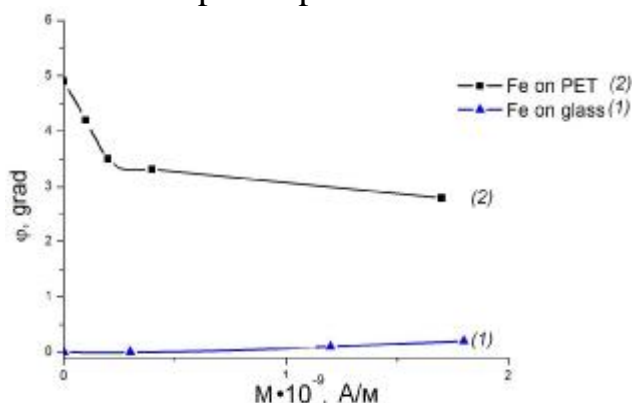


Figure – The dependence of the Faraday angle φ from magnetization of samples

References:

1) A.K. Zvezdin, V. A. Kotov, Magnitooptika tonkih pljonok, M. Nauka, 1988, 190 s.

Influence of Phonons on Optical Properties of Quantum Dot Semiconductor Heterostructures

Shevchuk I.S.

*Department of Theoretical and Applied Physics & Computer Simulation,
Ivan Franko Drohobych State Pedagogical University, Drohobych, Ukraine,
i.s.shevchuk@ukr.net*

A carefully controlled state formation of the quantum dot states is necessary for many devices of semiconductor quantum dots in quantum technology. Since quantum dots are placed in the semiconductor matrix, the interaction with phonons frequently plays a key role in the preparation process. The investigation of the fundamental properties of phonons is also essential to understand their part in the practical application in quantum information science. The active use of phonons in this field is presently highly discussed [1]. The optimized electron-LO-phonon coupling in semiconductor nanostructures is important to understand their optical properties and can be tuned by advanced fabrication techniques. If an electronic level separation in a quantum dot matches the energy of the longitudinal optical (LO) phonons, the electron-phonon interaction leads to formation of polarons i. e., coherent states composed of an electron and LO phonons [2].

In recent decades a significant effort has been placed in the research of the exciton-LO-phonon interaction in semiconductor quantum dots. The phonon sidebands are generally described in the adiabatic approximation with the use of a displaced harmonic oscillator model [3].

In the present work we investigate optical properties of semiconductor quantum dot heterostructures, in which a Fröhlich-type interaction between an electron (a hole, an exciton) and longitudinal optical phonons has been assumed. In order to understand the interactions of the coupled exciton-phonon subsystem, we study the effect of polarization phonons on the exciton spectra of quantum dots of realistic geometries in the multiband model and find a good agreement between theory and experiment. Further the phonon effects on the optical properties of spherical quantum dots are discussed.

1. Daniel Wigger, Helge Gehring, V. Martin Axt, Doris E. Reiter, Tilmann Kuhn. *Journal of Computational Electronics*, 15-4 (2016), 1158.
2. Tomoki Tasai, Mikio Eto. *Physica E*, 17 (2003), 139.
3. R.Heitz, I. Mukhametzhanov, O. Stier, A. Madhukar, D. Bimberg. *Physica E*, 7 (2000), 398.

Formation of Film Material on CoSb₃ Based Skutterudite for Thermoelectric Devices

Shkarban R.A., Makogon Yu.N., Sidorenko S.I.

*National Technical University of Ukraine «Igor Sikorsky Kyiv Polytechnic Institute»,
Kyiv, Ukraine, e-mail: ruslan.shkarban@gmail.com*

The solution of energy security problem by efficiency improving of alternative energy generation, the search for new, clean and renewable energy sources. This is a key scientific and technical task. One of the ways to increase the thermoelectric coefficient efficiency (ZT) is the application of skutterudite CoSb₃ antimony (conception the G. Slack). In addition, the transition from bulk materials to the nanoscaled allows to addition to increase ZT due to defectiveness in the structure.

The paper experimentally was confirmed the theoretical calculations of ZT increase in the transition to nanoscaled materials. The basic laws of phase composition and structure formation, electrical properties in as-deposited

Co-Sb(30 nm) films on SiO₂(100 nm)/Si(001) substrates and after annealing in vacuum and nitrogen atmosphere were defined.

The CoSb₃ films are thermally stable up to ~300°C. At annealing of Co-Sb films at temperatures above 300°C sublimation of not only excessive Sb but also of Sb from the crystalline phase CoSb₂ and CoSb₃ occurs.

ZT increases in CoSb₃(30 nm) nanoscaled film at 500°C up to ~1 that is in 8 times higher in comparison to bulk material is determined by nanoscaled factor and due to increased defectiveness of structure. This is the practical significance of the use of these materials for electronic devices with self-powered low-power and at the creation of the refrigerators in element base of the nanoscaled range for computer equipment and infrared sensors.

Theoretical Analysis of Nanostructure of Chalcogenide Amorphous Films

Bilozertseva V.I., Dyakonenko N.L., Korzh I.A.,
Lykah V.A., Sinelnik A.V.

National Technical University "Kharkiv Polytechnical Institute", Kharkiv, Ukraine

It was found that thin chalcogenide films $A^I\text{-Bi-C}^{VI}$ (A^I – Li, K, Na, Rb; C^{VI} – S, Se) deposited on a relatively cold substrate (300 K) have an amorphous structure [1]. Amorphous layers have not an atomically smooth surface, but consist of clusters measuring from 5 to 15 nm. The contrast on the electron-microscopic images of clusters is supposed to be caused by material density changes. There are narrow and wide regions of low density between clusters for different films.

Theoretical analysis of the amorphous structure was performed in order to explain the cluster formation reasons. Two order parameters were chosen: the average angle deviation of the covalent bond from the optimal value (φ) and the average interatomic distance (r).

There are many descriptions of interatomic interactions: the Morse potential, the Van der Waals model potential, the Lenard-Jones potential. The parameter φ together with the use of elliptic functions gives a good description of the disorientation of highly directional covalent bonds, as well as their periodicity. The variation of the free energy with respect to the order parameters leads to a system of two Lagrange type equations. The separation of variables in these equations is a nontrivial task, so the rectangular path was chosen, consisting of three straight segments, as can be seen on Fig.1. The path runs between two

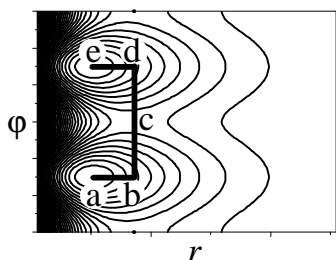


Fig. 1. The levels of potential as a function of order parameters r and φ ; the path of integration is also shown.

potential minima (a, e) and through saddle point (c). There are two segments (a-b and d-e) where only the interatomic distance changes and one segment (b-c-d) where only the angle varies with fixed interatomic distance. The application of this procedure of variable separation allows us to find the spatial dependence of the disordering parameters r and φ during the transition

from one cluster to another. Equations for the boundaries of clusters are obtained and it is shown that the boundaries of the cluster contain an increased number of disordered bonds.

1. Bilozertseva V.I., Khlyap H.M., Shkumbatyuk P.S., Dyakonenko N.L., Mamaluy A.O., Gaman D.O. Li-Be-Se semiconductor thin films: technology, structure and electrophysical properties // *Semiconductor Physics, Quantum Electronics & Optoelectronics*. – 2010. – V.13, №1. – P. 61-64.

Electrochemical Synthesis of Nb and Ta Nanoporous Oxide

Liashok L.V.¹, Gomozov V.P.¹, Skatkov L.I.², Vodolazchenko S.A.¹

¹ NTU “KhPI”, Kharkov, Ukraine

² PCB “Argo”, Beer Sheva, Israel

Electrochemical method of forming the porous anodic oxide film (AOF) to valve metals (Al, Ti, Nb, Ta and others) Attracts attention of many researchers as allows you to create oxide materials with controlled nanostructured surface morphology [1]. Nanoporous niobium and tantalum oxides has unique properties (pores of nanometer size, high chemical and thermal resistance, catalytic activity, etc.), which makes it promising from a practical point of view. These materials are characterized by the possibility of their effective application to create a wide range of devices such as gas sensors, solar cells, catalysts, thin-film lithium batteries and others. Thus, the development of technology of electrochemical formation of porous AOP on niobium and tantalum, and the study of their properties is of great scientific and technological interest. At the same time, the number of published studies on the synthesis and control of the morphology of porous tantalum and niobium oxides slightly because data objects are relatively new materials. This paper studies the role of activator and anodization regime in the formation of nanoporous oxide, niobium and tantalum amorphous or crystalline types. In this paper we have considered the original structure of the surface of the niobium and tantalum as the defect containing the natural oxide film, the legacy of the surface defects after the preparatory operations. Suppose that in this regard, along the surface of these metals at imposing building inhomogeneous electric field distribution, and the rate of electrochemical processes of growth and dissolution of the oxide in different parts of the surface are not the same and depend on the extent of its defects and composition of the fluid lining of the electric double layer. The defective areas dissolution process should proceed rapidly with nucleation pores. An analysis of the literature [1,2] shows that the OPA and sweat formed in fluoride electrolytes, slightly soluble oxide film.

Anionic composition of the electrolyte significantly affects the dynamics of the processes in the inhomogeneous energy passivation layer. By sorption capacity of fluoride ion exhibits an activating action. Depassivation of sample starts with the highest activity at sites, and then the process involved and less active sections. AOP fluoride interaction with surface leads to the formation of soluble complexes $[\text{NbF}_7]^{2-}$ and $[\text{TaF}_7]^{2-}$, which causes local dissolution of an oxide nucleation promoting the formation of pores and a porous structure AOF. Polarization measurements were carried out on potentiostat PI 50-1.1 at potential sweep rate $1 \cdot 10^{-2}$ V / s in potentiodynamic mode. The reference electrode - saturated with silver chloride. To develop the concepts of the general laws of the electrochemical behavior of niobium and tantalum in the acidic electrolyte 1 M H₂SO₄ and explain the effects of the cation nature consider

anodic polarization dependence. On the curves exhibit a maximum in the potential range from 0.05 to 0.45 V, which corresponds to the formation of barrier films on niobium, and the electrolytes 1 and 2 following the current rise, corresponding to an increase of the porous oxide, significantly higher than in solutions 3 and 4. such behavior of the system can be explained by the fact that the dissolution rate of the active surface of the centers in these electrolytes is comparable with the rate of production of the AOP. As noted above, the electrochemical formation of AOS on tantalum and niobium varying mode anodizing possible to obtain crystalline oxide structure. For the development of crystals takes a long time, so this crystallization is observed at voltstatic anodizing. Growing the crystals are in the form of irregular polyhedra.

1. Minagar S., Berndt C.C., Wang J., Ivanova E., Wen C. A review of the application of anodization for the fabrication of nanotubes on metal implant surfaces // *Acta Biomaterialia*. –2012. – Vol. 8, № 8. – P. 2875–2888.
2. Yu H, Zhu S, Yang X, Wang X, Sun H, Huo M (2013) Synthesis of Coral-Like Tantalum Oxide Films via Anodization in Mixed Organic-Inorganic Electrolytes. *PLoS ONE* 8(6): e

Novel Biosensors Based on Nano-Gold/Zeolite Modified ISFET for Concentration of Creatinine Determination

Ozansoy Kasap B.¹, Soldatkin O.O.^{2,3}, Marchenko S.V.², Dzyadevych S.V.^{2,3}, Akata Kurc B.^{1,4}

¹*Micro and Nanotechnology Department, Middle East Technical University, Ankara, Turkey,*
bernaozansoy@gmail.com

²*Institute of Molecular Biology and Genetics, NAS of Ukraine, Kyiv, Ukraine,*
alex_sold@yahoo.com

³*Taras Shevchenko National University of Kyiv, Kyiv, Ukraine,*

⁴*Central Laboratory, Middle East Technical University, Ankara, Turkey*

Zeolites are inorganic solids with large surface areas and well defined internal structures of uniform cages, cavities or channels of monodisperse dimension. In the field of biosensors, zeolites are promising materials for enzyme immobilization since they have large surface area, thermal/mechanical stabilities, ion exchange capacity, and controllable hydrophilicity/hydrophobicity.

The combination of advantages of using zeolites and gold nanoparticles were aimed to be used for the first time to improve the characteristic properties of ISFET based creatinine biosensors. The biosensors with covalently cross-linked creatinine deiminase using glutaraldehyde (GA) were used as a control group and the effect of different types of zeolites on biosensor responses were investigated in detail by using silicalite, zeolite beta (BEA), nano sized zeolite beta (Nano BEA) and zeolite BEA including gold nanoparticle (Gold-BEA). The presence of gold nanoparticles was investigated by ICP, STEM-EDX and XPS analysis. The chosen zeolite types allowed investigating the effect of aluminium in the zeolite framework, particle size and the presence of gold nanoparticles in the zeolitic framework.

After the synthesis of different types of zeolites in powder form, bare biosensor surfaces were modified by dip coating zeolites and creatinine deiminase (CD) was adsorbed on this layer. The sensitivities of the obtained biosensors to 1 mM creatinine decreased in the order of BEA-Gold>BEA>Nano BEA>Silicalite>GA. The highest sensitivity belongs to BEA-Gold, having threefold increase compared to GA, which can be attributed to the presence of gold nanoparticle causing favourable microenvironment for CD to avoid denaturation as well as increased surface area. BEA zeolites, having aluminium in their framework, regardless of particle size, gave higher responses than silicalite, which has no aluminium in its structure. These results suggest that ISFET biosensor responses to creatinine can be tailored and enhanced upon carefully controlled alteration of zeolite parameters used to modify electrode surfaces

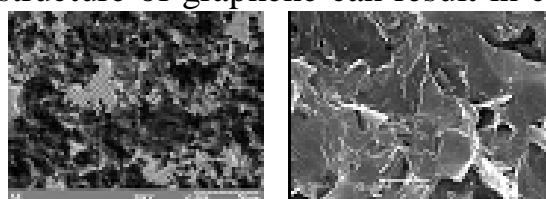
Filling with the Graphene Nanoplates as Effective Method of Considerable Adhesion Increase to Steel of Epoxy-Composite Tapes

Starokadomsky D., Tkachenko A., Shulga S.*

Acad. Chuiko Institute of Chemistry of Surface, NASU, Kyiv, Ukraine, stard3@i.ua

**Institute of General and Inorganic Chemistry, NASU, Kyiv, Ukraine*

Graphene is a new type of carbon materials, that forms 2D-structures. Structurally graphenes are monoatomic folias from sp²-hybridized atoms of C, packed in two-dimension cell structures with distance of C - C even 0,142 nm. He has very high electro- and thermo-conductivity. Therefore, the specific structure of graphene can result in creation of electroconducted composites and



substantial his strengthening, in particular strengthening of adhesion to the metallic surfaces.

Fig.1 SEM-image of our graphene

Tab.1. Strength of the adhesion tearing of steel cylinders (S= 5 cm²) glued by composites with 0.01 - 5 wt% of grapheme.

	Unfilled	0.05 wt%	2 wt%	5 wt%
Load of tearing Q, kgf	70	65	190	240
% to Q for unfilled	100%	93%	271%	343%

Our experiments allowed to set very considerable strengthening influence of graphene on epoxycomposite adhesion to steel surface (tab.1). This influence increases with the height of grapheme concentration. At small concentrations of graphene (for example the 0,05 masses%) influence on adhesion is insignificant (таб.1). A microscopy shows aggregative morphology of compositions (fig.2) with the presence of graphene particles to d≈0,4 mm and including of phials of air.

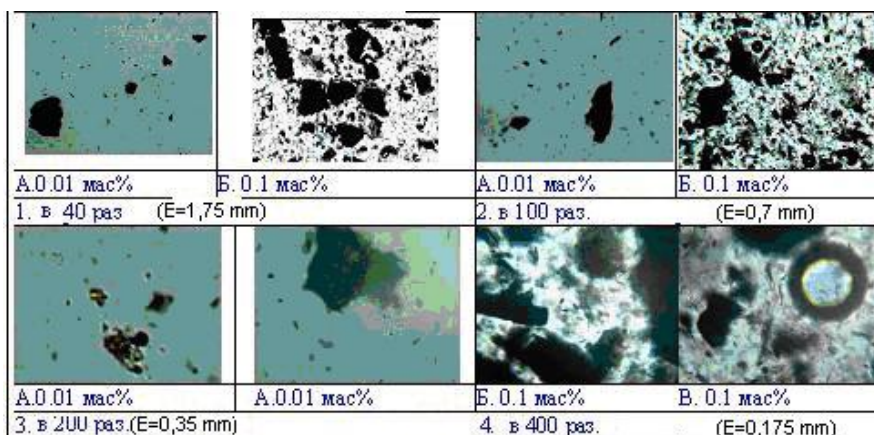


Fig.2. Micro-images of compositions before hardening (length of image E is 1)1,75; 2) 0,7; 3) 0,35 and 4) 0,175 mm).

Thus, grapheme is a perspective reinforcing filler for thermo- and electro-conducted epoxy-adhesives.

Effect of Low-Energy X-Rays on the Formation of Surface Nanorelief and on Change in the Physical Properties of Silicon Crystals

Steblenko L.P., Kuryliuk A.N., Krit A.N., Naumenko S.N.,
Kobzar Yu.L., Kravchenko V.N., Yurgelevich I.V.

Faculty of Physics, Taras Shevchenko National University of Kyiv, Kyiv, Ukraine
E-mail: kurylyuk_a2008@ukr.net

The present study was aimed at elucidation of the law of evolution of surface nanorelief and the features of change in microplastic and optical characteristics that occur in silicon crystals under action of low-energy X-rays ($E = 8 \text{ keV}$).

It is found that the X-ray treatment (XT) of Si crystals with different dopant type and, therefore, with different type of conductivity causes diametrically opposite changes in the roughness parameter (R_a), which was determined by means of atomic force microscopy.

Thus, roughness parameter R_a in n-type Si crystals after XT decreased from 12.5 to 4.7 nm. At the same time, roughness parameter in p-type Si crystals increased from 4.4 nm to 9.5 nm.

These results indicate that a consequence of XT-induced structural evolution is the reduction of defect content in the surface layer of n-type Si crystals and the growth of defect content in p-type Si crystals.

Increased defect content in the surface layer of p-type Si crystals after XT manifested itself in a change of the optical characteristics, in particular, in a change in the refractive index n . Due to XT the refractive index of p-type crystals decreased from 3.85 to 3.81, while that of n-type crystals remained unchanged.

It is found that the differences in surface nanostructuration affect not only the optical properties, but also the features of microplastic deformation.

Thus, after XT in p-type Si crystals one can observe a significant intensification of plastification processes, which shows up in the formation of slip lines and bands during deformation. At the same time, no similar processes in n-type Si crystals are observed.

Not excluded that a higher intensity of the development of plastic deformation processes in p-type Si crystals after XT may be associated with an increase in defect content in these crystals and participation of the defects in the processes of dislocation climb, which are known to contribute to plastification of the material.

Photoluminescence and Raman Spectra of As₂S₃ Doped with Mn

Paiuk O.¹, Stronski A.¹, Strelchuk V.¹, Kryskov Ts.², Vlček M.³

¹ V. Lashkaryov Institute of Semiconductor Physics NAS of Ukraine, Kyiv, Ukraine,
paiuk@ua.fm

² Kamianets-Podilsky National University, Kamianets-Podilsky, Ukraine

³ University of Pardubice, Pardubice, Czech Republic

As frequently pointed out by various researchers, chalcogenide glasses are promising materials for various applications because they are transparent over a wide spectral region, have high refractive indices, various photostimulated effects and are easy to fabricate. Chalcogenide glasses can be used in sensorics, infrared optics and optoelectronics. Special interest for applications is related with chalcogenide glasses doped with rare-earth and transition metal ions, because they alter physico-chemical properties of the host material due to structural and electronic changes of the glass network. The present work was devoted to studies of the influence of doping with Mn on structural and optical properties of As₂S₃ chalcogenide glasses.

Room temperature Raman spectra were recorded using Fourier spectrophotometer Bruker IFS-55 Equinox with FRA-106 attachment (with measurement step 1 cm⁻¹). Nd:YAG laser light at 1.06 μm wavelength was used for excitation. Introduction of manganese leads to the intensity increase of 192, 227, 236, 365 cm⁻¹ bands that correspond to the vibrations of non-stoichiometric molecular fragments As₄S₄. Intensity of band near 496 cm⁻¹, characteristic for vibrations of S–S bonds is decreasing. In 130–190 cm⁻¹ range bands appear, that can be connected with the creation of new sulphur containing structural units, similar to MnS molecular fragments.

Low-temperature photoluminescence was studied using the photoluminescence spectrometer HORIBA Jobin-Yvon T64000. Mentioned spectrometer was equipped with confocal microscope UV-Visible-NIR Olympus BX4 for micro sampling and Peltier cooled CCD detector TE-1024x256 Andor as a registration tool. As an excitation tool for photoluminescence the 488 nm (2.54 eV) line of Ar-Kr laser was applied. LTPL measurements were performed with a beam diameter of approximately 100 μm. PL measurements were carried out at liquid nitrogen temperature. For keeping samples at mentioned temperature they were fixed in micro-thermoelectrical cell Linkam Scientific Instruments THMS600. At 77 K, two luminescence peaks are observed at approximately 545 nm (2.28 eV) and 576 nm (2.15 eV). Band with λ_{max} = 576 nm can be connected with transitions in Mn²⁺ ions placed near structural defects [1]. The 545 nm (2.28 eV) band can be associated with radiative transitions of Mn ions placed near defects of structure (some authors mention also its complex structure) [1].

1. Yu. Yu. Bacherikov and S. V. Optasyuk Diffusion relaxation in ZnS after its thermo-doping by manganese at 800 °C // J.Appl. Spectroscopy.-2010.-V.77, N1.-P.104-112.

Composite Nickel Coatings Obtained by Pulse Current Programmable With External Laser Radiation

Tytarenko V.V., Zabludovsky V.A., Shtapenko E.Ph.

Dnepropetrovsk National University of Railway Transport named after academician V. Lazaryan, Dnipro, Ukraine

The electrolytic coatings based on nickel are widely used to protect metal surfaces from corrosion, mechanical damage, improve the strength characteristics and sliding strength of the products. The complex decision of the problem of improving the functional properties of the surface in this work is the modification of the metal matrix by ultrafine diamond (UDD) particles to obtain composite electrolytic coatings based on nickel and the use of a programmable pulsed current using laser radiation in the process of electrodeposition.

Deposition of composite coatings from an electrolyte water solution of nickel plating with the addition of UDD particles with a concentration of 2 g/l. Laser radiation with a wavelength of 1.06 μm was used. A programmable pulsed current with the same duration of trains of pulses unipolar current (36 min), frequency 50 Hz, average current density of 100 A/m^2 and successive increase in the duty cycle of trains of pulse current from 2 to 50; the pulse duration varied from 10 ms to 0.4 ms with a constant period of 20 ms. Microhardness of coverings measured on device PMT-3 at loading on indenter 0, 1 N. The sample life service tests were conducted on friction machine with reciprocating samples in conditions of unlubricated friction. The electron microprobe analysis was made by using the electron-scan microscope JSM-64901LV (Japan).

The results of the research showed that the use of laser radiation in the process of electrodeposition of composite nickel coatings by a programmable impulse current makes it possible to locally increase the concentration of nanodiamond particles in the coating from 0.19 to 0.32 at.%, which leads to an increase in microhardness from 4100÷4200 to 6400÷6500 MPa and wear resistance of coatings from 0.5 to 0.3 mg/h in comparison with electrodeposition without laser radiation.

Thus, the use of a programmable pulsed current using laser radiation in the course of electrodeposition allows layer-by-layer coating of a thickness of 15-20 μm , from the nickel coating layer with the smallest concentration of nanodiamond particles in the following layers with an increasing concentration of nanodiamond particles, which allows. This allows, first, to reduce the concentration of nanodiamond particles in the first layers of the coating and increase it in the following layers, improves the adhesion properties and increases the wear resistance of the coating, and secondly, with to lower the costs of nanodiamonds and thirdly to locally increase the concentration of nanodiamond particles in the coating.

High-Temperature Magnetic and Structural Properties of Core-Shell Magnetite Nanoparticles

Hurskyj S.T.¹, Syvorotka I.I.², Vasylechko L.O.¹, Ubizskii S.B.¹

¹ Lviv Polytechnic National University, Lviv, Ukraine

² Scientific Research Company «Carat», Lviv, Ukraine

Iron oxide-based nanoparticles have a number of applications in biomedical technologies, such as targeted drug delivery, magnetic cell separation, magnetic resonance imaging and magnetic fluid hyperthermia. Magnetite, maghemite, hematite, wüstite, β -Fe₂O₃ and ϵ -Fe₂O₃ are the main structural modifications of iron oxide. At high temperature structural transformations between these phases, can occur and change properties of material, in particular its magnetic behaviour. Such transformations in nanosized particles can be different from those of bulk material, but they are studied insufficiently. Therefore the purpose of this investigation was to identify the main peculiarities of the magnetic properties changes of core-shell magnetite nanoparticles occurring under heating and their relation to structural transformations.

Composite nanoparticles «magnetic core – polymer shell» grown by homogeneous nucleation method with average core diameter of ~ 8 nm [1] were used in this investigation. Temperature dependencies of magnetization as well as magnetisation reversal loops while heating and cooling in the range from room temperature to 650°C were measured by means of vibrating sample magnetometer method. The main properties of the core crystal structure of nanoparticles were studied in temperature range from 30°C to 910°C using X-ray diffraction of synchrotron radiation.

Results of this investigation have shown that the studied particles possess superparamagnetic properties at room temperature, but while being heated to ~ 300°C, they undergo irreversible changes of magnetic properties. Real structure and phase composition of magnetite nanoparticles' core were determined. At the temperature of ~ 700°C indistinctive structural phase transition from magnetite to wüstite was identified.

This work was fulfilled in frames of R&D project DB/KMON of Ukrainian Ministry of Education and Science. Authors are grateful to O.S. Zaichenko and N.Ye. Mitina for synthesis of core-shell nanoparticles.

1. P. Demchenko, N. Nedelko, N. Mitina, S. Lewińska, P. Dłużewski, J. M. Greneche, S. Ubizskii, S. Navrotskyi, A. Zaichenko, A. Ślawska-Waniewska, *J. Magn. Mat.* **379** (2015) 28-38.

Application of Darboux Transformation for Potential Reconstruction of Nanosystems with Known Energy Spectrum

Voznyak O.M.

Vasyl Stefanyk Precarpathian National University, Ivano-Frankivsk, Ukraine

With the development of low-dimensional nano-structures, which have quantum wells, quantum dots, quantum wires, or superlattices as the basis elements, there were created new quantum devices for optical, nanoelectronic, information technologies of new generation, measuring devices. At the moment engineers learned how to control creation of heterogeneous nano-structures with different shapes, growing on crystals surface of one semiconductor few atom height layers of other semiconductors. The different effective masses are typical for these layers. Generalized equation of Schrödinger with position-dependent mass is using for theoretical description of the quantum-mechanical properties of semiconductor heterostructures's. One more important task of quantum engineering is building multi-quantum wells that have selected spectral properties.

Constructing various nano-structures that have selected spectral properties is the one of the most popular problem of quantum engineering. Therefore, the task for the recovering of quantum potential wells having energy spectrum value is important for low dimensional-structures investigat. Darbu transformation as the tool for solving differential equations, proposed in XIX century and which is actively developing in recent years, provides the way to solve of the recovering quantum potentials with selected spectrum problems. In relation to Schrödinger time-independent equation, this approach is based on application of first order differential operator for finding exact solution of second order equation. Such operator, a namely transformation operator Darbu, using intertwining ratio, gives the method based on known solution Schrödinger equation data to found another potential, which has spectrum identical to known spectrum.

Considered method has been applied to constructing potentials with given spectrum for quantum-mechanical systems with the mass depending on coordinates. In this case, we obtained new exactly solvable potentials in first and second order Darbu transformation frames. Darbu transformation operator forcing on wave function of known solution gives wave function that fits Schrödinger equation with new potential, expression for which can be found by applying the same operator to known potential. Darbu transformation method also has been applied for finding reflectionless potentials and their wave functions having known solution of Schrödinger equation for free particle.

Synthesis, Structure and Electrochemical Properties of Molybdenum Disulfide Obtained by Template Method

Budzulyak I.M.¹, Grigorochak I.I.², Yablon L.S.¹, Khemii O.M.¹,
Morushko O.V.¹, Hanushchak M.A.

¹Vasyl Stefanyk Precarpathian National University, Ivano-Frankivsk, Ukraine

²Lviv Polytechnic National University, Lviv, Ukraine

Receipt of new and modification of existing functional materials is closely related to search and implementation capabilities of various technologies, including using of various methods of synthesis [1]. The template synthesis was used to produce molybdenum disulfide. We used silicate matrix MCM-41 with a pore size of ~ 3.7 nm as a template. Aqueous Na_2S was mixed with Li_2MoO_4 and an aqueous solution of hydrazine. Template was impregnated the resulting solution under vacuum. Then the template was placed in an autoclave of stainless steel and heated at 473 C for 24 h. After natural cooling to room temperature template encapsulated powder was washed in isopropyl alcohol and dried to constant weight. Hydrofluoric acid is used to remove the template. Then the black precipitate MoS_2 was collected, washed several times with distilled water and ethanol. X-ray analysis indicates that we have received MoS_2 of hexagonal system (space group $P63 / mmc$, unit cell parameters $a = 0.31631$ nm and $c = 1.22097$ nm, $\gamma = 120^\circ$). The surface of synthesized molybdenum disulfide consists of agglomerated nanoparticles with a diameter of 25-50 nm. The voltage open circle of electrochemical cell based on molybdenum disulfide electrode amounted to 3.2 V, and operating voltage was of 3 V. As shown in Fig. 1 the discharge curve is perfect and corresponds to filling all octahedral positions between layers of molybdenum disulfide. This can lead to a phase transition from 2H phase in 1T. The emergence of such two-phase region is due to the strong interaction between lithium cations with molybdenum disulfide ions. In such interactions some order may occur until the formation of compounds of constant composition which is in balance with the previous phase. The discharge specific capacity for a given electrochemical cell was 181 F/g.

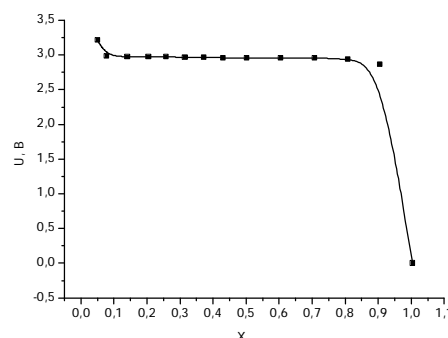


Fig. 1. The discharge curve of the electrochemical cell based on MoS_2 cathode, obtained by template method

1. Meng Wang, Guangda Li, Huayun Xu, Yitai Qian, and Jian Yang. Enhanced lithium storage performances of hierarchical hollow MoS_2 nanoparticles assembled from nanosheets // American Chemical Society Appl. Mater. Interfaces. – 2013, V. 5. – P. 1003–1008.

Properties of Nanostructured Epoxyurethane Polymers

Yashchenko L.M., Vorontsova L.O.

Institute of Macromolecular Chemistry of NAS of Ukraine, Kyiv, Ukraine

Currently, there is a growing interest in the problem of synthesis of nanoparticles and nanosystems and the study of their properties. Such systems include nanofilled epoxyurethane oligomers (nEUO).

This report demonstrates the results of several investigations in the field of epoxyurethane oligomer with polysiloxane particles and properties of polymer coatings based on them. Synthesis of polysiloxane particles (PSP) was performed by the sol-gel method "in-situ" in the medium of polyoxypropyleneglycol with the ratio of the tetraethoxysilane: water = 1:2. The synthesis of nEUO included the stage of obtaining the prepolymer with further introduction of epoxy resin ED-20. Iso-methyltetrahydrophthalic anhydride is the hardener. According to data of small-angle X-ray scattering the size of PSP is 5÷80 nm.

Considering nEUO as a base for protective coatings some physico-mechanical and optical properties of nanofilled epoxyurethane polymers (nEU) based on nEUO were investigated (Table, Fig. 1, 2).

Table. *Physico-mechanical properties of nEU*

Medium	The content of PSP, mass. %						
	0	0,001	0,01	0,1	0,5	1,0	2,0
	The degree of absorption, ΔM, %						
H ₂ O	1,26	0,92	0,93	1,25	1,39	1,86	1,86
H ₂ SO ₄	1,48	0,90	0,93	1,10	1,38	1,93	2,47
KOH	1,25	0,91	0,96	1,24	1,59	1,91	2,45
The adhesion strength (Al-substrate), S _s , MPa							
	29,6	33,8	37,8	32,6	23,0	20,0	28,6

It has been shown that the introduction of 0.001–0.5 mass. % of PSP increases adhesion strength, chemical resistance and optical clarity of the nanocomposites, which allows using them as a protective, optically transparent coating.

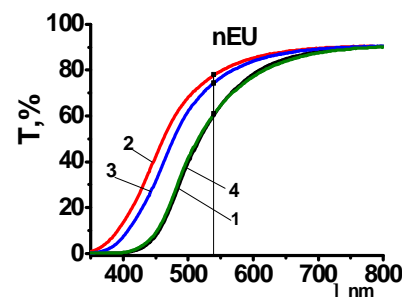


Fig.1. Transmission spectra of nEU: 1 – 0; 2 – 0,001; 3 – 0,01; 4 – 0,1 mass. % of PSP

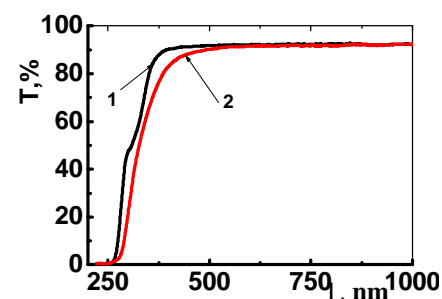


Fig.2. Transmission spectra of nEU (0,001 mass.% of PSP) before (1) and after (2) UV irradiation

Influence of Post-Annealing Effects on Electrochemical Properties of Microsized $\text{Bi}_2\text{Fe}_4\text{O}_9$

Yuryev S.O., Yushchuk S.I., Tsiupko F.I., Gorina O.M.

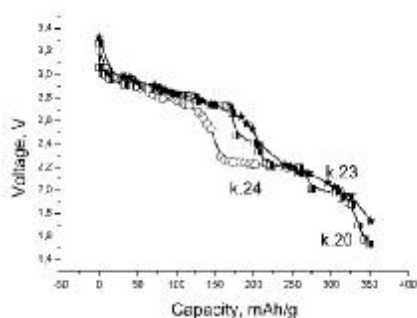
National University "Lvivska Polytechnica", Lviv, Ukraine, e-mail: syuryev@mail.ru

The aim of this work is to study the influence of thermal annealing microcapsules of powder $\text{Bi}_2\text{Fe}_4\text{O}_9$ ferrite on capacitive and electrical characteristics of the lithium current source with cathode based on it.

The powder of $\text{Bi}_2\text{Fe}_4\text{O}_9$ using the method of precipitation of hydroxides from solutions of iron (III) salts and bismuth with ammonium hydroxide at room temperature was synthesized. The particles size of the powder was less than $100 \mu\text{m}$. Individual portions of powder had been annealing in the air at $T=473, 673 \text{ K}$ for two hours.

X-ray diffraction analysis revealed that the crystal structure of $\text{Bi}_2\text{Fe}_4\text{O}_9$ can be seen as layered with the bulk layers perpendicular to the axis c . The distance between the layers was $3,94 \text{ \AA}$.

The obtained discharge curves of electrochemical cells with the cathodes basis on powder of $\text{Bi}_2\text{Fe}_4\text{O}_9$ are shown in Fig. The curve k.20 corresponds to unannealed sample of $\text{Bi}_2\text{Fe}_4\text{O}_9$. The curves k.23 and k.24 refer to the samples, subjected to annealing at $T=473$ and 673 K , respectively.



The curve k.24 has the steps which are related with the diffusion of the lithium ions at the grain boundaries and with the intercalation of the lithium ions in the crystal structure of $\text{Bi}_2\text{Fe}_4\text{O}_9$ in the channels formed by the ion layers.

The equivalent electrical circuits based on Nyquist diagrams of $\text{Bi}_2\text{Fe}_4\text{O}_9$ were obtained. It was founded that they all consist of series-connected resistances R , the RC – links and Warburg element. The value of Warburg elements are decreases with the increasing of annealing temperature of $\text{Bi}_2\text{Fe}_4\text{O}_9$ from 477 rel.ed. for the unannealed sample to 272 and 254 rel.ed. for annealed samples at $T=473$ and 673 K , respectively.

It is concluded that the annealing of the ferrite powder of bismuth at $T=673 \text{ K}$ leads to the formation of structural homogeneity of the material and the increase of the effect of intercalation of the lithium ions through the structure of $\text{Bi}_2\text{Fe}_4\text{O}_9$. The obtained value of capacitance in the neighbourhood of $350 \text{ mA}\cdot\text{h/g}$ at the discharge of up to $1,4 \text{ V}$ indicates the prospects of using the powders of $\text{Bi}_2\text{Fe}_4\text{O}_9$ as cathode material for the lithium current sources.

Hydrothermal Synthesis of β - $\text{FeF}_3 \cdot 3\text{H}_2\text{O}$ Followed by Heat Treatment in the Formation of HTB- $\text{FeF}_3 \cdot 0.33\text{H}_2\text{O}$ and r- FeF_3

Zbihlei L.¹, Moklyak V.², Hatala I.³

¹*Joint scientific-and-research laboratory of magnetic films physics (23) of the G.V. Kurdyumov Institute for Metal Physics NAS of Ukraine and Vasyl Stefanyk Precarpathian National University, Ivano-Frankivsk, Ukraine*

²*G.V. Kurdyumov Institute for Metal Physics of the NAS of Ukraine, Kyiv, Ukraine*

³*Vasyl Stefanyk Precarpathian National University, Ivano-Frankivsk, Ukraine*

In the last decades, research subjects have been shifted toward the nanostructuring of inorganic fluorides, especially iron fluoride, a recently reviewed field, due to potential applications in nanomedicine and electrical energy conversion. The synthesis of anhydrous iron trifluoride remains mostly unexplored. To the best of our knowledge, no account of its synthesis under molecular fluorine has been reported to date even though it appears to be the most practical way of obtaining anhydrous ferric fluoride species.

$\text{FeF}_3 \cdot \text{H}_2\text{O}$, $\text{FeF}_3 \cdot 0.33\text{H}_2\text{O}$, and FeF_3 have been synthesized via a hydrothermal method followed by heat treatment at different temperatures.

$\text{FeF}_3 \cdot 3\text{H}_2\text{O}$ was prepared by a simple hydrothermal methods. The first, 0.1 M aqueous solution of $\text{Fe}(\text{NO}_3)_3$ dropwise with vigorous stirring injected 25 % solution of ammonia and the resulted $\text{Fe}(\text{OH})_3$ precipitates were aged for 4 h. Then the precipitates were washed by deionized water to neutral pH=6.7 and separated by centrifugation. Secondly, excessive HF 40 % acid solution was added to the above precipitates $\text{Fe}(\text{OH})_3$ in the teflon wares, it will react immediately to form colorless FeF_6^{3-} due to its high stability ($K_f = 1015.04$). Next, the sealed Teflon ware was put into a stainless steel autoclave with continued stirring for 10 h at 70 °C, followed by cooling at the room temperature to obtain pink precipitates. The next step was made concentrating the solution by evaporation in air at 80 °C to precipitate $\text{FeF}_3 \cdot 3\text{H}_2\text{O}$. Finally, the unreacted HF and water were eliminated by heating in air and the residue was dried at 80 °C for 12 h in a vacuum drying oven. The crystal structure has been examined by X-ray diffraction method (XRD). From the XRD patterns and their Rietveld refinements, the β -form crystalline iron trifluoride (β - $\text{FeF}_3 \cdot 3\text{H}_2\text{O}$, PDF: 32-0464) with average size of 42 nm was received. Next, green $\text{FeF}_3 \cdot 0.33\text{H}_2\text{O}$ and brown FeF_3 compounds were obtained by heat treatment at 180 °C for 12 h and 400 °C for 4 h in a tube furnace with argon flow, respectively.

As a result, according to XRD data respectively received monophasic materials HTB- $\text{FeF}_3 \cdot 0.33\text{H}_2\text{O}$ structure of hexagonal bronze type (PDF: 76-1262) and anhydrous form of iron trifluoride romboedrycal structure r- FeF_3 (PDF: 33-0647). The average size appreciated by building Williamson-Hall are respectively of 26 and 23 nm.



POSTER REPORTS
Session 3
Physical-chemical properties of thin films



Optical Properties of Periodic 2D Structures

Bararash M.Yu¹., Gryn`ko D.A²., Litvin R.V³., Martynchuk V.E¹.,
Kolesnichenko A.A¹., Ryabov L.V¹., Balashov Yu.I¹., Danilova T.A¹.

¹ Technical Centre NAS of Ukraine, Kyiv, Ukraine

² Lashkariov Institute of Semiconductor Physics NAS of Ukraine, Kyiv, Ukraine

³ Frantsevich Institute for Problems of Materials Science NAS of Ukraine, Kyiv, Ukraine

Recently, an important part of nanotechnology and nanooptics – nanoplasmonics is rapidly developing in sphere of creating complex optical nanodevices, focusing on phenomena of conduction electrons oscillations in metallic nanostructures and nanoparticles and the interaction of these oscillations with light, atoms and molecules [1]. Plasmonic oscillations in nanoparticles significantly differ from the plasmons surface [2], therefore they are called localized plasmons.

The aim of current study is to investigate the optical properties of periodic metal-dielectric structures produced by the template method.

The optical extinction spectra of local gold films ordered by the template method (Fig. 1) have a number of differences in comparison with the wider bands spectrum, the spectra graphs have several curves, and the extinction maximum depends on the spatial frequency of the template. In case of unpolarized light, a wide band as shown on Fig. 1 appears. Curves on the spectra: 510 nm for graph 1, 750 nm and 520 nm for graph 2, numerical - for curve 3 - can be attributed to the opening of radiation mods channels - i.e. diffraction light dissipation on a spatially ordered system.

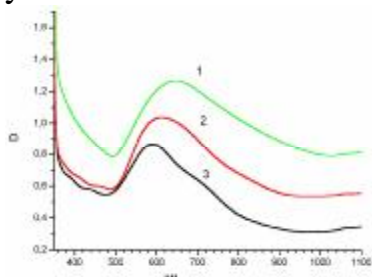


Fig.1. Optical extinction spectra of local gold films ordered by the template method. One-dimensional grid template with spatial frequency: 1- 1600 mm^{-1} , 2-500 mm^{-1} , 3- 160 mm^{-1} in unpolarized light.

Obviously, the gold nanowires formed by the template method are not solid and consist of a system of local areas. Therefore, the extinction spectra of gold nanoparticles system ordered by a template (Fig. 1), and the spectra of disordered system are very similar. This is related to nonresonant excitation conditions, when the wave vector of the incoming electromagnetic wave is not coordinated with the wave vector and the dispersion curve of the excitations. By changing the size and parameters of order, it is possible to control the magnitude and shape of the absorption spectrum.

1. M.Yu. Barabash, D.O. Hryn'ko, S.O. Sperkach. Formuvannya nanostruktur na templatakh vyromynyuvannyam iz vydymoho diapazonu – K.: IMF NANU, 2015. – 202 s.

2. M.Yu. Barabash, E.L. Martynchuk, D.O. Hryn'ko, R.V. Lytvyn. Zarodkoutvorenyya zolota v elektrychnomu poli na poverkhni templatu // Zhurnal Nano- ta Elektronnoyi fizyky. 2014. Vol.6, N 1. P.01029 (6c).

Template of Nanostructures Based on Amorphous Molecular Semiconductors

Barabash M.Yu., Litvin R.V., Kolesnichenko A.A.,
Martynchuk V.E., Ryabov L.V., Sezonenko A.Yu.

Technical Centre NAS of Ukraine, Kyiv, Ukraine

The template application is one of the most effective ways to obtaining modern functional nano- and the microstructured materials [1]. In current study the opportunity of electrographic process applying for producing planar templates with an artificial surface relief is shown. The amorphous molecular semiconductors (AMS) applying allows to provide cyclic obtaining of a geometrical relief with the modulated electrostatic charge on template surface in real time. It allows to optimize parameters of producing templates with various structure. The properties of new type of optical memory of AMS based on polyepoxipropilcarbazole is investigated. On the basis of this effect the templates with various relief and field topology were obtained. The research of surface potential relaxation, development of geometrical relief on AMS free surface has shown, that for AMS at temperatures lower then needed for a geometrical relief formation, a thermostimulated heterocharge (TSHC) is forming with charge value proportional to an initial charge. The surface potential relaxation depends on value and sign of the electric charge inside AMS and has three specific stages. An optimum value of temperature and time of TSHC formation was determined. While polymer template with TSHC obtaining it was established that the bandwidth of the transmitted frequencies coincides with the band of standard optical holograms method recording, there are no parasitic bands. TSHC presence inside template activates the local deposition of metal on its surface. Practical realization of the current effect allows to obtain templates with complex topology by holographic lithograph methods in real time.

1. M.Yu. Barabash, E.L. Martynchuk, D.O. Hryn'ko, R.V. Lytvyn. Zarodkoutvorennya zolota v elektrychnomu poli na poverkhni templatu // Zhurnal Nano- ta Elektronnoyi fizyky. 2014. Vol.6, N 1. P.01029 (6c).

Physical Processes in Planar Electrostatic Templates Generated by Tangential Intensities

Zabolotnyi M.A.¹, Barabash M.Yu², Vlaykov G.G², Litvin R.V²,
Kolesnichenko A.A², Martynchuk V.E², Ryabov L.V².

¹ Taras Shevchenko National University of Kyiv, Kyiv, Ukraine

² Technical Centre NAS of Ukraine, Kyiv, Ukraine

Currently, an important place in the development and uses of nanotechnology is the development of methods for the spatial self-consistent periodic nanostructures creation [1-3]. This interest is caused by possibilities of near-field technology to determine photoelectrical and electrotransport properties of thin organic polymer and composite layers using synergistic plasmonic effects [3-5]. This problem is solving by templates usage [3,6]. Thus surface morphology or topology of the template is used to generate the specified objects, ie, template work as mask that can be created by lithography methodics.

Thin layers of photoconductive thermoplastic materials can be considered as a perspective medium, rather than electrophotographic and photoplastic processes [3,6] are an instrument for the templates formation. It is interesting to find out the nature of the physical processes that determine the character of spatial relief amplitude, formed on the free surface of the deformable medium under the action of tangential components of external forces. Let's consider the kinetics of fluid particles trajectories moved in the process of free surface deformation. At layers with higher thickness closed trajectory occur, reducing the layer of material involved in the surface relief formation. In case of normal character of external deforming forces trajectories with such configuration do not occur [7].

A more detailed quantitative analysis can be performed using the law of energy conservation for the film deformed by normal forces.

$$W_f = \frac{1}{\lambda} \int_0^l P_H^{(1)} \cos^2(kx) h(k, t) dt = W_t + W_k + W_h, \quad (1)$$

where $\lambda=2\pi/k$, W_t – the density of energy dissipation, caused by internal friction of liquid at its flow during deformation by external forces of the free surface of the template layer and which is determined by the relation:

$$W_t = \frac{\eta}{\lambda} \int_0^\lambda dx \int_{-d}^0 dy \int_0^t dt \left[4 \left(\frac{\partial v_x}{\partial x} \right)^2 + 4 \left(\frac{\partial v_y}{\partial y} \right)^2 + \left(\frac{\partial v_x}{\partial y} + \frac{\partial v_y}{\partial x} \right)^2 \right]. \quad (2)$$

Variable W_k – the density of kinetic energy, determined by the relation:

$$W_k = \frac{\rho}{2\lambda} \int_0^\lambda dx \int_{-d}^0 dy [v_x^2 + v_y^2] \quad (3)$$

The change in free energy density of the deformed material surface W_h is caused by a change in the area of layer free surface during the formation of a spatial relief:

$$W_h \approx \frac{T_M k^2 h^2}{4} \quad (4)$$

In course of time (while t is comparable to τ_l) the circulation flow of liquid starts even with $kd < 0,7$ although it did not occur before. At the same time, there is an increase of spatial areas with turbulent flow where it previously existed. This leads to decrease in thickness of the liquid layer involved in formation of geometric relief on free surface and, consequently, to its amplitude decrease. Thus, in course of time, the extremum point in relief amplitude dependence on the spatial frequency of the external force moves to low-frequency values.

1. Suzdalev I.P. Nanotehnologija: fiziko-himija nanoklastero, nanostruktur i nanomaterialov.- M.: KomKniga., 2006, 592 s.

2. Paull J., Lyons K., Nanotechnology: the next challenge for organics //Journal of Organic Systems, – 2008.– vol. 3(1), P.3-22.

3. Vlaykov H.H., Barabash M.Yu., Zabolotnyy M.A.ta in. Formuvannya nanostruktur templantnym syntezom – K.: IMF NANU, 2010. – 230 s.

4. Kobajasi Naoja Vvedenie v nanotehnologii. –2-e izd. – M.: BINOM. Lab. Znaniy. 2008. 134 s.

5. Girard C., Joachim C., Gauthier S., The physics of the near-field // Rep. Prog. Phys. –2000.– Vol. **63**, P. 893–938.

6. Zabolotnyy M.A., Barabash Yu.M., Hryn'ko D.A., Barabash M.Yu., Kulysh N.P., Pryluts'kyy Yu.I., Elektrohafichnyy metod stvorennya dvovymirnoyi nadhratky z uporyadkovanykh nanoklastero na poverkhni fotoprovidnoho sharu, patent #55127, vid 10.12.2010.

7. Zabolotnij M.A., Barabash M.Ju., Grin'ko D.O., Martinchuk E.L., Dmitrenko O.P., Kulish M.P. Fizicheskie processy v termoplasticheskikh templatah // Polimernij zhurnal . 2011. t.33, № 4, S.361-369.

Spectroscopic Studies of Cu₆PS₅I-Based Thin Films Deposited by Magnetron Sputtering

Studenyyak I.P.¹, Bendak A.V.¹, Kutsyk M.M.¹,
Kúš P.², Azhniuk Yu.M.³, Zahn D.R.T.⁴

¹*Uzhhorod National University, Uzhhorod, Ukraine*

²*Comenius University, Bratislava, Slovakia*

³*Institute of Electron Physics, Ukr. Nat. Acad. Sci., Uzhhorod, Ukraine*

⁴*Chemnitz University of Technology, Chemnitz, Germany*

Crystalline Cu₆PS₅I belongs to the argyrodite family and is known as a superionic conductor with a mobile copper sublattice. Materials of this type are promising as solid electrolytes, supercapacitors, and electrochemical sensors. The optical properties of crystalline Cu₆PS₅I have been studied rather extensively. Here we report optical absorption and Raman spectra of Cu₆PS₅I-based thin films.

Cu₆PS₅I-based thin films were deposited on silicate glass substrates by non-reactive radio frequency magnetron sputtering, the film growth rate was 3 nm/min. The deposition was carried out at room temperature in Ar atmosphere. The chemical composition of the films obtained was checked by energy-dispersive X-ray spectroscopy (EDS Bruker XFlash 6) and appeared to differ from the stoichiometry, exhibiting excess of Cu and P and deficiency of S and I.

Optical transmission spectra were measured in the interval 77–300 K using an UTREX cryostat, a LOMO MDR-23 monochromator and a FEU-100 phototube. Micro-Raman studies were performed at room temperature using a Horiba LabRAM spectrometer with a CCD camera and a 514.7 nm Cobolt Fandango solid-state laser. The spectral resolution was better than 2.5 cm⁻¹.

The spectral dependence of the absorption coefficient and dispersion dependence of the refractive index are derived from the transmission spectra. A typical Urbach bundle is observed, the temperature behaviour of the absorption edge in the films is explained by a strong electron-phonon interaction.

The Raman spectrum of Cu₆PS₅I single crystal is dominated by a narrow (7 cm⁻¹) peak at 420 cm⁻¹ corresponding to a symmetric vibration of PS₄ tetrahedra while a less intense broader (27 cm⁻¹) peak at 309 cm⁻¹ results from unresolved degenerate E and F₂ bands. For the Cu₆PS₅I-based films, the maxima are much broader (30–40 and 80–90 cm⁻¹, respectively), which can be an evidence for a strongly amorphised structure. The most intense peak in the film spectra is shifted down to 392–396 cm⁻¹ which can be explained by tensile strain in the films. Evidently, the PS₄ structural groups are still to a noticeable extent preserved in the short-range order, even though the structure of these groups is noticeably distorted. An additional band in the film spectra near 425 cm⁻¹ is probably related to the vibrations of PS₃ groups formed in the sulphur-deficient films.

Formation of Nanostructures on the Surface of $\text{Cd}_{1-x}\text{Mn}_x\text{Te}$ Substrates

Bodul G.I.¹, Makhniy V.P.¹, Pavlyuk M.F.², Slyotov O.M.¹

¹ *Yuriy Fedkovych Chernivtsi National University, Chernivtsi, Ukraine*

² *Vasyl Stefanyk Precarpathian National University, Ivano-Frankivsk, Ukraine*

A specific set of physical and chemical parameters of crystals of $\text{Cd}_{1-x}\text{Mn}_x\text{Te}$ solid solutions determine the prospects of their use in magneto-optics, spintronics, laser technology and force optics. Fields of application of the material can be significantly extended by making on their base of surface-barrier diodes (SBD), that can be the basis of effective detectors of optical and ionizing radiation. A serious problem in the diodes creation is obtaining of the maximum height potential barrier φ_0 with a minimum concentration of defects at the interface, which is further complicated by the fact that defects of $\text{Cd}_{1-x}\text{Mn}_x\text{Te}$ crystal increases significantly with increasing of x . One way to solve these problems can be modification of substrate surface before applying the rectifying contact, in particular, creation of surface nanostructures (SNS), perspective of which was confirmed by increase of photoconversion efficiency of Au-CdTe contacts. This paper presents the results of studies of impact of modification on the surface morphology and optical transmission of $\text{Cd}_{1-x}\text{Mn}_x\text{Te}$ crystals. The plates of size $5 \times 5 \times 0,5 \text{ mm}^3$ were cut from bulk $\text{Cd}_{1-x}\text{Mn}_x\text{Te}$ crystals ($x = 0,04-0,045$). Substrate after etching in a bromine methanol had a mirror surface (type 1) and after annealing on air at certain conditions – matt (type 2). AFM images of the last indicates the formation of nanosized relief (Fig. 1 *b*) which is absent on plates with a smooth surface, Fig. 1 *a*. The formation of SNS is also confirmed by a shift to low-energy region of peaks of differential optical transmission spectra of samples of type 2 (*b*) comparatively with type 1 (*a*), Fig. 2. The mechanisms of SNS formation and possible ways of managing their parameters were discussed.

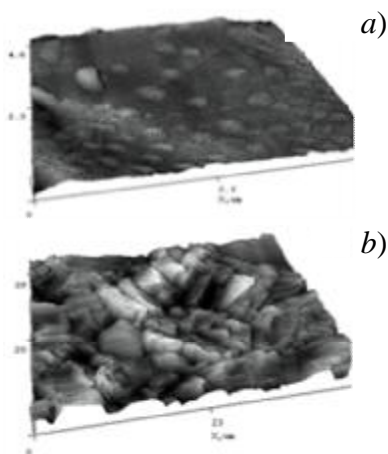


Fig. 1

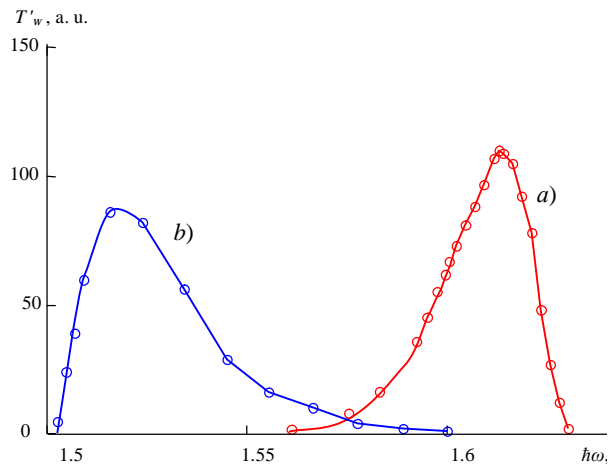


Fig. 2

Defect Structure of Arsenic Implanted HgCdTe Layers by HRTEM

Bonchuk O.Yu.¹, Savytsky H.V.¹, Swiatek Z.², Y.Morgiel², Izhnin I.I.^{3,4},
 Voitsekhovskii A.V.⁴, Korotaev A.G.⁴, Fitsych O.I.⁵, Varavin V.S.⁶, Dvoretzky
 S.A.^{4,6}, Yakushev M.V.⁶

¹Ya.S. Pidstryhach Institute for Applied Problems of Mechanics and Mathematics NASU,
 Lviv, Ukraine

²Institute of Metallurgy and Material Science PAN, Krakow, Poland

³Scientific Research Company "Carat", Lviv, Ukraine

⁴National Research Tomsk State University, Tomsk, Russia

⁵Hetman Petro Sahaidachny National Army Academy, Lviv, Ukraine

⁶A.V. Rzhov Institute of Semiconductor Physics SB RAS, Novosibirsk, Russia

The features of defect formation in arsenic ion-implanted (II) HgCdTe MBE layers grown on GaAs(Si) substrates with the (310) orientation were studied. Currently II is the most promising method for formation of high quality photodiodes p⁺-n junction. The II was carried out with As⁺ ions, the energy 190 keV, the dose 10¹³-10¹⁵ cm⁻². The defect structure in the II layers was investigated using a high-resolution transmission electron microscope Tecnai G2 from FEI Company. For the preparation of thin foils, the FIB method (Focused Ion Beam) was used in the FEI QUANTA 3D setup. Identification of the dominant types of defects: dislocations, stacking faults, micro-twins, plate precipitates, and specifics of their occurrence in the initial and modified layers were done. For example, Fig. 1 shows a dislocation structure in the ion range (a) and micrograph of plate the precipitates (b).

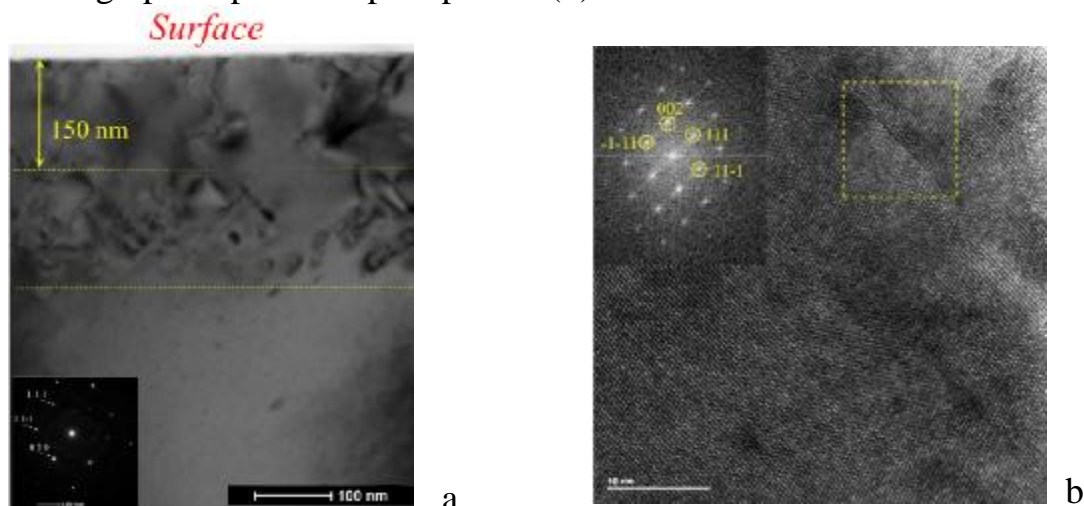


Fig. 1. Cross-sectional BF TEM micrographs of MBE HgCdTe /CaAs (310) layers implanted with As⁺ ions with fluence 10¹⁵ cm⁻² at 190 keV (a); high-resolution electron micrograph of the plate precipitates (b).

Strain Analysis of Synthetic Diamond and Diamond Films Using Electron Backscatter Diffraction

Borcha M.¹, Balovsyak S.¹, Fodchuk I.¹, Garabazhiv Y.¹,
Sumariuk O.¹, Tkach V.²

¹ *Yuriy Fedkovych Chernivtsi National University, Chernivtsi, Ukraine, ifodchuk@ukr.net*

² *Bakul Institute for Superhard Materials, NASU, Kyiv, Ukraine*

The strain state has been studied in local areas of a synthetic diamond crystal as well as diamond films produced by the temperature gradient method in the Fe–Al–C system through growing onto a diamond single crystal synthesized in the Ni–Mn–C system. Characteristic surfaces of the strain tensors and strain ellipsoids have been plotted; special features of strain distribution in the crystal have been analyzed.

We put forward a procedure [1, 2] whereby all the strain tensor components are determined from an analysis of distributions of intensity of reflected electrons in a single Kikuchi pattern. To determine five components of the symmetrical strain tensor we have analyzed the values of displacements of zone axes relative to their positions in the reference Kikuchi pattern taken from the most perfect region of the crystal. The diagonal components were found through the analysis of the change in the distribution of intensity for individual bands in the Kikuchi pattern.

We have studied the strain state in local regions of a synthetic diamond crystal produced by the temperature gradient method in the Fe–Al–C system through growing onto a diamond single crystal synthesized in the Ni–Mn–C system. Using a comprehensive analysis of the Kikuchi pattern (finding the positions of zone axes, analyzing the Kikuchi band intensity profiles) we have determined the values of strain components and plotted the characteristic surfaces of ellipsoids of strain in local regions of the synthetic diamond crystal. It has been demonstrated that all the regions studied have almost the same values of shear components suggesting no rotations along the given crystallographic directions, while other components exhibited significant variations. The most strained regions were identified. With a reference sample available, the proposed approach will permit improving the accuracy of determination of strain tensor components.

1. Dingley D.J., Wilkinson A.J., Meaden G., Karamched P.S. Elastic strain tensor measurement using electron backscatter diffraction in the SEM // *Journal of Electron Microscopy.* –2010. –V.**59**. – pp. 155-163.
2. Fodchuk M., Borcha M. D., Khomenko V. Yu., Balovsyak S. V., Tkach V. M., and Statsenko O. O. A Strain State in Synthetic Diamond Crystals by the Data of Electron Backscatter Diffraction Method // *Journal of Superhard Materials.* – 2016. – V.**38**, No 4. – pp. 271–276.

Structure and Photoelectrical Properties of β -Ga₂O₃ Thin Films

Bordun O.M., Bordun B.O., Medvid I.I., Kukharska L.V.

*Ivan Franko National University of L'viv, Lviv, Ukraine,
e-mail: bordun@electronics.lnu.edu.ua*

The thin films based on β -Ga₂O₃ are widely used as thin-film materials for field-effect transistors (FET), gas sensors and electrodes, which transparent in the UV region.

The thin films of β -Ga₂O₃ were obtained by radio-frequency ion-plasmas sputtering. The thickness of thin films ranged between 0.2 μ m and 1.0 μ m. The heat treatment of thin films was performed after deposition in oxygen atmosphere or in argon atmosphere as well as in hydrogen atmosphere. The X-ray diffraction studies showed the presence of the polycrystalline structure of thin films that preferentially oriented in the planes (400), (002), (111) and (512). The investigation of surface morphology of thin films by the atomic-force microscopy showed that the diameter of the grains on the surface of thin films without heat treatment is average equal to 30 nm and the average roughness of thin films is about 7 nm. The treatment of thin films in oxygen atmosphere leads to the increase size of grains through the processes of growth and sintering, thus, the average diameter of grains is increased to 45 nm.

The observation of the effect photoconductivity of β -Ga₂O₃ thin films regardless of the composition of the heat treatment atmosphere was found. The obtained results show that the lowest value of the photocurrent observed for thin films of β -Ga₂O₃ that were annealed in oxygen atmosphere and the these films have the smallest number of oxygen vacancies. The independently of the annealing atmosphere in the spectral range 220-270 nm for thin films of β -Ga₂O₃ are observed the two bands of photoconductivity that overlapping each other and the resulting spectrum of photoconductivity forms the superposition of these bands was shown. The excitation spectra of luminescence of β -Ga₂O₃ thin films were investigated. Considering that the band gap of β -Ga₂O₃ thin films is 4.80 eV (corresponding to 258 nm), we can see that the excitation these bands of luminescence and the formation of the corresponding bands of photoconductivity occurs in the region of band-to-band transitions with the formation of free charge carriers in the conduction band. According to the calculations of the electronic structure of β -Ga₂O₃, such electronic transitions carried out from 2p-states of O that form the top filled level valence band into the bottom of the conduction band that formed the hybrid 2p-states of O and 4s-states of Ga.

Structure and Electrical Properties of Chromium Nanometer Thick Films

Havrelyh V.M., Buchkovska M.D.

Ivan Franko Lviv University, Lviv, Ukraine

The impact of condensation regime and condition state of surface amorphous substrate on nucleation and growth parameters of chromium films and films ohmic conductivity were presented. The interest in chromium films is due to the fact that along with titanium and aluminum films it is widely used in film technology because of the high adhesion to the surface of the dielectric substrate. Chromium films was produced by condensation of thermally evaporated metal vapor on the surface of glass and carbon substrates at $T = 78$ K (method «quench condensed»), with speed of condensation not higher than 0,01 nm/s. Germanium films were received in a similar way. The study was conducted under ultrahigh vacuum conditions (pressure of residual gas during preparation and study of films was below 10^{-7} Pa).

It was shown that germanium underlayers with mass thickness changes the nucleation of chromium film and degree of substrate surface filling parameter with metal film. Germanium under layer with 2 nm mass thickness caused reduction of crystallites average linear sizes D_c of chromium films in 2 times. The most significant changes were observed in the range of germanium thickness 0-1 nm. Another feature of obtained experimental data was stability of D_c chromium parameter with thickness of germanium under layer.

Percolation model [1] showed that Ge under layers reduced the d_c percolation thickness of metal layer. Size dependence of electrical conductivity of chromium films were explained with quasi-classical and quantum size effect theories. The kinetic parameters of chromium films were calculated in the framework of such theories. The best fits with experimental data were carry out with theory of polycrystalline layer of heterogeneous thickness was observed [2].

According to the information of experimental studies the method of metal films production with predetermined structure and electrical properties with thickness 2-3 nm were developed.

1. M. Walther, D. Cooke, C. Sherstan, M. Hajar, M. Freeman, F. Hegmann. Terahertz conductivity of thin gold films at the metal-insulator percolation transition // Phys. Rev. B. – 2007.– Vol. 76, P. 125408(1-9).

2. ZV Stasyuk, A. Lopatinsky. Dimension kinetic phenomena in thin films of metals // Physics and Chemistry of Solid.- 2001.- V.2, №4.- S.521-541. (In Ukraine)

Luminescence Kinetics of the Metal Oxide Films

Burlak G., Vilinskaya L.

*The Odessa State Academy of Building and Architecture, Odessa, Ukraine,
demiga@yandex.ru*

It is known that porous anodic oxide films can be grown on materials such as silicon, indium phosphide, titanium, tantalum, tin, and others. One of the most promising materials for the creation of nanoporous oxide layer is aluminum and tantalum.

To clarify the mechanism of oxide films glow immersed in the electrolyte was studied the kinetics of luminescence. Studying the kinetics of the luminescence upon excitation pulses odnopolyarnymim positive voltage ("+" on the sample) with provodidlos Al_2O_3 films immersed in a series of aqueous solutions of electrolytes, for which the dependence of the luminescence intensity of the pH value goes through a maximum. In addition to the emission peak observed at half-time, when the applied voltage, and it appeared an additional peak that occurs at halftime, when the field is absent. Increasing the applied voltage leads to the flash and to the anode half-brightness increase in half-life, where the excitation electric field was absent. Thus, with increasing frequency of the exciting voltage from 25 to 250 Hz intensity of luminescence in the anode half-life is significantly reduced, and at half-time when no voltage lighting intensity up to a certain frequency value is essentially independent of its value, and then begins to decline and there is a shift of the maximum to the provisions of longer times relative to the half-cycle duration. Moreover, if the intensity of the luminescence of the anode half-life type of electrolyte used had no significant effect, the brightness at half-time, when the voltage is equal to zero, essentially dependent on the nature of the electrolyte. It should be noted that the glow when excited by an electric field is terminated until a zero voltage on the sample. At the time when the voltage becomes zero, reaches a certain concentration of the filled electron donor centers adsorptive nature. Next to the sample positive electrolyte ions begin to flow, forming on the surface of the oxide film acceptor levels with localized holes on them, with the result that it becomes possible to luminescence centers ionization. The recombination of the electrons coming from the donor centers with ionized luminescence centers leads to the emission of light. Within the framework of the theory of Langmuir mathematical model of the behavior of the curves brightness.

The analysis of the experimental and calculated curves gave a good agreement. It should be noted that the kind described vishe ikinetiki glow observed in all the phosphors in which the dependence of the luminescence intensity otvelichiny pH passes through a maximum as for the appearance of the glow at half-time, when the voltage is zero, responsible ions of both signs.

Structural and Optical Features of $\text{Cu}_2\text{ZnSnS}_4$ Films Deposited by Pulsed Spray Pyrolysis Technique

Dobrozhan O.A.¹, Danilchenko P.S.¹, Opanasyuk A.S.¹, Cheong H.²

¹ *Sumy State University, Sumy, Ukraine*

² *Sogang University, Seoul, Republic of Korea*

The quaternary compound semiconductor $\text{Cu}_2\text{ZnSnS}_4$ (CZTS) is a perspective material for the absorber layers in 3rd generation thin film solar cells. CZTS has *p*-type conductivity, high absorption coefficients ($\alpha > 10^4 \text{ cm}^{-1}$), as well as band gap ($E_g = 1.0\text{-}1.5 \text{ eV}$) close to Shockley-Queisser efficiency limit (32-34 %). The solar cells based on CZTS absorber layer showed the maximum efficiency of 12.6 %, but this value is significantly lower than ones demonstrated by other thin film solar cells with traditional CdTe (22.1 %) and CIGS (22.3 %) absorbers. This is due to CZTS films have the suboptimal structural characteristics and stoichiometry, secondary phases with different band gaps, the coexistence of kesterite and stannite phases with low transformation energy (3-4 meV/atom).

A range of applications (first of all in photovoltaics and thermoelectrics) require CZTS films deposited onto substrates with large surface area, including flexible ones. It could be achieved by applying the chemical pulsed spray pyrolysis technique which is non-vacuum, low-cost and versatile method allowing deposition of the different semiconductor materials at the moderate temperatures. One of the most important parameter of films is a thickness that could be varied by changing the volume of sprayed solution. The specified above determined the goal of work – the investigation of morphological, structural, optical properties and elemental composition of CZTS thin films obtained by pulsed spray pyrolysis at a different volume of sprayed initial precursor.

$\text{Cu}_2\text{ZnSnS}_4$ films were obtained at $T_s = 673 \pm 10 \text{ K}$ using a water-based precursor contained $\text{CuCl}_2 \cdot 2\text{H}_2\text{O}$, ZnCl_2 , $\text{SnCl}_2 \cdot 2\text{H}_2\text{O}$, NH_2CHNH_2 onto glass substrates. The volume of sprayed solution was set in the range of (2-5) ml with $\Delta = 1 \text{ ml}$. The main deposition parameters were used as follows: distance between the nozzle and substrate surface – 20 cm, carrier gas – 0.2 MPa, spraying velocity – 3 ml/min, the time between two spraying cycles – 10 s.

It was determined that the parameters of crystal lattice were changed in the range of $a = (0.5423\text{-}0.5480) \text{ nm}$, $c = (1.0823\text{-}1.1182) \text{ nm}$, $c/2a = (0.9970\text{-}1.0203) \text{ nm}$, volume of unit cell – $(0.3183\text{-}0.3358) \text{ nm}^3$. The chemical composition of films was varying for Cu = (26.43-28.56) at.%, Zn = (15.18-21.36) at.%, Sn = (14.33-15.39) at.% and S = (35.75-43.00) at.%. The samples, deposited in optimal conditions, had the almost single structure of kesterite, as well as stoichiometry and band gap, which are close to the optimal values for designing highly efficient solar cells. The research results can be applied in the development of 3rd generation thin film SC.

Inner Size Effect in Bi-Sn and Sn-Pb Films

Dukarov S.V., Petrushenko S. I., Bloshenko Z.V., Churilov I.G., Sukhov V.N.

*V. N. Karazin Kharkiv National University,
Kharkiv, Ukraine, petrushenko@univer.kharkov.ua*

This paper is devoted to the study of size effects in the melting of bilayer and multilayer Bi-Sn and Sn-Pb films on a substrate with a temperature gradient.

Samples were obtained by the method of successive condensation of components in a vacuum of 10^{-7} Torr. Bi-Sn and Sn-Pb films were deposited on lengthened steel plates previously deposited by a layer of amorphous carbon. The system of moving shields made it possible to create two series of samples with the same total thickness (200-400 nm) on the same substrate within a single vacuum cycle. These were bilayer and multilayer films in which 10 layers of each component were interchanged. The ratio of the layers thicknesses was chosen in accordance with the eutectic concentration. After condensation completion one end of the substrate was heated to a temperature providing melting of the most refractory component, and the other was at room temperature. A temperature gradient was established along the substrate, which made it possible to obtain a number of continuously varying states of the film. After annealing for 20 minutes, the samples were cooled to room temperature, taken from the vacuum chamber and studied by scanning electron microscope.

Both in bilayer and multilayer films, there is visually a boundary which corresponds to eutectic alloy formation temperature. As it has been shown by SEM studies, the samples are continuous polycrystalline films below this boundary, and they consist of individual spherical particles above it. The average size of crystallites in multilayer structures is greater than in bilayer samples of the same total thickness. This was explained by the increase in the diffusion coefficient in multilayer films.

The phase transition boundary is broadened in a certain range of temperatures, the magnitude of which is 2 K and 4.5 K in multilayered and 0.4 K and 0.9 K in bilayer Bi-Sn and Sn-Pb films, respectively. SEM studies show that in this interval the films undergo partial melting, in which the solid and liquid phases coexist simultaneously. In accordance with thermodynamic concepts, the lowering of the melting temperature of multilayer films is explained by the presence of additional energy of interphase boundaries in Bi-Sn and Pb-Sn films. Using the triple point model, the interface energy of the layers was estimated to be 33 mJ/m^2 and 45 mJ/m^2 for Bi-Sn and Sn-Pb films. Broadening of the melting boundary in bilayer samples is probably due to their polycrystalline structure. The additional energy, which is associated with grain boundaries, makes melting of individual crystallites energetically favorable below the equilibrium melting temperature.

Fe₃B Borides Formation Mechanism in Fe-B Alloys

Filonenko N.Yu.¹, Galdina A.N.²

¹ State Establishment “Dnipropetrovsk Medical Academy”, Dnipro, Ukraine

² Oles Honchar Dnipropetrovsk National University, Dnipro, Ukraine

The structure of hypoeutectic alloys includes two constituent – γ -Fe and $\gamma + \text{Fe}_2\text{B}$ eutectics, whereas the hypereutectic one – Fe_2B and eutectics [1]. The Fe_3B boride formation in binary Fe-B alloys is observed as a result of amorphous films annealing [2]. It is revealed that Fe_3B boride exists within the temperature interval from 1423 K to 1523 K in two modifications: orthorhombic high-temperature Fe_3B (o) and tetragonal low-temperature Fe_3B (t) [3]. The objective of this paper is investigation of the structural properties of hypoeutectic alloys in Fe-B system depending on heating temperature and cooling rate.

The investigation was performed for the specimens with boron content of 2.0-3.5 % (wt.), the rest is iron. To determine the effect of superheat and cooling rate on phase composition of alloys, we heated alloys to 50-350 K above liquidus curve and cooled with rate of 10^2 - 10^4 K/s. To ascertain the physical properties we use the microstructure analysis and the X-ray structural one.

The microstructure of hypoeutectic alloy of Fe-B system with boron content of 2.7 % (wt.) after crystallization from temperature 1553 K includes two constituents - α -Fe phase and α -Fe+ Fe_2B eutectics. With increase of cooling rate of alloy the sizes of α -Fe dendrites and their volume ratio decrease considerably, whereas degree of differentiation of eutectic colonies grows.

After the alloy with boron content of 2.7 % (wt.) was heated to temperature 1753 K and then was casted in copper wedge-shaped mould, in slim end of the wedge, where cooling rate was 10^4 K/s, we observed eutectics with rod morphology along with α -Fe phase and α -Fe+ Fe_2B eutectics. According to results of X-ray structural analysis in this end of the wedge the presence of Fe_3B boride with tetragonal lattice was revealed.

The analysis of obtained results enables to assume that heating temperature of liquid melt effects on phase formation on cooling, meaning that superheat of alloys to temperature over than 300 K from the liquidus curve and cooling with rate of 10^4 K/s enables to detect as-cast Fe_3B boride for the first time.

1. Samsonov G.V., Serebryakova T.I., Neronov V.A. Boridy. – Moscow: Atomizdat, 1999. – 220 p.
2. Abrosimova G.E., Aronin A.S. Fazovye prevrascheniya pri nagreve amorfnykh splavov Fe-B // Metallofizika. – 1988. – Vol. 10, №3. – P. 47-52.
3. Khan Y., Kneller E., Sostarich M. The phase Fe_3B // Z. Metallkunde. – 1982. – Bd. 73, №10. – P. 624-626.

Influence of Annealing in Vacuum on the Morphology of Titanium Nanofilms Applied to Non-Metallic Materials

Naydich U.V., Gab I.I., Stetsyuk T.V., Kostyuk B.D.

Frantsevych' Institute of Problems of Materials NAS of Ukraine, Kyiv, Ukraine

The changes of morphology of titanium nanofilms with thickness 100 nm deposited on a substrate made from leucosapphire, single crystals of ZrO_2 and SiC, and AlN ceramics and annealed in a vacuum at temperatures of $1300 \div 1600$ °C are researched. Films are deposited by electron beam evaporation on a well polished surface of the substrate ($R_z = 0,03 \div 0,05$ μm). Annealing time of the films was varied from two to twenty minutes at each temperature.

Annealed samples were studied using metallography, scanning and atomic force microscopy, while receiving photos. By using these micrographs the part of surface of the substrate was calculated, which was covered of islands dispersed titanium films. Calculations were performed using planimetric method. The data obtained by this method were treated as dependent of surface area of samples, which were covered with fragments of metal films after annealing, from annealing parameters (temperature and time).

It was established that the dispersion of titanium nanofilms with thickness of 100 nm deposited on leucosapphire and ZrO_2 , has approximately the same course and at short annealing (2 - 5 min) at 1400 °C they still almost solid, and with increasing annealing time at this temperature dispersion process is enhanced, although the fragments of the film even after 20 minutes of exposure cover more than 70% of the surface of the substrate and thus, in these conditions, the film is quite suitable for use in high-temperature soldering of oxides. With increasing of the annealing temperature to 1600 °C decay rate of the film is growing rapidly and it is completely decomposed after 10 minutes of exposure at that temperature, therefore not suitable for soldering. Film of titanium on aluminum nitride proved very refractory and after 20 minutes of annealing at 1600 C, it covers more than half of the area of the substrate and is quite suitable for high-temperature soldering of ceramics. In the film of titanium carbide on silicon at annealing above 1400 °C there is a noticeable interaction film material to the substrate. This interaction increases rapidly with increasing temperature and thus soldering of silicon carbide, which is metallized by titanium film, can only be done within 1400 °C. Using the resulting research data graphs, you can customize the desired temperature and time of soldering for studied non-metal materials metallized by titanium nanofilms.

Defect Subsystem in He-Implanted Epitaxial YIG Films

Fedoriv V.D., Kurovets V.V., Yaremiy S.I., Garpul O.Z.

Vasyl Stefanyk Precarpathian National University, Ivano-Frankivsk, Ukraine,
ogorishna@ukr.net

Study of defect subsystem evolution of the material is an important task for the targeted modification of the ferrite-garnet films properties by ion implantation. In this work, based on X-ray diffraction data, the changes of defect subsystem in epitaxial films YIG/GGG is analyzed in dependence on a dose of helium ions ($E = 100 \text{ keV}$, $D = 1 \cdot 10^{15} \text{ cm}^{-2} \div 1 \cdot 10^{16} \text{ cm}^{-2}$).

For correct analysis of X-ray diffraction data, the simulation of He^+ ions implantation to the target $\text{Y}_3\text{Fe}_5\text{O}_{12}$ was performed with using of the program SRIM. It is shown that primary knock-on target atoms created a significant number of secondary defects (60% of total). The theoretical concentration profile of radiation defects is expected and the model of defect subsystem is offered: point defects, radiation-disordered areas with an average linear size of 10 nm and dislocation loops (as a result of point defects association).

From the experimental dose dependence of maximum relative strain value of YIG/GGG films was calculated the effective radius of the defect, which is 0.11 nm, and the radius of instability zone – 0.36 nm.

Calculation by means of statistical dynamical theory of X-rays diffraction [1] showed that with the increase of implantation dose takes place increasing the concentration and reduction the radius of dislocation loops: the radius of dislocation loops changes from 5 nm for dose $1 \cdot 10^{15} \text{ He}^+/\text{sm}^2$ to 2 nm for dose $1 \cdot 10^{16} \text{ He}^+/\text{sm}^2$. The reason of this is increasing the number of large disordered regions (which are the centres of dislocation loops generation) with increasing of implantation dose, and the size of dislocation loops decreases due to the increasing number of possible runoffs for point defects. It was considered that the radius and concentration of dislocation loops was proportional to the defects profiles.

For estimation of defect subsystem was also used the approach [2]. It introduced the general characteristics of the defect subsystem: the static Debye-Waller factor $E = \exp(-L_H)$ and the correlation length τ . Established that with increasing of implantation dose from $1 \cdot 10^{15} \text{ He}^+/\text{sm}^2$ to $1 \cdot 10^{16} \text{ He}^+/\text{sm}^2$ the value E for reflection (444) in the most deformed layer changes from 0.95 to 0.80, and τ – from 10 nm to 3 nm, indicating a growth the defects in surface layers of YIG films.

1. Bragg diffraction of X-rays by single crystals with large microdefects. I. Generalized dynamical theory / V.B. Molodkin [et al.] // Phys. Stat. Sol. B. – 2001. – V. 227, № 2. – P. 429-447.

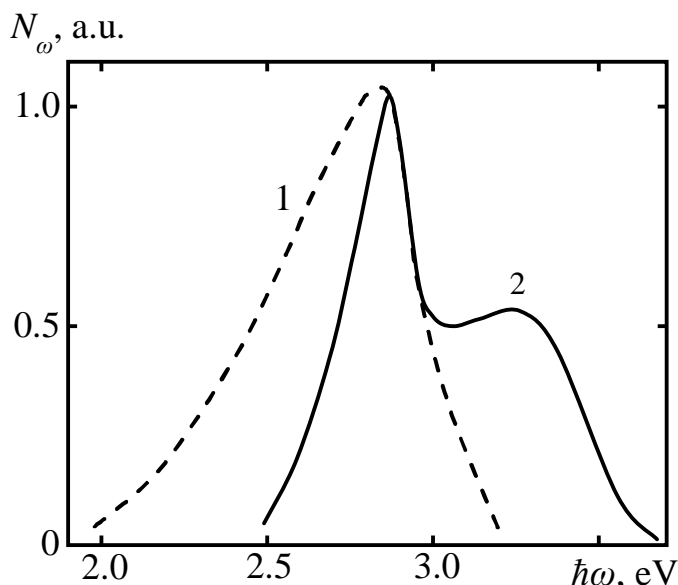
2. Punegov V.I. Correlation Length in the Statistical Theory of X-ray Diffraction by One Dimensionally Distorted Defect Crystals. I. Model of Discrete-Layer Structure / V.I. Punegov // Crystallography Reports. – 1996. – V. 41, № 1. – P. 19-25.

Luminescence of α -ZnSe Heterolayers with Modified Surface

Gavaleshko O.S., Kinzerska O.V., Herman I.I.

Yuriy Fedkovych Chernivtsi National University, Chernivtsi, Ukraine,
gavaleshkos555@gmail.com

Zinc selenide is one of the promising materials in functional electronics. ZnSe crystals are crystallized in the cubic modification and are basis for production a different type of LEDs and photosensitive structures. They are designed to generate and registrate optical radiation. However, still the important question is the expansion of its spectral range. One of the methods is receiving material with other crystal structure - hexagonal heterolayers α -ZnSe. In addition, surface modification of these layers will allow to change the emission spectra in favor of short-wave UV region. This work is dedicated to a search of possibility of obtaining α -ZnSe and influence of surface modification of heterolayers on their fluorescent properties.



Heterolayers α -ZnSe were obtained by isovalent substitution (IVS). Selection of the optimum temperature and time serial diffusion of elements Zn and Se allowed to grow heterolayers α -ZnSe. Investigation of X-diffraction confirms the formation of a hexagonal lattice. The research of reflectance R'_ω and luminescence N_ω was made on universal optical installation. The parameters of the energy structure in the center of the

Brillouin zone, which constitute $E_g = 2,89$ eV, $\Delta_{CR} = 0,07$ eV, $\Delta_{SO} = 0,37$ eV where identified. Heterolayers characterized by intense photoluminescence in marginal areas, curve 1, Fig. 1. Matte surface was created by chemical etching with etchant $H_2SO_4:H_2O_2 = 3:1$ [1]. The emission spectrum of modified layers differs from spectrum of base heterolayers by increase of efficiency and the formation of a new band with a maximum in the 3.35 eV, the curve 2, Fig. 1. The most likely, the reason of luminescence at $\hbar\omega \geq E_g$ can be the formation of the quantum-dimensional structures on the surface. In this paper analyzes of AFM topograms is made and the physical processes of formation of radiation in the short-wave region are discussed.

[1]. V.P. Makhniy, O.V. Kinzerska, I.M. Senko, A.A. Ascheulov. Luminescent properties of crystals ZnSe: Sb with modified surface // Science. Bulletin of Chernivtsi University. - 2014, v.3. № 1. Physics. Electronics. - p. 112 – 114.

Comprehensive Study of Crystalline and Magnetic Structure of Garnet Epitaxial Systems

Gutsuliak I.¹, Fodchuk I.¹, Dovganyuk V.¹, Kotsyubynskiy A.¹, Romankevych V.¹, Safriuk N.², Lytvyn P.², Kladko V.², Barchuk M.³, Syvorotka I.⁴

¹*Chernivtsi National University, Chernivtsi, Ukraine*

²*Institute of Semiconductor Physics of NASU, Kyiv, Ukraine*

³*Institute of Materials Science, TU Bergakademie Freiberg, Freiberg, Germany*

⁴*Scientific Research Company "Carat", Lviv, Ukraine, Jani_Urishyn@ukr.net*

The set of complementary techniques such as high-resolution X-ray diffraction, atomic force and magnetic force microscopy (MFM) accompanied by simulation were used to investigate a set of yttrium iron garnet epitaxial films of different thicknesses. We performed a series of reciprocal space maps (RSM) calculations taking into account a presence of the sample/substrate interlayer and changing the density of dislocations. The influence of film perfection on microstructure of magnetic domains and the RSM's shapes was studied.

From MFM analysis, it follows that the magnetic domain structure depends on the layers thickness. The sample with the thickness 6.4 μm possesses continuous parallel stripes with the periodicity of approximately 11 μm and some heterogeneity caused by small thickness of the film, which disappears with the overgrowth [1]. The stripes observed in thicker samples have a chaotic structure typical for the films with well-formed column structure. Experimental RSMs were recorded in symmetrical (444), (888) and asymmetrical (880) reflections by high-resolution X-ray diffractometer X'Pert PRO MRD. The sample with the thickness of 6.41 μm has a well-formed crystal structure. The RSM shapes of other samples are typical for a high content of defects in the near-surface layer, which is a common feature of selected growth conditions.

The simulation of RSMs is based on Krivoglaz kinematical theory [2] and performed using Monte-Carlo approach. Two sets of screw and edge dislocations with different densities were selected as the dominant type of defects. We achieved a good correspondence between simulated and experimental RSMs. It was established that stripe domain structure depends drastically on sample thickness, surface roughness and growth conditions.

1. Fodchuk I., Gutsuliak I., Dovganiuk V., Kotsyubynskiy A., Pietsch U. et al. Magnetic and structural changes in the near-surface epitaxial $\text{Y}_{2.95}\text{La}_{0.05}\text{Fe}_5\text{O}_{12}$ films after high-dose ion implantation // Applied Optics. – 2016. – V.55. – P. B144-B149.
2. Krivoglaz M. A. X-Ray and Neutron Diffraction in Nonideal Crystals. Berlin: Springer. 1996.

Study of Structural and Morphological Properties of Thermally Evaporated $(\text{Ge}_{40}\text{S}_{60})_{100-x}\text{In}_x$ Thin Films

Horvat H.¹, Khalakhan I.², Vlcek M.³, Rizak V.¹

¹*Uzhhorodskyy National University, Ukraine*

²*Charles University, Czech Republic*

³*University of Pardubice, Czech Republic*
galina.horvat@teib.info

Chalcogenide glasses are the most widely known families of amorphous materials and have been studied for several decades, because of their interesting fundamental properties and wide range of applications. They have been explored as promising candidates for optical memories, gratings, switching devices and optical communications.

Ge–S amorphous system are very good glass-former. The tendency of these system to form glasses, as well as the physical properties of the glasses, is determined by the character of the chemical bond formed between the atoms that make the glass and the composition of the elements. The addition of dopants such as Indium (In) controls its structure and physics properties. Moreover, the Ge–S–In system is of special interest, and it forms glasses over a wide composition range. It occurs up to 15 at.% In and 60–90 at.% Se and the rest is Ge. Various studies have reported on the structural, electrical and optical properties of Ge–S–In glasses. Bulk chalcogenide glasses $(\text{Ge}_{40}\text{S}_{60})_{100-x}\text{In}_x$ with different concentration of In ($0 \leq x \leq 10$ at.%) were synthesized by the usual melt quenching technique. Amorphous nature of glasses was checked by XRD technique. Thin films of $(\text{Ge}_{40}\text{S}_{60})_{100-x}\text{In}_x$ chalcogenide system were prepared by thermal evaporation technique onto Si substrates under at room temperature and base pressure of $\sim 10^{-4}$ Pa. onto Si substrates under high vacuum.

The structure and morphology properties $(\text{Ge}_{40}\text{S}_{60})_{100-x}\text{In}_x$ thin films were investigated as a function of In concentration. Study of the structure films to obtained by Raman spectroscopy [BRUKER IFS55 EQUINOX]. The surface morphology of the films was obtained by Atomic Force Microscopy [Multimode 8 (Bruker)] and Scanning Electron Microscopy [MIRA 3 (Tescan)].

From the SEM and AFM we are notice the difference in the film surface for different concentrations In. SEM and AFM micrographs reveals homogeneous surface of the film with rms surface roughness 0.5-0.91. The frequencies attributed to Ge-S bonds are observed at 361, at 368 cm^{-1} and at 430 cm^{-1} that arise from the connections between the GeS_4 tetrahedra and short S-S bonds between these tetrahedra. All these frequencies confirm the formation of Ge-S bonds.

Study of Some Photoelectrical Properties of Some Ternary Amorphous Thin Films

Iaseniuc O., Bordian O., Sibov-Medinschi G.L.

*Institute of Applied Physics, Academy of Sciences of Moldova, Chisinau, R. Moldova,
E-mail: oxana.iaseniuc@phys.asm.md*

Arsenic selenide and sulfide glasses are well known as high photosensitive materials with a wide range of application in optoelectronics and information storage systems. Besides, it was found that the impurities influence the electrical and photoelectrical characteristics of the amorphous material, due to the changes in the density of localized states. Introduction of the elements of IV group of periodic table in selenide and sulphide glasses, such as Sn and Ge, conduct to the appearance of tetrahedral structural units in the base glass, which change the coordination number. These particularities lead on non-monotonous dependence of physical properties on the glass composition.

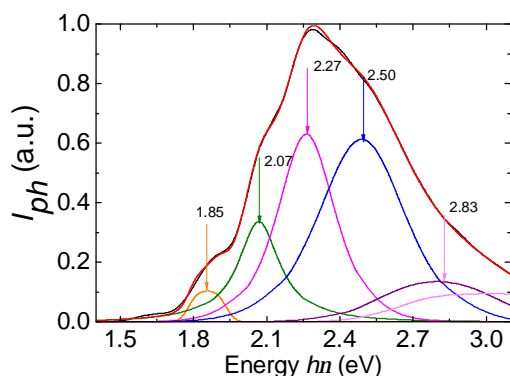


Fig.1. Deconvoluted photocurrent spectrum using Gaussian function for Al-(As₄S₃Se₃)_{0.90}Sn_{0.10}-Al thin films structure.

In the present paper is shown, that the spectral distribution of the stationary photoconductivity for both glass systems Ge_xAs_xSe_{1-2x} and (As₄S₃Se₃)_{1-x}Sn_x depends on the composition and polarity on the illuminated electrode. The experimental results are discussed in terms of multiple trapping models for amorphous materials, with exponential distribution of localized states in the band gap. Fig.1 represents the results of deconvoluted photocurrent spectrum using Gaussian function for Al(As₄S₃Se₃)_{0.90}Sn_{0.10}-Al thin films structure. The peak centered at $h\nu=2.27$ eV correspond to band-to-band photo-excitation of non-equilibrium carriers. The peaks situated around $h\nu=2.07$ eV and 1.85 eV can be attributed to some groups of localized levels induced by Sn impurities in the host chalcogenide glass. The observed peaks situated in the valence band around $h\nu=2.83$ eV for amorphous (As₄S₃Se₃)_{0.90}Sn_{0.10} thin films and around $h\nu=2.92$ eV for Ge_{0.07}As_{0.07}Se_{0.86} can be attributed to the electron states, which results predominantly from the p-orbital electron lone-pair of the chalcogen atoms and p- and σ -orbital states of chalcogen. In this approximation the shape of the spectra is governed by the short-range-order (SRO) [1].

1. Iovu, M.S., Shutov, S.D., Andriesh, A.M., Kamitsos, A.B., Popescu, E.I., Varsamis, C.P.E., Furniss, D., Seddon, J. of Optoelect. and Adv. Mater., 3(2), 443-454 (2001).

Structural and Optical Investigations of Amorphous and Nanocrystalline TiO₂ Thin Films

Studeniyak I.P.¹, Nahusko O.T.¹, Izai V.Yu.¹, Kranjčec M.², Kúš P.³, Mikula M.³

¹*Uzhhorod National University, Uzhhorod, Ukraine*

²*University North, Varaždin, Croatia*

³*Comenius University, Bratislava, Slovakia*

Titanium dioxide (TiO₂) thin films have many interesting applications in microelectronics, optics and medicine due to their excellent visible and near-IR transmittance, wide energy gap, relatively high refractive index and dielectric constant. The variety of applications of titanium dioxide films requires knowledge of their optical parameters. Here we report on the deposition, structural and optical studies of amorphous and nanocrystalline TiO₂ thin films.

TiO₂ thin films were deposited on glass substrates at room temperature by means of high target utilization sputtering (HiTUS) in reactive Ar+O₂ discharges. The plasma source power density was fixed at 2000 W yielding a deposition rate of approximately 1.5 nm/min. Target pulsed DC power was fixed at 70 W. Optical transmission spectra of TiO₂ thin films were studied in the temperature range 77–300 K using an MDR-3 grating monochromator.

XRD studies have shown that TiO₂ thin film with the minimal thickness of 14.7 nm is amorphous while with increasing thickness up to 222 nm the nanocrystalline inclusions of anatase and rutile phases of TiO₂ appear. Spectral dependences of the optical constants (refractive index and extinction coefficient) were measured by spectroscopic ellipsometry.

It is shown that the highest value of the absorption edge spectral position is observed for the thin films with approximately equal fraction of the anatase and rutile phases whereas it decreases with increasing rutile phase fraction, and the lowest absorption edge spectral position is revealed for the fully amorphous thin film. Urbach energy is highest for the thin film with the [excessive](#) content of rutile nanocrystal inclusions, and lowest for the thin film with approximately equal fractions of the anatase and rutile phases.

Temperature behaviour of the optical transmission spectra for nanocrystalline TiO₂ thin film was studied in the interval 77–300 K. A red shift of the optical absorption edge with increasing temperature was observed, the edge in the range of its exponential behaviour being well described by the Urbach rule. The temperature dependences of the energy position of the absorption edge and the Urbach energy for the TiO₂ thin film were analysed. The temperature-related and structural disorder affect the shape of the Urbach absorption edge, the contribution of the structural disorder to the Urbach energy for the TiO₂ thin film was estimated. The contribution of structural disordering into the TiO₂ thin film Urbach energy is shown to be 89.5%.

Effect of Annealing on the Phase State and Magnetoresistive Properties of Co/Ag/Ni_{0.8}Fe_{0.2} Pseudo Spin-Valve

Koloskova O.A., Pazukha I.M., Odnodvoretz L.V., Protsenko S.I.

Sumy State University, Sumy, Ukraine

In this work, a series of pseudo spin-valve (PSV) structures composed of two Co and Ni_xFe_{1-x}, where $x \approx 0.8$ (Py), ferromagnetic layers separated by non-magnetic Ag layer were investigated with the focus on effect of annealing on phase state and magnetoresistive properties in dependence of Ag layer thickness. The difference in coercivity between Py and Co layers allowed to realize a distinct magnetic reversal state in these samples.

Pseudo spin-valve structures Co(5nm)/Ag(d_{Ag})/Py(30nm)/S were prepared by electron-beam sputtering in HV chamber with a base pressure of 10^{-4} Pa at room temperature on an amorphous glass-ceramic substrate (S). The thickness of the Ag layer varied between 3 and 15 nm. To investigate the effect of annealing on phase state and magnetoresistance of PSV structures, the samples after deposition were annealed at the temperature of healing defects (it is close to 530 K) and 750K for 15 minutes. Transverse, longitudinal and perpendicular magnetoresistance (MR) loops were measured by using software-hardware complex with current-in-plane geometries in an external magnetic field up to 500mT at 300 K. The value of MR has been calculated as $\Delta R/R_s = [(R(B) - R_s)/R_s] \times 100\%$, where R_s and $R(B)$ are resistance at saturated field and a current value of resistance in a magnetic field, respectively. The phase state of the PSV structures was investigated by transmission electron microscopy (TEM-125K).

The analysis of TEM diffraction patterns of the as-deposited Co(5nm)/Ag(d_{Ag})/Py(30nm)/S for the whole range of non-magnetic layer thicknesses shows that samples have three-phase state. It corresponds to fcc-Ni₃Fe, hcp-Co and fcc-Ag. The annealing process in the temperature range up to temperature of the healing defects does not change the samples phase state. At the same time, after annealing to 700 K the formation of solid solution (s.s.) on the basis of Ag fcc lattice as a result of thermal diffusion occurs.

The study of MR loops for as-deposited samples allows conclude that a magnetoresistance value and shape of MR curves of PSV structures depends on not only researched geometry, but annealing temperature and non-magnetic layer thickness also. All samples in as-deposited and annealed to different temperatures states characterized by magnetic anisotropy. The formation of s.s.-Ag(Co) leads to change MR loop shape in perpendicular geometry. The maximum value of magnetoresistance has been received for Co(5nm)/Ag(15 nm)/Py(30nm)/S structure in perpendicular geometry after annealing up to 700 K.

The work was done in the frame of state project № 0116U002623.

Complex Spectroscopical Study of Top Surface Nanolayers of the $\text{As}_x\text{Se}_{100-x}$ Thin Films for Their Application in all optical Signal Processing

Kondrat O.¹, Holomb R.¹, Tsud N.² and Mitsa V.M.¹

¹ *Uzhhorod National University, Uzhhorod, Ukraine*

² *Charles University, Faculty of Mathematics and Physics, Department of Surface and Plasma Science, Prague, Czech Republic*

The dimensions of active elements used in modern electronics and photonics are of nanoscale order and the role of their surfaces becomes very important. Also, the local structure and structural defects (both charged defects and/or homopolar bonds) normally occurring at the surface can affect the "bulk" electronic, optical and other physico-chemical properties of ultrasmall active chalcogenide elements. Therefore, the characterization of the local structure at the surface of deposited nanolayers and the study of their relationship with the physico-chemical properties are of great scientific importance from both fundamental and applied points of view.

Synchrotron radiation photoelectron spectroscopy (SRPES) with a sampling depth of the measured photoelectron of approximately few monolayers (~5 angstroms) and X-ray photoelectron spectroscopy (XPS) with a sampling depth ~30 angstroms are an excellent method to study surface properties of materials. To investigate the structure of the samples at the extended scale range (*i.e.* medium range order) the Raman spectroscopy is suitable technique.

In this report the results of complex spectroscopical investigations of the "bulk" properties of $\text{As}_{20}\text{Se}_{80}$, $\text{As}_{40}\text{Se}_{60}$ and $\text{As}_{50}\text{Se}_{50}$ films and their top surface nanolayers using above mentioned methods are reported. Amorphous $\text{As}_x\text{Se}_{100-x}$, ($x = 20, 40, 50$) thin films with thickness of about $0.5 \mu\text{m}$ were prepared by thermal evaporation from bulk glass on clean (100) silicon crystal wafer substrates. The atomic stoichiometry, local structure and their characteristics as well as electronic properties of the surfaces of deposited As-Se nanolayers were examined and interpreted. Atomic concentrations and calculated As-to-Se ratios obtained from photoelectron spectra show that all surfaces are enriched by chalcogen. Each sample demonstrates depth dependence (gradient) of arsenic content, which increases with the depth. The lowest deficiency of arsenic in the subsurface region was found in the $\text{As}_{40}\text{Se}_{60}$ sample, which was attributed to the 3D network-like structure of arsenic triselenide. The properties observed in the surface layers of $\text{As}_{20}\text{Se}_{80}$, $\text{As}_{40}\text{Se}_{60}$ and $\text{As}_{50}\text{Se}_{50}$ films are connected with both their molecular structure and processes of arsenic oxidation and desorption of the oxidized products.

1. O. Kondrat, R. Holomb, A. Csik, V. Takats, M. Veres and V. Mitsa, Coherent light photo-modification, mass transport effect and surface relief formation in $\text{As}_x\text{S}_{100-x}$ nanolayers: absorption edge, XPS and Raman spectroscopy combined with profilometry study, *Nanoscale Research Letters* 2017, **12**:149, DOI: 10.1186/s11671-017-1918-y.

High Temperature Oxidation of NiSi and NiSi₂ Films

Dranenko A.S., Koshelev M.V.

*Frantsevich Institute for Problems of Materials Science of Natl. Acad. of Sci. of Ukraine,
Kiev, Ukraine*

Silicides of transition metals are widely used in the modern silicon film industry because they have metallic conductivity, high melting temperatures, high corrosion resistance, and oxidizability. Schottky diodes, ohmic contacts to shallow-lying active elements, inter-element junctions, gate electrodes in metal–oxide–semiconductor structures constitute by no means a complete list of silicide applications in the very-large-scale integrated circuit (VLSI) technology. Highly conductive nickel silicides are very promising: their conductivity is an order of magnitude higher than that of polysilicon and their properties remain stable to temperatures of about 1070 K

In this work the phase formation and thermal oxidation stability of NiSi and NiSi₂ thin films on n-type Si (111) substrates have been investigated. The objects to study were thin-film layers of Ni (200nm) on monocrystalline Si substrate of orientation (111) doped with phosphorus. Thin-film system Ni/Si obtained by electron-beam deposition in vacuum $2 \cdot 10^{-4}$ Pa. After deposition the samples were annealed in a furnace with oil-free vacuum pumping $1.33 \cdot 10^{-3}$ Pa in the temperature range 470 – 1270 K

For phase identification was performed in "Electronograph EMR-100" using reflection diffraction method. The thermogravimetric analysis (TGA) was carried out in "Derivatograph Q-1500D" thermoanalytical instrument. The sample mass of 20mg was heated in a platinum crucible in static air atmosphere at a rate 5 K/min and a maximum temperature of 1270 K.

According to data TGA, high-temperature oxidation of the NiSi films and the associated increase in weight begins at about 250 degree higher than the oxidation of a silicon substrate. The oxidation of NiSi film starts at 930 K, which is approximately 100 K below the temperature at which NiSi₂ films start oxidising. For both NiSi and NiSi₂ oxidation types the SiO₂ thin protective layers have been formed. When temperature increases, the mass increment NiSi films becomes greater than that of NiSi₂ films. This difference is three times as great at 1270 K, which is due to the difference in their structure and stoichiometry. Due to high silicon content, nickel disilicide forms dense layers of silica on the surface during oxidation, which has substantial impact on the oxidation rate.

InAs/i-GaAs Nano-Heterostructures Behavior Under Neutron Irradiation

Bolshakova I.¹, Vasyliiev O.¹, Kost Y.¹, Kuech T.², Radishevskiy M.¹, Shurygin F.¹

¹*Lviv Polytechnic National University, Lviv, Ukraine, inessa@mail.lviv.ua*

²*University of Wisconsin-Madison, Madison, USA*

InAs is a promising semiconductor for the radiation resistant Hall sensors development [1]. The fast neutrons create radiation defects of the donor and acceptor types in this material, whereas the thermal neutrons result in the nuclear doping with Sn impurity by means of transmutation reaction. During irradiation the Fermi level, E_F , is moving to conduction band, and when it approaches the threshold value of $E_F^{lim} = E_V + 0.52 \text{ eV}$ (E_V – valence band top), the Fermi level pinning takes place. The result is the stabilization of carrier concentration, n , with increase of neutron fluence, F . At irradiation of bulk single crystals InAs this E_F stabilization begins at $n = n^{lim} = 3 \times 10^{18} \text{ cm}^{-3}$ [2]. This work foresaw checking if n^{lim} has the same value for nanoscale InAs films.

The InAs/i-GaAs heterostructures were fabricated by MOCVD with Si doping to ensure the needed initial n levels. We grew 6 heterostructures with $n = (1.8 \div 3.8) \times 10^{18} \text{ cm}^{-3}$ and carrier mobility $\mu = (2850 \div 2600) \text{ cm}^2 \cdot \text{V}^{-1} \cdot \text{s}^{-1}$. Hall sensors were fabricated by mesa etching, Ti/Pt/Au contacts deposition and lift-off lithography. Sensors parameters (sensitivity and carrier mobility) were in-situ measured in on-line mode in the IBR-2 nuclear reactor. Such method allows to record the sensors parameters up to very high fluences $F = 2 \times 10^{19} \text{ n} \cdot \text{cm}^{-2}$.

We conducted three irradiation series of 14-days duration each. The neutron flux had 18.7% of thermal ($E < 0.5 \text{ eV}$), 48.5% of resonance ($E = (0.5 \div 10^5) \text{ eV}$) and 32.9% of fast ($E > 10^5 \text{ eV}$) neutrons. All sensors studied can operate up to $F = 2 \times 10^{18} \text{ n} \cdot \text{cm}^{-2}$ that exceeds by factor of two the maximum fluence of $F = 1 \cdot 10^{18} \text{ n} \cdot \text{cm}^{-2}$ that is foreseen at steady-state sensors locations of the ITER fusion reactor over the 20 years of its lifetime [3].

The dependences of sensor parameters on F for all n values are almost constant: the n is stable during the irradiation up to $F = 10^{17} \text{ n} \cdot \text{cm}^{-2}$; variation in parameters becomes evident with fluence increasing up to $F = 3 \times 10^{18} \text{ n} \cdot \text{cm}^{-2}$. The Fermi level pinning in InAs/i-GaAs heterostructures is not observed at the $n^{lim} = 3 \times 10^{18} \text{ n} \cdot \text{cm}^{-3}$ unlike that for the bulk InAs monocrystals [2].

1. Bolshakova I., Āuran I., Kost Ya. et al. // Key Engineering Materials. – Vol. 543. – 2013. – P. 273–276.
2. Brudnyĭ V. N., Kolin N. G., Smirnov L. S. // Semiconductors. – 2007. – Vol. 41, № 9, – P. 1011–1020.
3. Loughlin M. J. “Nuclear Environment at Magnetic Sensor Positions”. IDM Number ITER_D_2F6S7Y, 2008.

Ultrathin Thermo-Responsive Coatings - New Ellipsometric Technique for Characterization

Kostruba A.M.¹, Rachiy B.I.², Bahriychuk V.O.³, Kopylets V.I.⁴, Musiy R.Y.⁵

¹*Lviv University of Commerce and Economic, Lviv, Ukraine*

²*Vasyl Stefanyk Precarpathian National University, Ivano-Frankivsk, Ukraine*

³*The Company "Kartekiya-Build", Ternopil, Ukraine*

⁴*Karpenko Physico-Mechanical Institute of the NAS of Ukraine, Lviv, Ukraine*

⁵*Department of Physical Chemistry of Fossil Fuels InPOCC, National Academy of Sciences of Ukraine, Lviv, Ukraine, rostyslav_musiy@ukr.net*

Ellipsometry is a valuable tool for studying ultrathin thermo-responsive polymer films that permits to record real-time sub-nanometer transformations in structure of the films during changes in temperature of the liquid ambient. Thermo-responsive ‘smart’ coatings are able to change affinity toward proteins and cells under temperature stimuli and therefore have potential applications in biology and medicine.

Molecular films are often single layers. They can be porous with a significant volume fraction containing ambient. The ambient interface can be poorly defined, as surface coverage can be incomplete. Such films are called *ultrathin* to distinguish them from thicker films, which have a different optical behavior. Ultrathin films have a thickness $d \ll \lambda / 2\pi n_f$, typically < 15 nm in dry state. Since Δ is the main parameter that varies for ultrathin films by traditional ellipsometric measurement, the two unknowns, d and n_f , are strongly correlated. One of possible way to overcome the correlation problem was proposed in our earlier work. Testing this method on systems containing ultrathin thermo-responsive coatings in liquid ambient is the main objective of our research.

The usage of the transparent substrate can significantly increase the sensitivity of ellipsometric measurement and enables independence in determining the parameters of ultrathin film. Taking measurements provided constant amplitude ellipsometric parameter ($\Psi = \text{const}$) allows to solve the problem of the strong correlation between refractive index and thickness of ultrathin transparent film.

The error values of the thickness and refractive index of ultrathin transparent film obtained according to the proposed method is about an order of magnitude smaller than in the case of direct optimization methods in a range of 10-20 nm thickness and, despite a marked increase for the thickness of less than 10 nm, allow to conclude confidently the possibility of independent determination both these parameters.

Applications of Thin Films of Tin in Rechargeable Lithium-Ion Cells

Kublanovsky V.S.¹, Nikitenko V.M.¹, Globa N.I.²

¹*V.I. Vernadsky Institute of General and Inorganic Chemistry, NAS of Ukraine, Kyiv, Ukraine; e-mail: kublan@ukr.net*

²*Interdepartmental Division of Electrochemical Energy Generation, NAS of Ukraine, Kyiv, Ukraine, e-mail: gnl-n@ukr.net*

One of anode materials widely used in rechargeable lithium-ion cells (RLIC) is graphite providing modern RLIC models with more than thousand charge cycles. However, carbon materials based anodes do not meet the requirements to RLIC since they have low specific capacity ($372 \text{ mAh}\cdot\text{g}^{-1}$), low discharge rate, and relatively narrow temperature range of operation.

As a possible alternative for carbon material in RLIC, the use of thin electrolytic tin films or tin containing composite coatings, in particular tin-nickel alloy is proposed.

Tin films were deposited from complex (tartaric, citrate, and trilon-citrate) electrolytes, and efficacy were studied of lithium intercalation-deintercalation process in obtained tin films by methods of potentiodynamic and galvanostatic cycling in 1 M LiClO_4 solution in ethylencarbonate-dymethylcarbonate. It was shown that the nature of electrochemically active complex discharging at the electrode affects significantly not only tin current yield and process mechanism but also the electrochemical properties of tin films during lithium intercalation-deintercalation.

The values of lithium intercalation-deintercalation peak currents decreases depending on the ligand nature as follows: $\text{tart}^{2-} < \text{citr}^{3-} < \text{edta}^{4-}$. It allows one to suggest that discharging electrochemically active complexes are responsible for a morphology and properties of the tin films including their stability, specific capacity, and efficacy of their cycling within lithium power sources. The effect observed can be explained by changes in structure of the tin films obtained from complex electrolytes, according to the increase of nascent tin (II) complexes stability in the series mentioned above. This in turn is responsible for the average tin particles size and their packaging density.

The maximum specific capacity ($992 \text{ mAh}\cdot\text{g}^{-1}$) corresponding to the formation of intermetallic composition $\text{Li}_{22}\text{Sn}_5$ is not achieved for any of the investigated electrodes. The most stable capacitance characteristics under lithium intercalation-deintercalation conditions are shown by tin films obtained from citrate electrolyte ($500\text{-}400 \text{ mAh}\cdot\text{g}^{-1}$), tin (II) complexes stability constant in which has an intermediate value.

Luminescent Properties of Y_2O_3 Thin Films at Different Conditions of Obtained

Bordun I.O., Kukharskyy I.Yo., Tsapovska Zh.Ya.

Ivan Franko National University of L'viv, Lviv, Ukraine,

e-mail: kukharskij@electronics.lnu.edu.ua

The thin films based on Y_2O_3 are widely used for creating displays, scintillators, for the means for recording and visualizing information. In this work the spectra of photoluminescence (PL) and the excitation spectra of luminescence of Y_2O_3 thin films, obtained by different methods as well as the interrelation of the emission spectra with the methods and the conditions of obtained were investigated.

The thin films of Y_2O_3 with thickness from 0.3 to 1.0 μm were obtained by discrete evaporation in vacuum and by radio-frequency ion-plasmas sputtering on substrates of fused quartz ν - SiO_2 . After deposition, the thin films were subjected to heat treatment in oxygen atmosphere at 950°C. The X-ray diffraction studies of obtained thin films were performed.

The analysis of the PL spectra of Y_2O_3 thin films, obtained by discrete evaporation, showed that in these spectra are dominant the band of luminescence with maximum in the region at 3.20 eV. The relative contribution of the more low-energy bands of luminescence with maxima at 2.90 and 2.60 eV is determined by the excitation energy.

The thin films of Y_2O_3 , obtained by radio-frequency ion-plasmas sputtering in oxygen atmosphere, have weaker emission of the PL. Thus, in the luminescence spectra is the dominant band of luminescence with the maximum at 3.40 eV. The causes of sensitivity and the features of the structure of Y_2O_3 thin films according to content of oxygen in the spraying atmosphere were considered.

The nature of exuded bands of luminescence of Y_2O_3 thin films was considered. The band of luminescence with the maximum at 3.40 eV is associated with the luminescence of self-trapped excitons that describe the excited state molecular ion $(YO_6)^{9-}$. The band of luminescence with maximum at 2.90 eV is associated with the emission of the anionic lattice and the band with maximum at 2.60 eV is associated with emission of $Y^{3+} - O^{2-}$ donor-acceptor pair. The band of luminescence with maximum at 4.20 eV is likely not related with impurities or defects and the band of luminescence with maximum at 3.20 eV is likely caused the nonstoichiometry by the oxygen was found.

The kinetics of the decay of the luminescence of Y_2O_3 thin films at the maximum of the most intense band of emission that coincides with maximum of the summary spectrum of luminescence at 3.20 eV was investigated. The kinetics of the decay of luminescence the investigated of Y_2O_3 thin films, obtained by discrete evaporation, that have the most intense luminescence is well approximated monoexponential function with the constant of decay time equal to 111 μs .

Properties of the Nanocomposite Based on Poly (3-Methylthiophene)

Kukla O.L.¹, Mamykin A.V.¹, Ogurtsov N.A.², Pud A.A.²,
Bliznyuk V.N.³, Pyryatinski Yu.P.⁴

¹ V.E. Lashkaryov Institute of Semiconductor Physics, NAS of Ukraine, Kyiv, Ukraine

² Institute of Bioorganic Chemistry and Petrochemistry, NAS of Ukraine, Kyiv, Ukraine

³ Materials Science and Engineering, Clemson University, Clemson, USA

⁴ Institute of Physics of NAS of Ukraine, Kyiv, Ukraine

The polyvinylidene fluoride/poly(3-methylthiophene) (PVDF/P3MT) nanocomposite and neat P3MT has been synthesized through chemical oxidative polymerization of 0.1 M 3-methylthiophene solution in acetonitrile dispersion of PVDF particles using anhydrous oxidant FeCl₃ under Ar atmosphere.

The chlorine anions (Cl⁻) doped P3MT and PVDF/P3MT nanocomposites were investigated by various methods such as SEM and TEM microscopy, X-ray diffraction, FTIR, Raman, UV–Vis and photoluminescence spectroscopy and thermogravimetric analysis. Their thin films were studied for the gas sensor applications as chemoresisting elements. The films were deposited onto the gold raster electrodes formed on dielectric substrate.

It was demonstrated that the PVDF/P3MT-Cl⁻ nanocomposite particles have a core-shell like morphology, with the PVDF core and P3MT-Cl⁻ shell similar to earlier described PVDF-polyaniline nanocomposites [1]. The P3MT synthesis in the presence of submicron PVDF particles leads to the nanostructurization of the P3MT-Cl phase (the stabilization of primary particles and suppression of their aggregation) and improvement of the P3MT-Cl phase properties in the ultimate nanocomposite as compared with the neat polymer. Specifically, such changes both facilitate access of analyte molecules to the P3MT clusters on the sensor electrodes and improve its sensing properties. We studied the sensing behaviour of the PVDF/P3MT-Cl composite compared with that of neat P3MT-Cl for five volatile organic compounds (acetone, chloroform, n-heptane, toluene and 1-heptene).

It was found that the investigated films demonstrated high stability and reproducibility of sensor responses. Detection threshold of the films for the tested analytes was a few ppm, response time was about 10–20 s. Due to these properties, and the presence of cross-sensitivity of the films to different types of organic substances, these films are promising as sensing materials for the use in gas analytical systems of the “electronic nose” type.

1. Yu. Noskov, S. Mikhaylov, P. Coddeville, J. L. Wojkiewicz, A. Pud. Acid-dopant effects in the formation and properties of polycarbonate-polyaniline composites // Synth. Met. 2016, 217, 266-275.

Structure and Magnetic Properties of High-Entropy $\text{Co}_{19}\text{Cr}_{18}\text{Fe}_{22}\text{Mn}_{21}\text{Ni}_{20}$ Alloy Films Deposited by Ion Plasma Sputtering

Kushnerov O.I., Ryabtsev S.I., Bashev V.F.

Oles Honchar Dnipro National University, Dnipro, Ukraine

For a long time of the development of metallurgy, which is one of the most important directions of practical and research human activity, the majority of designed and, in particular, applied (in technology) alloys are based on a single and sometimes two or three metals. However, due to the ever-growing needs of technology in improved structural and functional metallic materials, new technologies are steadily being developed, and advanced alloyed steels and alloys are being designed. The first works related to designing and complex study of a new class of materials, i.e., the so-called high-entropy multicomponent alloys (HEAs) were published in 2004. As a rule, these compositions comprise 5–13 principal elements, the concentrations of which are equiatomic or close to equiatomic (5–35%). Choosing a number of components and their concentration allows one to achieve an increased entropy of mixing, which remains not only in the melt but after solidification. Because of the high entropy, usually simple substitutional solid solutions with BCC or FCC crystal lattices are formed during the solidification of such alloys. The HEAs are characterized by a number of useful characteristics, such as hardness, wear resistance, resistance to oxidation, corrosion, and ionizing radiation, biocompatibility, and high thermal stability.

In this study, $\text{Co}_{19}\text{Cr}_{18}\text{Fe}_{22}\text{Mn}_{21}\text{Ni}_{20}$ HEA thin films have been synthesized by ion plasma sputtering of mosaic targets consists of pure metals. The deposition process was carried out at room temperature with pure Ar atmosphere, the working pressure was controlled at $5 \cdot 10^{-2}$ Pa. The deposition rate for the HEA thin film was 0.2 nm/s. The as-deposited HEA film thickness was estimated to be ~ 110 nm. Single diffuse halo is observed on the XRD patterns of the as-deposited films, that confirms their amorphous structure. After the heat treatment in vacuum at 600°C , the $\text{Co}_{19}\text{Cr}_{18}\text{Fe}_{22}\text{Mn}_{21}\text{Ni}_{20}$ metallic film transforms from an amorphous form into a crystallized FCC solid solution structure with the lattice parameter $a=0.3613$ nm. The heating rate from room temperature to designated annealing one was $9^\circ\text{C}/\text{min}$.

The magnetic properties of the films were measured by a vibrating sample magnetometer at room temperature with the magnetic field applied parallel to the film plane. The results clearly reveal a typical ferromagnetic behavior of both as-deposited and annealed films. The coercivity H_c was 5 Oe for the as-deposited, and 110 Oe for the annealed films, so they can be referred to soft magnetic and hard magnetic materials respectively.

The Theoretical Study of Interplay of Crystal Lattice Defects with Al Impurity in ZnO:Al

Ovsiannikova L., Lashkarev G., Kartuzov V., Dranchuk M.

Frantsevich Institute for Problems of Material Science, NASU, Kiev, Ukraine,
avilon57@ukr.net

We successfully used fullerene like (FL) cluster model earlier for a solution of band engineering problems in ZnO alloys and precipitation of CdO phase in these materials[1-5]. For the development the technology of growing and for the control of properties for ZnO based materials doped by Al and other impurities for the aim of applications in photovoltaic and optoelectronic devices, the minimization of donor impurities compensation by native acceptor defects (V_{Zn} , O_i etc.) is required. Exponential dependence of defect concentration on their formation energy results in the situation when almost only defects with minimal energy are present in any semiconducting material. For determination the thermodynamic properties of defects we started the series of computational experiments.

Qualitative results for the behavior of Al impurity in fullerene like cluster based on ZnO were obtained. Al impurity tends to uniform distribution in such clusters. Analysis of the defect formation energy shows the advantage in the formation of interstitial O_i in a comparison with a formation of Zn vacancy when O_i is adjacent to Al. Uniform distribution of Al impurity and nonadjacent position of O_i to Al increase Al ionization energy. Thus FLM demonstrated again its capability of living, what allows to use it in future for the control of the electroactivity of donor impurities of the third group due to their compensation by intrinsic acceptor defects of ZnO crystal lattice and to look for technological ways for improving the electroactivity of the donor impurity in ZnO. Adjacent position of Al atom to O_i decreases the energy of its formation and increases Al ionization energy. The results of theoretical calculations of Al ionization energy and adjacent V_{Zn} and O_i allowed us to formulate recommendations to the conditions of technological processes for ZnO films deposition.

- [1] L.I. Ovsiannikova, *Acta Physica Polonica A* **122**, 1062 (2012)..
- [2] L.I. Ovsiannikova, *Acta Physica Polonica A* **126**, 1090 (2014)..
- [3] L. Ovsiannikova, V. Kartuzov, I. Shteplyuk, G. Lashkarev, *Acta Physica Polonica A* **129**, A-41 (2016)..
- [4] I.I. Shteplyuk, V. Khranovsky, G. Lashkarev, et al., *Solid-State Electronics*, **81**, 72-77 (2013)
- [5] L. Ovsiannikova, V. Kartuzov, G. Lashkarev, *45st "Jaszowiec" International School & Conference on the Physics of Semiconductors, Szczyrk, Poland, 2016*

Structural Transformations in Amorphous Semiconductor Films Based on GaSb

Lutsyk N.Yu, Mykolaychuk O.G.

Ivan Franko National University of L'viv, L'viv, Ukraine, E-mail: nyuluts@i.ua

Structure, substructure, concentration areas of existence of metastable solid solutions and an amorphous state and kinetics of structural transformations depending on technological conditions of evaporation of thin films of system GaSb-Sn were studied by methods of electronography (EG-100) and transmission electron microscopy (UEMB-100K). Films with the thickness near 500Å were prepared using method of a flash vacuum evaporation. Ceramic, glass and spallings NaCl monocrystals were served as substrates. The composition of films is more convenient to represent using the formula $(\text{GaSb})_{1-x}(\text{a-Sn}_2)_x$ because in the investigated system solid thin-film solutions are formed by substitution. The temperature of a substrate supported in a precipitation process of films has dominant effect on structure formation of explored films. Films precipitated on substrates at room temperature were amorphous up to 30% of Sn_2 concentration. Two-phase polycrystalline films (b -Sn and GaSb) are formed at higher concentrations of Sn. The linear relation of the proximate interatomic distance (from 0.272 nm in a-GaSb to 0.276 nm in $(\text{GaSb})_{0,7}(\text{Sn}_2)_{0,3}$) in amorphous films from composition is observed. The linear relation of the proximate interatomic distance in coordinate Sn_2 specifies random distribution of atoms with forming "alloyed" structure such as a solid solution.

Amorphous films at heat crystallized, but phases of a solid solution it is not observed. Initial crystallization phases are crystal grains b -Sn. The growth of crystallite sizes of b -Sn takes place with the temperature increase. A speed of continuous heating has essential influence on the density and sizes of metallic crystallites of b -Sn formed in the amorphous semiconductor matrix based on GaSb. With the increase of temperature of a substrate there is a forming the nonuniform amorphous films. With the further increase of temperature of substrates on the isotropic substrates, polycrystalline films of a metastable solid solution of substitution are formed for the concentration up to 20% of Sn_2 , and on spallings NaCl monocrystals textured and epitaxial films are formed. Disorder of solid solutions on phases GaSb and Sn at temperatures is higher 500K is observed.

Physical Properties of Thin Films of CZTS Obtained by the Method of High-Frequency Magnetron Sputtering

Mastruk E.V.

Yuriy Fed'kovytsch Chernivtsi National University, Chernivtsi, Ukraine

The synthesis of $\text{Cu}_2\text{ZnSnS}_4$ was carried out in a quartz ampoule in a tubular furnace. The synthesis temperature was selected experimentally, taking into account the melting points of the elementary substances and the substances that make up the compound. The synthesized material was crushed and ground in a porcelain mortar to a finely dispersed state and pressed into an aluminum beaker, which was placed on a magnetron. The films were deposited on glass and sital substrates. The analysis of the elemental composition confirms that the chemical composition of the resulting films corresponds to the loaded components.

The study of the kinetic coefficients of $\text{Cu}_2\text{ZnSnS}_4$ thin films was carried out in the temperature range 20 – 70 °C and magnetic fields 0.25 – 4 kOe. The temperature dependence of the electrical conductivity of thin films $\text{Cu}_2\text{ZnSnS}_4$ has a metallic character. Hall coefficient varies slightly with increasing temperature, which indicates the degeneracy of the charge carriers, their concentration at room temperature is $p = 5 \cdot 10^{18} \text{ cm}^{-3}$. The Hall mobility has a value $\mu = 1.9 \text{ cm}^2/\text{V}\cdot\text{s}$ at room temperature, and decreases with increasing temperature, which is due to the scattering of holes by phonons. Such low values of mobility can also be explained by the graininess of the films.

Investigation of the optical coefficients was carried out using a NIKOLET 6700 IR Fourier spectrometer and a SF2000 spectrophotometer in the IR and visible spectrum, respectively, with a total range of 0.2 to 26 μm . As the substrate temperature decreases, the edge of intrinsic absorption shifts to the short-wavelength region. This is due to the fact that $\text{Cu}_2\text{ZnSnS}_4$ is synthesized at temperatures close to 500 °C. At lower temperatures, the synthesis does not go completely, that is, not only $\text{Cu}_2\text{ZnSnS}_4$ but also its binary components Cu_2S , ZnS , SnS_2 are present in the films.

The films were deposited on glass and sital substrates. The time for the deposition of films was from 5 minutes to 1.5 hours, the temperature of the substrates was maintained at 400 to 600 °C. As a result, films of a small-crystal (100 nm) structure were obtained, which underpins electron microscopy. If the synthesis was not completely (at lower substrate temperatures), there are fine crystalline fractions (crystallite size 10-20 nm). Thus, when magnetron sputtering, CZTS from the target settles on the substrate in the form of its binary components, and only then further synthesis of $\text{Cu}_2\text{ZnSnS}_4$ takes place and at higher substrate temperatures (450 °C and higher).

On the other hand, as the temperature of the substrate increases, the process of film growth slows down, which is caused by the intensification of the desorption process of the atoms of the growing film from the surface of the substrate. In this case, the quality of the film deteriorates.

Electron Scattering on the Crystal Defects in Zinc Blende GaN Epilayers: Calculation from the First Principles

Malyk O.P., Syrotyuk S.V.

Lviv Polytechnic National University, Lviv, Ukraine

In the series of papers [1-5] the disadvantages of the long-range electron scattering models was shown and it was proposed a new approach for description of the transport phenomena on the base of the short-range principle. However, in the proposed approach the one disadvantage remains, namely the presence of some numerical fitting parameters which require the availability of experimental data to select their numerical values. At present investigation a new method is proposed that enables to eliminate the majority of the fitting parameters. In this method the calculation of the charge carrier transition probabilities was carried out on the base of wave function and self-consistent potential which were determined from the first principles using the projector augmented waves (PAW), as implemented in the ABINIT code [6].

The PAW basis functions have been generated for the following valence states: $3s^23p^64s^24p^13d^{10}$ for Ga and $2s^22p^3$ for N. The radii of the augmentation spheres have the following values: 1.8 and 1.2 a.u. for Ga and N. The exchange and correlation effects have been taken into account within the generalized gradient approximation hybridized with Hartree-Fock exact exchange of the Ga. The experimental value of the lattice parameter $a_0 = 4.5 \text{ \AA}$ was used in the calculation.

On the base of obtained wave function and self-consistent potential for zinc blende GaN in the framework of short-range scattering models the calculation of transition probabilities without fitting parameters for electron interaction with polar and nonpolar optical phonons, piezoelectric and acoustic phonons, ionized impurities are presented. The transition matrix elements were obtained by integration over the volume of the unit cell. To calculate the conductivity tensor components the method of a precise solution of the stationary Boltzmann equation was used. The temperature dependences of electron mobility and Hall factor in the range $30 \div 300 \text{ K}$ (for GaN) are calculated. The influence of the different scattering mechanisms on the charge carrier mobility is considered. The theoretical curves obtained in the short-range approach show much better agreement with measured data compared with long-range scattering models.

- [1] O.P. Malyk. // Mater. Sci. Eng. B. – 2006. – **129**. – P.161-171.
- [2] O.P. Malyk. // Phys. Status Solidi C – 2009. – **6**. – P. S86-S89.
- [3] O.P. Malyk. // Diamond Relat. Mater. – 2012. – **23**. – P. 23-27.
- [4] O.P. Malyk. // Can. J. Phys.– 2014. – **92**. –P. 1372-1379.
- [5] O.P. Malyk et al. // Phys. Status Solidi C.– 2016.–**13**.– P. 494-497.
- [6] X. Gonze et al. // Comput. Phys. Commun.– 2009.– **180**. –P.2582-2615.

The Influence of Conductive Polymer Filler on Microhardness of Composites with Dielectric Polymer Matrices

Martyniuk G.¹, Aksimentyeva O.²

¹Rivne State Humanitarian University, Rivne, Ukraine, e-mail: galmart@ukr.net

²Ivan Franko National University of Lviv, Lviv, Ukraine, e-mail: aksimen@ukr.net

Advances in modern science and technology make the need for new polymer composite materials, which would have complex of functional properties - electrical conductivity, mechanical strength, flexibility, etc. Special attention causes so-called "smart-materials" that have the ability to change their properties depending on changes in external conditions (the electric field, radiation, adsorption of gases). These materials include the conjugated polymers and their composites with polymer matrices. An important task when creating polymer-polymer composites is to determine their mechanical properties, in particular, microhardness, and connection the nature of polymer matrix and mechanical characteristics of composites.

We studied the effect of acid-doped polyaniline (PAN) as a conductive filler on the microhardness of its composites with polymer matrices of different structure – polyvinyl alcohol (PVA), polymethylmethacrylate (PMMA), polybutylmethacrylate (PBMA), epoxy resin ED-20 (ES). Composite samples for research were obtained by pressing fine powders of conducting polymers, dispersed in the matrix of PVA, PMMA, PBMA, under the pressure of 150 kg/cm² at softening point and flow temperature. The mechanical properties of the composites were studied by measuring microhardness and limit fluidity point on the Hepler consistometer.

It is established that the nature of the interaction between the polymer matrix and conductive polymer filler depends on its content and structure of the matrix, which manifested itself in an increase of microhardness (composites PBMA – PAN and ES–PAN and its decrease for PVS–PAN and PMMA–PAN composites. Microhardness value for polymer PBMA and epoxy resin ED –20 is smaller than filled composites and are $4.51 \cdot 10^{-9}$ N/m² and $9.05 \cdot 10^{-9}$ N/m². With introduction of filler increases microhardness to $7.5 \cdot 10^{-9}$ N/m² and $10.1 \cdot 10^{-9}$ N/m² at 15% content of conductive polymer, respectively. With increasing PAN content up to 20% is observed a noticeable drop in the values of the conical point of fluidity. Perhaps in this case a separate micro phase PAN is formed, causing loosening effect.

The values of the specific density of the obtained composites are well correlated with changes in microhardness, which proves the interaction between the polymer matrix and conductive polymer filler.

Properties of Films based on Copper Complex Adduct of Monoglycidyl Ethers Oxydiarylmethanes

Martynyuk M.I., Sirenko H.O., Drobot O.S.

Vasyl Stefanyk Precarpathian National University,
Ivano-Frankivsk, Ukraine, mar.martynyuk@mail.ru

This research is devoted to realization of the phenomenon of random transport of copper in dynamic contact of solid bodies, and also achievement of quasi anti-wear effect through creation of films on the surfaces of friction pair. Friction properties of films were studied using friction apparatus according to the friction scheme “plane surface – plane surface” of epoxy-filled composite, reinforced non-metallized and copper plated carbon fiber material (Cu^0 -CFM).

Parameters of tribological testing: sliding speed 0,54 m/s, normal load to one sample 100 N, specific load 3 MPa; run-in path 0-20 km, stationary friction path 40-100 km, parameters of effectiveness assessment of lubrication material – specific volume wear rate I , $\times 10^{-6} \text{ mm}^3 / (\text{N}\cdot\text{M})$. The scheme of contact of unidirectional composite NNNN and NLNN in contact with the surface of steel 45 counterbody (LD $4,5\pm 0,2$ Hpa; $R_a = 0,30\pm 0,05$ mkm); steel surface temperature 383 ± 10 K.

For investigation of friction pair anti-frictional properties, we have selected the following lubricants with and without copper compounds:

a) glycerin [Gl.]; [Gl.] with admixture of 5% disperse graphite [Gl. + Gr.]; [Gl.] with admixture of 5% copper graphite [Gl. + Cu^0 – Gr.]; [Gl.] with admixture of 5% organic copper compound MKF-18 [Gl. + MKF-18]; [Gl.] with admixture of 5% $(\text{CH}_3\text{COO})_2\text{Cu}$ [Gl.+CA];

b) plastic lubricant SMT-5 with disperse copper powder content [SMT-5];

c) mineral (compressor) oil KS-19 [KS-19]; [KS-19] with admixture of SMT-5 [KS + SMT-5]; [KS-19] with admixture of MKF-18 [KS-19+MKF-18];

d) copper complex of epoxidated benzyl phenol (EBP) adduct, polyethilenepolyamine (PEPA), $(\text{CH}_3\text{COO})_2\text{Cu}$ (CA) [EBP+ PEPA+CA].

The received results enabled making up minorant series according to wear intensity:

a) for composite with non-metallized CFM: [KS + MKF-18] > [KS + SMT-5] > [Gl.] > [KS-19] > [EBP+ PEPA-CA] > [Gl. + Gr.] > [SMT-5] > [Gl.+CA] > [Gl. + MKF-18] > [Gl. + Cu^0 – Gr.];

b) for composite with copper plated CFM: [KS-18] > [KS + MKF-18] > [KS + SMT-5] > [Gl. + CA] > [SMT-5] > [Gl. + MKF-18] > [Gl.] > [Gl. + Gr.] > [Gl. + Cu^0 – Gr.] > [EBP+ PEPA+CA].

These results have proved high efficiency of films on the surfaces of dynamic contact composite steel consisting of copper complex adducts of oxydiarylmethane, polyethilenepolyamine and copper acetate monoglycidyl ethers.

Ellipsometric Effects of the Porous Silicon Aging and Decorating

Odarych V.A.

Kyiv national University of Taras Shevchenko, Kyiv, Ukraine

Porous silicon (PC) are formed on the crystalline Si p-type surface by passing in a few minutes the electric current with a density of 10-40 mA/cm² through the electrolyte that showed 48% aqueous mixture of HF and acetone in equal proportions. Ellipsometric curves – dependence of the phase difference Δ between p - and s-components of the electric vector of the light wave ($\cos\Delta$) and the ratio of the reflectance of $\text{tg}\psi$ in p - and s-planes of the sample from the angle of incidence φ – are measured at different wavelengths of the visible range. The measurements were performed during long time (up to several years) after the samples preparation. It is observed that ellipsometric curve $\text{tg}\psi(\varphi)$ changes dramatically over time in air in contrast to the curve $\cos\Delta(\varphi)$, which varies little. This ellipsometric curves transformation (effect of aging) may be caused by change of surface layer parameters during the interaction of the electrochemical reactions products with the basic material, the atmospheric air (oxygen, water vapor) and atmospheric air with substrate (silicon). To specify the near-surface region structure the investigated samples were rinsed in 96% ethanol and after drying ellipsometric measurements were recovered. It is observed that after treatment with ethanol ellipsometric curves back around to what they were after samples preparation. Over time, within 7 to 10 days the relaxation effect occurs – curve $\text{tg}\psi$ returns to the state before contact with the ethanol. The effect (decoration effect) due to the fact that films of porous silicon have cavities which are filled with ethanol and thereby decorate hollow porous silicon layer. The first report of this effect speaks in [1]. Ellipsometric observations showed that after 7 to 10 days of stay in the open air the decoration effect disappears, when, obviously, the ethanol will evaporate. Experimental curves $\text{tg}\psi(\varphi)$ and $\cos\Delta(\varphi)$ can be described in a model of two-layer film, in which the upper layer has a refractive index smaller than the inner. In the result, it was found that the upper porous silicon layer consist of two layers, of which the first, outer, containing a mixture of silicon oxide and air in the amount of 0.8 air, and the second (inner) that is adjacent to substrate, incompletely oxidized and contains a mixture of silicon, silicon oxide and possibly air in the amount of 0.42. System containing a mixture of silicon and its oxide in an amount of 0.23 volume fraction of the mixture is substrate for them.

1. Odarych V., Rudenko O. Physics and Technology of thin films and nanosystems. Materials XIV International conference ICPTTFN-XIV. May, 20-25, 2013, Ivano-Frankivsk, Ukraine. P.321.

Electrical and Optical Properties of Graphite Thin Films, Prepared by the Electron-Beam Evaporation Technique

Orletskyi I.G., Ilashchuk M.I., Brus V.V., Maryanchuk P.D., Parfenyuk O.A.

Chernivtsi National University, Chernivtsi, Ukraine, i.orletskyi@chnu.edu.ua

Low-cost graphite thin films possess high electrical conductivity and chemical stability. Graphite films with a nanoscale thickness are transparent within wide spectral range. The mentioned features of graphite thin films make them perspective for practical application in optoelectronic devices.

This work reports the results of the investigation of electrical and optical properties of graphite thin films, deposited by means of the electron-beam evaporation technique as well as electrical properties of bulk graphite samples used as targets.

The analysis of electrical properties of the graphite bulk samples and thin films was carried out by the measurement of the temperature dependence of electrical conductivity, Hall coefficient and Hall mobility within the temperature range from 295 to 445 K. Transmittance spectra of the thin films were measured in the range of wavelengths 200 ÷ 1100 nm, by a CF-2000 spectrophotometer. The uniform morphology of the graphite thin films under investigation is proven by SEM images of the surface and cross-section. The determined thickness of the graphite films was 50 nm.

The both bulk samples and thin films were characterized by a high density of free electrons ($n = 8.6 \cdot 10^{19} \div 2.0 \cdot 10^{20} \text{ cm}^{-3}$) and the absence of its temperature dependence that is in good correlation with the band structure of graphite. The temperature dependence of the electron mobility and thus electrical properties was measured to be exponential. The electron mobility and electrical conductance of the bulk samples were about two orders of magnitude larger then that for the thin films at room temperature: $\sigma = 95 \div 110 \text{ } \Omega^{-1} \cdot \text{cm}^{-1}$, $\mu_H = 7.0 \div 8.0 \text{ cm}^2 \cdot \text{V}^{-1} \cdot \text{s}^{-1}$ and $\sigma = 1.5 \div 5.8 \text{ } \Omega^{-1} \cdot \text{cm}^{-1}$, $\mu_H = 1.0 \div 3.0 \cdot 10^{-2} \text{ cm}^2 \cdot \text{V}^{-1} \cdot \text{s}^{-1}$, respectively. Basing on the obtain results, the electrical characteristics of the both bulk samples and thin films were analyzed in the scope of the model developed for polycrystalline materials where the dominating role play the electrical conductance of grain boundaries. In this case $\sigma = \sigma_0 \exp(-E_b/kT)$, where E_b is the potential barrier, caused by the surface states at the grain boundaries. The absence of a hysteresis of the temperature dependence of the electrical conductivity of graphite thin films shows their high thermal stability.

The graphite thin films possessed high transparency in the spectral range of 300 ÷ 1100 nm. The transmittance coefficient linearly increases from 60 to 85% within the mentioned spectral range. High electrical conductance, thermal stability and transparency in the spectral range of the solar light make graphite thin films perspective for application in the form of the front layer of photovoltaic devices.

Electrical Conductivity of Amorphous Carbon Thin Films

Penyukh B.

Ivan Franko National University of Lviv, Lviv, Ukraine

The aim of the study is to investigate the influence of coating method on structure, surface morphology and conductivity thin films of carbon. The carbon thin films were deposited in high vacuum onto quartz substrates at 300 K by thermal evaporation methods from shot electric arc (condensation rate approx. 10 nm/min) or electron beam vapor (condensation rate approx. 0,5 nm/min). Films thickness (10-150 nm) was monitored by applying a quartz-crystal oscillator sensor. The planar electrical resistivity was measured by two probe method in temperature range 300-750 K using nickel film resistance thermometer. Surface morphology and structure of films were investigated by Jeol SEM microscope and Selmi TEM microscope.

Electron diffraction experiments indicate that carbon films coated by shot electric arc method consist of a mixture of diamond and graphite islands in amorphous lattice. On the other hand, samples coated by electron beam vapor method were fully amorphous. SEM microscopic studies gave similar results: dendrite inclusions in samples deposited at high evaporation rate and vary smooth surface of others.

Effects of annealing and temperature on electrical properties are studied, in light of the semiconducting nature of these films, through the electrical conduction mechanism. The results obtained are in good correlation with films structure and are discussed and compared with the literature.

Temporary Stability of Structure and Physical Properties of Films of Gd-Fe System

Prysyazhnyuk V.I., Mykolaychuk O.G.

Ivan Franko National University of Lviv, Faculty of Physics, Lviv, Ukraine

Thin layers of intermetallic compounds of type a rare-earth element – iron are interesting due to their structural features, electrical and magnetic properties.

Films of binary compounds of Gd-Fe system were obtained by means of a thermal vacuum evaporation of polycrystal mix material of a corresponding composition. The films with by thickness of 50-60 nanometers were evaporated on splitting of NaCl, then NaCl dissolved in water. The part of films was picked up at once on copper electron diffraction grids. The second series of films transplanted on copper grids, prestressly coated thin collodion supports and in such way was maintained 3-6 years. Then recurring researches were carried out. For electrophysical measurings the films are condensed on glassceramics substrates. The thickness of films changed within 100-200 nanometers. The temperature of substrates had two values 300 and 500 K. For structural investigation the electron microscope UEMV-100K and high-temperature attachment PRON-2 were used. Angle dependence of atomic factors of electron scattering was considered by atoms of gadolinium and iron. All measurements were repeated in 3-6 years after the first stage of measurings.

By us it is explored structure, electrophysical and magnetic properties of films of different compounds of Gd-Fe system in the range of 3-6 years. It is revealed high temporary durability of physical performances of films of Gd-Fe compounds and lack of an oxidizing.

Effect of Bi Doping on the Structure and Conduction Mechanism of Amorphous GeS Films

Romanyuk R.R.^{1,2}, Romanyuk L.M.³

¹Western Scientific Centre, Lviv, Ukraine, zncnan@mail.lviv.ua

²Ivan Franko National University of L'viv, Lviv, Ukraine

³Environmental College Lviv National Agrarian University, Lviv, Ukraine

The influence of Bi additions on the structure, electrical and photoelectrical properties of amorphous $(\text{GeS})_{1-x}\text{Bi}_x$ films ($0 \leq x \leq 0.15$) has been investigated. Bulk samples $(\text{GeS})_{1-x}\text{Bi}_x$ ($x = 0; 0.03; 0.07; 0.11; 0.15$) were obtained in ampoules by melting stoichiometric GeS with the addition of Bi of certain concentrations. The ampoules were subjected to vibration and hardening in cold water. The thin films under investigation (thickness of nearly $0.3\text{-}1.2 \mu\text{m}$) were obtained by using a method of discrete evaporation of a fine-dispersive mixture on the surface in a vacuum (10^{-4} Pa) from substrates of quartz and ceramics at 293 K followed by annealing in a vacuum at $T = 350$ K. A pre-sputtering method was applied to the substrate contact with copper. The photovoltaic properties of the samples were studied by using methods of unmodulated and modulated lighting depending on the temperature and the spectral composition of the exciting light. Temperature dependences of static conductivity and photoconductivity of amorphous films were investigated in the temperature range 150-350 K.

The temperature region of GeS amorphous structure existence was determined. The peculiarities of low order of amorphous thin films in dependences of technology preparation were studied. The topology and micro-local features of disordered structure $(\text{GeS})_{1-x}\text{Bi}_x$ films formation process were established using the method of analysis of experimental scattering curves as well as model interpretation of radial distribution function of atomic density.

Supplementing Bi to amorphous condensates leads to changes in the mechanism of conductivity and the conductivity type inversion. Bi-additives reduce the activation energy of photoconductivity and photosensitivity of GeS films. It is found that amorphous GeS films have an activation mechanism of conductivity in the temperature range $T=150\text{-}350$ K. Bi-additives in the GeS condensates cause an increase of conductivity and the appearance of hopping conductivity through localized states near the Fermi level with the variable length of hopping. Increasing the concentration of Bi reduces the photoconductivity and the spectral region of photosensitivity of GeS films. In the concentration range $0.11 < x < 0.15$ the conductivity type inversion from p - to n -type takes place. Changes of the physical properties of the films are explained in the framework of the heterogeneous structure of the condensates and defect states in the mobility gap.

Photo-Thermoinduced Effects in Ge, As, Sb Amorphous Chalcogenides

Rubish V.M.¹, Gorina O.V.¹, Mykaylo O.A.²,
Pop M.M.², Makar L.I.¹, Hasynets S.M.¹

¹ *Institute for Information Recording, NASU, Uzhgorod Ukraine*
center.uzh@gmail.com

² *Uzhgorod National University, Uzhgorod, Ukraine*

Amorphous arsenic chalcogenides films due to high light sensitivity are widely used as media for creating highly efficient holographic gratings and information optical recording.

Registration of information is based on difference in optical properties of irradiated and non-irradiated parts in these films. There are two main signs of changes in optical properties: shifts of the absorption edge (photodarkening or photobleaching) and growth (or reduction) of the refraction index. A level of photoinduced changes in optical parameters of films considerably depends on their chemical composition, conditions of preparation, thermal processing and irradiation in all these cases. Therefore, it is of great interest to investigate the photoinduced effects in films of another system.

In this work, we have adduced the results of studying the influence of illumination and annealing on transmission spectra of the films based on the systems As-S-Se, As-Sb-S, Ge-S, Ge-Se, Ge-S-Se.

Thin amorphous films (thickness $\sim 1-2 \mu\text{m}$) were deposited by vacuum thermal evaporation on cool silica substrates. A uniform thickness of layers was provided by planetary rotation of substrates. Light exposure of films was made using defocused radiation of a semiconductor laser ($\lambda = 530 \text{ nm}$). Optical transmission spectra of the films was measured at room temperature within the range 400 to 1100 nm by using a monochromator "МДР-3". The spectral resolution was no worse than 10^{-3} eV . Investigations have shown that with increasing of illumination time absorption edge of As-S-Se and As-Sb-S films is shifting into longwave region (photo-darkening the films takes place). Laser illumination of amorphous films in the Ge-S, Ge-Se and Ge-S-Se systems leads to the shift in transmission spectra to the shortwave region (photobleaching of films). The values of optical parameters (pseudogap width E_g and refractive index n) of films have been determined. It is shown that the level of photoinduced changes in optical parameters of annealed films is much lower than that in the as-prepared ones.

Optical characteristic changes of films are caused by structural transformations taking place in them under laser illumination and annealing.

Correlation Between the Mean Free Path of Charge Carriers and the Lateral Size of Objects on the Surface of a Thin Film SnTe<Sb>

Saliy Ya.P.

Vasyl Stefanyk Precarpathian National University, Ivano-Frankivsk, Ukraine

The work revealed the relationship between the mean free path of carriers and the lateral size of objects on the surface of a thin film SnTe <Sb>, deposited on substrates of mica and ceramics. There is also a correlation between the temperature dependences of these quantities.

Thin films p-type conductivity thickness $d = 200 - 2000$ nm were grown by thermal evaporation in a vacuum. Electro-physical studies were conducted in constant electric and magnetic field. We studied the morphology of the film surface using atomic force microscopy.

Monotonic increase mobility of free charge carriers with thickness are explained manifestation of classical size effect. Interpretation of dependence $\mu(d)$ was made in the framework of Fuchs-Sondheimer theory.

If the film thickness and the mean free path are commensurate, the dependence of the mobility on the size has the form: $\mu(d) = \mu_{\infty} / (1 + 3/8 (1 - p) l/d)$, where $\mu_{\infty} = e/m^*t$. In the coordinates $\mu^{-1}(d^{-1})$ the graphic will look like as a straight line.

If we present the relaxation time t through the mean of the free path l , then $\mu_{\infty} = el/m^*v = al$. The theoretical value is $a = e/m^*v = 0,6 \cdot 10^5$ m/V c.

Experimental values mobility of free charge carriers are splited into three groups depending on the temperature of deposition: these are films grown at temperature of 125 - 150 °C, 150 - 200 °C and 200 - 300 °C.

All experimental points have been approximated by the one dependence with a common coefficient a and with different pairs l and p for each group.

We got significance $a = 1 \cdot 10^5$ m/s in that less than two times higher than the theoretical estimate. The mean free paths of charge carriers in the groups were 30, 70 and 200 nm. Parameter p for the first and second group is 0, and for the third is 1. We observe that the films with close to the bulk material parameters are got at high deposition temperatures.

We have graphically compared the diameters, obtained by atomic force microscopy, of objects on the surface of the films grown at different temperatures, and received from electro-physical studies the mean free path of the charge carriers. The correlation between values of these parameters and the correlation between courses of their temperature dependences were discovered.

Thus for the first time, using the experimental size dependence of the charge carriers mobility in the films grown at different temperatures, the coefficient of proportionality between the volumetric mobility and the mean free path was discovered. The value of this coefficient is close to the theoretical one.

Limits the Use of Approximate Formulas of Theory Fuchs-Sondheimer for Classical Size Effect

Saliy Ya.P.

Vasyl Stefanyk Precarpathian National University, Ivano-Frankivsk, Ukraine

Fuchs-Sondheimer theory (FST) is basic in explaining of the classical size effect (CISE) in semiconductor and metal thin films. The main parameters of this theory are mean free path l of carriers in the bulk material and reflectivity degree p (share elastic component) of the carriers from the surface.

To obtain the unknown parameters p and l of approximating the experimental dependence of conductivity σ of the film thickness d are used the approximate functions, however their limits of use depend on these parameters. So we need to find such conditions of use approximate functions, which are independent of in advance unknown parameters.

To describe the CISE of conductivity σ of thin film with thickness d by FST [1] use the expression:

$$\sigma = \sigma_{\infty} \left\{ 1 - \frac{3}{2} (1 - p) / k \int_1^{\infty} (x^{-3} - x^{-5})(1 - e^{-kx}) / (1 - p e^{-kx}) dx \right\}, \quad (1)$$

σ_{∞} is the conductivity of an infinitely thick film, $k = d/l$.

The approximate functions are presented as

$$\sigma = \sigma_{\infty} / (1 + 3/8 (1 - p) l/d), \quad d \sim l, \quad (2)$$

$$\sigma = 3/4 \sigma_{\infty} (1 + p) / (1 - p) d/l \ln(l/d) \quad d \ll l. \quad (3)$$

However, the lack of information on the mean free path l does not allow us to prefer one of the formulas (2) or (3), therefore graphical comparison of functions represented by formulas (1 - 3) was made. By the nature of the behavior we choose the adequate approximate function to further determine the parameter l , which limits the application of approximate formulas.

A comparison of the graphs found that, for example, if $p = 0,5$ and the parameter l is known, should be used the approximate function (3) if $d < 0,01l$ or (2) if $d > 0,1l$.

Also found that should focus on changing the conductivity of the thickness, that is, if the dependence is changing in times, you should use the (3), if slightly changed - the (2). We can also determine the true approximation if we will present experimental data in the coordinates for which the graph of approximate function has view of direct line. These are σ/d as a function $\ln(d)$ if (3) and σ^{-1} as a function d^{-1} if (2).

Note, that the direct approximation of experimental data by functions (2, 3) with three independent parameters is impossible, because for these dependencies there are coordinates in which they become linear, and the approximation with the straight line needs only two parameters.

1. Sondheimer E.H. The mean free path of electrons in metals // *Advances in Physics.* – 1952. – V.1, №1. – P. 1–42.

Effect of Ni Concentration in Soft Magnetic Layer on Isotropic Magnetoresistance of Three-Layer Co/Cu/Fe_xNi_{100-x} Films

Shkurdoda Yu.O., Chornous A.M., Saltykov D.I., Shuliarenko D.O.

Sumy State University, Sumy, Ukraine.

Co/Cu/Fe_xNi_{100-x}/S (S is the substrate) film samples with the layer thickness of 1 – 30 nm were obtained in the vacuum chamber at a pressure of 10⁻⁴ Pa at the substrate temperature 300 K. Magnetoresistance measurement (MR) and thermomagnetic film processing were accomplished under conditions of the ultrahigh oil-free vacuum (10⁻⁶ – 10⁻⁷ Pa) in the magnetic field (B = 0.2 T).

Studies showed isotropic field dependence of MR for the films before and after annealed at the temperature of 400 K with non-magnetic layer thickness of d_N = 5 – 15 nm. It was a sign of the giant magnetoresistance effect. Dependence of the isotropic MR value on the nickel concentration in soft magnetic layer for the Co/Cu/Fe_xNi_{100-x}/S three-layer films before and after annealed at different temperatures with different thickness of the intermediate Cu layer are shown in fig. 1. Maxima at nickel concentrations of 80% can be observed at the concentration dependences of MR for the films before and after annealed at a temperature of 400 K regardless of the Cu layer thickness (fig. 1a, b curves 1, 2). Maximum on the concentration dependence after samples annealing at the temperature of 550 K is observed only for films with a non-magnetic layer thickness d_N > 8 nm. It should also be noted that this maximum shifts to the area with lower nickel concentrations (fig. 1b curve 3).

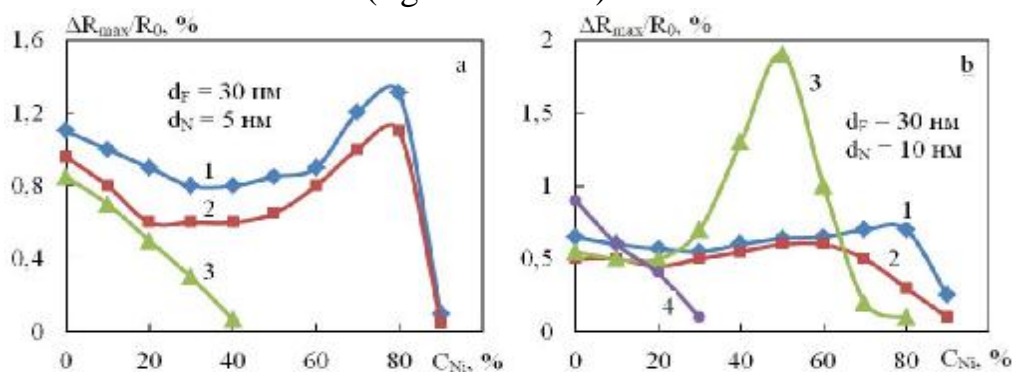


Fig.1. Dependence of the isotropic MR value on the Ni concentration in soft magnetic layer for three-layer Co/Cu/Fe_xNi_{100-x} films with different Cu layer thickness (1– as-deposited films; 2–T_{ann}= 400 K; 3–T_{ann}= 550 K; 4–T_{ann}=700 K).

For films annealed at the temperature of 550 K with d_N = 5 – 8 nm isotropic magnetoresistance value decreases only with the increase of C_{Ni} (fig. 1a curve 3). Similar dependence is also observed for films with d_N = 10 – 15 nm after annealing at the temperature of 700 K (fig. 1b curve 4). At the same time, Ni concentration range, in which the mechanism of spin-dependent scattering of electrons appears, is decreases.

The work been performed under the financial support of the Ministry of Education and Science of Ukraine (state registration number 0116U002623)

Luminescent Properties of $Zn_{0,88}Mg_{0,12}Se$ Diffusional Layers Doped with Rare-Earth Gd and Yb Elements

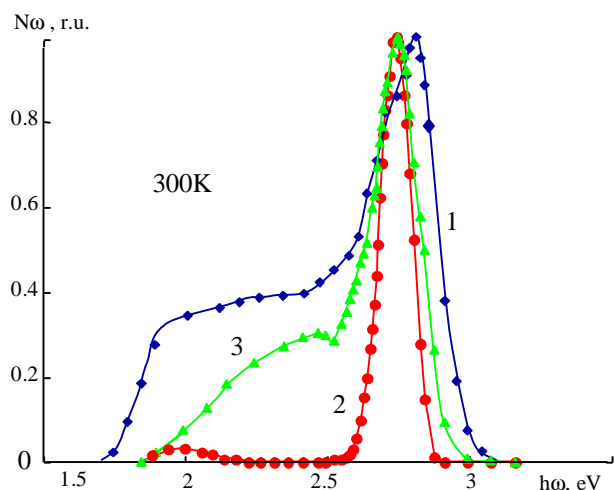
Makhniy V.P., Senko I.M., Slyotov O.M.

Yuriy Fedkovych Chernivtsi National University, Chernivtsi, Ukraine, illja.senko@yahoo.com

It is known, that doping of zinc selenide with isovalent impurity of Mg causes a significant increase of bound radiation and suppression of impurity luminescence bands [1]. In contrast the increase of concentration of Mg atoms in $Zn_{1-x}Mg_xSe$ solid solution causes diametrically opposite effects – the decrease of bound intensity and appearance of new low-energy emission bands. It is a result of a change in the chemical composition of material and appropriate transformation of quantitative and energy spectrum band of intrinsic point defects (IPD). On the other hand, the growth of molar part of Mg causes an increase of width of bandgap E_g of solid solution and expansion of the upper bound of the spectral and temperature ranges. In this regards, the actual task is a search and realization of different ways to decrease the concentration of IPD, caused by undesirable recombination channels in impurity absorption levels of a semiconductor. In such aspect promising can be crystals doped with rare-earth elements. They contribute to a sufficiently effective “purification” effect of material from uncontrolled impurities and defects [2]. In this work, luminescent properties of diffusional layer, obtained by diffusion of Gd and Yb impurities

from vapor phase in $Zn_{0,88}Mg_{0,12}Se$ monocrystalline substrates were studied.

It follows from the figure, that the strongest “purification” effect is observed in $ZnMgSe:Yb$ layers, curve 2. The Gd impurity “removes” the orange and somehow strengthens the green band (curve 3), which are also present in the base substrates, curve 1. The mechanism of formation and nature of the objects of research were observed.



[1] M.M. Slyotov Band luminescence of zinc selenide, doped with isovalent impurity of Mg / M.M Slyotov – Pisma JTF, - 2000 – t.27, bul. 2, p. 48-50.

[2] V.P.Makhniy Purification effects” in zinc selenide crystals doped with ytterbium from vapor phase / V.P.Makhniy O.V. Kinzerska, I.M. Senko //Telecommunications and Radio Engineering. – 2016 – 75(3), p. 279-284.

Optical Absorption and Compositional Disorder in Thin Films of As-Sb-S (Se)

Shpak I.I., Kunak S.J., Shpak M., Pop O.I.

Uzhgorod National University, Uzhgorod, Ukraine, shpak.univ@gmail.com

Found that when introduced into arsenic sulfide selenium (up to 15 at.%) and antimony (up to 12at.%) Absorption edge shifted to the long-wavelength region of the spectrum. The refractive indices n amorphous films $As_{40}S_{60-x}Se_x$ and $As_{40-y}Sb_yS_{60}$ determined at a wavelength of 710 nm with increasing concentration of Se and Sb increases, while dispersion curves $n(\lambda)$ shifted to lower energies.

Reducing optical pseudogap E_g with a slight change of inclination of the absorption edge in thin layers of the systems caused by restructuring in the transition from As_2S_3 to As_2Se_3 and Sb_2S_3 . This means that the type of structural variation in the composition of the matrix of amorphous films $As_{40}S_{60-x}Se_x$ and $As_{40-y}Sb_yS_{60}$ remains virtually unchanged. The main structural units forming the structure of the film is trigonal pyramid $AsS(Se)_{3/2}$, $SbS_{3/2}$ and $As(Sb)S_{3/2}$ in the presence of a significant number of molecular fragments homopolar bonds.

When irradiated with a laser ($\lambda = 530$ nm, $E = 95$ mW/cm²) thin layers set to shift to long-wavelength spectra of spectrum (is fotopotemninnya films), pointing to a decrease in the optical pseudogap. For all investigated films levels photoinduced changes of optical parameters decreases with increasing time of exposure. Changing the position and shape of the absorption edge, and n values E_g amorphous films caused by structural changes that occur in them under the influence of laser irradiation.

Amorphous films of As-S-Se and As-Sb-S characterized microheterogeneous structure, ie their structural matrix mainly based groups with ties heteropolyarnymy ($AsS(Se)_{3/2}$, $SbS_{3/2}$) in the presence of structural fragments called homopolar bonds. Irradiation of films leads to rupture and switchties arsenic and arsenic chalcogen-chalcogen in structural fragments As_4S_4 and chalcogen chains to form structural units of bonds heteropolyarnymy As-S, As-Se and Sb-S. This, in turn, leads to the polymerization of molecular groups located most optimal space in the grid trigonal pyramids with little change bond angles relations S (Se)-As-S(Se)-, S-As(Sb)-S . Higher, compared with $As_{40}S_{60}$, photosensitivity film $As_{40}S_{60-x}Se_x$ and $As_{40-y}Sb_yS_{60}$ with $x=12$ at.% and $y=4.6$ at.% Is explained by their greater of disordering matrix due to high content of structural fragments homopolar bonds.

Properties of α -ZnS_xSe_{1-x} Heterolayers

Slyotov M.M., Gavaleshko O.S.

Yuriy Fedkovych Chernivtsi National University, Chernivtsi, Ukraine

Zinc chalcogenides are widely used in devices of functional electronics. Further expansion of opportunities of their use in various systems of information transmission determines the necessity changes in properties of materials and produced on their basis of active elements for getting of a highly efficient optical communication. A significant attention is attracted by zinc selenide and sulfoselenide solid solutions, the bandgap E_g of which covers a short-wavelength range. However, it is possible to obtain new properties due to transition of their characteristic cubic (β) modifications to the hexagonal (α). Thus, searching of technology for obtaining of heterolayers II-VI compounds unlike widely used epitaxy of III-V materials is important.

Heterolayers of α -ZnS_xSe_{1-x} were obtained by isovalent substitution (IVS) [1]. Complex investigations of electro-physical, optical and luminescent properties were carried out. Using of highly sensitive methods of λ -modulation allowed to determine $E_g = 3.20$ eV, by which the composition of solid solution $x = 0.47$ was found. Investigation of optical reflection, allows to determine the energy structure which is typical for hexagonal lattice and its inherent value of spin-orbit interaction ($\Delta_{so} \approx 0.311$ eV) and crystal field splitting ($\Delta_{cr} \approx 0.066$ eV). It was found that obtained heterolayers are characterized by

intensive boundary photo-luminescence with a maximum $\hbar\omega_m = 3.155$ eV ($\lambda \approx 0.39$ μm). The spectrum covers violet and ultraviolet regions and formed by interband recombination of free carriers and dominant annihilation of bound exciton. The radiation is characterized by stability at change of temperature within 300-500 K. Characteristics and properties of radiation remains constant after repeated influence of temperature. Possibilities of practical use are discussed.

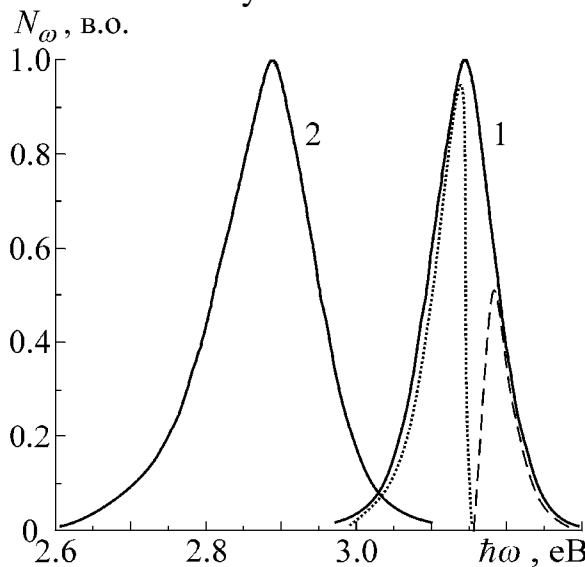


Fig. 1 Luminescence spectra of α -ZnS_xSe_{1-x} heterolayers (1) and α -ZnSe (2)

1. Makhniy V.P., Baranjuk V.Ye., Demich M.V., Melnik V.V., Malimon I.V., Slyotov M.M., Sobistchanskiy B.M., Stets E.V. Isovalent substitution – a perspective methods of producing heterojunction optoelectrical devices / SPIE. – 2000. – **4425**. – P. 272-276.

Study of Nanocolumnar Biaxial Films Using Conventional Multiangle-of-Incidence Monochromatic Ellipsometry

Sopinsky M.V.

V. Lashkaryov Institute of Semiconductor Physics, NAS of Ukraine, Kyiv, Ukraine

Oblique deposited films have a columnar microstructure which causes biaxial optical anisotropy. Such a films are the promising candidates for use in solar cells, as elements in narrow-band polarisation filters, phase elements, the elements of integrated photonic systems for communications, computation and other applications. Columnar biaxial thin films offer the designer greater flexibility – choosing the deposition angle allows tailoring principal refractive indices in predictable ways. There also are other applications of such a films. Specifically, oblique deposition of evaporated silicon monoxide makes it possible to vary the composition and structure of SiO_x films with inclined nanocolumns (those films are used for the formation of nc-Si-SiO_x nanocomposites).

In general, light reflection by nondepolarizing biaxial film is described by the (2×2) Jones reflection matrix with non-zero diagonal (r_{pp} , r_{ss}) and off-diagonal (r_{ps} , r_{sp}) terms. Measuring all four terms and solving the inverse problem of ellipsometry is the subject of generalized ellipsometry. This is much more difficult task from both experimental and theoretical point of view as compared to conventional ellipsometry that deals with diagonal terms only. That is why the goal of this work is to study the capabilities of conventional multi-angle-of-incidence monochromatic ellipsometry (CMAIME) to obtain the information on biaxial film. For this purpose the light incidence plane had been selected to match the vapor deposition plane. In this case $r_{ps} \equiv 0$, $r_{sp} \equiv 0$.

It has been established that for the known column tilt angle value the CMAIME makes it possible to determine the values of thickness and all three principal refractive indices of the film. To find the value of column tilt angle using just the dependence of ellipsometric parameters Δ and Ψ on the light incidence angle the necessary measurement precision should be better than the modern ellipsometers can provide. Without data on the column tilt angle value the CMAIME makes it possible to determine the values of the film thickness, refractive index for the axis perpendicular to vapor incidence plane, and the average refractive index in the vapor incidence plane.

The obtained values of the principal refractive indices of the oblique deposited at 60° biaxial SiO_x film have been considered on the basis of Bragg–Pippard model in which the columns are modeled as aligned ellipsoids of similar shape. Such a consideration has shown that the volume share of voids between the columns is less than 10% of the film’s volume, and the density of the columns is less than the density of normally deposited SiO_x film with the same stoichiometric index x .

Optical Percolation in Thin Gold Films

Bihun R.I., Stroganov O.V.

Ivan Franko Lviv national university, Lviv, Ukraine

The electrical properties of thin conductive layers and their interaction with electromagnetic radiation is a subject of interest in modern micro- and nanoelectronics industries [1]. The dimensional effect determines the physical properties of nanoscale metal films. Metal films of a few nanometers thickness are promising as ohmic conductors with high transparency, both in the visible and in infrared wavelengths. Since thin metal layer can be both in continuous and disperse phase (island) state, the question remains open about the conditions of transition from one state to another. The thickness of the metal film at which the transition from disperse to continuous state is observed called critical percolation thickness d_c . It is known that in the region of critical transition the metal film exhibits abnormal optical and electrical properties that can be explained within the percolation model [2-3]. The ability to control the d_c thickness percolation threshold will provide ohmic conductive metal connectors with high optical transparency in a range of thicknesses $d < 2-3$ nm.

Ultrathin metal films of Au and Ge underlayers were fabricated by the thermal evaporation on the glass substrate under high vacuum condition ($P \sim 10^{-7}$ torr) at the room temperature. Mass thicknesses of the films have been assessed by the shift of the resonance frequency of the quartz oscillator. Transmittance and reflectance spectra were measured by broadband spectrophotometer Shimadzu UV-3600.

The analysis of the size dependence of gold films transmittance (for wavelengths 1100 nm, 1500 nm, 1900 nm and 2500 nm) which were deposited on a clean glass substrate and on a glass substrate precoated with germanium underlayer with mass thickness of 0,5 nm have showed that the value of d_c for gold films deposited on a clean glass substrate is 6,4 nm, while for similar samples deposited on Ge underlayers with mass thickness of 0,5 nm, is $d_c = 4$ nm.

The analysis of infrared absorption of investigated gold samples showed the existence of maximum absorption for percolation transition thickness. In particular, it was found that for gold film deposited on a clean glass substrate the absorption maximum is $A = 0,21$, and for similar samples deposited on germanium underlayers the absorption maximum is $A = 0,3$. The observed behavior is caused by higher crystalline structure and more effective level of substrate occupation with gold film. Before percolation transition metal film is consisted with isolated islands, where the electronic subsystem is localized. The higher concentration of isolated islands, the more electrons is involved in plasmon resonance which leads to a high absorption ability of metal condensate.

1. A. Axelevitch, B. Gorenstein, G. Golan. *Physics Procedia.*– 2012.– V. 32.– P. 1-13.
2. P. Smilauer. *Contemporary Physics.*– 1991.– Vol. 32, № 2.– P. 89-102.
3. S. Ding, X. Wang, D. J. Chen, Q. Q. Wang. *Optics Express.*– 2006.– Vol. 14, Issue 4.– P. 1541-1546.

Photoinduce Mass-Transport in Amorphous Chalcogenides

Trunov M.L.¹, Rubish V.M.¹, Lytvyn P.M.²,
Durkot M.O.¹, Tarnaj A.A.¹, Pisak R.P.¹

¹ *Institute for Information Recording, NASU, Uzhgorod Ukraine*
center.uzh@gmail.com

² *V. Lashkaryov Institute of Semiconductors NAS Ukraine, Kiev, Ukraine*

Amorphous chalcogenides exhibit a number of remarkable changes of structural and optical characteristics at their laser irradiation. One of them is mass-transport included by bond-gap light. The prevailing opinion for a long time was that the modification of the surface of chalcogenide films due to their irradiation with light was only possible with their additional treatment using chemical etching. The discovery of the effect of photoinduced mass-transport under the influence of light at the absorption edge allowed obtaining surface topography purely by means of optical (one step) method and even at relatively low intensities of light waves. This method typically uses a projection of the interference pattern that is formed by the interaction of two or more coherent plane waves on the surface of chalcogenide amorphous films.

In this paper the experimental results showing the peculiarities of surface reliefs formation in chalcogenide As_xSe_{100-x} ($0 \leq x \leq 30$) amorphous films under laser exposure are presented.

Thin films (thickness $\sim 1-2 \mu\text{m}$) were deposited by vacuum thermal evaporation on Corning glass substrates. In the first series of studies the samples were irradiated from below through a transparent substrate using two coherent beams of solid-state laser with a wavelength of 650 nm ($E=1.9 \text{ eV}$) of equal power density that interfered on the film free surface and produced surface relief grating. In the second series of experiments the samples were irradiated from below through a transparent substrate using unfocused single beam of the same laser of random polarization.

It was shown that the parameters of induced mass-transport depend on irradiation conditions. Directions and velocity of the mass movement depends on the direction of polarization of exciting light, while the value of the induced surface distortion (trench or valley in the irradiated place) on the irradiation dose. It was established that under band-gap irradiation, the material of amorphous As_xSe_{100-x} films moves either towards the areas of maximum light intensity ($x > 4,5$), or, respectively, away from them ($x < 4,5$).

We have proposed a model of mass-transport in which the existence of moving anisotropic dipolar units and internal electric field in chalcogenide films as a main driving force of this movement is suggested.

It was shown that the studied materials have found applications in optical storage drives with high-density recording, holography and lithography, integrated optics.

Infrared Reflectance Spectroscopy of the GaN/AlN Superlattice Structures

Tsykaniuk B.¹, Kolomys O.¹, Strelchuk V.¹, Kladko V.¹, Li S.^{2,3}, Ware M.², Mazur Y.², Maidaniuk Y.², Benamara M.², Belyaev A.¹ and Salamo G.²

¹*V. Lashkaryov Institute of Semiconductor Physics, National Academy of Sciences of Ukraine, Kiev, Ukraine. btsykaniuk@gmail.com*

²*Institute for Nanoscience and Engineering, University of Arkansas, Fayetteville, USA.*

³*State Key Laboratory of Electronic Thin Film and Integrated Devices, University of Electronic Science and Technology of China, Chengdu, China*

Superlattice (SL) nitride structures have attracted a great deal of attention due to some unique properties and could be useful for infrared intersubband photonic devices operating in the telecommunication wavelength range (1.3-1.55 μm). IR reflectance spectroscopy is especially effective to provide information on the spatial variation of the thickness, lattice quality and dielectric function of various layers of multilayer structures.

The GaN/AlN SL samples were grown by plasma-assisted molecular beam epitaxy (PAMBE) under an activated nitrogen plasma flux in a metal-rich regime using GaN (4 μm)/c-plane sapphire templates as substrates. The SLs were deposited having GaN/AlN periods, repeated 5, 10, and 20 times, with quantum well and barrier thicknesses both maintained at 3 nm in all samples. Room temperature IR reflectance spectra were measured in mid-IR range (400-4000 cm^{-1}) using a FTIR spectrometer Bruker Vertex 70v. Spectral resolution was 1 cm^{-1} , number of scans – 64, angle of incidence - 11°. The reflection spectra are compared to the calculated spectra generated by the 2×2 transfer matrix method.

The complicated structure of the spectrum is observed in reststrahl region (400-1200 cm^{-1}) which is due combination of the overlapping AlN, GaN and Al₂O₃ reststrahl bands along with interference effect. Fit calculated spectra to this data can provide thickness information on the various layers of the samples and help to interpreted the complicated structure of reststrahl region in terms of the various material.

From the result of fitting procedure the dielectric permeability, dielectric function and appearance of phonon provisions.

The results of fitting procedures is set to dielectric permeability, dielectric function and phonon position of GaN template, GaN buffer, GaN-SL and AlN-SL are determination. With the appearance of the imaginary part of the dielectric function is obtained that with increasing of SL number the GaN well in SL is under compressive stress, while the AlN barrier is under tensile stress.

From the frequency shift of phonons of the GaN and AlN layers, the biaxial strains in the GaN/AlN superlattice layers were determined.

Photoconductivity and Photovoltaic Properties of Zinc Oxide Thin Films

Yavorskyi R.^{1,2}, Wisz G.², Virt I.^{2,3}, Nykyruy L.¹

¹*Vasyl Stefanyk Precarpathian National University, Ivano-Frankivsk, Ukraine,*
roctyslaw@gmail.com

²*Rzeszow University, Rzeszow, Poland*

³*Drohobych State University, Drohobych, Ukraine*

ZnO is one of the most promising materials for the fabrication of the next generation optoelectronic devices in the UV region and for application in optical or display devices [1].

ZnO thin films grown on silicon and ITO/glass substrates were obtained using PLD method in various substrate temperatures using pulse laser YAG:Nd³⁺ of wavelength 532 nm (second harmonics), time of impulse 6 ns and fluence 16 J/cm². The laser beam was focused on the target using a quartz lens with focal distance of 600 mm. The pressed ZnO powder was used as a target. The growth temperature T_s was kept at (25 – 400)°C and the deposition of the layers was carried out in vacuum at 10⁻⁸ mbar.

The correlation between the structural characteristics, properties and photovoltaic electric transport properties of films were evaluated by measuring of the photo response of films, especially, under UV irradiation. The photoconductivity response was performed with the illuminated light of 365 nm. The photocurrent for thin films with T_s = 300°C rises within 3 min and falls to 50 % of its maximum value within 6 min. The very pronounced photoconductivity effect is observed for samples with T_s = 300°C and 400°C after the annealing in oxide atmosphere. There is an extremely rapid excitation and fast relaxation occurring during the 280 sec. for the sample T_s = 400°C.

To determine of current-voltage characteristics, each sample was connected by soldering with metallic, silver wires used to measure the current on surface of cell. Samples were soldered in standard technique using classic soldering station. Examination of samples was made using solar simulator under constant condition for each sample. Properties of samples were investigated in dark and light conditions. Light conditions were obtained using lamp with power density 850 W/m².

It was shown, the efficiency decreased distinctly for the sample T_s=200°C with columnar type of growth. Layer with this structure is characterized by lower reflectance and acts as fibre, causing the increasing the amount of photons reaching the active region of p-n junction of silicon cells used as substrate.

[1] G.Wisz, I.Virt, P.Sagan, P.Potera, R.Yavorskyi. Structural, optical and electrical properties of Zinc Oxide layers produced by pulsed laser deposition method // *Nanoscale Research Letters*. – 2017. - 12: 253.

***In situ* Study of Size Dependence of Melting-Crystallization Phase Transformations in Bi-Ge System Fulfilled by Quartz Resonator Method**

Zelenina I.S., Minenkov A.A., Bogatyrenko S.I.

V.N. Karazin Kharkiv National University, Kharkiv, Ukraine

Nowadays there are a lot of data on the study of melting-crystallization phase transformations for free particles or thin films. Typically these objects are formed on non-interacting amorphous substrates. However, for binary systems such data is rather restricted, especially for the small characteristic sizes. Lack of data is due to the fact that nano-objects are extremely sensitive to various impurities. Hence, only *in situ* methods, i.e. those in which the formation and study of samples properties takes place in a single experimental cycle, allow to receive accurate information in proper way. Naturally, each *in situ* experimental method imposes certain experimental limitations. When using high-resolution transmission electron microscopy some difficulties with determination of the electron beam influence on the studied effects appear. Electric resistance measurement of the film system in which the film of a fusible component is between more refractory films can be used mainly for polycrystalline material with good electrical conductivity. Differential scanning nanocalorimetry (one of the most precise techniques) is well suited for materials with high thermal conductivity, i.g. as a rule for metals only. Therefore, there is a necessity to find a method that would allow investigating phase transitions in systems with practically any type of electrical conductivity and interaction between the components. In this study we have used a novel *in situ* method based on the quartz crystal as a phase transformations sensor to determine the size factor effect on Bi-Ge system liquid phase stability. The films under study were formed by sequential condensation of the components from independent sources in a high vacuum. Sample thickness was measured by changing resonant frequency of quartz crystal oscillation; whiles the boundaries of the liquid phase stability were traced using abrupt change in oscillation amplitude during heating and cooling. The temperature was controlled using a platinum resistor.

We have used two-, three- and multi-layer Bi-Ge films formed by successive condensation of components from independent sources in a high vacuum as objects under study. As a result of systematic research size dependences of melting and crystallization temperatures of Bi-Ge films have been built in a wide range (5-50 nm) of thicknesses. It has been found that the value of liquid phase supercooling in the Ge/Bi/Ge system with a layers mass thickness of 50 nm, is on about 30°C greater than value, which is typical for Bi/Ge samples. This result can be explained by the presence of the additional metal-semiconductor interface.

In addition, as a result of the experiments it was found that the method sensitivity limit allows us to investigate the melting and crystallization temperatures for films with thickness ranging from 10 to 100 nm, this result is in a good agreement with theoretical calculations. The technique, which significantly improves the sensitivity and allows the investigation in films with thickness less than 10 nm, have been suggested.



POSTER REPORTS

Session 4

Thin film compounds for electronic devices, nanoelectronics



Improvement of Methods for Study of Parameters of Semiconductor Structures

Berezhansky V.M., Boyko S.I., Kogut I.T., Holota V.I.

Department of Computer Engineering and Electronics, V.Stefanyk Precarpathian National University, Ivano-Frankivsk, Ukraine, E-mail: berezhansky@mail.ru

This paper describes practical implementation of the digital device used for measurement of electrical parameters and characteristics of semiconductor devices of various types.

Integrated structure manufacturing process requires ongoing monitoring of various electrical parameters of test structures that are made in a single technological cycle.

Improving manufacturing processes allows to create devices with fundamentally new characteristics. In process of introduction of new and improved to existing processes of integrated structures (diodes, field and bipolar transistors, thyristors, symistors et al.) manufacture it is always necessary to monitor electrical parameters of these structures. It is convenient to perform such control using computer processing of measured volt-ampere, volt-farad characteristics and others.

Computer processing allows to simultaneously conduct a statistical study of results and identify relationship between design and technological constraints of the process and real parameters of structures.

Structure of developed device consists of a microcontroller, precision digital-to-analog converter, generator of signals that are send to input of the analyzed element and module that transfers data to a computer.

The principle of the device is that the microcontroller controls the digital-to-analog converters that are built on resistor matrix to minimize the impact of noise compared to conventional digital-analog converters, and used to form various types of signals to be send to input study element.

As a result of statistical processing of test structures parameters can be made conclusions about the quality and characteristics of the major integrated circuit components, namely:

- to control the parameters of test structures in the manufacturing process;
- for inter-operation control of semiconductor devices in the manufacturing process;
- to analyze causes of production defects.

1. Simon M. Sze, Kwok K. Ng. Physics of Semiconductor Devices. John Wiley & Sons, 2006, - 832 p.

Evaluation of Ergonomic Parameters of Thin Film Displays

Bushma A.V.

Borys Grinchenko Kyiv University, Kyiv, Ukraine, o.bushma@kubg.edu.ua

The development of reliable and effective displays based on thin film elements implies the study of the functioning of the system elements under the influence of various operational factors. But also it requires the evaluation of ergonomic parameters of the quality of data representation: the accuracy of reading, the stability of perception, the impact on the visual analyzer of the operator, etc [1]. However, the analysis and evaluation of the ergonomic parameters of the information system requires considerable resources, since it involves the conducting of a large number of different tests, surveys, field trials including human participation. As a result, it is important to minimize the involvement and selection of experts and operators to determine the ergonomic characteristics of human-machine systems [2].

The work is devoted to the development of an effective and reliable method for estimating the ergonomic parameters of discrete semiconductor displays.

We propose a method for computer modeling of ergonomic studies based on the combination of imitation the flow of visual messages to the operator and the subsequent simulation of the operator's work when displaying data at a semiconductor display. Synthesis of test visual patterns is carried out by the simulator of the information area and the working environment of the operator. Mathematical modeling of pattern recognition of discrete messages on the information area is realized using an artificial neural network. Its analytical representation is based on the principle of the organization and functioning of biological neural networks - networks of nerve cells of a living organism, including the human brain. This approach provides a sufficiently high reliability of the simulation of the process of recognizing the visual patterns of data that are presented to the operator. Accumulation and processing of results is carried out by a specialized database management system.

The method of computer simulation of ergonomic studies on the reliability of the data obtained significantly exceeds the expert and calculation methods. So the resulting estimate of the ergonomic parameters of display devices is approaching a purely experimental one. At the same time, minimizing the need for human resources for research makes this method very promising.

1. Bushma A. V. Information security for optoelectronic ergatic system // Semiconductor physics, Quantum Electronics and Optoelectronics. - 2010. - Vol. 13, № 2. - P. 170-172.
2. Bushma A. V. Information processing in an optoelectronic display system // Semiconductor physics, Quantum Electronics and Optoelectronics. - 2011. - Vol. 14, № 2. - P. 222-227.

The Simulation of Integrated Resistive Elements for Microsystem-on-Chip

Holota V.I., Kogut I.T., Gryga V.M.

Vasyl Stefanyk Precarpathian University, Ivano-Frankivsk, Ukraine, gvi@pu.if.ua

The integral resistive elements are important element of microsystem-on-chip of sensory type. These elements can be formed on the basis of thin-films, in particular silicon-on-insulator (SOI), polysilicon films, polisilicon films with SOI structure or other type. The resistive elements on the basis of such films can be formed as elements of microsystems on a chip [1], in particular, on the surface of the special technological area that covered by the silicon oxide or integrated on membranes surface, or formed as movable beams. The resistive elements of such type can be sensible to the changes of external pressure, deformations, temperature and other external influences.

For registration of resistance changes under the action of external factors are developed direct measuring schemes of active pure resistance changes on the basis of integral SOI CMOS transistors and resistive structures and also a computer simulation is get an estimation of sensitivity parameters. The investigated functional schemes for measuring of resistance changing of integral resistive element are represented on Fig.1, a, b [2].

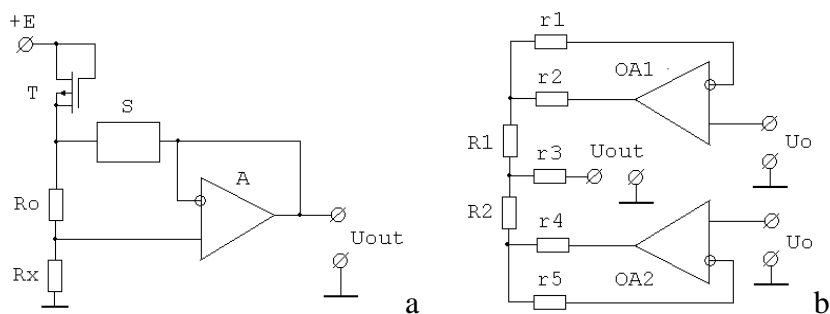


Fig. 1. The investigated functional schemes for measuring of active resistance changing of integral resistive elements realized in microsystem-on-chip with SOI structure.

The shown functional schemes are realized on the basis of integral SOI-structures. The sensitive resistive elements are formed on a technological area after the CMOS-process adapted to SOI-technology, and schemes of the primary signal processing are realized in microsystem matrix part on base cells [3].

In the scheme on Fig. 1, are proposed the stable current source on the basis of p-channel SOI MOS-transistor for displacement of resistance transformer, scheme of voltage stabilizing for forming of supporting voltage and operating amplifier on the basis of SOI CMOS-transistors.

Design results show that the proposed functional schemes with an integral resistive element and scheme of the primary signal processing on SOI structure provide the coefficient of sensitivity to 300-350.

1. Druzhinin A. Electrical and layouts simulation of analytical microsystem-on-chip elements for high frequency and low temperature applications / A. Druzhinin, Y. Khoverko, V. Dovhij, I. Kogut, V. Holota // UkrMiCo'2016. – Kyiv, 2016. – P. 29-32.

2. Vuytsik V., Holyaka R., Kalita V., Lopatyns'kyy I., Nevmerzhyts'ka O. Ananalohova mikroskhemotekhnika vymiryuvannya ta sensorykh prystroyiv / Za redaktsiyeyu Hotry Z., Holyaky R. – L'viv: Vydavnytstvo Derzhavnoho universytetu "L'vivs'ka politekhnika", 1999. – 364 c.

3. Patent # 62994 Ukrainy na korysnu model'. Komirka bazovoho matrychnoho krystalu / A. O. Druzhynin, I. T. Kohut, V. I. Holota, Yu. M. Khoverko, V. V. Dovhyy, A. M. Vuytsyk – MPK G01B 7/16(2006.01), G01L 9/14(2006.01), opubl. 26.09.2011, byul. #18/2011.

Structure and Physical Properties of Lead Chalcogenide Films Under the Influence of External Factors

Klanichka Yu.V., Klanichka V.M.

Vasyl Stefanyk Precarpathian National University, Ivano-Frankivsk, Ukraine

The regularity of reformation of chemical and phase compositions, real structure both as-grown films of lead chalcogenides and tin telluride and those influenced by thermal effect in atmospheric oxygen and vacuum is determined [1,2].

The heterogeneity in their thickness is found. It is demonstrated that degradation processes are determined by the condition of condensate crystal structure, temperature and annealing time. Within the limits of the average free path of charge carriers, drift barrier and Petric model of double layers kinetic parameters of films with different structure (monocrystal, polycrystal) are calculated and it is determined their dependence upon thickness.

It is demonstrated that due to the dispersion of charge carriers on grain boundary the average length of free run of the charge carriers in polycrystal films is vastly less than in monocrystal and depends significantly upon temperature. The electrical parameters of near-surface layers and the value of energetic barriers are determined.

The research was conducted as to the dependence of electrical parameters of polycrystal films of lead chalcogenides with different thickness $d=(20-250)$ nm from the oxygen pressure $P_{O_2}=10^{-4}-10^4$ Pa. There are two different mechanisms of oxygen acceptor interaction with the thin films surface which are connected with replacement of chalcogenide in anionic interlattice and rootage main matrix between nodes. It is also proposed their crystal-chemical models.

It is determined the degradation processes at isochronous and isothermal annealing of lead chalcogenides, tin telluride of different structure, type of conductivity, initial carrier concentration in the open air and explained by introphase and phase processes with oxygen involvement.

It is demonstrated that the complicated character of electric parameters change at vacuum annealing kept in the open air films is caused by the oxygen and chalcogenide desorption and demonstration of their own conductivity.

1. Boykov Yu.A., Kutasov V.A. Vlyyanye adsorbyrovannoho kysloroda na elektrofyzicheskye svoystva plenok PbTe // Fyzyka tverdoho tela. – 1983. – T.25, #4. – S.1248–1251.

2. Boykov Yu.A., Kutasov V.A. Yzmenenyia kontsentratsyy y podvyzhnosity nosyteley zaryada v plenkakh posle zavershenyya protsessa kondensatsyy // Fyzyka tverdoho tela. – 1981. – T.23, #8. – S.2527–2529.

The Development and Simulation of Capacitive Sensor Elements for Microsystems-on-Chip

Kogut I.T., Dovhyi V.V., Holota V.I.

Vasyl Stefanyk Precarpathian National University, Ivano-Frankivsk, Ukraine,

igorkohut2202@gmail.com

In this paper the results of investigated for using the ring oscillator which based on "silicon-on-insulator" structures (SOI) as the primary processing information circuit from integrated capacitive sensors in the Systems-on-Chip (SoC) are presented.

The proposed electrical circuits of the sensing element, which consist of 7-stage ring oscillator and the capacitive sensor is shown on Fig. 1, a. Developed layouts of the electrical circuit and scheme-topological simulation results are shown in Fig. 1, b and Fig. 1, c respectively.

For simulate this circuit directly from layouts were used capacitors formed by layers of metal-metal, metal-polysilicon, polysilicon-silicon-in-insulator. For Systems-on-Chip prototypes can be used in variable sensitive capacitance as movable membranes, beams and comb-type capacitors, the capacity of which is influenced by the environment, for example, gases.

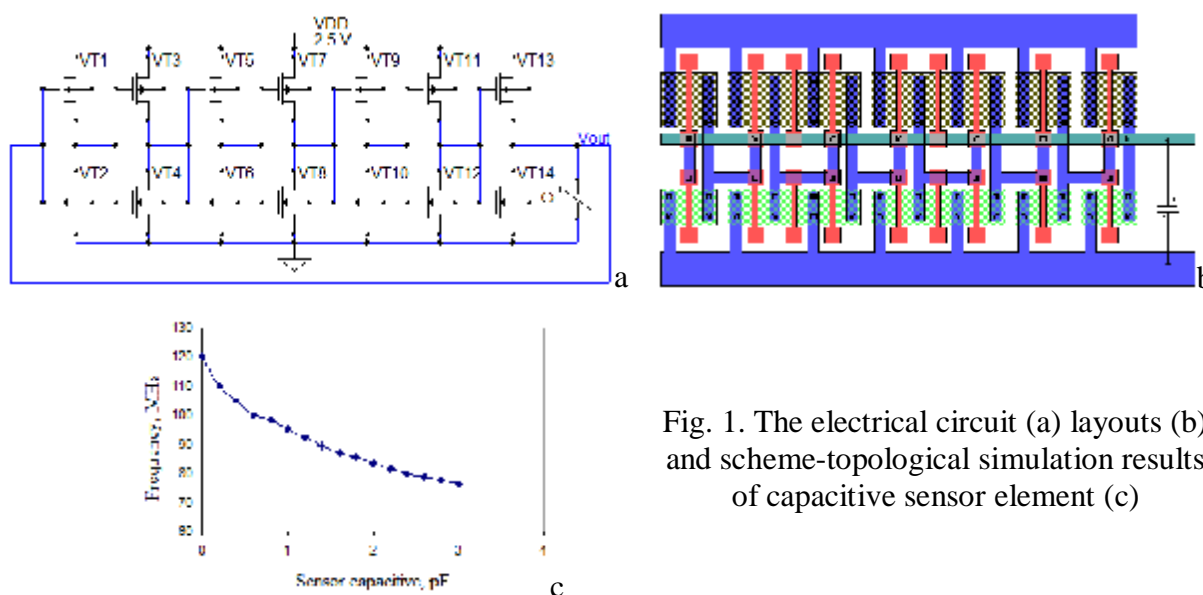


Fig. 1. The electrical circuit (a) layouts (b) and scheme-topological simulation results of capacitive sensor element (c)

The scheme-topological simulation results of the proposed sensor elements directly from the layouts are shown their high sensitivity. A small change in capacitance of the sensor leads to significant changes in the frequency of the ring oscillator. For example, by changing the capacitance from 1 pF to 2 pF the frequency oscillation ranges from 95 MHz to 83 MHz, which is approximately 10%. The obtained results can be used in the design of sensors System-on-Chip and others devices with SOI-structures.

1. Druzhinin A. Electrical and layouts simulation of analytical microsystem-on-chip elements for high frequency and low temperature applications / A. Druzhinin, Y. Khoverko, V. Dovhij, I. Kogut, V. Holota // UkrMiCo'2016. – Kyiv, 2016. – P. 29-32.

Study of Dependence of Electron Beam Induced Surface Relief Formation on Ge-As-Se Thin Films on the Film Elemental Composition

Kuzma V.^a, Bilanych V.^a, Kozejova M.^b, Hlozna D.^b, Mynda A.^b, Feher A.^b,
Rizak V.^a, Komanicky V.^b

^a Faculty of Physics, Uzhgorod National University, Uzhgorod, Ukraine

^b Faculty of Science, Safarik University, Kosice, Slovakiakuzmavasil.v@gmail.com

We studies interaction of electron beam with surfaces $\text{Ge}_x\text{As}_y\text{Se}_{100-x-y}$ films with different composition. The mean coordination number for studied films was in the interval from 2.27 to 2.80. It is shown that an extent and a value of local surface alterations cause by interaction of the film with electron beam follow the composition related parameters. Two intervals of the local electron irradiation doses, which are separated by a point of the surface relief inversion, are found. When local electron dose is from 9.3 to 0.3 $\text{C}\cdot\text{cm}^{-2}$ the electron beam induces formation of cones with Gaussian profile on surfaces of the films. In dose interval from 4.6 to 93.0 $\text{C}\cdot\text{cm}^{-2}$ we observe formation of craters. Surface relief relaxation times in these dose intervals can be also defined. We find that formation a surface relief in $\text{Ge}_x\text{As}_y\text{Se}_{100-x-y}$ thin films 1 μm thick has identical character. The mechanism of formation of such relief can be explained by the formation of a two-layer space charge region and its further electrostatic interaction. The size parameters of electron induced surface reliefs for the films with different concentration of constituting elements are function mean coordination number Z . It is shown that the extreme values of the size parameters of the surface relief, as well as inverse dose are observed in the films which have a minimum electrical conductivity.

Lateral Junctions Based on Graphene with Different Doping Regions

Balabai R.M., Lubenets A.G.

Kryvyi Rih State Pedagogical University, Kryvyi Rih., Ukraine

Laterally stitched heterostructures can only be grown by direct synthesis, since 2D layered materials (2DLMCs) are covalently bonded laterally. These heterostructures exhibit diode-like behaviors such as gate-modulated current rectifying properties and photovoltaic responses. Further work, especially on lateral heterostructures, is needed to both explore fundamental study and develop practical applications [1]. Most of the reports on 2DLMCs is currently based on the transferred heterojunctions, which may harm the electronic properties due to the dangling bonds and adsorbates at the interface.

Graphene is an ideal template to promote the nucleation and growth of other 2DLMCs crystals for producing functional hybrid structures via CVD method, which may result in the modulation of the electric and optical properties coupled with graphene [2]. For extension of information about electronic properties of lateral junctions based on graphene with different doping regions (see Fig. 1) they are calculated with such methods as electron density functional and first-principles pseudopotential based on own program code [3]. Fig. 1 demonstrates the charge regions of different densities, which can become the basis for creating a p-n junction.

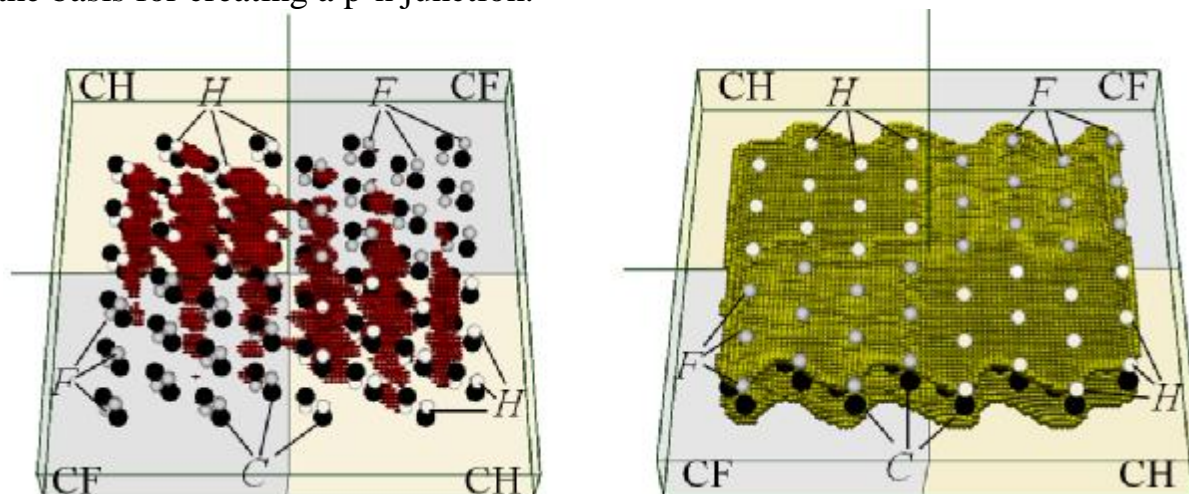


Fig. 1. Spatial distributions of the valence electrons density on the lateral coplanar 2D heterojunctions based on graphene with different doping regions: (left) within the interval of 1.0-0.9 of the maximum value, (right) within the interval of 0.6-0.5.

1. M.-Y. Li, C.-H. Chen, Y. Shi, L.-J. Li, *Mater. Today* (2015).
2. X. Zhou et al., *Adv. Sci.* 3, 1600177 (2016).
3. Ab initio calculation [E-resource]. – Access mode: <http://sites.google.com/a/kdpu.edu.ua/calculationphysics>.

CVC of Thin Film Heterostructures CdSe-Cu₂ZnSnS₄

Maistruk E.V., Koziarskyi I.P., Koziarskyi D.P.

Yuriy Fed'kovytch Chernivtsi National University, Chernivtsi, Ukraine

Investigated the electrical properties of heterostructures CdSe-Cu₂ZnSnS₄.

The heterostructures were formed on a ceramic glass substrate coated with a layer of molybdenum, which served as the rear contact. On the layer of Mo inflicted the thin film Cu₂ZnSnS₄ p-type conductivity and thickness $d = 2 \mu\text{m}$. Then deposited a thin film CdSe n-type conductivity thickness $d = 200 \text{ nm}$.

Films CdSe, Cu₂ZnSnS₄ obtained in the universal vacuum system YBH-70. To produce heterostructures used a target of pressed powders of synthesized CdSe and Cu₂ZnSnS₄. Targets sprayed in an atmosphere of Ar gas using magnetron sputtering in the AC voltage. Layers placed on the oven over the magnetron, which allow maintaining the temperature between room and 600°C. Cu₂ZnSnS₄ films temperature is maintained at 450°C, and for CdSe – 300°C. Before spraying process was obtained a residual pressure of $5 \cdot 10^{-3} \text{ Pa}$ in vacuum chamber. The process of sputtering films of CdSe and Cu₂ZnSnS₄ lasted 10 minutes and 60 minutes respectively.

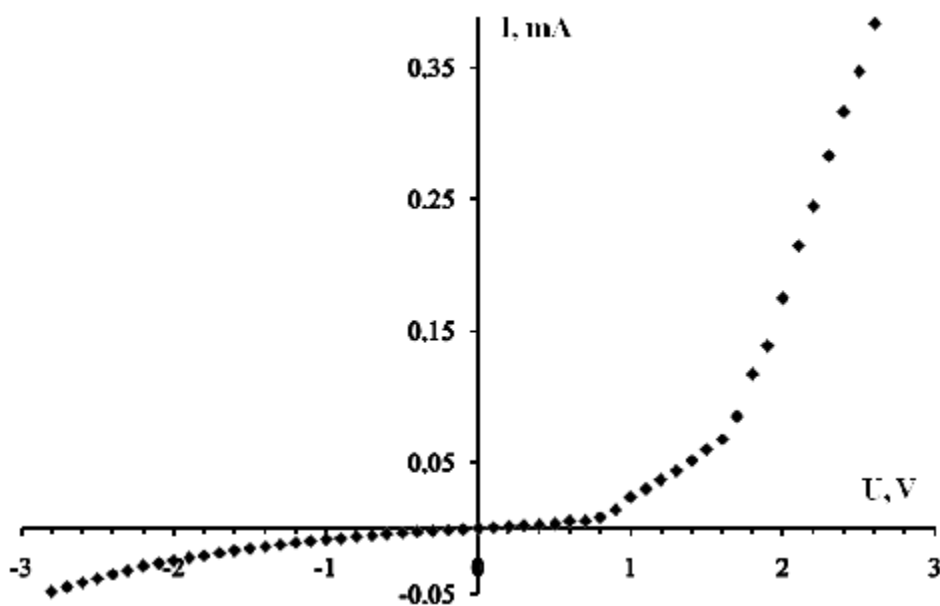


Fig.1. CVC of heterostructure n-CdSe/p-Cu₂ZnSnS₄ at 300°C

Height of the potential barrier of heterostructure n-CdSe/p-Cu₂ZnSnS₄ at room temperature is 0.7 eV.

Rectification coefficient of structure is $n=9.1$ at a voltage of 2.5 V at room temperature.

Defined transition series resistance $R_S=2.86 \text{ k}\Omega$. This value series resistance due to the high resistivity base material Cu₂ZnSnS₄.

Simulation of Performance of Measuring Computing System for High-Speed LSI/VLSI in Signaling CAD

Novosjadly S., Terletsky A., Fryk O.

*Vasyl Stefanyk Precarpathian National University, Ivano-Frankivsk, Ukraine,
andrii.terletskyi@pu.if.ua*

The performance of modern measuring computer systems is determined mainly by the performance of their components – LSI/VLSI and increasingly depends on the signal delay in interconnection (transmission lines) that take up to 65-75% of the integrated circuit. It was established, that bus time constant remains unchanged at increasing integration degree and the corresponding shrinkage of the interconnect, but the reliability of LSI/VLSI reduces because of electromigration processes in interconnection and contacts.

To improve the performance the operating temperature can be reduced down to cryogenic temperatures (77 K, 4,2 K). It reduces the resistance of the metal (policide) wiring and increases the reliability of LSI/VLSI due to reducing the intensity of electromigration processes, especially for GaAs-structures because they thermal conductivity is 2-3 times lower than the same for silicon. High-temperature superconductors (alloys of Al, Nb, V) are more promising for wiring both on the printed circuit board and on chip LSI/VLSI.

It were been a computer simulation: a) multiplexing circuit of measurement system; b) parameters of the GaAs-Schottky field-effect transistor as an active element of LSI/VLSI; c) comparing of parameters of aluminum (policide) and superconducting wiring in LSI/VLSI structures. In this case, to estimate the cutoff frequencies it was taking into account not only transmission lines parameters of computer system, but the characteristics of transistor as active structures elements of LSI/VLSI loaded on the line.

Simulation results show that system performance is determined by the time constant of transmission line delay and does not depend on the parameters of speed Schottky FET with Al-wiring at 300 K. For cryogenic (77 K) temperature the performance depends on both these factors, the delay in Schottky FET is the main factor limiting system performance in the case of superconducting wiring. Moreover the delay in Schottky FET is reduced due to use of superconducting materials to form electrodes of Schottky barriers.

1. Novosjadly S.P. Physical and technological bases submicron VLSI [Fizyko-tehnologichni osnovy submikronnoi tehnologii VIS] Ivano-Frankivsk, Simyk Publ., – 2003, – 351 p.

2. Novosjadly S.P. Sub- and nanomicon technology of VLSI structures. – Ivano-Frankivsk, MistoNV Publ., – 2010, – 455 p.

The Modifications of Structure of Carbon – Nitride CN_x Films Under the Pulsed Laser Irradiation Impact

Uvarov V.S.¹, Prudnikov A.M.¹, Fedorenko L.L.², Medvid A.³, Onufrijev P.³,
Pashchenko A.V.¹

¹ Donetsk Institute for Physics and Engineering named after O.O.Galkin NAS of Ukraine, Kyiv, Ukraine, grandevartist@yandex.ru, anatoliy.prudnikov@hotmail.com

²V.E. Lashkaryov Institute of Semiconductor Physics NAS of Ukraine, Kyiv, Ukraine, leonfdrn@gmail.com

³Riga Technical University, Riga, Latvia, medvids@latnet.lv

A lot of attention is paid to thin films due to the possibility of their wide applications in the hydrogen power engineering, production of electrochemical probes et al. Despite the large number of experimental and theoretical works concerning CN_x compositions, currently there are a number of unresolved problems that start their production technology to the peculiarities of the electronic structure.

The series of samples of the nanostructured carbon nitride CN_x films have been synthesized by reactive magnetron sputtering of the graphite target. Scanning electron microscopy and optical spectroscopy have been showed that different types of nanostructures (graphite-like, fullerene-like, diamond-like and nanocolumnar) are formed in the carbon nitride films.

The modification of the carbon nitride structure occurs at heating during growth process. However, there are unresolved problems in the technology of thermal annealing.

In this regard, the greatest advantages have a laser annealing. An obtain in the large structured regions of this material is provided by a computer scan mode.

The carbon nitride CN_x films on glass substrate have been irradiated by the nanosecond pulses of Nd^{3+} :YAG laser ($\lambda = 0.532 \mu m$, $t_p = 10 ns$). The intensity of the laser pulse varies in the range of 0.01 to 3 GW/cm².

After pulse laser annealing the structure features of carbon nitride CN_x films have been investigated by Raman spectroscopy. The two-peak structure with features of D and G near 1385 and 1580 cm⁻¹ has been observed. The use of a high power laser leads to a significant graphitization. A decrease in the intensity of the spectral "wing" in the region of 1000 cm⁻¹, where the characteristic frequencies of the C-N bond are located, testifies a decrease in the amorphization of the structure during a low laser power. G - peak with frequency of 1580 cm⁻¹ is due to the presence of sp²-hybridized carbon atoms and is a specific for a disordered graphite. The high intensity of the D mode 1385 cm⁻¹ indicates the presence of defectiveness of the nanocolumns structure after laser irradiation. It is connected with defects of the structure of nanocolumns as well as the mutual vibrations of both carbon and nitrogen atoms embedded in the nanocolumns structure forming the C = N bond.

Structural Properties of CdS:Dy Films Obtained by Close-Spaced Vacuum Sublimation

Yeromenko Y.S.¹, Opanasyuk A.S.¹, Opanasyuk N.M.¹, Gnatenko Yu.P.²

¹ *Sumy State University, Sumy, Ukraine*

² *Institute of Physics of National Academy of Sciences of Ukraine, Kyiv, Ukraine*

E-mail: yuri.yeromenko@gmail.com

Cadmium sulfide (CdS) is a well-known II-VI chalcogenide semiconductor compound with *n*-type conductivity. CdS is one of the most perspective materials for the optoelectronic devices and thin-film solar cells. The recent investigations show that the appropriate doping by the rare earth elements leads to the improvements of the properties of the window layers. Such impurities create the deep-level emission centers inside II-VI compounds, resulted in the optical conversion of the solar irradiance with the lowered frequency, which in turn can increase the efficiency of solar cells. However, there is a lack of the works devoted to the study of CdS thin films doped by the rare earth elements.

In this paper we investigated the effect of the substrate temperature on the structural properties of CdS:Dy thin films.

The thin films were deposited by the close-spaced vacuum sublimation (CSVS) method onto the cleaned glass substrates using the VUP-5M equipment. Samples were deposited on the cleaned glass substrates. The evaporator temperature was $T_e = 1173$ K, the substrate temperature was varied in the range of $T_s = 573-773$ K. The condensation time was $t = 4$ min. X-ray diffractometer DRON 4-07 in Ni-filtered K_α radiation of cobalt anode ($U = 30$ kV, $I = 20$ mA) was used to study the structural properties. The measurements were carried out in the range of 2θ angles from 25° to 95° , where 2θ – Bragg's angle. The obtained curves were normalized to (002) peak intensity of the hexagonal phase. The phase analysis was performed by comparing the interplane distances and relative intensities of the obtained samples with the data according to JCPDS standards. A detailed description and scheme of the device for deposition of the thin films, and the methodology of the studying of the structural properties are available in [1].

As the result of the investigations, it was established that CdS thin films had the hexagonal structure with [002] growth texture for the samples with different condensation temperatures. It was determined the substrate temperature effect on the lattice constants, coherent scattering domain sizes, microstrains, and other structural parameters of the material.

1. Substrate-temperature effect on the microstructural and optical properties of ZnS films obtained by close-spaced vacuum sublimation / D. Kurbatov, A. Opanasyuk, H. Khlyap [et al.] // *Phys. Status Solidi*. – 2009. – № 7. – P. 1549–1557



POSTER REPORTS

Session 5

Functional crystalline materials: growth, physical properties and applications



Processing of X-Ray Diffractograms of TiN Thin Films Using Wavelet Transforms

Balovsyak S., Fodchuk I., Roman Yu., Solodkyi M.

Chernivtsi National University, Chernivtsi, Ukraine, ifodchuk@ukr.net

X-ray diffractograms in the area of small reflection angles θ usually have strong high-frequency noise and non-homogeneous background, which gradually decreases with increasing angle θ (fig. 1). These effects, of course, make analysis of these curves more difficult. The wavelet filtration can be used for preliminary processing of diffractograms such as ones obtained from TiN thin films, what allowed us to reduce the influence of the aforementioned effects.

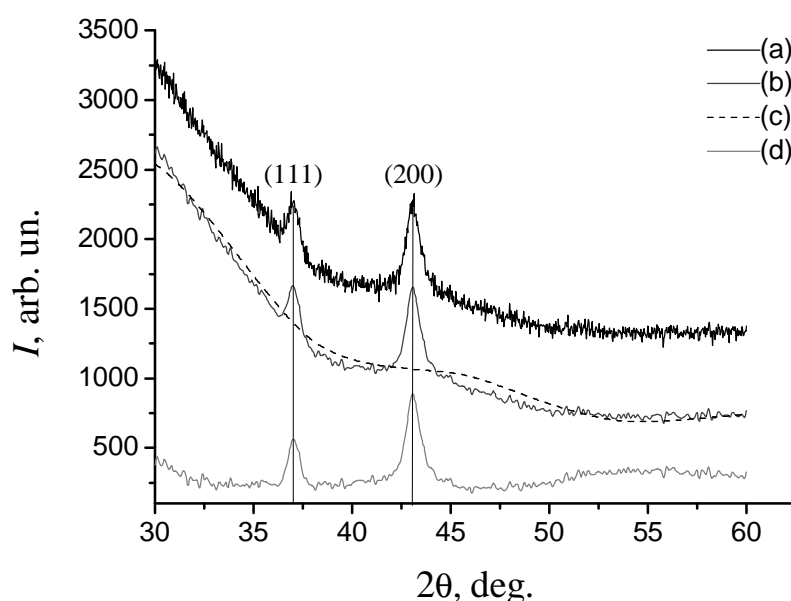


Fig. 1. X-ray diffractograms of TiN thin films: *a*) without processing; *b*) after elimination of high-frequency noise; *c*) background obtained by reduction of the contribution of average and high frequencies keeping only level D9 coefficients (biorthogonal wavelet); *d*) useful signal obtained subtracting *b* from *c*.

Wavelet analysis of X-ray curves is performed in Matlab by means of “Wavelet Toolbox” kit [1]. One-dimensional discrete wavelet transforms (DWT) are preferable, as soon as in comparison with a continuous wavelet transformation, it requires fewer resources, while ensuring the proper accuracy of obtained processing results.

The proposed approach greatly simplifies further analysis of curve and improves the accuracy of determining the characteristics of studied films. For TiN thin films for $a=0.42$ nm, grain size is $D \approx 13.5$ nm, and the value of microstrain is $\epsilon \approx 11.4 \cdot 10^{-3}$.

1. Gonzalez R., Woods R., Eddins C. Digital image processing in MatLab. - Moscow: Technosphere, 2006. - 616 p.

Crystal-Chemistry Defects and Their Complexes and Thermoelectric Properties of Solid Solutions on the Basis of PbTe, SnTe, GeTe

Boryk V.V.

Vasyl Stefanyk Precarpathian National University, Ivano-Frankivsk, Ukraine

On the basis of unique crystal-chemistry approaches which consider a complex spectrum of point defects in PbTe (V_{Pb}^{2-} , V_{Pb}^{-} , V_{Te}^{2+} , Pb_i^{2+} , Te_i^0 , $V_{Sn(Ge)}^{2-}$, $V_{Sn(Ge)}^{4-}$), in p-SnTe(GeTe), disproportionation charge conditions of M (Ga, In, Tl) impurities of in Plumbum Telluride crystals according to doping mechanisms of n- and p-PbTe: M for the first time are explained, formation of solid solutions in systems n- and p-PbTe-MTe (M_2Te_3) and their influence on physical and chemical properties of a material.

It is shown, that dominant doping of M (Ga, In, Tl) Plumbum Telluride it is necessary to consider as mechanisms replacement cation vacancies in crystals p-PbTe<Te>: M, or completion cation sublattice, in n-PbTe<Te>: M from the account of size disproportionation charge conditions of an impurity and their concentration N. Under conditions of realization thermodynamic n-p-(PbTe<Pb>: Tl) and p-n-(PbTe<Te>: In) transitions the certain value disproportionation charge conditions of impurity Z, which make $Z = 0.56$ ($N_{Tl^{1+}} = 1.7 \cdot 10^{19} \text{ cm}^{-3}$, $N_{Tl^{3+}} = 1.3 \cdot 10^{19} \text{ cm}^{-3}$) and $Z = 0.37$ ($N_{In^{1+}} = 1.1 \cdot 10^{19} \text{ cm}^{-3}$, $N_{In^{3+}} = 1.9 \cdot 10^{19} \text{ cm}^{-3}$) accordingly. Thus with increase in size of an initial deviation from stoichiometry on the side tellurium in basic matrix PbTe the size disproportionation ions impurity decreases.

For the first time are offered the crystal-quasichemical formulas, calculations and experimental researches dependences concentration of point defects, free carriers and Hall's concentration of charge from value of a deviation from stoichiometry and structure in n-PbTe<Pb>: Mn(Cr), p-PbTe<Te>: Mn(Cr), PbTe-MnTe ($MnTe_2$, CrTe, Cr_3Te_4), on the basis of which established defect subsystem and nature of doping and formations of solid solutions also conditions of realization thermodynamic p-n-transition are certain.

It is established that by the basic physical and chemical and technological directions of thermoelectric parameters of materials optimization of on the basis of PbTe, SnTe, GeTe, there is a reduction of size of heat conductivity (χ), growth of electric conductivity (σ) and activity of dot defects and maintenance of noncentral accommodation ions of impurity in solid solutions which opens prospect of their use in devices of alternative energy sources and refrigerating modules.

Multi-Layer Model of Growing Diamonds for HPA with a Large Reaction Volume

Burchenia A. V., Bovsunivskiyi O. V., Lysakovskiyi V. V.,
Kalenchuk V. A., Gordeev S. O., Hutsu O. S.

Institute for Superhard Materials NAS of Ukraine, Kyiv, Ukraine, bur4enia@bigmir.net

Intensive development of high pressure technology, that used to obtain diamond single crystals, led to creation of high-pressure apparatus (HPA) with a volume of working space 150 mm³ or more. There was a possibility of increasing growing layers for this kind of machines. In order to use multi-layer model needs to precise control of temperatures and temperature gradients. Ensuring of sufficiently close values of temperature and same values of temperature gradients in each of the growth layers is main challenge to implement multi-layer model.

The results of studies for diamond single crystals growth in HPA type "toroid" with volume of working space of ≈ 42 cm³ allowed to formulate requirements to the conditions needed for use multi-layers model for six-anvil HPA with a much larger working space (up to 180-200 cm³). Growth cell must meet the following requirements:

1. Temperatures in area of initiating growth on the surface of diamond seed must be in range of 1380–1450 °C;
2. Temperature difference in area of initiating growth of diamond between growth layers should not exceed 40 °C;
3. The magnitude of the temperature gradient within each growth layer should not exceed 3–5 °C/mm.

To conduct research for diamond single crystals growth we used six-anvil HPA model CSVII with volume of working space ≈ 180 cm³. Method of mathematical modeling was used for construction growth cell and selection of required configuration of resistive heating system. Calculation of distribution temperatures and temperature gradients showed that the temperature in the area of initiating growth of diamond for top and bottom growth layers will be 1385 and 1410 °C, respectively, and temperature gradients for upper and lower layers should not exceed 4.0 and 4.7 °C/mm, respectively. Required temperatures and temperature gradients were carried out by resistive heating system, which was formed from two dispersion-composite heating elements based on conductive and dielectric components. As a metal-solvent carbon was used alloy Fe + Al (4 wt. %).

At this conditions were obtained for 13 structurally perfect diamond single crystals with a total weight of 22.5 ct, the average weight of a diamond single crystal was 0.7 ct. The results of IR spectroscopy showed that the obtained samples can be attributed to the diamond crystals type IIa (nitrogen content not exceeding 5 ppm).

Optical Properties of RbPb₂Br₅ Optoelectronic Materials

Denysyuk N.M.¹, Khyzhun O.Y.¹, Tarasova A.Y.², Isaenko L.I.²

¹Frantsevych Institute for Problems of Materials Science, NAS of Ukraine, Kyiv, Ukraine

²Institute of Geology and Mineralogy, SB RAS, Novosibirsk, Russian Federation

Rubidium dilead pentabromide, RbPb₂Br₅, belongs to a fascinating family of lead-containing halides with the common formula APb₂X₅ (where A = K, Rb, Tl; X = Cl, Br) which, in recent years, have attracted significant attention from both scientific and technological viewpoints. The RbPb₂Br₅ compound crystallizes in tetragonal symmetry (space group *I4/mcm*) with the unit cell parameters $a = 8.4455 \text{ \AA}$ and $c = 14.5916 \text{ \AA}$ [1] or $a = 8.437 \text{ \AA}$ and $c = 14.572 \text{ \AA}$ [2].

Fig. 1. presents the measurements of the fundamental absorption edges made at 80 and 300 K have indicated that the edge position for RbPb₂Br₅ depends on the polarization. In particular, the fundamental absorption edges for RbPb₂Br₅ at 80 and 300 K are found to be shifted toward higher energies by 0.03–0.05 eV in the case of $E \parallel c$ compared to those in the cases of $E \parallel a$ and $E \parallel b$ polarizations. Furthermore, the band gap values, E_g , measured for RbPb₂Br₅ at 300 K for $E \parallel c$ are determined to be $3.47 \pm 0.1 \text{ eV}$, while for of $E \parallel a$ and $E \parallel b$ polarizations $E_g = 3.42 \pm 0.1 \text{ eV}$. The above E_g values are found to increase by about 0.19 eV as temperature of RbPb₂Br₅ decreased from 300 to 80 K.

The absorption coefficient spectrum near the fundamental absorption edge shown in Fig. 2. The evaluated optical band-gap energy (for absorption at $\alpha = 100 \text{ cm}^{-1}$) was varied within 2.52–2.57 eV for temperatures within the range 300–100 K.

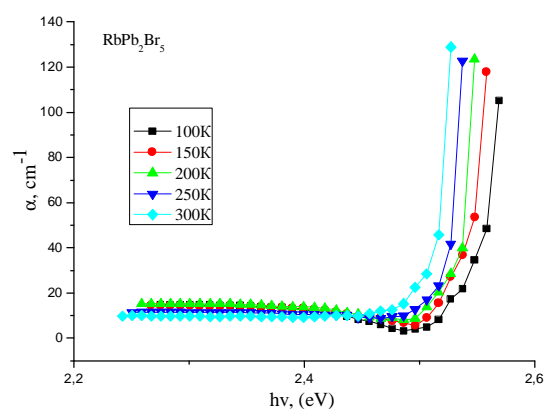
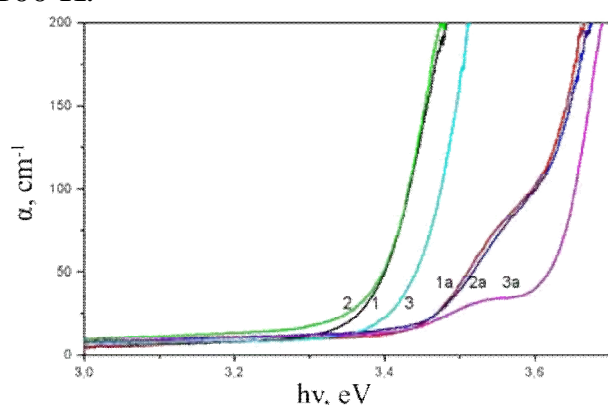


Fig. 1. Absorption edges of RbPb₂Br₅ measured at 300 K (1, 2, 3) and 80 K (1a, 2a, 3a) for polarizations $E \parallel a$ (1, 1a), $E \parallel b$ (2, 2a), and $E \parallel c$ (3, 3a). Fig. 2. Experimental frequency dependence of the absorption coefficient of the RbPb₂Br₅ single crystal.

1. D. Becker, H.P. Beck, Z. Anorg. Allg. Chem. 630 (2004) 1924–1932.
2. L.I. Isaenko, A.A. Merkulov, S.V. Melnikova, V.M. Pashkov, A.Yu. Tarasova, Cryst. Growth Des. 9 (2009) 2248–2251.

Influence of Conditions of Exploitations on Structure and Physical Properties of Polymeric Materials

Shunkina O.V., Domantsevych N.I., Yatsyshyn B.P.

Lviv University of Trade and Economics, Lviv, Ukraine

One of the areas is the use of polymeric materials are pipelines and pipeline equipment, which are made from different thermoplastic materials or their compositions. As a major matrix material, often for these purposes according to the needs of consumers, use high density polyethylene. The aim of this work was to study of the morphology and the mechanical properties of polymeric materials from a modified polyethylene composition low (brand PE2NT11-285D (PE 100)) and high (brand LDPE 15803-020) pressure, which were used in the pipe products for cold water systems.

The index of stability under constant internal pressure in the pipes, which were produced by 12 versions of the compositions of modified polyethylene, show according to results of investigations, that only 5 variants of these pipes have been in exploitation more than 6 years were suitable.

The greatest stability under constant internal pressure detected the pipes made of a composition which included LDPE 15803-020 (12 to 16 wt.%). The application of Irganox B225FF and Dynamar FX5911 (2 wt.%) slightly increased stability performance of products on value of 8 - 10%. The destruction accompanied with cracks, which appears on surface of tube, and causing pressure inside typical samples decrease. Initial samples of polyethylene pipes characterized by high values of tensile yield strength σ_{rt} (26 MPa to 33 MPa to PE2NT11-285D for composite polyethylene) and had elongation at breaking E_{rr} (up to 970 %). The modified samples had somewhat better results.

The structure of the surface of samples was smoother, with fewer defects as cracks and cavities, but on surface of modified samples which had increased amount of processing applications, thermal stabilizers, plasticizers were observed the formation such as balls. The tubes from modified plastic composite, which included a PE2NT11-285D and LDPE 15803-020, antioxidants, pigments and other processing application had most durable and higher resistant to conditions compare to another tubes material. Material of such pipes have surface structure with fewer defects and highest mechanical properties.

Features of Electrical Characteristics of Semi-Insulating CdTe:Cl Crystals

Fochuk P.¹, Nykoniuk Ye.², Zakharuk Z.¹, Solodin S.¹,
Dremlyuzhenko S.¹, Rudyk B.², Sklyarchuk V.¹

¹Chernivtsi National University, Chernivtsi, Ukraine

²National University of Water Management and Nature Resources Use, Rivne, Ukraine

Cadmium telluride crystals demonstrate a great ability for application in optoelectronics and X/γ-ray detectors. For detector applications the material with high resolution has to possess a high resistivity (10^9 - 10^{10} Ohm·cm), high mobility and lifetime of non-equilibrium charge carriers. Usually, semi-insulating CdTe obtain by doping, using CdCl₂. In this paper the results of investigations of CdTe:Cl crystal electrical characteristics are presented.

CdTe was synthesized using elementary Cd (6N) and Te (6N) at 1395 K. Polycrystalline CdTe ingot was purified by the traveling heater method. Concentration of Cl atoms in the melt was equal to $1 \cdot 10^{18}$ cm⁻³. The CdTe:Cl single crystals were grown by the vertical Bridgman method.

Temperature dependencies (TD) of electroconductivity σ , Hall coefficient R_H and carriers mobility $\mu = \sigma R_H$ were investigated in the temperature range 290-420 K, using the samples with dimensions of $12 \times 2 \times 1,5$ mm³.

On the TD of carries mobility the area of «normal» dependence of mobility was absent and, consequently, the high-temperature area of R_H , that determined the energy of ionization of «working» donors ε_D , also was not revealed. Therefore, ε_D can be assessed using the activation energy of the resistivity TD. Defined in such way the ε_D value was equal to 0.53 eV. Determined from TD of R_H low-temperature area ε_1 value was equal to 0.35 eV. The difference between these energies (0.18 eV) was less than the activation energy of the TD of mobility, which determines the drift barriers height $\varepsilon_b = 0.20$ eV. This means that the compensation degree of donors exceed 0.5, therefore the Fermi level should be located below the donors' one. Indeed, at 300 K Fermi level was located at $E_C - 0.54$ eV and donor level - at $E_C - 0.50$ eV.

The drift barriers in the samples are related to micro-inhomogeneities of spatial distribution of working donors and shallower ones too (or acceptors). This is evidenced by the presence of the abnormally series of powerful «jumps» of photoelectron inversely mobility that are not explained by recharging of isolated point defects. It should be noted that in these samples quasi-photochemical reactions were occurred. They were accompanied by irreversible changes in mobility of photoelectrons.

The Effect of PbO Addition and Burning Temperature on the Electrical Properties of SnO₂-based Varistor Ceramics

Gaponov O.V., Shuqing F.

Oles' Gonchar Dnipropetrovs'k National University, Dnipro, Ukraine

The SnO₂-based ceramics with high nonlinear current-voltage characteristics has been used as a varistor material for the last years. SnO₂-based ceramics can be used for producing the overvoltage-protective devices. In this article SnO₂-PbO-Co₃O₄-Nb₂O₅-Cr₂O₃ ceramics baked at 1050, 1150, 1250 and 1350°C with 0 - 8 mol. % PbO additions is studied. The structure of the investigated material consists of SnO₂ grains divided by the layers of Pb-rich intergranular phase. The width of this phase equals to several nanometers.

The addition of low-melt oxide PbO to the ceramics SnO₂-Co₃O₄-Nb₂O₅-Cr₂O₃ helps to improve the sintering of samples. The shrinkage of ceramics γ increases at the growth of PbO concentration and burning temperature T_b . The largest value $\gamma = 11.3$ is observed in 91.4 SnO₂ - 8 PbO - 0.5 Co₃O₄ - 0.05 Nb₂O₅ - 0.05 Cr₂O₃ (mol. %) ceramics produced at $T_b = 1350^\circ\text{C}$.

The increase of PbO concentration in ceramics as well as the burning temperature growth results in the decrease of electric field E_1 . The least value $E_1 = 1260$ V/cm has the ceramics with 2 mol. % PbO addition burned at 1350°C.

The optimal burning temperature for producing the high quality tin oxide varistors with large nonlinear current-voltage characteristics is 1150 - 1250°C. At $T_b = 1250^\circ\text{C}$ the value of nonlinear coefficient β in SnO₂-Co₃O₄-Nb₂O₅-Cr₂O₃ ceramics is up to 25 (fig. 1) at $E_1 = 6020$ V/cm and in ceramics with 0.5 mol. % PbO addition $\beta = 24$ at $E_1 = 5140$ V/cm. The least value of electrical conductivity of ceramics with 0.5 mol. % PbO addition has the sample obtained at $T_b = 1150^\circ\text{C}$.

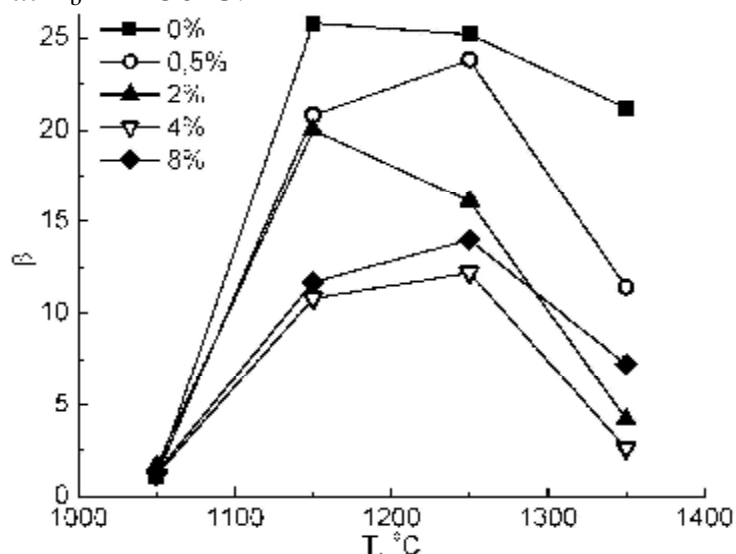


Fig. 1. The dependence of nonlinear coefficient β on burning temperatures in (99.4-x) SnO₂ - x PbO - 0.5 Co₃O₄ - 0.05 Nb₂O₅ - 0.05 Cr₂O₃ (mol. %) ceramics with different concentration of PbO addition

Thus, the SnO₂-based ceramics with 0.5 mol. % PbO additions baked at 1150 - 1250°C is perspective for producing the high-voltage varistors which can function in electric field about 5 kV/cm.

The Electrical Characteristics of SnO₂-Based Varistor Ceramics with Y₂O₃ Addition

Gaponov O.V.

Oles' Gonchar Dnipropetrovs'k National University, Dnipro, Ukraine

The ZnO- and SnO₂-based varistor ceramics has been used for producing the overvoltage-protective devices. In the presented paper the electrical characteristics of (99.9-x) SnO₂ - x Y₂O₃ - 0.05 Nb₂O₅ - 0.05 Cr₂O₃ (mol. %, x = 0, 0.3, 0.5 and 0.7) ceramics sintered at 1400°C have been considered in a wide range of current densities 10⁻⁹ - 10² A·cm⁻². The microstructure of the investigated materials consists of SnO₂ grains and particles of Y₂Sn₂O₇ pyrochlore phase. The size of these particles equals to several nanometers.

The studied materials have high nonlinear current-voltage characteristics. The Y₂O₃ addition to the SnO₂ - Nb₂O₅ - Cr₂O₃ ceramics helps to modify the structures of the samples and improves their electrical properties. The lowest shrinkage and grain average size and the highest grain specific resistance have the samples with 0.5 mol. % Y₂O₃ addition (fig. 1). Such ceramics has the largest values of nonlinear coefficient 48.6, qualifying electric field 14.6 kV·cm⁻¹ and activation energy of electric conduction 0.9 eV and the lowest values of leakage current 0.1 μA and electrical conductivity in low field 2.9·10⁻¹² Ohm⁻¹·cm⁻¹. The coordinated changes of tested parameters prove the barrier mechanism of electrical conductivity in SnO₂ - Y₂O₃ - Nb₂O₅ - Cr₂O₃ varistor ceramics.

Adding the yttrium oxide to tin-oxide ceramics allows to increase the nonlinear voltage-current characteristics and to decrease the leakage current of varistors. It helps to protect the electrical equipment from overvoltage.

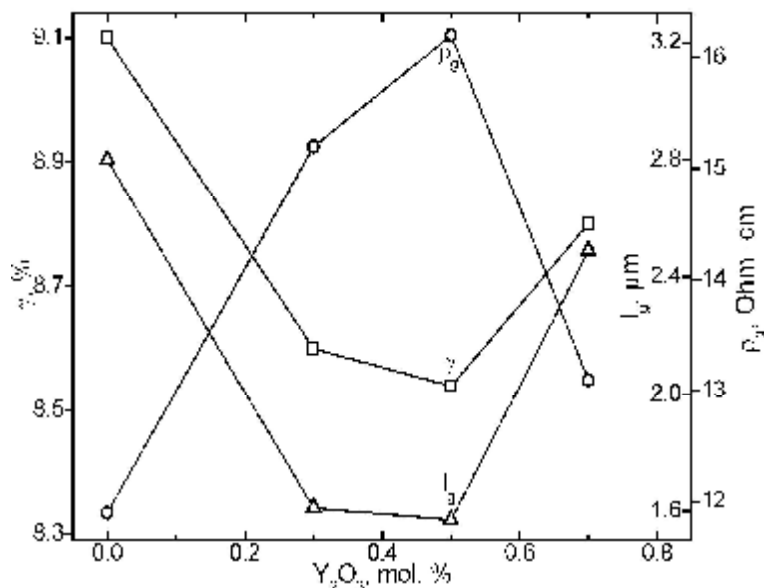


Fig. 1. The dependences of the linear shrinkage γ , grain average size l_g and grain specific resistance ρ_g on the concentration of Y₂O₃ addition in SnO₂ - Y₂O₃ - Nb₂O₅ - Cr₂O₃ varistor ceramics

A Phenomenological Model of Frequency Dispersion of the Conductivity of LiOH-Fe₂O₃-Al₂O₃ Ceramics

Gasyuk I.M.¹, Vakalyuk V.M.², Deputat B.Y.², Vakalyuk A.V.¹

¹*Vasyl Stefanyk Precarpathian National University, Ivano-Frankivsk, Ukraine*

²*Ivano-Frankivsk National Technical University of Oil and Gas, Ivano-Frankivsk, Ukraine*

The existence of unoccupied positions of face-centered cubic lattice in ligand field of O²⁻ anions surrounding as well as Li⁺ localization in their octa-positions give the opportunity to consider lithium-iron spinel not only as a possible lithium power source cathode but also as the Li⁺ ions electric transport environment. In order to ensure the prerequisites of lithium ion transferring the synthesis modification of Li_{0.5}Fe_{2.5}O₄ system have been made [1] by the replacement of certain amount of Fe³⁺ ions to Al³⁺ ions, which are more stable relatively to their ionic state. As a result, a series of systems has been obtained, phase composition and morphology of which enabled to predict the range of their uses in electrochemical devices. However, parameters of electric transport of these systems have been studied insufficiently.

Electrical impedance investigation method found a significant dependence of conductivity $\sigma(\omega)$ frequency dispersion of these substances in a wide temperature range. Considering the prevailing contribution of ionic Li⁺ component in the resulting charge transfer calculation of the frequency dispersion of lithium-iron-aluminum spinel conductivity has been made within the phenomenological model of the dynamic superionic conductivity [2]. This model considers the resonance growth of kinetic energy of ions in the charge-mass transfer process along with the energy dissipation in a periodic lattice field.

The values of carriers concentration, their macroscopic μ_1 and microscopic (translational) μ_2 mobility for a wide range of Al³⁺ ions concentration and temperature range of 125-425 °C have been obtained by approximation of the experimental dependencies with equation:

$$\sigma = \frac{ne^2}{m} \cdot \frac{\gamma(1-i\omega\tau)}{\gamma^2(\omega_0^2 - \omega^2) - i\omega\gamma(1+\gamma\tau) + \gamma^2 - \omega_0^2},$$

where γ is the frequency scattering on lattice defects; ω_0 is the frequency of natural oscillations of ions relatively to equilibrium positions; τ is the characteristic time of ions localization.

It is shown that with increasing aluminum amount in the samples macroscopic ion Li⁺ mobility μ_1 decreases and at temperatures about 200 °C curves $\mu_1(t)$ have distinct maxima. At the same time, translational mobility μ_2 increases from room temperature up to 200 °C, and then decreases sharply, that can be evidence of earlier observed manifestations of ferroelectric properties of samples and existence of the temperature transition to a ferroelectric state.

1. B.K. Ostafiychuk, I.M. Gasyuk, B.I. Deputat at all. X-ray diffraction study of lithium-iron spinel Li_{0.5}Fe_{2.5}O₄ doped by aluminum ions // Physics and chemistry of solid state.–2008., Vol.9, №1, – P. 24–29.

2. A.A. Volkov, G.V. Kozlov, S.P. Lebedyev at all. A phenomenological model of the dynamic superionic conductivity // Solid state physics. –1990. – Vol.32, №2 – P. 329–337.

Broadening Mechanisms of the Optical Spectra in Heavily Doped $n\text{-Ge}_{1-x}\text{Si}_x$ Solid Solution

Gentsar P.O., Vlasenko O.I.

V. Lashkaryev Institute of Semiconductor Physics NAS of Ukraine, Kyiv, Ukraine,
rastneg@isp.kiev.ua

In this paper, the following broadening mechanisms of the optical spectra of heavily doped semiconductors: 1) broadening mechanism associated with the fluctuations of the concentration of charged impurities that lead to the appearance of potential wells with linear dimensions of the order L_{TF} ; 2) broadening mechanism due to electron scattering at boundaries of grains; 3) broadening mechanism due to scattering of electrons on the impurities; 4) broadening mechanism due to scattering of electrons in a random potential that arises due to fluctuations of solid solution.

Based on the fundamental principle of physics - Heisenberg uncertainty principle for energy E and time t ($\Delta E \cdot \Delta t \geq \hbar$) the relaxation effects in the absorption of light by crystal describing broadening parameter $\Delta E = \frac{\hbar}{t}$, where t - time of energy relaxation of photogenerated free carriers. Broadening parameter ΔE can be written as $\Delta E = \frac{e\hbar}{m_e m_e}$. This relaxation time t_i because of scattering of electrons on the impurity is $t_i = \frac{\hbar}{\Delta E} = \frac{m_e^* m_e}{e}$, where m_e^* - the effective electron mass; m_e - electron mobility ($m_e = \frac{e\langle t \rangle}{m_e}$).

Evaluation of the relaxation time t_{AR} that have been caused the disordered solid solution obtained by the formula $t_{AR} = \frac{3m_{\parallel} m_{AR}}{(2K_m + 1)e}$, where K_m - number of equivalent minima in the conduction band of heavily doped $n\text{-Ge}_{1-x}\text{Si}_x$ solid solution.

Summarizing the above results, the effective relaxation time \bar{t} is $\bar{t} = (t^{-1} = t_i^{-1} + t_{AR}^{-1})$.

These calculations are compared with experimental data on optical studies (classical spectroscopy - reflection, modulation spectroscopy - electroreflectance) heavily doped $n\text{-Ge}_{1-x}\text{Si}_x$ solid solution with concentration of electrons $10^{19} - 10^{20} \text{ cm}^{-3}$ and the composition of the solution x from 0,6 to 0,8.

The Role of Surface Effects on Temperature Induced Hysteresis in Spin-Crossover Nanocrystals

Gudyma Iu.V., Maksymov A.Iu.

Department of General Physics, Yuriy Fedkovych Chernivtsi National University, Chernivtsi, Ukraine, yugudyma@gmail.com

Spin-crossover compounds are the class of magnetic molecular complexes based on transition metal ion with electronic configuration varying between $d^4 - d^7$ and surrounded by nonmetallic ligand environment. Under normal conditions, these complexes can exhibit a transition from a diamagnetic low-spin (LS) state, to a paramagnetic high-spin (HS) state, driven by various external stimuli like temperature, light irradiation, pressure, magnetic field and other.

In this work we study a magnetic spin-crossover nanosystem in the framework of microscopic Ising-like model with finite size, taking into account the energy perturbations of the external field, relative to transition metal ion. The main goal is to find out the influence of finite size effects and fluctuations strength of ligand field on the hysteretic properties of the spin-crossover system.

The behavior of spin-crossover compounds at molecular level may be described by the microscopic Ising-like model in the framework of mean field approach with the intermolecular interaction. The Hamiltonian of such model is the following

$$H = -J \sum_{\langle ij \rangle} s_i s_j - \sum_i h_i(t) s_i \quad (1)$$

Here, $s_{i,j}$ is a pseudospin scalar variable taking the values ± 1 for LS and HS states, respectively, J is the intermolecular interaction in spin-crossover materials which is assumed to be of a ferromagnetic nature ($J > 0$) and $h_i(t)$ is the external field relative to metal ion. We considered the case with the external site-dependent field $h_i(t) = \Delta - kT \ln g + x_i(t)$, where the stochastic process $x_i(t)$ reflects the external local random field statistically perturbed.

Based on the model (1) we have studied the 2D and 3D spin-crossover magnetic nanoparticles, described by an Ising-like Hamiltonian in framework of breathing crystal field concept. From Metropolis Monte Carlo simulations it is find out that increasing the fluctuations strength and lattice size side lead to an increase of the hysteresis width, which it is more pronounced for the three-dimensional system. In the case of cubic lattice the system dependence on its size achieves the saturation for smaller system size comparatively to the 2D system, where saturation on system size is not achieved for the chosen range of lattice side values.

1. Gudyma Iu., Maksymov A. Size effects in spin-crossover nanoparticles in framework of 2D and 3D Ising-like breathing crystal field model // *Appl. Surf. Sci.* – 2015. – Vol. **352**. – P. 60–65.

Growth Conditions of Flat Shaped Diamond Single Crystals

Hutsu O., Lisakovskiy V., Kalenchuk V., Burchenya A.

Institut for superhard materials named V. Bakul, Kyiv, Ukraine, 2wsxcvbnm@mail.ru

Structurally perfect single crystals of flattened diamond are widely applied in various branches of electronics, manufacturing, and optics. To obtain such diamonds, growth in the field of thermodynamic stability by the temperature gradient method is widely used. Using this method, the precision of temperature control of high-quality crystals of cubic habit is ± 3 °C; the production of diamond plates requires more detailed study of influence of axial and radial temperature gradients on the development of various crystallographic facets. For this purpose, a cell was developed where temperature gradients values do not exceed 3 °C /mm. The construction of the growth cell was calculated using finite element method. Temperature distribution in the growth volume was determined by varying materials with different thermal and electrophysical properties and the construction of the constituent elements. Results of modeling were experimentally tested on a six-punch high-pressure CS-VII apparatus with a plunger force of 6 x 28,5 MN and a diameter of 560 mm. The growing process was carried out at temperature and pressure of 1420 °C and 5.8 - 6 GPa, respectively; the duration of the cycles was 50 - 80 hours. The Fe - Ni - Sn system (11 at.%) was used as carbon solvent.

As a result of the experiments, the Ib type structurally perfect crystals with a mass of 0.2-0.3 ct were obtained. The size of the side of cube faces square of obtained crystals was 2.30 ÷ 2.55 mm. Flattening degree n of crystals along the four-fold axis, depending on the growing conditions, changed from 44 to 65%; while the average growth rate was 0.61 mg/hour.

Researches have shown that the value of the axial temperature differential in the growth volume, corresponding to 20 °C, makes it possible to obtain growth forms in plates of structurally perfect single diamond crystals.

Effect of Overdischarge on Electrochemical Properties of $\text{LiNi}_{0.5}\text{Mn}_{1.5}\text{O}_4$ Cathodes for LIB Application

Kosilov V.V., Potapenko A.V., Kirillov S.A.

Joint Department of Electrochemical Energy Systems, Kyiv, Ukraine

Dissimilarities in electrochemical properties of cathode materials based on substituted compounds such as $\text{LiNi}_{0.5}\text{Mn}_{1.5}\text{O}_4$ are due to using different methods of synthesis by manufacturers, which lead to differences in chemical and phase compositions of materials. In particular, specific capacity and power density values and the range of working potentials for various materials appear unequal. $\text{LiNi}_{0.5}\text{Mn}_{1.5}\text{O}_4$ commercial samples are widely applicable in lithium-ion batteries (LIB) and possess highly reproducible electrochemical characteristics. Therefore, the study of overdischarge effect of these materials is valuable from practical considerations.

The aim of this investigation was to assess the impact of overlithiation (overdischarge to 2.3 V) on the subsequent electrochemical behavior of $\text{LiNi}_{0.5}\text{Mn}_{1.5}\text{O}_4$ electrodes made by NEI Corporation (BE-30) and JDEES in the high-voltage region. From the practical point of view, the long-term cycling in different potential regions for $\text{LiNi}_{0.5}\text{Mn}_{1.5}\text{O}_4$ cathodes permits to draw a conclusion about their stability to overdischarge during the operation of lithium-ion batteries.

Electrochemical tests have been carried out in button-type 2016 cells with lithium anode. A Celgard 2400 separator has been impregnated with a solution of LiPF_6 in a mixture of ethylene carbonate and dimethyl carbonate (1:1). The internal resistance R_{DC} (Ohm) of cells has been estimated by the voltage drop on charge/discharge switching.

Single overdischarge experiments with $\text{LiNi}_{0.5}\text{Mn}_{1.5}\text{O}_4$ cathodes made by different manufacturers do not lead to a decrease in characteristics of electrodes. However, the practical application of the low discharge voltage is not appropriate for them. Multiple cycling with approaching the low-voltage region worsens the electrochemical properties, namely the resistance of the electrodes increases and their specific capacity falls. Degree of degradation is determined by the type of material. The nanosized sample (JDEES) shows a larger capacity in the low-voltage region compared with the microcrystalline sample (BE-30) at overdischarge up to 2.3 V, but upon prolonged cycling capacity decreases more rapidly. Most likely, nanosized materials are more susceptible to resistance growth than micro-sized ones due to the formation of a larger quantity of a solid electrolyte interphase on the surface of electrode materials of larger specific surface area.

The Influence of Surface on Transport Phenomena in n-PbTe Films

Ruvinskii M.A., Kostyuk O.B., Dzundza B.S., Makovyshyn V.I.

Vasyl Stefanyk Precarpathian National University 57, Shevchenko Str., Ivano-Frankivsk, 76018, Ukraine

Today the problem of calculating the conductivity of thin films is particularly relevant due to the fast development of micro and nonoelectronics. The necessity of modern society in new energy sources is accompanied by the fast development of thermoelectric material.

In this paper the influence of mechanisms of surface reflection of electrons on the experimental transport and thermoelectric properties of n-PbTe films on various substrates are considered based on the Fuchs-Sondheimer and Mayer models. The thickness dependence of conductivity, Hall coefficient and the Seebeck coefficient (Fig.1) of films based on PbTe are investigated. The probability of specular scattering of charge carriers both at the free surface of the film and the film-substrate boundary is defined. It was shown that for the films on sital substrates are implemented completely diffuse scattering of carriers ($p \approx 0$), and for the films obtained on fresh chips of mica the scattering coefficient $p \approx 0,4$.

Films for research are received by vapor deposition of synthesized material n-PbTe in a vacuum on the substrate of fresh chips (1000) of mica-muscovite and sital. The temperature of the evaporator was $T_e = 870$ K and the temperature substrates $T_s = 470$ K. The thickness of the films are set by the deposition time within (0,5-13) min and are measured by microinterferometer MII-4. Measurement of electrical parameters of the films was realized on air at room temperature and at constant magnetic field on the automated device.

The calculated values of the scattering coefficient depending on the roughness are also calculated. It is shown that for the coefficient p is traced a clear dependence on the thickness of condensate for studied samples: it increases with the decreasing film thickness. For thin films p is close to one, that indicating the mirror mechanism of carrier scattering from the surface.

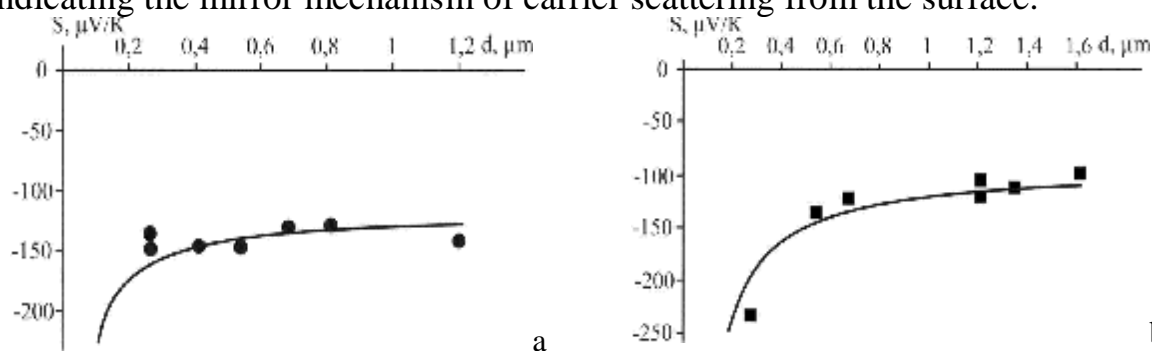


Figure 1. Thickness dependence of Seebeck coefficient S of the n-PbTe films on mica(a) and sital(b).

Features of Structural Inhomogeneities in Doped Cadmium Antimonide Crystals

Koval Yu.V.¹, Zakharchuk D.A.¹, Yashchynskyy L.V.¹, Panasjuk L.I.¹,
Fedosov S.A.²

¹*Lutsk National Technical University, Lutsk, Ukraine*

²*Lesya Ukrainka Eastern European National University, Lutsk, Ukraine*

It is known that monocrystals grown by Czochralski or zone melting, with the so-called layered structure (layers or bands of growth). Please note that during the layered inhomogeneity is different in the range of tens of microns to millimeters and growing proportion of temperature gradient in the crystallization front.

In this paper a study to identify structural inhomogeneities in CdSb monocrystals doped with Te. The method of optical topography revealed layered structure of the investigated single crystals with a period of about 300 microns.

Analysis of various methods used to study inhomogeneities in semiconductors, showed that in the case of semiconductors manyvalley required quantity control requirements can satisfy two-probe compensation method with the greatest possible resolution. Samples CdSb(Te) for research two-probe compensation method were cut parallel and perpendicular to the axis of crystal growth. The results of measurements are constructed experimental curves of the resistivity distribution along the length of the samples. In dependence $\Delta r/r_c = f(X)$ found a much higher resistivity deviation from the mean r_c in samples cut along the axis of the crystal growth than in samples cut perpendicular to this axis. Abrupt changes in gradient resistivity Dr in the direction of crystal growth due to the existence in this area of significant gradients of concentration of charge carriers Dn . Therefore, we can speak about the presence of crystal growth direction impurity concentration heterogeneities, with a frequency necessary to note in its distribution along the length of the samples.

When comparing the results obtained by optical topography and two-probe compensation method, suggested that the crystals is shown layered structure with several types of layers are characterized by different periods. To test this assumption a study of structure by means of scanning electron microscope (SEM). During these studies revealed layered structure of the investigated single crystals with the period of the order of 1,5 microns.

From the above results of studies suggest that in CdSb monocrystals doped layers are inhomogeneous distribution of impurities with different periods, and it must be considered when studying the anisotropy of physical properties data of monocrystals.

Deformation of Various Purity Auxetic at Different Structural Levels

Kurek I.G., Lysyuk O.V., Oliynich-Lysyuk A.V., Raransky M.D.

Yury Fedkovich Chernivtsy National University, Chernivtsy, Ukraine, a_oliynich@ukr.net

It is well known that plastic deformation of crystals occurs at different structural levels simultaneously or sequentially, starting from the surface, and relaxed by injection of defects in volume of crystallites in areas of maximum stress location. The result of the adaptation of defective subsystems of crystal to mechanical fields substantially depends on many factors, that is poorly predicted, especially at abnormal (auxetic) deformation due to the lack of information about the behavior of defects in crystals that are in auxetic condition.

Therefore, in this research conducted a comprehensive study of deformation processes in beryllium varying degrees of purity and type of auxetic at the micro and mezzo-levels. We studied the elastic energy absorption (IF), the behavior of effective torsion modulus (G_{ef}), the velocity of the defects in the temperature range of existence of normal and abnormal (auxetic) deformation. Briefly research results can be summarized as such.

- The most intensive sliding along grain boundaries is observed in high-Be (99.99%) in the vicinity of 290°C during the first 2-3 thermal cycles and accompanied by occurrence the asymmetric hysteresis maximum of IF and minimum on the temperature dependences of G_{ef} .

- Height of maximum is reduced almost 5 times with decreasing purity material at 0.06%. In this case on the temperature dependences of IF and of G_{ef} for coarsely crystalline MTC Be is observed a sharp increase in the studied variables in a narrow temperature range (see. Fig 1a), which may be associated with changes in the type of auxetic and formations of elastic doubles (fig.1b)

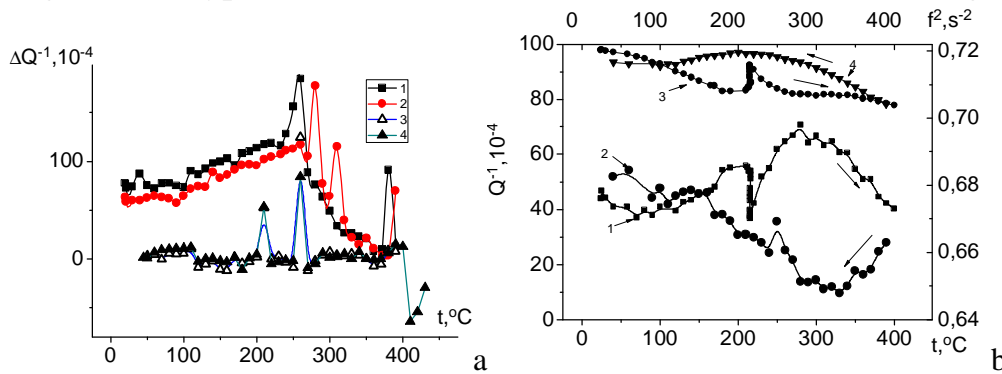


Fig.1a. Temperature dependences of the IF in the MTC Be (99.95% Be) at heating (1, 2) and cooling (3, 4). Fig.1b. Temperature dependences of IF (1,2) and G_{ef} (3,4) for MTC Be (99.93% Be) at heat. (1, 3), and at cool. (2, 4).

Phase Separation of Ge-S-Ag Glasses for Conductive-Bridge Memories

Lishchynskyy I.M.¹, Kaban I.G.², Varvaruk V.V.¹, Ivasiuk R.V.¹, Kushnir R.I.¹

¹*Vasyl Stefanyk Precarpathian National University, Ivano-Frankivsk, Ukraine*

²*Leibniz Institute for Solid State and Materials Research Dresden, Germany*

Due to continuously increasing digital information people are dealing with, the demand on memory devices being able to store, communicate, and compute this information is also increasing. Currently, flash memories based on a charge storage are widely used and continuously replace hard disc drives. However, flash memories are challenged by a down-scaling problem because of the charge leakage from the storage layer. In this view, alternative memory technologies such as for example phase-change memories (PCM), redox conductive-bridge memories (RCBM) and conductive-bridge memories (CBM) have been suggested [1].

The chalcogenide glasses (e.g. Ge-S-Ag used for the conductive-bridge memories), which are basically semiconductors, become superionic conductors upon doping with metal species. Ge-S-Ag glasses are very attractive first of all due to significantly higher glass transition temperature and consequently better thermal stability compared to the Ge-Se based glasses [2]. Also, Ge-S-Ag glasses are free of toxic elements.

We present the results of investigations of rapidly quenched $(\text{GeS}_2)_{100-x}\text{Ag}_x$ alloys ($x=0, 5, 10, 15$, and 20 at.%), $(\text{Ge}_{42}\text{S}_{58})_{100-x}\text{Ag}_x$ and $(\text{GeS}_3)_{100-x}\text{Ag}_x$ alloys ($x=0, 5, 10, 15, 20$, and 25 at.%) carried out at the Institute for Complex Materials, IFW Dresden and Vasyl Stefanyk Precarpathian National University.

The microstructure of the Ge-S-Ag glasses, and particularly phase separation, was studied using ZEISS Digital Scanning Electron Microscope (SEM) DSM 982 Gemini equipped with Bruker energy dispersive X-ray spectrometer. The SEM micrographs of the binary GeS_3 and the ternary $(\text{GeS}_3)_{75}\text{Ag}_{25}$ glasses revealed a homogenous microstructures, whereas the samples with $x=5, 10, 15, 20$ at.% were found to be phase separated. The SEM images and EDX analysis of the $(\text{Ge}_{42}\text{S}_{58})_{100-x}\text{Ag}_x$ samples showed that they are constituted of an amorphous single phase up to $x=20$ at.%. Ge crystals were detected in the glassy matrix at $x=25$ at.%. A homogenous single phase glassy state is observed for the binary GeS_2 and ternary $(\text{GeS}_2)_{95}\text{Ag}_5$ and $(\text{GeS}_2)_{80}\text{Ag}_{20}$ quenched alloys. On the other hand, the glasses with 10 and 15 at.% Ag are phase separated.

[1] J. S. Meena, S. M. Sze, U. Chand, T. Y. Tseng, *Nanoscale Research Letters* 9 (2014) 526.

[2] M. R. Latif, M. Mitkova, G. Thompa, E. IEEE Workshop on Microelectronics and Electron Devices, April 12, 2013.

Own Point Defects in Zinc Telluride

Lysak A.V., Pylyponyuk M.A., Kal'ka O.Yu., Seniv M.S.

Vasyl Stefanyk Precarpathian National University,
Ivano-Frankivsk, Ukraine, e-mail: oxana94@meta.ua

Zinc Telluride is a promising material of light-emitting diodes with high brightness. It is widely used as a barrier material to create all sorts of low-dimensional structures. It is needed reliable information about their defective condition for developing the science-based technology ZnTe material.

Stoichiometric Zinc Telluride can be changed by setting the partial pressure of the components on the solid phase or the temperature in the method of two-temperature annealing. Equilibrium of "crystal-vapor" can be described by equations quasichemical reactions. When you are calculated the system of equations you can determine the concentration of holes p through the constant quasichemistry reactions K and the partial vapor pressure of Zinc P_{Zn}

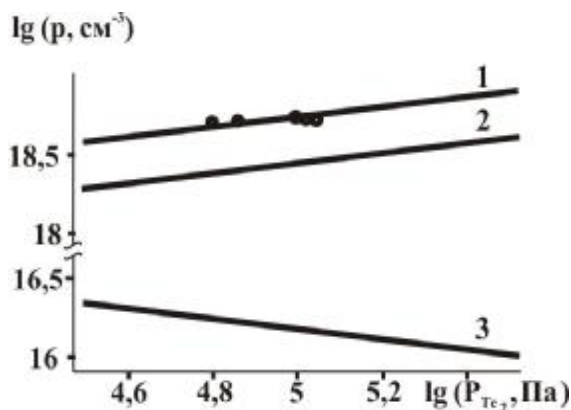


Fig. 1. Dependencies of concentration of holes p (1), Zinc vacancies $[V_{Zn}^{2-}]$ (2) and Tellurium vacancies $[V_{Te}^{2+}]$ (3) on the tellurium vapor partial pressure P_{Te_2} at the annealing temperature $T = 1244$ K. Points – experiment.

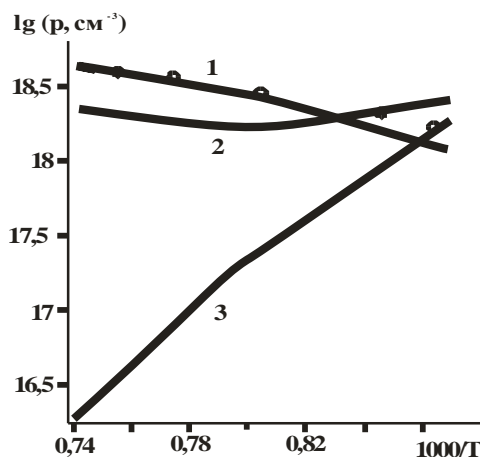


Fig. 2. Dependencies of concentration of holes p (1), Zinc vacancies $[V_{Zn}^{2-}]$ (2) and Tellurium vacancies $[V_{Te}^{2+}]$ (3) on the annealing temperature T at partial vapor pressure of tellurium $P_{Te_2} = 1.33 \cdot 10^4$ Pa. Points – experiment.

The calculation of defects concentration are showed that in crystals ZnTe vacancies of Tellurium $[V_{Te}^{2+}]$ are formed in small quantities and concentration of charge carriers which is determined by the mainly vacancies of Zinc $[V_{Zn}^{2-}]$. The increased of the Zinc vapor partial pressure P_{Zn} thus a constant annealing temperature T it reduces the hole concentration p , which is caused by a decrease in the concentration of Zinc vacancies $[V_{Zn}^{2-}]$ (fig. 1).

With the decrease of annealing temperature T by the constant partial pressure of Zinc vapor P_{Zn} the concentration of Zinc vacancies decreases $[V_{Zn}^{2-}]$, which reduces the hole concentration p (fig. 2).

Note that both isothermal and pressure dependence have good agreement with experiment.

Synthesis and Thermoelectric Properties of Solid Solutions of PbTe-SnTe

Matkivsky O.M.¹, Gorichok I.V.¹, Mateik G.D.², Yaworski Ya.S.¹

¹*Vasyl Stefanyk Precarpathian National University, Ivano-Frankivsk, Ukraine,*
e-mail: fcss@pu.if.ua

²*Ivano-Frankivsk National Technical University of Oil and Gas, Ivano-Frankivsk, Ukraine*

The efficiency of thermoelectric materials is determined by the dimensionless thermoelectric figure of merit $ZT = (\alpha^2 \sigma / k) T$, where α , σ , k , T - Seebeck coefficient, electrical conductivity, thermal conductivity and temperature, respectively. For the temperature range 200-500 C, particularly effective are materials on the basis of lead telluride, which $ZT \approx (0,7-0,8)$. However, there are some difficulties in obtaining samples of hole conductivity type. Part of this problem may be solved by the use of a material for district branches thermocouples solid solutions based on PbTe-SnTe.

Samples for research (SnTe, PbTe, $Pb_{0,4}Sn_{0,6}Te$, $Pb_{0,8}Sn_{0,2}Te$) prepared by pressing powders with pre-synthesized ingot. Among all the samples SnTe characterized by the highest electrical conductivity and thermal conductivity and simultaneously lowest Seebeck coefficient. At a temperature of 300 C of thermoelectric figure of merit $ZT \approx 0,1$, which is relatively low.

For a solid solution of $Pb_{0,4}Sn_{0,6}Te$ electrical conductivity decreases compared with Tin Telluride and thermoelectric coefficient at 300 C doubled. Also worth noting reduce the thermal conductivity of the samples due to a decrease in lattice component, due to the increased number of point defects and electronic component as the carrier concentration decreased from the values of $1.4 \cdot 10^{21} \text{ cm}^{-3}$ for SnTe, to $7.6 \cdot 10^{19} \text{ cm}^{-3}$ for the solid solution of $Pb_{0,4}Sn_{0,6}Te$.

For a solid solution of $Pb_{0,8}Sn_{0,2}Te$ electrical conductivity is reduced to values of $10-20 \text{ (Ohm cm)}^{-1}$, and Seebeck coefficient increases to 250 mkV/s at 150 C. But dependence of $\alpha(T)$ is non-monotonic and is characterized by a peak. A significant decrease in conductivity is due relatively low carrier concentration, which is $5 \cdot 10^{18} \text{ cm}^{-3}$.

Based on the dependencies found that the composition of $Pb_{0,4}Sn_{0,6}Te$ has the highest thermoelectric figure of merit that at $T = 300 \text{ C}$ is $ZT \approx 0,3$.

Energy of Substitution of Anions and Cations in Zinc and Cadmium Telluride

Pylyponiuk M.A., Prokopiv V.V., Horichok I.V., Arsenyuk I.

*Vasyl Stefanyk Precarpathian National University,
Ivano-Frankivsk, Ukraine, e-mail: HorichokIhor@gmail.com*

The relevance of the research of point defects is due to their considerable impact on all properties of semiconductor crystals. In this case, to establish the predominant type and the concentration of point defects is necessary to determine their energy creation. These values can be calculated as using the modern quantum chemical programs (GAMESS, Gaussian etc.), and based on the simplified models. Moreover, as it was shown in [1-2], the result, which is obtained on the basis of the semi-empirical method, is sufficient for the interpretation of many experimental data.

Considering the above, promising in terms of the definition of the energy parameters of defects is Harrison's method of connecting orbitals. This method is very simplified, so to get the quantitatively correct values is difficult, but to track the qualitative conformities in the investigated parameters is possible.

In the table is presented the results of calculation of the energy of the substitution defects in ZnTe i CdTe. Based on the data, which are presented in the table, it can be concluded that the halogen atoms are more inclined to substitution of matrix atoms than the atoms of the first group of Periodic Table. In the case of the metals of the first group the energy substitution on cationic and anionic sublattices, are positive, indicating that the disinclination to the formation of defects such as D_{Cd} ($D = Cu, Ag, Au$). This result may explain the ease of the transitions these atoms between nodal and internodal positions in CdTe, which causes to the time instability of the properties.

Table

Energy substitution (in eV) of cations and anions in zinc and cadmium telluride

	ZnTe		CdTe	
	E (D_{Zn})	E (D_{Te})	E (D_{Cd})	E (D_{Te})
Cu	7.49	34.84	7.92	34.47
Ag	6.28	33.72	6.71	33.42
Au	5.52	32.12	6.02	31.94
Cl	0.15	-1.40	1.40	-1.84
Br	-1.69	-0.88	-0.53	-1.20
I	-3.50	-0.21	-2.34	-0.40

1. I.V. Gorichok. Fizika tverdogo tela, 54 (7), 1373 (2012).
2. I.V. Horichok, H.Ya. Hurhula, V.V. Prokopiv, M.A. Pylyponiuk. Ukr. J. Phys. 61 (11), 992 (2016).

Semiconductive Phase Formation in V-Co-Sb Ternary System

Romaka L.¹, Romaka V.V.², Horyn A.¹, Stadnyk Yu.¹

¹ *Ivan Franko National University of Lviv, Lviv, Ukraine*

e-mail: romakal@franko.lviv.ua

² *Lviv Polytechnic National University, Lviv, Ukraine*

Semiconductor compounds included two transition metals and *p*-elements with the MgAgAs structure type (so called half-Heusler alloys) apply to the objects, which are intensively investigated as the prospective materials for the direct conversion of the heat energy into electric current. The most of the ternary systems V-*d*-metals-Sb is characterized by formation of the half-Heusler compounds (VCoSb, VFeSb, VNiSb, MgAgAs-type) with semiconductive properties and are interesting objects for investigation.

The phase equilibria in the V-Co-Sb ternary system were studied at 870 K by X-ray and metallographic analyses in the whole concentration range. The samples were prepared by arc melting the constituent elements and annealed at 870 K during 1400 hours. The interaction between the elements results in the formation of one ternary compound VCoSb with MgAgAs-type (half-Heusler phase, $a = 0.57799(7)$ nm). Under used conditions no homogeneity range and deviation of the stoichiometry was observed for VCoSb phase. The solubility of vanadium in the binary skutterudite CoSb₃ and its influence on the thermoelectric characteristics of V_{*x*}Co₄Sb₁₂ samples ($x = 0.02-0.20$) was studied by X-ray diffraction and electric property measurements. The effect of the doping of V on the electric transport properties of CoSb₃ skutterudite demonstrate that doping of the basic CoSb₃ skutterudite allows to considerably increase the power factor value *Z* at higher temperature for V_{*x*}Co₄Sb₁₂ sample in comparison with CoSb₃ binary. The performed electronic structure calculations are in good agreement with electrical studies.

Mechanism of Generation of Donor-Acceptor Pairs in (Zr,Ti)NiSn_{1-x}Ga_x Thermoelectric Materials

Romaka V.A.^{1,2}, Romaka L.P.³, Krayovskyy V.Ya.², Romaka V.V.²,
Stadnyk Yu.V.³, Horyn A.M.³

¹*Ya. Pidstryhach Institute for Applied Problems of Mechanics and Mathematics National
Academy of Sciences of Ukraine, Lviv, Ukraine;*

²*Lviv Polytechnic National University, Lviv, Ukraine;*

³*Ivan Franko National University of Lviv, Lviv, Ukraine*

Thermoelectric materials based on *n*-TiNiSn, *n*-ZrNiSn and *n*-HfNiSn semiconductors have high efficiency of the transformation of the heat energy into electrical power [1,2]. However, uncontrolled changes in the crystal and electronic structures during optimization of the characteristics by doping affect their properties and limit extensive application of these materials. The crystal and electronic structures, electrokinetic, and magnetic characteristics of *n*-TiNiSn and *n*-ZrNiSn doped by Ga acceptor impurity were investigated to resolve this problem.

The band structure calculations were performed for all variants of the distribution of atoms in the unit cell including different occupation of crystallographic positions by host and/or guest atoms, and taking into account the presence of the vacancies. The distribution of atoms in the ZrNiSn_{1-x}Ga_x and TiNiSn_{1-x}Ga_x unit cells, for which the modeled shift rate of the Fermi level ϵ_F obtained from the band structure calculations coincides with the shift rate determined from the $\ln\rho(1/T)$ dependencies, was established.

It was found that partial substitution of Sn ($5s^25p^2$) by Ga atoms ($4s^24p^1$) in the 4*b* crystallographic site generates simultaneously both structural defects of acceptor (Ga atoms in 4*b* site) and donor nature (vacancies in 4*b* site). The simultaneous generation of donor-acceptor pairs provides the principle of electro neutrality and structural stability of the ZrNiSn_{1-x}Ga_x and TiNiSn_{1-x}Ga_x thermoelectric materials and guarantees the stability and reproducibility of their characteristics.

[1] V.A. Romaka, V.V. Romaka, Yu.V. Stadnyk. *Intermetallic semiconductors: properties and applications* // Lvivska politekhnik, Lviv, 2011, 488 p.

[2] M. Gurth, G. Rogl, V.V. Romaka, E. Bauer, P. Rogl. // *Acta Materialia*, № 104, 210 (2016).

Influence of Mn-Admixture on Growth and Morphology of PbI₂ Crystals

Rybak O.V.

Lviv Polytechnic National University, Lviv, Ukraine

The doping of lead iodide by manganese provides for obtaining the new type of materials – layered semimagnetic semiconductors.

The doping of PbI₂ single crystals by Mn within the concentration range of 0,001–0,01 at.% was realized in the process of growth from vapour phase in the closed system at over-stoichiometric iodine vapour pressure. Under optimal conditions for the preparation of undoped lead iodide single crystals, we studied the effect of dopant concentration in the source material on the rate of PbI₂ transport and the dopant concentration in the single crystals. The present results demonstrate that, at dopant concentrations in the source material from 0,001 to 0,01 at.%, the mass transport rate is on the same order as in undoped crystals. The dopant concentration in the grown single crystals is proportional to that in the source material. As a result, thin monocrystalline PbI₂ layers of 4H-polytype 0,01-0,1 mm in thickness and having area of 10-1 mm² were grown.

In the most cases, under the optimal growth conditions, we obtained ribbon crystals. The following types of morphology can be distinguished: long ribbons and their intergrowths, elongated crystals with sharp terminations, bent ribbons. The surface of most regular crystals is perfect; striations are discernible only in SEM micrographs taken at large magnifications. On the surface of less perfect crystals (Fig. 1, 2) we observe growth patterns and vicinal developments in the form of regular or irregular triangles and hexagons. Fig.2 shows vicinal hillocks with a stepped structure. In fig.2 one can see details of a hexagonal pattern formed by a set parallel steps. On sufficiently perfect surfaces, we observe triangular pattern corresponding to stacking faults.

Manganese doping of PbI₂ in the range 0,001-0,01 at.% shifts the excitonic band in its low-temperature (5 K) photoluminescence spectrum to short wavelengths, reduces its intensity, and increases its full width at half maximum.

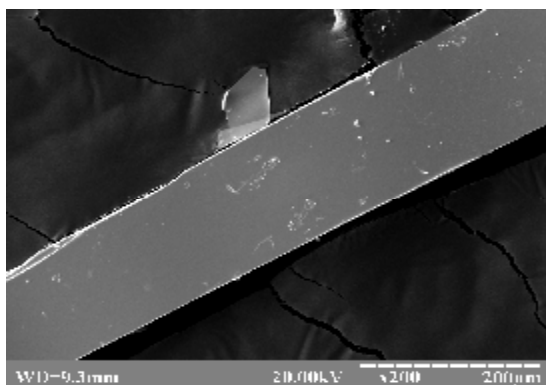


Fig.1.

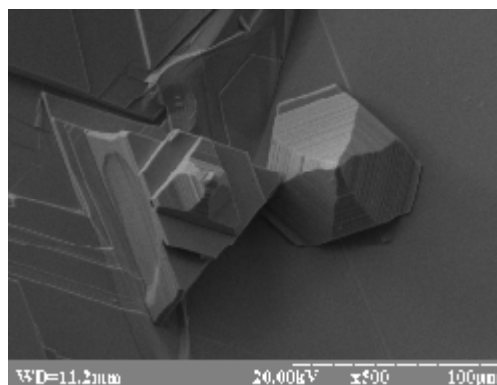


Fig.2.

Peculiarities of Phases Formation in Tm-Ni-Sb Ternary System

Rykavets Z.¹, Romaka L.², Shvachko S.¹, Stadnyk Yu.²,
Romaka V.V.¹

¹ Lviv Polytechnic National University, Lviv, Ukraine,
e-mail: romakav@lp.edu.ua

² Ivan Franko National University of Lviv, Lviv, Ukraine

Ternary systems that contain heavy rare-earth metal, nickel and antimony are of great interest due to the formation of ternary compounds of equiatomic composition crystallizing in the MgAgAs structure type (so called half-Heusler alloys). These alloys reveal p-type semiconducting properties and could be considered as high-performance thermoelectric materials for the direct conversion of the waste heat into electrical power.

The phase equilibria in the Tm–Ni–Sb ternary system were investigated at 870 K by means of X-ray and metallographic analyses in the whole concentration range. Alloys were prepared by arc melting (with excess of 3-5 at.% of Sb) and annealed at 870 K for 720 hours. The formation of the following phases was established: TmNiSb (MgAgAs-type), Tm₅Ni₂Sb (Mo₅SiB₂-type), and Tm₅Ni_{0.5}Sb_{2.5} (Yb₅Sb₃-type). The solubility of Tm in NiSb binary (NiAs-type) up to 5 at.% was observed. Lattice parameters change from $a = 0.3902(2)$, $c = 0.5122(4)$ nm in NiSb to $a = 0.3920(2)$, $c = 0.5143(3)$ nm in Tm_{0.1}Ni_{0.9}Sb). Metallographic analysis of annealed alloys revealed their dendrite structure. The lowest porosity was observed for the Ni-rich alloys, while with the increasing of Tm content up to 65 at.% the porosity increases.

The *ab initio* DFT+U spin-polarized calculations (FP-LAPW method, LSDA exchange-correlation potential, $U = 0.4$ Ha) of TmNiSb compound showed that only Tm atoms exhibit magnetism giving spin magnetic moment $1.93 \mu_B$ and confirming Tm³⁺ state. The presence of the energy gap at Fermi level predicts semiconducting properties of TmNiSb.

Microwave Ferromagnetic Materials with Spinel Structure: Influence on Properties of Synthesis Features

Solopan S.O., Skorokhod A.A., Fedorchuk O.P.

Vernadsky Institute of general and inorganic chemistry of the Ukrainian National Academy of Sciences Ukraine, Kiev, Ukraine; e-mail solopan@ukr.net

Modern radar and communication systems work in the microwave range and they have very important role in the efficient functioning the national economy, military capability etc. Ukraine is among the ten countries, which have the complete technological process - from the development of new materials to the creation of a variety of communication systems. Ferromagnetic microwave materials are one of the most important class of materials that determine the progress in developing new communications and radars. Application microwave ferromagnetic materials allows solving the problems of miniaturization, improving the reliability and sensitivity of different communication systems and radars, providing the solution generating elements of the transmission systems (reception) signals etc. However further progress in this area depends mostly on the development of new high-performance materials, establishing the nature of the dielectric and magnetic losses in ferromagnetic materials and opportunities for achieving the set parameters by changing the chemical composition and synthesis conditions of these materials. The development of synthesis methods and investigation the possibilities to control microwave parameters of ferromagnetic materials are of particular scientific and practical interest.

This study deals with synthesized microwave ferromagnetic materials based on complex oxides of iron and nickel with spinel structure NiFe_2O_4 , cationic partial substitution of nickel and iron by other elements, in particular, zinc, manganese and copper, by precipitation from aqueous solutions and solid state reaction method.

The investigation of chemical reactions during the synthesis and their influence on the electromagnetic characteristics ($4\pi M_s$, ϵ , $\text{tg}\delta$, ΔH) in the microwave range (eg, at a frequency of 9.4 GHz) were performed.

The effect of previous heat treatment (500-800 °C) on the particles sizes of obtained powders synthesized by different methods, their phase composition and saturation magnetization were established. It was shown that the powder synthesis temperature subsequently influence on the ceramics density and it electrical properties in the microwave range.

The Formation Mechanisms of PbTe-CdTe Solid Solutions

Tsymbalyuk T.P., Hurhula G.Y., Yaremiichuk O.V., Zapukhlyak Z.R.,
Levkun M.P.

Vasyl Stefanyk Precarpathian National University, Ivano-Frankivsk, Ukraine

Lead telluride is the basic matrix for creating a large group of semiconductor materials that is used for infrared optoelectronic devices and thermoelectric generators that function in the temperatures interval from room to 900 K. One of the possible ways to improve thermoelectric parameters there is doping of heterovalent atoms of substitution during formation of solid solutions. This leads to the generation of vacancies in the Lead or Tellurium sublattices. The solubility of Cadmium in PbTe far superior solubility of many heterovalent elements. The investigated $Pb_{1-x}Cd_xTe$ solid solutions, accordance with Hume-Rothery rule relate to solutions of replacement, where impurity of Cadmium occupies the regular knots of Lead.

The limiting content of Cadmium in $Pb_{1-x}Cd_xTe$ solid solutions (its solubility at 670°C in PbTe) corresponding to $x = 0.08$ (4 mol.% of Cd), that good agree to known data well enough [1].

The main objective of this paper is research of point defects in solid solutions based on Lead and Cadmium Telluride by using of crystal-quasi-chemical formulas and calculation of the concentration of dominant defects, basic carriers and Hall concentration of carriers due to deviation from stoichiometry and composition of solid solutions.

The crystal-quasi-chemical formulas and equations of electroneutrality for solid solutions of n-PbTe-nCdTe, n-PbTe-p-CdTe, p-PbTe-nCdTe and p-PbTe-p-CdTe with different initial deviation from the stoichiometric composition of basic compounds (n - and p-type conductivity), which are in good agreement with the results of measuring concentrations Hall was developed at first. The existence of p-n-transition in solid solutions n-PbTe-p-CdTe and p-PbTe-n-CdTe were established. In particular, for n-PbTe-p-CdTe is observed n-p-transition at 0.15 mol. of Cd, and for p-PbTe-n-CdTe the p-n-transition is observed at 0.0015 mol. of Cd.

The two-dimensional technological diagrams that define the chemical composition of $Pb_{1-x}Cd_xTe$ solid solutions with predetermined type of conductivity and Hall concentration of current carriers were received.

[1] A.J. Rosenberg, R. Grierson, J.C. Woolley, P. Nicolic, Trans. Met. Soc. AIME 230(2), 342 (1964).

The Fourier Energy Spectrum for X-Ray Moiré Images Arising Under the Action of Concentrated Forces in Si

Yaremchuk I., Balovsyak S., Fodchuk I., Novikov S.

Chernivtsi National University, Chernivtsi, Ukraine, ifodchuk@ukr.net

The X-ray moiré intensity distributions that occur from the action of concentrated forces on the initial plate of the three-crystal *LLL*-interferometer are analyzed using radial distribution F_R of Fourier energy spectrum P_s . In general, the boundaries for visualization of deformation moiré stripes nonlinearly depend on phase moiré period, magnitude of local concentrated forces, and the nature of their distribution. In general, the boundaries of visualization of deformation moiré stripes are nonlinearly dependent on the phase moiré period, the magnitude of the load of local concentrated forces and the nature of their distribution. In particular, Fig.1, a-c shows moiré images in case of parabolic distribution of concentrated forces magnitude. The deformation moiré stripes are formed on the ends of distribution – in the region of more significant magnitude of concentrated forces. A fine moiré structure is formed in the region of smaller deformation fields. Approximated radial distributions F_{Rp} in Fig. 1d demonstrate a high sensitivity to the magnitude and nature of the concentrated forces distribution and make it possible to determine the average period T_{rc} of moiré stripes and the corresponding average spatial frequency $\nu_{rc}=1/T_{rc}$.

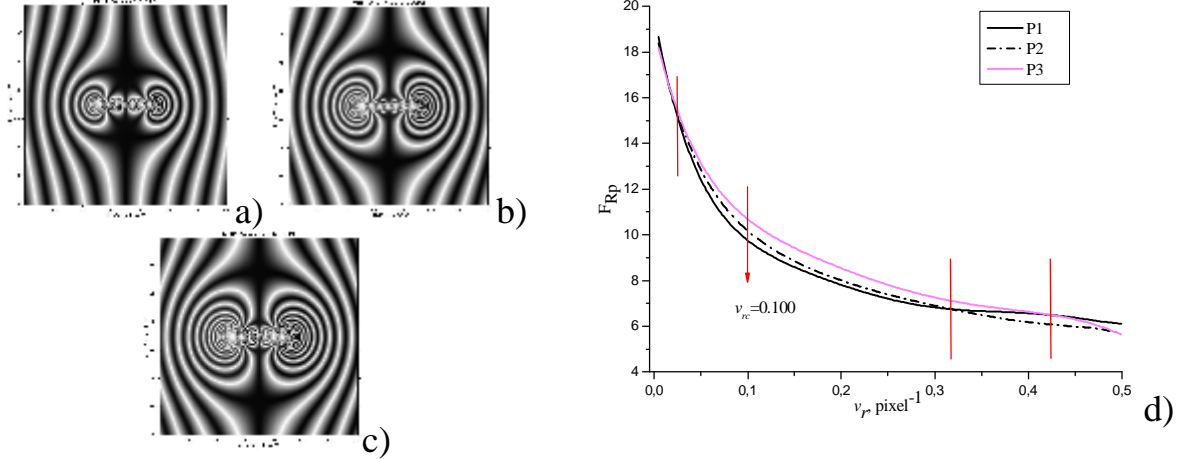


Fig. 1. Calculated X-ray moiré images of the set of 7 concentrated forces, placed through 800 microns on output surface of analyzer of silicon *LLL*-interferometer (a-c), 220 reflection, CuK_α -radiation; total magnitude of concentrated forces $P1=63$ (a); $P2=110$ (b); $P3=138$ (c); approximated radial distributions F_{Rp} of energy spectra P_s of moiré images (d), lines P1-P3 correspond to images in (a-c).

Dependencies $F_{Rp}(\nu_{rc})$ in Fig. 1d clearly define the boundaries of close-range and long-range strain fields in dependence on the force distribution and total magnitude of concentrated forces P_{sum} .

Crystal-Quasichemical Description for Nonstoichiometric GeTe

Yurchyshyn L.D., Mezhylovska L.I., Ivanyshyn I.M.,
Lishchynska S.I., Pletenytska L.S.

Vasyl Stefanyk Precarpathian National University, Ivano-Frankivsk, Ukraine, ld67@ukr.net

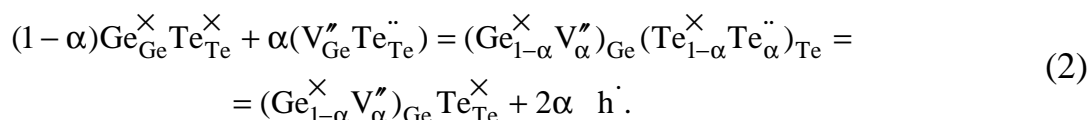
In the project crystal-quasichemical formulas for nonstoichiometric p-GeTe are proposed.

Overstoichiometric Tellurium in crystal GeTe may finish anion crystal sublattice (Mechanism A1), or be inculcated in tetrahedral cavities of Germanium atoms solid structures (Mechanism A2).

For the first mechanism in case of only two-charged Germanium vacancies existence stoichiometric Germanium telluride $V_{Ge}'' V_{Te}''$ antistructure creates a cluster with vacancies in cation crystal sublattice:

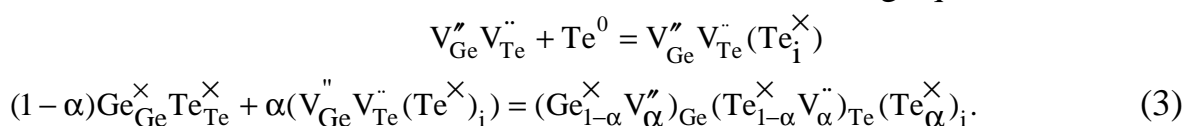


After superpositioning the received cluster to quasichemical stoichiometric composition formula we have



Thus, Tellurium redundancy stipulates for vacancies creation in cation crystal sublattice V_{Ge}'' and, correspondingly, acceptor level that is the reason of point conduction, that is, p-type material.

At Tellurium inculcationing into tetrahedral cavities of crystal lattice GeTe Germanium atoms solid structures we'll receive the following equation:



As we can see neutral Tellurium atoms inculcation in tetrahedral cavities of Germanium crystal sublattice causes appearance of both cation and anion vacancies. Though, such inculcation expects considerable elastic crystal lattice deformations that are caused by the difference of Tellurium $r_{Te} = 0,164^{\circ}nm$ atom sizes and tetrahedral cavities of Germanium that should cause GeTe compound crystal lattice characteristic decrease that is not observed.

The Kinetics of Electronic Processes in Single Crystals of n-Si at T>300K

Panasjuk L.I., Zakharchuk D.A., Koval Yu.V., Yashchynskyy L.V.

Lutsk National Technical University, Lutsk, Ukraine, zachdim@mail.ru

The peculiarity of modern technology experiment is the transition to a comprehensive study of various physical quantities that can not be defined at a high level without the presence of advanced semiconductor sensors designed for measuring static and dynamic pressures.

Previously [1,2] the crucial role of f-transitions in intervalley scattering of electrons in n-Si at temperatures up to 300K was first demonstrated. In the same work a small contribution to g-transitions in this type of scattering was shown. It is unknown, however, the way the electron mobility at T>300K will change where there is the possibility of g-transitions, which, moreover, are not completely eliminated under strong uniaxial pressure X [001].

The change in mobility with increasing temperature may be due to the inclusion of intervalley scattering g-transitions. Their contribution may increase with increasing temperature because of LO-phonon with energy 720K, deformation constant potential of which is $\approx 7,5 \times 10^8$ eV/cm. To change value for g-and f-transitions in intervalley scattering at T>300K, we used the direction of uniaxial pressure X [110] I. In this orientation uniaxial pressure two g-transitions in the directions [100] and [010] are added. Furthermore, eight f-transitions are excluded from strong intervalley scattering in uniaxial pressures and thus their intensity compared to unstrained crystals reduces to three times. The experiment conducted in the temperature range T=300K - 450K showed that even in such a ratio g-and f-slope conversion dependence $\lg \mu = \lg T$ is unchanged and equals to -2,3. This shows the crucial role of f-transitions in intervalley scattering of electrons in n-silicon and the minor role of g-transitions in this temperature range.

Thus, we can conclude that f-transitions and temperature T>300 K will play a major role in intervalley scattering of electrons in n-silicon. This lets you exclude such transitions of intervalley scattering and effectively increase the mobility of electrons in n-Si with the help of strong uniaxial pressure oriented in [001] direction.

1. P.I. Baranskii, I.V. Dakhovskii, V.V. Kolomoets, et. al. Fiz. Tekh. Polupov. 10, 1480 (1976).
2. V. Kolomoets, V. Baidakov, A. Fedosov // Phys. Status Solidi B. - 2009. - Vol. 246. - P. 652 - 654.

Crystal-Quasichemical Description for Cadmium, Lead and Tin Tellurides

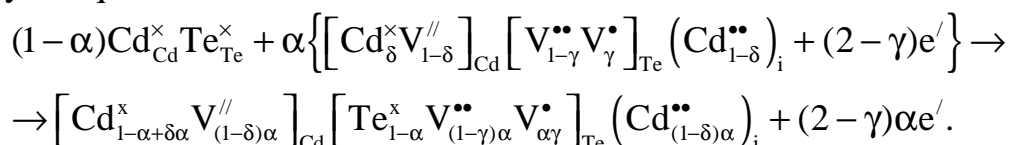
Prokopiv V.V.(Jr), Voznyak O.M., Zapukhlyak R.I., Dron R.P.

Vasyl Stefanyk Precarpathian National University,
Ivano-Frankivsk, Ukraine, e-mail: ruslan.zapukhlyak@pu.if.ua

Cadmium, lead and tin tellurides belongs to connections with noticeable deviation from stoichiometric. The change of composition within the limits of area of homogeneity is conditioned defects grades, which determine the type of conductivity of crystal, mobility of transmitters and their concentration, energy of radiate transitions and other electric and optical properties.

The area of existence of CdTe is asymmetric. For temperatures more small than 1000 K greater part of area of homogeneity of connection loafs surplus of Cd, and for temperatures more high 1000 K – displaced in the side of Te.

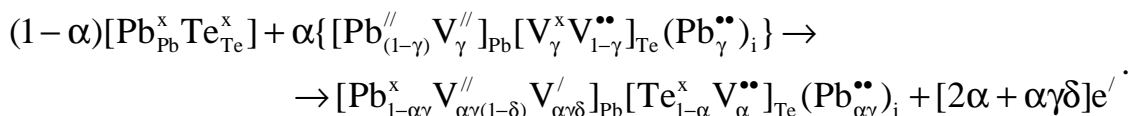
Crystal-quasichemical formula of n-CdTe:



For p-CdTe a crystal-quasichemical formula will be written down an analogical method.

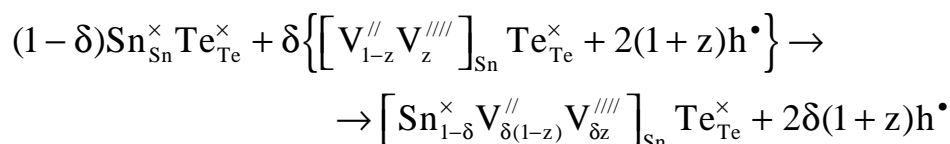
The analysis of phase diagram of Pb-Te specifies in the presence of one connection of PbTe, which smelts congruent at a temperature 1190 K. Maximum size of area of homogeneity of lead telluride is observed at a temperature 1133 K and is $1,310^{19}$ and $6,310^{18} \text{ cm}^{-3}$ for the superstoichiometrical atoms of tellurium and lead accordingly.

Crystal-quasichemical a formula of n-PbTe (surplus of lead is within the limits of area of homogeneity) taking into account disproportionation vacancies in cationic sublattice will be:



Crystal-quasichemical presentation of unstoichiometrical p-PbTe is like set (surplus of tellurium is within the limits of area of homogeneity).

In the system of Sn-Te there is one connection of SnTe that melt congruently at 1063 K. Area telluride lies the homogeneity of tin fully on the side of surplus of tellurium in relation to stoichiometrical composition and has a maximal slowness from $50,1 \pm 0,1$ to $50,9 \pm 0,1\%$ of atomic maintenance of tellurium at 873 K. Crystal-quasichemical the formula of p-SnTe will be written down as follows:





POSTER REPORTS

Session 6
Innovative methods for teaching



Blended Learning in Scientific and Educational Space of Ukraine

Denysenko O.¹, Tsotsko V.²

¹*National Metallurgical Academy of Ukraine, Dnipro, Ukraine*

²*Dnipropetrovsk State Agrarian and Economic University, Dnipro, Ukraine*

The solution to the problem of rationality (a kind of “guidelines for action”) through the lens of education is connected [1], first of all, with the development and implementation of new pedagogical technologies. Innovative education is oriented not so much to conveying knowledge as to mastering basic concepts which will allow an individual to acquire knowledge independently in the future, and the educational potential for the intellectual development of such individual will serve as his/her educational center.

Analysis of the current state of the scientific and educational space of Ukraine calls for the development of a proper environment for distance education which could perform a number of functions related to supporting independent and joint educational and scientific activities, as well as the decision-making process optimizing such activities.

Multilevel resource threshold is an active factor in the current state and extent of the introduction of information technologies in the learning process. Certain optimistic hopes [2] for the instinctive result of practically resourceless “tunneling” of teachers to the level of creation and use of distance courses in practical work [3] give rise to the ideas formulated in [1].

Blended (hybrid) learning is a learning methodology and approach that combine traditional methods of teaching in class and e-learning activities [2]. Its strengths are a mix of different technologies joined into one integrated learning approach. Blended learning is also often called hybrid learning. This is due to the fact that blending learning focuses on mechanical blending. A hybrid is a combination of new, advanced technology and traditional one and creation of an innovation in relation to the traditional technology.

1. Dolska O.O. Transformations of rationality in the field of education: Abstract dissertation for the degree of Doctor of Philosophy : speciality 09.00.10 „Philosophy of Education” . – Kharkov., 2010. – 31 p.
2. Denysenko O.I. Blended training with a distance course "Mechanics. Molecular physics and thermodynamics.". – Access mode: <https://www.researchgate.net/publication/315830902> .
3. Mechanics. Molecular Physics and thermodynamics. Distance course. – Access mode: <https://www.researchgate.net/publication/314048267> .

Formation of Paramagnetic Crystal Structures Based on Lead Telluride

Mikityuk V.¹, Frasunyak V.¹, Zayachuk D.²

¹*Yuriy Fedkovych Chernivtsi National University, Chernivtsi, Ukraine*

²*Lviv Polytechnic National University, Lviv, Ukraine*

In general case pure *PbTe* is diamagnetic. There are several different ways to change the diamagnetic state of semiconducting crystal in paramagnetic. One of them is the use of impurities with nonzero magnetic moment. Another way is the use of certain intrinsic defects, the probability of formation of which can be changed by technological means. In this report we present the summarized results of our investigation of formation of paramagnetic crystal structures based on lead telluride caused by special doping with rare-earth impurities or existence of uncontrolled background impurities and intrinsic defects.

We used *Eu* as the rare-earth impurity in *PbTe*. It can be contained in the crystals matrix of doped *PbTe* as an isolated center in Eu^{2+} state that corresponds to the charge state of Pb^{2+} ion replaced by it. Moreover *Eu* impurity in *PbTe* crystal can be the component of any complex where magnetic ordering is possible. We shown that paramagnetism of doped *PbTe:Eu* crystals is mainly caused by the single centers of *Eu* ions and their pairs, which are the constituents of the complexes of the magnetic impurities with the background Oxygen impurities in the crystal matrix of lead telluride. We also shown that introduction of the *Eu* impurities and especially formation of the *Eu* complexes appreciably effect the temperature independent constituent of the magnetic susceptibility (MS) of the crystal matrix of the doped *PbTe:Eu* crystals. It can change not only its value, but even sign from minus to plus, i.e., it can convert the crystal matrix from diamagnetic to paramagnetic state.

Another structural unit giving the paramagnetic contribution to MS of *PbTe* crystal is *Te* precipitates. The contribution is temperature-independent and increases when concentration of *Te* precipitates increases. Therefore, the value of temperature-independent component of MS in *PbTe* samples can be used as an indicator of *Te* precipitates in the samples.

Also there exist two different types of paramagnetic centers in *PbTe* crystals associated with point defects of crystal matrix. One of them (type I paramagnetic centers) determines the behavior of MS in the medium and high temperature range, another one (type II centers) dominate at lower temperatures. The characteristic feature of type I paramagnetic centers is independence of their MS of temperature and at the same time strong dependence on applied magnetic field starting from zero. Type II paramagnetic centers create the temperature-dependent Curie-like component of the total MS. We suggest that type I and II paramagnetic centers in *PbTe* are native defects of crystal lattice, namely interstitial *Pb* and vacancies in metal sublattice, respectively.

Features of Application of Innovative Teaching Technologies in Higher Education

Prokopiv L., Stynska V.

*Vasyl Stefanyk Precarpathian National University, Ivano-Frankivsk,
Ukraine, prk1@i.ua*

In modern pedagogical science, there are many issues related to teaching subjects at university. Problems of quality of students' knowledge are solved through innovative learning. Due to such education there is a development of the student mental activity, critical thinking skills and abilities are manifested, search operation experience is acquired etc.

We have approved and implemented innovative teaching technologies, which have proved their effectiveness, in the educational process of university.

Group and individual technology. The focus is shifted to creative improvisation. Important methods of group learning are mutual learning, formation of skills to conduct a dialogue and a discussion.

"The method of the press" is used when there are controversial issues and need to take and argue a clear position on the issue under discussion. Proven method steps are: position (I believe that ... (express your views, explain what your opinion is)), reasoning (...because... (the appearance of thoughts, evidence to support your position), example (bringing the facts which show evidence, they strengthen the position)), conclusions.

Group training (for example, prompting the facts and arguments). Its purpose is solving problems: acquire knowledge, abilities and skills formation, development of attitudes that determine the ability of the personality, support of individuality and active position of the individual.

Brainstorming allows discuss and comprehend in detail each of the participants' suggested solutions to the problem. To solve the problem as much as possible alternative means, which are subsequently analyzed by the students, are offered. One option is to offer a student or a group of students to consider the position in specified view.

Synectics is "the combination of heterogeneous elements". It is based on the targeted use of intuitive and imaginative and metaphorical thinking of participants. This is a methodology of stimulation of search of innovative solutions.

"A decision tree" is used in the analysis of situations and helps to achieve a complete understanding of the causes that led to making important decisions.

Thus, in modern pedagogy innovative teaching technologies, which are aimed at the quality of teaching students, development of their mental activity, search operation, acquiring skills that will be useful later in life, have their place.

Physics. Dialogic Teaching of the Course

Tsotsko V.¹, Denysenko O.²

¹*Dnipropetrovsk State Agrarian and Economic University, Dnipro, Ukraine*

²*National Metallurgical Academy of Ukraine, Dnipro, Ukraine*

Teaching the course of physics should be in line with modern creative forms - intense, dynamic and bright. The birth of thought and new knowledge requires a certain conflict, a clash of characters. It is not an overstatement to say that a great number of monographs were written by a team of contributors, for example, the Course of Theoretical Physics, a classical textbook on theoretical physics, was written by L. Landau in collaboration with his student E. Lifschitz.

According to the great physicist and Nobel laureate R. Feynman, the best teaching can be done only when there is a direct individual relationship between a student and a good teacher—a situation in which the student discusses the ideas, thinks about the things, and talks about the things. It can be added that it is a good idea for a student to find out the opinion of another teacher alternatively, as well as to listen to the dialogue between two teachers.

An interactive, dialogic form of teaching is offered, when two or even several teachers give classes by delivering the material through discussion, clarifying and supplementing it with new elements, exchanging ideas and entering into polemics. Students are encouraged to take part in the discussion, ask questions and put forward their own counterarguments. Of course, it is necessary to prepare well for such classes and they should be pre-announced. But how interesting it is to be a character in the play and not just a raw material for the replication of knowledge!

The idea of dialogue as a means of teaching is a kind of extrapolation of pair commenting of sporting events or modern interactive news or cultural television programs that have raised their expressiveness by several orders of magnitude. Such form of teaching makes it possible to invite bright personalities, such as scientists, experienced practitioners and experts, to visit the class which will arouse even more interest for learning in students.

The dialogic form of teaching has a number of advantages.

Errors in the delivered material virtually disappear. The depth and scope of the acquired knowledge increase. A multifaceted approach to solving a problem is implemented, new ideas are generated and thinking is activated. The variety of accents in the knowledge system leads to an understanding of the variability of the natural phenomena and the development as such. In dialogic teaching, a competition of personalities is simulated and a real process of improvement of teaching takes place. The students are faced with the issue of freedom of choice of information.

The dialogic form of teaching is more costly of course, but it is worth it for the sake of increasing its expressiveness and attractiveness of learning, and improving the quality of studies.

Play as Means of Study of Educational "Science" in Elementary School

Vysochan L.

Vasyl Stefanyk Precarpathian National University, Ivano-Frankivsk, Ukraine

Formulation of the problem. Coverage values and objectives of the game using the lessons of science. An important tool to enhance the learning of primary school children have a game. She held during walks, excursions, and the lesson to summarize the knowledge of specific objects and natural phenomena that form specific basic concepts of science. Analysis of the research. Outstanding teachers attached great importance to the inclusion of the game in training activities. Even Karl Ushinskiy advised to introduce elements of curiosity, game highlights in serious academic work of students so that learning process was more productive. Well-known educator ST Shatsky December called vital laboratory childhood: "When a person is playing, it increases their emotions. Our school we have to do is just such a place of recovery. " LS Vygotsky, considering the role of play in the mental development of the child, said that in connection with the transition to school, playing not only persists, but rather it permeates all activities of the student. "At school age, - he said - is not a game dies and enters in relation to reality. It has continued in its internal schooling and work. The development of game theory, clarifying the role, structure and their implications for education and training of children engaged psychologist Jean Piaget, L. Vygotsky, AN Leontiev, DA El'konin. More known dydakty warned against odoroslennya training and educational work with students, insisted on organizing role play. A. Makarenko believed didactic and role play as important for the development of the child as an adult - the real work. It contribute to this story games and exercises from natural materials. Their goal - to teach children to find the desired object using the analyzer - (touch, taste, smell), in terms of the essential features; describe the items and find them by description; find the part of the whole and the part for the whole; to group items by location. During the game the students made a habit of focus, to think independently, develop attention. Inspired by the game, kids do not notice enrole Thus, the most important secret of the game is that it is necessarily based on interest and pleasure. It gives joy and admiration, because the process of the game is full of surprises, and the result - always a mystery. Force can not play, you can grab the game.

Literature.

1. L. Artemov Parenting behavior in kids games / LV Artemov. - Soviet school. - 1964.

2. Béguey VM Oliyarm.P., Stepanova LV, Faychak Z.YE. Playing forms of organization of learning activities of students in the school and degree / Ed. VM Beheya.- Lviv, 1996.
3. State standard primary education - [electronic resource] access mode www.mon.gov.ua/new-stmp/ 2011 / 20.04.12.
4. L. Smith Modern educational technology in elementary school: Educational textbook / LV Blacksmith. - K .: Publishing house "elementary school", 2006.
5. Guidelines of the Ministry of Education and Science of Ukraine on teaching subjects in elementary school general educational institutions of Ukraine in 2016/2017 academic year: for of a comprehensive. teach. bookmark. Ukraine. - K .: Publishing house "Education", 2016. - S. 144.
6. The curriculum for secondary schools with the Ukrainian language learning 1-4 cells. - K .: An outstanding house "Education". 2012-392s.
7. Primary school [electronic resource] access mode www.mon.gov.ua
8. Savchenko OJ Didactic Elementary School: Textbook for students of pedagogical faculties / AJ Savchenko. - K .: outline, 1997.
9. Sukhomlinsky VA I give my heart to the children / VA Sukhomlinsky. - Select. op. In 5 t. - K .: Soviets. HQ., 1977.

Self-organization of heterocyclic amines on patterned silicon substrates as new technology for creation of hybrid solar cells

Smertenko¹ P.S., Gorbach¹ T.Ya., Roshchina¹ N.M., Naumov¹ V.V., Wisz² G.

¹ V.Lashkaryov Institute of Semiconductor Physics, NAS of Ukraine, Kyiv, Ukraine

² University of Rzeszow, Rzeszow, Poland

The self-organization and self-assembly approach allowed developing different technologies for preparation of huge number of structures: from membranes and sub-micron lithography masks to formation of helices, nanotubes and biomaterials. Self-assembles and self-organized layers are potential objects for photovoltaics, optoelectronics, biosensing, and gene and drug delivery applications due to: (i) unique properties of both the isolated molecule and self-organized molecular assemblies or aggregations; (ii) the combination of a high absorption coefficient of organics and good *Si* transport properties; (iii) hybrid compatibility with well explored *Si* planar technology. At the first time we used heterocyclic amines for self-organization of organic layers on nanostructures silicon substrate [1]. In Fig. 1 the optical image of surface morphology of hybrids with various HCAs is represented. There is wide variety of morphology: net-like, ring-like, fibers, stars.

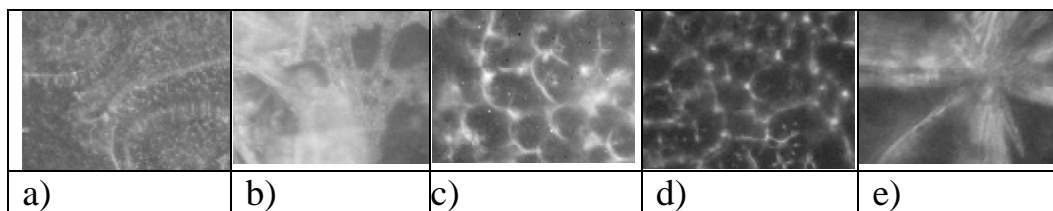


Fig.1. Morphology of hybrids on Si: a) thiamine diphosphide, b) clonidin, c) metamizole sodium, d) procainamide, e) sulfacil sodium.

New knowledge about the mechanisms of self-organization of organic molecules on the surface of inorganic materials during the formation of hybrid organic-inorganic structures allow the better understanding of many processes in pairs, such as the passivation of surface, changing of the charge trap states, influence of chemicals on the energy level alignment, altering the work function of surfaces, direction for the charge carriers injection and extraction, control of the organic layers morphology.

1. Gorbach T., Kostylyov V. and Smertenko P. New organic materials for organic-inorganic silicon-based solar cells. *Mol. Cryst. Liq. Cryst.* **535** 174-178 (2011).
2. Gorbach T.Ya., Kostylyov V.P., Melakh V.G., Roshchina N.M., Smertenko P.S, Wisz G. Formation of self-organized organic-inorganic hybrids. *Reports of Ukrainian Material Research Society* **8** 46-55 (2015).

Position of Ukrainian Science in global innovation trends

Smertenko P.S.

V.Lashkaryov Institute of Semiconductor Physics, NAS of Ukraine, Kyiv, Ukraine

Now Ukraine is under reformation practically in all spheres of political, economical and social life. Ukrainian science has been stagnating last decades and need radical conversion. Unfortunately there are no official ideas how to do this. We presume some steps to overcome this gap. Main aim of this report is not to give some knowledge in innovations of technology transfer but to shake the mentality and imagination to inspire us to think about cardinal changes in management of Ukrainian science and research institutions, to show ways for harmonized and synchronized with the world R&D activity. The main obstacle is the lack of innovation environment practically in all circles closed to science. There are some conditions for creative environment, free cooperation and arisen of crazy ideas: (i) high level of confidence; (ii) tolerant attitude to defeat and mistakes; (iii) corporative culture when the main type of relations is equality of treatment; (iv) the team is motivated for result. Innovations are guaranteed by: (i) generation of new knowledge in R&D, engineering and management; (ii) presence of high educated self programmed; (iii) existence of entrepreneurs who cam and wish to take a risk to turn business project into real innovations

On the base of overall analyses the next task can be emphasized.

- 1 To see ourself from outside.
- 2 Look through SWOT, PEST analysis and others.
- 3 Developing the strategy and tactics of innovation development.
- 4 Assistance to create the innovation environment.
- 5 Holding of non-formal training for scientists to enhance the grant writing skill and commercialization of R&D results.
- 6 Studying, dissemination and implementation of best practices.
- 7 Organization and stimulation of experience exchange.
- Work throught the mechanim for commercialization of R&D results, IP etc.
- 8 Support of real innovators, work through the stimulation and motivation mechanisms.
- 9 Attract the potential of technoparks for increase the innovation potential.
- 10 Heighten information providing of innovation process.
- 11 Orientation to young innovators with innovation thinking.
- 12 Realize exhibition activity on both internal and inernational level.
- 13 Implementation of effective TT mechanisms.
- 14 Active involving of young scientists for writing of international projects.
- 15 Enhance PR actions, including web-sites, leaflets etc.

So, now we are living in not simple conditions and only not simple decisions can help to survive and develop. Not simple decisions are innovations both R&D and managerial.

Miniband electroconductivity in heterosystem InAs/Ga_xIn_{1-x}As of periodic cubic quantum dots

Boichuk V.I., Bilynskyi I.V., Pazyuk R.I.

Drohobych Ivan Franko State Pedagogical University, Drohobych, Ukraine

In recent years the growing interest of researchers, engineers and technologists has been drawn to low-dimensional systems, among which superlattices constitute a special class of periodical system quantum dots. Quantum dot superlattices are rather important to fundamental science as completely new types of artificial materials with unusual physical properties.

The electrical properties of GaAs/Al_xGa_{1-x}As spherical quantum dot superlattices of various dimensionality are studied, depending on the Fermi energy and temperature, concentration of aluminum in the matrix in the tight binding approximation [1].

In this paper properties of the system of spatially assembled cubic quantum dots that are embedded in the matrix (i.e., quantum dot superlattice of various dimensionality) have been investigated. The energy bands spectra of the system have been studied. The temperature dependence of the Fermi energy of the that systems with impurities has been received and analyzed. We have taken account of the dependence of electron relaxation time on temperature caused by scattering of carriers on both phonons and donor centers. The effect of the impurity system on electroconductivity of the CQDS is investigated.

We have considered an InAs/Ga_xIn_{1-x}As nanoscale heterostructure. The energy spectra of electrons and holes of the quantum dot superlattice have been determined in the effective mass approximation and modified Kronig-Penney model. In the frame of this model, the spectra of charges of 3D-, 2D- and 1D-superlattices can be obtained by changing respective distances between the elements of the superlattice.

In case of the matrix doped by donor impurities, in the presence of impurities of one type we have studied the dependence of the Fermi level, concentration of charge carriers on temperature ($40 \leq T \leq 800$ K), concentration of impurities (10^{14} cm^{-3} , 10^{16} cm^{-3} , 10^{18} cm^{-3}), energy of impurity levels on the bottom of the conduction band of the semiconductor matrix (-750 meV, -150 meV). It has been shown that in the presence of deep impurities (-750 meV) the temperature dependence of conductivity of the superlattice has characteristic peaks, which are defined by concentrations of impurities and dimensionality of the superlattice. A different temperature dependence of conductivity has been observed for impurities with the energy of occurrence -150 meV.

[1] V.I. Boichuk, I.V. Bilynskyi, R.I. Pazyuk. *Physics and Chemistry of Solid State*, 17 (3), 320 (2016).

Influence of Surface Pd Films on Mechanism of Conductivity of Nanocomposites Based on Porous Silicon with Nafion and TiO₂ Inclusions

Gorbanyuk T.I.¹, Drozhcha I.I.¹, Lytovchenko V.G.¹, Nicolskii S.A.²

¹*V. Lashkarev Institute of Semiconductor Physic, NASU, Kyiv, Ukraine, e-mail tania2gor@gmail.com*

²*Institute of High Technologies, Taras Shevchenko National University of Kyiv, Academician Glushkov avenue 4G, 03022 Kyiv, Ukraine.*

One of all promising class of materials for the development of membrane electrode block is a composites based on porous silicon. The filling of silicon mesopores by material with ionic conductivity will provide reinforced solid electrolyte. As the mesoporous silicon has also high resistance, it allows isolating a cathode and an anode in the membrane electrode block. Combining different porous layers (two electrodes and membrane) in a single silicon wafer will yield a monolithic membrane electrode block with enhanced reliability. Using of a proton conducting membrane from Nafion perforated polymer [1] allows effective separate the protons and oxygen atoms in an electrode block that often used in a portable fuel cell.

In the present work presents the results of such an investigation in which the conductivity of nanocomposite based on porous silicon with Nafion/TiO₂ inclusions and nanostructured surface palladium films have been studied under H₂O adsorption. The morphology of Nafion/TiO₂ and Pd/Nafion/TiO₂ surface was characterised by scanning electron microscopy (SEM) and atomic force microscopy (AFM). Palladium layers were deposited by the magnetron deposition technique at room temperature. It was found that nanostructured palladium films on Nafion/TiO₂ surface lead to enhanced proton conductivity depends on the presence of TiO₂.

1. J. Zeng, B. He, K. Lamb, R. D. Marco, P. K. Shenc, and S. P. Jiang, Phosphoric acid functionalized pre-sintered meso-silica for high temperature proton exchange membrane fuel cells // Chem. Commun., — 2013, — v. 49, — No 41, — pp. 4655–4657

AUTHORS INDEX

- Afanasieva T.V. 105
 Akata Kurc B. 252
 Akinshau K.A. 208
 Aksimentyeva O.I. 74, 219, 298
 Alekseeva T.T. 99
 Andrearczyk T. 79
 Antonenko O.I. 228
 Arsenyuk I. 350
 Azhniuk Yu.M. 268
 Babich V.M. 58
 Babichuk I.V. 32
 Babkina N.V. 99
 Bahriyчук V.O. 289
 Baibara A.E. 22, 122
 Bairachny B.I. 194
 Bakhtinov A.P. 148
 Balabai R.M. 59, 206, 209, 325
 Balakin D.Yu. 131
 Balashov Yu.I. 264
 Balitska V. 225
 Balovsyak S. 271, 331, 357
 Bandura Kh.V. 60
 Barabash M.Yu. 265,266
 Baran J. 88
 Bararash M.Yu. 264
 Barchuk M. 156, 281
 Bardashevskа S.D. 106
 Barilka A.G. 209
 Barta A. 241
 Bartsikhovskiy V.V. 94
 Bashev V.F. 293
 Baturin V.A. 11, 185
 Bazylyak L.I. 231
 Beketov G.V. 107, 141, 149
 Belous A.G. 61, 108
 Belyaev A. 315
 Belyaev O.E. 113
 Benamara M. 315
 Bendak A.V. 268
 Bengus S.V. 146
 Bercha S. 241
 Berezhansky V.M. 319
 Berezovskyi I.S. 204
 Bersirova O.L. 45
 Bezruka N.A. 235
 Bihun R.I. 35, 313
 Bilanych V. 324
 Bilogorodskyy Y. 140
 Bilozertseva V.I. 249
 Bilynskyi 370
 Bliznyuk V.N. 292
 Blonskyi I. 5
 Bloshenko Z.V. 276
 Bodul G.I. 269
 Bogatyrenko S. 109
 Bogatyrenko S.I. 129, 317
 Bohdan R. 118
 Boichuk A.M. 150, 370
 Boichuk V.I. 6, 78
 Boichyshyn L.M. 188
 Boiko V. 63, 245
 Bojchuk V.M. 167
 Bokshyts Yu.V. 26
 Bolshakova I. 288
 Boltovets P.M. 210
 Bonchyk O.Yu. 270
 Borchа M. 110, 271
 Bordian O. 283
 Bordun B.O. 272
 Bordun I.O. 291
 Bordun O.M. 272
 Borkovskaya O.Yu. 62
 Boryk V.V. 332
 Bovgyra R.I. 240
 Bovsunivskyi O.V. 333
 Boyko S.I. 319
 Brovko O. 216
 Brus V.V. 54, 301
 Bryzhko V.S. 85
 Buchkovska M.D. 273
 Budjak Ya.S. 111
 Budzulyak I.M., 106, 222, 237

- Budzulyak S.I. 18, 106
 Budzulyak I.M. 259
 Bugaiova M.E. 22
 Bugayova M. 122
 Bukartyk N.M. 18
 Bulaniy M.F. 20
 Burchenya A. 342
 Burlachenko J. 230
 Burlak G. 274
 Burlaka I.M. 113
 Burunkova J. 118
 Bushkov N.I. 180
 Bushma A.V. 320
 Buzhuk Ya.M. 215
 Burchenia A.V. 333
 Bylina I.S. 181
 Calvez L. 5
 Chayka M.V. 182
 Cheong H. 275
 Chernikova H.M. 209
 Cheshko I.V. 84
 Chey C. 243
 Chornous A.M. 308
 Chugunova S.I. 157
 Chukova O.V. 26
 Churilov I.G. 276
 Csarnovics I. 118
 Csik A. 42
 Dan'kiv O.O. 85
 Danilchenko P.S. 275
 Danilenko I.A. 93
 Danilova T.A. 264
 Demianenko E.M. 72
 Denysenko O.I. 362, 365
 Denysiuk M.I. 161
 Denysyuk N.M. 334
 Denysyuk R.O. 182
 Deputat B.J. 211
 Deputat B.Y. 339
 Dmitriev A.I. 22
 Dmitruk N.L. 7, 62
 Dmytrenko O.P. 116
 Dobrozhan A.I. 152
 Dobrozhan O.A. 275
 Dolgov N.A. 46
 Dolynska L.V. 18
 Domagala J.Z. 79
 Domantsevych N.I. 202, 335
 Dominik A.M. 91
 Doroshkevich A.S. 93
 Dovbeshko G. 63, 245
 Dovganyuk V. 156, 281
 Dovhyi V.V. 323
 Dranchuk M. 123, 294
 Dranchuk M.V. 185
 Dranenko A.S. 287
 Dremlyuzhenko S. 336
 Drobot O.S. 299
 Dron R.P. 158, 360
 Drozhcha 371
 Druzhinin A.A. 80
 Dub M.M. 112
 Dubelt S.P. 205
 Dubikovskiy O.V. 58
 Dubiv T.O. 197
 Duchon T. 241
 Dudka O.I. 41
 Duffy R. 130
 Dukarov S.V. 134, 276
 Dukarov S.V. 38
 Durkot M.O. 314
 Dveriy O.R. 215
 Dvoretzky S.A. 270
 Dyadenchuk A.F. 213
 Dyakonenko N.L. 175, 249
 Dymko L.M. 54
 Dzeryn M. R. 183
 Dzumedzey R.O. 158
 Dzundza B.S. 214, 344
 Dzyadevych S.V. 252
 Dzyubinska N. 70
 Efremov A. 233
 Eremin O.G. 117
 Ermakov V.M. 18
 Evtukh A.A. 64, 94
 Fediv V.I. 221

- Fedorchenko S.V. 60
 Fedorchuk O.P. 355
 Fedorenko L.L. 328
 Fedoriv V.D. 279
 Fedorus A.G. 105
 Feher A. 324
 Figielski T. 79
 Filatov S.A. 33
 Filonenko N.Yu. 277
 Filonenko O. 65
 Fitsych O.I. 270
 Fochuk P. 336
 Fochuk P.M. 70
 Fodchuk I. 110, 156, 271, 281, 331, 357
 Frasunyak V.M. 363
 Frugynskyi M.S. 55
 Fryk O. 327
 Gab I.I. 278
 Gaidai S.I. 193
 Gaidar G.P. 66
 Gal' Yu.M. 30
 Galanov B.A. 157
 Galdina A.N. 277
 Galiy P.V. 215
 Galushchak M.O. 9
 Gaponov O.V. 337, 338
 Garabazhiv Y. 271
 Garpul O.Z. 279
 Gasyuk I.M. 144, 150, 339
 Gasyuk M.I. 211
 Gavaleshko O.S. 280, 311
 Gazova Z. 241
 Gentsar P.O. 340
 Getmanchuk I.P. 228
 Gilmutdinova V.R. 153
 Globa N.I. 290
 Glotov V.I. 130
 Gnatenko Yu.P. 329
 Gnatyuk O. 63
 Godlewski M. 123
 Golubenko A.A. 157
 Gomeniuk Yu.V. 130
 Gomozov V.P. 250
 Gorbach L. 216
 Gorbach T.Ya. 368
 Gorban' V. F. 176
 Gorbanyuk T.I. 24, 371
 Gorbulik V.I. 115
 Gordeev S.O. 333
 Gorichok I.V. 349
 Gorina O.M. 205, 261
 Gorina O.V. 305
 Gorskyi P.V. 67, 68
 Granozzi G. 10
 Grigorchak I.I. 259
 Gryga V.M. 321
 Gryn`ko D.A. 264
 Guba S.K. 217
 Gubanova A. 88, 238
 Gudyma Iu.V. 341
 Gudymenko O. 18, 58, 223, 238
 Gule E.G. 221
 Gun'ko V.M. 131
 Gutsuliak I. 156, 281
 Gwóźdź K. 121
 Hadzaman I. 225
 Haluschak M.O. 170
 Hanushchak M.A. 259
 Harchenko M.M. 152
 Hasynets S.M. 305
 Hatala I. 262
 Havrelyh V.M. 273
 Havrikov D.S. 113
 Herman I.I. 280
 Hlozna D. 324
 Holod A.G. 87
 Holomb R. 286, 218
 Holota V.I. 319, 321, 323
 Holovatsky V.A. 102
 Honchar F.M. 197
 Horbenko Yu.Yu. 74, 183, 219
 Horichok I.V. 158, 169, 350
 Horvat H. 282
 Horvat Yu.A. 31
 Horyn A. 351, 352

- Hrubiak A. 60, 69, 82
 Hrushka V.I. 220
 Hurhula G.Y. 356
 Hurskyj S.T. 257
 Hutsu O. 333, 342
 Iakovyshen R.S. 184
 Iarmolenko D.O. 113
 Iaseniuc O. 283
 Ievtushenko A.I. 11, 185
 Ignatova T.D. 228
 Ihnatolia P. 218
 Il'chuk H. 47, 121
 Ilashchuk M.I. 171, 301
 Ilchuk H.A. 18
 Initsky R.V. 150
 Initsky R.V. 222, 237
 Isaenko L.I. 334
 Isaieva O.F. 221
 Ishchenko O.O. 108
 Ivakhnenko S.A. 157
 Ivakhnenko S.O. 160
 Ivakin E.V. 13
 Ivanchyshyn I.B. 78
 Ivanits'ka V.G. 70
 Ivanyshyn I.M. 358
 Ivasiuk R.V. 347
 Izai V.Yu. 284
 Izhnin I.I. 270
 Izotov V.Yu. 113
 Jakiela R. 79
 Jaworski Y.A.S. 349
 Kaban I.G. 347
 Kachkovsky O.D. 116, 184
 Kachmar A.I. 222, 237
 Kadan V. 5
 Kal'ka O.Yu. 348
 Kalashnyk Yu.Yu. 159
 Kalchenko V.I. 114
 Kalenchuk V. 333, 342
 Kalytchuk I.V. 196
 Karachevtseva L. 71, 187, 223
 Karas N. 71
 Karpenko O.S. 72
 Karpenko O.Y. 11, 185
 Karpets M.V. 103, 211
 Karpyna V. 11, 123, 185
 Kartel N.T. 72
 Kartuzov V. 294
 Kasumov A.M. 246
 Kaykan Y.S. 211
 Kazantseva Z.I. 114
 Keush L. 224
 Khalachan I. 241, 282
 Kharchenko M.F. 124
 Khemii O.M. 259
 Khmelenko A.V. 56
 Khmelenko O.V. 20
 Khmil' D.N. 154
 Khoverko Yu.N. 80
 Khrypunov G.S. 16, 151, 152
 Khyzhun O.Y. 163, 334
 Kidalov V.V. 213
 Kinzerska O.V. 280
 Kirichenko M.V.
 Kirichenko M.V. 16, 151
 Kirillov A.K. 93
 Kirillov S.A. 242, 343
 Kisialiou I.G. 13
 Kizjak A.Yu. 64, 94
 Kladko V. 18, 58, 156, 223, 281, 315
 Klanichka V.M. 322
 Klanichka Yu.V. 322
 Klepikova K.S. 16
 Kleto G.I. 142
 Klimkiewicz R. 63
 Klimovskaya A.I. 159
 Klochko N.P. 16, 151
 Klots O.M. 164
 Klym H. 225
 Klyui N.I. 15, 115, 166
 Knoff W. 22, 122
 Kobylianskaya S.D. 108
 Kobzar P.Y. 116
 Kobzar Yu.L. 254
 Kocherba G.I. 117
 Kogut I.T. 319, 321, 323

- Kohdas M. G. 86
 Kokenyesi S. 118
 Kolesnichenko A.A. 264, 265, 266
 Kolkovskyi M.I. 73
 Kolkovskyi P.I. 73
 Kolomys O. 315
 Koloskova O.A. 285
 Koltsov I.V. 113
 Kolupaev B.B. 234
 Kolupaev B.S. 226
 Kolyadina E.Yu. 27
 Komanicky V. 324
 Komarov A. 243
 Konakova R.V. 27
 Kondrat O. 218, 286
 Konin K. 223
 Kononenko Ya.A. 103
 Konopelnyk O.I. 74
 Konstantinova T.E. 93
 Kopach G.I. 152
 Kopach V.R. 16, 151
 Kopylets V.I. 227, 289
 Korbutyak D.V. 18
 Korchemskaya E. 53
 Korchovyi A.A. 11, 49
 Korniy S. 227
 Korotaev A.G. 270
 Korovin A.V. 7, 62, 75
 Korsun V.E. 16
 Korzh I.A. 249
 Koshel V.I. 214
 Koshelev M.V. 287
 Koshets I.A. 114
 Kosilov V.V. 343
 Kosminska Yu.O. 76
 Kosovan R.P. 193
 Kost Y. 288
 Kostiv V.T. 188
 Kostruba A.M. 289
 Kostylyov V.P. 19
 Kostyuk B.D. 278
 Kostyuk D.M. 84
 Kostyuk O.B. 119, 138, 344
 Kosyanchuk L.F. 228
 Kosynska O.L. 189
 Kotova N.V. 62
 Kotsyubinsky V.O. 60, 73, 240
 Kotsyubynskiy A. 281
 Kotsyubynsky V. 69, 82, 103
 Kotyk M.V. 48
 Kouhar V.V. 26, 229
 Koval Yu.V. 346, 359
 Kovalenko A.V. 20, 56
 Kovalenko T.V. 160
 Kovalska E. 63
 Kovalyuk Z.D. 148
 Kozak I.M. 41
 Kozejova M. 324
 Koziarskyi D.P. 326
 Koziarskyi I.P. 326
 Kozoriz V.S. 189
 Kranjčec M. 284
 Kraszkiewicz P. 63
 Kravchenko S.O. 210
 Kravchenko V.N. 254
 Kravtsova D.Yu. 59
 Krayovskyy V.Ya. 352
 Krit A.N. 254
 Krivoruchko Ya.S. 96, 98
 Kroitor O. 110
 Kropyvnytska K.M. 6
 Kruglenko I. 230
 Krukovskyi R. 47
 Krukovskyi S. 47
 Krupa M. 21
 Krushinskaya L. 22, 122
 Krymus A.S. 161
 Kryshtal A. 109, 129
 Kryskov Ts. 120, 255
 Kshevetsky O. 110
 Kublanovsky V.S. 45, 290
 Kuech T. 288
 Kukharska L.V. 272
 Kukharskyy I.Yo. 291
 Kukla O.L. 292
 Kulinich A.V. 108

- Kulish M.P. 116
 Kulish N.P. 184
 Kulyk Yu.O. 235
 Kunak S.J. 310
 Kurchak A.I. 37
 Kurdyukov V.V. 116, 184
 Kurek I.G. 346
 Kurovets V.V. 279
 Kurta S. 77
 Kuryliuk A.N. 254
 Kúš P. 268, 284
 Kushlyk M.O. 168
 Kushnerov O.I. 293
 Kushnir R.I. 347
 Kusnezh V.V. 121
 Kutsyk M.M. 268
 Kuzma O.V. 190
 Kuzma V. 324
 Kuzyk O.V. 85
 Kylivnyk Yu. 101
 Kyrnychuk O.S. 153
 Kyrylenko V.K. 31
 Kytsya A.R. 231
 Lashkarev G. 11, 22, 122, 123, 185,
 246, 294
 Lavrenova T.I. 232
 Lepikh Ya.I. 232
 Leschiy R.M. 193
 Leshko R.Ya. 6, 78
 Levchenko I.V. 49
 Levchenko K. 79
 Levchuk V.V. 226
 Levkovets S.I. 163
 Levkun M.P. 356
 Li S. 315
 Liakh-Kaguy N.S. 80
 Liashok L.V. 250
 Liptuga A.I. 107, 115
 Lisakovskiy V. 342
 Lishchynsky I.M. 158
 Lishchynskya S.I. 358
 Lishchynskyy I.M. 347
 Litvin R.V. 264, 265, 266
 Litvinenko O. 71
 Lobanov V. 65, 72, 96, 98
 Loboiko V.I. 205
 Lopatynskiy I. 55, 197
 Lopjanko M.A. 170,191,193
 Lotsko O.P. 18
 Lozinska Yu.V. 115
 Lozinskii V.B. 115
 Lubenets A.G. 325
 Luchytskyi R.M. 162
 Luka G.55
 Lukianov A.M. 115
 Lukianova O.V. 16, 151
 Lukienko I.M.
 Lusakowska E. 55, 79
 Lutchytskyi R.M. 165
 Lutsyk N.Yu. 295
 Lutsyk O. 216
 Luzhnyi I. 163
 Lykah V.A. 249
 Lysak A.V. 348
 Lysakovskiy V.V. 160, 333
 Lysenko V.S. 130
 Lysyuk O.V. 346
 Lytovchenko V.G. 15, 19, 24, 371
 Lytvyn O.S. 185
 Lytvyn P. 233, 281
 Lytvyn P.M. 11, 31, 314, 159
 Lytvynenko A.A. 41
 Lytvynenko O. 187
 Lyuba T.S. 120
 Lyubchenko E.A. 175
 Lyubov V.M. 16, 151
 Magunov I.R. 117, 173
 Maidaniuk Y. 315
 Maistruk E.V. 296, 326
 Maizelis A.A. 194
 Makar L.I. 305
 Makara V. 140
 Makauz I. 118
 Makhniy V.P. 125, 269, 309
 Makhnovets H.V. 164
 Makogon Yu.N. 248

- Makoviychuk M.I. 81
 Makovyshyn V.I. 344
 Maksimtsev Yu.R. 234
 Maksymiuk N.T. 170
 Maksymov A.Iu. 341
 Malanych G.P. 49, 195
 Malashkevich G.E. 26
 Malyk O.P. 111, 297
 Malynych S.Z. 7
 Mamontova I.B. 62
 Mamykin A.V. 235, 292
 Manorik P.A. 39
 Mar'yan M. 126
 Mar'yanchuk P.D. 70
 Marchenko S.V. 252
 Marenkov V.I. 50
 Martynchuk V.E. 264, 265, 266
 Martyniuk G. 298
 Martynyuk M.I. 299
 Maryanchuk P.D. 54, 133, 301
 Maslyanchuk O. 156
 Maslyuk V. 123
 Mateik G.D. 349
 Matkivsky O.M. 158, 349
 Matkovsky A.K. 131
 Matolin V. 241
 Matveeva L.A. 27, 33
 Mazur P. 215
 Mazur T.M. 125, 169
 Mazur Y. 315
 Mazur M.P. 196
 Medvid I.I. 272
 Medvid A. 328
 Melnichuk L.Yu. 127
 Melnichuk O.V. 127
 Menshikova S.I. 128
 Metsan Kh.O. 30
 Mezhylovskaya L.I. 358
 Mikityuk V.I. 363
 Mikula M. 284
 Milenin G.V. 136
 Milenin V.V. 136
 Milman Yu.V. 157
 Minenkov A.A. 129, 317
 Mironchuk V.I. 220
 Mironyuk I.F. 236
 Mista W. 63
 Mitsa V. 218, 286
 Moiseeko V. 245
 Mokhnatska L.V. 82
 Mokhnatskyi M.L. 83
 Moklyak M. 69
 Moklyak V. 69, 262
 Molnar S. 118
 Morgiel Y. 270
 Morozovska A.N. 37
 Morozovska D. 223
 Morushko O.V. 259
 Mostovyi A.I. 54
 Mudryy S.I. 170
 Muronchuk G.L. 164
 Myronyuk I.F. 235
 Musiy R.Y. 289
 Mygushchenko R.P. 152
 Mykaylo O.A. 305
 Mykolaychuk O.G. 295, 303
 Mynda A. 324
 Myroniuk D. 123
 Myrovych O.V. 201
 Myrytyn I. 77
 Myslin M.V. 236
 Mytsyk B. 5
 Nahusko O.T. 284
 Nakhodkin N.G. 89
 Napolitani E. 130
 Nasieka Iu. 238
 Nasyeka Yu.M. 106
 Naumenko S.N. 254
 Naumov V.V. 368
 Naumovets A.G. 105
 Naydich U.V. 278
 Nazarov A.N. 130
 Nazarova T.M. 130
 Nechyporenko G.V. 173
 Nedilko S.G. 26
 Negriyko A. 245

- Neluba P.L. 27
 Nenchuk T.M. 215
 Netyaga V.V. 148
 Nevgasimov A.O. 134
 Nichiporuk Yu.M. 131
 Nikitenko V.M. 290
 Nikolenko A. 243
 Nicolskii 371
 Nitsuk Yu.A. 100
 Novikov S. 357
 Novosjadly S. 327
 Nowak S. 95
 Nur O. 243
 Nykoliuk M.O. 222, 237
 Nykoniuk Ye. 336
 Nykyrui L.I. 13, 316
 Nykyrui R.I. 196
 Nyzhnykevych V.V. 162, 165
 Oberemok O.C. 159
 Oberemok O.S. 58
 Odarych V.A. 300
 Odnodvoretz L.V. 132, 135, 285
 Odynets I.V. 166
 Ogurtsov N.A. 292
 Okholin P.N. 130
 Oksanich A.P. 86, 87
 Olar O.I. 221
 Oleskiv R.B. 201
 Olifan O.I. 11
 Olikh Ya.M. 171
 Oliynich-Lysyuk A.V. 346
 Onufrijev P. 328
 Onyshchenko V. 71, 187
 Opanasyuk A.S. 275, 329
 Opanasyuk N.M. 329
 Optasyuk S.V. 120
 Orletskyi I.G. 301
 Ostafiychuk B.K. 73, 240
 Ostrovskii I.P. 80
 Ovsiannikova L. 294
 Ozansoy Kasap B.
 Paiuk O. 88, 238, 255
 Panasjuk L.I. 346, 359
 Pandyak N.L. 188
 Parashchuk T.O. 167
 Parasyuk O.V. 163
 Parfenyuk O.A. 301
 Parkhomenko H.P. 133
 Pashchenko A.V. 328
 Pavlenko E.L. 184
 Pavlenko O.L. 116
 Pavlova S. 5
 Pavlyk B.V. 168
 Pavlyuk M.F. 196, 269
 Payentko V.V. 131
 Pazyuk 370
 Pazukha I.M. 285
 Pedchenko Yu.M. 159
 Peleshchak R.M. 30, 85, 220
 Penyukh B. 302
 Perederii O. 245
 Perekrestov V.I. 76
 Perevoznikov S.S. 52
 Petrenko I.V. 154
 Petrenko L.G. 175
 Petrosyan L. 123
 Petrovich R.Y. 217
 Petrus R.Y. 18, 121
 Petrushenko S. I. 38, 134, 276
 Pietruszka R. 123
 Pisak R.P. 314
 Piskach L.V. 163
 Płaczek-Popko E. 121
 Plakhtiy E.G. 20
 Pletenytska L.S. 358
 Pobigun O.I. 231
 Pogosov V.V. 75
 Pokhmurskii V. 227
 Polit J. 95
 Pop M.M. 305
 Pop O.I. 310
 Poplavsky I.O. 214, 215, 240
 Poplavskyy O.P. 214
 Popov V.G. 58
 Popovych A. 241
 Popovych D.I. 240

- Popovych N. 241
 Posudievsky O. 245
 Potapenko A.V. 242, 343
 Potyak V.Yu. 158
 Poznyak S.K. 52
 Pritchyn S.E. 86, 87
 Prohorenko S.V. 141
 Prokopenko I. 233
 Prokopiv L.M. 364
 Prokopiv V.V. 125, 169, 350
 Prokopiv V.V.(Jr) 360
 Protsenko I.Yu. 135
 Protsenko S.I. 84, 285
 Prudnikov A.M. 328
 Prysyzhnyuk V.I. 303
 Ptashchenko F.O. 153
 Ptashchenko O.O. 153
 Pud A.A. 292
 Pukha V.E. 90
 Pylypko V.G. 142
 Pylyponiuk M.A. 348, 350
 Pyryatynski Yu.P. 292
 Pytiuk O.Yu. 97
 Rachiy B.I. 222, 237, 289
 Rachkovsky O.M. 120
 Radchenko M. 22, 122
 Radelytskyi I. 79
 Radishevskiy M. 288
 Raransky M.D. 346
 Rarata S. 243
 Red'ko R.A. 136
 Red'ko S.M. 136
 Reshetnyak O.V. 188
 Reshytko B.A. 61
 Revutska L.O. 88
 Ribun V. 77, 200, 241, 282, 324
 Rodionova T.V. 89
 Rodych V.M. 197
 Rogachova O.I. 128
 Rogozin I.V. 137
 Romaka L. 351, 354
 Romaka L.P. 352
 Romaka V.A. 352
 Romaka V.V. 351, 352, 354
 Roman Yu. 156, 331
 Romankevych V. 281
 Romanyuk B.M. 58
 Romanyuk L.M. 304
 Romanyuk R.R. 304
 Romerowicz-Misielak M. 95
 Roshchina N.M. 368
 Rubish V.M. 31, 305, 314
 Rudchenko S.O. 90
 Rudko G.Yu. 221
 Rudyk B. 336
 Rudyk Yu.I. 91
 Rumiantsev D.V. 105
 Rutkovsky A.V. 46
 Ruvinskii B.M. 138
 Ruvinskii M.A. 138, 244, 344
 Ryabov L.V. 264, 265, 266
 Ryabtsev S.I. 293
 Rybak A. 5
 Rybak O.V. 353
 Rykavets Z. 354
 Ryzhuk A.O. 161
 Sachenko A.V. 19
 Sadkovska L.V. 173
 Sadova N.N. 232
 Sadowski J. 79
 Safriuk N. 156, 171, 281
 Safryuk N.V. 18
 Sai P.O. 139
 Sakalosh I.I. 200
 Salamo G. 315
 Saliy Ya.P. 306, 307
 Saltykov D.I. 308
 Samojlenko D.V. 193
 Samsonik A.L. 38
 Savchuk A. 53
 Savka S.S. 240
 Savytsky H.V. 270
 Selikhova A.V. 113
 Semkiv I.V. 197
 Semko T.O. 170
 Seneta M.Ya. 30

- Seniv M.S. 348
 Senko I.M. 309
 Serba O.A. 19
 Serednytski A.S. 240
 Sergeeva L. 216
 Sergeyeva T. 216
 Seti Ju.O. 92, 97
 Severin I. 245
 Sezonenko A.Yu. 265
 Shabel'nyk Yu.M. 135
 Shapoval K.O. 246
 Shenderovskiy V.A. 32, 196
 Shendyukov V.S. 52
 Sheregii E.M. 95
 Shergii E.M. 141
 Shevchenko G.P. 26
 Shevchuk I.S. 247
 Shevchuk O.M. 18
 Shirinyan A. 140
 Shkarban R.A. 248
 Shkolnikova T.V. 204
 Shkurdoda Yu.O. 308
 Shpak I.I. 310
 Shpak M. 310
 Shpilevsky E.M. 33
 Shportko K.V. 88
 Shpotyk O. 5
 Shpotyuk O. 225
 Shtapenko E.Ph. 256
 Shtefan V.V. 204
 Shulga S. 253
 Shuliarenko D.O. 308
 Shumakova M.O. 135
 Shumsky V.P. 228
 Shunkina O.V. 335
 Shuqing F. 337
 Shurygin F. 288
 Shvachko S. 354
 Shylo A.V. 93
 Shynkarenko O.V. 107
 Shynkarenko O.V. 141
 Shynkarenko V.V. 27, 139
 Sibov-Medinschi G.L. 283
 Sichka M.Yu. 200
 Sidletsky. V.A. 226
 Sidorenko S.I. 248
 Sinelnik A.V. 249
 Sirenko H.O. 198, 199, 299
 Skatkov L.I. 250
 Skipochka D.G. 189
 Sklyarchuk V. 336
 Skorokhod A.A. 355
 Slobodzyan D.P. 168
 Slynko V.E. 42
 Slyotov M.M. 125, 311
 Slyotov O.M. 269, 309
 Smertenko 368, 369
 Snopok B.A. 210
 Soldatkin O.O. 252
 Solodin S. 336
 Solodkyi M. 110, 156, 331
 Solomenko A.O. 177
 Solopan S.O. 356
 Solovan M.M. 54
 Soltys L.M. 198
 Sopinsky M.V. 312
 Stadnyk Yu. 351, 354
 Stadnyk Yu.V. 352
 Stan'ko M.H. 220
 Starokadomsky D. 253
 Stasyuk Z.V. 35
 Steblenko L.P. 254
 Steblova O.V. 64, 94
 Stelmakh Y. 122
 Stelmakh Ya.A. 22
 Stepanchikov D. 53
 Stetsenko A.N. 124
 Stetsyuk T.V. 278
 Stolyarchuk I.D. 95
 Story T. 22, 122
 Stratiychuk I.B. 49
 Strebezhev V.M. 142
 Strebezhev V.V. 142
 Strelchuk V. 63, 243, 255, 315
 Strikha M.V. 37
 Strizheus D. 105

- Stroganov O.V. 313
 Stronska O. 187
 Stronski A. 88, 238, 255
 Stubrov Yu. 63, 106
 Studenyak I.P. 268, 284
 Studzinski S.L. 116
 Stynska V.V. 364
 Sukach A.V. 143, 149
 Sukhov V.N. 38, 134, 276
 Sulym P.O. 144
 Sulyma I.V. 199
 Sumariuk O. 271
 Suprun O.M. 157
 Swiatek Z. 270
 Syrotyuk S.V. 297
 Syvorotka I. 281
 Syvorotka I.I. 257
 Takacs V. 118
 Tarasova A.Y. 334
 Tarnaj A.A. 314
 Tartachnyk V.P. 154
 Tatarchuk T.R. 236
 Telbiz G.M. 39
 Temchenko V.P. 115
 Terebinska M.I. 96, 98
 Terletsy A. 327
 Tetyorkin V.V. 143, 149
 Timofeeva I. 123
 Tkach M.V. 92, 97
 Tkach O. 110
 Tkach O.P. 135
 Tkach S.V. 11
 Tkach V. 271272
 Tkach S.V. 185
 Tkachenko A. 253
 Tkachuk A.I. 143, 149
 Tkachuk I.G. 148
 Tkachuk O.I. 96, 98
 Tokarev S.V. 18
 Tokarev V.S. 18
 Toma I.P. 78
 Tomashyk V.M. 49, 182, 195
 Tomashyk Z.F. 182
 Trikur I.I. 200
 Troitskiy G.A. 93
 Trotsenko S.P. 143, 149
 Trunov M.L. 31, 314
 Trzyna M. 79
 Tsapovska Zh.Ya. 291
 Tsebrienko T.V. 99
 Tsiupko F.I. 261
 Tsotsko V.I. 362, 365
 Tsud N. 218, 241, 286
 Tsybulskaya L.S. 52
 Tsykaniuk B. 315
 Tsymbalyuk T.P. 356
 Tsyzh B. R. 183
 Tur Y. 55, 145
 Turovska L.V. 169, 201
 Tymochko M.D. 171
 Tytarenko V.V. 256
 Ubizskii S.B. 257
 Uhorchuk V.V. 211
 Uhryn Yu.O. 30
 Ukrainets N.A. 121
 Ulyanytsky K.S. 54
 Uvarov V.S. 328
 V'yunov O.I. 108
 Vakalyuk A.V. 339
 Vakalyuk V.M. 339
 Vaksman Yu.F. 100
 Varavin V.S. 270
 Varvaruk V.V. 347
 Vasilkovskaya M. 123
 Vasylechko L.O. 257
 Vasyliiev O. 288
 Vasylyeva H. 101
 Velchenko A.A. 85
 Veleschuk V.P. 154
 Veltruska K. 241
 Venger E.F. 127
 Venger I.V. 127
 Venhryn Yu.I. 240
 Veres M. 218
 Vikhor L.N. 68
 Vilinskaya L. 274

- Virt I. 55, 145, 316
 Vlasenko O.I. 154, 340
 Vlasenko O.V. 132
 Vlasenko Z.K. 154
 Vlaykov G.G. 266
 Vlček M. 238, 255
 Vlchek M. 282
 Vodolazchenko S.A. 250
 Vodopyanov V.N. 148
 Voitkiv H. 178
 Voitsekhivska O.M. 92, 97
 Voitsekhovskii A.V. 270
 Volochanska B.P. 167, 172
 Vorontsova L.O. 260
 Voroshchenko A.T. 159
 Vorovskiy V.Yu. 20, 56
 Voznyak O.M. 258, 360
 Vysochan L. 366
 V'yunov O.I. 61
 Ware M. 315
 Willander M. 243
 Wisz G. 316, 368
 Wojnarowska R. 141
 Wojnarowska-Nowak R. 95
 Wosinski T. 79
 Yablon L.S. 259
 Yakhnevych M.Ya. 102
 Yakushev M.V. 270
 Yanitskyi V.Y. 48
 Yaremchuk I. 357
 Yaremiichuk O.V. 356
 Yaremiy I.P. 84
 Yaremiy S.I. 279
 Yarovets I.R. 215
 Yashchenko L.M. 260
 Yashchynskyy L.V. 346, 359
 Yasinko T.I. 31
 Yatsyshyn B.P. 202, 335
 Yatsyshyn M.M. 188
 Yavorskyi R. 203, 316
 Yavorskiy Y.S. 13
 Yavorskyi Y.V. 41, 103
 Yepifanova A.S. 204
 Yeromenko Y.S. 329
 Yukhymchuk V.O. 39, 130
 Yurchenko O.M. 163
 Yurchyshyn L.D. 358
 Yurgelevich I.V. 254
 Yuriychuk I.M. 142
 Yurkovych N. 126
 Yuryev S.O. 205, 261
 Yushchuk S.I. 205, 261
 Yuzepovich O.I. 146
 Zabludovsky V.A. 256
 Zabolotnyi M.A. 266
 Zahn D.R.T. 268
 Zaitsev R.V. 16
 Zakharchenko N.M. 132
 Zakharchuk D.A. 346, 359
 Zakharuk Z. 336
 Zamuruieva O.V. 164
 Zapukhlyak R.I. 360
 Zapukhlyak Z.R. 356
 Zaretska N.S. 103
 Zatovsky I.V. 40, 166
 Zaulychnyy Ya.V. 41, 103
 Zavaliy I.Yu. 231
 Zayachuk D.M. 42, 363
 Zbihlei L. 262
 Zdeshchyts A.V. 206
 Zelenina I.S. 317
 Zhuk D. 118
 Zinchenko V.F. 117, 173
 Zmiiovska E.O. 121, 197

**Штрихи життєвого та творчого шляху
Фреїка Дмитра Михайловича
(5.04.1943-5.06.2015)**



Фреїк Дмитро Михайлович народився 5 квітня 1943 р. у селі Кінашів, Галицького району, Івано-Франківської області. Батьки – Фреїк Михайло Ількович та мати Фреїк (Рекута) Юстина Степанівна – селяни.

Семирічну освіту отримав у місцевій, а середню – у Більшівцівській середній школі Івано-Франківської області. У 1959-1964 рр. навчався на фізико-математичному факультеті Івано-Франківського державного педагогічного інституту, який закінчив з відзнакою за спеціальністю „Фізика і загально-технічні дисципліни”. З 1964 р. по 1968 р. навчався в аспірантурі Львівського університету за спеціальністю „Фізика твердого тіла”, яку завершив захистом кандидатської дисертації (1968 р.).

У 1968 р. повернувся до Івано-Франківського педагогічного інституту на посаду викладача кафедри фізики. У 1984 р. захистив докторську дисертацію. З 1978 р. – завідувач кафедр методики фізики, фізики, фізики і хімії твердого тіла. Водночас з 1999 р. – директор Фізико-хімічного інституту при Прикарпатському університеті.

Професор Фреїк Д.М. – визнаний вчений з міжнародним іменем у галузі напівпровідникового матеріалознавства – фізики і технології кристалів, тонких плівок і наносистем сполук АІВVI та АІVВVI.

Одним із перших в Україні, ще у 70-і роки минулого сторіччя, Фреїк Д.М. розпочав дослідження методів вирощування і вивчення структури та фізичних властивостей тонких плівок халькогенідів металів другої та четвертої груп – на той час нового типу матеріалів з напівпровідниковими властивостями.

Продовжує успішно працювати заснована професором Фреїком Д.М. наукова школа з широкого кола співробітників, докторантів, аспірантів, магістрантів і студентів, яка широко відома своїми працями науковій громадськості як нашої держави так і далеко за її межами. Фреїк Д.М.

співавтор понад 700 монографій, наукових статей, авторських свідоцтв на винаходи та патентів України. Під його науковим керівництвом захищено 60 докторських і кандидатських дисертаційних робіт. Здійснено виконання ряду наукових проектів. Заснований за його ініціативою на фізико-технічному факультеті досі працює щотижневий науковий семінар з проблем фізичного матеріалознавства, який є справжньою школою для молодих науковців. Він засновник і головний редактор до кінця своїх днів наукового журналу „Фізика і хімія твердого тіла”, який є фаховим виданням із фізико-математичних, хімічних та технічних наук.

Фреїк Д.М. здобув міжнародне визнання: нагороджений медаллю РАН "Академік Курнаков Микола Семенович" (1978 р.), Міжнародним грантом Дж. Сороса (1995 р.), академік Міжнародної термоелектричної академії наук (2002 р.), член американського Товариства з вирощування кристалів (2003 р.), Соросівський професор (1997 р.), Видатний вчений ХХ століття (біографічний центр Кембридж, Англія) (1999 р.), Лауреат премії "Галицькі кмітливіці-2001 і 2007", „Людина-2001" (Кароліна, США), нагороджений відзнакою "За вклад у науку" ДФФД МОН України (2008) і МОН України "За наукові досягнення", та відзнакою державного департаменту інтелектуальної власності України "Творець", орденом «За заслуги III ступеня» (2009), дипломом «Відомий науковець року» (2011), Лауреат щорічної премії імені Г. Терсенова (2012 р.) Івано-Франківської ОДА і обласної ради та ТВР і СНІО України», обраний академіком Академії наук вищої школи України (2007) і Технологічної академії України.

Фреїк Д.М. – був ініціатором створення ряду громадських організацій: Івано-Франківського відділення Українського фізичного товариства, Асоціації „Вчені Прикарпаття", Івано-Франківського відділення наукового товариства ім. Т.Г. Шевченка. Був головним редактором Вісника Прикарпатського університету „Математика. Фізика", головою спеціалізованої вченої ради із захисту дисертацій зі спеціальностей фізика і хімія поверхні та хімії твердого тіла, членом ряду спеціалізованих рад у інших вузах України, експертом ВАК України, членом наукової ради НАН України з фізики напівпровідників і діелектриків.

Слід відзначити продуктивну роботу у редакційних колегіях наукових журналів:

- „Фізична інженерія поверхні, „Вісник ЧНУ. Фізика. Електроніка";
- “Фізика і хімія твердого тіла”;
- “Вісник Прикарпатського університету. Серія Фізика”;
- Journal of Precarpathian University;
- Прикарпатський вісник НТШ. Фізика і хімія твердого тіла;

та в оргкомітетах міжнародних конференцій:

- New Electrical and Electronic Technologies and their Industrial Implementation,

- Фізики напівпровідників,
- International Symposium "Thin Films in Electronics",
- International Conference on Modification of Properties of Surface Layers on Non-Semiconducting Materials Using Particle Beam).

Фреїк Д.М. – не тільки визнаний вчений, але і висококваліфікований викладач, який зробив вагомий внесок у підготовку спеціалістів вищої кваліфікації як для освіти так і для промислового потенціалу України.

Професор Дмитро Фреїк був завжди у творчому піднесенні, сповнений оптимізму в науці і задоволений потенціалом створеної ним наукової школи, яка успішно розв'язує важливі проблеми фізико-хімічного матеріалознавства.

Фреїк Д.М. – ініціатор і організатор відомих міжнародних конференцій з фізики і технології тонких плівок та наносистем, які стали фактично синтезуючим центром науки у нашій державі із цього напрямку. Чергова з них XVI присвячується світлій пам'яті професора Дмитра Фреїка.

02.05.2017

Л. Межиловська

Фінансова підтримка МКФТТПН-XVI –
компанія [ТОВ «Матеріалз Лаб»](#)



ТОВ «Матеріалз Лаб» спеціалізується на аналізі та підготовці до використання нових технологій, розробці і впровадженні рішень для різних лабораторій та виробництв, постачає й обслуговує аналітичне, дослідницьке, промислове обладнання провідних світових виробників. Надає консультації та комплексні рішення і здійснює ремонт відповідно до поставлених технологічних завдань.

ТОВ "Матеріалз Лаб" – активно розвивається на ринку планування та організації наукових і прикладних досліджень, а також їх забезпечення аналітичним, лабораторним та промисловим обладнанням наступних виробників:

- 1) **Pfeiffer Vacuum GmbH** (Німеччина) (винахідник турбомолекулярного насосу, виробник вакуумного обладнання);
- 2) **Presi** (Франція) (виробник високоякісного обладнання для металографічної пробопідготовки);
- 3) **Linseis** (Німеччина) (розробник та виробник передових інноваційних продуктів в області термічного аналізу та теплофізичних властивостей матеріалів);
- 4) **CILAS** (Франція) (винахідник та виробник обладнання для визначення розміру частинок за допомогою лазера);
- 5) **Alexanderwerk AG** (Німеччина) (світовий лідер у виробництві та розробці компакторів, грануляторів та ущільнювачів);
- 6) **Seron Technologies Inc** (Південна Корея) (провідний світовий виробник електронних мікроскопів);
- 7) **KRUSS GmbH** (Німеччина) (прилади для дослідження поверхневих явищ);
- 8) **SOL Instruments** (Білорусь) (розробка і виробництво наукоємного обладнання для оптичних та фотометричних вимірювань, аналізу елементного складу матеріалів та мікроскопічних досліджень);
- 9) **PROTO Manufacturing** (США) (світовий лідер у виробництві рентгенівських дифрактометрів та систем визначення залишкових напруг)

10) **AMETEK Scientific Instruments** (США) (винахідник синхронного підсилювача, виробник обладнання для електрохімії та відновлення слабого сигналу);

та інші.

Співробітники компанії – висококваліфіковані дипломовані фахівці, які беруть безпосередню участь у спільній роботі з науковими і технічними центрами України і Європи в широкому спектрі досліджень в інноваційних напрямках. Інженери ТОВ «Матеріалз Лаб» мають великий досвід роботи в науково-дослідних інститутах Національної Академії Наук України, є власниками патентів на наукові розробки різних сучасних технологій та нових класів матеріалів.

Наукове видання

ФІЗИКА І ТЕХНОЛОГІЯ ТОНКИХ ПЛІВОК ТА НАНОСИСТЕМ
Матеріали XVI Міжнародної конференції, присвяченої пам'яті
професора Дмитра Фреїка
МКФТТПН-XVI

PHYSICS AND TECHNOLOGY OF THIN FILMS AND NANOSYSTEMS
Materials of XVI International Conference
dedicated to memory Professor Dmytro Freik
ICRTTFN-XVI

Технічний редактор *Роман Дзумедзей*
Відповідальний за випуск *Любомир Никируй*

Усі матеріали подано у авторській редакції

Підписано до друку 22.04.2017.
Формат 60x84/16. Ум. др. 23,75 арк. Гарнітура «Times New Roman».
Папір офсетний, друк цифровий. Тираж 300 примірників.

Видавець
ДВНЗ «Прикарпатський національний університет
імені Василя Стефаника»,
вул. С. Бандери, 1, м. Івано-Франківськ, 76000.
Тел. (0342) 71-56-22.
E-mail: vdvcit@pu.if.ua

*Свідоцтво суб'єкта видавничої справи
ДК №2718 від 12.12.2006.*

Друк: підприємець Голіней О.М.
76008 м. Івано-Франківськ, вул. Галицька, 128
Тел. +38 (0342) 58-04-32, +38 050 540 30 64
E-mail: gsm1502@ukr.net